Short Papers in Geology and Hydrology Articles 60-121

GEOLOGICAL SURVEY RESEARCH 1963

GEOLOGICAL SURVEY PROFESSIONAL PAPER 475-C

Scientific notes and summaries of investigations prepared by members of the Conservation, Geologic, and Water Resources Divisions

UNITED STATES DEPARTMENT OF THE INTERIOR

STEWART L. UDALL, *Secretary*

GEOLOGICAL SURVEY

Thomas B. Nolan, *Director*

FOREWORD

This collection of 62 articles is the second of a series to be released in 1963 as chapters of Professional Paper 475. The articles report on scientific and economic results of current work by members of the Geologic, Water Resources, and Conservation Divisions of the United States Geological Survey. Some of the papers present the results of completed parts of continuing investigations; others announce new discoveries or preliminary results of investigations that will be discussed in greater detail in reports to be published in the future. Still others are scientific notes of limited scope, and short papers on methods and techniques.

Chapter A of this series will be published later in the year, and will present a synopsis of work of the Geological Survey during the present fiscal year.

Thomas B. Nolan,

Director.

III

CONTENTS

STRUCTURE OF PRECAMBRIAN CRYSTALLINE ROCKS
IN THE NORTHERN PART OF GRAND TETON NATIONAL PARK, WYOMING

By JOHN C. REED, JR., Denver, Colo.

Abstract.—Metasedimentary gneisses of high metamorphic grade in the northern part of Grand Teton National Park have been subjected to at least two periods of Precambrian deformation. The older was preceded or accompanied by formation of foliated granitic gneiss; the younger was followed by emplacement of quartz monzonite and mica pegmatite. Previously published isotopic age determinations are somewhat anomalous, but they suggest that pegmatite associated with the younger granitic rocks may be as old as 2,660 million years.

The Precambrian crystalline rocks of the Teton Range, Wyo., (fig. 60.1) were first noted and briefly described by members of the Hayden survey (F.H. Bradley, 1873; St. John, 1879). Since that time the surrounding Paleozoic and younger rocks have been extensively studied, but the Precambrian crystalline rocks in the core of the range have received surprisingly little attention. Horberg and Fryxell (1942) briefly described some of the metasedimentary rocks in the Precambrian complex, and C. C. Bradley (1956) made a detailed study of structures in the Precambrian rocks in a small area in the central part of the range. Giletti and Gast (1961) made isotopic age determinations on minerals from pegmatite and gneiss from Death Canyon in the southern part of the range, and Eckelmann (1963) studied zircons from a few of the gneisses and granitic rocks.

In the summer of 1962 the writer began a study of the Precambrian rocks of Grand Teton National Park. Fieldwork during the summer was concentrated in the northern part, and mapping was completed between Webb Canyon and the divide south of Snowshoe Canyon (fig. 60.2). Tentative conclusions regarding the Precambrian structural history of the crystalline rocks in the area are summarized in this article. No doubt some of these will have to be modified as a result of more detailed petrographic studies and geologic mapping in other parts of the Teton Range.

The oldest rocks mapped are a heterogeneous sequence of interlayered medium- and fine-grained amphibole gneiss, biotite-amphibole gneiss, biotite gneiss, and amphibolite, containing thin beds of amphibole schist, biotite schist, biotite-muscovite schist, and locally, sillimanite schist. The sequence also contains layers and lenses of fine-grained light-gray or white quartz-feldspar gneiss and quartzite. In one exposure northwest of Lake Solitude (fig. 60.1), south of the area mapped, a thin layer of dark-gray marble occurs in similar layered gneiss. Pods and sill-like bodies of coarse-grained amphibolite, hornblendite, and altered ultramafic rocks are locally common in the layered gneiss.

The gneisses and schists are all of high metamorphic grade, probably in the sillimanite zone. They are conspicuously layered and generally display a strong foliation parallel to layering. Individual layers range from fractions of an inch to tens of feet in thickness, and some can be traced for hundreds of feet. In detail, however, many layers are discontinuous, and some are pulled apart into isolated pods and lenses. Locally, some layers are found in small isoclinal folds, whereas adjacent layers above and below seem undisturbed (fig. 60.3). It seems unlikly that the layering in the gneiss is relatively undisturbed bedding as suggested by Horberg and Fryxell (1942). Rather, the layers appear to represent a sequence of isoclinally folded and intensely sheared beds in which individual folds have been largely sheared out and obliterated, so that no lithologic contact represents an original bedding plane. Thus, inferences as to stratigraphic sequence and original thickness are meaningless.

Nevertheless, the character of the layering, the mineralogy of many of the gneisses and schists, and the occurrence of quartzite and marble strongly support Horberg and Fryxell's conclusion that these rocks were derived from sedimentary rocks; they were probably

EXPLANATION

Quaternary deposits

Tertiary volcanic and
sedimentary rocks

Mesozoic sedimentary rocks

Paleozoic sedimentary rocks

Precambrian rocks

Contact

Fault

*Dashed where approximately
located; dotted where concealed*

0   5   10 MILES

FIGURE 60.1.—Generalized geologic map of the Teton Range, showing distribution of Precambrian crystalline rocks and location of the area studied (fig. 60.2). Modified from Love (1956).

110°50' 110°45'

43° 55'

EXPLANATION

PALEOZOIC

Sedimentary rocks

Diabase

Quartz monzonite and pegmatite
Dikes shown by dotted lines

PRECAMBRIAN

Foliated granitic gneiss
Containing concordant layers of amphibolite (black)

Layered gneiss and schist
Generalized trend of layering and foliation shown by lines

Contact
Dashed where approximately located

Fault
Dashed where approximately located, dotted where concealed. U, upthrown side; D, downthrown side

Strike and dip of bedding

Inclined   Vertical
Strike and dip of layering

Inclined   Vertical
Strike and dip of foliation

Webb Canyon
Colter Canyon
Ranger Peak
Waterfalls Canyon
Doane Peak
Eagles Rest Peak
Rolling Thunder Mountain
Snowshoe Canyon
Reynolds Peak
Bivouac Peak
Jackson Lake
TETON FAULT

0   1   2   3   4 MILES

Inclined   Horizontal
Direction and plunge of lineation marked by alinement of mineral grains or elongate aggregates

Strike and dip of axial plane of minor fold

Inclined   Horizontal
Direction and plunge of axis of minor fold or crenulation

FIGURE 60.2.—Geologic map of the Precambrian rocks in the northern part of Grand Teton National Park. Surficial deposits not shown. Geology mapped in 1962 by J. C. Reed, Jr., assisted by J. H. Dieterich and T. B. Ranson.

derived from a sequence composed largely of shale, calcareous shale, and siltstone, containing some interbedded sandstone and a few layers of impure limestone or dolomite. Some of the amphibolite and amphibole gneiss may have been formed from mafic lava or tuff.

In addition to the partly obliterated isoclinal folds described above, the layered gneiss displays many subisoclinal folds with diverse axial orientations. These differ from the isoclinal folds in being more open and in the continuity of layers in their limbs (fig. 60.4). Locally they have refolded the older isoclines. The diverse orientation of the younger folds suggests that they may be of several generations, but their pattern is complicated by post-Precambrian folding and faulting and has not as yet been satisfactorily worked out.

FIGURE 60.3.—Layered gneiss about half a mile S. 65° E. of summit of Ranger Peak. Interlayered amphibole-biotite gneiss (light gray), amphibole schist (dark gray), and quartz-feldspar gneiss (white). Note the rootless isoclinal fold (upper center) and the many discontinuous layers.

FIGURE 60.4—Subisoclinal fold in thinly interlayered amphibole gneiss and quartzite. About 500 feet north of lower fork of Snowshoe Canyon.

Medium-grained granitic biotite gneiss forms large bodies associated with the layered-gneiss sequence and forms smaller sill-like bodies within the layered gneiss. The rock is strongly foliated but is generally without layering, although locally it is crudely layered, especially near contacts with the layered gneiss. Contacts are concordant with the layered gneiss, and foliation in the granitic gneiss is parallel to foliation and layering in the layered gneiss. Near the contacts some fine-grained layered gneiss is interleaved with the granitic gneiss. The granitic gneiss contains layers of fine- to medium-grained amphibolite a few feet to several hundred feet thick, some of which have been traced for several miles. The amphibolite in these layers is similar to that which forms thinner layers in the layered-gneiss sequence. The granitic gneiss has nowhere been found in dikes or other crosscutting bodies.

The structural concordance between foliation in the granitic gneiss and in the layered-gneiss sequence, the lack of crosscutting, the absence of inclusions, and the continuity of the amphibolite layers suggest that the granitic gneiss may have formed through some sort of transformation in situ of selected parts of the sedimentary sequence from which the layered gneiss was formed, and that the amphibolite bodies represent layers of a composition that was especially resistant to the process.

Parallelism between foliation and lineation in the granitic gneiss and similar structures formed during the early deformation in the layered gneiss indicates that the granitic gneiss, whatever its origin, was emplaced before or during the earliest recognized period of deformation. Open folds in the foliation and in some of the amphibolite layers are similar to the second-generation folds in the layered gneiss and show that the granitic gneiss was clearly formed before this deformation.

Fine-grained light-gray or white muscovite-biotite-quartz monzonite and associated muscovite- and biotite-bearing pegmatite form large irregular masses in the southern part of the area mapped. Dikes of similar pegmatite and aplite cut the layered gneiss and granitic gneiss. Similar rocks are widespread farther to the south, where reconnaissance shows that they form a major part of the Precambrian complex south of Leigh Canyon.

The quartz monzonite locally displays faint flow structure that is discordant with the structures of the enclosing rocks. The larger bodies contain abundant angular blocks of layered gneiss, amphibolite, and granitic gneiss ranging from less than a foot to hundreds of feet in length (fig. 60.5). At the margins of the larger bodies of quartz monzonite and pegmatite the enclosing rocks are crisscrossed by swarms of pegmatite and aplite dikes, so that the contacts are arbi-

trarily placed where the granitic rocks form about half of the total mass. The dike swarms dwindle out gradually away from the granitic bodies, but a few scattered dikes of mica pegmatite occur throughout the area mapped.

Contacts of the dikes of quartz monzonite and pegmatite, and of the inclusions in the granitic bodies, are knifesharp. Undeformed pegmatite and aplite dikes cut through second-generation folds in the layered gneiss, and some of the angular included blocks of layered gneiss contain similar folds, showing that the pegmatite and quartz monzonite were emplaced after the second episode of Precambrian folding.

Adjacent to the large granitic bodies some of the layered gneiss contains abundant granitic folia and feldspar porphyroblasts. The metamorphic grade of the layered gneiss, however, seems to remain nearly the same throughout the area. The discrimination between the metamorphic effects associated with the emplacement of the younger granitic rocks and those to be attributed to the older metamorphism will have to await further petrographic study.

One dike of fine- to medium-grained gray diabase cuts the Precambrian rocks between Raynolds Peak and Bivouac Peak. The dike ranges from a few feet to about 50 feet in thickness. The dike rock and the trend of the dike are similar to the conspicuous well-known diabase dikes farther south that are truncated by Cambrian rocks, and the dike in the Raynolds Peak area is therefore believed to be of the same age. The dike has chilled borders, and rocks adjacent to it are baked and stained bright red brown. The chilled margins and the sharp truncation of all older structures indicate that the dikes were emplaced long after the quartz monzonite and pegmatite, as has been pointed out by Bradley (1956).

FIGURE 60.5.—Angular inclusions of granitic gneiss in fine-grained quartz monzonite about 0.2 mile northwest of Lake Solitude (fig. 60.1). Note rotation of foliation in the blocks, and very faint flow structure in the enclosing quartz monzonite. Dike of light-colored biotite-garnet pegmatite cuts foliation of granitic gneiss in block in upper left, but is truncated by the quartz monzonite. A small dike of younger muscovite pegmatite (below hammer) cuts both quartz monzonite and granitic gneiss, but is inconspicuous in the granitic gneiss in this photograph.

The observations and conclusions summarized above suggest the following tentative Precambrian structural history for the northern part of the Teton Range:

1. Deposition of a great but unknown thickness of sedimentary rocks composed of shale, calcareous shale, and siltstone, some interbedded sandstone and impure limestone, and possibly some volcanic rocks.
2. Deep burial and regional metamorphism of these rocks, accompanied by intense shearing and isoclinal folding, and probably by emplacement of small bodies of ultramafic rocks. At about the same time, granitization in situ of selected parts of the sequence to form granitic gneiss.
3. One or more periods of folding with less intense shearing. Older isoclinal folds refolded.
4. Emplacement of discordant bodies and dikes of fine-grained quartz monzonite and pegmatite.
5. Long interval of cooling, consolidation, and fracturing.
6. Emplacement of diabase dike.
7. Long interval of erosion and subsidence followed by deposition of Middle Cambrian Flathead Sandstone.

At present it is impossible to assign absolute ages to the various Precambrian events. The only absolute age determinations available from the Teton Range are for pegmatite and gneiss in Death Canyon. The pegmatite is probably the same age as the mica pegmatites associated with the quartz monzonite in the area mapped. Rubidium-strontium age determinations by Giletti and Gast (1961) on muscovite and microcline from the pegmatite give 2,660 and 1,990 million years, respectively. Determinations on biotite from the enclosing rocks, however, give 1,360 million years. This anomaly casts considerable doubt on the significance of these determinations. It is hoped that further geochronologic work will permit assignment of absolute ages to events recognized on the basis of other geologic evidence.

REFERENCES

Bradley, C. C., 1956, The Precambrian complex of Grand Teton National Park, Wyoming, in Berg, R. R., ed., Wyoming Geol. Assoc. Guidebook 11th Ann. Field Conf., Teton Range and Jackson Lake, Wyo.: p. 34–42.

Bradley, F. H., 1873, Report of Frank H. Bradley, geologist of the Snake River Division, in Hayden, F. V., Sixth Annual Report of the U.S. Geological Survey of the Territories * * * for the year 1872: Washington, U.S. Govt. Printing Office, p. 189–271.

Eckelmann, F. D., 1963, Zircon paragenesis in Precambrian crystalline rocks of the Teton Range, Wyoming, [abs.]: Geol. Soc. America Spec. Paper 73, p. 143.

Giletti, B. J., and Gast, P. W., 1961, Absolute age of Precambrian rocks in Wyoming and Montana: New York Acad. Sci. Annals, v. 91, p. 454–458.

Horberg, Leland, and Fryxell, Fritiof, 1942, Pre-cambrian metasediments in Grand Teton National Park, Wyoming: Am. Jour. Sci., v. 240, p. 385–393.

Love, J. D., compiler, 1956, Geologic map of Teton County, Wyoming, in Berg, R. R., ed., Wyoming Geol. Assoc. Guidebook 11th Ann. Field Conf., Teton Range and Jackson Lake, Wyo.: in pocket.

St. John, Orestes, 1879, Report of Orestes St. John, geologist of the Teton Division, in Hayden, F. V., Eleventh Annual Report of the U.S. Geological and Geographical Survey of the Territories * * * for the year 1877: Washington, U.S. Govt. Printing Office, p. 321–508.

PLUTONIC ROCKS OF NORTHERN ZACATECAS AND ADJACENT AREAS, MEXICO

By CLEAVES L. ROGERS; ROGER VAN VLOTEN; JESUS OJEDA RIVERA, EUGENIO TAVERA AMEZCUA, and ZOLTAN DE CSERNA; Denver, Colo.; Washington, D.C.; Mexico, D.F.

Abstract.—Plutonic rocks ranging in composition from dioritic to syenitic intrude Late Jurassic and Cretaceous marine sedimentary rocks in the central part of the Mexican geosyncline. The sediments were folded and uplifted in Eocene time; the deformed sediments were intruded by igneous masses during the late stages of the early Tertiary orogeny. Faulting and magmatic activity recurred during the middle and late Tertiary.

A number of small to moderately large plutons ranging in composition from dioritic to syenitic were examined during a reconnaissance study of phosphate deposits in a large area of north-central Mexico (fig. 61.1). This area, about 26,000 square kilometers in extent is mainly in northern Zacatecas and southern Coahuila States but extends eastward into Nuevo León and San Luis Potosí. Most of the igneous rocks are in Zacatecas.

The area contains a thick section of marine sedimentary rocks that range in age from Late Jurassic to Late Cretaceous and were folded and uplifted during the Eocene. It has been divided into three geologic belts (Rogers and others, 1962), designated, from north to south, as the valley and ridge belt, plain and range belt, and mineral belt. These belts are characterized, respectively, by folds alone; by folds with some faults; and by both folds and relatively common normal and reverse faults, and igneous plutons. Although igneous rocks are confined mainly to the mineral belt, a few small masses occur in the plain and range belt, as in the Sierra Mesquite del Sur of Coahuila.

The mineral belt is a rather broad zone occupying the site of the central part of the Mexican geosyncline (Imlay, 1938). Perhaps because this zone contains a relatively thin sedimentary section, the rocks yielded to the compressive orogenic forces not only by folding but also by extensive faulting. During the late stages of the early Tertiary orogeny these highly deformed sedimentary rocks were invaded by numerous igneous masses, and in middle and late Tertiary time there were several recurrent episodes of faulting and magmatic activity. During these later episodes numerous hypabyssal bodies were formed, and some of the magmas breached the surface. The igneous activity was accompanied by a period of extensive mineralization during which mineralizing solutions penetrated nearly every anticline in the belt. The central part of the mineral belt has played an important part in the Mexican mining industry since the early days of the Spanish conquest.

The intrusive rocks occur as sills, dikes, and small to moderately large stocks. The major areas of plutonic rocks that were observed by the authors are shown in figure 61.1, but there may be other bodies not found in the reconnaissance. The plutonic rocks that were mapped show variations in abundance and a systematic change in composition from west to east, and on this basis the mineral belt and plain and range belt have been divided into three petrographic provinces, labeled western, central, and eastern. To some extent, the older
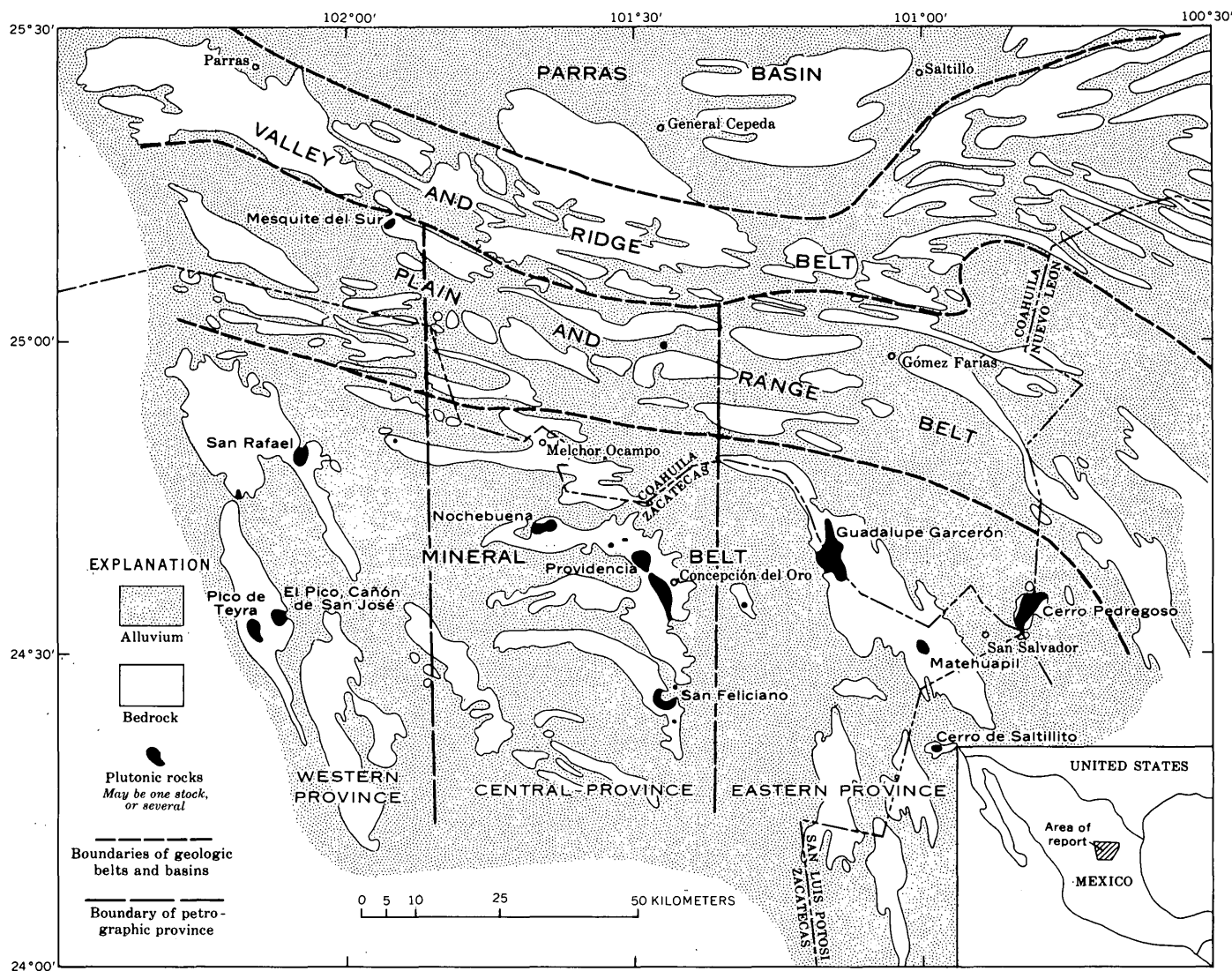
FIGURE 61.1—Sketch map of the area studied, showing principal occurrences of plutonic rocks.

hypabyssal bodies seem to reflect the same changes in composition as the plutonic rocks.

Plutonic rocks are relatively scarce in the western province and occur mainly in the vicinity of Pico de Teyra, an isolated mountain peak that forms the most prominent landmark in this part of the mineral belt. The rocks are mainly quartz monzonite, with local monzonitic and granodioritic facies (see Rogers and others, 1961, table 12, p. 125); they also include some albitic pegmatite and aplite, and one albitite pluton measuring several kilometers in diameter. A small isolated mass in the Sierra de San Rafael about 25 kilometers north of Pico de Teyra has been classed as a latite. Mineralization is meager in this province, and there are no mines. The province contains a few small talc deposits whose origin may be related to hydro-

thermal activity penecontemporaneous with the intrusion of magmas.

The western province extends northward into the plain and range belt, where Imlay (1937, p. 620–622) has described several small masses of monzonite and a dike of light-colored granite, which probably should be classed as an aplite.

The greatest concentration of intrusive rocks is in the central province, a major mining district that produces a variety of base and precious metals, including copper, lead, zinc, iron, silver, and gold. The largest mines are in contact-metasomatic deposits lying along or close to the margins of the three largest plutons, which have been designated the Concepción del Oro, Providencia, and Nochebuena stocks. The rocks of these plutons contain more quartz and plagioclase than the rocks of

the western province and range in composition from granodiorite to diorite. They are characterized by moderately abundant associated aplite but have no associated pegmatite or lamprophyre. The hypabyssal rocks of the central province fall within the same general compositional range and are mainly dacitic to andesitic. The igneous rocks within this province have been previously described by Rosenbusch (in Burckhardt, 1906, p. 23–28), Bergeat (1910), Imlay (1938, p. 1670–1672), and Rogers and others (1956, p. 35–47).

The plutonic rocks of the eastern province are monzonite and syenite (see Rogers and others, 1961; tables 13, 14, and 15); the hypabyssal rocks range from trachyte to latite and andesite. The most conspicuous pluton, the Guadalupe Garcerón stock, is largely monzonitic in composition but is heterogeneous in appearance. It is characterized by abrupt changes in grain size, color, and the ratio of light to dark constituents, and it is cut by numerous small leucocratic and melanocratic dikes that range in composition from monzonitic to syenitic. The stock appears to have been formed by successive surges of magma that were increasingly syenitic. The Matehuapil stock is similar to this mass, but the Cerro Pedregoso stock is relatively homogeneous and composed largely of porphyritic syenite. The albite in these rocks occurs as independent grains as well as in microperthitic intergrowth with the orthoclase, and its relative abundance suggests that the rocks may be transitional in composition and related to the alkalic rocks described by Watson (1937) in the Sierra de San Carlos, Tamaulipas, about 150 kilometers to the east. Alkalic rocks also occur in the Tampico embayment of southern Tamaulipas, and have been described briefly by Muir (1936).

The eastern province is sparsely mineralized, but it contains numerous prospects and several small mines that have produced copper and other metals. The area contains a little barite, which is being mined in the Sierra de Gómez Farías (fig. 61.1) in the northern part of the province and in the vicinity of Galeana, Nuevo León, about 30 kilometers to the east of the mapped area. Galeana is the major barite-producing district in Mexico.

The plutons described are believed to be for the most part contemporaneous and to have been emplaced at a relatively shallow depth shortly after the folding of the Mesozoic sediments toward the end of the early Tertiary orogeny.[1] They share many of the common characteristics ascribed by Buddington (1959) to plutons of the epizone. The plutons are largely discordant with the country rock which they have intruded, and

some have exerted an active upward thrust that domed and in places faulted the overlying rocks. Faulting of this type can be observed around the Concepción del Oro and Providencia stocks (fig. 61.2) and in the vicinity of Pico de Teyra (Rogers and others, 1961, pl. 1.). Other bodies, such as the Guadalupe Garcerón and Matehuapil stocks, appear to have exerted a lateral pressure which in places strongly folded the adjacent country rock without faulting.
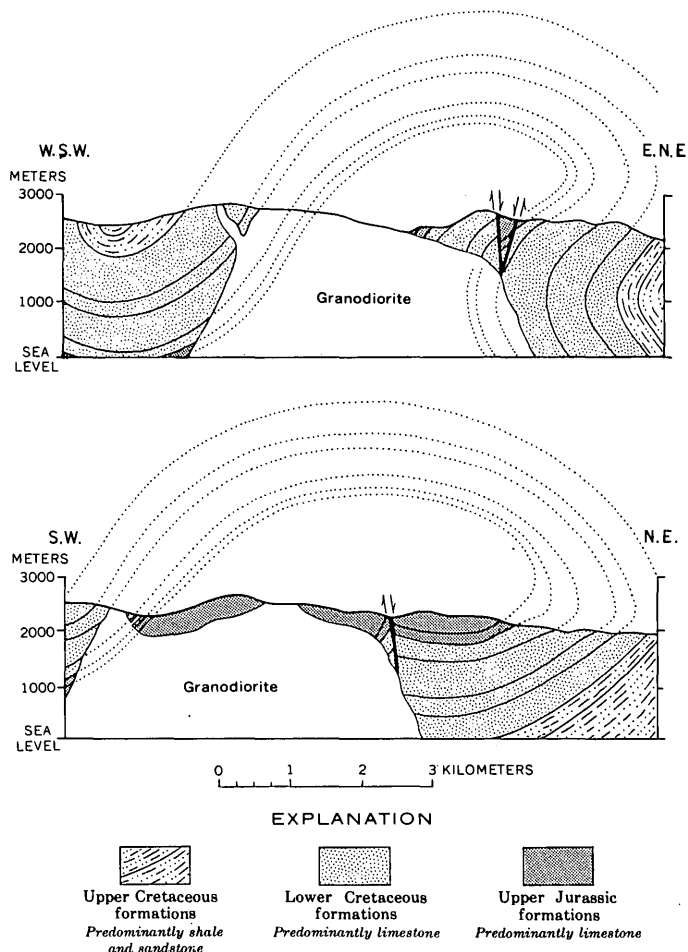
FIGURE 61.2—Structure sections through Concepción del Oro granodiorite stock, showing reconstruction of fold. The stock has been emplaced discordantly in the core of an overturned anticline and appears to have domed and faulted the roof by upward magma pressure.

The plutons have sharp contacts with the enclosing rock. They have metamorphic aureoles of varying width and intensity, and the Concepción del Oro and Providencia stocks are bordered by intermittent skarn zones.[2] Roof pendants are common in some masses.

---

[1] The Concepción del Oro stock has been dated recently by Buseck (1962) by the K-Ar method at about 40 million years, which would place intrusion at the end of the Eocene.

[2] Most of the plutons have intruded carbonate rocks of Late Jurassic or Early Cretaceous age, but some are in contact with Upper Cretaceous shales or with redbeds and metasediments, largely schists and phyllites, of the basement complex.

Many plutons are composite in character and appear to be the product of successive surges of magma, which generally were increasingly felsic. Late-stage dikes are mostly aplitic, although they include some dark rocks rich in mafic minerals. Associated hypabyssal rocks in part resemble rocks of the plutons in composition. Weakly to strongly developed primary foliation occurs in the marginal zones of some plutons. Primary lineation was not observed, but it might be revealed by a more detailed study of the rocks.

REFERENCES

Bergeat, Alfred, 1910, La granodiorita de Concepción del Oro en el Estado de Zácatecas y sus formaciones de contacto: Inst. geol. México Bull. 27.

Buddington, A. F., 1959, Granite emplacement with special reference to North America: Geol. Soc. America Bull., v. 70, no. 6, p. 671–748.

Burckhardt, Carlos, 1906, Géologie de la Sierra de Mazapil et Santa Rosa: Internat. Geol. Cong., 10th, Mexico City, Guide des Excursions, no. 26.

Buseck, P. B., 1962, Contact metasomatic ores at Concepción del Oro, Mexico [Abs.], in Geological Society of America, Abstracts for 1961: Spec. Paper 68, p. 144.

Imlay, R. W., 1937, Geology of the middle part of the Sierra de Parras, Coahuila, Mexico: Geol. Soc. America Bull., v. 48, p. 587–630.

—— 1938, Studies of the Mexican geosyncline: Geol. Soc. America Bull., v. 49, p. 1651–1694.

Muir, J. M., 1936, Geology of the Tampico region, Mexico: Tulsa, Okla., Am. Assoc. Petroleum Geologists, p. 143–151.

Rogers, C. L., Cserna, Zoltan de, Tavera, Eugenio, and Ulloa, Salvador, 1956, General geology and phosphate deposits of Concepción del Oro district, Zacatecas, Mexico: U.S. Geol. Survey Bull. 1037–A, 102 p.

Rogers, C. L., Cserna, Zoltan de, van Vloten, Rogelio, Tavera, Eugenio, and Ojeda, Jesús, 1961, Reconocimiento geológico y depositos de fosfatos del norte de Zacatecas y areas adyacentes en Coahuila, Nuevo León y San Luis Potosí: Consejo de Rec. Nat. no Renovables Bull. 56, 322 p.

Rogers, C. L., Cserna, Zoltan de, Ojeda, Jesús, Tavera, Eugenio, and Vloten, Roger van, 1962, Tectonic framework of an area lying within the Sierra Madre Oriental and adjacent Mesa Central, north-central Mexico: U.S. Geol. Survey Prof. Paper 450–C, p. C21–C24.

Watson, E. H., 1937, Igneous rocks of the San Carlos Mountains, pt. 2 of The geology and biology of the San Carlos Mountains, Tamaulipas, Mexico: Michigan Univ. Sci. Ser., v. 12, p. 99–156.

THE ORDOVICIAN-SILURIAN CONTACT IN DUBUQUE COUNTY, IOWA

By JESSE W. WHITLOW and C. ERVIN BROWN,

Beltsville, Md., and Washington, D.C.

Abstract.—The lower Silurian Edgewood Dolomite disconformably overlies the Upper Ordovician Maquoketa Shale in and near Dubuque County. Although the rocks above and below the contact are similar in lithology, this elusive contact can be recognized by a thin persistent basal conglomerate in the Silurian rocks, and locally by rare erosional remnants of the iron-rich Neda Member of the Maquoketa Shale.

The Mosalem Member of the Edgewood Dolomite of Early Silurian age disconformably overlies the Maquoketa Shale of Late Ordovician age in and near Dubuque County, Iowa. Features of the contact in the Dubuque South quadrangle and the location of outcrops of the Neda Member of the Maquoketa Shale, which occurs as sparse erosional remnants on the surface of disconformity, have been shown previously by us (1960, pl. 2). In that report we also described fragments of the Maquoketa Shale in basal Silurian beds, but did not recognize the regional distribution of the fragments. Exposures of the conglomeratic beds beyond the Dubuque South quadrangle indicate the possible use of the beds regionally as a marker for a gradational contact that is otherwise virtually undetectable. Location of outcrops of both the conglomeratic beds and the Neda Member of the Maquoketa Shale seen in Dubuque County is shown on figure 62.1.

The ancient erosion surface on the Maquoketa Shale has 135 feet of relief in the Dubuque South quadrangle; therefore, at most places the thin uppermost unit, the Neda Member, has been removed, exposing the underlying Brainard Member as shown in figure 62.2. The Neda Member consists of interlayered grayish-red soft shale, dolomitic grayish-green shale, and layers of reddish-brown limonitic oolites. Irregularly shaped phosphatic nodules that have a distinctive yellowish-brown glazed surface and contain embedded oolites are scattered in the oolitic layers. A 5-foot section of the Neda at locality 3 is the thickest seen by the authors. The easternmost traces of the member in Dubuque County are at localities 4 and 5, and the northernmost exposure seen is at locality 1. To the west the eroded edge of the Neda is about 2 miles southwest of locality 3, and 1 mile west of locality 2. The member was first discovered in Iowa by J. V. Howell (1916) in road ditches on Lore Hill (locality 1), about 4 miles west of the Dubuque city limits. Agnew (1955), in a study of well logs and drill cuttings from Iowa, reported other occurrences of the Neda in the subsurface.

The Brainard Member at the Ordovician–Silurian contact ranges from argillaceous thin-bedded commonly fossiliferous dolomite where the upper beds are preserved, as at localities 3, 4, and 6, to soft unfossiliferous dolomitic shale where the upper beds are eroded away. The argillaceous thin-bedded dolomite of the Brainard at many places resembles the lower beds of the overlying Mosalem Member of the Edgewood Dolomite; Calvin (1898, p. 142) referred to the lower beds in the Mosalem as "transition beds" and included them in the Maquoketa.

The Mosalem Member of Early Silurian age, which consists mainly of wavy-bedded argillaceous dolomite, fills the hollows in the top of the Maquoketa Shale and consequently ranges in thickness from a few feet to as much as 94 feet in the Dubuque South quadrangle. The basal conglomeratic zone is about 1 foot thick and contains fragments of shale, dolomite, and phosphatic nodules from the Maquoketa Shale set in an argillaceous and dolomitic matrix. The matrix also contains iron sulfide, glauconite, and minor quantities of barite. The dolomite and shale fragments are mainly from the Brainard Member, and are as much as 1 inch in maxi-
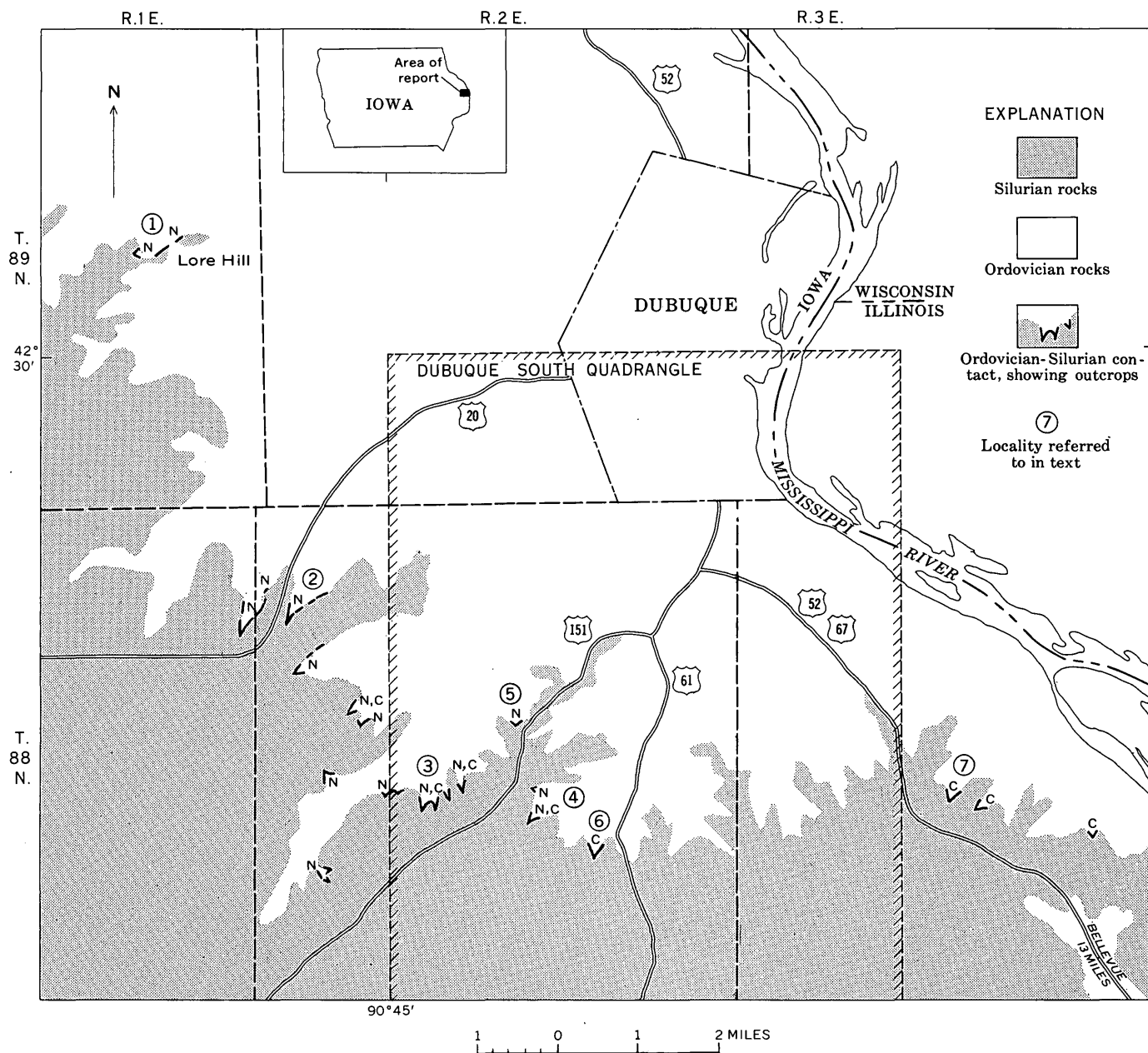
FIGURE 62.1.—Map showing approximate location of the Ordovician-Silurian contact and outcrops studied in Dubuque County, Iowa. *N*, Neda Member of the Maquoketa Shale of Late Ordovician age; *C*, basal conglomerate of the Mosalem Member of the Edgewood Dolomite of Early Silurian age.
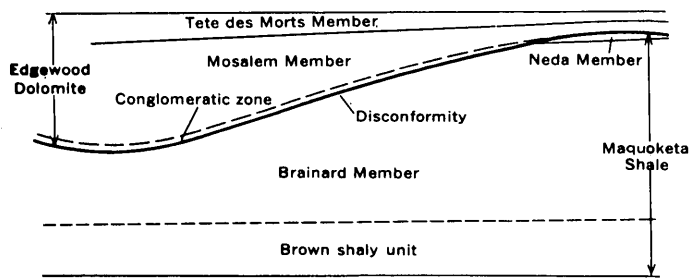
FIGURE 62.2—Diagrammatic section showing stratigraphic relations at the Ordovician–Silurian contact in and near Dubuque County, Iowa. Vertical scale, 1 inch=about 200 feet.

mum dimension. These fragments are difficult to see megascopically because they are texturally similar to the matrix. Phosphatic nodules and limonitic oolites derived from the Neda Member were recognized at localities 3 and 4, where the Silurian overlies the Neda, and at locality 6, where the Neda is missing. Fragments of phosphatic nodules are present not only in the basal conglomerate but are also scattered throughout the overlying few feet of dolomite. The thickness of the zone containing phosphatic debris increases with increasing thickness of the Mosalem. Locally, as at locality 6, weathered iron sulfide causes iron staining of the basal detrital beds. Glauconite was noted in drill cuttings and in unweathered outcrops of the basal Mosalem, but was not seen in weathered outcrops. Phosphatic nodules were found in the basal beds of the Mosalem in cuttings from holes drilled in the Dubuque South quadrange for the U.S. Geological Survey.

Thin-bedded conglomeratic silty dolomite, about 18 inches thick, was found at the base(?) of the Mosalem Member in 1962 by Whitlow at a large roadcut along U.S. Highway 67, a quarter of a mile south of Bellevue, Jackson County, Iowa, about 21 miles southeast of Dubuque. The rock is lithologically similar to the conglomeratic layers in Dubuque County. Except for

scattered phosphatic fossil fragments, the detrital character of the rock is difficult to see in outcrop but is evident on freshly broken surfaces. If this thin zone is the basal conglomerate of the Mosalem Member, the Maquoketa at Bellevue is only about 100 feet thick. This is less than reported by Kay (1935), who included in the Maquoketa Shale some of the shaly dolomite beds overlying the conglomerate.

Phosphatic material and fragmental debris in the basal beds of the Silurian rocks have rarely been reported in Iowa or in northwestern Illinois. Agnew (1955, p. 1718) reported the phosphatic material in basal Silurian beds at only one place in Iowa, and Trowbridge and Shaw (1916, p. 72) described shale pebbles in basal Silurian beds at two places in northwestern Illinois. Although previous notice of these features is rare, the authors believe that the phosphatic conglomeratic beds or traces of the iron-rich Neda Member can probably be found regionally in Iowa and Illinois and can be used as a marker horizon for the Ordovician-Silurian contact either in outcrop or subsurface studies.

REFERENCES

Agnew, A. F., 1955, Facies of Middle and Upper Ordovician rocks of Iowa: Am. Assoc. Petroleum Geologists Bull., v. 39, p. 1703–1752.

Brown, C. E., and Whitlow, J. W., 1960, Geology of the Dubuque South quadrangle, Iowa-Illinois: U. S. Geol. Survey Bull. 1123–A, 93 p. [1961].

Calvin, Samuel, 1898, Geology of Delaware County, in Annual Report, 1897, with accompanying papers: Iowa Geol. Survey, v. 8, p. 122–199.

Howell, J. V., 1916, An outlier of the so-called Clinton Formation in Dubuque County, Iowa: Iowa Acad. Sci. Proc. 23, p. 121–124.

Kay, G. M., 1935, Ordovician system of the Upper Mississippi Valley, in Kansas Geol. Soc. Guidebook 9th Ann. Field Conf., Iowa City, Iowa, to Duluth, Minn.: p. 281–295.

Trowbridge, A. C., and Shaw, E. W., 1916, Geology and geography of the Galena and Elizabeth quadrangles: Illinois Geol. Survey Bull. 26, p. 61–82.

Article 63

SPIRORBAL LIMESTONE IN THE SOURIS RIVER(?) FORMATION
OF LATE DEVONIAN AGE AT COTTONWOOD CANYON,
BIGHORN MOUNTAINS, WYOMING

By CHARLES A. SANDBERG, Denver, Colo.

Abstract.—A small outlying deposit 30 miles southeast of the main body of the marine Souris River Formation may have been laid down in the upper reaches of an estuary. Its abundant and unusual biota includes *Spirorbis*, fish remains, carbonized wood, plant impressions, spores, and megaspores.

A thin deposit of carbonaceous spirorbal limestone and silty calcitic dolomite, containing an abundant and unusual Late Devonian flora and fauna, crops out on the steep north wall of Cottonwood Canyon on the west side of the Bighorn Mountains in sec. 34, T. 57 N., R. 93 W., Big Horn County, Wyo. (fig. 63.1). This is the first recognized occurrence of Upper Devonian rocks that are not certainly marine in the Williston basin or in adjacent parts of Montana and northern Wyoming. The deposit tentatively is considered to be part of a small outlier of the Souris River Formation, which is of early Late Devonian (Frasnian) age outside the Williston basin. The outlier extends at least as far southeast as a well drilled 15 miles from Cottonwood Canyon.

The Souris River Formation has been traced from its type area in the Williston basin into south-central Montana by Sandberg (1961b, pl. 10). It consists of marine thinly interbedded shaly dolomite, argillaceous limestone, shale, siltstone, and anhydrite, and its age and stratigraphic relations in south-central Montana are the same as those of the deposit in Cottonwood Canyon. Two southward-projecting tongues of the main body of the Souris River lie about 30 miles northwest and 110 miles northeast of Cottonwood Canyon (fig. 63.1).

At Cottonwood Canyon, the Souris River(?) Formation underlies a cliff of massive dolomite, 25 feet high, which is at the base of the Jefferson Formation of early Late Devonian (Frasnian) age, and overlies thin ledges of white dolomite at the top of the Bighorn Dolomite of Late Ordovician age. The Souris River(?) has a maximum observed thickness of 16 feet, of which the lower 11 feet forms a partly covered slope and the upper 5 feet forms weakly resistant ledges. The upper part originally was described by Blackstone and Mc-Grew (1954, p. 39) as a 6-foot bed of "reddish weathering pyritic limestone" and black shale 50 feet above the base of the Jefferson. However, regional correlation of the Jefferson between its type section at Logan, in southwestern Montana, and 12 measured sections in the Bighorn and Pryor Mountains (Sandberg, 1961b, pl. 10) demonstrates that the 25-foot-thick massive dolomite is the basal bed of the Jefferson. Blackstone and McGrew (1954) noted the slight disconformity between it and the underlying pyritic limestone but placed the base of the Jefferson much lower. It is likely, however, that they did not observe the ledges of white Bighorn Dolomite about 10 feet below the pyritic limestone, because the pre-Devonian erosion surface is very irregular and drops sharply eastward from the outcrop of the Souris River(?) Formation. Just 225 feet to the east, the eroded top of the Bighorn is 135 feet lower stratigraphically.

The following section of Souris River(?) Formation is exposed for a distance of 75 feet along the canyon wall between talus slides to the east and west. Results of calcium-magnesium analyses of 13 selected samples by James A. Thomas are incorporated in the lithologic descriptions.

Devonian:
  Jefferson Formation.
  Disconformity.
  Souris River(?) Formation:

	Thickness (feet)
Dolomite, calcitic, carbonaceous, pale-yellowish-brown, pale-brown, and light-brownish-gray, microcrystalline, slightly silty. Thin bedded to platy but thinly laminated and fissile at base. Contains abundant spores, megaspores, fish plates, and carbonized plant fragments and large flattened stems. Grades eastward to medium-bedded brownish-gray to brownish-black carbonaceous dolomitic limestone containing pyrite concretions and scattered white coiled worm tubes of *Spirorbis* sp. about 1 mm in diameter. Weathers to yellowish-gray or grayish-orange smooth, powdery surface; forms reentrant _____	1½
Limestone, spirorbal, medium-dark-gray, medium to coarsely fragmental, slightly silty, slightly dolomitic, pyritic. Oxidation of pyrite to hematite colors rock pale brown or grayish red to depth of ¼ to ½ in. from weathered surfaces. Composed largely of *Spirorbis* tubes ½ to 1 mm in diameter. Interbedded with thin lenses of fissile moderate-yellowish-brown and grayish-brown microcrystalline silty calcitic dolomite containing scattered *Spirorbis* tubes. Contains carbonized macerated plant remains and large flattened stems as much as 2 in. wide, fish plates and teeth, and rounded pebbles of carbonized wood as much as 1 in. in diameter. Pyrite coats many *Spirorbis* tubes and partly replaces some carbonized-wood pebbles. Weathers pale brown and yellowish gray; thin bedded to thinly laminated; forms weakly resistant ledges_____	2½
Limestone, carbonaceous, argillaceous, dark-gray and brownish-gray, microcrystalline to cryptocrystalline. Contains spores, megaspores, carbonized macerated plant remains, and scattered white *Spirorbis* tubes. Weathers to very-light-gray or yellowish-gray smooth, rounded surface; medium bedded; forms weakly resistant ledge_____	1
Dolomite, calcitic, carbonaceous, silty, dark-yellowish-brown, pale-brown, and grayish-brown, microcrystalline, earthy, porous, friable. Contains fish plates and teeth, carbonized plant remains, spores, megaspores, and scattered *Spirorbis* tubes. Weathers yellowish gray; thin bedded to laminated; nonresistant; forms partly covered slope with 1½-foot-thick ledge near middle_____	9
Dolomite, silty, pale- to dark-yellowish-brown and yellowish-gray mottled with pale-yellowish-brown; in part carbonaceous. Dark-yellowish-orange porous finely to very finely crystalline rhombic sandy dolomite at base. Contains fish plates and teeth, spores, megaspores, and carbonized plant stems. Weathers to yellowish-gray or yellowish-orange smooth surface; thin bedded; forms weakly resistant ledge_____	2
Total Souris River (?) Formation_____	16

  Unconformity.
Ordovician:
  Bighorn Dolomite.
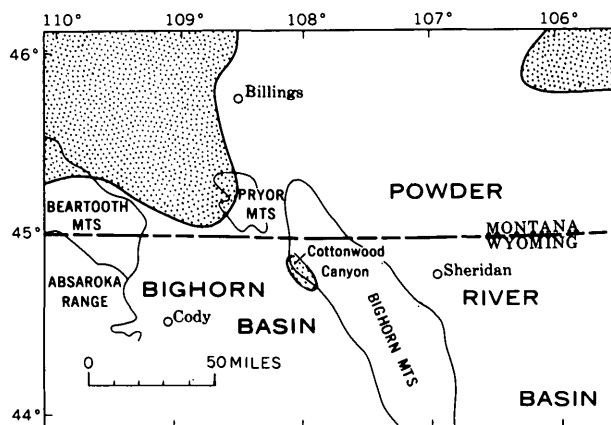
FIGURE 63.1.—Index map showing distribution of Souris River Formation and equivalents (stippled) in southern Montana and northern Wyoming.

The Souris River(?) Formation has a minimum width of 350 feet at Cottonwood Canyon, as indicated by blocks of spirorbal limestone found in the talus slide for 275 feet west of its outcrop. At the east side of the other bounding talus slide, 225 feet east of the outcrop, the Beartooth Butte Formation crops out slightly below the basal cliff of the Jefferson. The Beartooth Butte in Cottonwood Canyon is of Early Devonian age (Blackstone and McGrew, 1954; D. H. Dunkle, written communication, Oct. 14, 1959). It consists largely of coarse dolomite conglomerate and fills a deep channel in the underlying Bighorn at this locality (Sandberg, 1961a, p. 1305). The Beartooth Butte occupies most of the 150-foot interval between the Jefferson and Bighorn. However, the upper 20 feet of this interval, into which the Souris River(?) Formation might extend, and the basal 5 feet of Jefferson are covered. Reconnaissance of the canyon for about 4 miles to the east failed to disclose additional exposures of the Souris River(?) Formation.

The most abundant fossil in the Souris River(?) Formation at Cottonwood Canyon is *Spirorbis* sp. Tubes of this polychaete worm, about ½ to 1 mm in diameter, are abundant throughout. Some beds of limestone, particularly those near the top of the deposit, are composed almost exclusively of whole and fragmentary worm tubes and are termed spirorbal limestone (fig. 63.2). The deposit also contains fish remains, rounded pebbles of carbonized wood, impressions of large plant stems, macerated plant remains, spores, and megaspores. Fish remains include the antiarch *Bothriolepis* cf. *B. coloradensis* Eastman, palaeoniscoid teeth cf. *Rhadinichthys* sp., coccosteid plates, and weathered heterostracan carapaces (F. C. Whitmore, Jr., written communication, July 14, 1961), and the crossopterygian *Holoptychius* cf. *H. giganteus* Eastman (D. H. Dunkle, written communication, Feb. 5, 1963). *Callixylon*-type
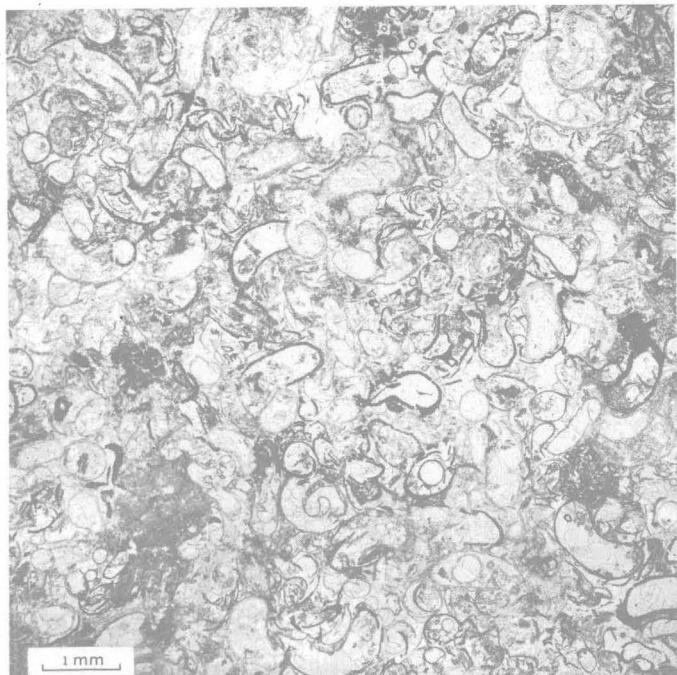
FIGURE 63.2—Spirorbal limestone near top of Souris River(?) Formation, Cottonwood Canyon, Big Horn County, Wyo. Thin section (×10) parallel to bedding, in plain transmitted light. *Spirorbis* tubes are round or crescent shaped and are filled by secondary calcite. Black outlines on some tubes are pyrite coatings.

pitting of tracheids was observed in the wood fragments by R. A. Scott (oral communication, Jan. 1961). The microflora consists almost entirely of a single spore species, *Punctatisporites* cf. *P. planus* Hacquebard, but it includes a few individuals of many diverse palynomorph species (R. H. Tschudy, written communication, Feb. 14, 1962). The fish and spores indicate an early Late Devonian age.

This biota suggests a marginal marine environment but does not indicate whether deposition was in brackish or fresh water. The diverse microflora is related to land plants and does not include any exclusively marine forms. On the other hand, the fish include both marine and fresh-water forms. *Holoptychius* is believed to have lived in fresh water, although some remains have been found in shallow inshore marine sediments (D. H. Dunkle, written communication, Feb. 5, 1963). The other fish also do not give a clear paleoecologic picture, according to F. C. Whitmore, Jr. (written communication, July 14, 1961), who stated:

The Heterostraci lived in the seas or in lower reaches of streams; palaeoniscoids and euarthrodires lived in both marine and fresh water. *Bothriolepis* was a fresh-water form, but the single plate in this collection could have been washed into a marine deposit.

The abundance of *Spirorbis* sp. accords with a marginal marine environment, for *Spirorbis* sp. apparently was adapted to fresh water as well as to salt and brackish water (Pruvost, 1930).

The main body of the marine Souris River Formation was deposited as the shallow Late Devonian sea transgressed with minor pulsations westward and southward from the Williston basin into southern Montana (Sandberg, 1961b). Both the regional paleogeography and the mixed paleoecology of the fish fauna in the Cottonwood Canyon deposit suggest that rocks of this outlier were deposited in brackish or nearly fresh water in the upper reaches of a long, narrow estuary that extended into the retreating shoreline.

REFERENCES

Blackstone, D. L., Jr., and McGrew, P. O., 1954, New occurrence of Devonian rocks in north central Wyoming, *in* Billings Geol. Soc. Guidebook, 5th Ann. Field Conf., Pryor Mountains and northern Bighorn Basin: p. 38–43.

Pruvost, Pierre, 1930, La faune continentale du terrain houiller de la Belgique: Inst. royal colonial belge, sec. sci. nat. et med., Mém. 44, p. 103–282.

Sandberg, C. A., 1961a, Widespread Beartooth Butte Formation of Early Devonian age in Montana and Wyoming and its paleogeographic significance: Am. Assoc. Petroleum Geologists Bull., v. 45, p. 1301–1309.

—— 1961b, Distribution and thickness of Devonian rocks in Williston basin and in central Montana and north-central Wyoming: U.S. Geol. Survey Bull. 1112–D, p. 105–127. [1962]

DARK SHALE UNIT OF DEVONIAN AND MISSISSIPPIAN AGE IN NORTHERN WYOMING AND SOUTHERN MONTANA

By CHARLES A. SANDBERG, Denver, Colo.

Abstract.—A marine sequence of black and moderate-yellow-ish-brown quartzose shale and carbonaceous siltstone discon-formably underlies the Madison Limestone (Mississippian) and is separated from underlying Upper Devonian rocks by a regional unconformity. The stratigraphic relations, thickness, lithologic character, and age of this dark shale unit approximate those of the Englewood Formation.

A clastic marine sequence of black and moderate-yellowish-brown quartzose shale and carbonaceous siltstone that unconformably overlies Devonian rocks and disconformably underlies the Madison Limestone of Mississippian age in northern Wyoming and southern Montana is here informally termed a dark shale unit of Devonian and Mississippian age. This dark shale unit is the homotaxial equivalent of the Englewood Formation of the Black Hills, South Dakota and Wyoming.

The reference locality of the dark shale unit is in the eastern Beartooth Mountains at the mouth of Clarks Fork Canyon, north of the river, in the NE¼NE¼ sec. 7, T. 56 N., R. 103 W., Park County, Wyo., in the Deep Lake 15-minute quadrangle. It is approached on Wyoming State Highway 120, which extends north from Cody, Wyo. About 2½ miles beyond the Clarks Fork bridge, which is 26 miles from Cody, a trail easily traversed by automobile connects the highway to the mouth of the canyon, about 7 miles west. From this trail the reference section is reached by climbing a talus slope between the Jefferson Formation of Late Devonian age and the Madison Limestone, which dip 50° to 55° NE. At the head of this talus slope the following section of the dark shale unit is well exposed along a steep bench below a high cliff formed by the Madison.

The dark shale unit at most measured sections consists of dark-gray to black carbonaceous dolomitic quartzose shale and light-olive-gray, yellowish-brown, yellowish-gray, and dark-gray dolomitic siltstone that grade to very shaly and very silty dolomite. Commonly the unit forms partly covered slopes and weakly to moderately

Reference section of the dark shale unit of Devonian and Mississippian age in the NE¼NE¼ sec. 7, T. 56 N., R. 103 W., Park County, Wyo.

	Thickness (Feet)
Dark shale unit:	
Siltstone, dolomitic, greenish-gray, light-olive-gray, dark-gray, and dark-yellowish-orange, fissile, partly carbonaceous, nodular, very fine grained; grades to dolomitic quartzose shale. Botryoidal nodules, about 1 in. in diameter, are white crystalline quartz geodes with vugs and cracks partly filled by white calcite and grayish-red hematite. Contains several conodont species that are characteristic of the Lower Carboniferous of Europe (B. F. Glenister, written communication, Mar. 2, 1961). Weathers very dusky red purple, olive gray, light brown, and yellowish brown. Interbedded with fissile siltstone are 2 thick-bedded lenses, 0 to 4 ft thick, of slightly nodular coarser grained limonitic dolomitic siltstone that is light olive gray and moderate yellowish brown mottled with pale red purple, greenish gray, and pale reddish brown. Unit is weakly resistant and slope forming, except for lenses which form moderately resistant ledges, about 4 ft and 11 ft below top_____	19
Siltstone, dolomitic, limonitic, hematitic; dark yellowish orange to moderate yellowish brown, with grayish-red streaks and mottles in upper half; medium dark gray and olive gray, with yellowish-brown and dark-yellowish-orange laminae in lower half. Weathers moderate yellowish brown, dark yellowish orange, and light brown; upper half massive; lower half medium bedded; resistant; ledge forming_____	8
Siltstone, dolomitic, carbonaceous, medium-dark-gray to dark-gray; grades to dolomitic quartzose shale. Weathers yellowish gray and dark yellowish orange; thick bedded to laminated; moderately resistant; ledge forming_____	8
Shale, quartzose, dolomitic, carbonaceous, dark-gray to grayish-black. Contains abundant palynomorphs, including hystricosphaeres, *Micrhystridium*, *Tasmanites*, and a spore, *Leiosphaera* sp., which are indicative of marine deposition (R. H. Tschudy, written communication, Feb. 14, 1962). Upper 8 ft weathers dark gray to medium dark gray mottled locally with light olive gray; lower 5 ft weathers light olive gray; weakly resistant; slope forming_____	13
Total, dark shale unit_____	48

resistant ledges, but locally it forms the base of a cliff of Madison. At some localities it consists entirely or partly of microcrystalline to very finely crystalline hematitic slightly silty dolomite that is yellowish gray mottled with grayish red and contains scattered fine to coarse sand grains and fish plates and teeth. Thin partings of dark-gray carbonaceous shale commonly occur in this dolomitic facies. The base of the dark shale unit locally is a bed of phosphatic quartzitic sandstone, as much as 6 inches thick, containing abundant large conodonts, fish plates and teeth, black phosphate pellets, and angular pebbles derived from the underlying rocks.

The dark shale unit is present in north-central and northwestern Wyoming and south-central and southwestern Montana (fig. 64.1). It crops out in the Beartooth and northern Bighorn Mountains, in the Wind River, Teton, Absaroka, Gallatin, and Bridger Ranges, and in the Horseshoe Hills, near Logan, Mont. The dark shale unit is 48 feet thick at the reference locality. From there its thickness increases northeastward to a maximum of about 70 feet in the subsurface north of Billings, Mont. The thickness decreases northwestward

from the reference locality to about 12 feet in the western Beartooth Mountains and to about 4 feet in the Gallatin and Bridger Ranges and Horseshoe Hills. The unit also thins southward and eastward; its thickness is about 10 feet in the Bighorn Mountains and in the Absaroka, Wind River, and Teton Ranges.

At Logan, Mont. (fig. 64.1), the dark shale unit overlies the Sappington Sandstone Member at the top of the Three Forks Formation of Devonian and Mississippian age. There the dark shale unit previously was correlated by Knechtel and others (1954), with the Little Chief Canyon Member of the Lodgepole Limestone of Early Mississippian age, whose type locality is in the Little Rocky Mountains of north-central Montana. Regional stratigraphic studies by the author indicate, however, that the southern limit of the Little Chief Canyon lies very near the Little Rocky Mountains and 160 miles northeast of Logan, so the continued use of this name at Logan is inappropriate.

From Logan southeastward to central Wyoming, the dark shale unit truncates progressively older rocks ranging in age from earliest Mississippian to early Late
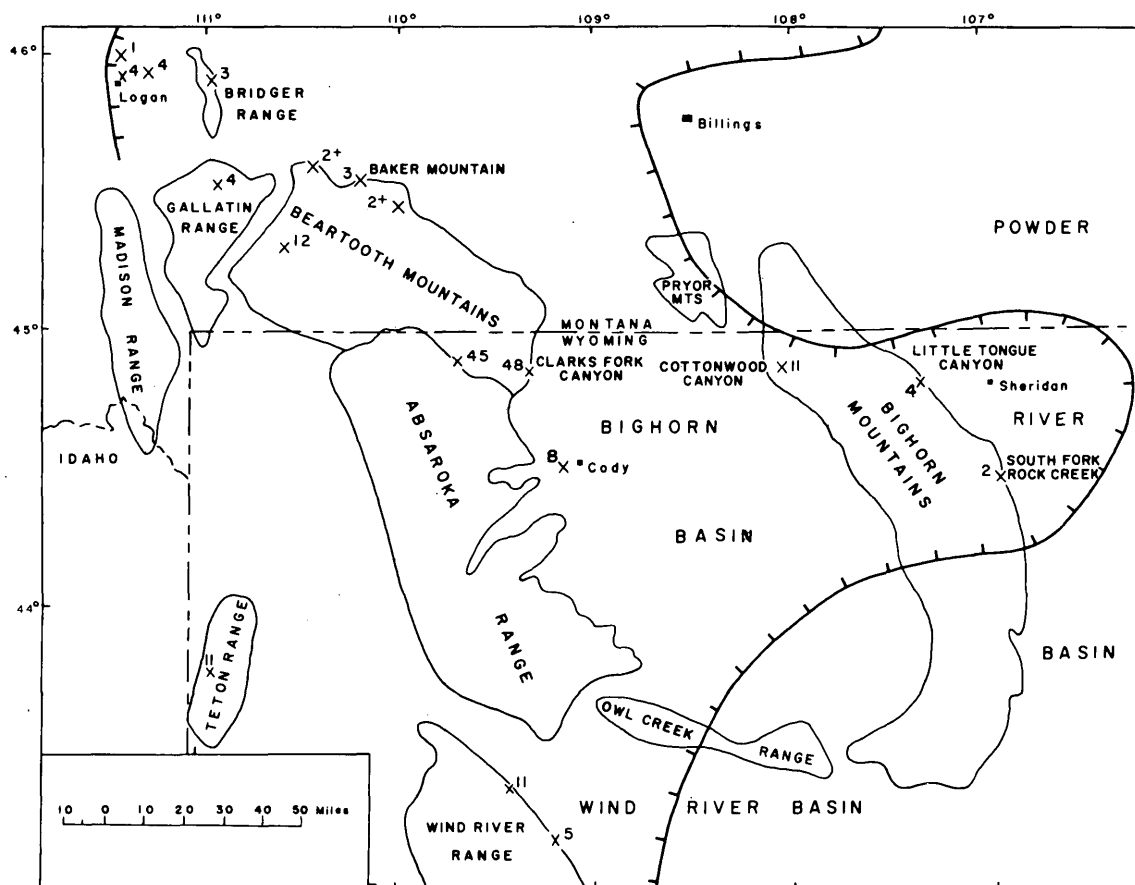
FIGURE 64.1.—Outcrops of the dark shale unit. Numbers indicate thickness, in feet, of measured sections. Approximate limit of unit shown by hachured line; unit absent on unhachured side.

Devonian (fig. 64.2). These rocks include all three members of the Three Forks Formation and the subsurface Birdbear Formation and upper part of the Duperow Formation and their equivalents in the outcropping Jefferson Formation. At its reference locality the dark shale unit overlies the lower, evaporitic member of the Three Forks, but only about 10 miles north, south, and east of this locality it rests on the Jefferson.
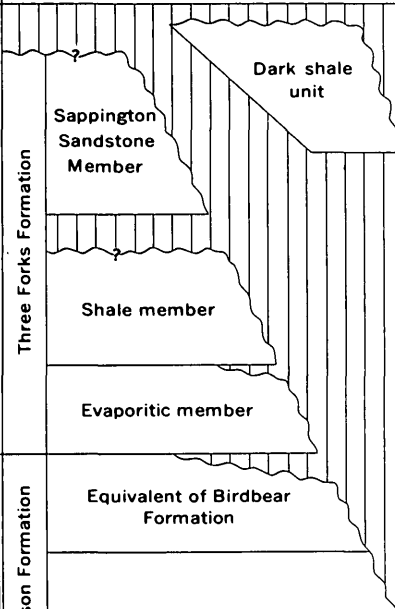
SYSTEM	SERIES	EUROPEAN STAGE	AMMONOID ZONE (Stufe)	FORMATION AND MEMBER
MISSISSIPPIAN	LOWER	TOURNAISIAN	Pericyclus (cuII^a)	Madison Limestone (base)
			Gattendorfia (cuI)	Dark shale unit
DEVONIAN	UPPER	FAMENNIAN	Wocklumeria (toVI)	Sappington Sandstone Member
			Clymenia (toV)	
			Platyclymenia (toIII-IV)	Shale member
			Cheiloceras (toII)	Evaporitic member
		FRASNIAN	Manticoceras (toI)	Equivalent of Birdbear Formation / Equivalent of Duperow Formation

(Three Forks Formation; Jefferson Formation)

FIGURE 64.2.—Age and stratigraphic relations of dark shale unit and adjacent formations. (Ammonoid zones after House, 1962; Collinson and others, 1962.)

The dark shale unit is disconformably overlain by the Madison Limestone, which truncates it west of Logan in southwestern Montana, in southeastern Montana, and in northeastern and central Wyoming (fig. 64.1). Conodont collections made independently by Gilbert Klapper and the author from the basal few feet of the Madison at 14 measured sections in Montana and Wyoming indicate an Early Mississippian age, equivalent to the Pericyclus-Stufe (cuIIα) of the Lower Carboniferous in Europe (Klapper, written communication, Oct. 12, 1962).

The age of the dark shale unit ranges from very late Devonian, equivalent to the Clymenia-Stufe (toV) of the Famennian Stage in Europe, to earliest Mississippian, equivalent to the upper part of the Gattendorfia-Stufe (cuI) of the Tournaisian Stage of Lower Carboniferous in Europe (fig. 64.2). This precise determination is based largely on independent conodont collections of Klapper and the author. The conodonts were identified by Klapper (written communication, Oct. 12, 1962), who plans to publish systematic descriptions of the conodont faunas of the dark shale unit and adjacent formations.

In the Absaroka and Teton Ranges, Beartooth Mountains, and areas to the northwest (fig. 64.1), the dark shale unit appears to be entirely Early Mississippian. This determination is supported by conodonts collected from the basal sandstone of the dark shale unit at Baker Mountain by the author and previously determined to be of Early Mississippian (Kinderhook) age by W. H. Hass (written communication, Nov. 1, 1957).

In the Bighorn Mountains (fig. 64.1) the dark shale unit contains beds of very late Devonian as well as of earliest Mississippian age. Conodonts collected from the unit at South Fork Rock Creek by the author were determined to be of Early Mississippian (Kinderhook) age by W. H. Hass (written communication, Nov. 1, 1957). Conodonts from a thin bed directly below the Madison at Little Tongue Canyon were determined to include a mixed fauna of Upper Devonian and basal Kinderhook forms by Koucky and others (1961). This bed is here included at the base of the dark shale unit. Conodonts from thin beds of black shale at the top of the Devonian sequence in Cottonwood Canyon were reported to be Upper Devonian by Blackstone and McGrew (1954). Conodonts from these same beds were equated to the Clymenia-Stufe (toV) by Ethington and others (1961). These shale beds are here included in the lower part of the dark shale unit. In the upper beds of the dark shale unit at Cottonwood Canyon, Klapper (written communication, Oct. 12, 1962) found Lower Carboniferous (cuI) conodonts.

In the Wind River Range (fig. 64.1), south of other outcrops of the dark shale unit, the unit appears to be entirely of very late Devonian age. Upper Devonian (toV) conodonts were reported from the top of the Darby Formation at two localities by Klapper (1958). However, Klapper (written communication, Oct. 12, 1962) now recognizes the conodont-bearing beds as the dark shale unit.

The dark shale unit of Devonian and Mississippian age is the homotaxial equivalent of the Englewood Formation, formerly Englewood Limestone, of the Black Hills of South Dakota and extreme northeastern Wyoming. Their lithologic character, stratigraphic relations, thickness, and age are very similar.

The Englewood Formation contains variegated siltstone, shale, and sandstone, some grayish-red to pinkish-gray silty dolomite, similar to the dolomitic facies of the dark shale unit, and a little pinkish-gray and medium- to light-gray limestone. At its type locality near Englewood, S. Dak., the upper part of the Englewood Formation is entirely dolomite, as determined by calcium-magnesium analyses, and the lower part is siltstone.

The Englewood Formation underlies the Pahasapa Limestone of Mississippian age, which is equivalent to a large part of the Madison Limestone, and is separated from the Pahasapa at some localities in the northern Black Hills by an angular unconformity. Like the dark shale unit, the Englewood truncates progressively older beds southward. These range from the Three Forks Formation of Late Devonian age in the subsurface northeast of the Black Hills (Sandberg, 1961) to the Deadwood Formation of Late Cambrian age at the south end of the Black Hills.

The thickness of the Englewood Formation ranges from 18 to 54 feet at 6 sections measured by the author in various parts of the Black Hills.

The Englewood Formation, like the dark shale unit, contains conodont faunas equated to both the Upper Devonian (toV) and the Lower Carboniferous of Europe (Klapper and Furnish, 1962). On the basis of their age determinations in the Black Hills and the author's stratigraphic correlation between the Englewood Formation at Coldbrook Canyon in the south end of the Black Hills and equivalent rocks at Sand Canyon in the Hartville area, from which Love and others (1953) reported a Late Devonian brachiopod fauna, the age of the Englewood Formation is here recognized as Late Devonian and Early Mississippian.

The dark shale unit of Devonian and Mississippian age and the Englewood Formation are now separate rock bodies. They were deposited penecontemporaneously in two elongate, arcuate, shallow marine basins, each characterized by a northeast-trending axis, along which a narrow belt of thin sediments accumulated. Although these depositional basins are now only about 30 miles apart, it would be difficult to demonstrate that they had once coalesced. Any vestige of very thin deposits, which might have been laid down on a connecting shelf area, has been removed by slight pre-Madison erosion in the intervening Powder River Basin of northeastern Wyoming.

REFERENCES

Blackstone, D. L., Jr., and McGrew, P. O., 1954, New occurrence of Devonian rocks in north central Wyoming, in Billings Geol. Soc. Guidebook 5th Ann. Field Conf., Pryor Mountains–Northern Bighorn Basin, Montana: p. 38–43.

Collinson, Charles, Scott, A. J., and Rexroad, C. B. 1962, Six charts showing biostratigraphic zones, and correlations based on conodonts from the Devonian and Mississippian rocks of the upper Mississippi Valley: Illinois Geol. Survey Circ. 328, 32 p.

Ethington, R. L., Furnish, W. M., and Wingert, J. R., 1961, Upper Devonian conodonts from Bighorn Mountains, Wyoming: Jour. Paleontology, v. 35, No. 4, p. 759–768.

House, M. R., 1962, Observations on the ammonoid succession of the North American Devonian: Jour. Paleontology, v. 36, No. 2, p. 247–284.

Klapper, Gilbert, 1958, An Upper Devonian conodont fauna from the Darby formation of the Wind River Mountains, Wyoming: Jour. Paleontology, v. 32, No. 6, p. 1082–1093.

Klapper, Gilbert, and Furnish, W. M., 1962, Devonian-Mississippian Englewood Formation in Black Hills, South Dakota: Am. Assoc. Petroleum Geologists Bull., v. 46, No. 11, p. 2071–2078.

Knechtel, M. M., Smedley, J. E., and Ross, R. J., Jr., 1954, Little Chief Canyon Member of Lodgepole Limestone of Early Mississippian age in Montana: Am. Assoc. Petroleum Geologists Bull. v. 38, No. 11, p. 2395–2411.

Koucky, F. L., Cygan, N. E., and Rhodes, F. H. T., 1961, Conodonts from the eastern flank of the central part of the Big Horn Mountains, Wyoming, in Paleontological notes: Jour. Paleontology, v. 35, No. 4, p. 877–879.

Love, J. D., Henbest, L. G., and Denson, N. M., 1953, Stratigraphy and paleontology of Paleozoic rocks, Hartville area, eastern Wyoming: U.S. Geol. Survey Oil and Gas Inv. Chart OC–44.

Sandberg, C. A., 1961, Distribution and thickness of Devonian rocks in Williston basin and in central Montana and north-central Wyoming: U.S. Geol. Survey Bull. 1112–D, p. 105–127 [1962].

NOMENCLATURE FOR LITHOLOGIC SUBDIVISIONS
OF THE MISSISSIPPIAN REDWALL LIMESTONE, ARIZONA

By EDWIN D. McKEE, Denver, Colo.

Abstract.—New formal names given to the principal sub-divisions of the Mississippian Redwall Limestone in northern Arizona are, in ascending order: Whitmore Wash Member, Thunder Springs Member, Mooney Falls Member, and Horseshoe Mesa Member.

The Redwall Limestone of Mississippian age extends across much of northern Arizona and forms in outcrop one of the thickest, most massive cliffs of the region. Although superficially it seems to consist of a single uniform lithology, detailed examination indicates that it is readily divisible into four distinct lithologic units. These units have been recognized in the literature and referred to as informal members for more than 20 years. Various informal designations have been applied to them as follows (ascending order) : I, II, III, and IV (Gutschick, 1943, p. 5; Easton and Gutschick, 1953, p. 3) ; bottom, lower middle, upper middle, and top (McKee, 1958, p. 75) ; and A, B, C, and D (McKee, 1960b). The informal designations A, B, C, and D have been used in well-log descriptions by the American Stratigraphic Co. since 1960.

The application of formal names to members of the Redwall Limestone is desirable at this time because the validity of the units has been tested and established through a detailed study of the formation by E. D. McKee and R. C. Gutschick (report in preparation) and also because these units frequently are referred to in the petroleum industry, as a result of recent discoveries of oil and gas in them. The following names are here given to the four members of the Redwall, listed from oldest to youngest (fig. 65.1) : Whitmore Wash Member, Thunder Springs Member, Mooney Falls Member, and Horseshoe Mesa Member. These names are taken from geographic localities in which the rocks are well exposed and in which detailed sections have been measured; thus the names refer to appropriate type sections.

The Whitmore Wash Member, at the base of the formation, is exposed along the east side of the valley of that name in northwestern Arizona. The type section, 101 feet thick, is on the upthrown side of the Hurricane fault, about ¼ mile north of the Colorado River, where the member consists of very thick bedded (4 to 15 feet) dolomite that is very fine and even grained. In sections to the southeast along the south side of Grand Canyon, the member ranges in thickness from 72 to 85 feet and is also largely dolomite, but farther west it is limestone composed mostly of well-rounded bioclasts and locally of ooids. Medium-scale crossbedding is conspicuous in a few places.

The Thunder Springs Member of the Redwall Limestone consists of thin beds of chert alternating with thin beds of carbonate rock. The type section, 138 feet thick, is in the cliff of Redwall Limestone west of the springs at the head of Thunder River, about 2 miles north of the Colorado River in central Grand Canyon. Chert beds are the most conspicuous feature of this member (McKee, 1960) ; in the western part of Grand Canyon they are associated with limestone, but to the east with dolomite. Grains within the limestone range in size from fine to very coarse and consist of both bioclasts and peloids (intraformational clastic particles), commonly in an aphanitic calcite matrix. Uniformly fine grains are characteristic of the dolomite.

The Mooney Falls Member is the thickest, most massive, and most prominent unit of the Redwall Limestone. It forms a sheer cliff throughout the Grand Canyon and from east to west ranges in thickness from
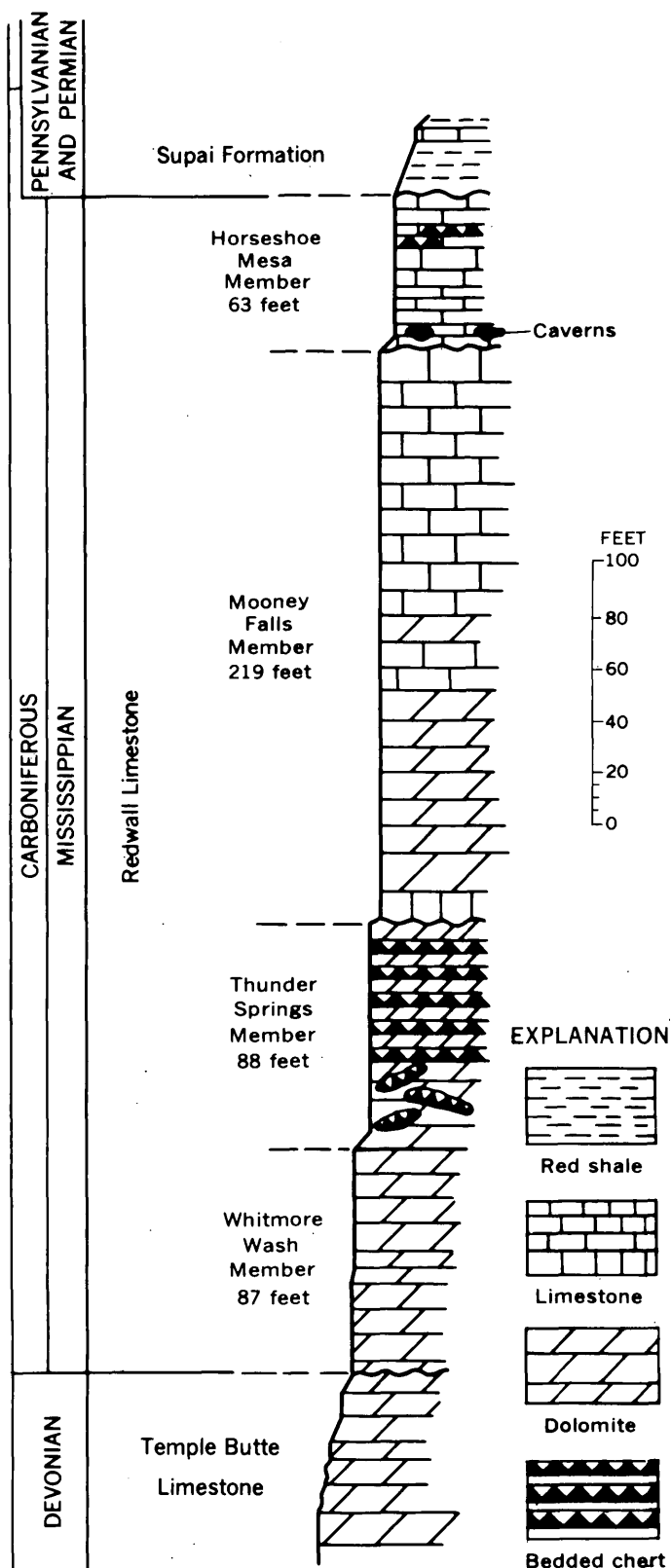
FIGURE 65.1.—Section showing stratigraphic relations and thickness of the members of the Redwall Limestone along the Bright Angel Trail, Grand Canyon.

about 200 feet to more than 350 feet. Its type section, 312 feet thick, is at Mooney Falls in Havasu Canyon, a major tributary of the Grand Canyon from the south. This member forms most of the walls of the narrow gorge in which the spectacular waterfalls are located, and it is well exposed for many miles in that area. Mostly the Mooney Falls Member is a very pure limestone remarkably free of all detrital matter, but locally, as in the lower part of the type section, it contains dolomite. Detailed study shows that particle size ranges widely from bed to bed and that a well-defined cyclic sequence of texture can be traced across the area (McKee, 1960). The thick, massive beds within this member locally contain abundant coral heads (*Syringopora*), as at the type section. Zones of certain colonial corals and of endothyrids are well marked and persistent in the upper half. Thin chert beds are common near the top, and large-scale cross-bedding is well developed in some areas. Oolitic units occur in the upper part of the member in western Grand Canyon.

The uppermost unit, the Horseshoe Mesa Member, is relatively thin bedded and in Grand Canyon commonly forms receding ledges at the top of the great cliff of the Redwall. The thickness of this unit has been much affected locally by pre-Supai erosion, but in general it is thin, ranging from 38 feet at the type section to 125 feet in the west. A type section has been selected at Horseshoe Mesa below Grandview Point on the south side of the Grand Canyon. The section is accessible from the Grandview trail, which crosses Horseshoe Mesa. At this locality, as in most of the region, the member consists largely of aphanitic limestone; encrusting and sediment-binding algal structures are common. The member is characterized by features typical of quiet-water conditions, although crossbedding, ripple marks, and oolite beds occur locally.

REFERENCES

Easton, W. H., and Gutschick, R. C., 1953, Corals from the Redwall Limestone (Mississippian) of Arizona: Southern California Acad. Sci. Bull., v. 52, pt. 1, p. 1–27.
Gutschick, R. C., 1943, The Redwall Limestone (Mississippian) of Yavapai County, Arizona: Plateau, v. 16, no. 1, p. 1–11.
McKee, E. D., 1958, The Redwall Limestone: New Mexico Geol. Soc., 9th Field Conf., p. 74–77.
——— 1960a, Cycles in carbonate rocks, in the Bradley volume: Am. Jour. Sci., v. 258–A, p. 230–233.
——— 1960b, Lithologic subdivisions of the Redwall Limestone in northern Arizona—their paleogeographic and economic significance: Art. 110 in U.S. Geol. Survey Prof. Paper 400–B, p. B243–B245.
——— 1960c, Spatial relations of fossils and bedded cherts in the Redwall Limestone, Arizona: Art. 210 in U.S. Geol. Survey Prof. Paper 400–B, p. B461–B463.

MISSISSIPPIAN ROCKS IN THE LARAMIE RANGE, WYOMING, AND ADJACENT AREAS

By EDWIN K. MAUGHAN, Denver, Colo.

Abstract.—Mississippian strata in the Laramie Range equivalent to the Madison Limestone are composed, in ascending order, of arkosic sandstone, limestone, and a unit containing fossiliferous chert lenses. These rocks are 500 feet thick west of Casper but wedge out southward by convergence of the basal sandy unit and upper cherty unit. This convergence suggests an actively rising positive area farther south in Colorado during Mississippian time.

Mississippian strata in the Laramie Range equivalent to the Madison Limestone are composed of a basal unit of arkosic conglomeratic sandstone; a middle unit of limestone; and an upper unit that contains yellowish-gray tabular fossiliferous chert lenses in a matrix of yellow siltstone in the southern part of the range, and limestone in the north (fig. 66.1). The basal sandstone is gradational with the overlying limestone unit, but the upper cherty unit seems to rest sharply upon the limestone. These rocks are 500 feet thick a short distance west of Casper but wedge out southward along both flanks of the Laramie Range. Similar rocks occur also in the subsurface in southeastern Wyoming and adjacent parts of northeastern Colorado and western Nebraska, as indicated on figure 66.2.

Thickness measurements given on figure 66.2 were obtained from sections measured by the author south of Marshall and Horseshoe Creek in the Laramie Range, and in the Medicine Bow Mountains; from subsurface logs of the American Stratigraphic Co., Denver, Colo., and Casper, Wyo.; from measured sections in many unpublished theses, mostly from the University of Wyoming; and from measured sections in published reports listed in the references at the end of this report.

The southernmost exposure of Mississippian rocks known in the Laramie Range is on the east flank of the range, at the North Fork of Crow Creek, Laramie County, Wyo. (Maughan and Wilson, 1960). On the west flank of the range, the Madison extends southward as far as Garrett, and possibly is continuous as far as the vicinity of Wheatland Reservoir (figs. 66.1 and 66.2). Isolated outcrops are found farther south, in secs. 13 and 9, T. 17 N., R. 72 W. Reworked fragments of Mississippian rock in the basal (Pennsylvanian) part of the younger Casper and Fountain Formations have been reported as far south as Bellevue, Colo., on the east side of the range (Henderson, 1909, p. 158–159), and at Rogers Canyon, central Albany County, Wyo., on the west flank of the range (Knight, 1929, p. 29–30). Fragments of Mississippian rock, mostly yellow-gray chert, are common in the basal part of the Casper Formation north of Rogers Canyon.

The basal sandstone unit in the Laramie Range is composed generally of arkosic conglomeratic sandstone that by some geologists has been correlated with the Flathead Quartzite or Deadwood Formation of Cambrian age. Well-rounded to subangular quartz and feldspar pebbles are common in a matrix which is dominantly quartz sand, but which includes silt- and clay-sized particles. Grains of feldspar and ferromagnesian minerals are also abundant. This arkosic sandstone was derived from weathering of the underlying Precambrian granite and metamorphic rocks. Its thickness at many places is indicated on figure 66.2. The unit commonly grades upward into moderately well sorted quartzose sandstone which, in turn, is increasingly calcareous upward and intertongues and grades into the overlying limestone unit. Laterally the sandstone intertongues and grades into limestone, as illustrated on figure 66.1. Locally, where the sandstone is moderately thick, as in the area a few miles southeast of Marshall, it is very well sorted orthoquartzite.

Fossils of Kinderhook age, "notably *Chonopectus fischeri*, were collected 13 feet above granite at the top of calcareous arkose" (Agatston, 1954, p. 514) in the

ART. 66 *IN* U.S. GEOL. SURVEY PROF. PAPER 475-C, PAGES C23–C27. 1963.

C23
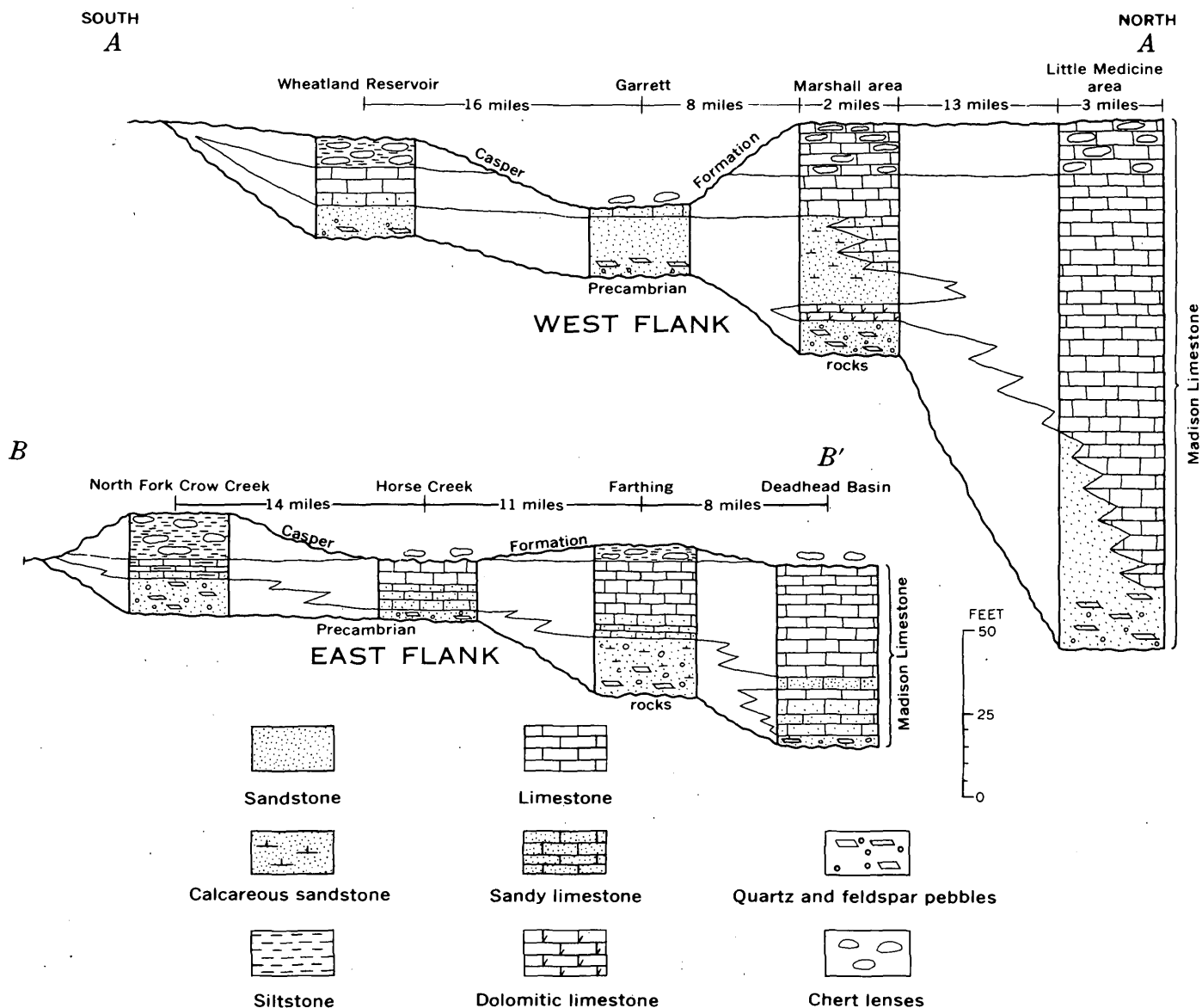
FIGURE 66.1.—Columnar sections showing tongue of Madison Limestone on east and west flanks of the Laramie Range, Wyo. Location of lines of section shown on figure 66.2.

vicinity of Farthing. These fossils, as well as the inter-tonguing of this sandstone with typical Madison Limestone, establish a Mississippian, probably Kinderhook, age for the basal sandstone in the Laramie Range; therefore, these strata should no longer be correlated with the Flathead or Deadwood. The basal sandstone unit in the Laramie Range correlates with a similar basal Mississippian unit in the Rawlins, Wyo., area. Paleontologic evidence (Thomas, 1951) indicates that at least the upper part of the sandstone near Rawlins is of Mississippian age. Other units that are probably correlated with the Mississippian sandstone in the Laramie

Range are the Gilman Sandstone Member of the Leadville Dolomite of central Colorado, the Englewood Limestone of the Black Hills, the Bakken Formation of northern Montana, and possibly the Sappington Sandstone Member of the Three Forks Shale of south-central Montana.

The Mississippian sandstone in the Laramie Range can be traced northeastward in the subsurface (fig. 66.2) into the Hartville uplift area in east-central Wyoming, where it is probably represented by a thin sequence of red shale, sandstone, and conglomerate that underlies limestone of the Guernsey Formation. The red shale

N

Casper

240/70+ *N o r t h*

220+

210/30

294/35

15/15 *White River*

293/88

220/55 160/52

144/53

Douglas

175/15+ 235/35

10/10

30/15

366/92 Alcova Reservoir

145
15/95
45

115/3

209/65

185/25

215/27

190/20

155

15/0 *River*

340+

Pathfinder Reservoir

Little Medicine

Macfarlane Ranch

230+

130+

160+ *Niobrara*

163/13

205 185
45/50

Marshall
45/25 28/42

3/18

210/10

64/30?

Garrett

135/35+

Alliance

120/25

20/10

115/5

□Wheatland

Seminoe Reservoir

Scottsbluff

40/15

Arlington
▲0 △10±

Wheatland Reservoir

Deadhead Basin

50/5 B'

R i v e r

75/30

0

28/17

Farthing

LARAMIE COUNTY

15/5 Horse Creek

20±

Rogers Canyon

Laramie

Lorenz Ranch

CHEYENNE

Lodgepole

Kimball

Creek

Crow

B'

WYOMING | NEBRASKA

10/5

COLORADO

28/55

Sterling

45/18

30/30

40/20

40/60+

30/15

42/23

□Bellvue
□Fort Collins

South Platte River

EXPLANATION

▲ Outcrop section   ● Subsurface section

Isopach

Thickness, in feet, of Mississippian rocks. Dashed
where approximate, dotted where eroded

120/27

Thickness, in feet of Mississippian rocks

Number above bar is thickness of limestone unit;
number below is thickness of sandstone unit of
Madison Limestone

10   0   10   20   30 MILES

FIGURE 66.2.—Distribution and thickness of Mississippian rocks in southeastern Wyoming, western Nebraska, and northeastern Colorado. Dark pattern, exposed Mississippian rocks; light pattern, exposed pre-Mississippian rocks; dotted isopachs across these areas indicate inferred thickness before erosion. Local outliers of Mississippian rocks lie beyond zero isopach. A–A' and B–B', lines of sections shown on figure 66.1. Compiled partially from Beckwith (1914), Condra and others (1940), and Lee (1927).

and conglomerate unit has been correlated or tentatively correlated with the Deadwood Formation (Jenkins and McCoy, 1958; Love and others, 1953), although originally it was recognized as a basal conglomerate of the Guernsey (Smith and Darton, 1903). Ballard (1942, p. 1567) affirmed that the sandy unit should be considered part of the Guernsey. Love and others (1953) date limestone near the base of the Guernsey as Late Devonian. If the sandstone in the Laramie Range is continuous with the sandy unit in the Hartville area, as the present work suggests, then the sandstone and its correlatives transgress the Devonian-Mississippian systemic boundary between the Hartville area and the Laramie Range.

It seems unlikely that rocks of Cambrian age are present in any part of the area shown on figure 66.2, except for anomalous remnants such as those reported by John Chronic (oral communication, 1962) in the southern part of the Laramie Range or, possibly, for wedges of Cambrian sandstone which may extend a short way into the northwestern part of the area from central Wyoming. Additional study of sandstone exposed at the base of undoubted Mississippian rocks in the vicinity of the Alcova and Seminoe Reservoirs is needed before use of the names Flathead or Deadwood can be continued in that area, because that sandstone also may be a locally thick sandy facies of the Madison Limestone, as it is in the Laramie Range.

The middle, limestone unit of the Madison is at least 200 feet thick in the northern part of the Laramie Range and as much as 360 feet in the subsurface to the northwest. The unit is composed almost exclusively of limestone and dolomitic limestone typical of the Madison and has been described previously by several authors (Barnett, 1914; Rapp and Maxson, 1953; and Mytton, 1954). This limestone thins southward chiefly by intertonguing of the lower part with the underlying sandstone unit (fig. 66.1). Abrupt thinning occurs in the vicinity of Marshall; south of Marshall this unit is no more than 30 feet thick.

The upper, cherty unit, although relatively thin, varies considerably in thickness from place to place owing to erosion before deposition of the overlying Casper Formation. The cherty unit seems to thicken slightly northward. In the northern part of the range and in adjacent areas some of the thickening of the Mississippian rocks (fig. 66.2) seems to be due to preservation of Mississippian strata younger than the chert bed. That younger beds are present northward is consistent with the concept of regional southward truncation of the upper part of the Madison Group postulated by Andrichuk (1955, fig. 5).

Fossils collected from the chert at North Crow Creek (USGS loc. 18622–PC) are *Spirifer* aff. *S. madisonensis* (Girty); *Composita* aff. *C. subquadrata* (Hall); *Dielasma* sp.; and indeterminate pelecypods. This fauna suggests that these strata "might be roughly correlated with the upper parts of the Pahasapa Limestone and Madison Group" (J. T. Dutro, Jr., written communication, 1959). The late Early Mississippian age, which may be implied from this statement, is supported by the occurrence in the chert of *Endothyra* sp. of probable Osage age (identified by B. L. Skipp, oral communication, 1962).

The thinning of the Madison described here compares with northward thinning of the Leadville Dolomite along the east flank of the Front Range north of Colorado Springs, Colo., and with thinning of the Leadville eastward and northeastward in the Pando area, central Colorado (Tweto, 1949, p. 186). The Madison thins from Rawlins southward to the vicinity of Savery, Wyo. (Ritzma, 1951), and a thin wedge (possibly an isolated remnant) is exposed at the north end of the Medicine Bow Mountains near Arlington, Wyo. (R. S. Houston, oral communication, 1963).

These stratigraphic relations suggest that a large positive area in the central Rocky Mountain region was inundated from the north in latest Devonian to earliest Mississippian time. The transgression culminated in Osage time when the sea extended partly across this area, but probably not far beyond the zero isopach of figure 66.2. Convergence of the basal sandy unit and upper cherty unit of the Madison southward along the Laramie Range (fig. 66.1) suggests that the positive area, although partly submerged in Wyoming, was actively rising farther south in Colorado during Mississippian time.

REFERENCES

Agatston, R. S., 1954, Pennsylvanian and Lower Permian of northern and eastern Wyoming: Am. Assoc. Petroleum Geologists Bull., v. 38, p. 508–583.

Andrichuk, J. M., 1955, Mississippian Madison Group stratigraphy and sedimentation in Wyoming and southern Montana: Am. Assoc. Petroleum Geologists Bull., v. 39, p. 2170–2210.

Ballard, Norval, 1942, Regional geology of Dakota basin: Am. Assoc. Petroleum Geologists Bull., v. 26, p. 1557–1584.

Barnett, V. H., 1914, The Douglas oil and gas field, Converse County, Wyoming: U.S. Geol. Survey Bull. 541–C, p. 49–88.

Beckwith, R. H., 1941, Structure of the Elk Mountain district, Carbon County, Wyoming: Geol. Soc. America Bull., v. 52, p. 1445–1486.

Condra, G. E., Reed, E. C., and Scherer, O. J., 1940, Correlation of the formations of the Laramie Range, Hartville uplift, Black Hills, and western Nebraska: Nebraska Geol. Survey Bull. 13, 52 p.

Henderson, Junius, 1909, The foothills formation of north-central Colorado: Colorado Geol. Survey, First Rept. 1908, p. 145–188.

Jenkins, M. A., and McCoy, M. R., 1958, Cambro-Mississippian correlations in the eastern Powder River Basin, Wyoming and Montana, *in* Wyoming Geol. Assoc. Guidebook 13th Ann. Field Conf., Powder River Basin, Wyoming, 1958: p. 31–35.

Knight, S. H., 1929, The Fountain and the Casper Formations of the Laramie Basin: Wyoming Univ. Pubs. in Sci., Geology, v. 1, p. 1–82.

Lee, W. T., 1927, Correlation of geologic formations between east-central Colorado, central Wyoming and southern Montana: U.S. Geol. Survey Prof. Paper 149, 80 p.

Love, J. D., Henbest, L. G., and Denson, N. M., 1953, Stratigraphy and paleontology of Paleozoic rocks, Hartville area, eastern Wyoming: U.S. Geol. Survey Oil and Gas Inv. Chart OC–44, 2 sheets.

Maughan, E. K., and Wilson, R. F., 1960, Pennsylvanian and Permian strata in southern Wyoming and northern Colorado, *in* Weimer, R. J., and Haun, J. D., eds., Guide to the Geology of Colorado: Geol. Soc. America, 1960 Ann. Mtg.. Denver, Colo., guidebook for field trips, p. 34–42.

Mytton, J. W., 1954, The petrology and residues of the Madison Formation of the northern part of the Laramie Range, *in* Wyoming Geol. Assoc. Guidebook 9th Ann. Field Conf., Casper Area, Wyoming, 1954: p. 37–43.

Rapp, J. R., and Maxson, Horace, 1953, Reconnaissance of the geology and ground-water resources of the La Prele area, Converse County, Wyoming: U.S. Geol. Survey Circ. 243, 33 p.

Ritzma, H. R., 1951, Paleozoic stratigraphy, north end and west flank of the Sierra Madre, Wyoming-Colorado, *in* Wyoming Geol. Assoc. Guidebook 6th Ann. Field Conf., South-central, Wyoming, 1951: p. 66–67.

Smith, W. S. T., and Darton, N. H., 1903, Description of the Hartville quadrangle [Wyoming]: U.S. Geol. Survey Geol. Atlas, Hartville folio, no. 91.

Thomas, H. D., 1951, Summary of Paleozoic stratigraphy of the region about Rawlins, south-central Wyoming, *in* Wyoming Geol. Assoc. Guidebook 6th Ann. Field Conf., South-central Wyoming, 1951: p. 32–36.

Tweto, Ogden, 1949, Stratigraphy of the Pando area, Eagle County, Colorado: Colorado Sci. Soc. Proc., v. 15, no. 4, p. 149–235.

Article 67

TRIASSIC UPLIFT ALONG THE WEST FLANK
OF THE DEFIANCE POSITIVE ELEMENT, ARIZONA

By EDWIN D. McKEE, Denver, Colo.

Abstract.—A cross section of the Moenkopi Formation from Winslow to Fredonia, Ariz., has been redrawn with the lower massive sandstone used as a datum plane. The cross section indicates that uplift, followed by erosion, occurred on the west flank of the Defiance positive element in Triassic time after Moenkopi deposition but before deposition of the Chinle Formation.

A positive area in northeastern Arizona where Precambrian rocks are overlapped by Permian strata was first noted by Gregory (1917, p. 17). Some details of the west flank of this structure, termed the Defiance positive element, were described by McKee (1951, p. 484-486, 488) and illustrated by isopach maps. Notable features are the radiating ridges or prongs extending out from the positive element with somewhat different locations during different geologic periods.

The Defiance positive element seems to have been repeatedly uplifted. Movement along its west flank during the Triassic Period is well documented by the stratigraphic relations of the Moenkopi Formation as shown

in a cross section across the central part of northern Arizona from Winslow to Fredonia (figs. 67.1, 67.2). Data for the section were obtained during field investigations in the 1940's and were illustrated later by the author (1954, p. 21-22). The relations were also shown in section *B-B'* of plate 3 of McKee and others (1959), but in this section some of the pertinent conclusions are obscured by what seems to have been an unfortunate choice of datum plane.

Certain features of the stratigraphic history become conspicuous when the data obtained in earlier investigations are replotted with the widespread "lower massive sandstone" unit (McKee, 1954) as a datum plane (fig. 67.2). First, the base of the formation rises relatively evenly from northwest to southeast, apparently the result of transgression. Second, the area between Black Point and Fredonia is one in which considerable erosion took place, cutting to and below the upper massive sandstone unit, after the Moenkopi was deposited and before the overlying Chinle Formation began to be
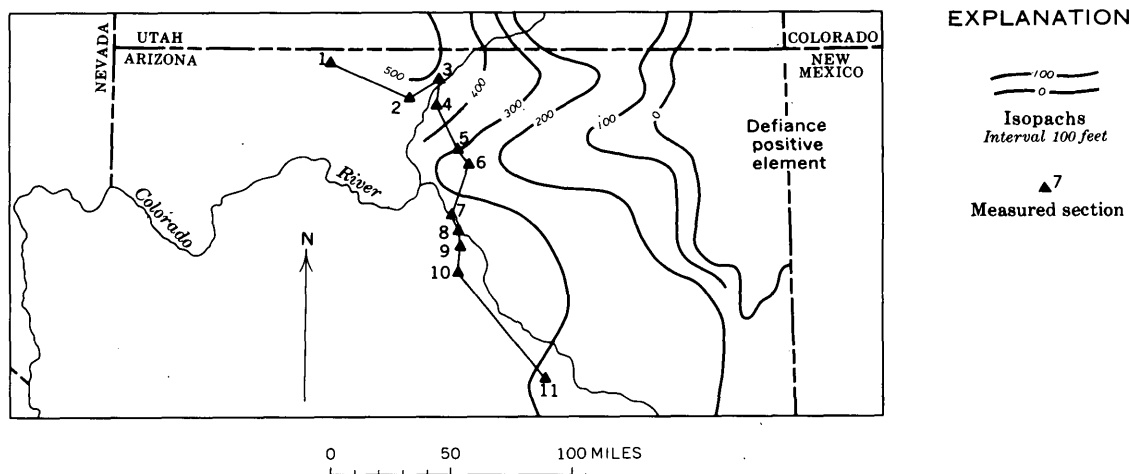
FIGURE 67.1.—Index map showing line of section and localities on figure 67.2, and isopachs of Moenkopi Formation adapted from McKee and others (1959, pl. 3). *1*, Fredonia; *2*, west of Navajo Bridge; *3*, Lees Ferry; *4*, south of Navajo Bridge; *5*, North Cedar Ridge; *6*, North Gap; *7*, 12 miles northwest of Cameron; *8*, 6 miles west-northwest of Cameron; *9*, Poverty Tank; *10*, Black Point; *11*, Winslow.
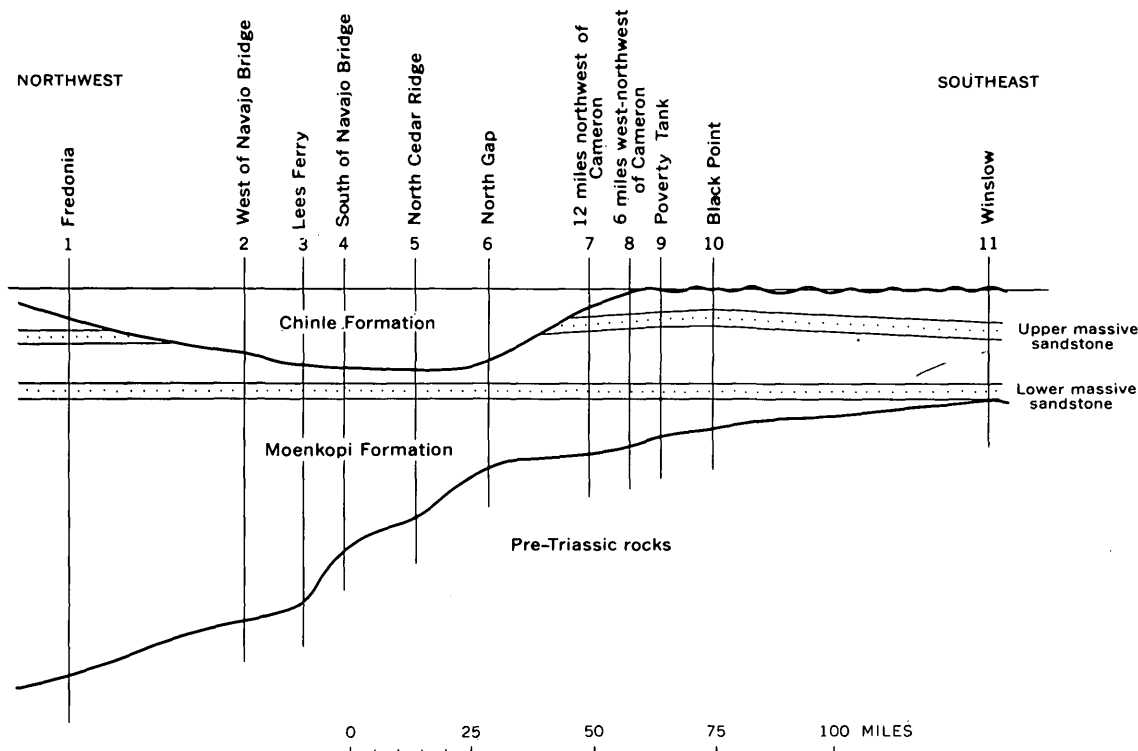
FIGURE 67.2.—Section of Moenkopi Formation from Fredonia to Winslow, Ariz. The lower massive sandstone is used as datum plane.

formed. This surface of erosion is interpreted as evidence of an uplift, probably a gentle upwarp, of a westward-extending prong of the Defiance positive element.

The time of uplift of the western prong of the Defiance positive element can be dated within relatively narrow limits in the Triassic. The uppermost part of the Moenkopi Formation in the area concerned is considerably higher stratigraphically than the zone of *Tirolites* that marks the late part of the Early Triassic (Smith, 1932, p. 15), which suggests that the uppermost part of the Moenkopi may be of Middle Triassic age. Supporting evidence is the presence of the amphibian *Cyclotosaurus* high in the Moenkopi Formation near Holbrook, Ariz.; this genus is characteristic of the Middle and Upper Triassic of Europe and South Africa, according to Welles (1947). Above the unconformity at the top of the Moenkopi Formation in this area is the Chinle Formation, considered to be of Late Triassic age by most geologists (McKee and others, 1959, p. 38–39). Thus the uplift and resulting erosion must have taken place later than the end of Early Triassic and before the early part of Late Triassic time.

Crustal disturbance and warping of beds apparently also took place in other parts of southwestern United States during the interval between deposition of the Moenkopi and Chinle Formations. In eastern Utah a renewal of movement along the general axis of the Moab anticline apparently was sufficiently intense to raise the Moenkopi Formation completely above the base level of erosion, as shown by angular discordance (McKnight, 1940, p. 50). In the Capitol Reef area of Utah, farther west, the writer has observed a discordant contact between these formations, and similar relations have been reported from other areas. Furthermore, uplift of considerable magnitude must have occurred at this time in many places adjacent to the region, as shown by much conglomerate in basal Upper Triassic strata (McKee, 1951, p. 494).

REFERENCES

Gregory, H. E., 1917, Geology of the Navajo country: U.S. Geol. Survey Prof. Paper 93, 161 p.
McKee, E. D., 1951, Sedimentary basins of Arizona and adjoining areas: Geol. Soc. America Bull., v. 62, p. 481–506.
——— 1954, Stratigraphy and history of the Moenkopi Formation of Triassic age: Geol. Soc. America Mem. 61, 133 p.
McKee, E. D., and others, 1959, Paleotectonic maps of the Triassic System: U.S. Geol. Survey. Misc. Geol. Inv. Map I-300, 33 p. [1960].
McKnight, E. T., 1940, Geology of area between Green and Colorado Rivers, Grand and San Juan Counties, Utah: U.S. Geol. Survey Bull. 908, 147 p.
Smith, J. P., 1932, Lower Triassic ammonoids of North America: U.S. Geol. Survey Prof. Paper 167, 199 p.
Welles, S. P., 1947, Vertebrates from the Upper Moenkopi Formation of northern Arizona: California Univ. Pub., v. 27, no. 7, p. 241–294.

Article 68

REVISED STRATIGRAPHIC NOMENCLATURE AND AGE OF THE TUXEDNI GROUP IN THE COOK INLET REGION, ALASKA

By ROBERT L. DETTERMAN, Menlo Park, Calif.

Abstract.—The Tuxedni Formation is raised to group rank in the Cook Inlet region. Names are given to three formerly unnamed members, and these and three other members are raised to formation rank. In ascending order they are designated the Red Glacier Formation, Gaikema Sandstone, Fitz Creek Siltstone, Cynthia Falls Sandstone, Twist Creek Siltstone, and Bowser Formation.

The Tuxedni Formation was defined as the Tuxedni Sandstone by Martin and Katz (1912, p. 59–64) to include all the marine sandstone and shale of Middle Jurassic age exposed on the south shore of Tuxedni Bay, Alaska. The formation was subdivided as the result of mapping by oil company and Geological Survey geologists during and immediately after World War II (fig. 68.1).

Recent mapping in the Cook Inlet region and southern Alaska has shown that the formation should be considered a group. Therefore, in this article the Tuxedni Formation is raised to the rank of group and its former members to the rank of formation, except for the former Bowser Member, which is subdivided and raised to two formations. In ascending order, the formations are the Red Glacier Formation, Gaikema Sandstone, Fitz Creek Siltstone, Cynthia Falls Sandstone, Twist Creek Siltstone, and Bowser Formation. The marine rocks of the Tuxedni Group are abundantly fossiliferous. Ammonites studied and described by R. W. Imlay (1961, 1962a, 1962b, and report in preparation) indicate that the Tuxedni Group is of Middle and Late Jurassic age. ·

The name Red Glacier Formation is here introduced to replace the term lower member of the former Tuxedni Formation in the older reports. The formation is named after Red Glacier, and the type section is designated as exposures along both sides of the glacier (fig. 68.2). The upper 3,310 feet is exposed along the south side, 4½ miles S. 62° E. of Iliamna Volcano, and the lower 1,230 feet is on the north side of the glacier, 6½ miles N. 86° E. of Iliamna Volcano. The Red Glacier Formation is 1,980 feet thick at Tuxedni Bay, 18 miles northeast of Red Glacier, and about 6,500 feet thick in the subsurface under Iniskin Peninsula, 18 miles southwest of Red Glacier.

The Red Glacier Formation consists mainly of arkosic sandstone and shale with minor amounts of sub-graywacke-type sandstone, conglomerate, and limestone in the lower part, and sandy siltstone in the upper part. At the type locality the lower 200 feet is light-brown arkosic sandstone. This is overlain by 200 feet of black silty shale, 200 feet of arkosic sandstone, 1,000+ feet of soft black silty shale in which a small fault cuts out part of the section, 720 feet of light-brown arkosic sandstone, 1,060 feet of interbedded sandstone and siltstone, and at the top by 1,160 feet of sandy siltstone. The base of the formation rests unconformably on the Talkeetna Formation of Early Jurassic age. The upper contact is gradational into the overlying Gaikema Sandstone.

The Gaikema Sandstone Member, named by Kirschner and Minard (1948) after Gaikema Creek on Iniskin Peninsula, is herein designated the Gaikema Sandstone. The type locality is designated as the left bank of the creek, starting 5,000 feet from the mouth and continuing for 1,800 feet upstream. The section at the type locality is 850 feet thick and consists of resistant cliff-forming sandstone, in part conglomeratic. Siltstone, shale, and cobble-boulder conglomerate are subordinate constituents.

Measured sections of the Gaikema Sandstone range in thickness from 500 to 870 feet. At the type locality the lower 180 feet is medium-bedded olive-gray to yellowish-green sandstone containing beds of silty shale, siltstone, and conglomerate. This is overlain by 220

Martin and Katz (1912) Moffit (1927)	Kellum (1945)	Kirschner and Minard (1948)	Hartsock (1954)	This article		Stage	Standard zones in Europe (Imlay, 1952)
UPPER JURASSIC Chinitna Shale	Not examined	Chinitna Siltstone	Chinitna Formation	Chinitna Formation	Generalized geologic section	Callovian	Only those zones present in Cook Inlet region are shown
		Tonnie Silt-stone Member ?		Tonnie Silt-stone Member			
	Tuxedni Formation — Upper sandstone member	Tuxedni Formation — Bowser Member	Bowser Member	Bowser Formation			*Macrocephalites macrocephalus*
						Bath-onian(?)	*Clydoniceras discus*
							Oppelia aspidoides
	Upper sandy-shale member			Twist Creek Siltstone			*Strenoceras subfurcatum*
							Stephanoceras humphriesanum
MIDDLE JURASSIC Tuxedni Sandstone	Cynthia Falls Sandstone Member	Cynthia Falls Sandstone Member	Cynthia Falls Sandstone Member	Tuxedni Group — Cynthia Falls Sandstone		Bajocian	*Otoites sauzei*
	Lower sandy-shale member	Lower sandy-shale member	Siltstone member	Fitz Creek Siltstone			*Sonninia sowerbyi*
	Kialagvik Formation — Sandstone member	Kialagvik Formation — Gaikema Sand-stone Member	Gaikema Sand-stone Member	Gaikema Sand-stone			*Tmetoceras scissum*
	Sandy-shale member	Sandy-shale member	Lower member	Red Glacier Formation			
LOWER JURASSIC Porphyries and tuffs	Volcanic rocks	Volcanic rocks	Volcanic rocks	Talkeetna Formation			

EXPLANATION

Bedded sandstone

Massive sandstone

Conglomerate

Siltstone

Sandy siltstone

Shale

Tuff and lava flows

Limestone concretions

2000 FEET
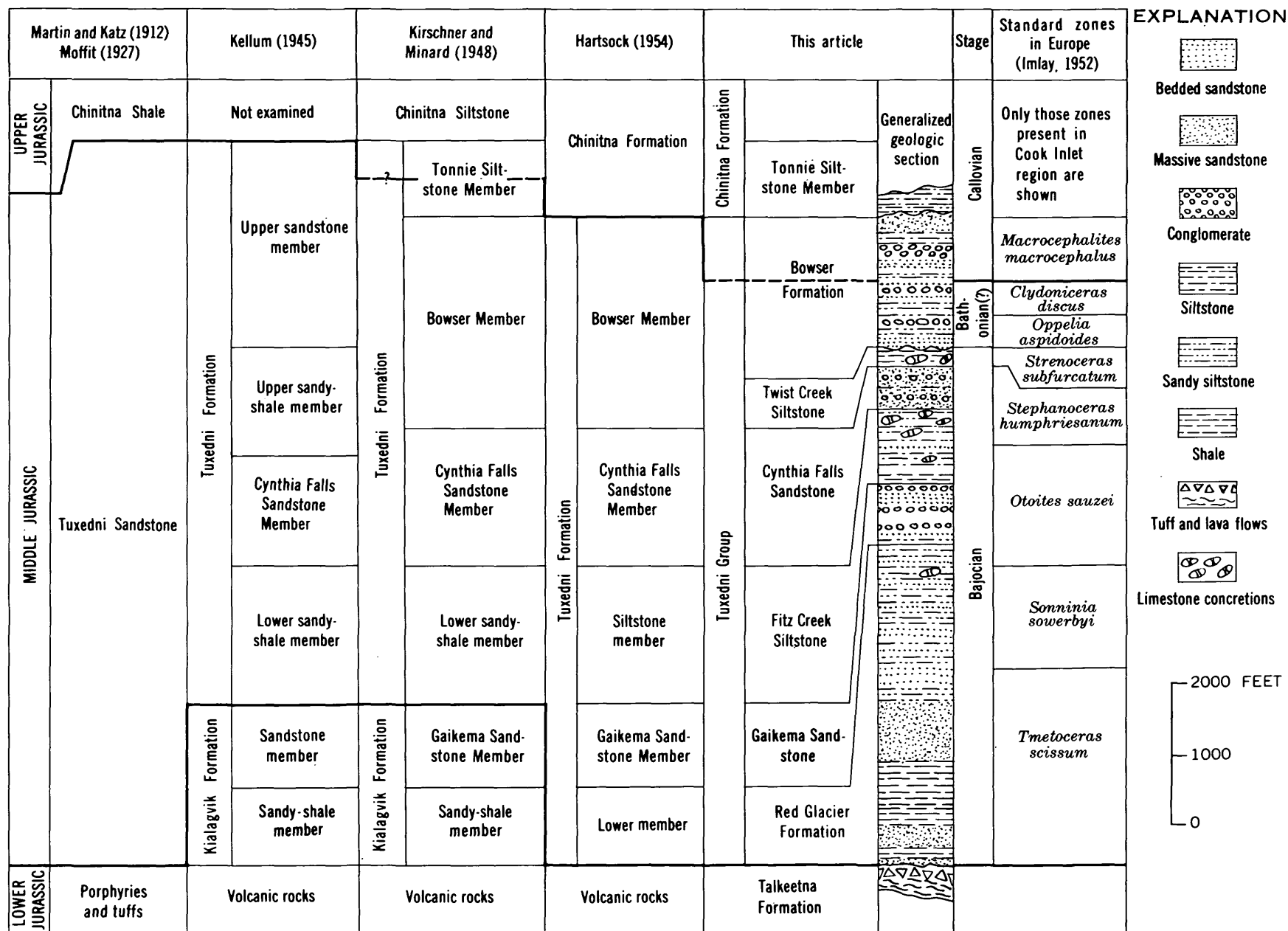1000
0

FIGURE 68.1—Revision of stratigraphic nomenclature of the Tuxedni Group in Cook Inlet region, Alaska.
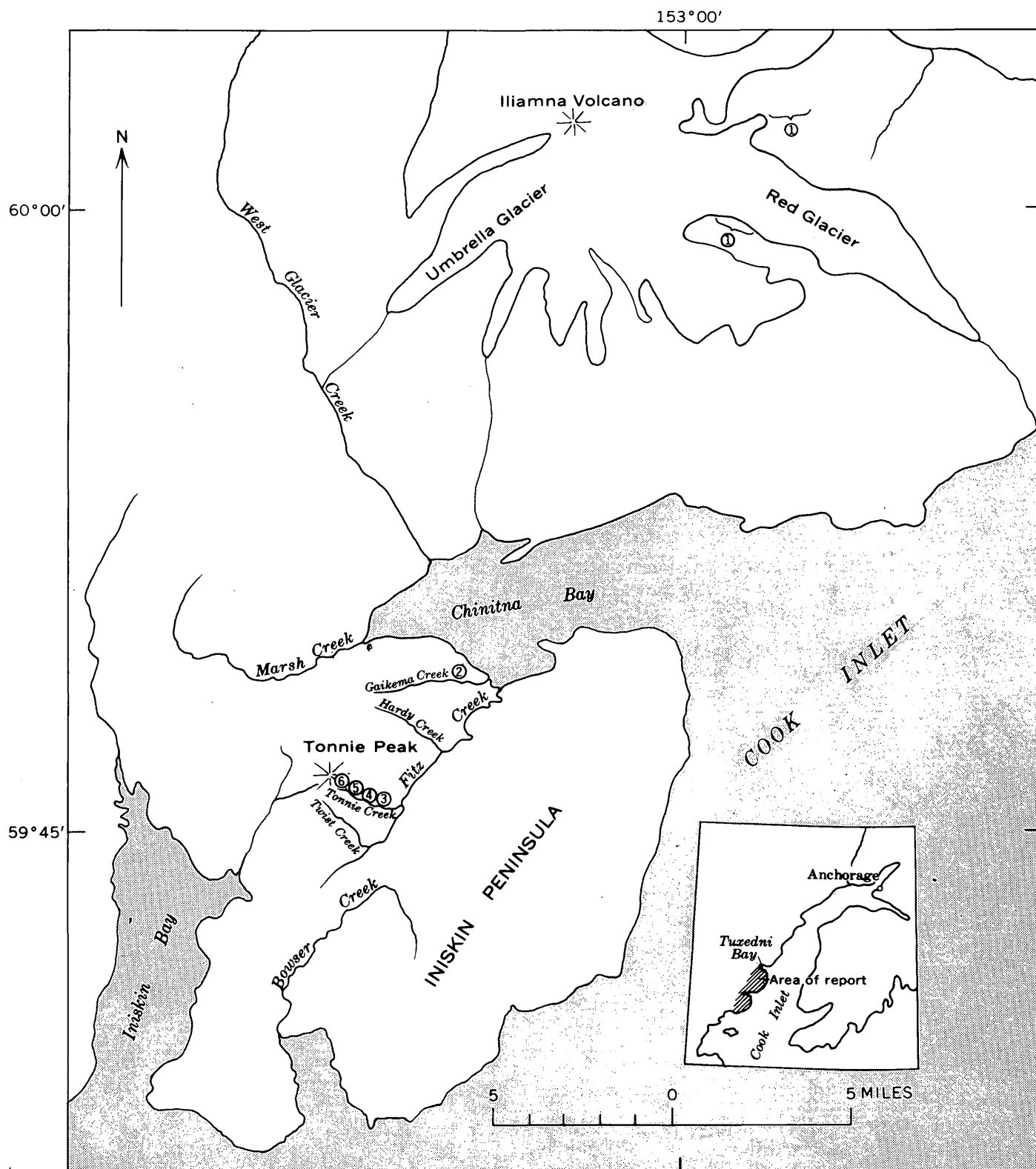
DETTERMAN

C31

FIGURE 68.2.—Index map showing type localities of formations in the Tuxedni Group, Cook Inlet region, Alaska. *1*, Red Glacier Formation. *2*, Gaikema Sandstone. *3*, Fitz Creek Siltstone. *4*, Cynthia Falls Sandstone. *5*, Twist Creek Siltstone. *6*, Bowser Formation.

feet of medium-bedded greenish-gray sandstone, 110 feet of cobble-boulder conglomerate and coarse-grained arkosic sandstone, 220 feet of thin- to medium-bedded olive-green sandstone, and at the top by 120 feet of medium-bedded medium-grained dark-olive-green sandstone containing a few beds of cobble-boulder conglomerate. The lower contact is gradational into the Red Glacier Formation, and the upper contact with the Fitz Creek Siltstone is conformable and sharp.

The Fitz Creek Siltstone is here named to replace the term siltstone member of the former Tuxedni Formation of older reports. The formation is named after Fitz Creek, the principal stream on Iniskin Peninsula. The type locality is on Tonnie Creek, a tributary of Fitz Creek, starting 7,000 feet S. 55° E. of Tonnie Peak and continuing upstream for 1,400 feet. The formation is 1,090 feet thick at the type locality.

The formation is composed mainly of massive bluish-gray arenaceous siltstone that commonly weathers rusty brown and contains many small ovoid fossiliferous limestone concretions. Interbedded with the siltstone are fine-grained sandstone and, locally, conglomerate. Measured sections range from about 650 to 1,280 feet in thickness. The lower 80 feet of the type section is a massive bluish-gray siltstone, with a 70-foot covered interval above the siltstone. The covered interval is overlain by 340 feet of siltstone, 70 feet of very fine grained silty sandstone, and at the top by 530 feet of massive bluish-gray arenaceous siltstone. The upper and lower contacts are conformable.

Formational status is given the former Cynthia Falls Sandstone Member of Kellum (1945). The formation was named after Cynthia Falls, a prominent waterfall on Hardy Creek, Iniskin Peninsula. The type section is on Tonnie Creek, starting 5,600 feet S. 50° E. of Tonnie Peak and continuing upstream for 600 feet. Massive- to thick-bedded coarse-grained greenish-gray graywacke-type sandstone is the main constituent. Interbedded with the sandstone are thin layers of pebble-cobble conglomerate and arenaceous siltstone. Much of the sandstone is mottled green and white. The white spots are formed by the abundant zeolite minerals in the sandstone.

The Cynthia Falls Sandstone is 600 to 700 feet thick in the Cook Inlet region. The type section is 600 feet thick; it consists of 270 feet of massive coarse-grained greenish-gray-mottled sandstone at the base, overlain by 50 feet of brownish-gray arenaceous siltstone and 280 feet of massive sandstone containing a few layers of pebbles. The contacts with the underlying and overlying formations are conformable.

The Twist Creek Siltstone is herein named for the sequence of rocks included by Imlay (1962b) as the lower part of the former Bowser Member of the Tuxedni Formation. The formation is named after Twist Creek on Iniskin Peninsula, and the type section is on Tonnie Creek, starting 5,000 feet S. 47° E. of Tonnie Peak and continuing upstream for 500 feet. The Twist Creek Siltstone is uniformly soft, poorly consolidated siltstone and shale with a few thin graywacke-type sandstone interbeds. The siltstone is thin bedded to massive, arenaceous, dark gray, and weathers rusty dark brown. Many thin beds of volcanic ash are intercalated with the siltstone, and small discoidal limestone concretions occur abundantly throughout. The formation is 240 feet thick at the type locality and has a maximum thickness of about 410 feet near Red Glacier.

A major unconformity exists between the Twist Creek Siltstone and the overlying Bowser Formation. As a result of this unconformity the Twist Creek is missing in the southwestern part of Iniskin Peninsula.

The Bowser Member of the Tuxedni Formation, named by Kirschner and Minard (1948), is here restricted to the upper part of the member and raised in rank to the Bowser Formation of the Tuxedni Group. The formation is named after Bowser Creek. The formation is exposed at many localities along the creek, but the type locality is on Tonnie Creek, starting 4,500 feet S. 47° E. of Tonnie Peak and continuing upstream for 1,500 feet.

Rocks assigned to the Bowser Formation include massive units of cliff-forming graywacke-type sandstone, pebble-cobble conglomerate, thin-bedded shale, and massive siltstone. Measured sections of the formation range in thickness from about 1,250 feet to as much as 1,850 feet. The type section is 1,830 feet thick and consists of 70 feet of thin-bedded sandstone overlain by 280 feet of massive siltstone, 70 feet of cobble conglomerate, 260 feet of gray siltstone, 250 feet of sandstone with pebble-conglomerate layers, 130 feet of dark-gray siltstone, 170 feet of thin-bedded light-gray sandstone, 170 feet of cobble conglomerate, 250 feet of massive olive-gray siltstone, and at the top by 180 feet of massive coarse-grained dark-gray sandstone. The contact with the overlying Chinitna Formation, of Late Jurassic age, is locally unconformable.

Ammonites from the lower part of the Bowser Formation have been identified by Imlay (1962a) as of Bathonian (Middle Jurassic) or Callovian (Late Jurassic) age, and from the upper part as of definite Callovian age. Therefore the age of the Bowser Formation is herein considered to be Middle(?) and Late Jurassic.

REFERENCES

Hartsock, J. K., 1954, Geologic map and structure sections of the Iniskin Peninsula and adjacent area, Alaska: U.S. Geol. Survey open-file report, 1 map, cross section.

Imlay, R. W., 1952, Correlation of the Jurassic formations of North America exclusive of Canada: Geol. Soc. America Bull., v. 63, p. 953–992.

—— 1961, New genera and subgenera of Jurassic (Bajocian) ammonites from Alaska: Jour. Paleontology v. 35, p. 467–474.

—— 1962a, Jurassic (Bathonian or early Callovian) ammonites from Alaska and Montana: U.S. Geol. Survey Prof. Paper 374–C, 32 p.

Imlay, R. W., 1962b, Late Bajocian ammonites from Cook Inlet region, Alaska: U.S. Geol. Survey Prof. Paper 418–A, 15 p.

Kellum, L. B., 1945, Jurassic stratigraphy of Alaska and petroleum exploration in northwest America: New York Acad. Sci. Trans., ser. 2, v. 7, p. 201–209.

Kirschner, C. E., and Minard, D. L., 1948, Geology of the Iniskin Peninsula, Alaska: U.S. Geol. Survey Oil and Gas Inv. Prelim. Map 95, scale 1 inch to 4,000 feet [1949].

Martin, G. C., and Katz, F. J., 1912, A geologic reconnaissance of the Iliamna region, Alaska: U.S. Geol. Survey Bull. 485, 138 p.

Moffit, F. H., 1927, The Iniskin-Chinitna Peninsula and the Snug Harbor District, Alaska: U.S. Geol. Survey Bull. 789, 71 p.

REDEFINITION AND CORRELATION OF THE OHIO CREEK FORMATION (PALEOCENE) IN WEST-CENTRAL COLORADO

By D. L. GASKILL and L. H. GODWIN, Denver, Colo.

Abstract.—The redefined Ohio Creek Formation includes strata formerly mapped as Ohio Creek Conglomerate as well as underlying conglomeratic sandstone beds formerly included with the upper part of the Mesaverde Formation. These conglomeratic beds in the West Elk Mountains are similar to strata described elsewhere in the Piceance Basin at equivalent stratigraphic positions.

A sequence of conglomeratic sandstone beds of probable Paleocene age, similar to the unnamed Tertiary(?) sandstone of the Colorado Book Cliffs area (Erdmann, 1934, p. 53–55), underlies the Ohio Creek Conglomerate of Lee (1912) in the Ruby–West Elk Mountain area of Gunnison County, Colo. (fig. 69.1).
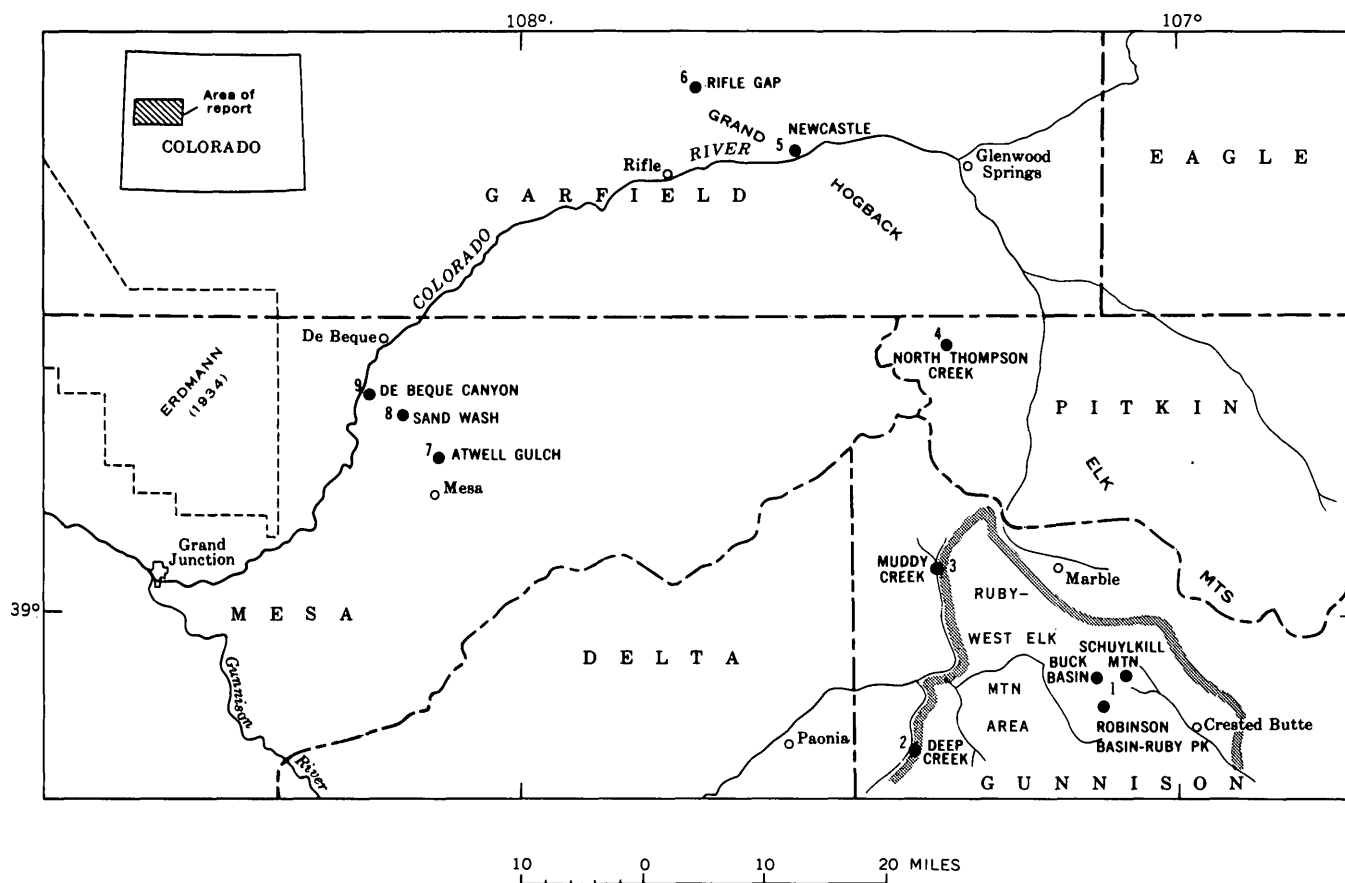

FIGURE 69.1.—Index map showing Ruby–West Elk Mountain area (shaded outline in lower right corner) and localities referred to in text and on figure 69.2.

In the Ruby–West Elk Mountain area this conglomeratic sandstone sequence is about 380 to 430 feet thick and consists of very thick massive beds of white to medium-gray very coarse to fine-grained sandstone interbedded with shale and siltstone. Locally some carbonaceous shale and coal are present. Small well-rounded pebbles of light- to dark-gray chert predominate in the conglomeratic sandstone beds. Pebbles of gray, purple, and pink quartzite, quartz, shale, and silty clay are common, and a few pebbles of varicolored reddish- to yellowish-orange chert and igneous rock may be present. Most of the pebbles range from a quarter of an inch to 1 inch in diameter and occur in thin discontinuous layers, thin to thick lenses, or pockets in a matrix of coarse sand and granules. Abundant pebble- to boulder-size sandstone concretions cemented with limonite are present at several localities. The sandstone beds in many localities are more conglomeratic at or near their base. Many exposures contain only a few scattered pebbles.

The conglomeratic beds of this sequence generally differ from the overlying Ohio Creek Conglomerate of Lee only in the scarcity, smaller size range, and less variety of color of the pebble components.

Incomplete exposures of the Ohio Creek Formation of Eldridge (1894) in the type area at the head of Ohio and Carbon Creeks, Gunnison County, Colo., seem to include both the Ohio Creek Conglomerate of Lee and the lower conglomeratic sandstone sequence described above. Similar conglomeratic beds are present at an equivalent stratigraphic position near Mesa, Colo., and along the Grand Hogback (Hill, 1890, p. 391; Gale, 1910, p. 79; Lee, 1912, p. 48; Donnell, 1953, p. 17, 1959, p. 76, 1960, p. 48, 79, 1961, p. 843, 844; Young, 1959, fig. 4, p. 23; F. G. Poole, oral communication, March 7, 1963; and several theses [1]).

We here redefine the Ohio Creek Formation so that it includes the Ohio Creek Conglomerate of Lee, the underlying conglomeratic sandstone sequence of the Ruby–West Elk Mountain area, and equivalent beds elsewhere in the Piceance Basin. Beds included in the redefinition below Lee's Ohio Creek Conglomerate were formerly mapped as Mesaverde Formation undifferentiated (Lee, 1912) or Barren member of the Mesaverde (Johnson, 1948). In the Ruby–West Elk Mountain area the following threefold division of this interval

[1] Mull, C. G., 1961, Geology of the Grand Hogback monocline near Rifle, Colorado: Colorado Univ. Master's degree thesis.

Newman, K. R., 1961, Micropaleontology and stratigraphy of Late Cretaceous and Paleocene formations: Colorado Univ. Ph. D. dissert., available on microfilm from University Microfilms, Inc., Ann Arbor, Mich.

Phipps, J. B., 1961, Geology of area near Newcastle, Colorado: Colorado Univ. Master's degree thesis.

Poole, F. G., 1954, Geology of southern Grand Hogback area, Garfield and Pitkin Counties, Colorado: Colorado Univ. Master's degree thesis.

is possible: a lower conglomeratic sandstone-shale unit, 150 to 250 feet thick; a middle nonconglomeratic locally coal-bearing sandstone-shale unit of Mesaverde-like lithology, 100 to 230 feet thick; and an upper conglomeratic sandstone unit, 10 to 55 feet thick (the Ohio Creek Conglomerate of Lee). The sandstone of these units is predominantly white to light gray, very coarse to medium grained, quartzose, feldspathic, and friable. Erosional disconformities, like those in the underlying Mesaverde Formation, commonly separate many beds. Individual beds in the lower and middle units may or may not have a wide lateral extent. Similar sandstone beds with very coarse grained sand to granule lenses containing silty clay pellets are found at many places below the lowest conglomeratic sandstone.

The lower contact of the formation is gradational with the underlying Mesaverde beds and is arbitrarily placed at the base of the lowest conglomeratic sandstone bed. In the Ruby–West Elk Mountain area the upper conglomeratic sandstone unit is generally overlain by a thick gray to greenish-gray commonly maroon-stained shale, greenish coarse-grained sandstone, or sandy micaceous claystone, siltstone, and dense siliceous mudstone. Locally a basal conglomerate of the Wasatch directly overlies the upper sandstone unit.

The upper contact seems to be conformable with the overlying beds in places, but is locally disconformable.

The basal conglomerates of the Wasatch are distinctive beds easily differentiated from the Ohio Creek beds. They form very thick to thin beds of well-cemented poorly sorted generally well rounded pebbles in a coarse angular-grained quartzose feldspathic matrix. Igneous pebbles of dacite, andesite, gneiss, and granite predominate. Varicolored chert, quartzite, and quartz pebbles are scattered throughout or locally concentrated in many of the conglomerate lenses.

A typical stratigraphic section for the redefined Ohio Creek Formation is located at the head of Deep Creek (W½ sec. 12, T. 14 S., R. 90 W.), about 10 miles east of Paonia, Colo. (2, figs. 69.1 and 69.2), (Lee, 1912, pl. VI–A). A reference locality for the upper conglomeratic sandstone unit is well exposed on both sides of Muddy Creek below the McClures Pass road in the SW¼ sec. 29 and NE¼ sec. 31, T. 11 S., R. 89 W. (3, figs. 69.1 and 69.2).

Stratigraphic sections of the lower and middle units are best exposed on the south face of Schuylkill Mountain (W½ sec. 11, T. 13 S., R. 87 W., unsurveyed) and in Buck Basin on the west slope of the Ruby Range (SE¼ sec. 8, T. 13 S., R. 87 W., unsurveyed) (1, figs. 69.1 and 69.2).

The Ohio Creek Formation is believed to be of Paleocene age on the basis of a fossil flora collected about 20

RUBY-WEST ELK MOUNTAIN AREA
Gunnison County, Colo.

GRAND HOGBACK AREA
Pitkin and Garfield
Counties, Colo.

MESA-DE BEQUE AREA
Mesa County, Colo.

1
RUBY RANGE
COMPOSITE SECTION
T. 13 S., R. 87 W.

Wasatch beds measured
on Ruby Peak (secs. 21,
28); Ohio Creek beds
measured in Robinson
basin (sec. 21) and on
Schuykill Mtn. (W½
sec. 11)

6
RIFLE GAP
Sec. 18,
T. 5 S., R. 92 W.

FEET
0

100

200

300

5
NEWCASTLE
Sec. 2,
T. 6 S., R. 91 W.

2
DEEP CREEK
W½ sec. 12,
T. 14 S., R. 90 W.

3
MUDDY CREEK
NE¼ sec. 31,
T. 11 S., R. 89 W.

4
NORTH THOMPSON
CREEK
Sec. 28,
T. 8 S., R. 89 W.

7
ATWELL GULCH
SW¼ sec. 8,
T. 10 S., R. 96 W.

8
SAND WASH
Sec. 26,
T. 9 S., R. 97 W.

9
DE BEQUE CANYON
NW¼NW¼ sec. 16,
T. 9 S., R. 97 W.

Igneous sill

Wasatch Formation
Conglomerate facies

Ohio Creek Formation
Upper unit
Middle unit
Lower unit

Mesaverde
Formation

EXPLANATION

Sandstone

Sandstone with
large concretions

Conglomeratic sandstone

Conglomerate

Siltstone and sandy shale

Shale and claystone

Covered

Coal

Carbonaceous shale

3
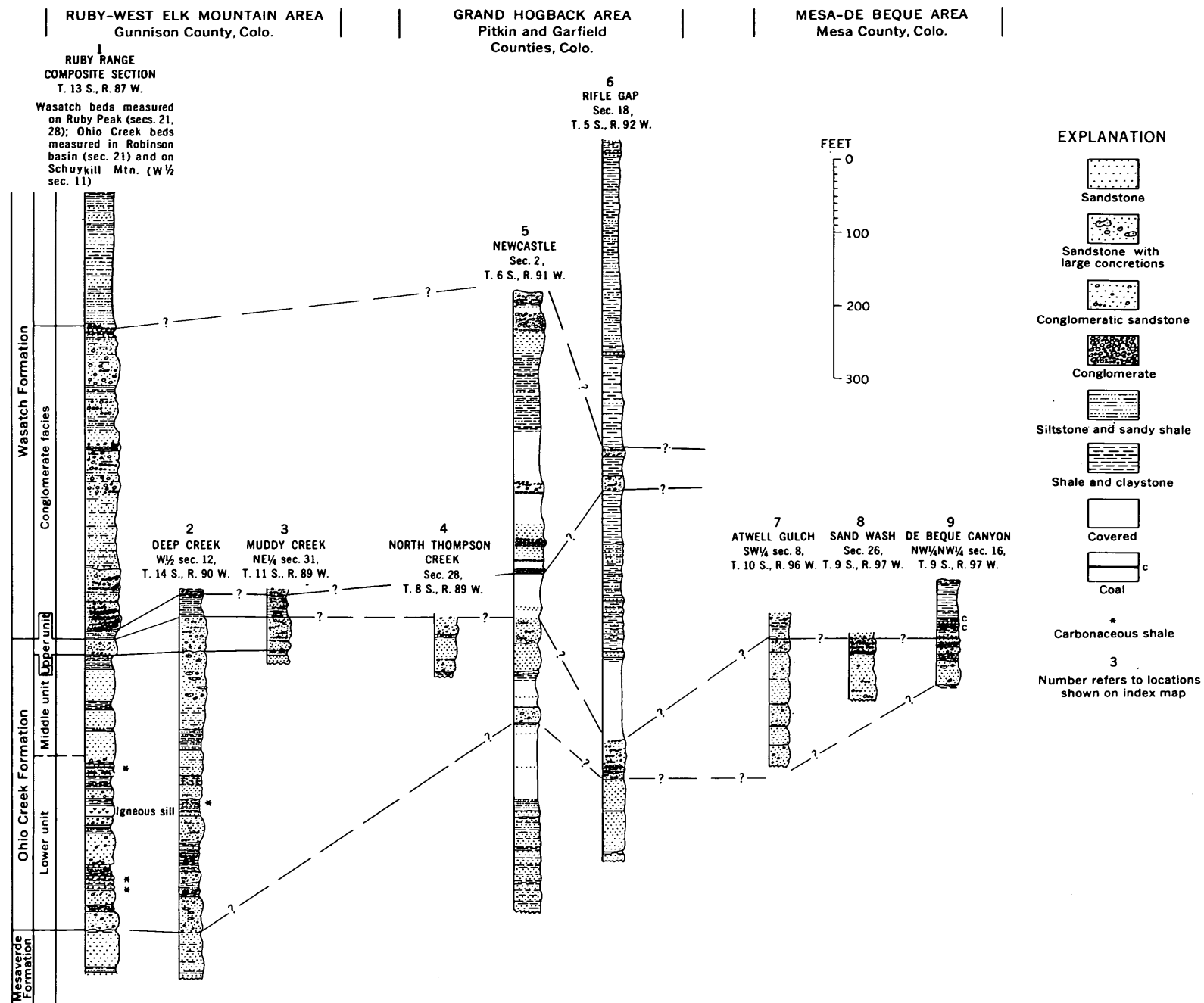Number refers to locations
shown on index map

FIGURE 69.2.—Stratigraphic sections of the Ohio Creek Formation in Gunnison, Pitkin, Garfield, and Mesa Counties, Colo.

feet above the base of the formation in the N½ sec. 1, T. 13 S., R. 88 W. (Gaskill, 1961). Reevaluation of this fossil locality shows the flora to be near the base of the lower conglomeratic sandstone unit and not in the Ohio Creek Conglomerate of Lee as indicated by Gaskill (1961).

Reconnaissance examination of scattered outcrops along the Grand Hogback and in the Mesa-DeBeque, Colo., area has convinced the authors that beds present at each of the numbered localities shown on figure 69.1 are equivalent, in part, to the redefined Ohio Creek Formation. Some of these conglomeratic sandstone beds, correlated with the Ohio Creek Formation on figure 69.2, closely resemble the upper conglomeratic sandstone unit in the Ruby–West Elk Mountain area. Other beds, generally those lower in the section, are similar to the lower conglomeratic sandstone unit in the Ruby–West Elk Mountain area. The DeBeque Canyon sequence is identical with the general description of Erdmann's unnamed Tertiary(?) sandstone unit in the Colorado Book Cliffs. However, because of the lithologic similarity of these fluvial deposits and their regional distribution and different source areas, it will probably be necessary to trace beds along outcrops in order to correlate individual units in the Ruby–West Elk Mountain area with those elsewhere in the Piceance Basin.

REFERENCES

Donnell, J. R., 1953, Columnar section of rocks exposed between Rifle and DeBeque Canyon, Colorado, and road logs north of Rifle, Colorado, in Rocky Mountain Association of Petroleum Geologists Guidebook, Field conference in northwestern Colorado, 1953: p. 16–17.

Donnell, J. R., 1959, Mesaverde stratigraphy in the Carbondale area, northwestern Colorado, in Rocky Mountain Association of Petroleum Geologists, Symposium on Cretaceous rocks of Colorado and adjacent area, 11th Field Conf., Washakie, Sand Wash, and Piceance Basins, 1959: p. 76–77.

——1960, Road logs, Rifle to Craig, Colorado; Rangely to Grand Junction, Colorado, in Rocky Mountain Association of Petroleum Geologists, Geologic road logs of Colorado: p. 48, 79.

——1961, Tertiary geology and oil-shale resources of the Piceance Creek Basin between the Colorado and White Rivers, northwestern Colorado: U.S. Geol. Survey Bull. 1082–L, p. 835–891.

Eldridge, G. H., 1894, Descriptions of the sedimentary formations, in Emmons, S. F., Cross, Whitman, and Eldridge, G. H. Anthracite-Crested Butte [Colorado]: U.S. Geol. Survey Geol. Atlas, Folio 9, p. 6–10.

Erdmann, C. E., 1934, The Book Cliffs coal field in Garfield and Mesa Counties, Colorado: U.S. Geol. Survey Bull. 851, 150 p. [1935].

Gale, H. S., 1910, Coal fields of northwestern Colorado and northeastern Utah: U.S. Geol. Survey Bull. 415, 265 p.

Gaskill, D. L., 1961, Age of the Ohio Creek Conglomerate, Gunnison County, Colorado: Art. 96 in U.S. Geol. Survey Prof. Paper 424–B, p. B230–B231.

Hill, R. C., 1890, Orographic and structural features of Rocky Mountain geology: Colorado Sci. Soc. Proc., v. 3 p. 362–458.

Johnson, V. H., 1948, Geology of the Paonia coal field, Delta and Gunnison Counties, Colorado: U.S. Geol. Survey unnumbered coal-investigations map.

Lee, W. T., 1912, Coal fields of Grand Mesa and the West Elk Mountains, Colorado: U.S. Geol. Survey Bull. 510, 237 p.

Young, R. G., 1959, Cretaceous deposits of the Grand Junction area, Garfield, Mesa and Delta Counties, Colorado, in Rocky Mountain Association of Petroleum Geologists, Symposium on Cretaceous rocks of Colorado and adjacent areas, 11th Field Conf., Washakie, Sand Wash, and Piceance Basins, 1959: p. 22–23.

TERTIARY VOLCANIC STRATIGRAPHY
IN THE WESTERN SAN JUAN MOUNTAINS, COLORADO

By R. G. LUEDKE and W. S. BURBANK, Washington, D.C.,

and Exeter, N.H.

Abstract.—Eruptive materials, genetically related to the western San Juan eruptive centers, are divided into three principal stratigraphic units: San Juan Formation, Silverton Volcanic Group, and Potosi Volcanic Group; the second and third units are further subdivided into formations. These stratigraphic units are, in part, renamed and redefined.

Volcanism in the middle and late Tertiary built a tremendous pile of eruptive materials upon an extensively eroded basement of Precambrian, Paleozoic, and Mesozoic rocks to form most of the western San Juan Mountains (fig. 70.1). The volcano-tectonic structures consisting of a younger comagmatic pair of calderas superimposed upon an older volcanic depression (super caldera) are related to this volcanism.

The volcanic rocks form a layered succession aggregating nearly 1½ miles in thickness and having a volume greater than 1,000 cubic miles. The types of deposits are many, but tuff breccia, lava flows, and welded ash-flow tuffs (terminology of Smith, 1960a) predominate. Eruptive materials composing these deposits range in composition from basalt to rhyolite but are predominantly rhyodacitic and quartz latitic. The volcanic rocks are quite heterogenous, as indicated by lithologic, petrographic, and meager chemical data. We therefore believe it desirable to refer to the different units, with one exception explained herein, either as formations or as rock types rather than as petrographic types.

The eruptive materials are divided from older to younger into three principal units: the San Juan Formation, the Silverton Volcanic Group, and the Potosi Volcanic Group. The second and third units are subdivided into several formations each. Changes in nomenclature of these volcanic units throughout the period of geologic investigations in the western San Juan Mountains are shown in the accompanying table. The unit definitions and name changes here proposed are restricted to eruptive centers of the western San Juan Mountains. The centers are confined mainly to the headwater basins of the Uncompahgre and Animas Rivers and the Lake Fork of the Gunnison River (fig. 70.1). The interrelations of the several eruptive units to those of other centers of the San Juan Mountains are not as yet fully established.

Only a few poorly preserved plant and animal fossils have been found so far in the volcanic units of the western San Juan Mountains, and these are too inadequate to permit age assignments closer than middle and late Tertiary.

SAN JUAN FORMATION

Cross (1896, p. 226) initially named the oldest of the local volcanic units the San Juan Formation for exposures in the vicinity of Telluride. The name was changed by Cross and others (1905, p. 7), after their study of the limited exposures in the Silverton quadrangle, to the San Juan Tuff, which it has been called until the present article. The unit consists predominantly of rhyodacitic tuff breccia with minor associated volcanic conglomerates and air-fall tuffs, rhyobasaltic and rhyodacitic lava flows and flow breccias, and rhyodacitic to quartz latitic welded ash-flow tuffs. The lower few hundred feet of the formation contains erratically distributed foreign fragments derived from the underlying prevolcanic terrane. Because of the
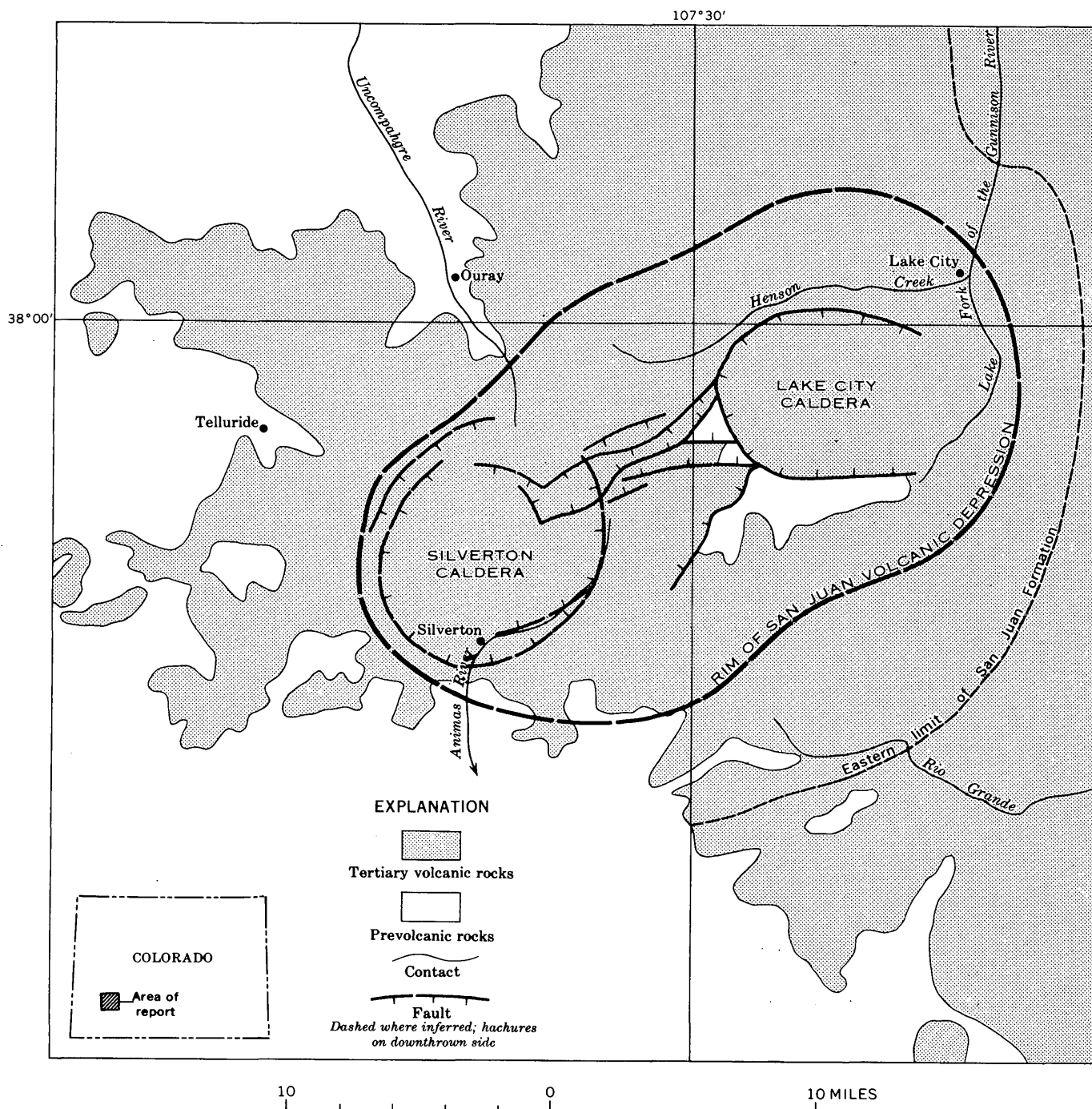
FIGURE 70.1.—Generalized geologic map of part of the western San Juan Mountains, Colo., showing location of the San Juan volcanic depression and the Silverton and Lake City calderas within it. Depression rim is locally a fault zone, fault-line scarp, or topographic escarpment.

variations in type of eruptive materials, the original name proposed by Cross is preferred and is here reassigned.

The San Juan Formation has a maximum thickness of more than 3,000 feet, was deposited over an estimated 2,400 square miles, and had a volume of about 600 cubic miles. Typically it appears from a distance as a single unit in which rude bedding is readily discernible. Most of the tuff breccia beds were probably deposited as mudflows (Burbank, 1930, p. 189), but the origin of some features of the formation is obscure.

The source of the volcanic materials is believed to have been a cluster of volcanoes centered within the headwater areas of the Uncompahgre and Animas Rivers and the Lake Fork of the Gunnison River. Most if not all of the volcanoes are presumed to have been destroyed during explosive activity that led to the widespread dispersal of mudflows and ash beds. The engulfment of the vents during the late San Juan eruptions initiated the formation of the San Juan volcanic depression.

SILVERTON VOLCANIC GROUP

This group of volcanic deposits, recognized and referred to by Cross (1896, p. 228), first was named the Intermediate Series (Cross and Purington, 1899, p. 5). The name was changed to the Silverton Series by Cross (in Ransome, 1901, p. 32) and, later, to the Silverton Volcanic Series (Cross and others, 1905, p. 7) for its extensive exposures in the Silverton quadrangle. In 1961, the name was changed to Silverton Volcanic Group in keeping with the code adopted by the American Commission on Stratigraphic Nomenclature, in which "group," a rock-stratigraphic term, is substituted for "series," a time-stratigraphic term.

The Silverton Volcanic Group is divided into four formations which are, from the base upwards, the Picayune Formation, Eureka Tuff, Burns Formation, and Henson Formation (see table). The sequence of major eruptions, characterized by the individual formations, is an alternation of explosive episodes of ash and pumice and less violent outporings of lava and ash. The bulk of the Silverton consists of thin to thick flows and breccias interbedded with air-fall and partly reworked tuffs, local volcanic piles and domes, and related intrusive bodies.

The Silverton Volcanic Group is confined to an area of about 425 square miles, mainly within the San Juan volcanic depression. Some of the materials overflowed the contemporary rims of the depression, particularly to the west. The total volume of intradepression eruptive materials forming this group is estimated to be about 400 cubic miles, compared with 15 or 20 cubic miles which overflowed.

Picayune Formation.—The Picayune Formation was first named and described by Cross and others (1905, p. 7), for exposures at the mouth of Picayune Gulch northeast of Silverton in the Silverton quadrangle, and since has undergone several name changes (see table). The formation consists of thin to thick flows, breccias, and tuffs that range widely in composition from basaltic andesite to rhyolite. The heterogeneous sequence of rocks is exposed in limited outcrops throughout the volcanic depression. It is best developed, with a thickness of about 2,000 feet, near Lake City (Cross and Larsen, 1935, p. 60).

Eureka Tuff.—The second formational unit of the Silverton Volcanic Group, named the Eureka Rhyolite by Cross and others (1905, p. 7), for exposures in the vicinity of Eureka Gulch northeast of Silverton, is redefined as the Eureka Tuff. The more descriptive rock term is substituted for the generally incorrect lithologic term. Also, the formation has been restricted to one principal rock type except where impracticable to do so. The Eureka Tuff, now restricted, consists predominantly of a succession of even bedded rhyodacitic to rhyolitic welded ash-flow tuffs that range in thickness from 0 to locally more than 1,000 feet. The welded tuffs indicate a period of ash-flow eruptions of great magnitude, and have a volume of probably 100 cubic miles or more. The Eureka is an excellent example of Smith's (1960b, p. 158) ash-flow composite sheet.

Burns Formation.—The Burns Formation was originally named for exposures in Burns Gulch northeast of Silverton (Cross and others, 1905, p. 8) and, as defined, consisted of only a few thick flows between conspicuous tuff layers at the bottom and top. The 500-foot-thick type section, however, is not characteristic of the formation as a whole. The Burns Formation as redefined is a heterogeneous and complex accumulation of thin to thick lava flows, breccias, and tuffs associated with local volcanic piles, volcanic domes, and minor welded ash-flow tuffs. About 200 feet of tuffaceous and varved shale and limestone is interlayered with the predominant volcanic rocks in the center of the depression. The formation has a total cumulative thickness of several thousand feet. Except for a local thick rhyolitic mass near the western edge of the depression, the Burns Formation consists of rhyodacitic eruptive materials.

Henson Formation.—The Henson Formation as here defined includes the two upper units of the Silverton Volcanic Series as mapped originally by Cross and others (1907, p. 9). The present formation includes (1) the Henson Tuff, named for exposures in the headwaters of Henson Creek west of Lake City, and (2) the unnamed unit of interbedded lava flows and tuffs provisionally called pyroxene andesite or more recently

Nomenclature of Tertiary volcanic units in the western San Juan Mountains

Telluride quadrangle (Cross and Purington, 1899)	Silverton quadrangle (Cross and others, 1905)	Ouray quadrangle (Cross and others, 1907)	San Juan region (Cross and Larsen, 1935)		San Juan region (Larsen and Cross, 1956)		Western San Juan region [1] (this report)	
Potosi rhyolite series	Potosi volcanic series	Potosi volcanic series	Potosi volcanic series	Piedra rhyolite Huerto andesite Alboroto quartz latite Sheep Mountain andesite Treasure Mountain quartz latite Conejos andesite	Potosi volcanic series	Piedra rhyolite Huerto quartz latite Alboroto rhyolite Sheep Mountain quartz latite Treasure Mountain rhyolite Conejos quartz latite	Potosi Volcanic Group	Sunshine Peak Rhyolite Gilpin Peak Tuff
			Sunshine Peak rhyolite		Sunshine Peak rhyolite			
Intermediate series	Silverton volcanic series	Pyroxene andesite flows and tuffs Burns latite complex Eureka rhyolite Picayune andesite	Silverton volcanic series	Henson tuff Pyroxene andesite Burns latite Eureka rhyolite Picayune andesite	Silverton volcanic series	Henson tuff Pyroxene andesite Burns latite Eureka rhyolite Picayune volcanic group	Silverton volcanic series	Henson tuff Pyroxene-quartz latite Burns quartz latite Eureka rhyolite Picayune quartz latite	Silverton Volcanic Group	Henson Formation Burns Formation Eureka Tuff Picayune Formation
San Juan formation	San Juan tuff	San Juan tuff	San Juan tuff		San Juan tuff		San Juan Formation	

[1] As a result of studies in progress, other new units will be established in the Potosi Volcanic Group. Units that were previously assigned to the Potosi Volcanic Series of former usage will be redefined, restricted, or abandoned.

pyroxene-quartz latite (see table). Tuff beds originally assigned to the Henson tuff actually are interbedded with the lava flows, rather than exclusively overlying them. The tuff beds in all occurrences are identical, and it is impracticable if not impossible to distinguish between them, particularly in belts of complexly faulted and tilted rocks. Moreover, similar or identical tuff beds are found throughout most of the volcanic depression. The entire sequence of eruptive rocks in the Silverton Volcanic Group above the Burns Formation is accordingly assigned to the Henson Formation. Thus defined, the Henson Formation includes andesitic to rhyodacitic tuffs, flows, and breccias, a few local rhyolitic flows and tuffs, and a local quartz latitic welded ash-flow tuff (Luedke and Burbank, 1961). The maximum thickness of the formation is about 1,000 feet.

POTOSI VOLCANIC GROUP

The third and youngest major unit of volcanic rocks in the western San Juan Mountains is the Potosi Volcanic Group, which was named for exposures on Potosi Peak southwest of Ouray (Cross and Purington, 1899, p. 5). From the first description of this sequence of layered volcanic rocks by Cross (1896, p. 229) to the completion of work upon them by Cross and his associates (Larsen and Cross, 1956), the group name and its subdivisions have been extended throughout the San Juan Mountains. Use of the name Potosi here does not imply any specific correlations outside the local occurrences described in this report and covering the type locality of the name.

The Potosi as represented in the area of the Silverton and Lake City calderas is presently divided into two formational units, the Gilpin Peak Tuff and the Sunshine Peak Rhyolite. Both formations consist principally of welded ash-flow tuffs, which possibly could have covered an area of more than 1,000 square miles and had a volume of 200 to 300 cubic miles.

The Gilpin Peak Tuff and Sunshine Peak Rhyolite are related genetically to the development of the Silverton and Lake City calderas, respectively.

Gilpin Peak Tuff.—The Gilpin Peak Tuff was formerly called the Treasure Mountain Quartz Latite (Cross and Larsen, 1935, p. 76–78) and Treasure Mountain Rhyolite (Larsen and Cross, 1956, p. 117–124); the formation is here renamed for a specific sequence of rocks exposed in a 1,400-foot-thick section at Gilpin Peak, near the head of Canyon Creek, about 7 miles

west-southwest of Ouray in the western San Juan Mountains. The former name has been used elsewhere in the San Juan Mountains for similar rocks from other volcanic centers; correlation of these other units with the local Gilpin Peak Tuff is now considered doubtful and without value in working out the complex sequences of local centers.

The Gilpin Peak Tuff so far can be subdivided into 7 mappable units; 6 are moderately crystal-rich welded ash-flow tuffs, and 1 consists of reworked air-fall tuff moderately rich in fossil plant fragments. The units are even bedded and range in thickness from 0 to about 500 feet. The bulk of the rock is probably quartz latite but may range from rhyodacite to rhyolite. The welded tuffs of the Gilpin Peak are an excellent example of Smith's (1960b, p. 158) composite sheet of ash-flow deposits and represent a wide range in local conditions during a complex cooling history, as he suggests.

Sunshine Peak Rhyolite.—The Sunshine Peak Rhyolite was named by Cross and Larsen (1935, p. 67) for the exposures on Sunshine Peak southwest of Lake City, and included both extrusive and intrusive rhyolitic rocks. Parts of the rocks comprising this unit were originally described by Cross (*in* Irving and Bancroft, 1911, p. 30–31) as intrusive rhyolite, locally resembling the Eureka Rhyolite of the Silverton Series. Larsen and Cross (1956, p. 89) later stated that the formation resembles Alboroto rocks of the Potosi Series, and possibly forms a basal part of that unit. However, the Sunshine Peak Rhyolite was not included in the Potosi, owing to its somewhat restricted occurrence and uncertainty of age, but was placed arbitrarily between the Silverton and Potosi Volcanic Series (Larsen and Cross, 1956, p. 88–89). In contrast, we have found that the Sunshine Peak Rhyolite, as shown on their geologic map, is interbedded with and equivalent to their so-called Alboroto rocks southeast of Lake City. We therefore are excluding the name Alboroto in the western San Juan Mountains, using instead a local name, Sunshine Peak Rhyolite, for these deposits, and are placing the Sunshine Peak in the Potosi Volcanic Group. The lithologic term will be retained pending completion of studies in progress.

The Sunshine Peak consists of moderately crystal-rich welded ash-flow tuffs. The rocks have a probable composition ranging from quartz latite to rhyolite. The deposits are even bedded and range in thickness from 0 to a few hundred feet.

REFERENCES

Burbank, W. S., 1930, Revision of geologic structure and stratigraphy in the Ouray district of Colorado, and its bearing on ore deposition: Colorado Sci. Soc. Proc., v. 12, no. 6, p. 151–232.

Cross, Whitman, 1896, Igneous rocks of the Telluride district, Colorado: Colorado Sci. Soc. Proc., v. 5, p. 225–234.

Cross, Whitman, and Larsen, E. S., 1935, A brief review of the geology of the San Juan region of southwestern Colorado: U.S. Geol. Survey Bull. 843, 138 p.

Cross, Whitman, and Purington, C. W., 1899, Description of the Telluride quadrangle [Colorado]: U.S. Geol. Survey Geol. Atlas, Folio 57.

Cross, Whitman, Howe, Ernest, and Irving, J. D., 1907, Description of the Ouray quadrangle [Colorado]: U.S. Geol. Survey Geol. Atlas, Folio 153.

Cross, Whitman, Howe, Ernest, and Ransome, F. L., 1905, Description of the Silverton quadrangle [Colorado]: U.S. Geol. Survey Geol. Atlas, Folio 120.

Irving, J. D., and Bancroft, Howland, 1911, Geology and ore deposits near Lake City, Colorado: U.S. Geol. Survey Bull. 478, 128 p.

Larsen, E. S., Jr., and Cross, Whitman, 1956, Geology and petrology of the San Juan region, southwestern Colorado: U.S. Geol. Survey Prof. Paper 258, 303 p.

Luedke, R. G., and Burbank, W. S., 1961, Central vent ash-flow eruption, western San Juan Mountains, Colorado: Art. 326 in U.S. Geol. Survey Prof. Paper 424–D, p. D94–D96.

Ransome, F. L., 1901, A report on the economic geology of the Silverton quadrangle: U.S. Geol. Survey Bull. 182, 265 p.

Smith, R. L., 1960a, Ash flows: Geol. Soc. America Bull., v. 71, p. 795–842.

———— 1960b, Zones and zonal variations in welded ash flows: U.S. Geol. Survey Prof. Paper 354–F, p. 149–159.

FENTON PASS FORMATION (PLEISTOCENE?), BIGHORN BASIN, WYOMING

By W. L. ROHRER and E. B. LEOPOLD, Denver, Colo.

Abstract.—The Fenton Pass Formation, which is made up of Pleistocene(?) andesitic conglomerate and sandstone, is named for Fenton Pass on Tatman Mountain. Two members of the formation are recognized at the type locality: the lower member, a channel conglomerate that rests unconformably on the Tatman Formation, and the upper member, a flood-plain deposit.

The sequence of andesitic conglomerate and silty sandstone that caps Tatman Mountain near Fenton Pass (fig. 71.1) is here named the Fenton Pass Formation. The conglomerate occurs on both sides of Fenton Pass, which is about 35 miles northwest of Worland. The exposure in the N½SE¼SE¼ sec. 24, T. 50 N., R. 98 W., sixth principal meridian, Park County, Wyo., is designated the type section and is slightly more than 1 mile west of the pass. The Fenton Pass Formation, which is probably Pleistocene in age, unconformably overlies the Tatman Formation of Eocene age. The new name replaces the name Tatman Mountain Gravels, to avoid confusion with the Tatman Formation. A description of the type section follows.

Fenton Pass Formation:

|	*Thickness (feet)*
Sandstone member:	
Sandstone, grayish-brown, fine-grained to very fine grained, silty and clayey; composed mainly of angular grains derived from andesitic rocks but includes scattered rounded pebbles and cobbles; caliche layer at base; calcareous cement, poorly indurated, very porous_____	10
Conglomerate member:	
Conglomerate of well rounded pebbles, cobbles, and boulders; composed mainly of andesite, some quartzite, traces of chalcedony and waterworn pieces of silicified coniferous wood; calcareous cement, well indurated at base; angular unconformity at base__	36
Total thickness of formation_____	46
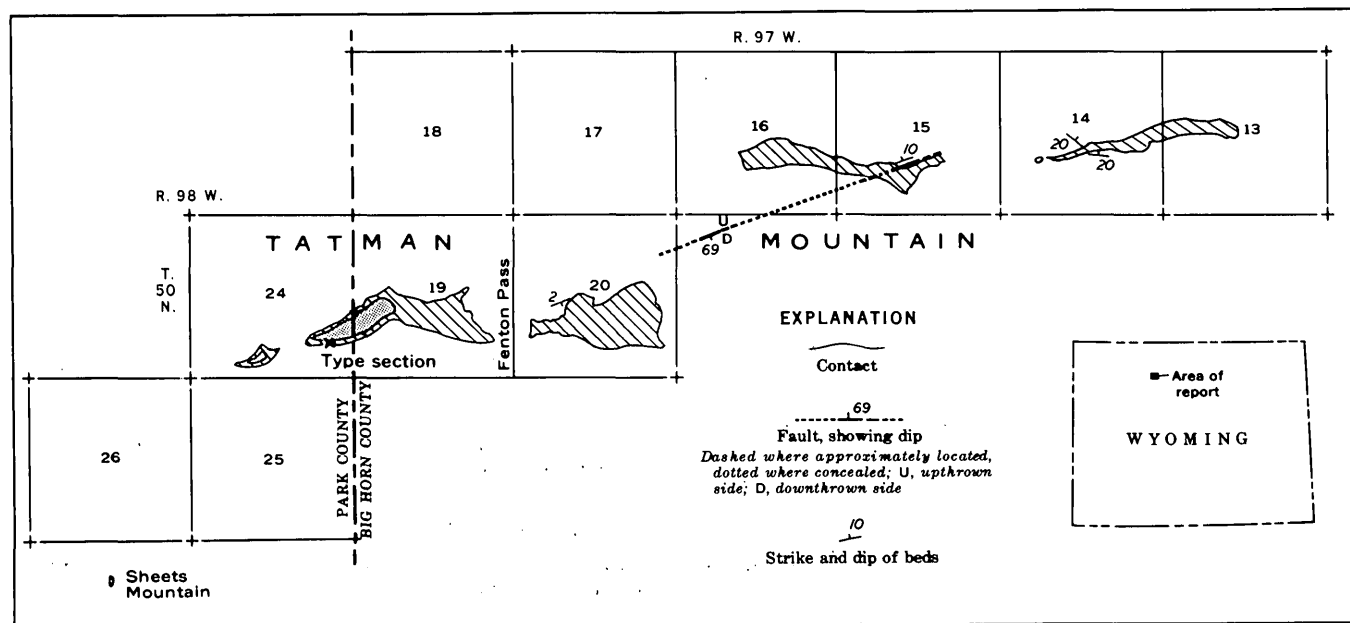
FIGURE 71.1.—Map showing Fenton Pass Formation and location of type section, central Bighorn basin, Wyoming. Sandstone member (shaded); conglomerate member (diagonal pattern).

The silty sandstone of the upper member is here recognized as a distinctive unit in the Fenton Pass Formation, as shown on figure 71.2. Hitherto, the whole formation was referred to as gravels, and the sandstone member at the top was not recognized as a separate unit.

The areal extent of the formation is shown in figure 71.1. Apparently the Fenton Pass Formation is restricted to a broad terrace that is cut in rocks of early Eocene age and is the highest and oldest within the Bighorn basin (Mackin, 1937, p. 866). The rocks lying upon this planed surface were called Quaternary by Fisher (1906), Eocene by Loomis (1907), Oligocene by Sinclair and Granger (1911), Miocene by Alden (1932), post-Miocene by Mackin (1937), Quaternary by Love and others (1955), and Pliocene by Schulte (1961).
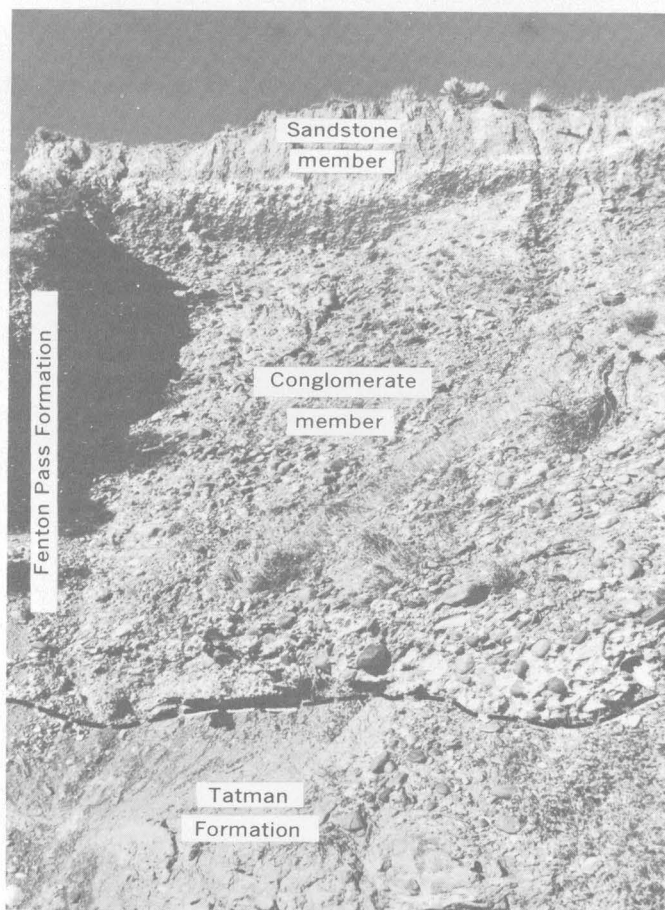

FIGURE 71.2.—Type section of the Fenton Pass Formation, showing lithology and basal unconformity (dashed line).

No megafossils except silicified wood have been observed in the Fenton Pass Formation. Two samples of sandstone from the upper member at the type section were examined for pollen: sample D1909 from 2 feet above the base, and sample D1910 from the caliche layer at the base. Pollen and spore tallies from these samples are listed in the following table.

Pollen and spores of the sandstone member of the Fenton Pass Formation at the type section

[×, form present in the Tatman Formation]

	Fenton Pass Formation		Tatman Formation
	D1909 [1]	D1910 [1]	D1911 [1] D1810 [1]
Group 1. Late Cenozoic pollen forms			
Pinus (pine)	18	33	×
Picea cf. engelmanii (spruce)	1	4	
Ephedra cf. torreyana } (Mormon's tea)	1	------	
Ephedra cf. nevadensis }	2	------	
cf. Juniperus (juniper?)	1	1	
Chenopodiaceae or Amaranthus	57	8	
Sarcobatus vermiculatus (greasewood)	1	------	
Compositae undetermined (sunflower family)	2	4	
cf. Taraxacum	1	------	
Gramineae (grass family)	1	------	
Eriogonum	1	1	
Alnus (alder)	2	------	
cf. Populus	1	------	
Total	89	51	
Minimum percentage of late Cenozoic forms	61.4	42.2	
Group 2. Redeposited pollen (probably all from Eocene Tatman Formation)			
cf. Bignoniaceae	2	------	×
cf. Celtis	1	------	×
Carya (hickory)	1	3	×
Platycarya cf. strobilacea	3	10	×
Betula claripites	1	1	×
Betulapollenites	3	------	×
cf. Podocarpus	1	1	×
cf. Jatropha	1	------	×
Tilia (linden)	1	1	×
cf. Engelhardtia	------	4	×
Monocolpopollenites cf. areolatus	4	------	
Pistillipollenites mcgregorii	2	1	×
Eucommiidites	3	4	×
Tricolporopollenites n. sp	2	------	×
Total	25	25	
Minimum percentage of Eocene forms.	17.2	20.7	
Group 3. Late Cenozoic or redeposited Eocene forms			
Pollen:			
Tsuga (hemlock)	------	1	×
Juglans (walnut)	1	------	×
Ulmus or Zelkova (elm)	2	1	×
Fern spores, algae:			
Polypodiaceae?	8	4	×
Pterospermopsis	1	1	×
Botryococcus	1	1	×
Pediastrum	1	8	×
Undetermined pollen	17	26	
Undetermined spores	------	3	
Total	31	45	
Percentage of forms of uncertain age	21.4	37.1	

[1] USGS paleobotanical localities.

Each sample contained a mixture of Eocene and late Cenozoic forms. The late Cenozoic forms (group 1 of the table) are dominant (61 percent) in sample D1909, but are less abundant (only 42 percent) in sample

D1910. The Eocene forms (group 2) make up 17 percent and 21 percent, respectively, of each sample. The forms considered to be of unequivocal late Cenozoic age have better preserved wall structures than the Eocene pollen and represent genera that grow in the region today. Pollen of the family Compositae noted here have not yet been found in strata older than Miocene and are not common until Pliocene time. The Eocene components are mainly forms known from the underlying Tatman Formation. One of these forms, *Platycarya*, is a tree genus that is now monotypic and limited to Japan and North China; fossil pollen of the genus in this country seems to be limited to the Eocene.

The remaining forms of pollen are listed in group 3 of the table. These forms are found in the Tatman Formation of Eocene age and are also known from younger, late Tertiary strata in the region. Although these forms may possibly be of late Tertiary age, their poor preservation and their known occurrence in the Tatman Formation indicate that they probably belong to the Eocene fraction of this assemblage.

Precautions were taken in the field and laboratory against possible contamination. The pollen is therefore interpreted as a mixture of late Cenozoic and Eocene forms. The presence of Eocene pollen results from reworking of older pollen-bearing sediments. The incorporation of older pollen-bearing sediments in younger deposits is common in the Quaternary of Europe (Iversen, 1936). If the primary pollen in the Fenton Pass Formation is limited to the forms which now occur in the region (group 1), the age of the formation is probably Pleistocene. However, if the tree forms listed in group 3 are in place, the deposit could be Pliocene. The presence of members of the highly evolved family Compositae precludes a pre-Miocene age. The physiographic age, extrapolated from terraces of late Pleistocene age (Moss and Bonini, 1961, p. 550), indicates that the formation can be no older than early Pleistocene.

The lower member of the Fenton Pass Formation rests unconformably upon shales and sandstones of the Tatman Formation, which generally dip southward about 50 feet per mile. Adjacent to faults the dip may be reversed. Locally a sharp angular relation is present, as shown in figure 71.3. Gentle ridges and swales, which are oriented N. 45°–60° E. and which represent flood-plain irregularities, remain on the surface of the upper member.
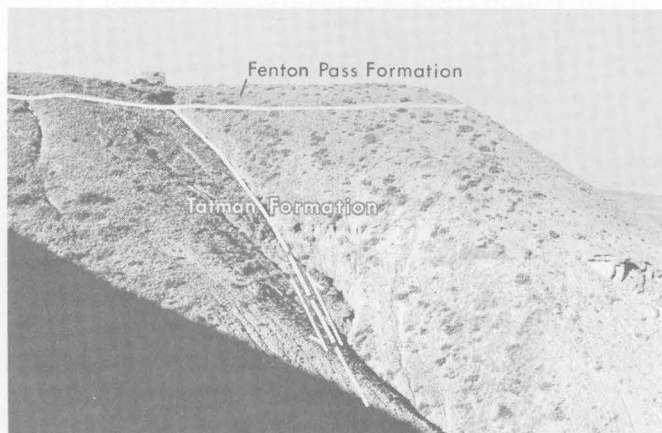
FIGURE 71.3.—Faulting in the Tatman Formation. The normal fault offsetting Tatman strata occurred before deposition of the Fenton Pass Formation. Maximum displacement along the fault is about 250 feet. The angle of view relative to the fault trace makes the fault appear to be a reverse fault. Dip of sandstone at right edge of picture is 10° N.

The following brief summary of the geologic history of the Fenton Pass Formation is based on data presented by previous investigators as well as data collected by us. Some time after the early Eocene, probably during the Miocene, the Tatman Formation was faulted in the central part of the Bighorn basin, resulting in the development of adjacent minor folds. The start of the present erosional cycle may be genetically related to the deformation. Eventually, the folded and faulted strata of the Tatman Formation were truncated by an eastward-flowing stream which had a gradient of about 40 feet per mile in the Tatman Mountain area. Deposition of the conglomerate and sandstone members of the Fenton Pass Formation accompanied the cutting of this surface of unconformity during the early Pleistocene.

Correlatives of the Fenton Pass Formation are uncertain. The upper part of the Cypress Hills Gravels has been tentatively correlated with the gravel on Tatman Mountain (Mackin, 1937, p. 869). The Flaxville Formation, which has a late Miocene or early Pliocene fauna except for a Camelops tooth of probable Pleistocene age (Mackin, 1937, p. 871), may also be a correlative if the exception is valid. Study of pollen in the units may yield a more definite answer to the correlation.

REFERENCES

Alden, W. C., 1932, Physiography and glacial geology of eastern Montana and adjacent areas: U.S. Geol. Survey Prof. Paper 174, 133 p.

Fisher, C. A., 1906, Geology and water resources of the Bighorn basin, Wyoming: U.S. Geol. Survey Prof. Paper 53, 72 p.

Iversen, Johanes, 1936, Sekundäres Pollen als Fehlerquelle: Danmarks geol. Undersogelse, raekpe IV, no. 15, p. 3–24.

Loomis, F. B., 1907, Origin of the Wasatch deposits: Am. Jour. Sci., 4th ser., v. 23, art. 34, p. 356–364.

Love, J. D., Weitz, J. L., and Hose, R. K., 1955, Geologic map of Wyoming: U.S. Geol. Survey.

Mackin, J. H., 1937, Erosional history of the Big Horn basin, Wyoming: Geol. Soc. America Bull., v. 48, no. 6, p. 813–893.

Moss, J. H., and Bonini, W. E., 1961, Seismic evidence supporting a new interpretation of the Cody terrace near Cody, Wyoming: Geol. Soc. America Bull., v. 72, no. 4, p. 547–555.

Schulte, J. J., 1961, Highlights of Cenozoic geologic history of the Big Horn Canyon region, Montana and Wyoming in Billings Geol. Soc. Guidebook 12th Ann. Field Conf., Float trip, Big Horn River from Kane, Wyo., to Yellowtail Dam site, June 1961: table 1, p. 16–17.

Sinclair, W. J., and Granger, Walter, 1911, Eocene and Oligocene of the Wind River and Big Horn basins, Wyoming: Am. Mus. Nat. History Bull., v. 30, art. 7, p. 83–117.

NUSSBAUM ALLUVIUM OF PLEISTOCENE(?) AGE AT PUEBLO, COLORADO

By GLENN R. SCOTT, Denver, Colo.

Abstract.—The Nussbaum Formation at Pueblo, Colo., is re-designated Nussbaum Alluvium because of its fluviatile origin. The age, which has been considered Pliocene(?), is changed to Pleistocene(?) because of the geomorphic and stratigraphic relation of the Nussbaum with known Pleistocene and Pliocene deposits, and because of the resemblance and sequential relation of the formation to adjacent Pleistocene alluvium.

The Nussbaum Formation was named by Gilbert (1897) for its outcrop on Baculite Mesa (fig. 72.1) in the Pueblo quadrangle and was assigned by him to the "Neocene epoch." Hills (1889) subsequently assigned the Nussbaum to late "Neocene," and later, Stose (1912) changed the age to Pliocene(?), where it has been placed until now. This article shows that the age is early Pleistocene and changes the name to alluvium to emphasize the fluviatile origin of the formation. In the ensuing discussion the extent of the Nussbaum is limited to the type locality at Baculite Mesa. Acknowledgment is made to J. H. Irwin, H. E. McGovern, and W. G. Weist, Jr., U.S. Geological Survey, who supplied information on the Ogallala Formation and surficial deposits east of Pueblo, Colo.

From 1896 to 1912 the name Nussbaum Formation was widely applied to small deposits of high-level gravel on the High Plains in southeastern Colorado. The deposits thus named are now known to embrace a wide range of ages. In 1924 the formation was considered by the Colorado Geological Survey (Toepelman, 1924) to be synonymous with the Arikaree Sandstone (Miocene) and the Ogallala Formation (upper Mio-
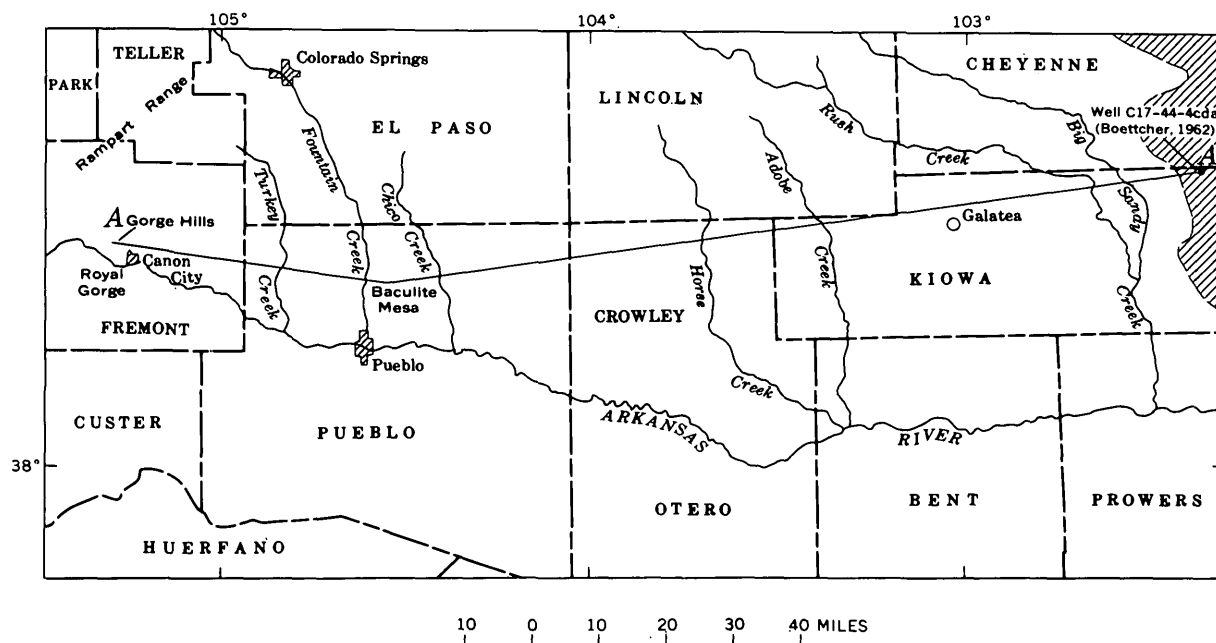

FIGURE 72.1.—Index map showing Baculite Mesa and location of profile *A–A'* of figure 72.2. Known Ogallala Formation crosshatched in northeast corner.

cene and Pliocene(?)). As a result of this extension of usage the formation came to include deposits of gravel, both consolidated and unconsolidated, that ranged from Miocene to Kansan in age. Burbank and others (1935) listed the Arikaree, Ogallala, and Nussbaum Formations as separate units on the geologic map of Colorado, but implied, by juxtaposing the latter two units, that the Nussbaum was partly equivalent to the Ogallala Formation. This intent seems certain because they included in the Ogallala Formation some outcrops that previously had been designated as Nussbaum. Some of these outcrops are still considered to be Ogallala Formation, but others now are known to be of Pleistocene age.

The identification of most of the outcrops that have been mapped as Nussbaum in southeastern Colorado and most of the area mapped as Ogallala between Big Sandy Creek and the Arkansas River should be viewed with skepticism (Elkin, 1958, p. 9). Probably most of these outcrops or areas eventually will have to be reassigned to other formations.

DESCRIPTION

The Nussbaum at its type locality is a stream-laid deposit of loose coarse sand, as much as 100 feet thick, that contains pebbles. Near the top it contains a layer of pebbly silt more than 10 feet thick. This silt layer resembles layers of locally derived silt containing pieces of limestone that lie in the upper part of the Slocum, Louviers, and Broadway Alluviums (see table) near Pueblo. The Nussbaum Alluvium is composed chiefly of fragments of granite and hard sedimentary rocks. The major part of the alluvium is lacking in caliche; however, the basal 2 to 4 feet of alluvium is commonly cemented by calcium carbonate to hard conglomerate or coarse sandstone. The cement probably was precipitated by ground water that contained calcium bicarbonate derived from the leaching of underlying Cretaceous rocks.

No fossils from the Nussbaum have been identified despite searches by G. K. Gilbert, G. W. Stose, G. E. Lewis, and many others. Two bones have been found in a gravel pit operated by the city of Pueblo at the south end of Baculite Mesa. One bone was lost, and a large bone left lying in the pit overnight slaked beyond recognition by morning. It is noteworthy, however, that neither of these bones was permineralized, as is characteristic of many bones from the Ogallala Formation.

The Nussbaum caps Baculite Mesa at the type locality, northeast of Pueblo, where it unconformably overlies the Pierre Shale (Upper Cretaceous) on a well-formed erosion surface. The erosion surface slopes 30 feet per mile to the south and 20 feet per mile to the east.

The gradient of this surface and the lithology of fragments in the Nussbaum suggest that the streams that deposited the alluvium flowed southeastward from an area of weathered Pikes Peak Granite (Precambrian) near Turkey Creek on the southeast flank of the Rampart Range. The location of the ancestral Arkansas River into which the above streams flowed is unknown. As indicated by the position of high-level terraces south of the present river, on which gravel brought in from the west by the Arkansas is now perched, the ancestral Arkansas River must have flowed about 5 miles south of the modern river.

The extent of deposits truly equivalent to Nussbaum Alluvium as redefined here is unknown because very few of the outcrops previously mapped as Nussbaum have been restudied. Outcrops of high-level gravel that have been mapped as Nussbaum are scattered throughout the area from the Arkansas River south to New Mexico and from the Rocky Mountain front east to Baca County, Colo. Most of these outcrops are no longer considered to be equivalent to the Nussbaum Alluvium and some have been reassigned to other formations. For examples of such changes compare Levings (1951), Harbour and Dixon (1956), Burbank and others (1935), and McLaughlin (1954) with earlier maps that showed outcrops of Nussbaum.

EVIDENCE FOR A CHANGE IN AGE

A Pleistocene age for the Nussbaum has been suggested by Hills (1899, 1900, and 1901), Tator (1952, p. 273), and Mitchell and others (1956, p. 134). The Pleistocene age was preferred by them because the alluvium is lithologically like other Pleistocene alluvium and lies at a topographic level comparable to that of other Pleistocene alluvium.

Refutation of a Pliocene(?) age, which has been used for the Nussbaum, requires that the correlation of the Nussbaum with the Ogallala Formation be disproved. Evidence to disprove this correlation is based on the lithologic dissimilarity of the two deposits and their topographic disparity.

The most significant ways in which the Nussbaum and the Ogallala differ are as follows: The Nussbaum is for the most part a uniform coarse sand containing small pebbles; the Ogallala characteristically is poorly sorted and consists of calcareous clay, sand, gravel, and fresh-water limestone. The coarse sediments in the Nussbaum are unconsolidated except for the basal conglomerate; the coarse sediments in the Ogallala commonly are firmly cemented and contain hard layers of caliche, called mortar beds, more than 50 feet thick (Boettcher, 1962, p. 14). The Nussbaum contains a thick diffuse layer of calcium carbonate near its top, which presumably formed as a pre-Wisconsin soil; the

Ogallala has a thick hard caprock of calcium carbonate at the top. The Nussbaum is only 100 feet thick; the Ogallala is nearly 400 feet thick east of Big Sandy Creek (Boettcher, 1962, p. 12) and locally is 200 feet thick near the mountains at Raton Mesa (Levings, 1951, p. 23). These distinct differences can hardly be the result of facies differences within the Ogallala, for the Ogallala is characterized by mortar beds and the other features listed above wherever it has been described in southeastern Colorado.

Two profiles (fig. 72.2) were drawn to determine topographic relations of the Nussbaum and the Ogallala Formation. A lower profile was constructed along a line from the mountain front at Canon City, Colo., to southwest of Big Sandy Creek, near Galatea, across the highest outcrops of Pleistocene high-level gravel, including the Nussbaum Alluvium at Baculite Mesa. A higher one was drawn from a well-defined pre-Pleistocene (Rocky Mountain?) erosion surface in the Royal Gorge area west of Canon City to water well C17–44–4cda (Boettcher, 1962, p. 9) in known Ogallala deposits east of Big Sandy Creek. The two profiles converge somewhat toward the east. The higher profile, which shows the inferred original level of the Ogallala Forma-

tion, is more than 500 feet above the Nussbaum Alluvium at Baculite Mesa and more than 250 feet above lower Pleistocene alluvium near Galatea.

The geomorphic history of the upper Tertiary and Quaternary deposits further supports differentiation of the Nussbaum and the Ogallala, and placement of the Nussbaum in the Pleistocene. The Nussbaum Alluvium at Baculite Mesa lies only 100 feet above the uppermost of a sequence of deposits of Pleistocene and Recent age and is nearly identical in lithology to the later deposits. The age and height above modern stream level of successive deposits younger than the Nussbaum are listed in the table, which suggests that the Nussbaum is the earliest of a closely spaced sequence of alluvial deposits. Evidence (Scott, 1963) from the Denver area shows that a great erosional hiatus separated this sequence from the earlier Ogallala Formation. Near Denver the Rocky Mountain (Pliocene and Miocene) surface, which underlies the Ogallala Formation (Lee, 1922, p. 15–17), is 2,000 feet above modern streams (Scott, 1963), whereas the oldest of a sequence of Pleistocene deposits, which probably is equivalent to the Nussbaum Alluvium, lies only 450 feet above modern streams. The cutting of canyons more than 1,500 feet
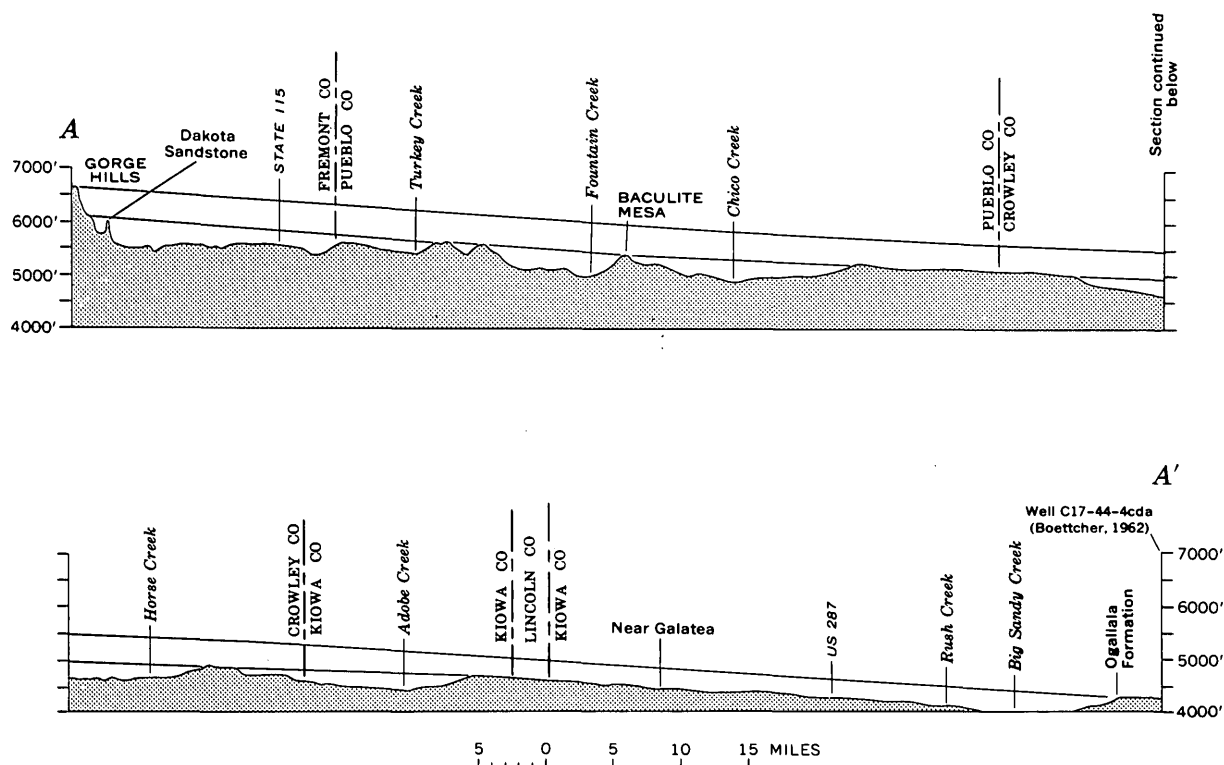
FIGURE 72.2.—Probable profiles of deposition in Nussbaum time and Ogallala time. Lower profile drawn across outcrops possibly equivalent to the Nussbaum Alluvium from Canon City, Colo., to near Galatea. Upper profile drawn from a low pre-Pleistocene (Pliocene?) erosion surface near Royal Gorge to inferred original level of Ogallala Formation above the Nussbaum Alluvium at Baculite Mesa, and on to the Ogallala Formation east of Big Sandy Creek.

Quaternary alluvium exposed near Pueblo, Colorado

System	Series	Glaciation	Stage	Alluvium	Height of surface above modern stream (feet)
Quaternary	Recent		Late	Post-Piney Creek	0–10
				Piney Creek	20
	Pleistocene	Wisconsin	Late	Broadway	40
			Early	Louviers	70–80
		Sangamon or Illinoian		Slocum	110–120
		Yarmouth or Kansan		Verdos	200–220
		Aftonian or Nebraskan		Rocky Flats	250–260
	Pleistocene(?)			Nussbaum	320–360

deep probably required all of late Pliocene time. The advent of a closely spaced sequence of nearly identical alluvial deposits suggests that conditions of deposition changed after the hiatus and then remained much the same during deposition of the alluvial sequence. I believe that this change marked the onset of Pleistocene time and that the Nussbaum is the earliest Pleistocene alluvium.

REFERENCES

Boettcher, A. J., 1962, Records, logs, and water-level measurements of selected wells and test holes and chemical analyses of ground water in eastern Cheyenne and Kiowa Counties, Colorado: Colorado Water Conserv. Board Basic-Data Rept. 13, 18 p.

Burbank, W. S., Lovering, T. S., Goddard, E. N., and Eckel, E. B., 1935, Geologic may of Colorado: U.S. Geol. Survey.

Elkin, A. D., 1958, Geology of eastern Elbert County, Colorado, in relation to soil development: U.S. Dept. Agriculture Soil Conserv. Service, 17 p.

Gilbert, G. K., 1897, Description of the Pueblo quadrangle [Colorado]: U.S. Geol. Survey Geol. Atlas, Folio 36.

Harbour, R. L., and Dixon, G. H., 1956, Geology of the Trinidad-Aguilar areas, Las Animas and Huerfano Counties, Colorado: U.S. Geol. Survey Oil and Gas Inv. Map OM–174.

Hills, R. C., 1899, Description of the Elmoro quadrangle [Colorado]: U.S. Geol. Survey Geol. Atlas, Folio 58.

—— 1900, Description of the Walsenburg quadrangle [Colorado]: U.S. Geol. Survey Geol. Atlas, Folio 68.

—— 1901, Description of the Spanish Peaks quadrangle [Colorado]: U.S. Geol. Survey Geol. Atlas, Folio 71.

Lee, W. T., 1922, Peneplains of the Front Range and Rocky Mountain National Park, Colorado: U.S. Geol. Survey Bull. 730–A, p. 1–17.

Levings, W. S., 1951, Late Cenozoic erosional history of the Raton Mesa region [Colorado–New Mexico]: Colorado School Mines Quart., v. 46, no. 3, 111 p.

McLaughlin, T. G., 1954, Geology and ground-water resources of Baca County, Colorado: U.S. Geol. Survey Water-Supply Paper 1256, 232 p. [1955]

Mitchell, J. G., Greene, John, and Gould, D. B., 1956, Catalog of stratigraphic names used in Raton Basin and vicinity [Colorado-New Mexico], in Rocky Mountain Association of Geologists, Guidebook 1956: p. 131–135.

Scott, G. R., 1963, Quaternary geology and geomorphic history of the Kassler quadrangle, Colorado: U.S. Geol. Survey Prof. Paper 421–A, 70 p.

Stose, G. W., 1912, Description of the Apishapa quadrangle [Colorado]: U.S. Geol. Survey Geol. Atlas, Folio 186.

Tator, B. A., 1952, Piedmont interstream surfaces of the Colorado Springs region, Colorado: Geol. Soc. America Bull., v. 63, no. 3, p. 255–274.

Toepelman, W. C., 1924, Preliminary notes on the revision of the geological map of eastern Colorado: Colorado Geol. Survey Bull. 20, 21 p.

AGE OF THE MURRAY SHALE AND HESSE QUARTZITE
# ON CHILHOWEE MOUNTAIN, BLOUNT COUNTY, TENNESSEE

By R. A. LAURENCE and A. R. PALMER, Knoxville, Tenn.,
and Washington, D.C.

Abstract.—Well-preserved specimens of *Indiana tennesseensis* (Resser) have been discovered in place in the lower part of the Murray Shale. They show that the age of the Murray Shale and the overlying Hesse Quartzite should now be considered as definite, rather than questionable, Early Cambrian.

The discovery of well-preserved fossils in the lower part of the Murray Shale at Murray Gap, on Chilhowee Mountain, Blount County, Tenn., indicates an Early Cambrian age for the Murray Shale and the overlying Hesse Quartzite. These two formations were previously considered to be Early Cambrian(?) because of the uncertainty as to the location of the site and the stratigraphic position of the collections reported by Walcott (1890, p. 536–537, 588) and Keith (1895, p. 3).

Roadcuts on the newly constructed Foothills Parkway and a county access road at and near Murray Gap in 1962 exposed much of the 350-foot thickness of the Murray Shale (fig. 73.1). The Murray may be divided into three units of approximately equal thickness: a lower unit consisting of bluish-gray noncalcareous shale with scattered quartz grains and muscovite flakes up to about 1 mm across and occasional biotite flakes and glauconite grains; a middle unit which is principally a dark-gray muscovite-bearing fine siltstone and which, when weathered, yields buff chips similar to the weathered shale of the bottom unit; and an upper unit consisting of siltstone, shale, and fine-grained sandstone with many glauconitic layers.

Identifiable fossils were found only in the bottom unit, from about 20 to 60 feet above the top of the underlying Nebo Quartzite. The two upper units yielded only numerous fossil tracks and trails. No fossils were found in the older Nichols Shale, which is separated from the lithologically similar lower unit of the Murray by 300 feet of Nebo Quartzite (Neuman and Wilson, 1960).

EXPLANATION

Contact	Thrust fault	Fault
	Barbs on upper plate	*Approximately located*
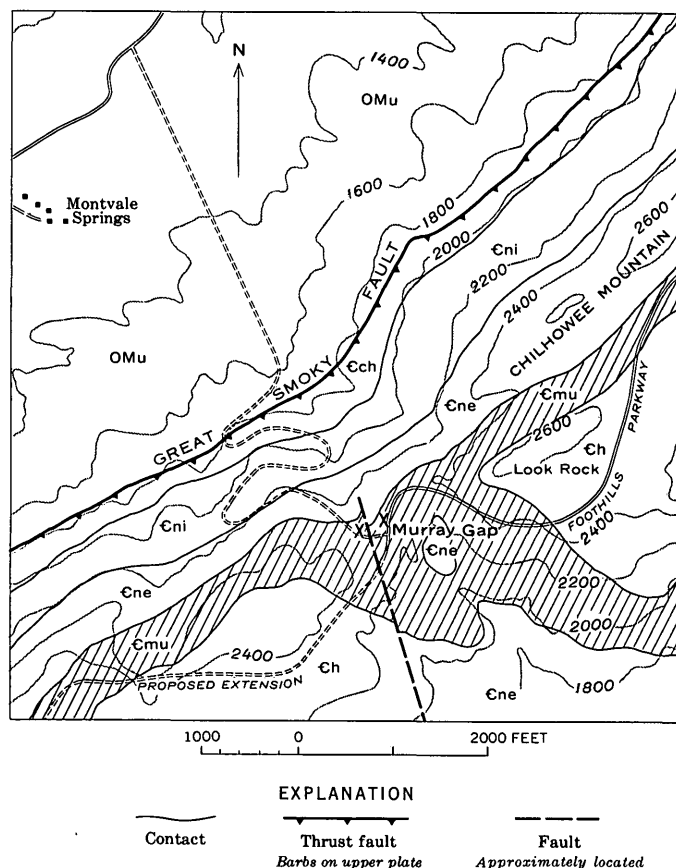
FIGURE 73.1—Map showing fossil localities and distribution of rocks of Chilhowee Group in the vicinity of Murray Gap, Chilhowee Mountain, Tenn. Geologic units, youngest to oldest: OMu, post-Cambrian rocks; €h, Hesse Quartzite; €mu, Murray Shale; €ne, Nebo Quartzite; €ni, Nichols Shale; €ch, Cochran Formation. Fossil localities indicated by X, Base from Blockhouse quadrangle; geology modified from Neuman and Wilson (1960). Contour interval 200 feet.

ART. 73 *IN* U.S. GEOL. SURVEY PROF. PAPER 475-C, PAGES C53–C54. 1963.

C53

The critical fossil in dating the Murray Shale, and the only fossil present other than problematic tubular structures and trails, is a large ostracode identified as *Indiana tennesseensis* (Resser). Species of *Indiana* are known from Lower Cambrian beds in eastern and western North America, and in western Europe. Although the specimens from the Murray Shale are not associated with trilobite remains, they are here assigned to the Lower Cambrian because of the occurrence of the genus elsewhere in Lower Cambrian beds and the absence of any known fossils with a mineralized carapace in beds of undoubted Precambrian age.

The specimens of *I. tennesseensis* described by Resser (1938) were collected by Walcott and Keith in 1893 from the "Upper shales of Chilhowee, Tenn." according to data placed in the locality file of the U.S. National Museum in 1927. Resser assigned them to "Lower Cambrian? Antietam?" in 1938, apparently questioning the stratigraphic occurrence because the specimens did not look like any Lower Cambrian fossils known to him. The discovery of these specimens in place and well down in the Chilhowee Group leaves no doubt about their stratigraphic occurrence. Both the lithology of the enclosing rock and the morphologic details of specimens in Walcott's original collection are the same as those of the specimens collected in 1962. The more recently collected specimens of the *I. tennesseensis* are better preserved than the type material; the species is redescribed below.

Genus INDIANA Matthew, 1902

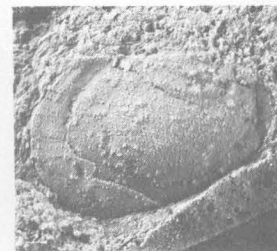#### Indiana tennesseensis (Resser)

Figures 73.2A, 73.2B

Indianites tennesseensis Resser, 1938, p. 107, pl. 3, fig. 47.

Description.—Carapace inequilateral, leperditiform, thin, apparently only weakly calcified. Valves equal in size, length up to 10 mm. Hinge straight, simple; length about eight-tenths length of valve; both anterior and posterior ends terminate in acute cardinal angles. Greatest height posterior to midlength; height beneath anterior end of hinge about two-thirds greatest height. Posterior end of valve with strong posterior swing so that most posterior point is well behind end of hinge. Anterior end barely produced in front of hinge end.

External surface without nodes or ridges, but many valves have a distinct, shallow groove paralleling free margin at a distance about four-fifths maximum height of valve. Both valves evenly covered with close-spaced fine papillae.

FIGURE 73.2.—*Indiana tennesseensis* (Resser). *A*, Left valve, USNM 143799. *B*, Right valve, USNM 143800. Both specimens ×5, from USGS collections 3796–CO and 3911–CO, respectively, Murray Gap, Chilhowee Mountain, Tenn.

Discussion.—All the specimens of *I. tennesseensis* are crushed to some degree, but about 20 valves are reasonably complete and form the basis for the description given above. The best specimens are illustrated. This material is much superior to specimens in the older collection. The holotype (USNM 94759), however, shows the papillate surface and groove paralleling the free margin that characterize the specimens described and illustrated here. These characteristics distinguish *I. tennesseensis* from all other species assigned to *Indiana*. The only other described Cambrian ostracode with a papillate surface is *Cambria sibirica* (Neckaja and Ivanova, 1956), from the Lower Cambrian of Siberia. This species also has an outline similar to that of *I. tennesseensis*, but differs by having prominent ridges on the valves and a reportedly sinuous hinge line.

Lower Cambrian ostracodes are so rare that an adequate classification at the generic level is not possible. The change in generic assignment of *I. tennesseensis* from *Indianites* to *Indiana* results from the genera being based on the same type species and not on any reevaluation of the characteristics or content of *Indiana*.

REFERENCES

Keith, Arthur, 1895, Description of the Knoxville sheet (Tennessee and North Carolina): U.S. Geol. Survey Geol. Atlas, Folio 16, 6 p.

Neckaja, A. I., and Ivanova, V. A., 1956, First discovery of an ostracode from the Lower Cambrian of eastern Siberia: Doklady Akad. Nauk SSSR, 111, no. 5, p. 1095–1097 [in Russian].

Neuman, R. B., and Wilson, R. L., 1960, Geology of the Blockhouse quadrangle, Tennessee: U.S. Geol. Survey Geol. Quad. Map GQ–131 [1961].

Resser, C. E., 1938, Cambrian system (restricted) of the southern Appalachians: Geol. Soc. America Spec. Paper 15, 140 p.

Walcott, C. D., 1890, The fauna of the Lower Cambrian, or *Olenellus* zone: U.S. Geol. Survey 10th Ann. Rept., pt. 1, p. 509–763.

CONODONTS FROM THE FLYNN CREEK CRYPTOEXPLOSIVE STRUCTURE, TENNESSEE

By JOHN W. HUDDLE, Washington, D.C.

Abstract.—A limestone breccia in the base of the Chattanooga Shale in the crater of the Flynn Creek cryptoexplosive structure, about 5 miles south of Gainesboro, Tenn., contains a mixture of early Late Devonian and Ordovician conodonts. The age of the breccia is early Late Devonian, and the well-preserved Ordovician conodonts in the samples probably include reworked specimens in the matrix and specimens from pebble-size fragments in the breccia. Most of the Ordovician conodonts probably came from the Leipers and Catheys Limestones.

The Flynn Creek cryptoexplosive structure lies about 5 miles south of Gainesboro, Tenn. (fig. 74.1). It is about 2 miles in diameter, slightly elliptical, and at least 170 feet deep. The structure was described by Wilson and Born (1936), and the stratigraphy of the Chattanooga Shale by Conrad and others (1957) and Conant and Swanson (1961). The following discussion is based on these reports.

The oldest rocks exposed in the crater are jumbled blocks of Middle and Upper Ordovician limestone (fig. 74.2). These formations lie in normal stratigraphic sequence immediately outside the disturbed area. Overlying the jumbled blocks of Ordovician limestone is a sedimentary breccia called "bedded breccia" by Wilson and Born (1936, p. 821) and "fresh water limestone" by Conrad and others (1957, p. 16). Conant and Swanson (1961, p. 11) established that the bedded breccia is a marine basal unit of the Chattanooga Shale.

This assignment was based on conodonts identified by W. H. Hass. Conant and Swanson (1961, p. 23, 25) showed that the basal sandstone of the Chattanooga Shale varies with the character of the underlying rock, and they considered the bedded breccia to be an expectable variant of the basal sandstone in the Chattanooga Shale. Overlying the bedded breccia is a greatly overthickened lower (Dowelltown) member of the Chattanooga Shale which fills the crater. The upper (Gassaway) member of the Chattanooga Shale extends across the crater with normal thickness.

The bedded breccia (fig. 74.3) grades from a basal coarse-grained unit up into a fine-grained laminated sandy limestone unit. The lower part consists of more or less rounded fragments of Ordovician limestone as much as 4 inches in diameter that rest in a matrix composed mainly of fine-grained to very fine grained dolomitic limestone. This rock lies with sharp contact on more angular, chaotic, and unbedded breccia of Ordovician limestone. The entire unit is 15 feet thick at one locality but is absent in others.

The age of the bedded breccia is important in dating the explosion, as the breccia is the oldest unit not involved in the Flynn Creek structure. Fauna consists of a mixture of Devonian and Ordovician species of conodonts. A study of the fauna was undertaken to see if any part of the bedded breccia is Ordovician in age
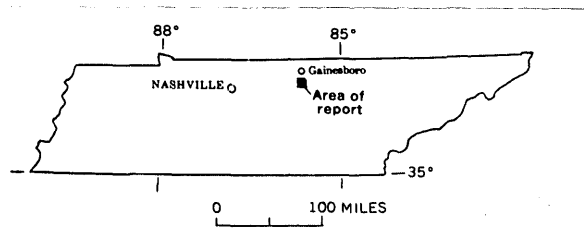

FIGURE 74.1—Map of Tennessee, showing location of the Flynn Creek cryptoexplosive structure.
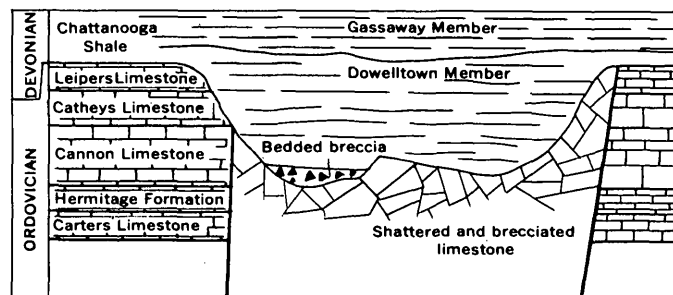

FIGURE 74.2.—Diagrammatic section, showing the Flynn Creek structure after Chattanooga Shale deposition (not to scale).
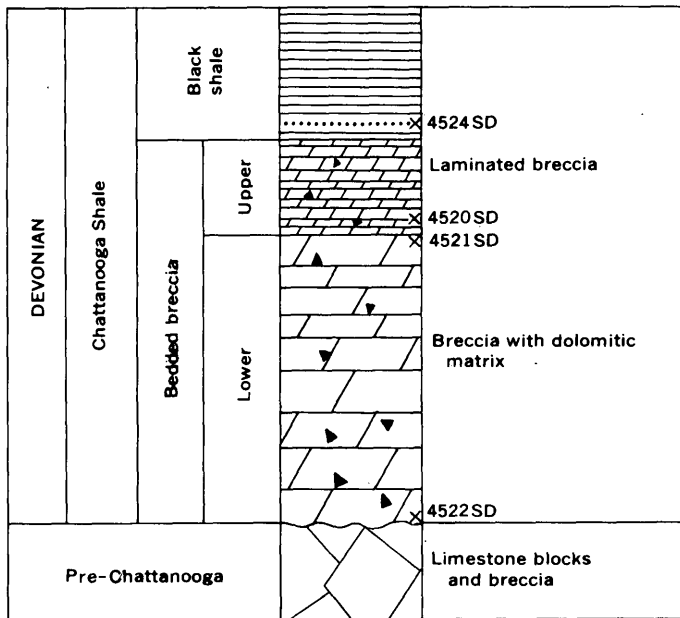
FIGURE 74.3.—Generalized section of the lower part of the Chattanooga Shale, showing the stratigraphic position of collections. (Exact position of 4523SD unknown).

and whether or not any of the conodonts present suggest the former presence of pre-Chattanooga, post-Leipers formations in the area of the crater.

Conodonts were collected from the bedded breccia by W. H. Hass on November 14, 1958, with the help of L. C. Conant, R. A. Laurence, S. H. Maher, H. C. Milhous, R. G. Stearns, and C. W. Wilson, Jr. Hass made preliminary identification of the conodonts and plans for this paper before he died in 1959. His identifications were checked, and additional material was studied by the writer, who prepared this article from Hass' notes and from the literature cited. The conodonts identified are listed in the accompanying table.

Conodonts identified from the Flynn Creek cryptoexplosive structure, Tennessee

[Numbers in table are number of specimens identified from each locality; numbers in notes at end of table are USGS collection numbers]

Species	1	2	3	4	5
Devonian species					
Ancyrodella rotundiloba (Bryant)	86	18	6	3	52
Bryantodus radiatus (Bryant)	21	3			6
Euprioniodina prona Huddle		1			
Hibbardella sp	5				
Hindeodella sp	5				
Icriodus sp	7				
Ligonodina sp	8				
Neoprioniodus alatus (Hinde)	5				9
Ozarkodina sp		1			
Palmatolepis (fragments)	1		2		6
Polygnathellus collingatus Ulrich and Bassler	11				9
Polygnathus alata Huddle	1				2
Polygnathus caelata Bryant	5	1			

Conodonts identified from the Flynn Creek cryptoexplosive structure, Tennessee—Continued

[Numbers in table are number of specimens identified from each locality; numbers in notes at end of table are USGS collection numbers]

Species	1	2	3	4	5
Devonian species—Continued					
Polygnathus cristata Hinde	4				
Polygnathus foliata Bryant		1			8
Polygnathus linguliformis Hinde	36	6	3	6	29
Polygnathus ordinata Bryant	40	13	5	4	60
Polygnathus pennata Hinde	102	6	2	11	92
Polygnathus n. sp	10				
Polygnathus n. sp	1				
Polygnathus n. sp	5				
Prioniodina n. sp	2	3			
Prioniodina n. sp	7				
Ordovician species					
Aphelognathus sp	43	16	24	30	
Cordylodus sp	18	8	6	19	
Drepanodus sp		1			
Drepanodus cf. *D. subrectus* (Branson and Mehl)		1			
Eoligonodina cf. *E. flexuosus* (Branson and Mehl)			11	5	
Eoligonodina cf. *E. richmondensis* Branson, Mehl, and Branson	33	8	12		
Eoligonodina cf. *robusta* Branson, Mehl, and Branson	1				
Microcoleodus panderi? Branson, Mehl, and Branson	2				
Oistodus cf. *O. abundans* Branson and Mehl			4		
Oistodus cf. *O. inclinatus* Branson and Mehl	6				
Panderodus cf. *P. gracilis* (Branson and Mehl)	3			2	
Polycaulodus sp	2				
Prioniodina oregonia Branson, Mehl, and Branson	15	5	6		
Prioniodina sp	2				
Rhipidognathus cf. *R. curvata* Branson, Mehl, and Branson			2		
Rhipidognathus cf. *R. paucidentata* Branson, Mehl, and Branson	1	1		2	
Rhipidognathus cf. *R. symmetrica* Branson, Mehl, and Branson	9			11	
Rhipidognathus fragments		1	11		
Trichonodella cf. *T. nitida* Branson, Mehl, and Branson	2	2	15		
Trichonodella cf. *T. undulata* Branson, Mehl, and Branson	9	2		7	
Trichonodella sp				2	
Zygognathus cf. *Z. pyramidalis* Branson, Mehl, and Branson	20	8	13	3	
Zygognathus sp			7	1	

1. 4520SD; road cut at mouth of Cub Hollow opposite Antioch School, Gainesboro quadrangle, Tennessee; base of upper laminated part of bedded breccia 4–5 feet below lowest black shale in Chattanooga Shale.
2. 4521SD; same locality as 4520SD; bedded breccia 5.7–6.2 feet below lowest black shale in the Chattanooga Shale.
3. 4522SD; same locality as 4520SD; base of bedded breccia 14.5–15.0 feet below lowest black shale in the Chattanooga Shale.
4. 4523SD; road cut at mouth of Steam Mill Hollow, 4,000 feet west of Antioch School, Gainesboro quadrangle, Tennessee; bedded breccia.
5. 4524SD; Flynn Creek, about 100 feet north of road near mouth of Lacy Branch, Gainesboro quadrangle, Tennessee; sandstone, 0.2 feet thick, 0.25 feet above base of lowest black shale in the Chattanooga Shale.

Many unidentifiable fragments of conodonts were found in addition to the species listed in the table. A few of the specimens are nearly whole, but most are broken. They are fresh, unworn, and, except for breakage, show no evidence of reworking. Some specimens, mainly Devonian ones, are slightly weathered. Nearly complete specimens are more common in the Devonian species than in the Ordovician. However, this may be due to the fact that the Devonian species are stronger and heavier than those from the Ordovician. Many unidentifiable fragments can be classed as probably Devonian or Ordovician on the basis of thickness of the bar, blade, or plate. In general, the Ordovician conodonts have light, slender bars and expanded thin-walled basal cavities.

All the Devonian species found in the bedded breccia are also found in the Genesee Formation of Middle and Late Devonian age, and most of them are found in the Genundewa Limestone Member of the Genesee Formation in New York. The list of species in the table is somewhat longer than that given by Hass (1956) for the basal sandstone of the Chattanooga Shale, but his age determination is confirmed. The new species of *Polygnathus* and *Prioniodina* listed here are identical with species that are abundant in the Genesee Formation. Devonian species of conodonts occur throughout the bedded breccia but are most abundant in the base of the laminated part of the bedded breccia at locality 4520SD at Antioch School. Only one specimen of *Ancyrodella rotundiloba* was found in the upper 2½ feet of laminated breccia. All the species that are abundant in the bedded breccia are also found in the lower part of the black shale at locality 4524SD.

Ordovician conodonts are common in the lower unit of the bedded breccia and in the base of the upper laminated unit. No Ordovician, and only one Devonian, conodont has been found in the upper 4 feet of the laminated unit in the localities sampled. Many of the specimens were not identified because they are fragmentary and comparative material was not available. Most of the Ordovician conodonts listed occur in Middle and Late Ordovician rocks in Kentucky and Indiana (Branson and Mehl, 1951; Pulse and Sweet, 1960; Sweet and others, 1959). Sweet (written communication, 1963) reports that the species of *Aphelognathus*, *Cordylodus*, *Drepanodus* listed in the table, *Oistodus abundans*, *O. inclinatus*, *Panderodus gracilis*, and some species of

Zygognathus occur as low as the base of the Cannon Limestone in the Tennessee Ordovician section; that *Rhipidognathus* is common in the Cannon, Catheys, and Leipers Limestones; and that big species of *Eoligonodina*, *Trichonodella* cf. *undulata*, *T.* cf. *nitida*, and *Prioniodina oregonia* are abundant in the Catheys and Leipers Limestones.

The conodont fauna of the bedded breccia indicates an early Late Devonian age. All the Devonian conodonts in the lower part of the bedded breccia at locality 4522SD are regarded as indigenous. There is no evidence that these conodonts came from the overlying rocks by stratigraphic leakage. The Ordovician conodonts could all have come from the Leipers and Catheys Limestones locally. Probably most of them were derived from the explosion breccia which provided most of the material reworked into the bedded breccia. Some of the well-preserved Ordovician conodonts probably were enclosed in pebble-size fragments in the bedded breccia. Other conodonts were transported as particles and included in the matrix. None of the bedded breccia is considered Ordovician in age and there is no evidence of the former presence of a pre-Chattanooga, post-Leipers formation near the Flynn Creek structure. This is a good example of mixed conodont fauna, but no improvement in dating the age of the explosion was made.

REFERENCES

Branson, E. B., Mehl, M. G., and Branson, C. C., 1951, Richmond conodonts of Kentucky and Indiana: Jour. Paleontology, v. 25, no. 1, p. 1–17.

Conant, L. C., and Swanson, V. E., 1961, Chattanooga Shale and related rocks of central Tennessee and nearby areas: U.S. Geol. Survey Prof. Paper 357, p. 1–91.

Conrad, S. G., Elmore, R. T., and Maher, S. W., 1957, Stratigraphy of the Chattanooga Shale in the Flynn Creek structure, Jackson County Tennessee: Tennessee Acad. Sci. Jour., v. 32, no 1, p. 9–18.

Hass, W. H., 1956, Age and correlation of the Chattanooga Shale and the Maury Formation: U.S. Geol. Survey Prof. Paper 286, p. 1–47.

Pulse, R. R., and Sweet, W. C., 1960, The American Upper Ordovician standard. III. Conodonts from the Fairview and McMillan Formations of Ohio, Kentucky, and Indiana: Jour. Paleontology, v. 34, no. 2, p. 237–264.

Sweet, W. C., Turco, C. A., Warner, Earl, Jr., and Wilkie, L. C., 1959, The American Upper Ordovician standard. I. Eden conodonts from the Cincinnati region of Ohio and Kentucky: Jour. Paleontology, v. 33, no. 6, p. 1029–1068.

Wilson, C. W., Jr., and Born, K. E., 1936, The Flynn Creek disturbance, Jackson County, Tennessee: Jour. Geology, v. 44, no. 7, p. 815–835.

Article 75

MIDDLE TRIASSIC MARINE OSTRACODES IN ISRAEL [1]

By I. G. SOHN, Washington, D.C.

Abstract.—The first Middle Triassic marine ostracodes in the world are recorded from the Makhtesh Ramon, in southern Israel. Their age is established by associated megafossils.

This is a preliminary note recording the presence of well-preserved ostracodes in Middle Triassic marine sedimentary rocks of the Makhtesh Ramon, in southern Israel. The ostracodes occur in the vicinity of Har Gevanim, in the same beds from which Parnes (1962) described an ammonite fauna. On the basis of the megafossils, these beds belong to the Anisian and Ladinian Stages (Muschelkalk). The location of the outcrops is shown on figure 75.1.

Definite Middle Triassic marine ostracodes are as yet undescribed anywhere in the world, and only a few genera of marine Triassic ostracodes are known (see accompanying table).

Range of Triassic marine ostracode genera
[Data from Kollmann, 1960; Moore, 1961]

	Pre-Triassic	Triassic			Post-Triassic
		Lower	Middle	Upper	
Bairdia McCoy, 1844	×				×
Bairdiocypris Kegel, 1932	×			×	
Bythocypris Brady, 1880				×	×
Cytherella Jones, 1849				?	×
Cytherissinella Schneider, 1956		×			
Fabalicypris Cooper, 1946	×			?	
Gemmanella Schneider, 1956		×			
Glyptobairdia Stephenson, 1946				cf.	×
Healdia Roundy, 1926	×			×	
Hungarella Méhes, 1911				×	
Monoceratina Roth, 1928	×				×
Ogmoconcha Triebel, 1941				×	×
Parabairdia Kollmann, 1960				×	
Paracytheridea Müller, 1894				cf.	×
Ptychobairdia Kollmann, 1960				×	
Pulviella Schneider, 1957		×			
Renngartenella Schneider, 1957		×			
Triassinella Schneider, 1956		×			

The genera *Bairdia* and *Monoceratina* are presumed to have lived in the Triassic because species are assigned to them from both pre- and post-Triassic sedimentary rocks. *Cryptophyllus* Levinson, 1951, is also in this category, but Jones (1962, p. 5) suggests that the Upper Jurassic (Redwater Shale) species may have been reworked from older, possibly Paleozoic, beds. Kollmann (1960, p. 87) also lists small specimens of Kirkbyidae, a Paleozoic family, in sample 214/2 from Lanzing, Austria (Upper Triassic).

Preliminary work disclosed well-preserved ostracodes in three samples of weathered and marly fossiliferous limestone. The most common genus is a minute dimorphic sulcate form with a healdiid muscle scar, represented by growth stages, that probably belongs to a new genus. Individuals of several additional genera are present, including one that resembles *Monoceratina* Roth, 1928, and a second that resembles *Ogmoconcha* Triebel, 1941.

This find is incidental to my work on Lower Cretaceous ostracodes in Israel. I am grateful to M. I. Price, Naphtha Oil Co., for taking me to the outcrops, and to I. Zak, Geological Survey of Israel, for stratigraphic information.

REFERENCES

Jones, P. J., 1962, The ostracod genus *Cryptophyllus* in the Upper Devonian and Carboniferous of Western Australia: Australia Bur. Mineral Resources, Geology and Geophysics Bull. 62, no. 3, 37 p., 3 pls.

Kollmann, Kurt, 1960, Ostracoden aus der alpinen Trias Österreichs I. *Parabairdia* n.g. und *Ptychobairdia* n.g. (Bairdiidae) : Jahrb. geol. Bundesanstalt, Wien, Sonderband 5, p. 79–105, pls. 22–27, 3 figs.

Moore, R. C., ed., 1961, Treatise on invertebrate paleontology, Pt. Q. Arthropoda, 3. Ostracoda: Geol. Soc. America and Univ. Kansas Press, 442 p., 334 figs.

Parnes, Abraham, 1962, Triassic ammonites from Israel: Geol. Survey of Israel Bull. 33, 76 p., 9 pls., 12 figs.
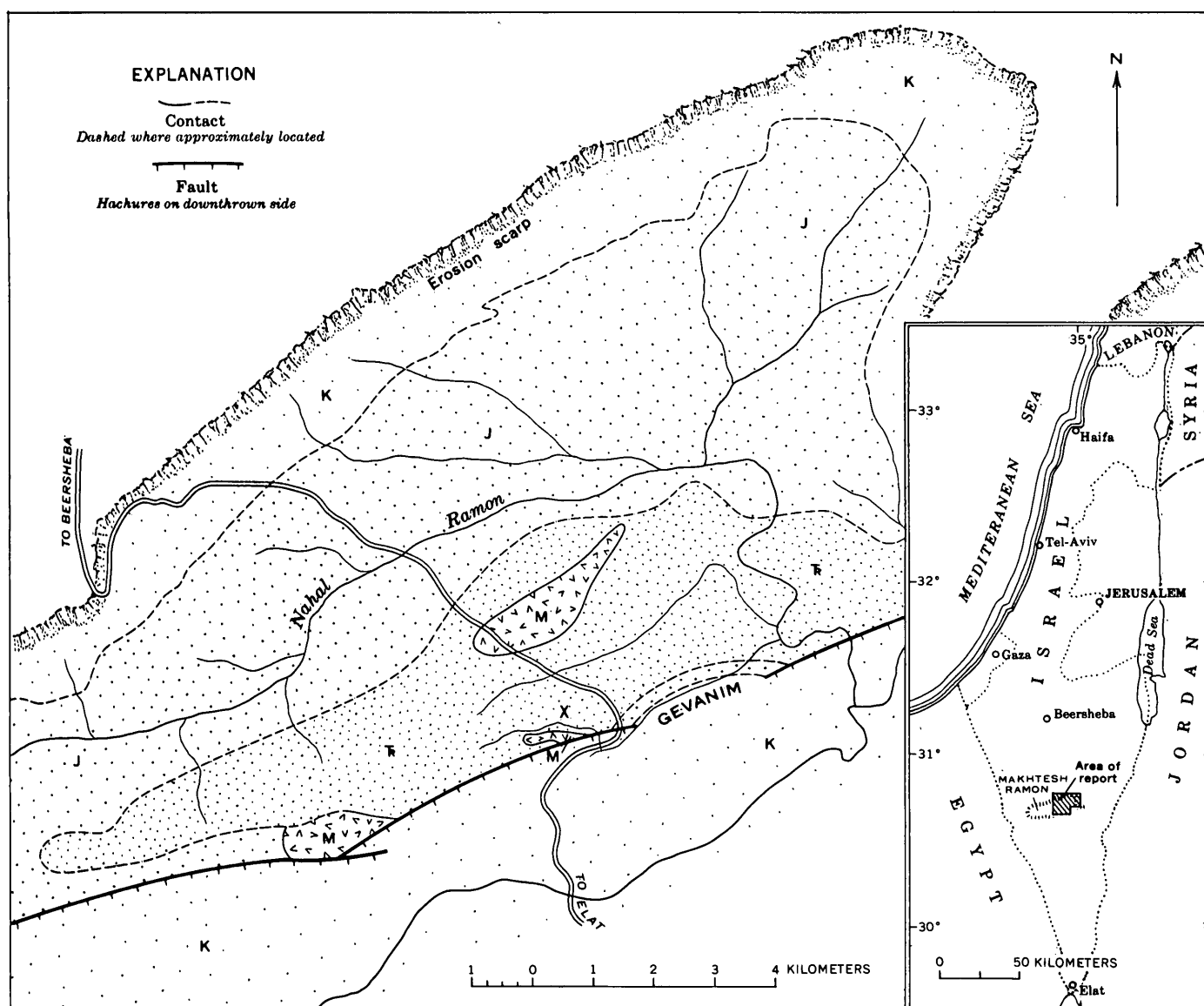
FIGURE 75.1.—Sketch map showing the geology of the Makhtesh Ramon (after Parnes, 1962) and the location of ostracode-bearing Middle Triassic sedimentary rocks. K, Cretaceous sedimentary rocks; J, Jurassic sedimentary rocks; ℞, Triassic sedimentary rocks; M, igneous intrusive rocks; X, location of outcrops containing Middle Triassic marine ostracodes.

Article 76

OCCURRENCE OF THE LATE CRETACEOUS AMMONITE
HOPLITOPLACENTICERAS IN WYOMING

By W. A. COBBAN, Denver, Colo.

Abstract.—*Hoplitoplacenticeras*, a genus well established in Europe as an index fossil to the upper part of the Campanian Stage, has been discovered in the *Baculites asperiformis* Range Zone near the top of the Steele Shale in Carbon County. The Wyoming specimen is compared to *Hoplitoplacenticeras coesfeldiense* (Schlüter) var. *schüteri* Mikhailov.

While mapping in south-central Wyoming, E. N. Harshman, of the U.S. Geological Survey, collected a fragment of *Hoplitoplacenticeras*, thus providing the first record of this genus in the western interior of the conterminous United States. Aside from its great rarity, the find is of considerable importance because of the association of the *Hoplitoplacenticeras* with *Baculites asperiformis* Meek, one of the western interior zone fossils (Cobban, 1962, p. 708). The fossil was found in a bed of concretionary sandstone near the top of the Steele Shale at USGS Mesozoic locality D2923 in the NW¼SE¼SW¼ sec. 35, T. 27 N., R. 79 W., Carbon County, Wyo. Associated fossils included numerous baculites and bits of carbonized wood, and a few fish scales and small pelecypods.

The fragment of *Hoplitoplacenticeras*, 59 mm high and 73 mm wide, consists of the middle part of an adult living chamber, and part of the septate whorls. The suture is not visible. Only one side of the living chamber is preserved, and the younger part of it is broken near the venter and the parts separated. The septate whorls have been pushed into the living chamber, and the height of the outer septate whorl has been shortened on one side along a fracture. A slightly oblique view of the specimen is shown in a drawing prepared by John R. Stacy (fig. 76.1).

The cross section of the outer septate whorl is very narrow, and the flanks are flattened. The venter is flat and bordered by nodes. The flanks of the outer septate whorl have broad, straight, slightly prosiradiate ribs.
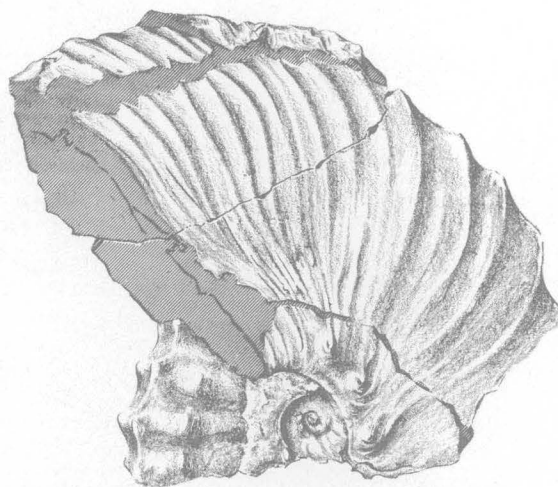
FIGURE 76.1.—*Hoplitoplacenticeras* cf. *H. Coesfeldiense* (Schlüter) var. *schlüteri* Mikhailov. USNM 132373.

Only 4 ribs are visible but, judging from their spacing, about 10 or 11 would be present on a half whorl. Each rib has a low, weak clavate node high on the flank, and each rib terminates in a strong clavate node at the margin of the venter. In the illustration the lateral nodes appear to be located about at the base of the upper third of the flank owing to the shortening caused by the fracture lower on the flank. On the opposite and undamaged side of this whorl (not visible in the illustration), these nodes are located at the base of the upper quarter of the flank. Small sharp umbilical nodes are present; these are widely spaced and only two are visible on the exposed part of the outer septate whorl.

The living chamber has flattened flanks and well-defined umbilicus and venter. The older part is ornamented by low, broad, prosiradiate, sinuous ribs that terminate in moderately strong clavate nodes at the edge of the venter. There is no trace of the weak lateral

nodes present on the outer septate whorl. Strong, sharp, bullate umbilical nodes are present on the older part of the living chamber. On the younger part, the ribbing abruptly becomes much denser and the ventral and umbilical nodes weaken and disappear.

The fragment from Wyoming very closely resembles the adult from Germany figured by Schlüter (1872, p. 56, pl. 17, figs. 1, 2) as a variant of his *Ammonites coesfeldiensis*. The only conspicuous difference is the persistence of the lateral nodes onto the part of the living chamber of the German specimen that is the equivalent of the Wyoming specimen. This difference may have little meaning inasmuch as the species of *Hoplitoplacenticeras* are extremely variable, as demonstrated by Paulcke (1907, p. 181–220) for material from Argentina. Schlüter's specimen differs from the typical form of *H. coesfeldiense* by its wider umbilicus and more coarsely sculptured septate whorls. Mikhailov (1951, p. 82), in the course of describing Russian specimens, named Schlüter's specimen *H. coesfeldiense* var. *schlüteri*. Naidin and Shimanskii (1959, p. 193) accepted Mikhailov's assignment, although Glazunova and others (1958, pl. 55) had earlier regarded Mikhailov's variety as a species. Schlüter's *Ammonites dolbergensis* (1876, p. 159, pl. 44, figs. 1–4) resembles the septate whorls of *H. coesfeldiense* var. *schlüteri*, and if these forms prove to be the same, Schlüter's name will take priority over Mikhailov's.

Aside from the occurrences in Germany, Russia, and Argentina, *Hoplitoplacenticeras* is known from France (Grossouvre, 1893, p. 116–123), Sweden (Ødum, 1953, p. 23), Poland (Nowak, 1909, p. 765), Spain (Basse, 1931, p. 36), Libya (Maxia, 1943, p. 470–473), Madagascar (Basse, 1931, p. 35–37), British Columbia (Usher, 1952, p. 93, 94), and Texas (Young, 1963, p. 63, 64).

In all of these areas the genus is restricted to rocks of late Campanian age. Schlüter (1876, p. 245–254) recognized a "zone des *Ammonites Coesfeldiensis*" in his sequence of Late Cretaceous fossil zones for northwest Germany, and Grossouvre (1901, p. 801, table 35) proposed a "Zone à *Hoplites Vari*" as marking the lower part of the upper Campanian. Since the time of Schlüter and Grossouvre's publications, one or the other of these species of *Hoplitoplacenticeras* has been used as a zonal fossil in the Campanian Stage. Spath (1926, table opposite p. 80) accepted *Hoplitoplacenticeras vari* as one of the Campanian zones in his compilation of Late Cretaceous ammonite levels. Jeletzky (1951, p. 18) and Seitz (1952, p. 149) have used *H. vari* as the basal zone of the upper Campanian. Muller and Schenck (1943, text fig. 6), in their proposal for the

standard of the Cretaceous, recognized *H. coesfeldiense* as one of the zones of the Campanian and, in the upper part of this zone, *H. vari* was used as a subzone. Schlüter (1876, p. 252) noted that *H. coesfeldiense* and *H. vari* occurred together in his zone of *H. coesfeldiense* but that *H. vari* ranged on up into the next higher zone (*Bostrychoceras polyplocum*). This longer range of *H. vari* has been verified by Mikhailov (1951, p. 108). Giers (1934, p. 476) also noted the association of *H. coesfeldiense* and *H. vari*, and that *H. dolbergense* occurred a little below them.

In the western interior region, rocks near the boundary of the lower and upper Campanian have been zoned best by means of baculites. Above rocks containing the well-known *Scaphites hippocrepis* of early Campanian age, the following sequence of baculites (from oldest to youngest) has been determined (Cobban, 1962, p. 705): *Baculites obtusus* Meek, *B. mclearni* Landes, *B. asperiformis* Meek, *B.* sp. (smooth), and *B. perplexus* Cobban. The discovery of *Hoplitoplacenticeras* cf. *H. coesfeldience* var. *schlüteri* in the *B. asperiformis* Range Zone suggests that this baculite zone lies at or very near the boundary between the lower and upper Campanian. If *H. coesfeldiense* var. *schlüteri* and *H. dolbergense* are the same, a very low position in the upper Campanian is indicated.

The Wyoming specimen is in the U.S. National Museum, Washington, D.C. (USNM 132373). A plaster cast is at the Federal Center, Denver, Colo.

REFERENCES

Basse, Éliane, 1931, Monographie paléontologique du Crétacé de la Province de Maintirano: Service des Mines, Govt. Gén. Madagascar et Dépendencies, 86 p., 13 pls.

Cobban, W. A., 1962, Baculites from the lower part of the Pierre Shale and equivalent rocks in the western interior: Jour. Paleontology, v. 36, no. 4, p. 704–718, pls. 105–108.

Giers, Rudolf, 1934, Die Schichtenfolge der Mukronatenkreide der Beckumer Hochfläche: Centralbl. Mineralogie, 1934, B, p. 471–476.

Glazunova, A. E., Luppov, N. P., and Savel'ev, A. A., 1958, Nadseme stvo Noplitaceae, *in* Luppov, N. P., and Drushchitz, V. V., Molluski–Golovonogne II [Superfamily Hoplitaceae, *in* Mollusca–Cephalopoda II] *of* Orlov, Y. A., ed., Principles of paleontology–Handbook for paleontologists and geologists of the U.S.S.R.: Moscow, State Sci. and Tech. Publishing House of Lit. on Geology and the Preservation of Mineral Resources [Gosgeoltekhizdat], v. 6, pt. 2, p. 112–116, pls. 53–55 [in Russian].

Grossouvre, Albert de, 1893, Les ammonites de la craie supérieure, pt. 2, Paléontologie, *of* Récherches sur la craie supérieure: Carte Geol. France, Mém., 264 p., pls. 1–39.

——— 1901, Classification des couches supracrétacées, chap. 22 *in* Pt. 1, Stratigraphie générale, *of* Récherches sur la craie supérieure: Carte Géol. France, Mém., p. 751–830.

Jeletzky, J. A., 1951, Die Stratigraphie und Belemnitenfauna des Obercampan und Maastricht Westfalens, Nordwestdeutschlands und Dänemarks sowie einige allgemeine Gliederungs–Probleme der jüngeren borealen Oberkreide Eurasiens: Geol. Jahrb., no. 1, 142 p., 7 pls.

Maxia, Carmelo, 1943, Ammoniti maestrichtiane della Tripolitania: Soc. geol. italiana Boll., v. 61, p. 469–487, pl. 8.

Mikhailov, N. P., 1951, Ammonity werchnego mela yuzhnoj chasti jewropejskoj chasti SSSR i ich stratigraficheskoe znatschenie [The ammonites of the Upper Cretaceous of the southern part of the European part of the USSR and their stratigraphic significance]: Akad. Nauk SSSR, Inst. geol. nauk Trudy, no. 129, geol. ser. no. 50, 143 p., 19 pls. [in Russian].

Muller, S. W., and Schneck, H. G., 1943, Standard of Cretaceous System: Am. Assoc. Petroleum Geologists Bull., v. 27, no. 3, p. 262–278.

Naidin, D. P., and Shimanskii, V. N., 1959, Golovonogne Molluski, in M. M. Moskvin, (ed.), Atlas verkhnemelovoi fauny Severnogo Kavkaza i Kryma [Cephalopod Mollusca, in Atlas of the Upper Cretaceous fauna of the Northern Caucasus and Crimea]: Trans. All-Union Sci.-Research Inst. Natural Gases (VNIIGAZ), [Moscow] p. 166–220, 23 pls. [in Russian].

Nowak, Jan, 1909, O kilku glowonogach i o charakterze fauny z Karpackiego Kampanu [On some cephalopods and the character of the fauna of the Carpathian Campanian]: Kosmos, v. 34, p. 765–787, 1 pl. [Polish with German summary].

Ødum, Hilmar, 1953, The macro-fossils of the Upper Cretaceous, pt. 5 of De geologiska resultaten från borrningarna vid Höllviken: Sveriges geol. undersökning, ser. C. Arsbok 46 (1952) N:o3, no. 527, 37 p., 4 pls.

Paulcke, W., 1907, Die Cephalopoden der oberen Kreide Südpatagoniens: Freiburg Naturf. Gesell. Berichte, v. 15, p. 167–244, pls. 10–19.

Schlüter, Clemens, 1871–1876, Cephalopoden der oberen deutschen Kreide: Palaeontographica, v. 21 (1871–1872), p. 1–120, pl. 1–35; v. 24 (1876), p. 121–264, pls. 36–55.

Seitz, Otto, 1952, Die Oberkreide-Gliederung in Deutschland nach ihrer Anpassung an das internationale Schema: Deutsche geol. Gesell. Zeitschr., v. 104, p. 148–151.

Spath, L. F., 1926, On new ammonites from the English Chalk: Geol. Mag., v. 63, no. 740, p. 77–83.

Usher, J. L., 1952, Ammonite faunas of the Upper Cretaceous rocks of Vancouver Island, British Columbia: Canada Geol. Survey Bull. 21, 182 p., 31 pls.

Young, Keith, 1963, Upper Cretaceous ammonites from the Gulf Coast of the United States: Texas Univ. Pub. 6304, 373 p., 82 pls.

PALEOTEMPERATURE INFERENCES FROM LATE MIOCENE MOLLUSKS IN THE SAN LUIS OBISPO–BAKERSFIELD AREA, CALIFORNIA

By W. O. ADDICOTT and J. G. VEDDER, Menlo Park, Calif.

Abstract.—Tropical molluscan taxa in upper Miocene strata near Bakersfield, Calif., suggest a marine hydroclimate warmer than existed in the San Luis Obispo area, 100 miles to the west. A late Miocene temperature regime analogous to that of the present-day outer coast of southwestern Baja California, Mexico, is indicated.

Certain faunal data critical to the interpretation of late Miocene water-temperature distribution in California apparently have been overlooked in Hall's (1960, 1962) study and definition of molluscan provinces of this age along the San Andreas fault. Approximately 60 molluscan taxa of late Miocene age from the southern San Joaquin basin not listed by Hall include several species and genera suggestive of a tropical marine climate. Most of the additional taxa are listed in published reports that discuss subsurface occurrences of late Miocene mollusks in the southern San Joaquin basin; a few are previously unreported species from surface localities in this area. The modification of Hall's paleotemperature interpretation required by these data invalidates the use of his inferences as definitive evidence for large lateral displacement along the San Andreas fault.

A critical area in Hall's interpretation (1960) is the San Luis Obispo–southern San Joaquin Valley region (fig. 77.1). According to Hall, a composite subtropical fauna from 5 areas on the west side of the fault is opposed by a composite warm-temperate fauna from 2 widely separated areas east of the fault. Temperature inferences were made by comparing certain species and genera with the modern faunas of northern and southern Baja California. The living mollusks of these geographic areas along the outer coast of Baja California are considered sufficiently distinct by Hall (1960, map 1) to include them in a newly recognized tripartite subdivision of the California province (lat 23° N. to 34½° N.) of Dall (1909) and others. The boundary
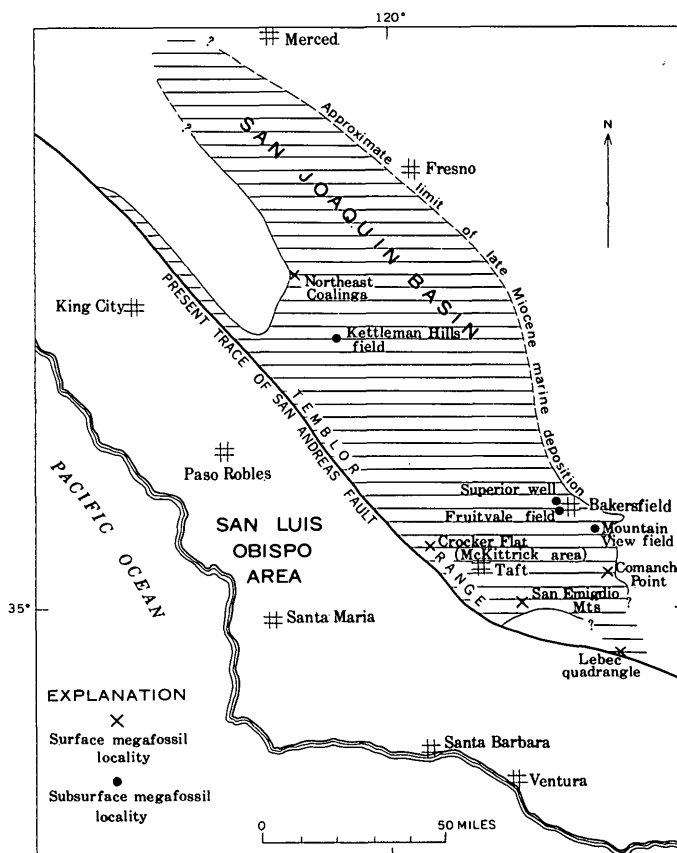
FIGURE 77.1—Late Miocene molluscan fossil localities and marine deposition in southern San Joaquin Basin.

separating Hall's Magdalenan (subtropical) and Ensenadian (warm-temperate) subprovinces is placed near Cedros Island (lat 28° N.). Provincial boundaries can be conveniently expressed by mean winter surface-water isotherms which are generally normal to the coastline of western North America. Northern end points of range for tropical (Panamic) and subtropical

ART. 77 *IN* U.S. GEOL. SURVEY PROF. PAPER 475-C, PAGES C63–C68. 1963.

C63

taxa measured in these terms have been used to interpret Cenozoic paleotemperatures (Durham, 1950a; Hall, 1960; Valentine, 1961). The principal indicator for a subtropical marine environment in the San Luis Obispo region seems to be the occurrence of an undescribed pelecypod referred to the subgenus *Arca* s.s., which today is limited, in the eastern Pacific, to latitudes south of the 18°C minimum winter surface-water temperature isotherm (Hall, 1960, p. 298). Supporting evidence presented by Hall for interpreting subtropical water temperatures west of the fault was the diversity of species of *Turritella* (four species) and the abundance of *Anadara* and *Lyropecten*. In the southern San Joaquin basin, Hall (1960, p. 286) lists 20 molluscan taxa which he regards as a warm-temperate fauna. All but one of these forms occur in the Comanche Point area, where 27 taxa previously have been reported (Clark *in* Merriam, 1916; Nomland, 1917; and Hoots, 1930). Other published occurrences of marine molluscan fossils considered were from the San Emigdio area (2 species listed by Pack, 1920, p. 42, which were regarded as Pliocene forms by Hoots, 1930, p. 258); the Crocker Flat landslide area (3 species listed by Simonson and Kreuger, 1942, p. 1620); and 11 taxa from the Lebec quadrangle identified by Corey (*in* Crowell, 1952, p. 13).

Faunal data from east of the fault not included by Hall consist of an assemblage of 55 taxa of mollusks identified by H. R. Gale (*in* Preston, 1931, p. 15, 16) from well cores in upper Miocene strata west of Bakersfield (see table 77.1). This assemblage includes 48 taxa previously unreported from surface localities in the southern San Joaquin basin and contains a number of tropical and subtropical species and genera.

The mollusks identified by Gale (*in* Preston, 1931, p. 15, 16) are from the Fruitvale oil field 3 miles west of Bakersfield, Calif. (fig. 77.1). Northwest of the Fruitvale field, Grant and Gale (1931, p. 408) list 15 species of mollusks from the Santa Margarita Formation in the Superior Ansolabehere No. 1 well (sec. 9, T. 29 S., R. 27 E., M.D.B. and M.). All of these species are recorded in Gale's larger list. Other subsurface occurrences of megafossils of probable late Miocene age are from the Mountain View oil field southeast of Bakersfield, where the Wharton sand (local usage) has been compared with the type Santa Margarita Formation on the basis of the molluscan assemblage (Miller and Ferguson, 1943). In the southeast part of the Mountain View field, Miller and Bloom (1937, p. 10) describe "marine fingers" in the lower part of the Chanac Formation with marine fossils including "*Clementia pertenuis*, large variety."

Miocene mollusks identified by Gale from the Fruitvale field are from the upper 500 to 600 feet of the Santa Margarita Formation, which is described as a gray, fine- to medium-grained sand with abundant fossil remains (Preston, 1931, p. 12). Beck (1952) assigns the Santa Margarita Formation penetrated by wells in the area southwest and southeast of Bakersfield to the upper Mohnian Stage (Kleinpell, 1938). A recent correlation section (Church, Krammes, and others, 1957) places the upper part of the Santa Margarita Formation at the Fruitvale field within the upper Mohnian Stage. As stated by Gale (*in* Preston, 1931, p. 15), the molluscan assemblage is indicative of "post-Temblor Miocene" or a late Miocene age in the usage of the Pacific coast larger invertebrate chronology.

Recent collecting at Comanche Point has nearly doubled the number of taxa from that locality (see table 77.2) and further increases the known late Miocene fauna from the southern San Joaquin basin to about 80 taxa.

Analysis of the supplementary faunal data strongly suggests that interpretation of temperature affinities of late Miocene molluscan assemblages, as they are now known, cannot be used as definitive evidence for large lateral displacement along the San Andreas fault as was proposed by Hall (1960). The tropical faunal element near Bakersfield indicates water temperatures higher than those suggested by the San Luis Obispo fauna west of the San Andreas fault (table 77.3), in contradistinction to Hall's (1960, p. 288) conclusion that "cooler temperatures must have prevailed [in the southern San Joaquin basin] because of the total absence of distinct Magdalenan faunal [=subtropical] elements." Further evidence for subtropical to tropical marine water temperatures east of the fault is found in the Coalinga area, where two taxa characteristic of the Panamic molluscan province have been described from the Santa Margarita Formation (Nomland, 1917, p. 301).

Discussion.—For the purpose of this discussion the species identified by Gale and other workers are considered to have been competently determined. Information on the geographic ranges of living species and genera is from Grant and Gale (1931), Burch (1944–46), and Keen (1958). Although definitive criteria for Hall's (1960) subdivision of the Californian molluscan province into Magdalenan, Ensenadian, and Southern Californian subprovinces are not readily apparent, particularly along the unprotected outer coast, these units are used provisionally in the following discussion and are referred to as provinces as a matter of convenience.

A large lucinid, *Miltha xantusi* (Dall), one of the most abundant species in the well cores, is reported living off Cape San Lucas, Baja California, near the boundary of the Panamic and Magdalenan provinces and has been collected intertidally at La Paz (Pilsbry and Lowe, 1933). A similar form is present at Coman-

che Point. The extinct gastropod *"Phos" dumbleana* Anderson *in* Hanna is an indicator of tropical hydroclimate at the generic level. Although this species is probably better assigned to the genus *Tritiaria*, it is here referred to *"Phos"* in deference to the most recent treatment of living eastern Pacific species by Strong and Lowe (1936). Another extinct species listed by Gale, *Ficus* (*Trophosycon ocoyana* (Conrad), supports the interpretation of subtropical to tropical marine waters in the southern San Joaquin basin during late Miocene time. In the eastern Pacific the genus *Ficus* is restricted to the Panamic province; its northernmost occurrence along the outer coast of Mexico is off Cape San Lucas, at or south of the tropical-subtropical provincial boundary. This species occurs in well cores from the Reef Ridge Shale of late Miocene age at Kettleman Hills oil field (Barbat and Johnson, 1934). *Ficus* also has been reported from the Santa Margarita Formation northeast of Coalinga by Nomland (1917, p. 301) as *"Ficus*, cf. *nodiferous* Gabb."* The genus *Turricula*, represented in the Santa Margarita fauna from the Fruitvale field by the extinct species *Turricula ochsneri* (Anderson and Martin), is characteristic of the Panamic province. This species seems to be very closely related to *Turricula* (*Turricula*) *libya* Dall, which is living in the Panamic province off Cape San Lucas. *Calyptraea mamillaris* Broderip, the second most abundant gastropod in cores from the Santa Margarita Formation at the Fruitvale field, is not known to be living farther north than Magdalena Bay along the southern coast of Baja California (Keen, 1958, p. 311). A similar form is present at Comanche Point.

Turritella cf. *T. vanvlecki* Arnold, also listed by Gale, is very closely related to the living *T. gonostoma* Valenciennes. Both species have been placed in a group of approximate subgeneric rank, the *Turritella broderipiana* stock, by Merriam (1941, p. 51). In the eastern Pacific, living representatives of this stock range throughout the Panamic province. *Turritella gonostoma*, which typifies this stock, is the most northerly ranging species occurring in the living fauna as far north as San Juanico Bay (lat 26° N.) on the outer coast of southern Baja California (Keen, oral communication, 1962).[1] Another species referable to this stock, *Turritella freya* Nomland, is described from the Santa Margarita Formation north of Coalinga. Other species of *Turritella* occurring east of the San Andreas fault in strata of this age are *Turritella* cf. *T. cooperi* Carpenter, identified by Merriam (1941, p. 49, fig. 8; p. 118) from the San Pablo "formation" (Cierbo Sandstone) on the

north side of Mount Diablo, and an unnamed *"Turritella,* sp. (large)"* in the Santa Margarita Formation north of Coalinga (Nomland, 1917, p. 301). There are thus at least 3 and possibly 4 species of *Turritella* in upper Miocene strata on the east side of the San Andreas fault.

Cancellarids commonly found in middle Miocene strata of California also are listed from the subsurface section of upper Miocene rocks near Bakersfield. Using the classification of Marks (1949), *Cancellaria lickana* Anderson and Martin is best assigned to *Cancellaria* s.s., which, in the eastern Pacific, is restricted to the Magdalenan and Panamic provinces. *Cancellaria* cf. *C. pacifica* Anderson is representative of the subgenus *Euclia*, which lives in tropical seas. *Cancellaria joaquinensis* Anderson, a form that seems to have no Recent analogs in the eastern Pacific, may be intermediate between *Cancellaria* s.s. and *Euclia*. *Cancellaria joaquinensis* closely resembles *Cancellaria pabloensis* Clark from the Mount Diablo, Coalinga, and Comanche Point areas. Two other species referable to *Cancellaria* s.s. have been collected recently at Comanche Point (see table 77.2).

Corey (*in* Crowell, 1952, p. 13) lists an *Oliva* sp. from the Santa Margarita Formation of the Lebec quadrangle, about 20 miles south of Comanche Point on the east side of the San Andreas fault. Living representatives of this genus are characteristic of the Panamic molluscan province, but one species ranges northward into the Magdalenan province. Gale (*in* Preston, 1931) lists a taxon as *?Olivella biplicata* Sowerby but indicates parenthetically that the specimen might be an *Oliva*, *O. futheyana* Anderson.

The late Miocene Lyropectens are related to the Recent Panamic–Magdalenan species *Lyropecten* (*Nodipecten*) *subnodosus* (Sowerby), which is assigned to *Lyropecten* s.s. by some authors (Hertlein [as subgenus of *Pecten*], 1935, p. 317; Durham, 1950b, p. 65; Keen, 1958, p. 74). The common occurrence of late Miocene species of *Lyropecten* s.s. in the southern San Joaquin basin further suggests water warmer than that postulated by Hall. It should be noted that Lyropectens are among the most abundant fossils at nearly all late Miocene localities in the Coalinga area, along the west side of the Temblor Range from Recruit Pass south to Bitterwater Creek, at Comanche Point, and in the Lebec area.

A point to be considered in paleoecologic interpretation is the difference in opinion of various workers in ascribing temperature ranges to certain critical molluscan taxa. *Dosinia ponderosa* Gray, for example, is closely related to late Miocene species. Grant and Gale (1931, p. 352–354) consider late Miocene forms as variants of the living *Dosinia ponderosa*, which ranges from

[1] A more northerly occurrence reported from Scammons Lagoon (lat 28° N.) in the "Hemphill collection" (Grant and Gale, 1931, p. 773) is questionable inasmuch as Phleger and Ewing (1962) list *T. gonostoma* as a characteristic element in late Pleistocene deposits that lie a few feet above sea level.

Scammons Lagoon, near the latitude of the Magdalenan–Ensenadian provincial boundary, southward to Peru. Valentine and Meade (1961) treat this species as a Panamic form which extended its range north of the provincial boundary by inhabiting protected, warm-water environments. Hall (1960), however, identifies the northern end point of range of this taxon with the Ensenadian molluscan province. Doubtless, arguments can be made for either interpretation, but the former seems to be more acceptable in light of Emerson's (1956) discussion of the latitudinal coexistence of tropical species in protected embayments and cooler water assemblages in outer coast environments in the Magdalenan province. It is apparent that use of the indicated minimal temperatures of tropical (Panamic) or warm-temperate (Ensenadian) provinces in interpreting late Miocene occurrences of this taxon will yield widely divergent estimates of paleotemperature.

Conclusion.—The distribution of tropical and subtropical marine species and genera is not compatible with Hall's (1960) interpretation of late Miocene surface-water temperatures from which he has postulated large right-lateral movement along the San Andreas fault. The relationship of the critical San Luis Obispo–southern San Joaquin basin late-Miocene faunas suggests a complex distribution of marine surface-water temperatures. The pattern probably was related more to the configuration of an irregular, embayed coastline protected to the west and to the north by large insular or peninsular blocks separated by narrow straits rather than to the present latitudinal distribution of winter surface-water temperatures along a fairly regular, open coast.

If large right-lateral slip has occurred along the San Andreas fault since deposition of upper Miocene strata, a paleogeographic restoration would place the molluscan fauna of the San Joaquin basin with its tropical element considerably farther north than the presumed subtropical fauna of the San Luis Obispo region. Whether or not the fault has had relatively great lateral movement, the presence of tropical and subtropical molluscan species at the same latitude in late Miocene time seems to be indicated. This can be satisfactorily explained by reference to the modern occurrence of many Panamic species in shallow embayments along the west coast of southern Baja California. If the southern San Joaquin basin was a protected embayment during late Miocene time, it seems likely that relicit faunal elements may have persisted there long after more temperate faunas had spread southward along the open outer coast.

The intent of this discussion is not to conclude whether paleoecologic interpretation can be used to prove or to disprove lateral movement along the San

Andreas fault; rather, it is to point out that the faunal assemblages, as they are now known, do not necessarily support the contention that late Miocene molluscan provinces were alined from north to south through the present area of California in a manner which approximated the present latitudinal distribution of winter oceanic surface-water temperatures. Instead, a fairly complex temperature regime, possibly analogous to that of the outer coast of southern Baja California but with much larger protected embayments, existed in the central California region during late Miocene time.

TABLE 77.1.—*Miocene mollusks from the Fruitvale field*

[Gale *in* Preston (1931). Generic designations as listed by Gale; arrangement revised]

Gastropods

Calliostoma sp.
Tegula sp.
?*Melanella californica* (Anderson and Martin)
Turritella cf. *T. vanvlecki* Arnold
Calyptraea mamillaris Broderip
Polinices (*Polinices*) *diabloensis* (Clark)
Polinices (*Neverita*) *reclusianus* (Deshayes)
Ficus (*Trophosycon*) *ocoyana* (Conrad)
Forreria wilkesana (Anderson)
Mitrella tuberosa (Carpenter)
Phos dumbleana Anderson *in* Hanna
Nassarius (*Uzita*) *antiselli* (Anderson and Martin)
Nassarius (*Uzita*) cf. *N. arnoldi* (Anderson)
?*Olivella biplicata* Sowerby
Olivella pedroana (Conrad)
Cancellaria joaquinensis Anderson
Cancellaria lickana Anderson and Martin
Cancellaria cf. *C. Pacifica* Anderson
Cancellaria cf. *C. nevadensis* Anderson and Martin
?*Daphnella* sp.
?*Mangelia* cf. *M. kernensis* Anderson and Martin
Turricula ochsneri (Anderson and Martin)
Pseudomelatoma penicillata (Carpenter)
Terebra pedroana Dall
Turbonilla sp.

Pelecypods

Glycymeris septentrionalis (Middendorff)
Ostrea cf. *O. lurida* Carpenter
Pecten (*Aequipecten*) *discus* Conrad
Anomia sp.
Lucina (*Here*) *richthofeni* Gabb
Lucina (*Miltha*) *xantusi* (Dall)
Lucina (*Myrtea*) *acutilineata* Conrad
?*Lucina* (*Myrtea*) *californica* Conrad
Lucina (*Myrtea*) *nuttalli* Conrad
Taras harfordi (Anderson)
Cardium sp.
Dosinia ponderosa longidens Grant and Gale
Irus lamellifer perlamellifer Grant and Gale
Chione sp.
Venerupis (*Protothaca*) *staminea* (Conrad)
Amiantis callosa stalderi (Clark)
Petricola carditoides (Conrad)
Mactra (*Spisula*) *hemphill* Dall
Mactra (*Spisula*) sp.
Anatina (*Raeta*) *plicatella longior* Grant and Gale

TABLE 77.1.—*Miocene mollusks from the Fruitvale field*—Continued

Pelecypods—Continued

Tellina idae Dall
Apolymetis biangulata (Carpenter)
Macoma identata (Carpenter)
?Macoma inquinata (Deshayes)
Macoma wilsoni (Anderson and Martin)
Gari edentula (Gabb)
Solen sicarius Gould
Corbula (*Lentidium*) *luteola* Carpenter
?Myra sp.
Panope generosa Gould

TABLE 77.2.—*Mollusks from the Santa Margarita Formation at Comanche Point*

[Combined lists of previous collectors. Clark *in* Merriam, 1916; Nomland, 1917, Clark *in* Hoots, 1930. Generic designations revised in part]

Gastropods

Calyptraea sp.
"*Natica*" sp.
Nassarius pabloensis (Clark)
"*Fusinus*" *fabulator* Nomland
Conus sp.
Bulla sp.

Pelecypods

Pinna alamedensis Yates
Ostrea titan Conrad
Ostrea cf. *O. vespertina* Conrad
Chlamys hastatus (Sowerby)
Aequipecten raymondi (Clark)
Lyropecten crassicardo (Conrad)
Lyropecten crassicardo biformatus (Nomland)
Lyropecten estrellanus (Conrad)
Lucina excavata Carpenter [=*Phacoides richthofeni* (Gabb)]
Miltha sanctaecrucis Arnold [possible misidentification of *Miltha xantusi* (Dall)]
Cardium sp.
Dosinia arnoldi Clark
Dosinia sp.
Amiantis stalderi (Clark)
Saxidomus nuttalli Conrad
Clementia (*Egesta*) *pertenuis* (Gabb)
Chione sp.
Apolymetis biangulata (Carpenter) [=*Metis alta* (Conrad)]
Solen sp.
Siliqua cf. *S. lucida* (Conrad)
Teredo sp.

[Supplementary list from USGS loc. M1619 (near head of second east-draining gully due north of hill 1039, NW¼SW¼ sec. 24, T. 32 S., R. 29 E., collected by J. G. Vedder, 1962. Most of the taxa listed above are present at this locality]

Gastropods

Astraea cf. *biangulata* (Gabb) [?=*A. raymondi* (Clark)]
Littorina mariana Arnold?
Calyptraea mammilaris Broderip?
Crepidula cf. *C. adunca* Sowerby
Crepidula princeps Conrad?
Polinices sp. [may be *Natica* of Clark]
Neverita reclusiana (Deshayes) [may me *Natica* of Clark]

TABLE 77.2.—*Mollusks from the Santa Margarita Formation at Comanche Point*—Continued

Gastropods—Continued

"*Trophon*" sp.
Pterynotus sp.
Mitrella aff. *M. tuberosa* (Carpenter)
Olivella aff. *O. pedroana* (Conrad)
Cancellaria (*Cancellaria*) cf. *C. sanjosei* Anderson and Martin
Cancellaria (*Cancellaria*) n. sp.? cf. *C. decussata* Sowerby
Cancellaria (*Cancellaria?*) cf. *C. pabloensis* Clark
Crassispira n. sp.? cf. *C. ericana* Hertlein and Strong
Conus n. sp.? cf. *C. purpurascens* Sowerby [presumably *Conus* sp. of Clark]
Strioterebrum aff. *S. martini* (English)
Scaphander? sp.

Pelecypods

Anadara? sp.
Glycymeris aff. *G. subobsoleta* (Carpenter)
Hinnites? cf. *H. giganteus* (Gray)[1]
Pododesmus cepio (Gray)?
Lucinisca nuttalli (Conrad)
Miltha cf. *M. xantusi* (Dall)
Dosinia cf. *D. merriami* Clark [may be *Dosinia* sp. of Clark]
Protothaca? cf. *P. staminea* (Conrad)
Protothaca cf. *P. tenerrima* (Carpenter)
Tellina sp.
Corbula (*Caryocorbula*) n. sp.

[1] University of California Museum of Paleontology localities A–9417, A–9418.

TABLE 77.3.—*Late Miocene mollusks from the San Luis Obispo area*

[Compiled by Hall (1960, table 7)]

Gastropods

Astraea raymondi (Clark)
Bulla sp.
Calyptraea martini Clark
Crepidula sp.
Neptunea cierboensis (Clark)
Nucella rankini Eaton and Grant
Ocenebra selbyensis (Clark)
Trophon (*Forreria*) *carisaensis* (Anderson)
Trophon (*Forreria*) *carisaensis mirandaensis* Eaton and Grant
Trophon clarki cuyamanus Eaton and Grant
Trophon gillulyi Eaton and Grant
Trophon pabloensis Clark
Turritella carrisaensis Anderson and Martin
Turritella cooperi Carpenter
Turritella freya Nomland
Turritella margaritana Nomland

Pelecypods

Anadara obispoana (Conrad)
Anadara trilineata (Conrad)
Apolymetis biangulata (Carpenter)
Arca s.s. n. sp.
Chione sp.
Dosinia sp.
Gari sp.
Glycymeris sp.
Lucinisca nuttallii (Conrad)

TABLE 77.3.—*Late Miocene mollusks from the San Luis Obispo area*—Continued

Pelecypods—Continued

Lucinoma acutilineata (Conrad)
Ostrea bourgeoisii Remond
Ostrea titan Conrad
Ostrea titan eucorrugata Hertlein
Panope generosa Gould
Pecten (Lyropecten) crassicardo Conrad
Pecten (Lyropecten) estrellanus Conrad
Pecten (Chlamys) hodgei Hertlein
Pecten (Aequipecten) raymondi Clark
Saxidomus nuttallii (Conrad)
Schizothaerus nuttallii (Conrad)
Solen sp.
Tivela sp.
Trachycardium quadragenarium (Conrad)
Yoldia sp.

REFERENCES

Barbat, W. F., and Johnson, F. L., 1934, Stratigraphy and Foraminifera of the Reef Ridge shale, upper Miocene, California: Jour. Paleontology, v. 8, p. 3–17.

Beck, R. S., 1952, Correlation chart of Oligocene, Miocene, Pliocene, and Pleistocene in San Joaquin Valley and Cuyama Valley areas: Am. Assoc. Petroleum Geologists, Soc. Econ. Paleontologists and Mineralogists, Soc. Exploration Geophysicists Guidebook, Joint Ann. Mtg., Los Angeles, Calif., p. 104.

Burch, J. Q., ed., 1944–46, Distributional list of the west American marine mollusks from San Diego, California, to the Polar Sea: Conchological Club Southern California Minutes, nos. 33–63.

Church, H. V., Jr., and Krammes, Kenneth, (chairmen) and others, 1957, Cenozoic correlation section, south San Joaquin Valley: Am. Assoc. Petroleum Geologists, Geol. Names and Correlations Comm., San Joaquin Valley Subcomm. on the Cenozoic.

Crowell, J. C., 1952, Geology of the Lebec quadrangle, California: California Div. Mines Spec. Rept. 24, 23 p.

Dall, W. H., 1909, Report on a collection of shells from Peru, with a summary of the littoral marine Mollusca of the Peruvian zoological province: U.S. Nat. Museum Proc., v. 37, p. 147–294.

Durham, J. W., 1950a, Cenozoic marine climates of the Pacific Coast: Geol. Soc. America Bull., v. 61, p. 1243–1264.

Durham, J. W., 1950b, Megascopic paleontology and marine stratigraphy, pt. 2 *of* The 1940 E. W. Scripps cruise to the Gulf of California: Geol. Soc. America Mem. 43, 216 p.

Emerson, W. K., 1956, Pleistocene invertebrates from Punta China, Baja California, Mexico, with remarks on the composition of the Pacific Coast Quaternary faunas: Am. Mus. Nat. Hist. Bull., v. 111, art. 4, p. 317–342.

Grant, U. S., IV, and Gale, H. R., 1931, Catalogue of the Marine Pliocene and Pleistocene Mollusca of California: San Diego Soc. Nat. Hist. Mem., v. 1, 1,036 p.

Hall, C. A., Jr., 1960, Displaced Miocene molluscan provinces along the San Andreas fault, California: California Univ., Dept. Geol. Sci. Bull., v. 34, no. 6, p. 281–308.

——— 1962, Reply [to a review of Hall (1960) by J. W. Durham and S. R. Primmer, in the same issue]: Am. Assoc. Petroleum Geologists Bull., v. 46, no. 10, p. 1953–1960.

Hertlein, L. G., 1935, The Templeton Crocker expedition of the California Academy of Sciences, 1932—No. 25, The Recent Pectinidae: California Acad. Sci. Proc., 4th ser., v. 21, p. 301–328.

Hoots, H. W., 1930, Geology and oil resources along the southern border of San Joaquin Valley, California: U.S. Geol. Survey Bull. 812–D, p. 243–332.

Keen, A. M., 1958, Sea shells of tropical west America; marine mollusks from Lower California to Columbia: Stanford, Calif., Stanford University Press, 624 p.

Kleinpell, R. M., 1938, Miocene stratigraphy of California: Tulsa, Okla., Am. Assoc. Petroleum Geologists, 450 p.

Marks, J. G., 1949, Nomenclatural units and tropical American Miocene species of the gastropod family Cancellariidae: Jour. Paleontology, v. 23, no. 5, p. 453–464.

Merriam, C. W., 1941, Fossil Turritellas from the Pacific coast region of North America: California Univ., Dept. Geology Sci. Bull., v. 26, no. 1, p. 1–214.

Merriam, J. C., 1916, Mammalian remains from the Chanac Formation of the Tejon Hills, California: California Univ., Dept. Geology Bull., v. 10, no. 9, p. 111–127.

Miller, R. H., and Bloom, C. V., 1937, Mountain View oil field: California Div. Oil and Gas, Summary of Operations, California Oil Fields Ann. Rept. 22, no. 4, p. 5–36.

Miller, R. H., and Ferguson, G. C., 1943, Mountain View oil field: California Div. Mines Bull. 118, p. 565–570.

Nomland, J. O., 1917, Fauna of the Santa Margarita beds in the North Coalinga region of California: California Univ., Dept. Geology Bull., v. 10, no. 18, p. 293–326.

Pack, R. W., 1920, The Sunset-Midway oil field, California, pt. 1, Geology and oil resources: U.S. Geol. Survey Prof. Paper 116, 179 p.

Phleger, F. B., and Ewing, G. C., 1962, Sedimentology and oceanography of coastal lagoons in Baja California, Mexico: Geol. Soc. America Bull., v. 73, p. 145–182.

Pilsbry, H. A., and Lowe, H. N., 1933, West Mexican and Central American mollusks collected by H. N. Lowe, 1929–1931: Acad. Nat. Sci. Philadelphia Proc., v. 84, p. 33–144.

Preston, H. M., 1931, Report on Fruitvale oil field: California Div. Oil and Gas, Summary of Operations, California Oil Fields Ann. Rept. 16, no. 4, p. 5–24.

Simonson, R. R., and Krueger, M. L., 1942, Crocker Flat landslide area, Temblor Range, California: Am. Assoc. Petroleum Geologists Bull., v. 26, no. 10, p. 1608–1631.

Strong, A. M., and Lowe, H. N., 1936, West American species of the genus *Phos*: San Diego Soc. Nat. Hist. Trans., v. 8, p. 305–320.

Valentine, J. W., 1961, Paleoecologic molluscan geography of the Californian Pleistocene: California Univ., Dept. Geol. Sci. Bull., v. 34, no. 7, p. 309–442.

Valentine, J. W., and Meade, R. F., 1961, Californian Pleistocene paleotemperatures: California Univ., Dept. Geol. Sci. Bull., v. 40, no. 1, p. 1–46.

LATE PLEISTOCENE DIATOMS FROM THE ARICA AREA, CHILE

By ROBERT J. DINGMAN and KENNETH E. LOHMAN, Washington, D.C.

Abstract.—The extensive Tertiary(?) sequence of ash-flow and detrital deposits in the Arica area was studied. Samples from within the Lluta Formation and from strata underlying it were barren of microfossils. Samples from two deposits of diatomaceous earth overlying the formation or interbedded in the upper part indicate a probable late Pleistocene age.

A thick sequence of ash flows and interbedded fanglomerate locally associated with deposits of diatomaceous earth mantles much of northern Chile, western Bolivia, northwestern Argentina, and southern Peru. In general the sediments are coarse grained, poorly sorted, and poorly stratified. The crossbedding of the water-laid sediments indicates deposition from areas that correspond to the present areas of high relief. For example, in northern Chile the direction of deposition was westward from the Andes Mountains, and the sequence is preserved in the attitude in which it was deposited, with few exceptions. Along much of the western slope of the Andes the uppermost ash-flow bed is a moderately welded tuff that forms the present land surface and slopes uniformly 3° to 5° W. Below an altitude of approximately 2,000m the tuff bed is mantled by a thick series of detrital material. Bowman (1909) misinterpreted this depositional surface in the Pica area of Chile as a peneplain, and upon this interpretation based his still widely accepted theory of Pleistocene uplift of the Andes.

The volcanic-clastic sequence has been described by many geologists and has been assigned many names. The most complete description was made by Galli and Dingman (1962) in the Pica area, where the deposits were named the Altos de Pica Formation. The Altos de Pica Formation in the type locality is 735 m thick and consists of 3 coarse-grained sedimentary members interbedded with 2 intercalated welded-tuff members. Doyel and Henriquez (written communication, 1962) proposed the name Lluta Formation for the same sequence in the Arica area. The presence of the pyroclastic members within the sequence suggested the name given to the formation by Bertrand (1885), "Traquítica"; and by Bruggen (1918), "Liparítica" and "Riolítica". The last two formation names are still in general use, although they are misnomers inasmuch as volcanic rocks make up less than 10 percent of the formation in many areas.

The determination of the age of this sequence, which extends over many thousands of square kilometers and may be 2,000 m thick in some localities, has been one of the main problems of Chilean geology. The sequence is generally considered to be of Tertiary or possibly Quaternary age (table 78.1). It is of continental origin and contains no diagnostic vertebrate or invertebrate fossils, nor is it known to interfinger with marine deposits. All the ages assigned in table 78.1 are, therefore, only estimates by the various authors. The only fossil evidence is the classification by Douglas (1914) of fragments of a jawbone from the Stratos de Río Mauri as being from a Nesodon similar to that of a Miocene species from the Santa Cruz Formation of Argentina.

In June 1960 an attempt was made to date the Lluta Formation of the Arica area by means of diatoms. Samples were collected from the shales of the (marine?) Arica Formation, which underlies the Lluta Formation with marked angular unconformity; from dolomitic beds intercalated within the Lluta For-

ART. 78 *IN* U.S. GEOL. SURVEY PROF. PAPER 475–C, PAGES C69–C72. 1963.

C69

TABLE 78.1.—*Tertiary and Quaternary formations in northern Chile and adjoining areas*

Period	Epoch	Bolivia (Douglas, 1914)	Bolivia (Ahlfeld, 1946)	Peru (Jenks, 1948)	Chile (Bruggen, 1950)	Argentina (Groeber, 1957)	Chile (Galli and Dingman, 1962)	Chile (Doyel and Henriguez, written communication, 1962)	Chile (Dingman, 1963)
Quaternary	Pleistocene					Riolítica Formacion [1] (Chile)	Altos de Pica Formation	Lluta Formation [1]	Unnamed formation of ash-flow deposits [1]
Tertiary	Pliocene		Estratos del Río Mauri [1]			Araucaniano Formacion			
Tertiary	Miocene	Mauri Volcanic Series [1]			Liparítica Formacion [1] Riolítica Formacion [1] (1950)			—??—	San Pedro Formation Tambores Formation
Tertiary	Oligocene		Corcoro System	? Chacani Volcanics ?				Putani Formation Arica Formation	
Tertiary	Eocene								
Tertiary	Paleocene				San Pedro Formacion				

[1] Stratigraphically and lithologically equivalent to the Altos de Pica Formation.

mation; and from deposits of diatomaceous earth that overlie or are intercalated in the uppermost beds of the Lluta Formation (table 78.2). The locations of the sampled localities are indicated in figure 78.1.

All 17 of the samples listed in table 78.2 were disaggregated, concentrated for diatoms, and systematically examined under the microscope. Five samples (5272, 5273, 5283, 5287, and 5288,) proved to be devoid of diatoms. Because many of the remaining 12 samples had very similar diatom assemblages, 7 were selected for intensive study. The diatoms found in them are listed in table 78.3. It will be noted that several were selected from each of the two productive localities.

Unfortunately, two of the barren samples (5272 and 5273) came from the older marine(?) sediments that unconformably underlie the Lluta Formation; thus no inferences can be made concerning these beds except that they are older, according to the field evidence.

All samples containing diatoms were obtained from the two deposits of diatomaceous earth listed in table 78.2. The larger of these deposits is 7½ km north-

northeast of Arica and 4 km east of the coast on a head-land approximately 240 m above sea level. The diatoms from this outcrop were studied by Frenguelli (1938), who gave a different location for the deposits. However, the samples examined by Frenguelli were obtained from Dr. Humberto Fuenzalida, present director of the School of Geology at the University of Chile, who had been given them by Senor Tomas Vila. Senores Fuenzalida and Vila have agreed (oral communication, 1963) that the earlier samples were obtained from the same deposit that was sampled during this investigation.

This deposit probably formed in a shallow freshwater lake that may have been a sag pond along one of the north-trending faults of the area. The deposit overlies an ash-flow bed of the Lluta Formation and may be overlain by the upper detrital member of the formation. Unfortunately, the upper part of the Lluta Formation is lithologically identical with the more recent colluvial deposits of the area so that it is possible that the coarse sediments that overlie the eastern part

TABLE 78.2.—*List of samples collected for diatom determination*

USGS diatom locality	Location on fig. 78.1	Location and description of samples
5272 [1]	5	4 km northeast of Arica, Chile; clay pit in the Arica Formation 200 m east of Esso oil tanks. Sample from unconsolidated marine(?) sediments of probable early to middle Tertiary age which are overlain with marked angular unconformity by the Lluta (upper Tertiary to Recent) Formation.
5273 [1]	5	Same locality as 5272.
5274	1	Approximately 7½ km northeast of Arica, Chile; 3 km east of Pan-American highway. Samples from deposit of diatomaceous earth overlying or intercalated in the Lluta Formation. Samples 5274–5279 were taken by channeling the exposed vertical face of the deposits. Sample 5274 from 0–1.6 m above base of sampled interval.
5275	1	Same locality as 5274. Interval 1.6–2.25 m.
5276	1	Same locality as 5274. Interval 2.25–4.45 m.
5277	1	Same locality as 5274. Interval 4.45–5.85 m.
5278	1	Same locality as 5274. Interval 5.85–7.1 m.
5279	1	Same locality as 5274. Interval 7.1–7.65 m.
5280	1	Same locality as 5274. Layer of very pure diatomaceous earth.
5281	1	Same locality as 5274. Layer of very pure diatomaceous earth.
5282	1	Same locality as 5274. Caprock overlying deposit of diatomaceous earth.
5283 [1]	3	Arica, Chile. Dolomite quarry in Quebrada Diablo, 20 km east of Arica. Dolomite is intercalated in the Lluta Formation.
5284	2	Boca Negra, Chile. Deposit of diatomaceous earth in the Lluta Valley. Deposit overlies or is intercalated in uppermost part of the Lluta Formation.
5285	2	Same locality as 5284.
5286	2	Same locality as 5284.
5287 [1]	4	5.1 km south of the Chaca, Chile, police station. Impure dolomite bed intercalated in the Lluta Formation, on south side of Quebrada Chaca.
5288 [1]	4	Same locality as 5287.

[1] No diatoms found.

of the diatomaceous deposit may be younger in age than the Lluta Formation. The same stratigraphic situation exists at Boca Negra, where the diatomaceous-earth deposit overlies the uppermost ash flow and is overlain by coarse sediments.

The extensive assemblage of diatoms obtained contains three extinct species, *Mastogloia atacamae*, *Melosira spinigera* and *Navicula fuenzalida*, the first two of which were originally described from a lacustrine limestone in the Calama basin, Chile. The limestone has been called early Pleistocene by Frenguelli (1936) on the basis of somewhat tenuous stratigraphic correlations. These two species occur rarely in the present material. The last species was described from the
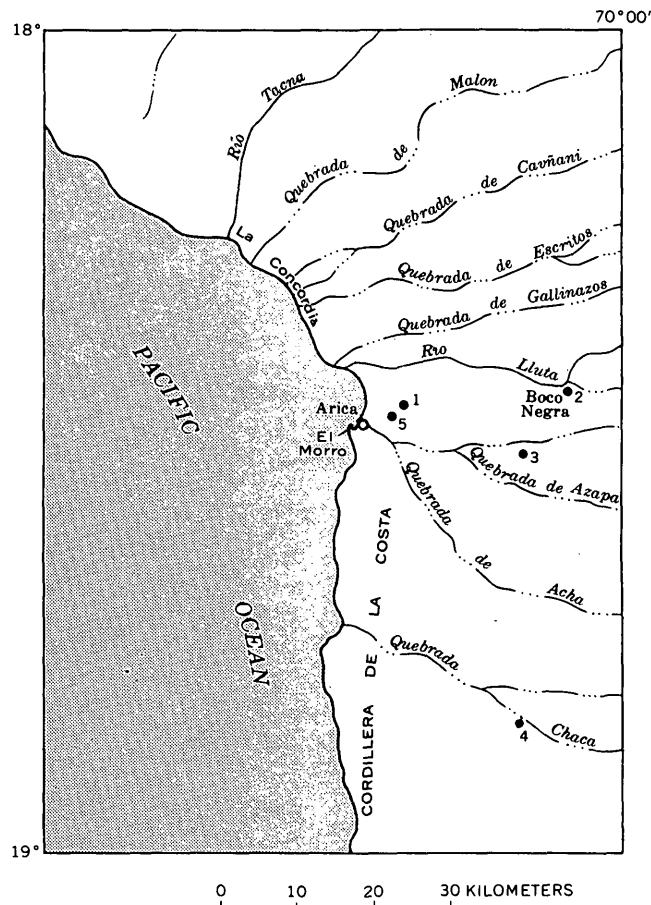

FIGURE 78.1.—Map of the Arica area, Chile, showing the locations from which samples were collected. *1*, Arica diatom deposit; *2*, Boca Negra diatom deposit; *3*, Dolomite beds; *4*, Chaca diatom deposit; *5*, Tertiary sediments.

diatomite near Arica by Frenguelli (1938), who considered it to be late Pleistocene. Because the last species, *Navicula fuenzalida*, occurs commonly in the Lluta Formation, more importance can be attached to it. The balance of the species found, with the exception of two thought to be new, are represented in living assemblages. The diatoms indicate a late Pleistocene age for the diatomaceous earth.

Some species of diatoms from the Lluta Formation (marked by the footnote reference in table 78.3) also occur in the Calama basin in the limestone considered by Frenguelli (1936) to be early Pleistocene. However, the most abundant species in all the collections studied for this report is *Denticula elegans*, a Recent form that goes back to late Tertiary. It is rare in the Calama basin. Although the diatomaceous deposits in which these collections were made may be early Pleistocene in age, the evidence for a late Pleistocene age is much more compelling. The diatom assemblages indicate deposition in a nonmarine, though somewhat saline, shallow lake, whose waters were cool to cold.

TABLE 78.3.—*Diatoms identified from the Lluta Formation in the Arica area*

[A, abundant; C, common; F, frequent; R, rare.   Numbers in boxheads are USGS diatom localities]

Diatom	8 km northeast of Arica					Boca Negra	
	5274	5276	5279	5280	5282	5284	5286
Achnanthes cf. *A. microcephala* Kützing [1]		F					R
Amphora acutiscula Kützing							R
lineata Ehrenberg						R	
salina Wm. Smith		F					
cf. *A. salina* Wm. Smith		R		F		R	
sp	R						
Anomoeoneis sphaerophora (Kützing) Pfitzer	F	F					
Caloneis formosa (Gregory) Cleve							R
Cocconeis placentula var. *euglypta* (Ehrenberg) Cleve [1]	F			F	R	R	F
Cymbella cf. *C. gracilis* (Rabenhorst) Cleve							F
turgida (Gregory) Cleve [1]		R					
sp	C						
Denticula elegans Kützing [1]	A	A	R	A	F	A	A
kittoniana Grunow							F
tenuis var. *crassula* (Naegli) Hustedt							F
valida Grunow [1]	F						
Epithemia turgida var. *granulata* (Ehrenberg) Kützing [1]	R			F			
Fragilaria construens var. *subsalina* Hustedt		F					
Gomphonema intricatum Kützing		F					
lanceolatum Ehrenberg	R						
lanceolatum var. *insignis* (Gregory) Cleve				F			
longiceps var. *gracilis* Hustedt				R			
Mastogloia atacamae Hustedt [1]							R
Mastogloia elliptica (Agardh) Cleve		F				R	C
elliptica var. *dansei* (Thwaites) Cleve	F	F					C
sp							R
Melosira spinigera Hustedt [1]						R	
Navicula cari Ehrenberg				F			
cryptocephala Kützing	F	F					
cryptocephala var. *veneta* (Kützing) Grunow		R					
cuspidata Kützing							F
fuenzalida Frenguelli		F			R		
lanceolata (Agardh) Kützing		R					
pupula var. *capitata* Hustedt	F	F					
cf. *M. simplex* Krasske				R			
sp		R					R
Nitzschia cf. *N. sublinearis* Hustedt	R						
sp							R

See footnotes at end of table.

TABLE 78.3.—*Diatoms identified from the Lluta Formation in the Arica area*—Continued

[A, abundant; C, common; F frequent; R, rare.   Numbers in boxheads are USGS diatom localities]

Diatom	8 km northeast of Arica					Boca Negra	
	5274	5276	5279	5280	5282	5284	5286
Pinnularia major (Kützing) Cleve				R			
viridis (Nitzsch) Kützing				R			
sp	R						
Rhopalodia gibberula (Ehrenberg) Muller	F						
gibberula var. *rupestris* Grunow [1]		R					
musculus (Kützing) Muller				R			
Synedra tabulata (Agardh) Kützing				R			
ulna (Nitzsch) Ehrenberg [1]	C	C		C	R		C

[1] Also occur in lacustrine limestone of the Calama basin.

REFERENCES

Ahlfeld, Friedrich, 1946, Geología de Bolivia: La Plata, Argentina, Mus. La Plata Rev. (nueva serie), Sección Geol., v. 3, p. 3–370.

Bertrand, A., 1885, Memoria sobre las Cordilleras del Desierto de Atacama i rejiones limitrofes: Santiago, Chile, Imprenta Nac.

Bowman, Isaiah, 1909, The physiography of the central Andes: Am. Jour. Sci., 4th ser., v. 29, no. 165, p. 197–217.

Bruggen, Juan, 1918, Infrome sobre el agua subterránea de la rejion de Pica: Santiago, Chile, Soc. Nac. de Minería.

—— 1950, Fundamentos de la geologia de Chile: Santiago, Chile, Instituto Geográfico Militar.

Dingman, R. J., 1963, Quadrangulo Tulor, Antofogasto Province, Chile: Santiago, Chile, Instituto Inv. Geol., Carta Geol. de Chile, v. 4 [In press]

Douglas, J. A. 1914, Geological sections through the Andes of Peru and Bolivia, pt. I—From the coast of Africa in the north of Chile to La Paz and the Bolivian "Yungas": Geol. Soc. London Quart. Jour., v. 70, p. 1–53.

Frenguelli, Joaquin, 1936, Diatomeas de la Caliza de la Cuenca de Calama: Mus. la Plata Rev. (nueva serie), Seccíon paleontologia, v. I, p. 3–34.

—— 1938, Analisis microscopico del tripoli de Arica: Santiago, Chile, Dept. Minas y Petroleos, Ministerio de Fomento.

Galli, C. O., and Dingman, R. J., 1962, Quadrangulos Pica, Alca, Matilla y Chacarilla: Santiago, Chile, Instituto Inv. Geol., Carta Geol. de Chile, v. 3, nos. 2, 3, 4, and 5, 125 p., 11 pl.

Groeber, Pablo, 1957, Chile, pt. 7 of Amerique Latine, in Hoffstetter and others, Lexique Stratigraphique International: Paris, France, Comm. Stratigraphy, Internat. Geol. Cong., v. 5, p. 195.

Jenks, W. F., 1948, Geologia de la Hoja de Arquipa: Lima, Peru, Dirección de Minas y Petroleo Bull. 9.

POSSIBLE PLEISTOCENE-RECENT BOUNDARY
IN THE GULF OF ALASKA, BASED ON BENTHONIC FORAMINIFERA

By PATSY B. SMITH, Menlo Park, Calif.

Abstract.—Of 10 cores from sediments in the Gulf of Alaska, 7 contained boreal faunas throughout, similar to those living in the area today, and 3 contained boreal foraminiferal faunas at the top and Arctic faunas in the lower part. It is inferred from the cores that the change in faunas marks a possible Pleistocene-Recent boundary in the sediments.

In the spring of 1961, 10 cores were taken by scientists on the U.S. Coast and Geodetic Survey ship *Pioneer* from sediments in the Gulf of Alaska, west and southwest of Kodiak Island (fig. 79.1). The coring was done under the direction of Lt. Comdr. H. P. Nygren, oceanographer of the *Pioneer*, and the samples were examined by G. W. Moore, U.S. Geological Survey, Menlo Park, Calif. Eight cores were obtained with a Phleger coring tube and two with a modified Ewing piston coring tube. Five of the cores are from the Continental Shelf (at depths of 76 to 240 meters) and five are from the north scarp of the Aleutian Trench (at depths of 810 to 5,540 meters) (table 79.1).

The top centimeter of each core was preserved in ethanol so that living Foraminifera could be recognized

TABLE 79.1.—*Location and length of cores and description of the top centimeter of sediment*

Core No.	Location		Depth (m)	Core length (cm)	Sediment	Color [1]
	Latitude (north)	Longitude (west)				
1	57°18′	155°20′	230	56	Clayey silt	Dark greenish gray.
3	54°33′	157°24′	2,070	6	___do___	Olive gray.
4	55°31′	156°16′	240	122	Medium sand	Grayish olive.
5	55°17′	155°09′	1,950	33	Clayey silt	Do.
6	55°52′	154°25′	810	54	Clayey very fine sand.	Grayish olive green.
7	56°25′	155°36′	76	15	Very fine sand	Dark greenish gray.
8	55°36′	158°23′	146	101	Sandy silt	Olive gray.
9	54°55′	157°59′	117	72	Pebbly medium sand.	Dark greenish gray.
10	54°51′	155°24′	4,170	13	Clayey silt	Do.
11	54°27′	155°23′	5,540	43	___do___	Olive gray.

[1] Color of the wet sediment follows the convention of Goddard and others (1948)
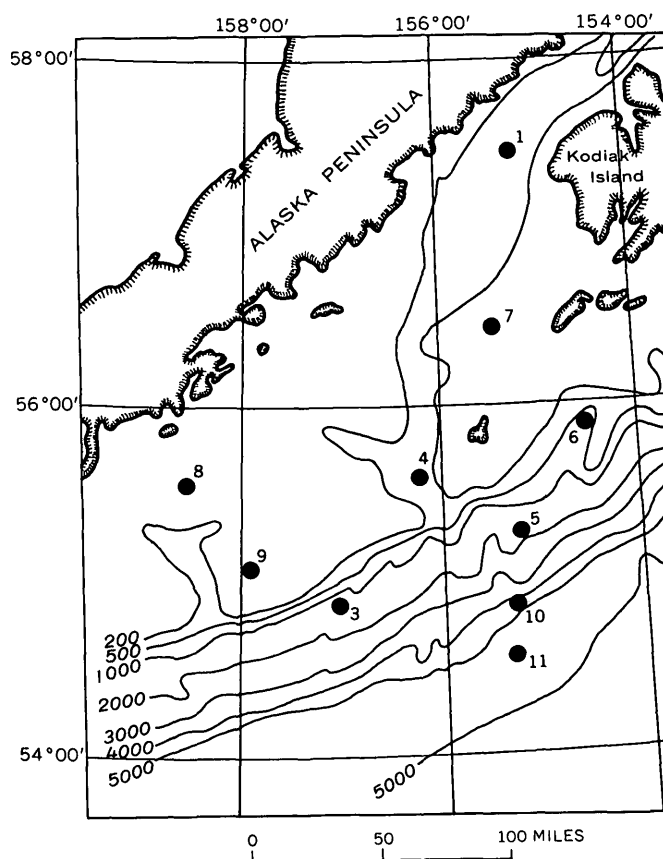

FIGURE 79.1.—Map of part of the Gulf of Alaska, showing station locations. Depth contours in meters.

by a stain test for protein. Generally, 1-centimeter samples were taken at 10-centimeter intervals from the remainder of each core. From these samples, distribution of successively older faunas was determined and the age and depositional environment of the cored sediments were interpreted.

Living and dead faunas (table 79.2) from the tops of all the cores are similar to those from the boreal waters of the Continental Shelf and Slope off Washington, Oregon, and California. A few species characteristic of arctic waters are present in the samples from the Continental Shelf and Slope in the Gulf of Alaska, but most forms characteristic of Arctic water are not present (Phleger, 1952; Loeblich and Tappan, 1953; Green, 1960).

The shallow (76–240 meters) benthonic faunas of the shelf samples (cores 9, 8, 7, 4, 1) are similar to those of the Continental Shelf off Washington, Oregon, and northern California (Enbysk[1]; Bandy, 1953). Characteristic species are most of the Nonions and Nonionel-

[1] Enbysk, B. J., 1960, Distribution of Foraminifera in the northern Pacific: Univ. Washington, Ph. D. thesis.

las, *Buliminella elegantissima*, *Uvigerina hollicki*, *Virgulina pauciloculata*, and *Epistominella pacifica* (generally a bathyal species off California).

The present bathyal faunas in the Gulf of Alaska (cores 6, 5, 3) (810–2,070 meters) have a wider distribution than the shallow faunas; many of the species occur at similar depths not only off Washington, Oregon, and California, but also off the coast of Central America (Smith, 1963). Included in these faunas are *Bolivina argentea*, *B. spissa*, *Bulimina marginospinata*, *B. subacuminata*, and most commonly, *Uvigerina peregrina*.

The present abyssal faunas (cores 10, 11) (4,170 and 5,540 meters) are composed almost entirely of arenaceous species, very similar to faunas found in deep north Pacific waters from the Aleutian Trench to Hawaii.

TABLE 79.2.—*Foraminifera in the top centimeter of each core*

[Abundance given as percentage of dead faunas. Number of living specimens shown in parentheses]

Depth zone	Shelf					Bathyal			Abyssal	
Core No.	7	9 [1]	8	1	4	6	5	3	10	11
Species — Depth (m)	76	117	146	230	240	810	1,950	2,070	4,170	5,540
Arenaceous										
Adercotrema glomeratum (Brady)			1	2. 5	<1(4)					1
Alveophragmium nitidum (Goes)			4. 5	1	<1	1			15	8
A. ringens (Brady)										<1
A. subglobosum (G. O. Sars)									10	1
A. weisneri (Parr)										<1
Ammobaculites agglutinans (d'Orbigny)										9
A. cf. A. americanus (d'Orbigny)										3
A. agglutinans filiformis Earland										6. 5
Ammoglobigerina globigeriniformis (Parker and Jones)								<1	10	2
Ammomarginulina foliacea (Brady)									5	2
Bigenerina minutissima (Earland)			<1							<1
Cornuspira involvens (Reuss)							2			
Cyclammina cancellata Brady										<1
C. trullissata (Brady)						<1			5	<1
Cystammina galeata (Brady)									5	
Eggerella bradyi (Cushman)							7	10	30	1
Eggerella propinqua (Brady)						1				
E. scabra (Williamson)	1		2(1)	2	7			1. 5		
Gaudryina sp					<1					
Glomospira gordialis (Jones and Parker)										2
Haplophragmoides canariensis (d'Orbigny)			1							
Hyperammina and Astrorhiza spp										Frag. A
Involutina tenuis (Brady)										2
Jaculella acuta Brady										<1
Karreriella apicularis (Cushman)										<1
Nodellum membranaceum (Brady)										<1
Placopsilina bradyi Cushman and McCulloch										7
Psammosphaera fusca Schulze										6
Reophax bacillaris Brady			1		<1					
R. difflugiformis Brady						<1	2		10	16
R. distans Brady										2
R. nodulosus Brady										2. 5
R. scorpiurus Montfort			1							2
R. scotti Chaster							5. 5			
Spiroplectammina biformis (Parker and Jones)			1. 5	<1	1	1			5	
Textularia torquata Parker			1		<1	<1				
Trochammina grisea Heron-Allen and Earland										<1
T. cf. I. inflata (Montagu)					<1	<1				
T. kellettae Thalmann					1	1(1)		2		
T. cf. T. malovensis Heron-Allen and Earland										1

See footnote at end of table

TABLE 79.2.—*Foraminifera in the top centimeter of each core*—Continued

[Abundance given as percentage of dead faunas. Number of living specimens shown in parentheses]

Species / Depth zone	Shelf					Bathyal			Abyssal	
Core No.	7	9¹	8	1	4	6	5	3	10	11
Depth (m)	76	117	146	230	240	810	1,950	2,070	4,170	5,540
Calcareous benthonic										
Angulogerina angulosa (Williamson)		(1)			5(4)	2		5.5		
Astrononion gallowayi Loeblich and Tappan			1		<1(1)	1	2			
Bolivina argentea Cushman						<1				
B. decussata Brady	10	(3)	2	<1(1)	9(4)	2.5		<1		
B. pacifica Cushman and McCulloch	1	(3)	1(2)	<1	<1	1		<1(2)		
B. pseudobeyrichi Cushman					<1	<1				
B. spissa Cushman						17(11)		<1		
Buccella frigida (Cushman)		(1)	3.5	<1	<1					
Bulimina cf. *B. auriculata* Bailey		(1)								
B. marginospinata Cushman and Parker						1(2)	5.5			
B. subacuminata Cushman						13(5)				
Buliminella elegantissima (d'Orbigny)	1		<1(1)		1					
B. subfusiformis Cushman						3(2)		<1		
Cassidulina cushmani R. E. and K. C. Stewart						8(3)				
C. islandica nørvangi Thalmann			2	4(6)	1			21		
C. norcrossi Cushman			1(1)	<1	1		2	<1		
C. cf. *C. subglobosa* Brady									(1)	
Cibicides lobatulus (Walker and Jacob)		(2)			<1(1)	<1				
Ehrenbergina sp						1				
Elphidium cf. *E. incertum* (Williamson)				<1	<1					
E. magellanicum Heron-Allen and Earland	10									
Epistominella exigua (Brady)	37	(1)	17(4)	13(43)	33(15)	<1		32(1)		
E. pacifica (Cushman)				15(9)	4.5(3)	<1				
Eponides tenera (Brady)							4			
Eponides tumidulus (Brady)			2.5							
Globobulimina pacifica Cushman					<1(4)	<1				
Lagenid spp	1		<1	<1	1	2.5	2			
Loxostomum amygdaliformis (Brady)		(1)								
Nonion cf. *N. depressulum* (Walker and Jacob)					2.5(6)			6		
N. grateloupi (d'Orbigny)	1		<1	4	<1					
N. labradoricum (Dawson)		(8)	5(3)	1	<1(2)		2			
Nonionella auricula Heron-Allen and Earland						1	15(8)	1		
N. bradii Chapman	7		9(6)	6	12					
N. globosa Ishiwada			8(5)	<1	<1	1(2)	2			
N. miocenica stella Cushman					2.5(20)					
Pullenia bulloides (d'Orbigny)							4			
P. subcarinata (d'Orbigny)		(1)			<1	1	2			
Quinqueloculina spp			1	1	<1					
Robulus sp					1(2)					
Rosalina sp	1									
Uvigerina hollicki Thalmann		(1)	5.5(4)	17(18)	19(5)					
U. peregrina Cushman						14(15)	4	3.5		
Valvulineria sp					1	2(1)	2	<1(2)		
Virgulina pauciloculata Brady	10	(1)	25(11)	8	<1(1)			2		
V. seminuda Natland							4			
V. spinosa Heron-Allen and Earland			<1	1.5	<1			<1		
Planktonic										
Globigerina bulloides d'Orbigny	16			4.5	<1	4	9	<1		
G. pachyderma Ehrenberg				11	4	11	9	10		
Globigerinita uvula (Ehrenberg)	3			<1	2	<1				
Total dead population	67		196	260	1,200	190	26	175	20	928

¹ Only living specimens counted, as reworked Pleistocene(?) specimens are present.

Faunas from below the top of the cores were also examined. Cores 1, 5, 6, and 7 contained faunas over the length of the core similar to those at the top. Cores 4, 8, and 9 contained boreal faunas at the top but arctic benthonic faunas in the lower part. In core 4 (table 79.3) the change in faunas occurs between 26 and 29 centimeters; in core 8, between 80 and 90 centimeters; and in core 9, within the first 2 centimeters. All three cores contain similar faunas, and except for the depth of the faunal break the three cores are similar. The upper layer, characterized by a Recent fauna, generally thins toward the edge of the shelf. The bathyal and abyssal faunas in cores 3, 5, 10, and 11 show no significant change from top to bottom.

TABLE 79.3.—*Distribution of Foraminifera in core 4*

[Abundance given as percentage of dead faunas. Number of living specimens in top 2 cm is shown in parentheses]

Species / Depth in core (cm)	Recent 0-2	Recent 2-14	Recent 14-26	Pleist. 26-29	29-32	41-42	51-52	61-62	71-72	81-82	91-92	101-102
Arenaceous												
Adercotrema glomeratum (Brady)	<1(4)	<1										
Alveophragmium nitidum (Goes)	<1	<1										
A. ringens (Brady)		<1										
Eggerella bradyi (Cushman)		<1										
E. scabra (Williamson)	7(5)	<1										
Gaudryina sp	<1	<1	1	<1	<1							
Haplophragmoides spp		<1										
Karreriella bradyi (Cushman)				2	<1							
Reophax bacillaris Brady	<1											
R. difflugiformis Brady		<1										
Spiroplectammina biformis (Parker and Jones)	<1	<1										
Textularia torquata Parker	<1											
Trochammina cf. T. inflata (Montagu)	<1											
T. kellettae Thalmann	1	<1	<1	<1			<1	<1		<1		
Calcareous benthonic												
Angulogerina angulosa (Williamson)	5(4)	23	30	8	5	<1		<1	<1	<1	<1	<1
Astacolus sp								<1				
Astrononion gallowayi Loeblich and Tappan	<1(1)	1	2					<1		<1		
Bolivina decussata Brady	9(4)	4	1.5	6	6	<1	<1	<1		<1	<1	<1
B. pacifica Cushman and McCulloch	<1	<1	<1	<1	<1	<1	<1	<1		<1	<1	
B. pseudobeyrichi Cushman	<1	<1	<1									
B. spissa Cushman		<1	<1									
Buccella frigida (Cushman)	<1			1	2							
B. inusitata Anderson		1.5	1	3	7.5	2	3.5	5	3	5	5	4.5
Buliminella elegantissima (d'Orbigny)	1(1)	<1	<1	<1	<1							
B. subfusiformis Cushman		<1										
Cassidulina islandica Nørvang		1	<1	10	3	3	3	3	2.5	10.5	3.5	2.5
C. islandica nørvangi Thalmann	1	<1	<1	10	9	11	8.5	8	11	17	8.5	11
C. norcrossi Cushman	1	3	6	2	1	<1	1	<1		<1	<1	1
Cibicides lobatulus (Walker and Jacob)	<1(1)	<1	<1	8	7.5	<1	1	2	2.5	5	3	4.5
C. pseudoungerianus (Cushman)		<1	1	<1			<1					
Dentalina spp				<1		1	<1		<1	<1	1	
Dyocibicides biserialis Cushman and Valentine				3	<1							
Elphidium cf. E. bartletti Cushman				1.5	5	2	7	6	6	4.5	3	5.5
E. clavatum Cushman			<1	10	12	30	30	26	40	13	32	31
E. cf. E. incertum (Williamson)	<1	<1										
Elphidiella groenlandica (Cushman)				5	1.5	2	1.5	2	1	5	15	4
Epistominella exigua (Brady)	33(15)	6	4	11	9	23	16	15	16	17	13	8
E. pacifica (Cushman)	45(3)	12	7	<1	<1	1	1	1				
Globobulimina pacifica Cushman	<1(4)	<1	<1	<1	<1							
Gyroidina broekiana (Karrer)		<1	<1	<1								
Lagenid spp	1	1.5	2	2	1.5	3.5	2.5	4	3.5	3.5	5	3
Nonion cf. N. depressulum (Walker and Jacob)	2.5(6)		<1		1.5							
N. grateloupi (d'Orbigny)	<1			1	1.5	2	2		<1	<1	1	<1
N. labradoricum (Dawson)	<1(2)	1	<1	<1		6.5	3.5	4	<1	2	4	2
Nonionella auricula Heron-Allen and Earland					1							
N. bradii (Chapman)	12	2.5	<1						1	1	2	1.5
N. globosa Ishiwada	<1	<1					<1					
Parafrondicularia advena Cushman				<1								
Patellina corrugata Williamson							<1					
Pullenia subcarinata (d'Orbigny)	<1	<1	<1	<1	<1							
Pyrgo spp				4								
Quinqueloculina stalkeri Loeblich and Tappan				<1	<1	1						
Q. spp	<1	<1		<1								
Robertinoides sp				<1								
Rodulus sp	<1(2)	<1	<1		<1							
Triloculina spp							<1	<1	1		<1	1
Uvigerina hollicki Thalmann	19(5)	28	30	1	<1	<1	<1				<1	
Valvulineria sp		<1									1	<1
Virgulina pauciloculata Brady	<1(1)	<1		<1	<1	<1	<1					
V. spinosa Heron-Allen and Earland	<1	<1										

TABLE 79.3.—*Distribution of Foraminifera in core 4*—Continued

[Abundance given as percentage of dead faunas. Number of living specimens in top 2 cm is shown in parenthesis]

Age / Species — Depth in core (cm)	Recent			Pleistocene(?)								
	0-2	2-14	14-26	26-29	28-32	41-42	51-52	61-62	71-72	81-82	91-92	101-102
Planktonic												
Globigerina bulloides d'Orbigny	<1	1	<1	5	9	4	6	6	3	7	11	12
G. pachyderma Ehrenberg	4	7	6.5	8	9	6	4	6	8	5	3.5	5.5
Globigerinita uvula (Ehrenberg)	2			1	<1							
Total population in 10 cc of sediment	1,200	1,280	250	900	1,000	500	350	325	190	700	440	460

The distribution of species in core 4 is tabulated in table 79.3. The faunas of the upper 26 centimeters of this core contain a high percentage of *Angulogerina angulosa, Epistominella pacifica*, and *Uvigerina hollicki*. The faunas below 29 centimeters are characterized by *Cassidulina islandica* and subsp. *nørvangi, Elphidium* cf. *E. bartletti, E. clavatum*, and *Elphidiella groenlandica*. These species are characteristic of Recent faunas of the Point Barrow region (Loeblich and Tappan, 1953) and the Canadian and Greenland Arctic (Phleger, 1952). The species characterizing the upper part of the core, with a few exceptions, form only a very small percentage of the faunas from the lower part.

In core 4, woody material is common below the faunal break and rare above. Chlorite is the predominant clay mineral below and montmorillonite above. G. W. Moore (written communication, 1961) considers the chlorite to have been derived from the erosion of rocks on Kodiak Island by former glaciers. Perhaps the woody material was also delivered to the marine environment by these glaciers.

The evidence suggests that while the sediment sampled by cores 4, 8, and 9 was being deposited, the water temperature and characteristics abruptly changed from Arctic to boreal. The most probable explanation for this change is that the lower sediment containing the abundant Arctic species was deposited when glaciers and pack ice were nearby and that the upper sediment was deposited when conditions resembled those of today. Thus, the faunal break in the cores marks a possible Pleistocene-Recent boundary in the sediments in the Gulf of Alaska.

REFERENCES

Bandy, O. L., 1953, Ecology and paleoecology of some California Foraminifera, pt. I, The frequency distribution of Recent Foraminifera off California : Jour. Paleontology, v. 27, no. 2, p. 161–182, pl. 21–25, 4 figs.

Goddard, E. N., and others, 1948, Rock-color chart : Washington, Natl. Research Council, 11 p.

Green, K. E., 1960, Ecology of some Arctic Foraminifera : Micropaleontology, v. 6, no. 1, p. 57–78, 1 pl., 9 text figs., 6 tables.

Loeblich, A. R., Jr., and Tappan, Helen, 1953, Studies of Arctic Foraminifera : Smithsonian Misc. Coll., v. 121, no. 7, 142 p., 24 pl.

Phleger, F. B., 1952, Foraminifera distribution in some sediment samples from the Canadian and Greenland Arctic : Cushman Found. Foram. Research, Contr., v. 3, p. 80–88, pl. 13, 14, 1 table, 1 text fig.

Smith, P. B., 1963, Recent Foraminifera off Central America. Ecology of benthonic species : U.S. Geol. Survey Prof. Paper 429-B. [In press]

Article 80

PETROLOGY OF RHYOLITE AND BASALT, NORTHWESTERN YELLOWSTONE PLATEAU

By WARREN HAMILTON, Denver, Colo.

Abstract.—Late Pliocene and Quaternary rhyolite ash-flow tuffs and lava flows are compositionally uniform and have a very high silica content. Olivine basalt and olivine basaltic andesite are greatly subordinate in outcrop abundance but may be widespread beneath young rhyolite lava flows.

The Yellowstone Plateau is an upland 50 miles across in northwestern Wyoming and adjacent Montana and Idaho. The northwest part of the plateau (fig. 80.1) consists in the north of welded rhyolite ash-flow tuffs of late Pliocene or early Pleistocene age, which have been warped down beneath the West Yellowstone basin and raised up on the flanks of the Madison Range to the west. The rhyolite ash-flow tuff section is broken by an arcuate fault, locally composite and everywhere concealed by younger rhyolite in the area of figure 80.1, along which the rocks on the southeast side were dropped more than 1,500 feet (Boyd, 1961). Enormous steep-fronted lava flows that erupted during late Pleistocene time, after the faulting, overlap the fault scarp. The Central Plateau, forming the central part of the Yellowstone Plateau, consists of rhyolite lava flows extruded from scattered vents (fig. 80.1) which apparently overlay a large magma chamber. The lava flows of the Madison Plateau were extruded from a crestal fissure zone trending north-northwestward (Hamilton, 1960, fig. 1). Minor volcanism has continued into Recent time in the Madison Plateau, south of the area of figure 80.1 (Hamilton, 1960). An extrusive rhyolite obsidian dome of middle(?) Pleistocene age stands at the east edge of the West Yellowstone basin (fig. 80.1).

The rhyolite of all occurrences generally contains crystals of high quartz and clear sanidine, and commonly of oligoclase (Boyd, 1961). The mafic minerals are sparse iron oxides and clinopyroxene, and rare fayalite; biotite and hornblende are nearly lacking (Boyd, 1961; Hamilton, 1960). The rhyolite lava flows have lithoidal interiors which grade upward into obsidian breccias consisting of flow-contorted obsidian blocks in a matrix of unconsolidated, sandlike glass shards (Boyd, 1961; Hamilton, 1960).

A few small flows of nearly holocrystalline olivine-augite-labradorite basalt and olivine-augite-calcic andesine basaltic andesite lie upon the rhyolite ash-flow tuff. Similar basalt is probably widespread beneath the young rhyolite lava flows. The large moraines of Bull Lake (early? late Pleistocene) age of the southern part of the West Yellowstone basin were deposited by ice that flowed from the central part of Yellowstone Plateau, since buried by young rhyolite lava flows (Richmond and Hamilton, 1960). Blocks in the moraines are almost entirely of olivine basalt, although such basalt forms only a minute proportion of the exposed rocks of the plateau. During Bull Lake time the central part of the plateau may have been surfaced largely by basalt erupted in the interval between extrusion of the rhyolite ash flows and the rhyolite lava flows. No mafic rocks younger than the rhyolite lava flows are known.

The accompanying table presents 3 new analyses of basalt and basaltic andesite and 8 of rhyolite from the northwestern part of the Yellowstone Plateau. The mafic rocks analyzed are all from flows; of the specimens of rhyolite, 3 are from lava flows, 1 is from an extrusive obsidian dome, and 4 are from welded ash-flow tuff.
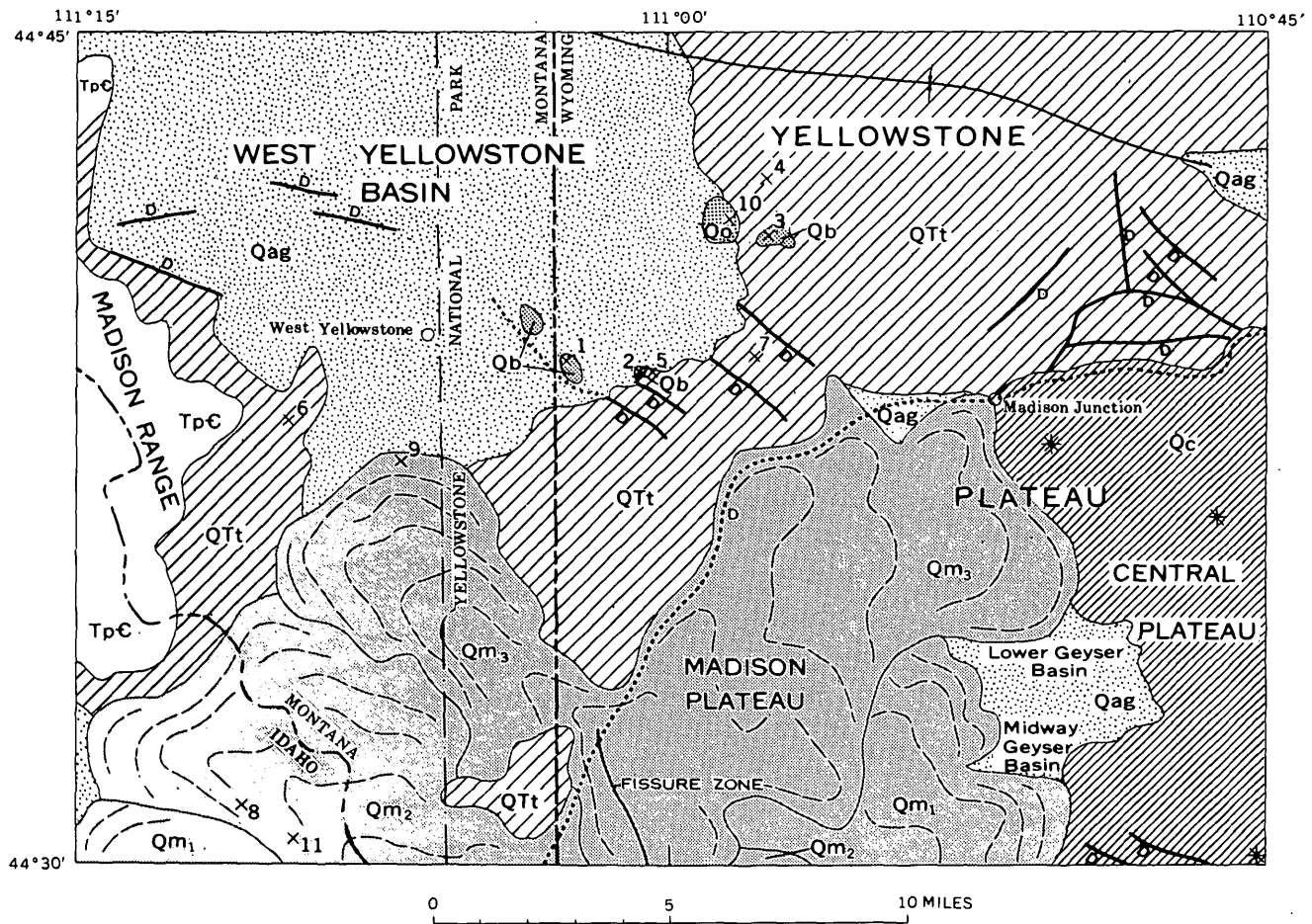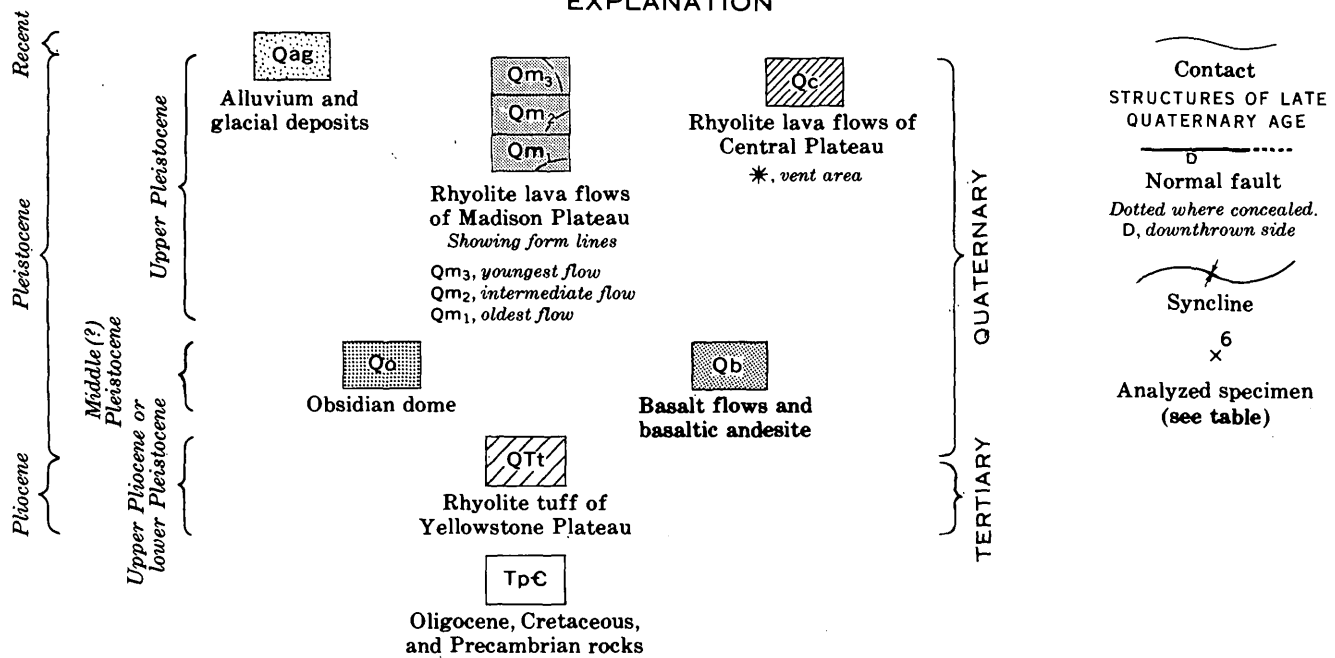
FIGURE 80.1.—Geologic map of the northwest part of the Yellowstone Plateau, Idaho, Montana, and Wyoming. Geology by Warren Hamilton in 1959, with additions from Boyd (1961) and W. Bradley Myers (written communication, 1962).

Chemical analyses of basalt and rhyolite of the northwest part of Yellowstone Plateau

[Major oxides determined by rapid colorimetric methods by Paul Elmore, I. Barlow, S. Botts, and G. Chloe, Washington, D.C., 1961. Fluorine and chlorine determined by Vertie C. Smith, Denver, Colo., 1961. Other minor elements determined by semiquantitative spectrographic methods by Paul R. Barnett, Denver, Colo., 1961; values reported as midpoints of logarithmic-third divisions]

	Basalt and basaltic andesite			Rhyolite ash-flow tuff				Rhyolite lava-flow and dome rocks				Averages of column 4-11	Range of columns 4-11
	1	2	3	4	5	6	7	8	9	10	11	12	13
Field number	YS 6 H 3303	YS 20C H 3310	YS 5 H 3302	YS 4 H 3301	YS 20A H 3309	YS 8 H 3305	YS 24 H 3311	YS 26A H 3313	YS 7A-2 H 3304	YS 3 H 3300	YS 27 H 3314		
Laboratory numbers	158059	158055	158047	158046	158054	158050	158056	158058	158049	158045	158048		
Major oxides, in weight percent													
SiO$_2$	46.7	48.1	51.5	75.8	76.1	77.3	77.3	75.7	75.8	76.4	76.7	76.4	75.7-77.3
Al$_2$O$_3$	15.7	15.7	15.5	12.4	12.7	12.5	12.2	11.9	12.0	12.2	11.9	12.2	11.9-12.7
Fe$_2$O$_3$	1.2	4.2	2.0	1.2	1.7	.8	1.3	.5	.8	.5	.5	.9	}0.9-1.9 as
FeO	13.0	9.4	9.0	.40	.10	.17	.08	1.0	1.2	.84	1.2	.6	}FeO
MgO	6.8	6.8	6.0	.15	.16	.07	.08	.06	.18	.21	.13	.13	0.07-02
CaO	9.3	9.2	8.5	.27	.34	.24	.22	.34	.57	.57	.38	.4	0.2-0.6
Na$_2$O	3.2	3.3	3.0	3.3	3.3	3.3	3.6	3.3	3.4	3.0	3.4	3.3	3.0-3.6
K$_2$O	.46	.56	1.1	5.0	5.0	4.8	4.6	5.0	4.9	5.0	5.0	4.9	4.6-5.0
H$_2$O	.30	.18	1.2	.72	.30	.58	.30	1.1	.32	.68	.60	.6	0.3-1.1
TiO$_2$	2.4	2.2	1.8	.14	.14	.10	.10	.12	.20	.13	.14	.13	0.1-0.2
P$_2$O$_5$	.39	.33	.28	.02	.02	.02	.02	.02	.02	.04	.01	.02	0.01-0.04
MnO	.22	.21	.17	.03	.04	.04	.02	.04	.06	.03	.04	.04	0.02-0.06
Total	99.7	100.2	100.1	99.4	99.9	99.9	99.8	99.1	99.5	99.6	100.0		
Minor elements, in weight percent													
Ba	0.03	0.03	0.07	0.07	0.07	0.003	0.007	0.015	0.03	0.07	0.015	0.04	0.007-.07
Be	<.0001	<.0001	<.0001	.0003	.0003	.0003	.0003	.0003	.0003	.0003	.0003	.0003	.0003
Ce	<.01	<.01	<.01	.015	.015	<.01	<.01	.015	.015	.015	.015	~.01	<.01-.015
Cl	.01	.01	.02	.01	.03	.02	.02	.09	.08	.09	.09	.05	.01-.09
Co	.007	.007	.007	<.0002	<.0002	<.0002	<.0002	<.0002	<.0002	<.0002	<.0002	<.0002	
Cr	.015	.015	.015	<.0001	.00015	<.0001	<.0001	<.0001	.00015	<.0001	<.0001	<.0001	<.0001-.00015
Cu	.007	.007	.003	.00015	.003	.00015	.00015	.00015	.0003	.0003	.00015	~.001	.00015-.003
F	.03	.03	.03	.01	.01	.03	.03	.14	.14	.12	.14	.08	.01-.14
Ga	.0015	.0015	.0015	.0015	.0015	.0015	.0015	.003	.0015	.003	.0015	.002	.0015-.003
La	<.002	<.002	<.002	.007	.007	.007	.003	.007	.015	.007	.015	.008	.003-.015
Mo	<.0002	<.0002	<.0002	.0003	<.0002	.0003	.0003	.0003	.0003	.0003	.0003	.0003	<.0002-.0003
Nb	<.0005	<.0005	<.0005	.003	.003	.003	.003	.003	.003	.0015	.003	.003	.0015-.003
Nd	<.005	<.005	<.005	.007	.007	<.005	<.005	.007	.015	<.005	.015	~.004	<.005-.015
Ni	.007	.015	.007	<.0002	<.0002	<.0002	<.0002	<.0002	<.0002	.0003	<.0002	<.0002	
Pb	<.0005	<.0005	<.0005	.0015	.0015	.0007	.0015	.0015	.0015	.0015	.0015	.0015	.0007-.0015
Sc	.003	.003	.003	<.0005	<.0005	<.0005	<.0005	<.0005	<.0005	<.0005	<.0005	<.0005	
Sn	<.0002	<.0002	<.0002	.0007	.0007	<.0002	.0015	.0007	.0007	.0007	.0007	.0007	<.0002-.0015
Sr	.07	.07	.07	.0015	.003	.0015	.0007	.0007	.0007	.003	.0007	.001	.0007-.003
V	.03	.03	.03	<.0005	<.0005	<.0005	<.0005	<.0005	<.0005	<.0005	<.0005	<.0005	
Y	.003	.003	.003	.003	.003	.003	.003	.0015	.007	.007	.003	.004	.0015-.007
Yb	.0003	.0003	.0003	.0003	.0007	.0003	.0003	.0003	.0007	.0007	.0003	.0005	.0003-.0007
Zr	.007	.007	.015	.03	.03	.015	.015	.015	.03	.015	.015	.02	.015-.03

Descriptions of analyzed specimens follow (see analyses in table and locations on figure 80.1):

1. Olivine-augite basalt. Dense medium-light-gray flow rock of subophitic texture. Flow-alined laths of labradorite are partly enclosed in plates of light-green augite. Forsteritic olivine forms granules and microphenocrysts. Ilmenite and magnetite are euhedral. Collected from quarry (in hill 6809, south of Madison River, West Yellowstone quadrangle) 2.6 miles east of West Yellowstone.

2. Olivine-augite basalt. Very fine grained (0.01–0.1 mm) medium-gray flow rock with small irregular vesicles; intergranular texture. Sodic labradorite occurs as tiny zoned laths, greenish augite is in granules, and olivine forms subhedral prisms. Magnetite and ilmenite are irregular. Sparse microphenocrysts of labradorite are 0.5 mm long. Collected from highway cut 4.1 miles east of West Yellowstone.

3. Olivine-augite basaltic andesite. Finely vesicular medium-light-gray flow rock. Microphenocrysts of labradorite lie in a groundmass consisting of laths of calcic andesine, granules of augite, magnetite, and sparse olivine. Collected near Cougar Creek road (northwest of hill 7210, Madison Junction quadrangle), 6.8 miles east-northeast of West Yellowstone.

4. Devitrified welded rhyolite ash-flow tuff. Light-gray rock consisting of crystals and fragments of sanidine (abundant) and oligoclase (An$_{20}$, sparse) in thoroughly divitrified hazy aggregate of minute grains of quartz, feldspar, and opaque dust. One fragment of clinopyroxene noted in thin section. Outlines of squashed shards faintly visible. Collected 7.9 miles east-northeast of West Yellowstone (on north side of Cougar Creek near Cougar Creek patrol cabin, Madison Junction quadrangle).

5. Partly devitrified welded rhyolite ash-flow tuff. Light-purplish-gray porcelaneous rock streaked by white, consisting of large squashed shards and crystal fragments of sanidine (abundant), quartz (common), and oligoclase (An$_{25}$, uncommon). Much hematite dust and minor anhedral magnetite is in the glass, which is partly devitrified. Overlain by basalt (specimen 2). Collected from highway cut 4.1 miles east of West Yellowstone.

6. Devitrified welded rhyolite ash-flow tuff. Light-purplish-gray rock streaked by white, consisting of thoroughly devitrified welded tuff containing fragments of sanidine (abundant), quartz (sparse), and clinopyroxene (rare). Collected 3 miles west-southwest of West Yellowstone (from roadcut on west side of the South Fork of Madison River, West Yellowstone quadrangle).

7. **Spherulitic rhyolite.** Very light purplish gray rock, consisting largely of 3-mm spherulites enclosing phenocrysts of sanidine (abundant) and quartz (sparse). Spherules were produced by devitrification of a glassy rock that could have been a flow but was probably a welded tuff. Collected 6.5 miles east of West Yellowstone (from cliffs southwest of Madison River, Madison Junction quadrangle).

8. **Unconsolidated rhyolite shards.** Angular shards and splinters of clear to smoky glass, some subpumiceous, 0.2 to 5 mm long. No welding or rounding. This is the matrix material of the obsidian breccia at the top of a very thick rhyolite flow. Collected 10.1 miles south-southwest of West Yellowstone (from roadcut of Black Canyon forest access road, West Yellowstone quadrangle).

9. **Rhyolite obsidian.** Black glass, containing phenocrysts of sanidine (abundant) and quartz (common), and numerous spherulites. Flow structures are shown by abundant microlites of clinopyroxene (0.001×0.003 mm) and feldspar; flow structures pass uninterrupted through devitrification spherulites. The sample is from an obsidian block in breccia at top of a rhyolite flow and was collected from the front of the flow, 2.3 miles south of West Yellowstone.

10. **Rhyolite obsidian.** Granular black obsidian, crowded with 1- to 5-mm pink spherulites and sanidine crystals. Strong swirled flow structure, shown by microlites of clinopyroxene and feldspar(?), passes uninterrupted through the devitrification spherulites. Scattered phenocrysts of sanidine and sparse fragments of micropegmatite; rare phenocrysts of grid-twinned albite and fayalite ($-2V = 50°$). Collected from obsidian dome (hill 7085, Madison Junction quadrangle) 6.5 miles east-northeast of West Yellowstone.

11. **Rhyolite obsidian.** Granular-structured undevitrified black obsidian with many sanidine phenocrysts. Flow structures are defined by microlites. Collected (along Black Canyon forest access road) from block in obsidian breccia at top of rhyolite flow, 10.6 miles west of south from West Yellowstone.

The basalt and basaltic andesite have a high content of iron and moderate content of magnesium, calcium, alkalies, and titanium. Their minor-element content is typical of nonalkaline mafic rocks.

Rhyolite throughout the Yellowstone Plateau is highly silicic and varies little from the average (columns 12 and 13 of table); relative to calc-alkaline rhyolite of andesitic associations, this rhyolite is a little high in both silica and sodium content, and a little low in aluminum, magnesium, calcium, and potassium content. The relatively high ratio of alkalies to aluminum in the rhyolite of the Yellowstone Plateau is reflected mineralogically in the presence of clinopyroxene and fayalite and in the absence of biotite and hornblende.

The average of the new analyses (column 12) is practically the same as the average of 10 prior modern analyses of rhyolite from varied occurrences and different parts of the plateau (Hamilton, 1959, table 1). The ranges of oxides are a little greater in those 10 analyses;

for example, SiO_2 ranges from 73.1 to 78.0 percent in them, whereas it ranges only from 75.7 to 77.3 in the new analyses. The greater ranges in the older group may reflect analytical biases of the several laboratories involved, and the true range throughout the plateau may be generally closer to that of the new analyses.

Comparison of samples of welded rhyolite ash-flow tuff (columns 4–6 and probably 7) with the rocks of lava flows and the dome (columns 8–11) shows that the two groups are virtually identical in most components, varying through the same narrow ranges in each. There are, however, differences in some components. The lava flows appear to contain slightly less alumina and slightly more calcium. The lava-flow rocks contain a much greater quantity of halogens: they contain an average of 4 times as much chlorine and 7 times as much fluorine as do the welded ash-flow tuffs. Presumably chlorine and fluorine were lost with the steam during transport and welding of the ash-flow tuffs. The total iron content is the same in each type, but 75 to 95 percent of it is oxidized in the ash-flow tuffs, whereas only 30 to 40 percent is oxidized in the lava-flow rocks. The degree of oxidation of iron appears from this sampling to provide a tentative means to distinguish welded ash-flow tuffs from lava-flow rocks. Presumably the high oxidation of the iron is due to the high content of supercritical water of the ash-flow magmas.

Rhyolite and low-alkali olivine basalt are closely associated throughout the Snake River province of Pliocene and Quaternary volcanism, of which the Yellowstone Plateau is the high, east end. Rocks intermediate between basaltic andesite and quartz latite are lacking. The contrasted basic and silicic magmas have come from the same chambers in some instances. Field and petrologic characteristics are satisfied by the explanation that tholeiitic basaltic magma has here fractionated as a liquid, before appreciable crystallization, into olivine-basaltic and rhyolitic magmas.

REFERENCES

Boyd, F. R., 1961, Welded tuffs and flows in the rhyolite plateau of Yellowstone Park, Wyoming: Geol. Soc. America Bull., v. 72, no. 3, p. 387–426.

Hamilton, Warren, 1959, Yellowstone Park area, Wyoming: a possible modern lopolith: Geol. Soc. America Bull., v. 70, no. 2, p. 225–228.

——— 1960, Late Cenozoic tectonics and volcanism of the Yellowstone region, Wyoming, Montana, and Idaho, in Billings Geol. Soc. Guidebook 11th Ann. Field Conf., West Yellowstone-earthquake area, 1960: p. 92–105.

Richmond, G. M., and Hamilton, Warren, 1960, The late Quaternary age of obsidian-rhyolite flows in the western part of Yellowstone National Park, Wyoming: U.S. Geol. Survey Prof. Paper 400–B, p. B224–B225.

Article 81

THE CANYON MOUNTAIN COMPLEX, OREGON, AND THE ALPINE MAFIC MAGMA STEM

By T. P. THAYER, Washington, D.C.

Abstract.—The Canyon Mountain Complex shows relations between peridotite, gabbro, quartz diorite, and albite granite that characterize a Lower to Middle Triassic magma series in eastern Oregon. Because of their similarities, these Oregon rocks, the Troodos Complex in Cyprus, and certain other alpine peridotite-gabbro complexes are believed to belong to a distinctive alpine mafic magma stem.

At least two major types of nonalkalic ultramafic rock associations are now recognized: stratiform and alpine. The stratiform ultramafic rocks show remarkable layering, are associated with large volumes of gabbroic rocks, and, it is generally agreed, were formed by fractional crystallization of basaltic magma in place. The alpine ultramafic rocks may or may not be closely associated with gabbroic rocks and occur along geosynclinal belts that have undergone an alpine type of deformation. Although there are differing opinions (Hess, 1955), rapidly mounting field evidence points to emplacement of the many alpine ultramafic rocks as crystal mushes (Thayer, 1960) or fragmented solid masses (De Roever, 1957), as postulated by Bowen and Tuttle (1949). The presence of gabbro as an essential constituent of several peridotite-rich alpine complexes (Guild, 1947; Flint and others, 1948; Rossman and others, 1959; Thayer, 1963) suggests that there may be more siliceous members in the petrogenetic series. This, in turn, leads to the concept of an alpine magma stem.

The Canyon Mountain Complex in eastern Oregon is one of three examples in which mapping has demonstrated the existence of a complete series of rocks ranging in composition from peridotite to albite granite (Gilluly, 1937) or closely related albite- and quartz-rich rocks. The complex consists mainly of peridotite and gabbro which form Canyon Mountain (after which the complex is here named) and occupies an area about 12 miles long by 5 miles wide across the John Day quadrangle, Oregon (fig. 81.1). It is faulted off at the east end and along half of the north side; elsewhere it intrudes volcanic and sedimentary rocks, of which at least part are Late Permian in age. On the west, Upper Triassic pillow lava, conglomerate, and graywacke lie unconformably on serpentine that forms part of the present border of the complex.

The complex, which is believed to have been emplaced as a crystal mush during Early to Middle Triassic time, consists of the following rocks: olivine-rich peridotite, about 50 percent; gabbro and norite, about 40 percent; pyroxene-rich peridotite and pyroxenite, 6 percent; quartz diorite and albite granite, 4 percent. The olivine-rich peridotite averages about 80 percent olivine; it includes large masses of dunite and some small pyroxene-rich lenses and contains podiform chromite deposits. The gabbro ranges from olivine-rich to olivine-free varieties, in which the ratio of orthopyroxene to clinopyroxene varies widely and unzoned plagioclase ranges in composition from about An_{85} to An_{60}. The pyroxene-rich peridotite and pyroxenite lie compositionally and spatially between the gabbro and olivine-rich peridotite. In many places all varieties of the three rocks intergrade and are intricately interlayered. The distribution (fig. 81.1, and Thayer, 1956), composition, texture, and structure (Thayer, 1963) of the gabbro and peridotite are characteristic of the alpine type. The attitude of the constituent rock units and their contacts against country rocks is consistently steep or vertical. Quartz diorite cuts the gabbro and nearby country rocks as sharply bounded dikes, small pipes, and irregular masses. The quartz diorite consists mainly of zoned andesine-oligoclase and hornblende that show hypidiomorphic texture, and quartz (No. 1 in table). As shown on the map, the quartz diorite occurs mostly in or near the contact zone between gabbro and country rocks.
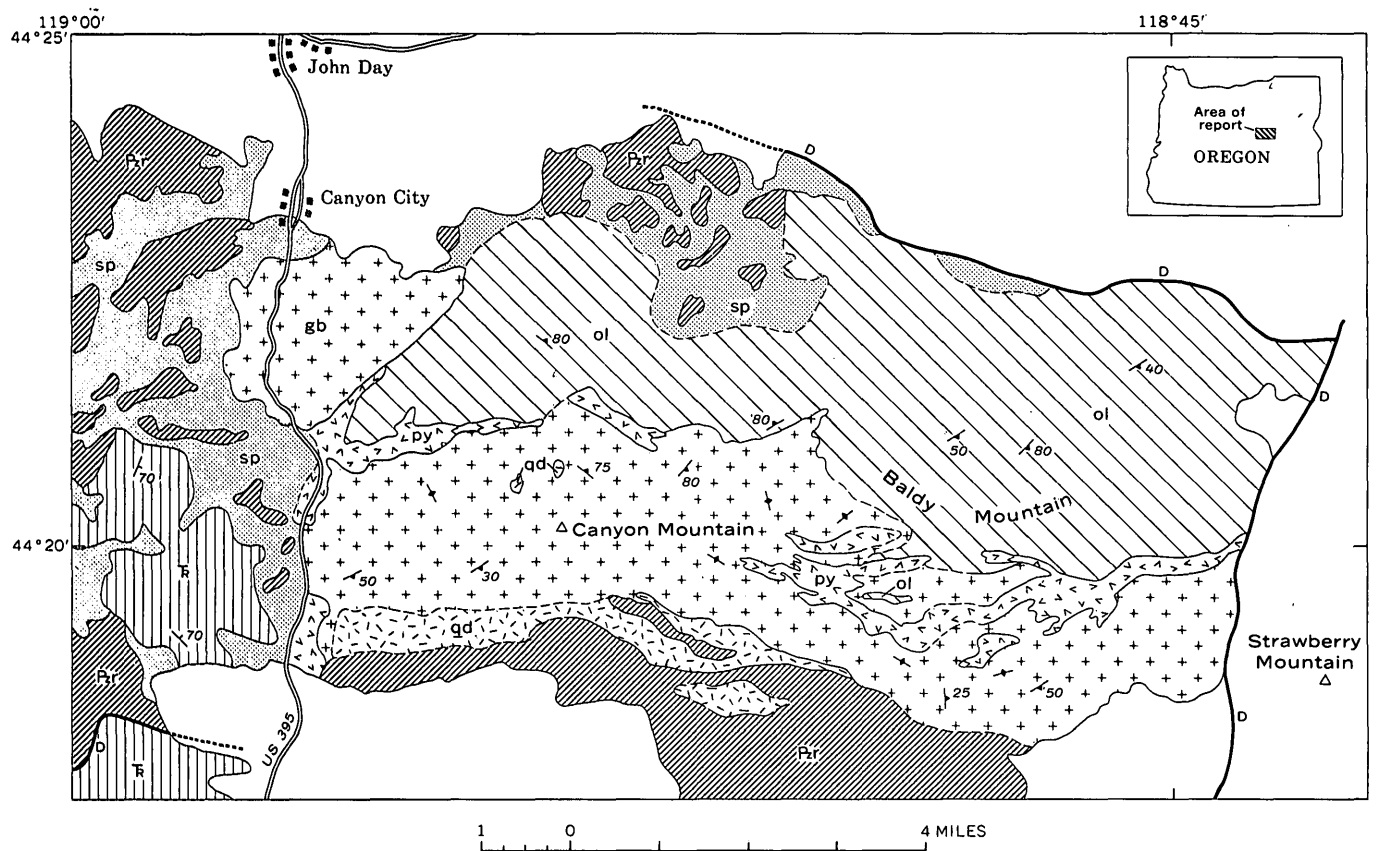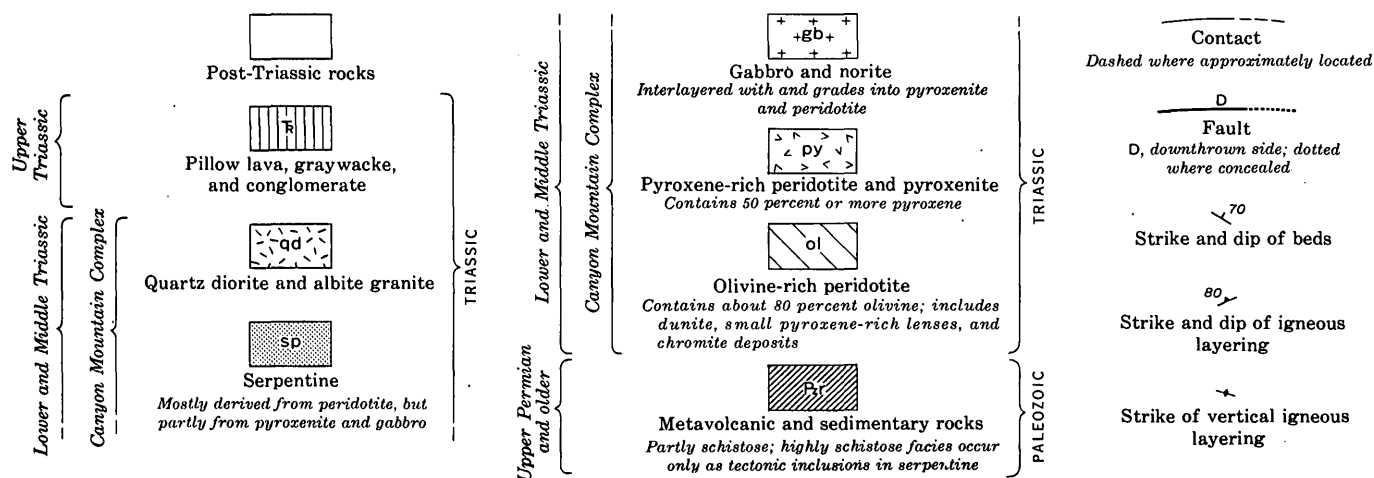
FIGURE 81.1.—Geologic map of the Canyon Mountain Complex, Grant County, Oreg.

Parts of the quartz diorite, gabbro, and country rocks have been metasomatically altered to albite granite of the kind described by Gilluly (1933) near Sparta, 80 miles to the east. Much of the albitized gabbro closely resembles quartz diorite (Gilluly, 1937, p. 35) in hand specimen. In parts of the gabbro, the same kind of alteration that transformed quartz diorite into albite granite instead formed massive coarse-grained hornblende rocks that resemble pegmatite, but are in no wise related to many small masses of pyroxenic truly gabbroic pegmatite (Guild, 1947).

Similar relations between the same kinds of rocks have been mapped and described in the Baker (Gilluly, 1937) and Sparta quadrangles (Gilluly, 1933; Prostka,

1962) in Oregon, and in Cyprus (Wilson and Ingham, 1959; Bear, 1960; Gass, 1960). In the summer of 1962 the writer found like relations between gabbro, diorite, and albitic alteration in the Hindubagh igneous complex, Pakistan (Bilgrami, 1961) and in the Guleman district, eastern Turkey. The gabbro and peridotite in these areas is of the alpine type, and podiform chromite deposits have been mined in all except the Baker-Sparta area.

Close affinity between the quartz diorites and albite granites in eastern Oregon and between trondhjemites and quartz-albite porphyries of the Troodos Complex in Cyprus is indicated in the accompanying table. In view of the spotty variation in such rocks and the concomitant problems of sampling, the rocks are notably similar even though those near Sparta are consistently richer in K_2O. Despite differences in interpretation of textures and field relations, geologists in all three areas agree that the rocks, from peridotite to soda-rich varieties, are comagmatic (Gilluly, 1937, p. 40; Wilson and Ingham, 1959, p. 124; Bear, 1960, p. 43; Gass, 1960, p. 90). The evidence seen in Pakistan and Turkey implies, furthermore, that the same kinds of rocks and relations will be found in still other alpine mafic complexes.

These complexes as a class seem to have been emplaced in two rather distinctive stages: an early stage during which peridotite and gabbro were emplaced together more or less as a unit, and a somewhat later quartz

Analyses of quartz diorite, trondhjemite, and albite-rich rocks from eastern Oregon and Cyprus

	1	2	3	4	5	6	7
SiO_2	58. 74	54. 67	67. 81	73. 06	78. 27	77. 04	75. 8
Al_2O_3	17. 17	15. 95	14. 13	12. 30	11. 43	11. 88	12. 9
Fe_2O_3	. 82	2. 08	1. 50	2. 32	1. 44	1. 05	1. 6
FeO	4. 53	7. 48	4. 04	2. 23	. 14	1. 32	2. 0
MgO	5. 30	4. 09	1. 56	. 65	. 57	. 04	. 39
CaO	5. 91	7. 97	3. 76	3. 56	. 92	1. 28	. 79
Na_2O	3. 99	2. 71	3. 36	3. 90	4. 70	4. 45	5. 8
K_2O	. 13	1. 16	1. 62	. 18	. 53	1. 64	. 20
H_2O^{-1}	. 24	0	. 06	. 52	. 53	0	1. 0
H_2O^{+1}	2. 89	1. 26	1. 24	1. 09	1. 39	. 54	
TiO_2	. 25	1. 16	. 79	. 28	. 25	. 37	. 14
CO_2	. 01	1. 24	. 45	-----	-----	. 14	. 28
P_2O_5	. 04	. 11	. 06	. 07	. 05	. 04	. 04
MnO	. 08	. 17	. 13	. 05	. 03	0	. 06
	100. 10	100. 05	100. 51	100. 21	100. 25	99. 79	101

1. Quartz diorite, north slope of Canyon Mountain, Oreg., F. H. Neuerburg, analyst.
2. Quartz diorite, Sparta quadrangle, Oregon (Gilluly, 1933, p. 70).
3. Partly albitized quartz diorite, same locality as 2.
4. Hornblende trondhjemite, Troodos Complex (Wilson and Ingham, 1959, p. 98).
5. Quartz-albite microporphyry, Troodos Complex (Gass, 1960, p. 83).
6. Albite granite, Sparta quadrangle, Oregon (Gilluly, 1933, p. 70).
7. Albite granite, Canyon Mountain, Oreg. K. E. White, S. D. Botts, analysts; analyzed by methods described in U.S. Geol. Survey Bull. 1036-C.

diorite–albite granite stage in which fluid magma was accompanied or followed closely by pervasive albitization. Great disparities in proportions of the various rocks in different complexes, plus other features, preclude differentiation in place. The rest magma in the peridotite and gabbro, if late dikes are a true sample (Thayer, 1960, p. 252), was no more siliceous than the solid constituents. The diorite, therefore, cannot have been derived from the gabbro by filter pressing during emplacement. Field relations in Canyon Mountain indicate some time lapse between emplacement of the gabbro and quartz diorite, but in the Sparta quadrangle the gabbro and quartz diorite seem to have been nearly contemporaneous (H. J. Prostka, oral communication, 1963). Close areal correlation of albitization effects with quartz diorite masses in the gabbro in Canyon Mountain shows that the two are genetically related. The presence of pyroxene instead of talc or amphibole in the peridotite and gabbro implies a dearth of water during their consolidation that contrasts markedly with the evidence of abundant water during and after emplacement of the diorite.

The magmatic history of these rocks, from dunite to albite granite, seems to have been quite different from that of normal intermediate to granitic rocks. The peridotite and gabbro apparently were emplaced as crystal mushes that were formed, deep in the crust or mantle, from previously differentiated rocks by incipient melting just sufficient to render them mobile en masse under high tectonic pressures. These mushes seem to have been emplaced at early stages in the evolution of most eugeosynclines, before severe metamorphism and complete dehydration of the country rocks. The dioritic rocks were emplaced as fluid magmas, but whether they were generated by refusion of upper layers of a deep stratiform-type complex or fusion of eugeosynclinal country rocks is pure conjecture. The albitizing solutions may have been derived partly from the diorite, and partly from alteration of country rocks (Gilluly, 1933, p. 76).

The Canyon Mountain Complex represents the older of two plutonic magma series of Mesozoic age in northeastern Oregon. The older series is post-Permian and pre-Upper Triassic; the younger one is Lower to middle Cretaceous, the same as the Idaho batholith (Larsen and Schmidt, 1958). Dioritic rocks constitute only a small part of the older magma series, in the Canyon Mountain area less than 5 percent and in the Baker quadrangle 10 percent or less. The Bald Mountain batholith, which belongs to the younger magma series, contains only about 3 percent of rocks more mafic than diorite (Taubeneck, 1957, p. 226); its final product was quartz monzonite. The contact relations around the

respective plutons could scarcely differ more: extensive albitization and brecciation without development of foliation is found around the older series, and strong foliation without much albitization around the younger series. There must have been fundamental differences in the nature of the magmas during emplacement, which presumably were related to different stages in the development of the Blue Mountain eugeosyncline. Identification and mapping of the two magma series close to the Idaho batholith might be very uncertain and difficult.

In summary, most of the peridotite and gabbro in northeastern Oregon, as exemplified by the Canyon Mountain Complex, is part of a pre-Upper Triassic magma series in which peridotite and gabbro predominate, soda-rich dioritic rocks form a small part, and late-stage metasomatic albitization is characteristic. The similarity to the Troodos Complex in Cyprus, and to like rocks in some other alpine-type complexes, is believed to show that they all belong to a distinctive line of magmatic descent, for which the name "alpine mafic magma stem" is suggested. The "primary" peridotite rocks of Hess (1938) are at the ultramafic end of this magma stem, and soda-rich rocks represented by the albite granite of Gilluly (1933) and quartz-albite porphyries of the Troodos area are at the silicic end.

REFERENCES

Bear, L. M., 1960, The geology and mineral resources of the Agros-Apsiou area: Cyprus Geol. Survey Dept. Mem. 7, pt. 1, p. 11–50.

Bilgrami, S. A., 1961, Distribution of Cu, Ni, Co, V, and Cr in rocks of the Hindubagh igneous complex, Zhob Valley, West Pakistan: Geol. Soc. America Bull., v. 72, p. 1729–1738.

Bowen, N. L., and Tuttle, O. F., 1949, The System MgO–SiO₂–H₂O: Geol. Soc. America Bull., v. 60, p. 439–460.

Flint, D. E., Albear, J. F. de, and Guild, P. W., 1948, Geology and chromite deposits of the Camagüey district, Camagüey Province, Cuba: U.S. Geol. Survey Bull. 954–B, p. 39–63.

Gass, I. G., 1960, The geology and mineral resources of the Dhali area: Cyprus Geol. Survey Dept. Mem. 4, 116 p.

Gilluly, James, 1933, Replacement origin of the albite granite near Sparta, Oregon: U.S. Geol. Survey Prof. Paper 175–C, p. 65–81.

——— 1937, Geology and mineral resources of the Baker quadrangle, Oregon: U.S. Geol. Survey Bull. 879, 119 p.

Guild, P. W., 1947, Petrology and structure of the Moa district, Oriente Province, Cuba: Am. Geophys. Union Trans., v. 28, p. 218–246.

Hess, H. H., 1938, A primary peridotite magma: Am. Jour. Sci., 5th ser., v. 35, p. 321–344.

——— 1955, Serpentines, orogeny, and epeirogeny in Poldevaart, A., Crust of the earth: Geol. Soc. America Spec. Paper 62, p. 391–407.

Larsen, E. S., Jr., and Schmidt, R. G., 1958, A reconnaissance of the Idaho batholith and comparison with the southern California batholith: U.S. Geol. Survey Bull. 1070–A, p. 1–33.

Prostka, H. J., 1962, Geology of the Sparta quadrangle, Oregon: Oregon Dept. Geology and Mineral Industries Geol. Map Ser. 1, 6 p.

Roever, W. P. de, 1957, Sind die alpinotypen Peridotitmassen vielleicht tectonisch verfractete Bruchstücke der Peridotitschalle?: Sond. Geol. Rundschau, v. 46, p. 137–146.

Rossman, D. L., Fernandez, N. S., Fontanos, C. A., Zepeda, Z. C., 1959, Chromite deposits on Insular Chromite Reservation Number One, Zambales, Philippines: Philippine Bur. Mines Spec. Projects Ser., Pub. 19, Chromite.

Taubeneck, W. H., 1957, Geology of the Elkhorn Mountains, northeastern Oregon: Bald Mountain batholith: Geol. Soc. America Bull., v. 68, p. 181–238.

Thayer, T. P., 1956, Preliminary geologic map of the John Day quadrangle, Oregon: U.S. Geol. Survey Mineral Inv. Map MF–51.

——— 1960, Some critical differences between alpine-type and stratiform peridotite-gabbro complexes: Internat. Geol. Congress 21st, Copenhagen 1960, Rept. pt. XIII, p. 247–259.

——— 1963, Flow-layering in alpine peridotite-gabbro complexes: Internat. Miner. Assoc. Symposium on layered intrusions, Third General Meeting, 1962. [in press]

Wilson, R. A. M., and Ingham, F. T., 1959, The geology and mineral resources of the Xeros–Troodos area: Cyprus Geol. Survey Dept. Mem. 1, 183 p.

Article 82

MODAL COMPOSITION OF THE IDAHO BATHOLITH [1]

By CLYDE P. ROSS, Denver, Colo.

Abstract.—Modal analyses of 56 rock samples suggest that the Idaho batholith may be slightly more calcic than previous estimates indicate. Relatively silicic rocks and calcic rocks occur in the outer parts of the batholith.

Data on the modal composition of components of the Idaho batholith have been assembled as a part of a renewed study. Many of the published modal analyses from the batholith and from other rocks in Idaho have been brought together by E. S. Larsen, Jr., and R. G. Schmidt (1958, p. 15). D. L. Schmidt (1958) has studied rocks from areas in the western part of the batholith and near Hailey, in the southern part, and has kindly made his analyses available to me. A number of other modal analyses, mostly my own, are recorded here for the first time; some of these resulted from reconnaissance in 1959–61.

The most thorough study of the modal composition of any part of the Idaho batholith is that by Anderson and Rasor (1934). They studied rocks from more than 50 localities in and around the Boise Basin in the southwestern part of central Idaho and plotted their results on a triangular diagram. Their data are not reproduced in the present article only because the numerous analyses from a small part of the batholith would crowd and tend to unbalance the illustrations.

Figure 82.1 shows the localities from which the samples were collected and the relation of the samples to the Idaho batholith and its border zone. The boundaries of the batholith and, especially, those of parts of its border zone are expected to be modified very extensively when detailed mapping is done. Figure 82.2 shows graphically the proportion of quartz, potassium feldspar, plagioclase, and other constituents (largely biotite) in the samples that have been studied, other than

those of Anderson and Rasor (1934) from the Boise Basin.

As shown in figure 82.1, most of the samples came from that part of the batholith south of lat 45°30′ N. As the samples were gathered for varied purposes over a period of more than 60 years, they are not systematically distributed and hence fail to give a statistically satisfactory concept of the composition of the batholith. Also, for the same reasons, the methods of analysis vary so widely that the results are not strictly comparable. Some of the modal compositions represented in figure 82.2 were computed from chemical analyses (Lindgren, 1904, p. 18–19), but most were determined by the methods of Rosiwal or of Chayes (1956). A few are based on estimates. The discrepancies that arise from these differences are not large enough to be significant in the present discussion.

The rocks represented in figure 82.2 are all regarded as components of the Idaho batholith proper (fig. 82.1). Outlying masses and intrusions within the area of the batholith that are not known to be distinctly related to the batholith are not included. This has resulted in elimination of a few analyses attributed to the batholith in previous compilations but now known to be from younger rocks. Conceivably a few analyses that are shown on figure 82.2 are also from rocks of postbatholithic age; future detailed work should eliminate them. All analyses on figure 82.2 are of rocks of dominantly granitoid texture. A few of the rocks are gneissic, but those that are unquestionably metamorphosed derivatives of sedimentary rocks are not included.

GEOLOGIC SETTING

The Idaho batholith, as shown on figure 82.1, lies mainly in central Idaho, but its northeastern part extends a short distance into Montana. Its exposures cover about 16,000 square miles and embrace an irregular area up to 120 miles in width and 240 miles in

C86

ART. 82 *IN* U.S. GEOL. SURVEY PROF. PAPER 475–C, PAGES C86–C90. 1963.
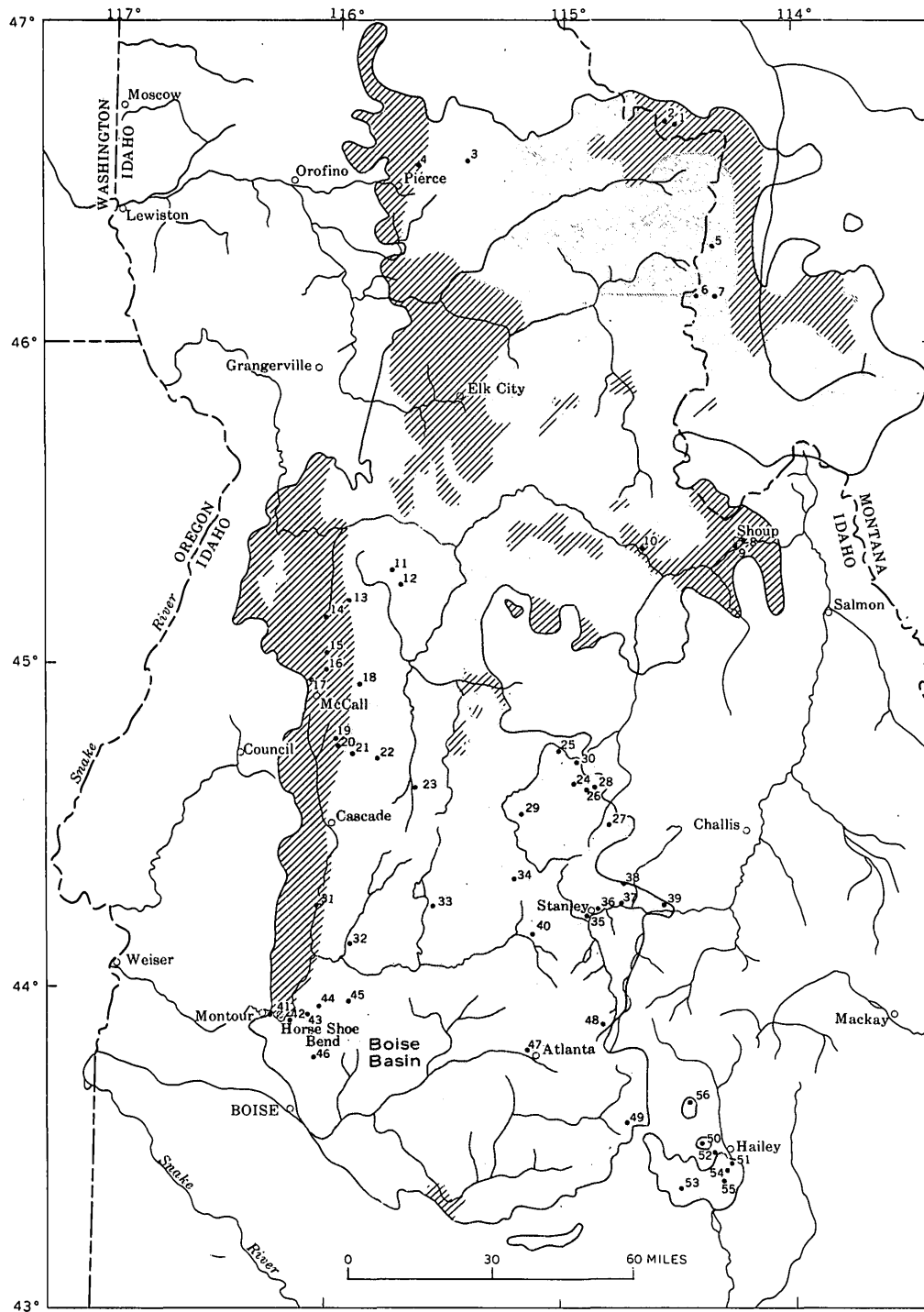
FIGURE 82.1.—Sketch of the Idaho batholith (shaded) and its border zone (diagonal pattern) showing the location of samples for which modal analyses are plotted on figure 82.2. Source of samples as follows: Anderson and Wagner (1946) 53; Chase[1], 7; Choate (1962), 38; Davidson (1939), 8, 9; Hewett, in Umpleby and others (1930), 55; Larsen and Schmidt (1958), 3, 4, 6, 31, 32, 36, 40, 47; Leischner[2], 1, 2; Lindgren (1900), 41, 46, 50, 51; Lindgren (1904), 5; Schmidt (1958), 15, 17, 20, 21, 22, 23; Schmidt[3], 54; other samples by the author.

[1] Chase, R. B., 1961, Geology of Sweethouse Canyon, Bitterroot Range, Montana: Montana State Univ. unpub. M.A. thesis.
[2] Leischner, L. M., 1959, Border-zone petrology of the Idaho batholith in vicinity of Lolo Hot Springs, Montana: Montana State Univ. unpub. M.S. thesis, 76 p.
[3] Schmidt, D. L., 1962, Quaternary geology of the Bellevue area in Blaine and Camas Counties, Idaho: Univ. of Washington unpub. Ph D. thesis.
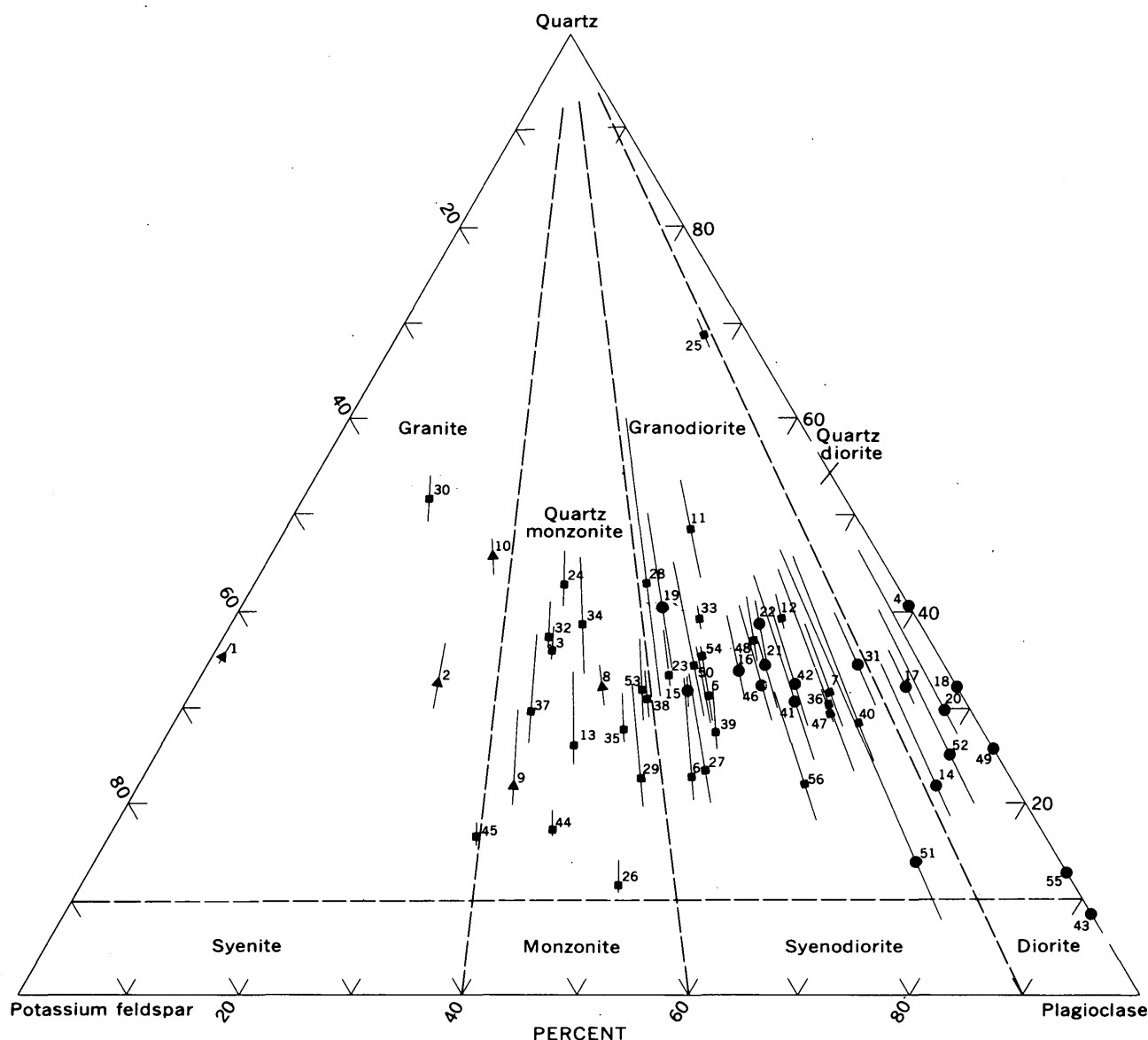
FIGURE 82.2.—Diagram of modal analyses from the Idaho batholith. Square, sample from inner facies; circle, sample from calcic border facies; triangle, sample from silicic border zone. Length of inclined lines indicates percentage of essential constituents (mainly biotite) not otherwise represented in the diagram. Numbers indicate sample locations as shown in figure 82.1.

length. Much the greater part belongs to the main, inner facies of fairly uniform rather light-colored granitoid rock. An outer mass, somewhat older and more diversified, may have originally constituted an envelope that enclosed much of the main facies. Most of the outer zone is rather calcic and is commonly referred to as the calcic border zone. Locally, however, silicic rocks are conspicuous along the border of the batholith. This distinction is not made on figure 82.2, but the principal area of these silicic rocks is near Shoup, Idaho, on the east side of the batholith.

The Idaho batholith intrudes sedimentary and volcanic rocks ranging in age from Precambrian to Triassic, and is in turn cut by dikes and other small intrusions. Most of these are of early to possibly middle Tertiary age but may include some rocks as old as Late Cretaceous (Anderson, 1952, p. 263). Most of the younger intrusive rocks are fine grained and porphyritic, but some in central Idaho have a coarsely granitic texture and can easily be confused with the rocks of the batholith. Possibly a few of the analyses reported here are of granitic rocks of Tertiary age.

On the basis of its geologic relations the Idaho batholith has been deduced to be not older than Early Cretaceous or, at most, Late Jurassic (Ross and Forrester, 1958, p. 24–25) : possibly much of it did not con-

solidate until the middle of the Cretaceous. Determinations of absolute age by the lead-alpha method (Larsen and Schmidt, 1958, p. 18–19; Larsen and others, 1958, p. 50–51, 54–55) average about 105 million years, if a few determinations on rocks not belonging to the Idaho batholith proper are eliminated.

MINERALOGY

The rocks are mineralogically rather simple. The principal components of the quartz monzonite and granodiorite of the main inner facies are quartz; potassium feldspar; plagioclase; commonly biotite or, more rarely hornblende; and muscovite or pyroxene. Much of the potassium feldspar is microcline, some of which is perthitic. Sphene and apatite are among the most abundant accessory minerals. Dike rocks such as pegmatite, aplite, and lamprophyre are not considered.

Most of the rocks of the calcic border zone are granodiorite and quartz diorite. Many of them are similar in mineral composition to rocks of the main mass except that commonly the most abundant plagioclase is akin to andesine, and hornblende is the principal dark mineral. Some contain no potassium feldspar; a few contain pyroxene. The border zone as plotted on figure 82.2 includes metamorphosed sedimentary material, not considered here, that is gradational with the granitoid rocks.

The few siliceous rocks that border the batholith, as noted by Davidson (1939) and Leischner[2], are largely granite and augen gneiss in which such components as quartz, microline, perthite, albite, oligoclase, and biotite are plentiful. Micropegmatite intergrowths are also conspicuous in many of them.

MODAL ANALYSES

The modal analyses of rocks referred to in this article are shown graphically in figure 82.2, which is plotted in accord with a method proposed by Johannsen (1932). According to the subdivision of rock names indicated in the figure, the samples from the main, inner facies are mainly granodiorite, although many are quartz monzonite. Most published summaries indicate that the main mass of the batholith is dominantly quartz monzonite. Thus the diagram suggests that the main mass may be somewhat more calcic than most published reports indicate. It is interesting, however, to note that most of the samples plotted contain more than 20 percent quartz and a few contain more than 45 percent. Many have a dark-mineral content of scarcely more than 10 percent, and several samples have less than 5 percent.

All of the analyses corresponding to diorite and quartz diorite are of samples from the calcic border zone. Some from that zone are as siliceous as granodiorite and quartz monzonite. As the calcic zone is known to be cut by offshoots of the main interior mass (Ross and Forrester, 1958, p. 22), some of the more siliceous rocks here grouped with the calcic border zone may be apophyses of the inner facies. This statement is not intended to apply to the rock of the approximate composition of granite referred to below.

Attention may be called to samples 1, 2, 8, 9, and 10 (fig. 82.2), which represent the siliceous variant of the rocks along the batholith border. These show that the Idaho batholith, as now mapped, includes rocks distinctly more siliceous than is apparent from most published descriptions. The siliceous and calcic components of the outer parts of the batholith have not been observed in contact with each other. The relation between the two is among the unsolved questions regarding the Idaho batholith.

The diagram presented by Anderson and Rasor (1934), while corresponding to a much smaller part of the batholith than figure 82.2, has much similarity to the figure. Their compilation is especially like the denser portion of figure 82.2. It shows a slightly larger proportion of quartz monzonite, no granite or diorite, and little quartz diorite.

The part of the batholith north of lat 45°30′ N. is poorly represented by samples. Reconnaissance in the summer of 1962 and a little published data (Lindgren, 1904, p. 17–23; Shenon and Reed, 1934, p. 16, 17, 19–21; Anderson, 1930, p. 17–23) show that gneissic rocks are fairly common and that in some areas, notably in the northernmost parts, the rock varies in texture and composition even within a single outcrop.

REFERENCES

Anderson, A. L., 1930, Geology and mineral resources of the region about Orofino, Idaho: Idaho Bur. Mines and Geology Pamph. 34.

―― 1952, Multiple emplacement of the Idaho batholith: Jour. Geology, v. 60, p. 255–265.

Anderson, A. L., and Rasor, A. C., 1934, Composition of the Idaho batholith in Boise County, Idaho: Am. Jour. Sci., 5th ser., v. 27, p. 287–294.

Anderson, A. L., and Wagner, W. R., 1946, A geological reconnaissance in the Little Wood River (Muldoon) district, Blaine County, Idaho: Idaho Bur. Mines and Geology Pamph. 75, 22 p.

Chayes, Felix, 1956, Petrographic modal analysis—an elementary statistical appraisal: New York, John Wiley and Sons, 113 p.

Choate, Raoul, 1962, Cinnabar district east of Stanley: Idaho Bur. Mines and Geology Pamph. 126.

Davidson, D. M., 1939, Geology and petrology of the Mineral Hill mining district, Lemhi County, Idaho [abs.]: Minnesota Univ. summaries of Ph. D. theses, v. 1, p. 218–221.

---

[a] Leischner, L. M., 1959, Border-zone petrology of the Idaho batholith in vicinity of Lolo Hot Springs, Montana: Montana State Univ. unpub. M.S. thesis, 76 p.

Johannsen, Albert, 1922, On the representation of igneous rocks in triangular diagrams: Jour. Geology, v. 30, p. 167–169.

Larsen, E. S., Jr., and Schmidt, R. G., 1958, A reconnaissance of the Idaho batholith and comparison with the southern California batholith: U.S. Geol. Survey Bull. 1070–A.

Larsen, E. S., Jr., Gottfried, David, Jaffe, H. W., and Waring, C. L., 1958, Lead-alpha ages of the Mesozoic batholiths of western North America: U.S. Geol. Survey Bull. 1070–B, p. 35–62.

Lindgren, Waldemar, 1900, The gold and silver veins of Silver City, De Lamar and other mining district in Idaho: U.S. Geol. Survey 20th Ann. Rept., pt. 3, p. 65–256.

Lindgren, Waldemar, 1904, A geological reconnaissance across the Bitterroot Range and Clearwater Mountains in Montana and Idaho: U.S. Geol. Survey Prof. Paper 27, 123 p.

Mackin, J. H., and Schmidt, D. L., 1956, Uranium- and thorium-bearing minerals in placer deposits in Idaho, in Contributions to the geology of uranium and thorium by the U.S. Geological Survey and Atomic Energy Commission for the United Nations International Conference on Peaceful Uses of Atomic Energy: U.S. Geol. Survey Prof. Paper 300, p. 375–380.

Ross, C. P., 1962, Stratified rocks in south-central Idaho: Idaho Bur. Mines and Geology Pamph. 125, 126 p.

Ross, C. P., and Forrester, J. D., 1958, Outline of the geology of Idaho: Idaho Bur. Mines and Geology Bull. 15, 74 p.

Schmidt, D. L., 1958, Reconnaissance petrography of the Idaho batholith in Valley County, Idaho: U.S. Geol. Survey open-file report.

Shenon, P. J., and Reed, J. C., 1934, Geology and ore deposits of the Elk City, Orogrande, Buffalo Hump, and Tenmile districts, Idaho County, Idaho: U.S. Geol. Survey Circ. 9.

Umpleby, J. B., Westgate, L. G., and Ross, C. P., 1930, Geology and ore deposits of the Wood River region, Idaho, with a description of the Minnie Moore and near-by mines, by D. F. Hewett: U.S. Geol. Survey Bull. 814, 250 p.

SOLUTION BRECCIAS OF THE MINNELUSA FORMATION IN THE BLACK HILLS, SOUTH DAKOTA AND WYOMING

By C. G. BOWLES and W. A. BRADDOCK, Denver, Colo.

Abstract.—Solution features in the Minnelusa Formation (Pennsylvanian and Permian age) have been formed since early Tertiary time by the removal of as much as 250 feet of anhydrite and gypsum by ground water. Breccia pipes and sinks in Permian to Lower Cretaceous formations are attributed to collapse in the Minnelusa.

Breccias in the Minnelusa Formation were recognized by Darton (1905, p. 29) as "a distinctive feature throughout the southern Black Hills." Breccia was observed in parts of seven 7½-minute quadrangles (Braddock, 1963; D. A. Brobst, and J. B. Epstein, 1963; V. R. Wilmarth, oral communication, 1957; and Wolcott and others, 1962) during recent mapping of the Minnelusa in the area between Hot Springs, S. Dak., and Stockade Beaver Creek, 6 miles east of Newcastle, Wyo. (fig. 83.1).

The Minnelusa Formation has been divided into 6 units totaling 700 to 1,100 feet in thickness (fig. 83.2). The units, numbered from youngest to oldest, correspond closely to the 6 divisions of Condra and Reed (1940). In outcrop, units 6, 5, and 4 in the lower part of the Minnelusa consist, respectively, of a basal sandstone, a lavender to cream-colored limestone, and a sequence of interbedded red shales and gray to purple limestones and dolomites. Outcrops of units 3 and 2 of Middle and Late Pennsylvanian age are composed of cherty yellow dolomites and limestones, yellow sandstones, and black shales. Rocks of Permian age, designated unit 1, crop out as thick red and yellow sandstones, thin gray or yellow limestones and dolomites, and red mudstones. The base of unit 1 is the lower contact of the "Red Marker" (Thompson and Kirby, 1940, p. 145), a red mudstone that may be traced in both surface and subsurface rocks in the southern Black Hills.

Brecciation, with few exceptions, is restricted to the upper part of the Minnelusa Formation and decreases in intensity downward from unit 1 to unit 3. In unit 1, layers of breccia are composed of angular carbonate and clastic fragments which have moved very little relative to one another; thus, bedding is preserved. Unit 1 also contains vertical pipes of breccia, against which recognizable bedding terminates. Unit 2 is characterized by contorted and locally brecciated strata and by breccia "sills" as much as 3 feet thick (fig. 83.3). The weathered sills, composed of fragments of dolomite, limestone, and sandstone, are heavily cemented by calcium carbonate and form rounded tufalike ledges that are connected by pipes of similar breccia. Presumably the sills were formed where dolomite beds bridged cavernous areas, permitting lateral movement of breccia fragments outward from the pipes into the caverns to form tabular bodies. In unit 3 the rocks are slightly brecciated and stylolites have formed along bedding planes in the carbonate rocks. Strata in units 4, 5, and 6 commonly are undisturbed, except in areas where solution of the underlying Pahasapa Limestone of Mississippian age has caused collapse and draping.

In the subsurface within a mile or two of the Minnelusa outcrop, units 1, 2, and 3 are unbrecciated and are thicker than the equivalent surface exposures. The additional thickness, amounting to as much as 250 feet, is due to intercalated beds of anhydrite. In cores from the USGS No. 2 Pass Creek drill hole (fig. 83.1) about 200 feet of anhydrite was recovered in unit 1, 25 feet of anhydrite in unit 2, and 10 feet of anhydrite at the top of unit 3 (fig. 83.2). Within unit 3, additional beds
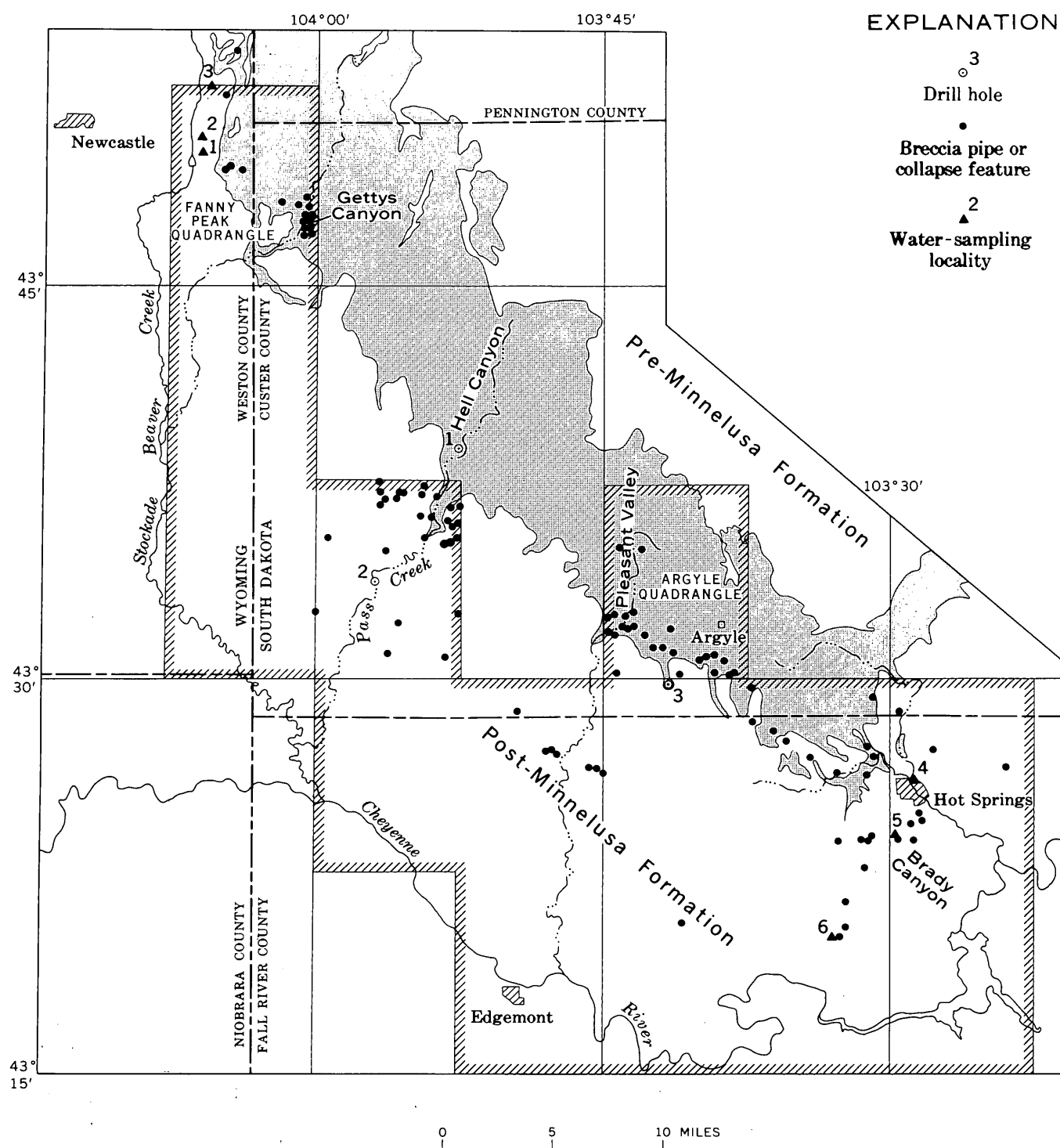
FIGURE 83.1.—Map showing outcrop of the Minnelusa Formation (shaded), location of breccia pipes and collapse features in Permian and younger rocks, and distribution of springs emitting sulfate water, southern Black Hills of South Dakota and Wyoming. Hachures outline area mapped in 1953–59; data compiled from published and unpublished reports of the U.S. Geological Survey.
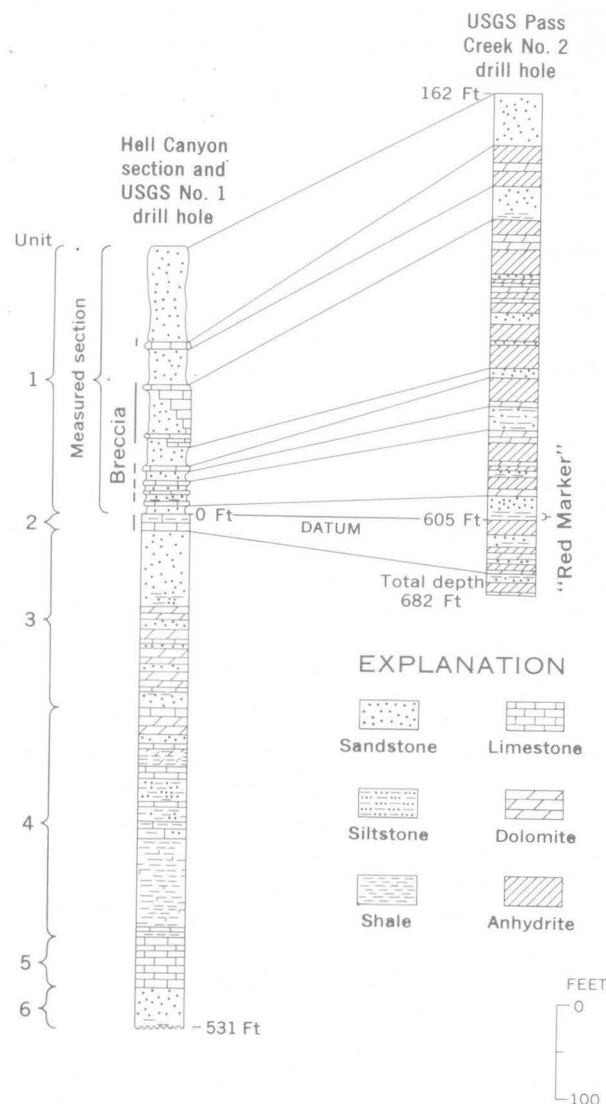
USGS Pass
Creek No. 2
drill hole

162 Ft

Hell Canyon
section and
USGS No. 1
drill hole

Unit

Measured section

Breccia

0 Ft   DATUM   605 Ft   "Red Marker"

Total depth
682 Ft

531 Ft

EXPLANATION

Sandstone   Limestone

Siltstone   Dolomite

Shale   Anhydrite

FEET
0

100

FIGURE 83.2.—Stratigraphic sections of the Minnelusa Formation of Pennsylvanian and Permian age showing correlation of brecciated rocks in outcrop with anhydrite-bearing strata of the subsurface in Custer County, S. Dak. The locations of the stratigraphic sections are: Hell Canyon section, NW¼ sec. 3 and NE¼ sec. 4, T. 5 S., R. 2 E.; USGS No. 1 Hell Canyon drill hole, sec. 3, T. 5 S., R. 2 E.; USGS No. 2 Pass Creek drill hole, sec. 1, T. 6 S., R. 1 E.

FIGURE 83.3.—Breccia sills (a) connected by pipes (b) in unit 2 of the Minnelusa Formation in Red Canyon, NE¼ sec. 11, T. 6 S., R. 3 E., Custer County, S. Dak.

of anhydrite were identified by Gordon Hurd (1942, written communication) in cores and cuttings from the Continental Oil Co. State No. 1 drill hole, sec. 36, T. 8 S., R. 3. E. Correlation of beds from the thicker subsurface sections into the brecciated section indicates that the breccia has resulted from collapse induced by solution of anhydrite.

The breccia layers are composed predominantly of fragments of Minnelusa rocks, but fine-grained detritus from the overlying formations is also incorporated in the upper part of the formation. Petrologic studies of the Minnelusa breccia show that dolomite has been replaced, and sandstone and breccia have been cemented, by calcite (Art. 84). The intensely brecciated rocks are firmly cemented, in contrast to the thick, moderately to weakly brecciated sandstones, which are loosely cemented. In many places the only evidence of disturbance in the sandstones is a slight development of boxwork structure resulting from differential weathering of the poorly cemented sandstones and the well-cemented joints. Within the brecciated rocks, cavities ranging from several inches to 4 feet across are lined with calcite crystals. In core from the USGS No. 3 Minnekahta drill hole south of Argyle, S. Dak. (fig. 83.1), calcite crystals rim breccia fragments and, in turn, are enclosed by a matrix of silt and clay. The abundance of this fine-grained matrix suggests that in places silt and clay from the overlying Opeche Formation of Permian age and possibly the Spearfish Formation of Permian and Triassic age have been incorporated within the breccia following the initial collapse and brecciation.

The breccia pipes (fig. 83.4) are cylindrical masses of blocks and fragments derived from overlying beds and are firmly cemented by calcite. Intense cementation causes the pipes to weather out in relief along the canyon walls or to form free-standing masses of breccia. The maximum height of the pipes is not known, but within the Minnelusa Formation breccia pipes 200 feet high and "tens to several hundred feet" in diameter (Brobst and Epstein, 1963) are exposed in canyon walls. Many of the pipes were undoubtedly formed well below the ground surface, as indicated by
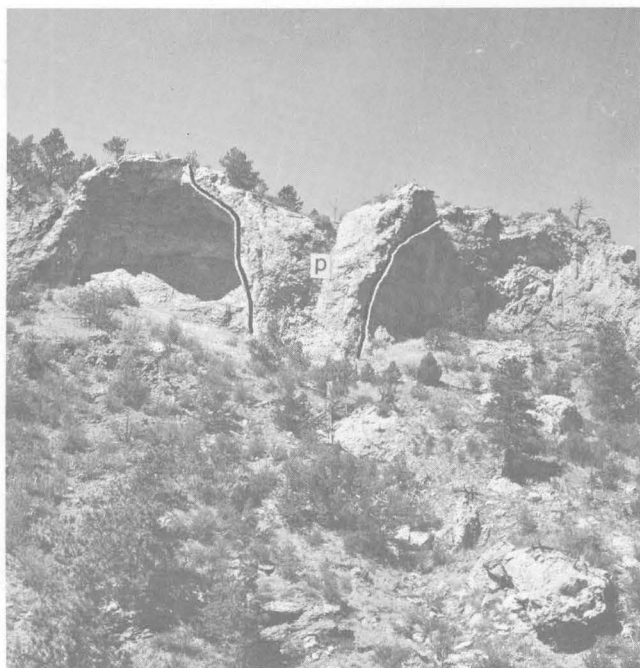
FIGURE 83.4.—Breccia pipe (p) in the upper part of the Minnelusa Formation in Gettys Canyon, SE¼ sec. 16, T. 3 S., R. 1 E., Custer County, S. Dak. Photograph by J. B. Epstein.

FORMATION		AGE	ABUNDANCE	
			1	2
Lakota Formation		Early Cretaceous		
Morrison Formation	Unkpapa Sandstone	Late Jurassic		
Sundance Formation				
Spearfish Formation		Permian and Triassic	?	
Minnekahta Limestone		Permian		
Opeche Formation				
Minnelusa Formation		Pennsylvanian and Permian		
Pahasapa Limestone		Early Mississippian		

1. Related to solution within the Pahasapa Limestone.
2. Related to solution within the Minnelusa Formation.

FIGURE 83.5.—Stratigraphic distribution of breccia layers and pipes and other collapse features in the southern Black Hills, South Dakota and Wyoming.

large blocks of Minnekahta Limestone of Permian age that were dropped 150 feet or more below the normal stratigraphic position and incorporated in pipes near Argyle, S. Dak. Other pipes probably were formed after the overlying formations were removed by erosion (Epstein, 1958). Many pipes in Gettys Canyon, SE¼ sec. 16, T. 3 S., R. 1 E., are funnel shaped (fig. 83.4), suggesting that they originated as sinks formed above the water table and later filled by debris from the outcrop.

Collapse features in more than 1,000 feet of overlying rocks ranging in age from Permian to Early Cretaceous (fig. 83.5) appear to be related to the solution breccias of the Minnelusa Formation. These pipes, sinks, and collapse features (fig. 83.1) must have resulted from the solution of calcium sulfate in the Minnelusa Formation, because no comparable solution has occurred in the overlying rocks. Even the gypsum beds of the Spearfish Formation, which total more than 100 feet in thickness, crop out almost continuously. The absence of widespread solution within the Spearfish may be attributed to the lower permeability of the siltstones of that formation, a property which has restricted the migration of solvents. In contrast, the Minnelusa contains highly permeable sandstones that aided solution of anyhdrite and gypsum. Where collapse in the Minnelusa initiated upward stoping through the overlying formations, ground water circulating through the pipes probably leached blocks of gypsum from the Spearfish, thus reducing the volume of the breccia and thereby increasing the stoping. Near the margin of the pipes, collapse of the siltstones probably sealed off the gypsum beds from further solution by ground water.

Solution in the Minnelusa began in early Tertiary time and has progressed downdip from the brecciated outcrops. Inclusions of fragments of Minnekahta Limestone within the collapse structures indicate that solution and collapse were not penecontemporaneous with deposition of the Minnelusa. Only after the Laramide uplift of the Black Hills was the Minnelusa exposed to erosion and subjected to solution by ground water. Collapse and brecciation in the Argyle quadrangle occurred before deposition of the Chadron Formation in Oligocene time. During Recent time two sinks, the largest measuring 240 feet in diameter and 60 feet in depth, have formed downdip in Cretaceous strata at the head of Brady Canyon, 2 miles south of Hot Springs, S. Dak. (D. E. Wolcott, 1957, oral communication). Analyses of present-day spring water ascending from the Minnelusa (Gott and Schnabel, 1963) show that solution of anhydrite, replacement of dolomite, and recementation of the collapse breccias by calcite are continuing in the Minnelusa Formation at the present time (Art. 84).

REFERENCES

Braddock, W. A., 1963, Geology of the Jewel Cave SW quadrangle, South Dakota: U.S. Geol. Survey Bull. 1063-G. [In press]

Brobst, D. A., and Epstein, J. B., 1963, Geology of the Fanny Peak quadrangle, Wyoming and South Dakota: U.S. Geol. Survey Bull. 1063-I. [In press]

Condra, G. E., and Reed, E. C., 1940, Correlation of the Carboniferous and Permian horizons in the Black Hills and Hartville uplift: Kansas Geol. Soc. Guidebook 14th Ann. Field Conf., Aug. 26 to Sept. 1, 1940, p. 127-128.

Darton, N. H., 1905, Geology and underground water resources of the Central Great Plains: U.S. Geol. Survey Prof. Paper 32, 433 p.

Epstein, J. B., 1958, Geology of part of the Fanny Peak quadrangle, Wyoming-South Dakota: U.S. Geol. Survey open-file report.

Gott, G. B., and Schnabel, R. W., 1963, Geology of the Edgemont NE quadrangle, South Dakota: U.S. Geol. Survey Bull. 1063-E, p. 127-190.

Thompson, W. O., and Kirby, J. M., 1940, Cross sections from Colorado Springs to Black Hills showing correlation of Paleozoic stratigraphy: Kansas Geol. Soc. Guidebook 14th Ann. Field Conf., Aug. 26 to Sept. 1, 1940, p. 145 pl. XV.

Wolcott, D. E., and others, 1962, Geologic and structure map of the Minnekahta NE quadrangle, Fall River and Custer Counties, South Dakota: U.S. Geol. Survey Mineral Inv. Field Studies Map MF-242.

Article 84

CALCITIZATION OF DOLOMITE BY CALCIUM SULFATE SOLUTIONS IN THE MINNELUSA FORMATION, BLACK HILLS, SOUTH DAKOTA AND WYOMING

By W. A. BRADDOCK and C. G. BOWLES, Denver, Colo.

Abstract.—From early Tertiary time to the present, anhydrite and gypsum have been dissolved from the Minnelusa Formation in a zone near the outcrop. The residual rocks have been oxidized, dolomite and anhydrite cements of sandstones have been replaced by calcite, and bedded dolomites have been converted to limestone.

Anhydrite beds in the upper part of the Minnelusa Formation have been removed by solution in a zone near the outcrop of the formation in the Black Hills. The removal of several hundred feet of rock has resulted in the formation of depression features, breccia layers and breccia pipes (Art. 83, fig. 83.1). A description of the solution breccias and a summary of the stratigraphic units in the Minnelusa Formation are given in Article 83.

In the zone in which anhydrite has been removed, the remaining rocks have been oxidized, dolomite and anhydrite cements of sandstones have been replaced by calcite cement, and bedded dolomites have been converted to limestones.

These conclusions are based upon examination of samples collected from the brecciated part of units 1 and 2 of the Minnelusa Formation in the vicinity of Hell Canyon and in the USGS No. 3 Minnekahta drill hole (Art. 83, fig. 83.1). Samples were also studied from the USGS No. 2 Pass Creek drill hole in the NW¼ sec. 1, T. 6 S., R. 1 E. This core test is downdip from the zone of intense leaching, and it penetrated rocks of unit 1.

The rocks cored in the No. 2 drill hole are mostly unaltered and include 235 feet of anhydrite. The sandstone in the core is dominantly light to dark gray, although some beds are irregularly spotted red, yellow, or purple in streaks paralleling the stratification, and others are mottled red along fractures. The cement of the gray to mottled sandstone is predominantly coarsely crystalline anhydrite containing small rhombs of dolomite. Pyrite occurs as interstitial filling in some of the gray sandstone. Carbonate rock in the core is very fine grained, dark gray, and consists largely or entirely of dolomite.

Rocks in all but one outcrop of the Minnelusa in the southern Black Hills are altered and contain neither anhydrite nor gypsum. The brecciated sandstone beds in the leached area are dominantly yellow and red. In outcrop the sandstone is friable and weakly cemented by coarsely crystalline calcite; it contains authigenic hematite crystals but no pyrite. Much of the brecciated carbonate rock is red and contains abundant spots and dendrites of manganese oxide. In the outcrop the carbonate rock ranges from calcitic dolomite to medium-grained limestone that contains less than 1 percent dolomite. These mixed carbonate rocks are the product of replacement of dolomite by calcite and the precipitation of calcite in vugs and fractures.

The determination of calcite and dolomite was made by studying the rate of solution of the minerals in dilute HCl, staining the calcite in thin sections with hematoxyline, measuring the refractive indices, and studying X-ray diffractometer patterns.

Progressive stages of calcitization exhibited by the dolomite breccias are significant in the interpretation of the origin of medium-grained limestone. The initial stages of calcitization of dolomites are shown by the photomicrographs (figs. 84.1A and B) of the dolomite
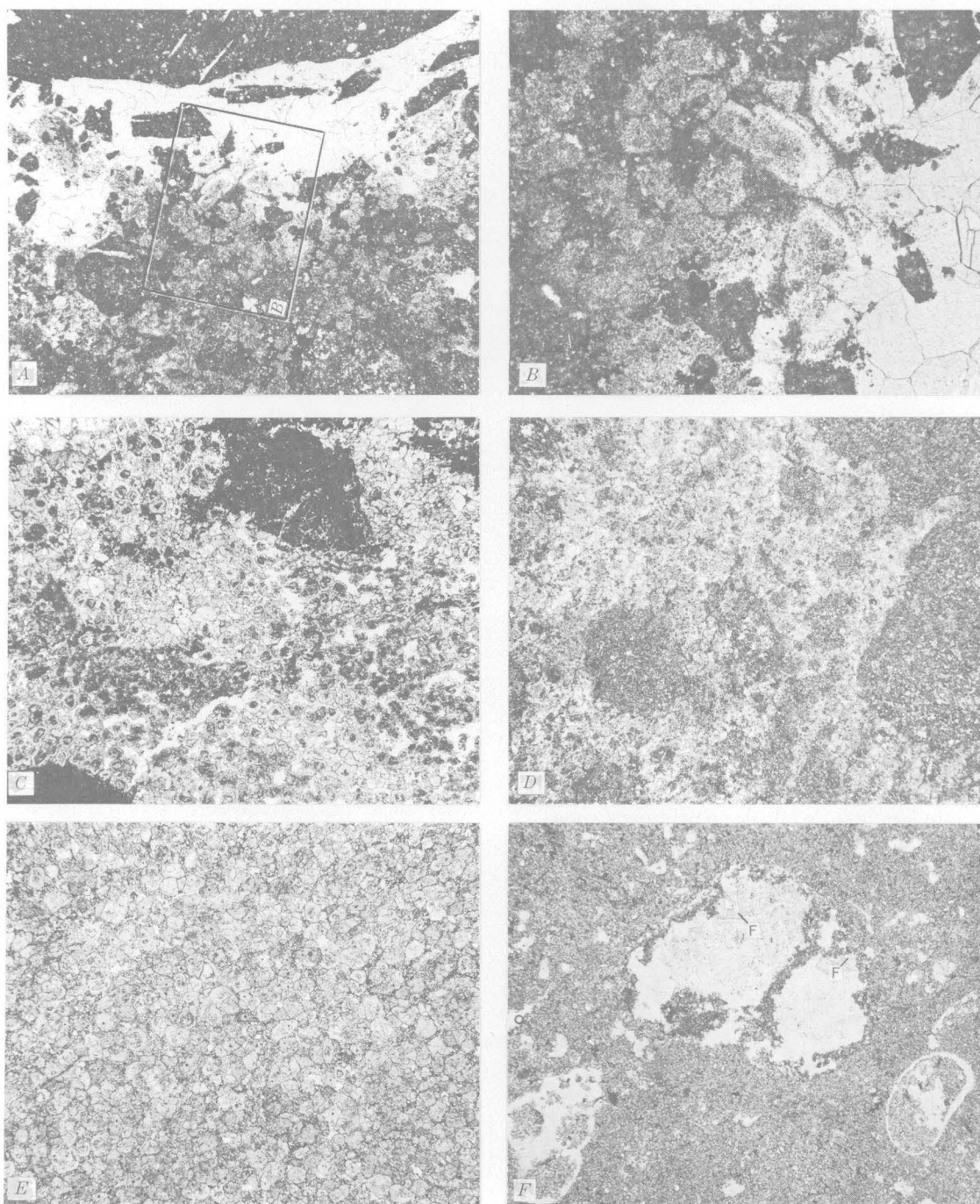
FIGURE 84.1.—Photomicrographs of carbonate rocks in the Minnelusa Formation, Custer County, S. Dak.

A, Dolomite breccia cemented and partly replaced by calcite. The dolomite (dark gray) below the fracture (white) has been extensively calcitized. The light gray patches are individual calcite crystals that poikalitically enclose abundant small dolomite grains. Area of figure 84.1B shown by outline. ×10.

B, Enlargement of the center of figure 84.1A. ×30.

C, Dolomite breccia. Some dolomite rock fragments (dark gray) have sharp boundaries, and other fragments are quite diffuse. Many of the coarse calcite crystals (light gray) have cores containing relict dolomite grains. ×10.

D, Calcitic dolomite. Residuals of dolomite rock (dark gray) are largely replaced by calcite (light gray). ×10.

E, Medium-grained limestone containing only traces of dolomite. ×10.

F, Gypsiferous dolomite. White areas are gypsum. Areas marked F are fluorite. The dolomite bed from which this sample was taken has been replaced by calcite in the zone of brecciation to form the limestone shown in figure 84.1E. ×10.

breccias. Fractures in the dolomites are filled with coarse-grained calcite. Where there has been little replacement by calcite, the breccia fragments are clearly defined and have sharp margins. With more advanced replacement, coarse calcite crystals have developed within the dolomite rock fragments and have poikalitically enclosed many smaller grains of dolomite. The formation of large calcite crystals with inclusion-filled cores and abundant fine grains of dolomite along their margins appears to be typical of the replacement process (figs. 84.1A, B, and C). With even more advanced replacement, the dolomite rock fragments have become quite diffuse (figs. 84.1C and D), and where calcitization is nearly complete the rock is a medium-grained limestone (fig. 84.1E).

Progressive degrees of alteration of an 8-foot carbonate bed were observed from the USGS No. 2 drill hole to an outcrop in Hell Canyon, 5 miles updip. At the crest of a small anticline, 2 miles updip from the drill hole, slight alteration is indicated by the hydration of anhydrite masses to gypsum as shown in figure 84.1F. Between the anticline and the outcrop in the zone of intense alteration in Hell Canyon, the dolomite bed has been completely converted to a medium-grained limestone (fig. 84.1E).

The alteration discussed above not only has affected surface exposures, but is believed also to have occurred throughout the subsurface part of the formation from which anhydrite has been leached. Specimens cored 25 to 180 feet below the surface in the USGS No. 3 Minnekahta drill hole show similar evidence of alteration.

It is clear that as the sandstone and dolomite were fractured by the subsidence resulting from leaching of anhydrite, oxidizing and calcium-rich solutions gained ready access to them and precipitated appreciable quantities of calcite along fractures and porous zones. In addition, these solutions brought about the extensive replacement of the fractured dolomite by calcite, a process which at completion produced limestone.

We conclude from the study of collapse features (Art. 83) that evaporitic rocks of the Minnelusa Formation have been dissolved by ground water, beginning in early Tertiary time and continuing to the present. Water analyses confirm our belief that solution is occurring now. Present day spring waters ascending from the Minnelusa contain in solution much calcium sulfate and some magnesium and bicarbonate (see table), indicating that the major ions are derived from the solution of calcium sulfate (anhydrite and gypsum), dolomite, and possibly limestone.

Ground water that dissolves the sulfate and carbonate rocks of the Minnelusa also precipitates $CaCO_3$ and replaces Mg with Ca. If the composition of the spring waters resulted only from the process of solution of the above-described rocks, then the concentration of calcium would at least be equivalent to the total concentration of sulphate and magnesium, which it is not. Also, too little bicarbonate is present to support the assumption that solution is the only process affecting the spring water. These deficiencies can be explained by the precipitation of $CaCO_3$, the exchange of Ca and Mg during calcitization of dolomite, or by a combination of both processes, as found in the Minnelusa rocks (fig. 84.1).

Yanat'eva (1956) showed that calcium sulfate solutions, similar in composition to the spring waters from the Minnelusa Formation, will calcitize dolomite and precipitate calcium carbonate. In a solution of calcium sulfate at 25°C and a low partial pressure (0.0012 at-

Chemical analyses of spring water from the Minnelusa Formation, Black Hills, South Dakota and Wyoming [1]

[All data from Gott and Schnabel, 1963; ppm, parts per million; epm, equivalents per million [2]]

Chemical constituent	1		2		3		4		5		6	
	ppm	epm	ppm	epm	ppm	epm	ppm	epm	ppm	epm	ppm	epm
Calcium (Ca)$^{+2}$	532	26.6	472	23.6	402	20.1	252	12.6	508	25.4	568	28.3
Sulfate (SO₄)$^{-2}$	1,420	29.6	1,260	26.2	1,040	21.7	639	13.3	1,610	33.5	1,540	32.1
Magnesium (Mg)$^{+2}$	83	6.8	78	6.4	56	4.6	51	4.2	112	9.2	92	7.6
Bicarbonate (HCO₃)$^{-1}$	225	3.7	227	3.7	190	3.1	232	3.8	112	1.8	235	3.9
Carbonate (CO₃)$^{-2}$	0	0	0	0	0	0	0	0	0	0	0	0
Sodium (Na)$^{+1}$	5	.2	6	.2	4	.2	86	3.7	21	.9	54	2.4
Chloride (Cl)$^{-1}$	4	.1	5	.1	1	.0	112	3.2	13	.4	62	1.8
Other dissolved solids	25	------	21	------	17	------	40	------	18	------	31	------

1. Sample 2208. SE¼ sec. 31, T. 45 N., R. 60 W., Weston County, Wyo.
2. Sample 2209. NE¼ sec. 31, T. 45 N., R. 60 W., Weston County, Wyo.
3. Sample 2210. SW¼ sec. 17, T. 45 N., R. 60 W., Weston County, Wyo.
4. Sample 2247. Evans Plunge, Hot Springs, Fall River County, S. Dak.
5. Sample 2249. NW¼ sec. 35, T. 7 S., R. 5 E., Fall River County, S. Dak.
6. Sample 2250. Cascade Springs, SW¼ sec. 20, T. 8 S., R. 5 E., Fall River County, S. Dak.

[1] Locations of springs shown on fig. 83.1 of Article 83 as numbered water-sampling localities.
[2] Equivalents per million = parts per million × 1/combining weight.

mosphere) of carbon dioxide, dolomite was many times more soluble than calcite. Dolomite and gypsum were unstable, and the reaction

$$CaCO_3 \cdot MgCO_3 + CaSO_4 \rightleftharpoons 2CaCO_3 + MgSO_4 (+ \ water)$$
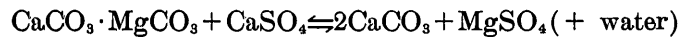
occurred, causing calcitization of dolomite and the accumulation of magnesium sulfate in solution.

REFERENCES

Gott, G. B., and Schnabel, R. W., 1963, Geology of the Edgemont NE quadrangle, South Dakota: U.S. Geol. Survey Bull. 1063–E, p. 127–190.

Yanat'eva, O. K., 1956, The nature of the solubility of dolomite in water and in calcium sulfate solutions at different partial pressures of CO_2: Zhur. Neorg. Khim. Trans., v. 1, no. 7, p. 1473–1478.

Article 85

APATITIZED WOOD AND LEUCOPHOSPHITE IN NODULES
IN THE MORENO FORMATION, CALIFORNIA

By R. A. GULBRANDSEN, D. L. JONES, K. M. TAGG, and D. W. REESER,
Menlo Park, Calif.

Abstract.—Nodules containing apatitized wood fragments occur in the Moreno Formation of Cretaceous age. Pyrite, deposited in open space in the wood, and apatite are primary minerals formed in a marine environment; leucophosphite and gypsum are secondary minerals formed during weathering. X-ray data for leucophosphite are presented for this new occurrence of the mineral.

Apatitized fossil wood in itself is rare, but in association with leucophosphite in gypsum-encased nodules, as described here, it is unique. Simpson (1912) reviewed early reports of phosphatized fossil wood, and since then only a few occurrences have been described (Simpson, 1920; Read, 1936; Hofmann, 1944; Maslennikov and Kavitskaya, 1956; Goldberg and Parker, 1960). The wood in the samples described here has been replaced by carbonate fluorapatite, hereinafter referred to as apatite. Leucophosphite, a hydrous potassium ferric phosphate, is new in this mode of occurrence and previously has been found only in a pegmatite (Lindberg, 1957) and in deposits formed by reactions of iron-rich materials with bird guano (Simpson, 1931–32) and bat dung (Axelrod and others, 1952).

The Moreno Formation, in which the fossil wood occurs, is of latest Cretaceous and earliest Paleocene(?) age. It crops out in the foothills along the western side of San Joaquin Valley, mainly in Fresno and Merced Counties, Calif. It consists of several thousand feet of dominantly purple and chocolate-brown organic-rich mudstone with intercalated sandstone lenses. Marine fossils occur throughout the section, although preservation of megafossils is generally poor. Foraminifera are locally abundant, and several rich floras of diatoms have been described (Hanna, 1927, 1934; Long and others, 1946).

The specimens of fossil wood were obtained from the lower part of the Moreno at the head of Escarpado Canyon, Fresno County (figs. 85.1 and 85.2), where Payne (1941; 1951) divided the formation, in ascending order, as follows: Dosados Sand and Shale, Tierra Loma Shale, Marca Shale, and Dos Palos Shale Members (fig. 85.3). The fossil wood was obtained from the upper part of the Dosados Sand and Shale Member and the lower part of the Tierra Loma Shale Member.
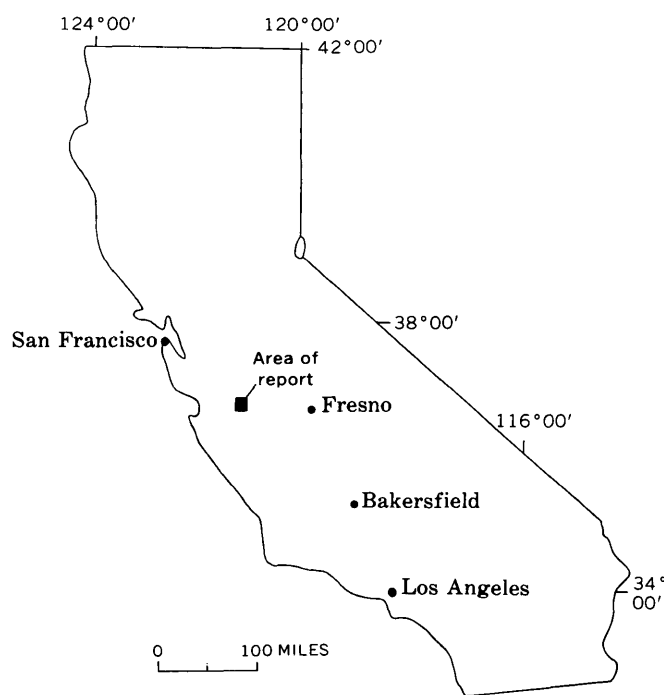
FIGURE 85.1.—Index map of California showing location of described area.
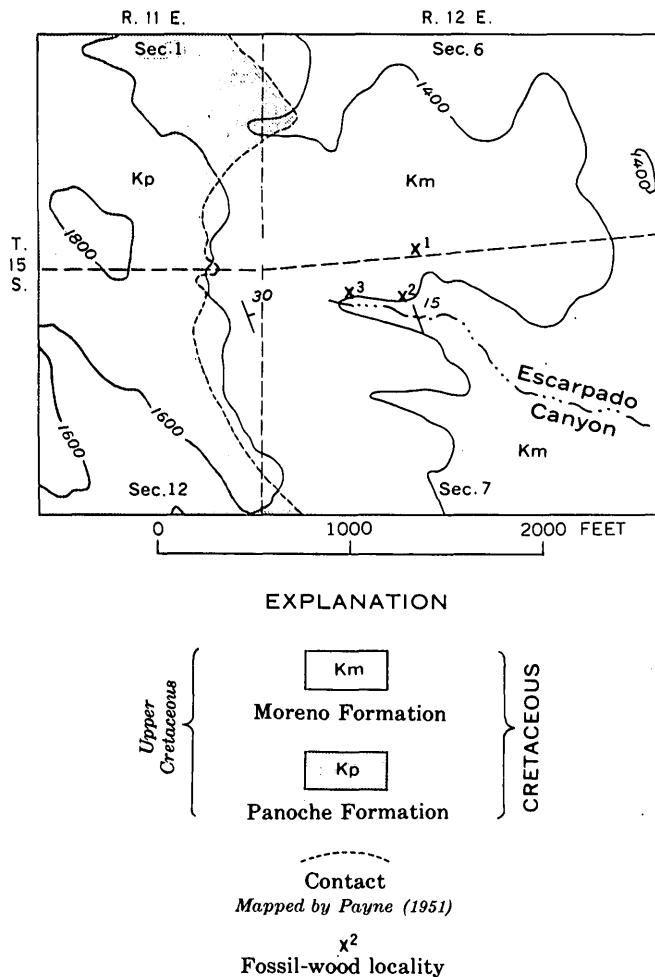
FIGURE 85.2.—Map showing location of fossil-wood localities in the Moreno Formation, Fresno County, Calif.

The wood is not ideal for fossil identification, as it is poorly preserved. Two of the better preserved specimens, examined by R. A. Scott, U.S. Geological Survey, could be identified with certainty only as dicotyledons; one is provisionally assigned to the family Sapotaceae, genus *Chrysophyllum*, a form now found only in tropical and subtropical regions.

The fossil wood occurs in gypsum-encrusted nodules in brown mudstone, and the nodules have considerable range in size and shape. The largest found was a slab $1 \times 1\frac{1}{2}$ feet in largest dimensions; the longest, a branch, was $1\frac{1}{2}$ feet long. A typical nodule (fig. 85.4) is composed of three parts: a core of fossil wood, an earthy zone, and a crust of gypsum. Nodules exposed to surface weathering usually lack all or part of the gypsum crust.

The core of a nodule is composed principally of gypsum, pyrite, and apatite. Apatite generally preserves in detail the cell structure of the wood (fig. 85.5) and apparently is an initial replacement mineral. Under the microscope most of it is seen as brown submicrocrystalline particles that are isotropic in aggregate; a very small amount is a colorless anisotropic filling of microscopic fractures. Some brown apatite masses reveal no cell structure. Pyrite is associated with the apatite and is regarded as contemporaneous; it occupies cell space and larger openings. Gypsum occurs as light-brown fine-grained crystals in veins and larger replacements of the apatitized wood, rarely preserving the cell structure. In some nodules, bassanite occurs in place of gypsum. Leucophosphite in the core is rare. Although the dissolution of apatite and pyrite is complete in many cores, a gross wood structure is still evident.

The earthy zone partly encases the core material and differs markedly from the enclosing mudstone in that it characteristically is a tan soft aphanite composed principally of cristobalite-opal, quartz, leucophosphite, and gypsum. The composition ranges widely, and either cristobalite-opal or brown gypsum may constitute most of the earthy matrix in some nodules. Montmorillonite and jarosite are present in small amount in the earthy zone of some nodules. Leucophosphite, which is regarded as a secondary mineral, occurs as spherulites and pellets that commonly are concentrated in a layer immediately beneath the gypsum crust but also are found in fractures and other areas within the earthy zone. Two unidentified minerals, one common but not abundant, appear to be confined to the earthy zone.

The crust is composed of white coarsely crystalline gypsum. The crystals are elongate perpendicular to the surface of the earthy zone, or wood core where the earthy zone is absent, thus delineating a sharp discontinuity between the crust and the rest of the nodule.

The mudstone in which the nodules were found is composed principally of mixed-layer montmorillonite-illite, quartz, plagioclase, K-feldspar, and mica; traces of cristobalite-opal and gypsum also are present. Gypsum occurs in veins and is strikingly abundant in surface exposures. Samples of mudstone from drill cores are similar in composition to surface samples except that pyrite is present and gypsum is absent.

All mineral identifications have been confirmed by X-ray analysis. X-ray data for the leucophosphite in the Moreno Formation are listed in the accompanying table along with data of the synthetic mineral and data from well-formed crystals in the Sapucaia pegmatite mine. The leucophosphite of the Moreno Formation is submicrocrystalline and produces a generally diffuse X-ray pattern. The d values and intensities of the principal peaks check well with the values measured on the other samples, despite the lack of sharp resolution and the partial interference, due to impurities, that is indicated for a few peaks.
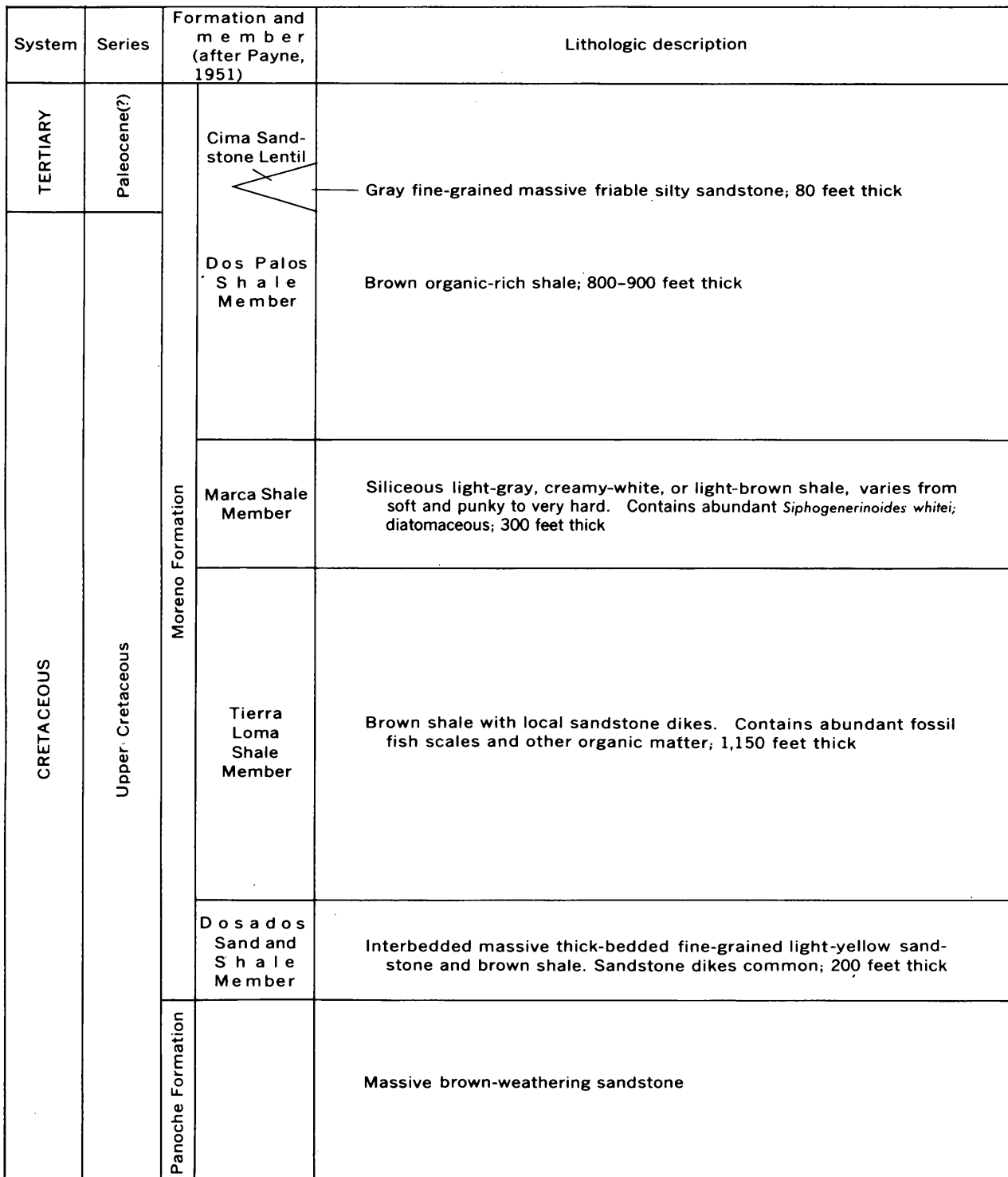
System	Series	Formation and member (after Payne, 1951)		Lithologic description
TERTIARY	Paleocene(?)	Moreno Formation	Cima Sandstone Lentil	Gray fine-grained massive friable silty sandstone; 80 feet thick
CRETACEOUS	Upper Cretaceous		Dos Palos Shale Member	Brown organic-rich shale; 800–900 feet thick
			Marca Shale Member	Siliceous light-gray, creamy-white, or light-brown shale, varies from soft and punky to very hard. Contains abundant *Siphogenerinoides whitei*; diatomaceous; 300 feet thick
			Tierra Loma Shale Member	Brown shale with local sandstone dikes. Contains abundant fossil fish scales and other organic matter; 1,150 feet thick
			Dosados Sand and Shale Member	Interbedded massive thick-bedded fine-grained light-yellow sandstone and brown shale. Sandstone dikes common; 200 feet thick
		Panoche Formation		Massive brown-weathering sandstone

FIGURE 85.3.—Diagrammatic columnar section of Moreno Formation in Escarpado Canyon, Fresno County, Calif. Modified from Payne (1951).
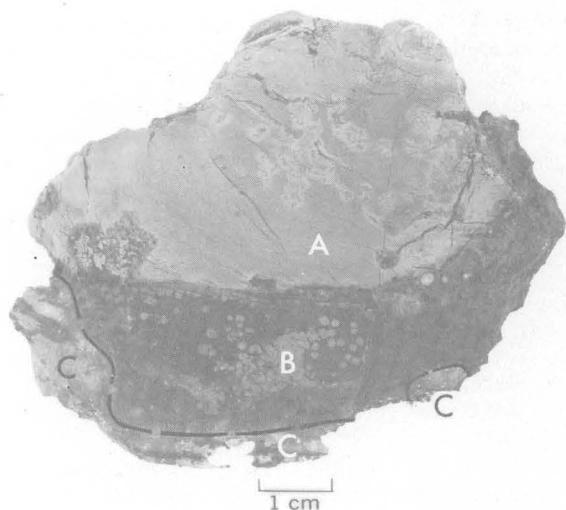
FIGURE 85.4.—Section of nodule showing apatitized wood, *A*; earthy zone with leucophosphite pellets, *B*; and gypsum crust, *C*.
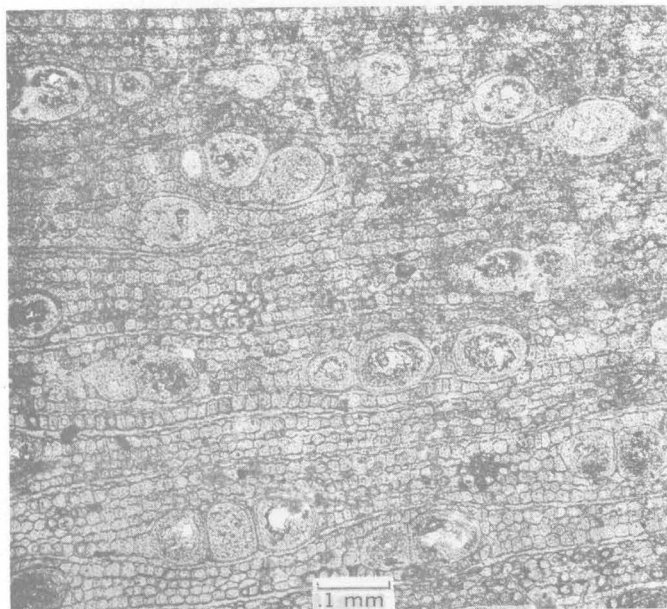
FIGURE 85.5.—Apatitized wood (family Sapotaceae?, genus *Chrysophyllum?*) showing preservation of intricate wood structure.

X-ray diffraction data for leucophosphite

[Lines less than 2.629 not included]

Moreno Formation [1]		Synthetic [2]		Sapucaia pegmatite mine, Brazil [3]	
d	I	d	I	d	I
7. 55	25	7. 50	0. 31	7. 60	3
6. 72	100	6. 77	1. 00	6. 79	10
				6. 09	1
5. 94	95	5. 92	. 76	5. 99	7
4. 70	30	4. 73	. 28	4. 76	3
4. 22	[4] 35	4. 23	. 21	4. 28	2
		4. 20	. 28	4. 21	2
4. 06	[4] 40	4. 05	. 14	4. 08	2
3. 76	20	3. 78	. 21	3. 79	3
				3. 65	1
				3. 54	1
3. 34	[5] 65	3. 34	. 35	3. 37	[6] 3
		3. 20	. 14	3. 25	½
		3. 09	. 14	3. 23	½
3. 03	55	3. 03	. 59	3. 06	7
2. 970	40	3. 00	. 28	3. 017	1
		2. 97	. 28	2. 990	1
				2. 956	1
2. 869	25	2. 90	. 37	2. 916	4
2. 798	35	2. 81	. 41	2. 829	4
2. 672	30	2. 66	. 35	2. 685	1
2. 629	30	2. 64	. 37	2. 655	3

[1] Escarpado Canyon, SW¼SW¼ sec. 6, NW¼NW¼ sec. 7, T. 15 S., R. 12 E., Fresno County, Calif. X-ray powder analysis on wide-range diffractometer, Ni-filtered Cu $K\alpha_1$ radiation, (λ=1.54050A).
[2] Haseman and others, 1950, p. 80. Product I.
[3] Lindberg, 1957, p. 219.
[4] Peak broad and intensity enhanced by cristobalite-opal and quartz impurities.
[5] Intensity enhanced by quartz impurity.
[6] Broad.

The origin of the nodules may be postulated from the nature and distribution of the minerals within the nodules themselves and from evidence in the sedimentary rocks in which the nodules occur. The presence of pyrite in the nodules and the abundant organic matter as well as pyrite in the surrounding sediments indicates that the wood was deposited in a reducing environment that had a pH lower than that of ordinary sea water. In addition, the wood itself probably created a local environment that favored deposition of apatite. Limited data from a modern occurrence of apatitized wood on the Pacific sea floor (Goldberg and Parker, 1960, p. 631) show that the bottom water contains almost no oxygen and is rich in phosphate. The cristobalite-opal composition of the earthy zone probably was derived from diatoms or other siliceous organisms that were attached to the wood before it sank or that drifted against it on the bottom. The abundance of such organisms is a feature of oceanic areas of modern phosphate deposition (McKelvey, 1959, p. 1783). Leucophosphite and gypsum represent in large part only a recombination of the elements already present in the phosphatized wood when uplift of the enclosing Moreno Formation exposed it to weathering. Oxidation of the pyrite locally produced sulfuric acid, which dissolved the apatite. Ensuing reactions produced the new solid phases, leucophosphite and hydrous calcium sulfate.

REFERENCES

Axelrod, J. M., Carron, M. K., Milton, Charles, and Thayer, T. P., 1952, Phosphate mineralization at Bomi Hill and Bambuta, Liberia, West Africa: Am. Mineralogist, v. 37, p. 883–909.

Goldberg, E. D., and Parker, R. H., 1960, Phosphatized wood from the Pacific sea floor: Geol. Soc. America Bull., v. 71, p. 631–632.

Hanna, G. D., 1927, Cretaceous diatoms from California: California Acad. Sci. Occasional Papers, no. 13, 48 p.

——— 1934, Additional notes on diatoms from the Cretaceous of California: Jour. Paleontology, v. 8, p. 352–355.

Haseman, J. F., Lehr, J. R., and Smith, J. P., 1950, Mineralogical character of some iron and aluminum phosphates containing potassium and ammonium: Am. Soil Science Soc. Proc., v. 15, p. 76–84.

Hofmann, Elise, 1944, Pflanzenreste aus dem Phosphoritvorkommen von Prambachkirchen in Oberdonau: Palaeontographica, v. 88, pt. B, p. 1–81.

Lindberg, M. L., 1957, Leucophosphite from the Sapucaia pegmatite mine, Minas Gerais, Brazil: Am. Mineralogist, v. 42, p. 214–221.

Long, J. A., Fuge, D. P., and Smith, James, 1946, Diatoms of the Moreno Shale: Jour. Paleontology, v. 20, p. 89–118.

McKelvey, V. E., 1959, Relation of upwelling marine waters to phosphorite and oil [abs.]: Geol. Soc. America Bull., v. 70, p. 1783.

Maslennikov, B. M., and Kavitskaya, F. A., 1956, O fosfatom veshchestve fosforitov [The phosphate substance of phosphorites]: Doklady Akad. Nauk SSSR, v. 109, no. 5, p. 990–992 [in Russian].

Payne, M. B., 1941, Moreno shale, Panoche Hills, Fresno County, California [abs.]: Geol. Soc. America Bull., v. 52, p. 1953–1954.

——— 1951, Type Moreno Formation: California Div. Mines Spec. Rept. 9, 29 p.

Read, C. B., 1936, The flora of the New Albany shale, pt. 1, *Diichnia kentuckiensis*, a new representative of the Calamopityeae: U.S. Geol. Survey Prof. Paper 185–H, p. 149–162.

Simpson, E. S., 1912, Unusual types of petrifaction from Dandarragan: Nat. History and Sci. Soc. Western Australia Jour., v. 4, p. 33–37.

——— 1920, On gearksutite at Gingin, Western Australia: Mineralog. Mag., v. 19, p. 23–39.

——— 1931–32, Contributions to the mineralogy of western Australia—series VII: Royal Soc. Western Australia Jour., v. 18, p. 61–74.

VARIATION IN ELEMENT CONTENT OF AMERICAN ELM TISSUE WITH A PRONOUNCED CHANGE IN THE CHEMICAL NATURE OF THE SOIL

By HANSFORD T. SHACKLETTE, Denver, Colo.

Abstract.—Chemical analysis of ash of an American elm tree whose base was flooded by galena and sphalerite tailings indicated that phosphorus and zinc were concentrated in the living wood, that calcium was depleted, and that potassium was concentrated in both living wood and nonliving cells.

Two large American elm (*Ulmus americana* L.) trees growing under sharply contrasting conditions were analyzed to detect differences in the element content of their tissues. The trees, near Tennyson, Grant County, in southwestern Wisconsin, were growing on a slope within 150 feet of each other and were 3½ feet in diameter at breast height. One was growing in normal soil, whereas the other had been enclosed on the lower side of the slope by an earth and rock dam to make a settling basin for tailings from an ore mill located a few hundred yards upslope. The dam was constructed and the basin put in use in 1952, 10 years before the field study reported here. Fine tailings suspended in water, resulting from the crushing of lead (galena) and zinc (sphalerite) ores and from their separation in the milling process, had been poured into the basin. The water had evaporated and the "fines" had settled into a firm deposit composed principally of dolomite, estimated to be 5 feet thick around the trunk of the enclosed tree. A partial chemical analysis of this soil material is given in table 86.1.

The change in soil level over the roots of the tree and the periodic flooding is slowly killing the tree, probably because of the effect of reduced soil aeration on the roots and not because of the heavy-metal content of the deposit. At the time of examination the last 2 years of growth had been greatly retarded, as determined by the length of branch-growth increments and the width of annual-growth rings. In addition, the leaves were markedly sparse and chlorotic; more so in 1962 than in 1961. The adjacent elm tree on unaffected soil was vig-

TABLE 86.1.—*Chemical analyses of American elm samples and soil samples*

[J. B. McHugh, J. H. Turner, and S. L. Power, U.S. Geological Survey, analysts]

Sample	Ash (percent of dry weight)	Ca	K	P	Cu	Pb	Zn
		Percent of ash, by weight					
Wood:							
Flooded tree, 1952–61	1.5	20	23.0	1.50	0.008	0.0050	0.070
Flooded tree, 1942–51	1.3	16	35.0	.60	.012	.0075	.050
Normal tree, 1952–61	2.5	41	9.4	1.20	.006	.0025	.060
Normal tree, 1942–51	1.0	19	25.0	.60	.015	.0100	.050
Branches (1–4 years old):							
Flooded tree	4.5	25	12.0	2.40	.008	.0150	.400
Normal tree	5.0	32	7.0	1.20	.004	.0150	.050
Average elm [1]	4.8				.009	.0080	.073
Leaves:							
Flooded tree	7.0	16	16.0	2.40	.006	.0050	.070
Normal tree	12.0	20	16.0	1.80	.004	.0025	.010
Average elm [1]	13.3				.004	.0025	.021
		Percent of dry weight					
Tailings fines		16	2.0	0.15	0.015	0.0200	1.000
Soil near normal tree, A₂ horizon		6	1.4	.06	.001	.0150	.020

[1] From 22 other American elm trees growing under normal soil conditions in Wisconsin.

orous and healthy, judging from its growth increments and leaf color.

Samples of the tree trunk at breast height were taken separately of the wood formed during the last 10 years and that formed during the 10 years before flooding to ascertain whether the change in chemical composition of the soil was reflected in the element content of the wood. An increment borer was used to determine, by ring count, the thickness of the wood formed during these 2 periods (2¼ and 2 inches, respectively). A 1-inch-diameter wood auger was then used to remove the wood for chemical analysis from that part of the trunk that grew during these two periods. The same procedure was followed in sampling the normal tree, the wood increments for the 2 periods being 2½ and 2 inches. In addition, samples of the leaves and of current to 4-year-old branches were collected from the 2 trees. The

A₂ soil horizon from near the normal tree was also sampled.

The tissue samples were air dried and then burned to ash in an electric oven in which the heat was increased 50°C per hour to 550°C and then held constant for 14 hours. The ash was analyzed by colorimetric methods (Ward and others, 1963) for calcium, potassium, phosphorus, copper, lead, and zinc. The sample of fines from the tailings and the sample of normal soil were sieved without grinding, and the minus-80-mesh fractions were analyzed by colorimetric methods. Results of these analyses are presented in table 86.1, as are also the averages of tissue analyses of 22 American elm trees which are growing under normal soil conditions in Wisconsin and which are cited to demonstrate the validity of using the normal tree of this study as a control.

Results.—The following results were noted in the study:

1. Flooding the American elm tree with ore-mill tailings resulted in a greater percentage of phosphorus and zinc in the ash of wood formed after the flooding occurred, but had no effect on the percentage of these elements in ash of the wood formed before flooding, as compared with the percentage in wood ash of the normal tree (table 86.2).

TABLE 86.2.—*Increase or decrease in percentage of elements in flooded tree samples as compared with normal tree samples*

[Percentage of ash by weight. +, increase; −, decrease]

Sample	Ca	K	P	Cu	Pb	Zn
Wood, 1952–61	−21	+13.6	+0.30	+0.002	+0.0025	+0.01
Wood, 1942–51	−3	+10.0	0	−.003	−.0025	0
Branches	−7	+5.0	+.12	+.004	0	+.35
Leaves	−4	0	+.60	+.002	+.0025	+.60

2. The percentage of calcium in the ash of all tissues was lower in the flooded tree (table 86.2), although the amount of this element in the soil was increased almost threefold (table 86.1). No explanation is offered for the reduction in calcium content of the tissue.

3. The percentage of potassium in the ash of both recently formed and older wood was significantly greater in the flooded tree (table 86.2). This indicates that the transport and deposition of this element is not exclusively related to metabolic processes of the tree, for the gain in potassium of the older wood presumably took place after the wood cells were dead. Wood cells of this age (10 years and older) are generally assumed to be nonliving, and in this tree the older wood sample was entirely "heartwood."

4. The differences in the copper and lead content of the ash appear to have no clear-cut relation to the increased amounts of these elements in the soil. The indicated increase of these elements in recently formed wood of the flooded tree compared with the amount in the normal tree is about the same as their decrease in the older wood (table 86.2). The apparent reduction of these elements in the ash of recently formed wood of the flooded tree as compared with the older wood of the same tree (table 86.1) is likewise probably within the limits of experimental error.

5. An increase in the zinc content of the soil resulted in an eightfold increase in the percentage of zinc in ash of the branches and a sevenfold increase in ash of the leaves (table 86.1). This is the most pronounced change in element content of any of the plant tissues.

Conclusions.—The addition of zinc and phosphorus to the soil in which the tree was growing resulted in an increase of these elements only in wood formed subsequently. Therefore, chemical analysis of tree rings may be a useful method of determining the year when the trees were exposed to increased amounts of these elements in the soil. In geochemical exploration it is important to know if a chemical anomaly in the soil is caused by naturally occurring element concentration or by manmade soil contamination; if the date of this increase in element content can be determined, it may be possible to determine the cause. If anomalies in certain elements at a site can be attributed to habitation by man, one may suspect that anomalies in some other elements are due to the same cause.

REFERENCES

Ward, F. N., Lakin, H. W., Canney. F. C., and others, 1963 Analytical methods used in geochemical exploration by the U.S. Geological Survey: U.S. Geol. Survey Bull. 1152, 100 p.

ORDOVICIAN AGE FOR SOME ROCKS OF THE CAROLINA SLATE BELT IN NORTH CAROLINA

By A. M. WHITE; ARVID A. STROMQUIST; T. W. STERN, and HAROLD WESTLEY;

Washington, D.C.; Denver, Colo.; Washington, D.C.

Abstract.—Two lead-alpha age determinations on zircon from felsic crystal–lithic tuff in part of the Carolina slate belt indicate an Ordovician age for these rocks. The results add to growing evidence of a Paleozoic rather than a Precambrian age for much of the southeastern Piedmont province.

Lead-alpha ages have been determined for zircon from two localities in the Carolina slate belt in the eastern part of the North Carolina Piedmont. Both samples of zircon are from the southeastern part of the Albemarle quadrangle (fig. 87.1), and the indicated age for each is Ordovician according to the Holmes time scale (Holmes, 1959, p. 204). Results of analyses and age calculations for the zircon are given in the accompanying table.

Lead-alpha age determinations of zircon from rocks of the Carolina slate belt

Sample No.	Alpha counts per milligram per hour	Pb(ppm)[1]	Calculated age [2] (m.y.)
ZU–1_____	52	9.6	440±60
ZU–2_____	201	40	470±60

[1] Average of duplicate determinations ZU–1 analyzed by Charles Annell and Harold Westley; ZU–2 by Harold Westley and I. H. Barlow.

[2] Ages (rounded to nearest 10 million years) calculated from the equations:

$$t = C\,Pb/a$$

where t is the calculated age, in millions of years; C is a constant based on the U/Th ratio and has a value of 2,485; Pb is the lead content, in parts per million; and a is the alpha counts per milligram per hour; and

$$T = t - \tfrac{1}{3} k t^2$$

where T is the age, in millions of years, corrected for decay of uranium and thorium; and k is a constant based on the U/Th ratio and has a value of 1.56×10^{-4}.

The Carolina slate belt of low-grade metasedimentary and metavolcanic rocks extends from Virginia south-ward across the Carolinas into Georgia, where the rocks are known as the Little River Series (Crickmay, 1952, p. 31). To the east it is bounded by rocks similar to those of the Charlotte belt (King, 1955, p. 346–350), by discontinuous outcrops of the Newark Group of Triassic age, and by overlap deposits of the coastal plain of Cretaceous and younger age. To the west, rocks of the slate belt are truncated by faults and metamorphosed along the border of a complex of plutons of the Charlotte belt.

Only rocks of the greenschist facies are commonly considered slate-belt rocks. They comprise a sequence of alternating rhyolitic to basaltic volcanic rocks interbedded with argillite, siltstone, sandstone, and their tuffaceous equivalents. The sequence is intruded by granitic to gabbroic sills, stocks, and batholiths of probable Paleozoic age (King, 1955, p. 349), and by Triassic diabase dikes that trend northwest to northeast.

Felsic flows and tuffs were selected as the most likely rocks to yield zircon, the sole mineral in these rocks on which age determinations are possible. Only 1 of 12 units sampled, however, yielded enough zircon for analysis. This unit, which is in the southeastern part of the Albermarle quadrangle, is part of a sequence of acid lithic tuffs in the lower volcanic unit as mapped by Stromquist and Conley (1959, p. 15, 16, and map) and by Conley (1962). It is the lowest stratigraphic unit in the Albemarle and Denton quadrangles and consists of felsic lithic tuff and crystal tuff with interbedded rhyolite flows. The tuffs are cut by several rhyolite dikes. The unit is traceable from the southern part of the Albemarle quadrangle to the area north of
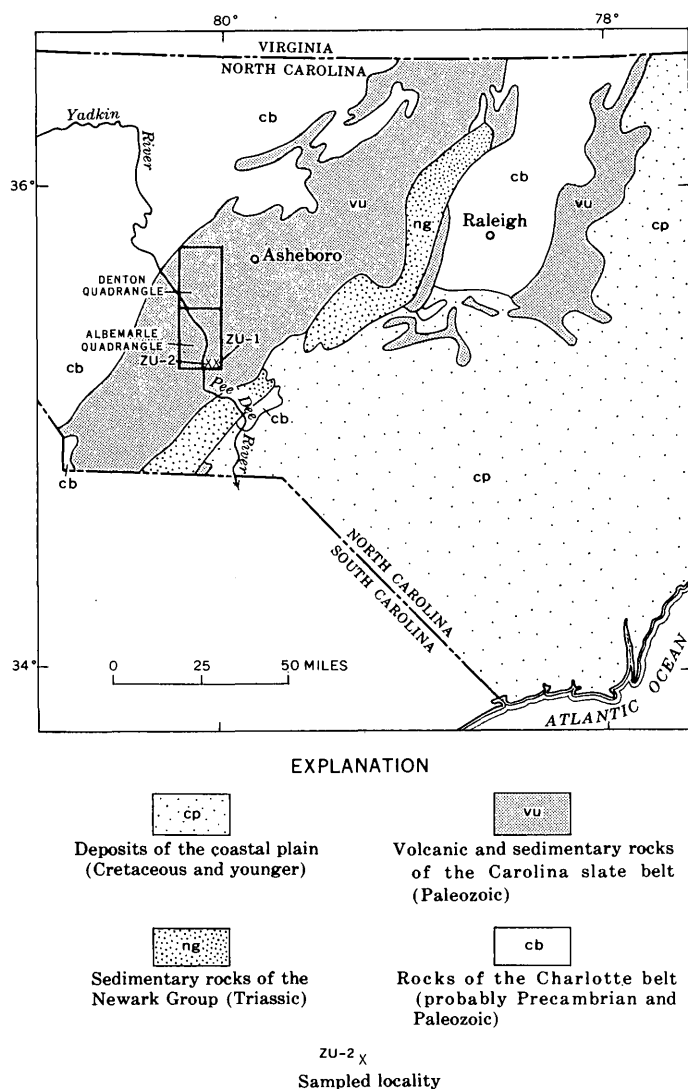
EXPLANATION

Deposits of the coastal plain
(Cretaceous and younger)

Volcanic and sedimentary rocks
of the Carolina slate belt
(Paleozoic)

Sedimentary rocks of the
Newark Group (Triassic)

Rocks of the Charlotte belt
(probably Precambrian and
Paleozoic)

ZU-2 ₓ
Sampled locality

FIGURE 87.1.—Index map of central North Carolina showing lo-
calities sampled for zircon. Geology generalized from geo-
logic map of North Carolina (Stuckey and Conrad, 1958) and
from King (1955).

Asheboro, and from the sedimentary rocks of the New-
ark Group on the east to the area near the Pee Dee
River on the west (fig. 87.1). The structure appears to
be that of a large southwest-plunging anticline. In the
upper part of the unit, poor bedding and a lack of
sorting of the constituent fragments and crystals sug-
gest subaerial deposition. Therefore, this unit probably
represents an old landmass built up from the sea floor
by a series of volcanic eruptions and flows. The unit
sampled is overlain by a younger sequence of volcanic
and sedimentary rocks extending at least to the bound-

ary of the slate belt with the Charlotte belt to the west.
Eastward, the younger unit may extend to the sedi-
mentary rocks of the Newark Group (fig. 87.1).

The tuff was sampled at exposures in roadcuts along
North Carolina Highway 27, 3.4 miles east of the Pee
Dee River and 1 mile north of the junction of Clarks
and Dumas Creeks (sample ZU-1), and 1.3 miles east
of the Pee Dee River and 0.7 mile southeast of White
Crest Church (sample ZU-2). Both localities are in
Montgomery County. About 700 pounds of saprolite
of felsic crystal–lithic tuff was panned to obtain zircon
for sample ZU-1, and about 300 pounds for sample
ZU-2. The zircon obtained from the tuffs is euhedral,
very fine grained, and pale pink. Detrital zircon of
more than one generation and from more than one
source is present in some slate-belt tuffs as well as in
alluvial deposits in the area (White and Stromquist,
1961), but the zircon reported here is believed to be
primary because of its euhedral crystal form and uni-
form grain size and color.

Rocks of the Carolina slate belt heretofore have been
dated only by inference and by speculation, for no de-
finitive fossil material has been reported from them.
Ordovician fossils have been found in the Arvonia and
Quantico slates of Virginia, but the geologic relations
of these rocks to the Carolina slate belt are not known.
For many years the slate-belt rocks were considered
Precambrian, and they were assigned a Precambrian age
on the geologic map of the United States (Stose and
Ljungstedt, 1932). Stuckey and Conrad (1958, p. 26–
29; map) designated them as Precambrian or lower
Paleozoic(?) on the geologic map of North Carolina.
An increasing amount of evidence favors a Paleozoic
age for the slate-belt rocks as well as for much of the
piedmont terrane west of the slate belt (King, 1951, p.
119–144; 1955, p. 332–373; Crickmay, 1952, p. 31; Over-
street and others, 1961, p. B104; Overstreet and others,
1962, p. C81). Moreover, stratigraphic equivalence of
some units within the piedmont, such as the Carolina
slate belt and the Kings Mountain belt to the west
(King, 1955, map), has been suggested (Keith and
Sterrett, 1931, p. 4; Kesler, 1936, p. 34; Overstreet and
Bell, 1960, p. B199). The Ordovician age reported here
for rocks of the Carolina slate belt supports the opinion
that many of the rocks in the southeast piedmont are
Paleozoic rather than Precambrian in age, and it per-
mits for the first time the assignment of a definitive age
to part of the Carolina slate belt.

REFERENCES

Conley, J. F., 1962, Geology of the Albemarle quadrangle, North Carolina: North Carolina Dept. Conserv. and Devel., Div. Mineral Resources Bull. 75, 26 p.

Crickmay, G. W., 1952, Geology of the crystalline rocks of Georgia: Georgia Geol. Survey Bull. 58, p. 1–54.

Holmes, Arthur, 1959, A revised geologic time scale: Edinburgh Geol. Soc. Trans., v. 17, pt. 3, p. 183–216.

Keith, Arthur, and Sterrett, D. B., 1931, Description of the Gaffney and Kings Mountain quadrangles [South Carolina–North Carolina]: U.S. Geol. Survey Geol. Atlas, Folio 222, p. 1–13.

Kesler, T. L., 1936, Granitic injection processes in the Columbia quadrangle, South Carolina: Jour. Geology, v. 44, no. 1, p. 32–42.

King, P. B., 1951, The tectonics of middle North America: Princeton, N.J., Princeton Univ. Press, p. 3–203.

————1955, A geologic section across the southern Appalachians—An outline of the geology in the segment in Tennessee, North Carolina, and South Carolina, in Russell, R. J., ed., 1955, Guides to southeastern geology: Geol. Soc. America Guidebook, 1955 Ann. Mtg., p. 332–373.

Overstreet, W. C., and Bell, Henry, 3d, 1960, Geologic relations inferred from the provisional geologic map of the crystalline rocks of South Carolina: Art. 87 in U.S. Geol. Survey Prof. Paper 400–B, p. B197–B199.

Overstreet, W. C., Bell, Henry, 3d, Rose, H. J., Jr., and Stern, T. W., 1961, Recent lead-alpha age determinations on zircon from the Carolina Piedmont: Art. 45 in U.S. Geol. Survey Prof. Paper 424–B, p. B103–B107.

Overstreet, W. C., Stern, T. W., Annell, Charles, and Westley, Harold, 1962, Lead-alpha ages of zircon from North and South Carolina: Art. 88 in U.S. Geol. Survey Prof. Paper 450–C, p. C81.

Stose, G. W., and Ljungstedt, O. A., 1932, Geologic map of the United States: U.S. Geol. Survey.

Stromquist, A. A., and Conley, J. F., 1959, Geology of the Albemarle and Denton quadrangles, North Carolina: Carolina Geol. Soc. Field Trip Guidebook, Oct. 24, 1959, North Carolina Div. Mineral Resources, Raleigh, N.C., 36 p.

Stuckey, J. L., and Conrad, S. G., 1958, Explanatory text for the geologic map of North Carolina: North Carolina Dept. Conserv. Devel., Div. Mineral Resources Bull. 71, p. 3–51, map.

White, A. M., and Stromquist, A. A., 1961, Anomalous heavy minerals in the High Rock quadrangle, North Carolina: Art 118 in U.S. Geol. Survey Prof. Paper 424–B, p. B278 and B279.

Article 88

GRAVITY SURVEY IN THE RAMPART RANGE AREA, COLORADO

By CARTER H. MILLER, Denver, Colo.

Abstract.—Gravity interpretation indicates that the Rampart Range is bounded on the east by a high-angle reverse dip fault and that an outlier of sedimentary rocks on the west is about 2,000 feet thick.

A gravity survey was made across the Manitou Park graben, Rampart Range, and the eastern foothills belt of Colorado (fig. 88.1) to obtain the depth and two-dimensional configuration of the sedimentary rocks in the graben and in the foothills belt. The configuration of the rocks in the foothills belt and in the graben is primarily controlled by the Rampart Range fault and the Ute Pass fault, respectively.

The Rampart Range extends about 40 miles northwest from Colorado Springs, Colo., to the South Platte River. The range is about 10 miles wide and is bordered on the west by the Manitou Park graben, which is approximately 3 miles wide, and on the east by the eastern foothills belt (fig. 88.1).

GEOLOGY

The Rampart Range is an anticlinal horst of part of the Precambrian Pikes Peak batholith. The range is bounded by the Rampart Range fault on the east and the Devils Head fault zone on the west (Boos and Boos, 1957, p. 2657–2661).

The Manitou Park graben is bounded by the Devils Head fault zone on the east and the Ute Pass fault on the west. The southern part of the graben contains outcropping Cambrian to Pennsylvanian sedimentary beds, which dip westward from the Rampart Range and are terminated at the Ute Pass fault. Some of the Pennsylvanian section, of which the valley floor of the Monitou Park graben is composed, has been removed by erosion. An anticline, consequent upon the Rampart Range, is indicated by projecting the attitude of

the beds southward around the end of the range.[1] A syncline in the graben is suggested by westward-dipping beds on the east side of the graben and, in places, by near-vertical beds on the west side.

The eastern foothills belt of the Front Range of Colorado is composed of a thick section of sedimentary rocks that dip steeply to the east, away from the Rampart Range. The foothills belt is bounded on the west by the Rampart Range fault. In parts of the belt the beds are overturned, which indicates that the fault is a high-angle reverse fault. The fault has cut out most of the sedimentary rocks older than Tertiary in that part of the belt covered by this survey.

THICKNESS AND DENSITY OF UNITS IN THE STRATIGRAPHIC SEQUENCE

The Pikes Peak Granite, of Precambrian age, is homogeneous in mineral content and density.

In the Manitou Park graben, Cambrian to Mississippian formations, which include the Sawatch Quartzite, Ute Pass(?) Dolomite (Peerless Formation of current usage), Manitou Limestone, Williams Canyon Limestone, and Madison(?) Limestone have a total thickness of approximately 240 feet.[2]

The thickness of two sections of the Pennsylvanian and Permian Fountain Formation, including the Glen Eyrie Shale Member, averages approximately 3,900 feet. One section was measured at Perry Park by Aslani[3] and the other was measured in the valley of Fountain Creek, near Colorado Springs (McLaughlin, 1947, 1944, 1948).

The stratigraphic section between the Fountain Formation and the Arapahoe Formation of Late Cretaceous

---

[1] Fowler, W. A., 1952, Geology of the Manitou Park area, Douglas and Teller Counties, Colorado: Colorado Univ. unpub. Ph. D. dissert., p. 24.

[2] Op. cit., p. 6–19.

[3] Aslani, Morad-Malek, 1950, The geology of southern Perry Park, Douglas County, Colorado: Colorado School of Mines unpub. thesis, no. 686, p. 30–32.
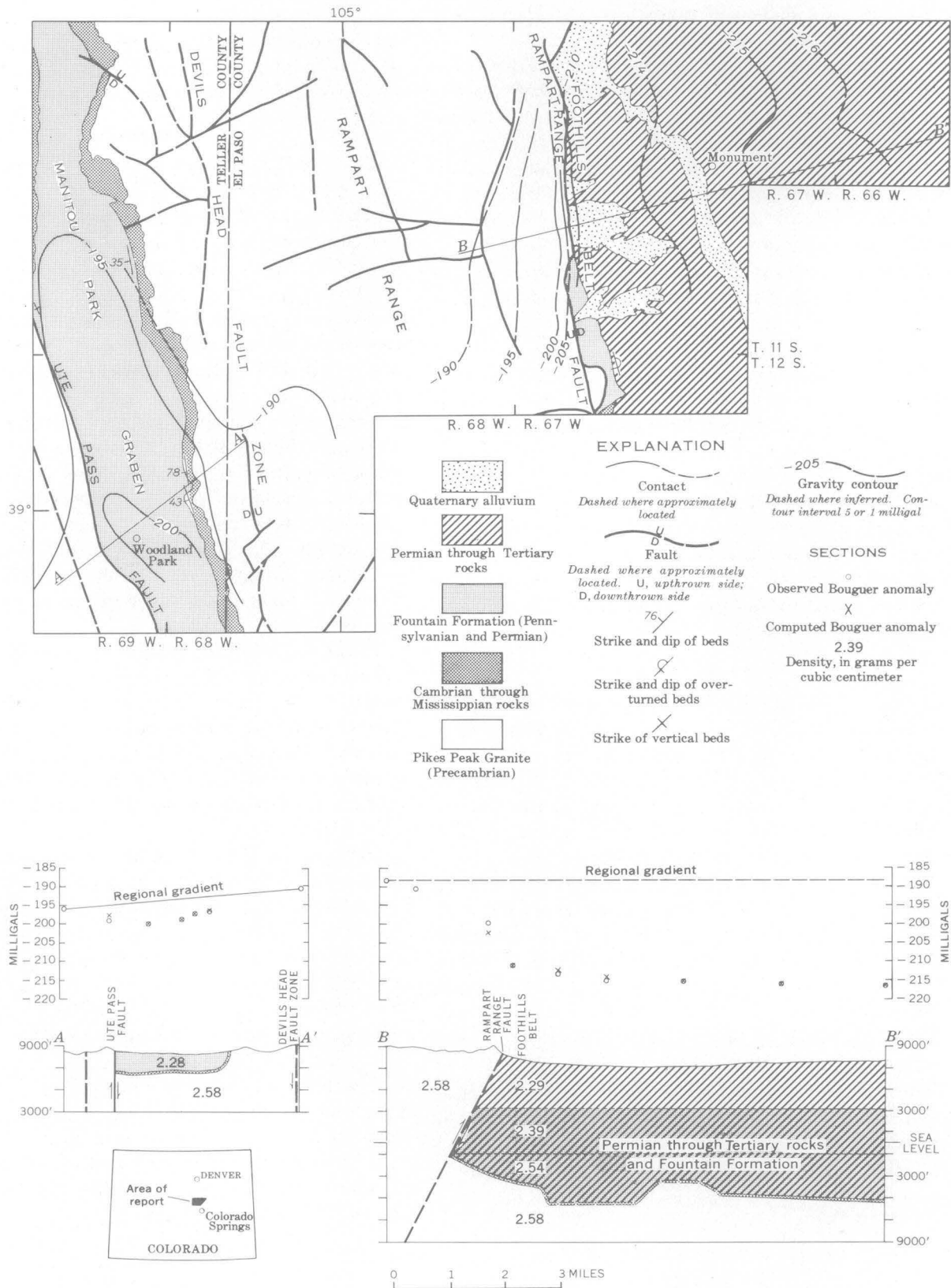
FIGURE 88.1.—Geologic and gravity map of part of the Rampart Range area (geology adapted from Boos and Boos, 1957, figs. 9 and 10). Sections show a two-dimensional analysis across Manitou Park and the eastern foothills belt.

age consists of shale and sandstone. At Perry Park the section is about 7,300 feet thick.[4]

The Arapahoe, Denver, and Dawson Formations range in age from Late Cretaceous through Paleocene. The formations are principally poorly cemented sandstone and conglomerate and have a total thickness of about 1,400 feet east of the Rampart Range. This thickness was estimated from a section measured by Reichert (1956, pl. 2, p. 108–111) in the Castle Rock quadrangle, Colorado.

The total thickness of the stratigraphic sequence east of the Rampart Range averages 12,800 feet. This thickness is presumed to be accurate within about 10 percent.

An average density of 2.58 g per cm³ for the Precambrian granite of the Rampart Range was determined from six fresh samples. An average density of 2.59 g per cm³ for the Cambrian to Mississippian sedimentary rocks was determined from eight samples picked at random from the section at Manitou Park. The density for the Pennsylvanian to Tertiary rocks is considered to be the same as the average density for shale and sandstone. The bulk density of shale is taken to be 2.31 g per cm³ and that of sandstone 2.28 g per cm³ (Birch and others, 1942, p. 22, 23).

GRAVITY DATA

A total of 130 gravity stations were established, and the data from 71 stations were used in this article. The survey was made with a Worden gravimeter that has a scale constant of approximately 0.227 milligals per scale division. The survey was tied to base stations that are part of a network established in 1961 by D. J. Stuart, of the U.S. Geological Survey.

Complete Bouguer anomalies were computed with elevation corrections of 0.062 mgal per ft and with terrain corrections that were computed or estimated through zone L of Hammer's tables (Hammer, 1939). These corrections were made using a density of 2.50 g per cm³.

Latitude corrections were based on the international gravity formula of 1930.

Elevations of the gravity stations were taken from bench marks and photogrammetric points shown on topographic maps published by the U.S. Geological Survey. The station elevations are thought to have an

[4] Op. cit., p. 41–70.

average error within ± 5 feet of the true value, which corresponds to a gravity error of less than ± 0.3 milligals. The latter value may be considered to be the largest error in the gravity computations.

INTERPRETATION

The two-dimensional graticule interpretations (fig. 88.1, A–A′, B–B′) were aided by independent control. In the Manitou Park graben, control was furnished by the known angle of dip of the beds on the east side of the graben and by the limited range of density of the Fountain Formation. The interpretation across the foothills belt was controlled by the known average thickness of the rocks (12,800 feet) and by theoretical limits of dip imposed by the observed gravity curve and density contrast.

Because the average density of the Cambrian to Mississippian formations is the same as that of the underlying Precambrian granite there is no gravimetric distinction between the two. Therefore, gravity computations were made to the base of the Fountain Formation. A density contrast of 0.3 g per cm³ between the Fountain Formation and Mississippian to Cambrian formations was used in the interpretation of the geology in the graben.

In the foothills belt, density is assumed to increase, as a result of compaction of the sedimentary rocks, at a rate of 0.025 g per cm³ per 1,000 feet of depth. Values for density contrast were chosen at 0.30, 0.20, and 0.05 g per cm³, corresponding to three intervals of depth of about 4,000 feet each. The intervals extend from the ground surface down to the base of the Fountain Formation.

Because the Pikes Peak batholith is extensive and is constant in density and mineral content it was assumed that the regional gradient is flat over a relatively small distance. Therefore, the regional gradient along cross section B–B′ is taken as a straight line of zero slope and of the same magnitude as the greatest gravity value along the cross section. This value is quite consistent with gravity values of other stations on the long axis of the Rampart Range.

The regional gradient along cross section A–A′ is taken as a straight line connecting the two greatest gravity values along the cross section.

The maximum computed depth to the base of the Fountain Formation in the Manitou Park graben is about 2,000 feet (fig. 88.1, A–A′).

CONCLUSIONS

The sedimentary rocks in the Manitou Park graben form a syncline, the west limb of which is truncated by the Ute Pass fault.

Overturned beds, which might indicate reverse faulting, are not predominant in the exposed parts of the foothills belt. However, the computed dip of the Rampart Range high-angle reverse fault, as defined by the observed gravity curve is limited to a reversed dip of 50° to 75° (fig. 88.1, B–B′).

The magnitude of the computed anomalies in the undulating basement rocks (fig. 88.1, B–B′) approaches the maximum error in the gravity computations and, therefore, the validity of these anomalies is questionable.

REFERENCES

Boos, C. M., and Boos, M. F., 1957, Tectonics of eastern flank and foothills of Front Range, Colorado: Am. Assoc. Petroleum Geologists Bull., v. 41, no. 12, p. 2603–2676.

Birch, A. F., Schairer, J. F., and Spicer, H. C., eds., 1942, Handbook of physical constants: Geol. Soc. America Spec. Paper 36, 325 p.

Hammer, Sigmund, 1939, Terrain corrections for gravimeter stations: Geophysics, v. 4, no. 3, p. 184–194.

McLaughlin, K. P., 1947, Pennsylvanian stratigraphy of Colorado Springs quadrangle, Colorado: Am. Assoc. Petroleum Geologists Bull., v. 31, no. 11 p. 1936–1981.

Reichert, S. O., 1956, Post-Laramie stratigraphic correlations in the Denver basin, Colorado: Geol. Soc. America Bull., v. 67, pl. 2, p. 108–111.

Article 89

GRAVITY SURVEY OF THE ISLAND OF HAWAII

By W. T. KINOSHITA,[1] H. L. KRIVOY,[2] D. R. MABEY,[1] and R. R. MacDONALD,[2]

[1] Menlo Park, Calif., [2] Hawaiian Volcano Observatory, Hawaii

Abstract.—Large gravity highs are centered over 4 of the 5 major volcanoes on the island of Hawaii. A lower amplitude gravity high occurs near the fifth volcano, Hualalai. These highs are attributed to intrusive rocks and denser parts of flows that are near the surface beneath the volcanoes and are convergent at depth.

Local gravity surveys in the vicinity of Kilauea volcano and its two major associated rift zones (Krivoy and Eaton, 1961) have been supplemented by a regional survey of the island of Hawaii (fig. 89.1). Measurements along the main roads and trails provided generally good coverage at elevations below 6,000 feet, but at higher elevations large areas are inaccessible and the gravity map is necessarily generalized. An average density of 2.3 g per cc was used for all above-sea-level material in the gravity reductions and terrain corrections. The reductions were made to sea level and the terrain corrections were made for above-sea-level terrain to a distance of about 100 miles from the station. Terrain corrections were made at about half the stations and interpolated at the remainder because the topography is such that a near-linear relation exists between station altitude and amount of correction in many parts of the island. A few corrections for submarine topography were made, and it was found that their effect on a map with a 10-mgal contour interval was negligible.

Because the total relief on Hawaii is more than 13,000 feet, the selection of a density to compute the Bouguer corrections determines to a large extent the character of the Bouguer anomaly map. The density of 63 dry samples, collected by R. R. Doell from the denser parts of numerous flows for remanent-magnetization studies, ranged from 1.8 g per cc to 3.0 g per cc but averaged 2.3 g per cc. Although the probable average density of the intrusive and nonvesicular flow rocks as shown by a few measurements is about 2.8 g per cc, these rocks constitute only a small part of the exposed rock on the island. Woollard (1951) found by a gravity-profile method that a density of 2.3 g per cc was the most applicable for his gravity study on Oahu.

The Bouguer gravity-anomaly map (fig. 89.1) shows pronounced gravity highs over Kohala Mountain, Mauna Kea, Mauna Loa, and Kilauea, 4 of the 5 major volcanoes which make up the island of Hawaii. Hualalai, the fifth volcano, lies at the north end of an elongate high of much lower amplitude than those over the other four. Other features of the gravity map include an east-trending gravity nose on the northeast slope of Mauna Kea, southwest-trending and east-trending gravity noses from the summit of Kilauea, a south-trending gravity nose from the summit of Mauna Loa, and low-gravity fields at Hilo and at the northwestern part of the island between Hualalai and Kohala Mountain.

The general correlation between the gravity highs and the topographic highs suggests that the density assumed in making the Bouguer corrections is too low, and that some discussion of these reductions is needed. There is little question that 2.3 g per cc is a reasonable approximation of the dry density of the exposed flows, and there is no reason to expect significant compaction of these flows between the surface and sea level. When this density is used in making the Bouguer correction, the anomalies obtained reflect the presence of masses with densities different from this value. In making the Bouguer reductions, no effort has been made to remove the part of the anomaly caused by density contrasts above sea level. An examination of the gravity map reveals several areas where substantial gravity differences do not correlate with surface topography. The most striking example is the +251-mgal value on the 8,000-foot summit of Hualalai, which is about the same as the gravity values at sea level along the southeast and east shores of the island.
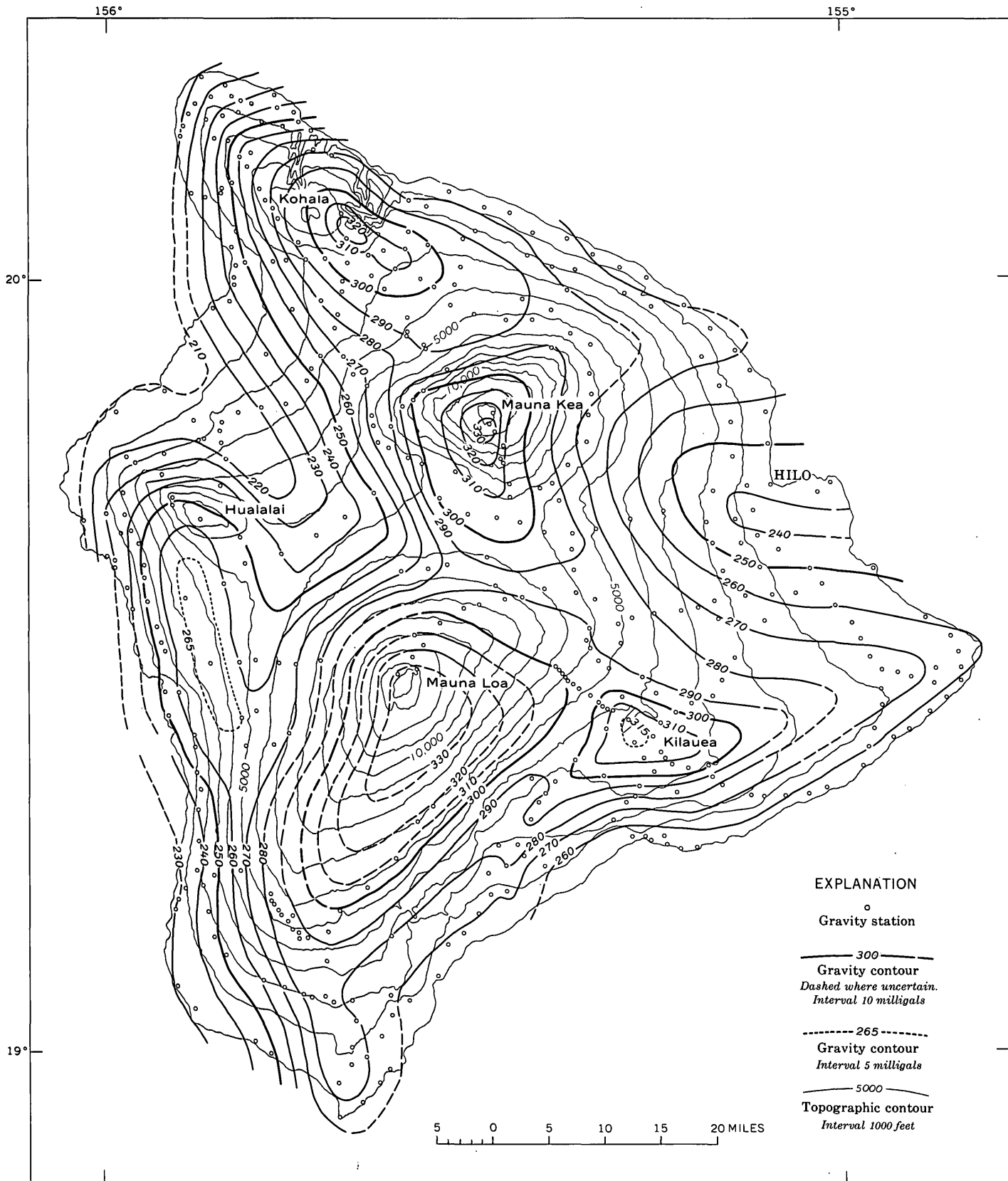
FIGURE 89.1.—Bouguer gravity-anomaly map of the island of Hawaii.

The four gravity highs over the individual volcanoes are part of a more extensive high that covers the central part of the island, so that although the total gravity relief is about 120 mgals, the gravity decreases only about 50 mgals between volcanoes. In this respect the island of Hawaii is quite different from Oahu, where Woollard (1951) found maximums of about 110 mgals over the volcanoes and no connecting high between volcanoes. Horizontal distances between the adjacent volcanoes on both islands are about the same.

Quantitative analyses of the gravity highs are incomplete, but some qualitative conclusions on the cause of the anomalies can be reached. The amplitude of the highs and steepness of the gradients indicate that the highs are probably produced by mass anomalies above the sea floor and maybe even above sea level. The central high on Hawaii indicates the presence of relatively dense rocks at depth between the 4 volcanoes and suggests the presence of one or more of the following rock configurations: (1) a continuous intrusive mass, extending from Kohala Mountain to Mauna Loa and Kilauea, with cupolas beneath the 4 volcanoes having gravity maximums, (2) flow rocks between volcanoes, with a bulk density approaching that of intrusive rocks, or (3) interfingering of intrusive rocks with flows from the 4 volcanic centers, the whole mass of which has a bulk density approaching that of intrusive rocks. East-west asymmetry of the gravity anomalies requires the denser rocks to have a greater lateral extent to the east than to the west in all three possibilities. The third possibility is favored by the writers because there is no evidence of interconnection between volcanoes above the sea floor. Furthermore, although some massive parts of flows have measured densities of 3.0 g per cc, there is no surface evidence that such flows accumulate only in certain areas.

The absence of a pronounced closed high over Hualalai is surprising because Hualalai is the third highest volcano on the island, and it is similar in most respects to the other volcanoes on Hawaii. Hualalai's summit lies at the northern end of an elongate gravity high that reaches a maximum value at least 8 miles to the south. This high has very small closure and its maximum value is about 85 mgals less than the maximums over Mauna Kea or Mauna Loa, but the local relief of about 55 mgals is about the same as the relief between the other volcanoes on the island. An interesting possibility is that Hualalai lies on the north rift zone of an older volcano buried by Mauna Loa lavas. The elongate, rather than bull's-eye, gravity-contour pattern could be produced by diametrically opposed north- and south-trending rift zones of the buried older volcano. The gravity effect of the southern rift zone could be masked by its proximity to the larger Mauna Loa anomaly. A recorded offshore eruption near the south end of this high in 1877 (Dana, 1891) occurred at about the same time as a Mauna Loa summit eruption, and possibly the two were related.

Relatively narrow, low-amplitude gravity noses occur over or near the more conspicuous rift zones of Mauna Loa and Kilauea. The east-trending high on the northeast slope of Mauna Kea lies between a rift zone pointed out by Stearns and MacDonald (1946) and an east-trending submarine ridge off the northeast coast of the island. These highs are probably produced by the greater abundance of intrusive rocks in the rift zones, although it is possible that ponded flows in parts of the rifts are responsible for at least a part of the gravity maximums.

The gravity lows at Hilo and at the western part of the island in an area bounded by Kohala Mountain, Mauna Kea, and Hualalai are over areas probably covered with thick accumulations of low-density flow rocks.

REFERENCES

Dana, J. D., 1891, Characteristics of volcanoes: New York, Dodd, Mead and Co., 399 p. [1890].

Krivoy, H. L., and Eaton, J. P., 1961, Preliminary gravity survey of Kilauea Volcano, Hawaii: Art. 360 in U.S. Geol. Survey Prof. Paper 424-D, p. D205-D208.

Stearns, H. T., and MacDonald, G. A., 1946, Geology and ground-water resources of the island of Hawaii: Hawaii Div. Hydrography Bull. 9, p. 168.

Woollard, G. P., 1951, A gravity reconnaissance of the island of Oahu: Am. Geophys. Union Trans., v. 32, no. 3, p. 358-368.

EVALUATION OF MAGNETIC ANOMALIES BY ELECTROMAGNETIC MEASUREMENTS

By F. C. FRISCHKNECHT and E. B. EKREN, Denver, Colo.

Abstract.—Good agreement was obtained between field data taken over magnetic nonconductive iron-formation in the Cuyuna Range, Minn., and laboratory data using a scale model made of powdered magnetite. Field data are presented also for a more complex situation in the Gogebic Range, Wis., in which the iron-formation is highly conductive electrically, as well as magnetic.

Electromagnetic measurements were made over parts of unoxidized iron-formation in the Cuyuna Range, Minn., and the Gogebic Range, Wis., to determine the practicability of estimating magnetite content by electromagnetic techniques.

Parts of the iron-formation in both areas are highly magnetic and contain magnetite disseminated in a quartz- or chert-rich matrix. The iron-formation in Wisconsin overlies quartzite, siltstone, and argillite and underlies slate that commonly contains conductive graphitic layers.

Both electromagnetic and magnetic methods respond to the magnetic susceptibility of a geologic body, and the relation between magnetic susceptibility and magnetite content is well known (Werner, 1945). The dominant cause of many anomalies obtained by magnetic methods is remanent magnetization, which is not predictably related to magnetite content. Because the electromagnetic methods are unaffected by remanent magnetization, they offer, in principle at least, a better means of estimating magnetite content than do the magnetic methods.

The chief problem in using electromagnetic methods to evaluate high-amplitude magnetic anomalies is that deposits of the Lake Superior type containing a high percentage of magnetite often are good electrical conductors, and, at the frequencies ordinarily used, electromagnetic response is due to the combined effects of susceptibility and conductivity.

Ward (1959, 1961) has outlined a theory for determining the conductivity, susceptibility, size, and depth of a buried sphere and suggests the extension of the technique to bodies of other shape. Ward shows that it is possible to determine the permeability contrast between the sphere and the surrounding rock by using the ratio of the response extrapolated to zero frequency to the response extrapolated to infinite frequency, without determining any of the other parameters. The permeability contrast may also be obtained readily from the zero frequency response alone, by comparison with model data.

As an example of the latter approach (fig. 90.1), a turam model profile was compared with a turam field profile and with a vertical-component magnetometer profile taken over the thin-bedded facies of the main iron-formation of the North Cuyuna Range, Minn. (Schmidt, 1959). In the turam method (Frischknecht and Ekren, 1961), the complex ratio of the voltages induced in two receiving loops is measured along traverses normal to a long wire carrying an alternating current. The profiles in figure 90.2 are the normalized vertical component of the alternating magnetic field calculated from the measured ratios. A 200×200-foot induction loop was used as the source, rather than a grounded wire, to avoid the effects of galvanic currents. The turam anomaly is typical of that obtained over a magnetic nonconducting body (Törnquist, 1958). Other data obtained by the turam and slingram methods substantiate the indication that conductivity effects were negligible. The model was made of powdered magnetite having a susceptibility of about 0.08 cgs units. The model and loops were scaled so that the model represents a prism having dimensions of about 70×300×750 feet buried at a depth of 100 feet. There is good agreement between the model profile and the field profile; therefore, the susceptibility, width, depth of burial, and dip of the scale model are probably a fairly accurate replica of the actual magnetic bed involved. The depth and the extent along strike of the iron-formation are no

doubt greater than in the model, but due to the relatively short distance between the transmitting loop and the iron-formation, only the nearest part of both the iron-formation and the model contributed significantly to the electromagnetic response.
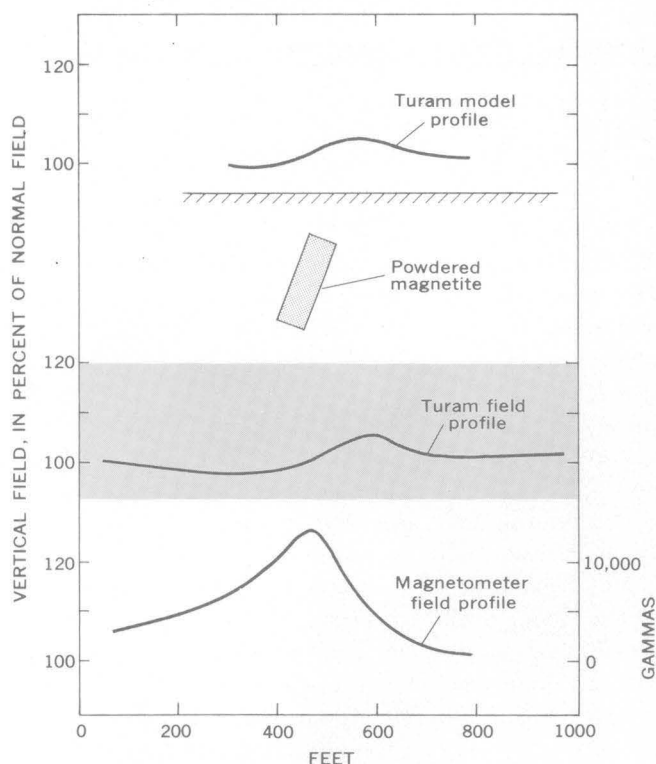

FIGURE 90.1.—Comparison of turam model profile with a turam field profile and a magnetometer profile taken over the Cuyuna Range, Minn.

In contrast with the amplitude of the electromagnetic field profile, which is largely the result of magnetic susceptibility, the amplitude of the magnetometer profile is greatly affected by remanent magnetization. From other studies, Gordon Bath, of the U.S. Geological Survey (oral communication, 1958), has deduced that the contribution of remanent magnetization to the anomaly is 3 to 5 times the contribution of induced magnetization. Because the anomaly represents about 25 percent of the earth's normal vertical field, the contribution of induced magnetization is about 6 percent of the earth's normal field. This agrees well with the magnitude of the electromagnetic anomaly, even though the inducing electromagnetic field did not have exactly the same direction as the earth's magnetic field.

In tracing the Ironwood Iron-Formation in the Gogebic Range, Wis., by means of slingram traverses, it was found by Frischknecht and Ekren (1961) that the response of the iron-formation depended partly on susceptibility, although conductive effects were usually predominant. Variable frequency measurements were made at a locality where the contact between the Ironwood Iron-Formation and the Palms Quartzite is exposed. A 50 × 50-foot horizontal transmitting loop was used. A small receiving coil, a fixed reference coil, and a ratiometer were used to measure the field at various frequencies and distances from the transmitting coil. Conventional turam equipment was used to verify the results obtained with the experimental apparatus operating at a single frequency of 500 cycles per second.

Figure 90.2 shows profiles obtained at 3 different frequencies: 40, 200, and 1,000 cps. Three anomalies, labeled A, B, and C, are recognized; only part of anomaly C was measured. There is, no doubt, some interdependence among these anomalies because of their proximity to each other.

Anomaly A is characterized by in-phase values greater than 100 percent and out-of-phase values that are essentially 0. These results are indicative of a member of the iron-formation having fairly high magnetic susceptibility and low electrical conductivity. The anomaly increases slightly at the higher frequencies, showing a small conductivity effect, but at 40 cps the anomaly is almost entirely caused by the high susceptibility of the formation. It is probably caused by iron-formation having considerable magnetite in the form of discontinuous grains which do not increase significantly the overall conductivity of the rock. The susceptibility and dimensions of the unit could be readily estimated by comparison with model experiments as in the preceding example.

Anomaly B is practically nonexistent at 40 cps. The out-of-phase component is positive at 200 cps and negative at 1,000, whereas the in-phase component is increasingly greater at 200 and 1,000. Anomaly B must therefore be caused by a part of the iron-formation having low magnetic susceptibility and intermediate electrical conductivity. A graphitic bed containing little magnetite probably is the cause.

Anomaly C is more complex than A or B. To facilitate the study of anomaly C, figure 90.3 shows the maximum in-phase and out-of-phase values of anomaly C and A plotted against frequency.

At frequencies below about 400 cps the in-phase component is greater than 100 percent, becoming larger as the frequency is decreased. Except for the inflection in the curve of the in-phase component at about 50 cps, both the in-phase and the out-of-phase curves resemble theoretical curves for a conductive permeable sphere (Ward, 1959). The disturbing body certainly is not spherical, but data are not available for other shapes.
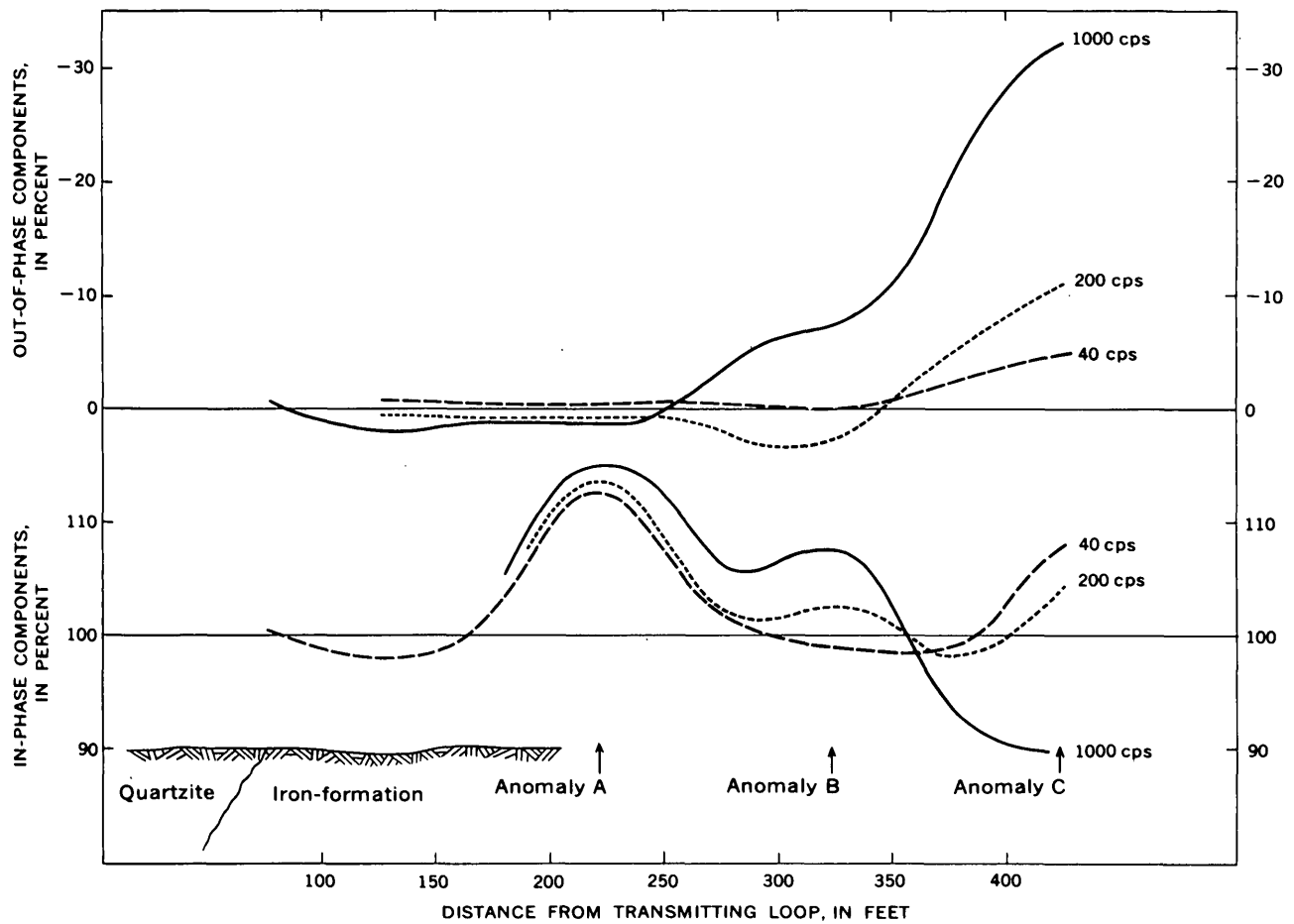
FIGURE 90.2.—Electromagnetic profiles at 3 frequencies across iron-formation on the Gogebic Range, Wis.
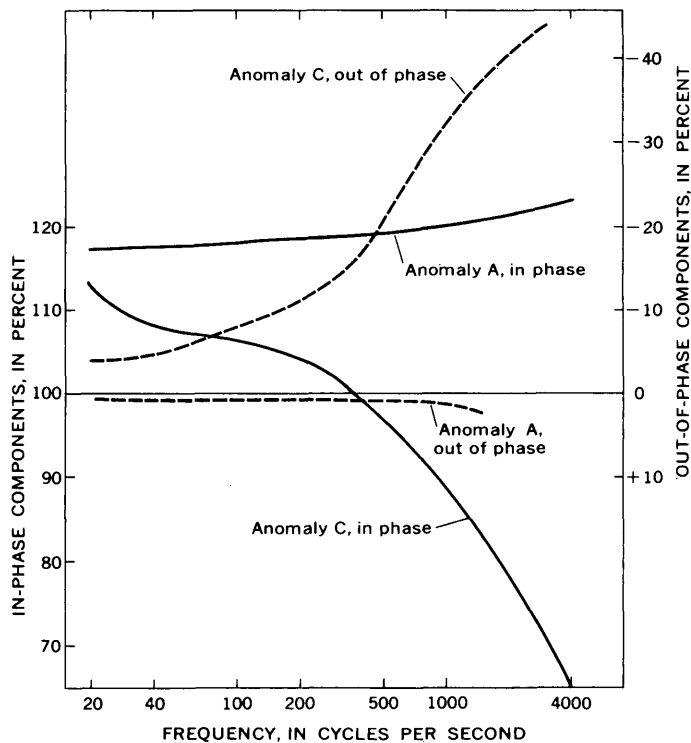
FIGURE 90.3.—Variation of electromagnetic anomalies with frequency on the Gogebic Range, Wis.

The body probably has a relatively high magnetic susceptibility and electrical conductivity. More detailed field work and model work are needed to explain the cause of the inflection in the in-phase curve and to interpret the anomaly further. In particular the measurements need to be extended to lower and higher frequencies. There is little difficulty in making measurements at higher frequencies than those used in these studies, but conventional electromagnetic equipment for use at lower frequencies is very bulky. One other possible approach to identify the effect of magnetic susceptibility is to use a very sensitive magnetometer and utilize the natural time-variant magnetic field (Ward and Ruddock, 1962).

REFERENCES

Frischknecht, F. C., and Ekren, E. B., 1961, Electromagnetic studies of iron formation in the Lake Superior region: Mining Eng., v. 13, no. 10, p. 1157–1162.

Schmidt, R. G., 1959, Bedrock geology of the northern and eastern parts of the North Range, Cuyuna district, Minnesota: U.S. Geol. Survey Mineral Inv. Map MF–182.

Törnquist, G., 1958, Geophysical history of the iron mine at Forsbo, Sweden, *in* Geophysical surveys in mining, hydrological and engineering projects: European Assoc. Expl. Geophysicists, p. 64.

Ward, S. H., 1959, Unique determination of conductivity, susceptibility, size and depth in multifrequency electromagnetic exploration: Geophysics, v. 24, no. 3, p. 531–546.

——— 1961, The electromagnetic response of a magnetic iron ore deposit: Geophys. Prosp., v. 9, no. 2, p. 191–202.

Ward, S. H., and Ruddock, K. A., 1962, A field experiment with a rubidium vapor magnetometer: Jour. Geophys. Research, v. 67, no. 5, p. 1889–1898.

Werner, S., 1945, Determinations of the magnetic susceptibility of ores and rocks from Swedish iron ore deposits: Sveriges Geologiska Undersöknin, Arsbok 39, no. 5, 79 p.

GLACIOLACUSTRINE DIAMICTON DEPOSITS IN THE COPPER RIVER BASIN, ALASKA

By OSCAR J. FERRIANS, JR., Washington, D.C.

Abstract.—The character, stratigraphic relations, and distribution of nonsorted and poorly sorted diamicton deposits, interbedded with stratified lacustrine sediments, indicate that many diamicton units were deposited in a lacustrine environment, and that turbidity currents and subaqueous mudflows were important as agents of deposition. Commonly, the diamicton is till like in character.

Numerous diamicton units interbedded with stratified lacustrine sediments occur within the unconsolidated deposits of Pleistocene age in the Copper River Basin, Alaska. The term "diamicton," proposed by Flint and others (1960a, b) for "nonsorted or poorly sorted terrigenous sediment that consists of sand and/or larger particles in a muddy matrix," is especially applicable to both the nonsorted, till-like units not deposited directly by glaciers, and to poorly sorted units of similar origin.

The Copper River Basin, in south-central Alaska, is approximately 5,500 square miles in areal extent and is surrounded by high mountains with numerous glaciers. The Wrangell Mountains lie to the east, the Chugach Mountains to the south, the Talkeetna Mountains to the west, and the Alaska Range to the north.

The distribution of glacial erratics and till around the margin of the basin and on top of bedrock hills within the basin indicates that the entire basin floor was covered with ice one or more times during early Pleistocene time. In addition, in the northeastern part of the Copper River Basin there is stratigraphic evidence of three younger, major glaciations during which ice did not completely cover the basin floor.

During each major glaciation, glaciers advancing in the mountains surrounding the Copper River Basin dammed the drainage of the basin, thus impounding an extensive proglacial lake (Nichols, 1956, p. 4; Ferrians and Schmoll, 1957; Nichols and Yehle, 1961, p. 1066).

The lake that existed during the last major glaciation covered more than 2,000 square miles of the basin floor, and numerous glaciers and sediment-laden glacial streams debouched into it. At Gakona, in the northeastern part of the basin, the age of the sediments that were deposited in this lake is bracketed between a maximum radiocarbon date of greater than 38,000 years B.P. (before present) and a minimum date of 9,400±300 years B.P. (Rubin and Alexander, 1960, p. 170 and 171, samples W-531 and W-714). Therefore, the last major glaciation in the Copper River Basin is comparable in age to the last major glaciation (Wisconsin) of central North America.

The conclusions presented in this article are based primarily on observations of the diamicton and associated materials deposited in the northeastern part of the Copper River Basin during the last major glaciation. The diamicton units were examined in detail at Gakona, where river bluffs 250 feet high provide nearly continuous exposure of these deposits for more than a mile.

The diamicton units range in thickness from less than 1 inch to as much as 150 feet. Some of the nonsorted, till-like diamicton deposits have only a few phenoclasts, some are intermediate in character, and others consist predominantly of phenoclasts. The poorly sorted diamicton deposits are relatively fine grained, with the coarser fraction generally limited to sizes smaller than cobbles. Locally, these poorly sorted deposits show well-developed graded bedding.

TYPES OF DIAMICTON AND ASSOCIATED DEPOSITS

Nonsorted diamicton

Numerous units of nonsorted, till-like diamicton alternate vertically with bedded lacustrine sediments and with poorly sorted diamicton (fig. 91.1). Locally these alternations may repeat several times within a

FIGURE 91.1.—Section of lacustrine deposits near Gakona consisting of (A) nonsorted till-like diamicton, (B) interbedded poorly sorted diamicton and well-stratified sediment, and (C) poorly sorted diamicton (sand and granules in a clayey-silt matrix).

FIGURE 91.2.—Section of lacustrine deposits near Gakona consisting of (A) well-stratified sediment interbedded with poorly sorted diamicton units at base—lower part deformed, (B) gravel unit which has the form of a channel filling (man standing on unit), and (C) thick unit of nonsorted diamicton with numerous thin zones of bedded silt, sand, and gravel, which give an overall bedded appearance to the unit.

stratigraphic thickness of a few feet. Generally, the contacts between these units are extremely sharp; the beds immediately underlying the diamicton units generally are not deformed, even though deformation is common within the rest of the lacustrine sequence. Many nonsorted diamicton deposits of this type occur as thick units consisting of a series of superimposed diamicton beds. The character of these beds makes them difficult to differentiate. These thick units generally include numerous thin, discontinuous deposits of horizontally bedded silt, sand, and gravel, which give them an overall bedded appearance (fig. 91.2). The variety of rock types, from various source areas, occurring in these diamicton deposits indicates that considerable mixing has occurred.

The stratigraphic relations, character, and distribution of these deposits indicate that they were deposited mainly by dense turbidity currents and (or) subaqueous mudflows. The intimate stratigraphic relation between the diamicton deposits and the bedded lacustrine sediments, plus the general lack of deformation of beds immediately underlying the deposits, precludes the possibility that they were deposited directly by glaciers. Kuenen and Migliorini (1950, p. 105) have shown experimentally that very dense turbidity currents could deposit materials that do not show graded bedding, and

Menard and Ludwick (1951, p. 12) suggest that several superimposed currents depositing simultaneously also could cause deposition of material that would not show graded bedding.

Some nonsorted diamicton units occurring within the lacustrine sequence contain rock types from a single source area and have phenoclasts that are angular to subangular, whereas stratigraphic units immediately below contain mixed rock types and have phenoclasts that are subrounded to rounded. The character of this type of diamicton is similar to that of a subaerial volcanic mudflow deposit that occurs in the Copper River Basin (Ferrians and others, 1958). A subaqueous mudflow is the most logical agent that could have transported these angular to subangular rock fragments several miles out onto the lake floor without abrading them, and without eroding the underlying sediments. Because large accumulations of glacial and fluvial phenoclastic material with mixed rock types could have been the source of other subaqueous mudflows, it seems likely that some nonsorted diamicton units not having

distinct mudflow characteristics also were deposited by subaqueous mudflows.

Other nonsorted diamicton units grade almost imperceptibly, both horizontally and vertically, into well-stratified fine-grained sediment. Many of these units occur as large lenses within bedded sediment and, consequently, are isolated from potential ice sources. Deposits of this type typically have a fine-grained matrix and relatively few pebble- and cobble-sized phenoclasts. The character of the pebbles and cobbles is quite similar to that of the ice-rafted pebbles and cobbles found in the associated laminated sediment. The isolation of these units from potential ice sources, the gradational contacts with laminated sediment, and the character of these deposits indicate that this type of nonsorted diamicton was formed by rapid, uniform deposition of fine-grained sediment, with the concurrent deposition of ice-rafted stones, and that it was not deposited directly by glaciers. The stratigraphic data suggest that the fine-grained fraction of this type of diamicton was transported to deep parts of the lake by turbidity currents generated by sediment-laden glacier-fed streams entering the lake.

Other, less important, depositional agents of nonsorted diamicton were glaciers and icebergs, which locally dumped phenoclastic material into the lake. Deposits of material dumped by glaciers characteristically have a chaotic stratigraphic relation with associated bedded sediment, because of subaqueous slumping and sliding. Material forming small pods of nonsorted diamicton is present locally within the bedded lacustrine sediments and probably was dumped into the lake by overturning icebergs which held large quantities of ablation debris in depressions on their upper surfaces.

Poorly sorted diamicton

Poorly sorted diamicton units occur interbedded with nonsorted diamicton and bedded lacustrine sediments (fig. 91.1). Generally, contacts are sharp between these units and dissimilar materials lying below and above them; bedded materials immediately underlying the diamicton units are not deformed. The variety of rock types occurring in these diamicton units indicates that considerable mixing has occurred. Some of these units display well-developed graded bedding (figs. 91.3 and 91.4) and, consequently, provide good evidence of deposition by turbidity currents. Many of these units that do not display well-developed graded bedding have stratigraphic relations and a lithologic composition similar to those that do; therefore, they also are considered to have been deposited by turbidity currents.

The end members of the continuum represented by typical deposits of subaqueous mudflows and turbidity

FIGURE 91.3.—Several fine-grained diamicton units, each of which grades upward from sand and granules in a clayey-silt matrix to massive fine sand, silt, and clay. The fine-grained diamicton units are overlain by a coarse-grained till-like diamicton unit which is graded also, to the extent that the cobble-sized phenoclasts are concentrated at the base. Slopewash occurs in the lower right corner. See figure 91.4 for closeup view of one of the fine-grained diamicton units.

currents can be distinguished by the presence or absence of well-developed graded bedding, by the character of the included phenoclasts, and by the degree of mixing. However, it is very difficult to distinguish between the two types of deposits in the intermediate range.

Bedded sand and gravel

Numerous relatively thin discontinuous deposits of bedded sand and gravel, ranging in thickness from less than 1 inch to several feet, are interbedded with the diamicton, especially within many of the thick units (fig. 91.2). Generally these deposits are relatively uniform in thickness, but locally they occur as what appear to be channel fillings (fig. 91.2). Commonly the included phenoclasts are not so well rounded as normal stream-deposited phenoclasts, indicating that the material was not transported far by water currents. The character of these bedded sand and gravel deposits and their association with lacustrine diamicton units, plus the lack of any evidence suggesting that deposition in the lake was interrupted by subaerial conditions, indicate that these deposits were laid down by turbidity currents with a velocity high enough, in relation to

density, to remove the fine-grained material and to deposit sand-, pebble-, and cobble-sized material.

FIGURE 91.4.—Closeup view of a fine-grained, poorly sorted diamicton unit which grades upward from sand and granules in a clayey-silt matrix to massive fine sand, silt, and clay. Base of overlying diamicton unit is at top of picture. This unit is one of several shown in figure 91.3.

DEFORMATION OF LACUSTRINE BEDS

Deformation of beds is common within the stratified lacustrine deposits; however, the bedded sediments that underlie the diamicton units deposited by turbidity currents and subaqueous mudflows generally are not deformed. Most of the deformation probably was caused by subaqueous slumping and sliding. Nichols (1960) has described two types of deformation of lacustrine beds in the southeastern part of the Copper River Basin, and has postulated that the deformation was caused by slumping, triggered by earthquakes.

CONCLUSIONS

Gould (1951) discusses turbidity currents formed by the sediment-laden Colorado and Virgin Rivers entering Lake Mead in the western United States. The glacier-fed sediment-laden streams debouching into the proglacial lake that existed in the Copper River Basin also must have created turbidity currents because of the heavy load of suspended sediment. Even today, the glacier-fed streams in the basin are heavily laden

with suspended sediment. For example, the Copper River near Chitina, in the southeastern part of the basin, discharged 71,395,000 tons of suspended sediment during the period June 17 to September 6, 1957 (U.S. Geological Survey, 1960, p. 40), an average of 870,670 tons a day.

Stratigraphic analysis of the lacustrine sediments indicates that much of the fine-grained bedded sediment, as well as the relatively fine-grained diamicton, was transported by turbidity currents generated by sediment-laden glacial streams entering the lake. Numerous thin sand beds interbedded with the varve-like clayey silt attest to the presence of currents, even in the relatively quiescent lacustrine environment. An apparent secondary preferred orientation of the A-axis of ice-rafted phenoclasts in these varve-like sediments may have been caused by currents, according to Schmoll (1961, p. C195). Kuenen (1951a, b) has postulated that even "glacial varves" can be deposited by turbidity currents formed by sediment-laden melt water entering lakes.

The rapid accumulation of deltaic material where major streams entered the lake, and of ice-deposited material where glaciers bordered the lake, created unstable slope conditions which resulted in slumping. Slumping of this type probably generated the subaqueous mudflows and dense turbidity currents that deposited many of the coarse-grained diamicton units.

In summary, the character, distribution, and stratigraphic relations of the various types of lacustrine diamicton conspicuous in the Copper River Basin indicate four agents of deposition, the first two of which were most important: (1) Turbidity currents; (2) subaqueous mudflows; (3) glaciers, which dumped phenoclastic material into the lake; and (4) icebergs, which dumped phenoclastic material into the lake.

REFERENCES

Ferrians, O. J., Jr., Nichols, D. R., and Schmoll, H. R., 1958, Pleistocene volcanic mudflow in the Copper River Basin, Alaska [abs.] : Geol. Soc. America Bull., v. 69, no. 12, p. 1563.

Ferrians, O. J., Jr., and Schmoll, H. R., 1957, Extensive proglacial lake of Wisconsin age in the Copper River Basin, Alaska [abs.] : Geol. Soc. America Bull., v. 68, no. 12, p. 1726.

Flint, R. F., Sanders, J. E., and Rodgers, John, 1960a, Symmictite: a name for nonsorted terrigenous sedimentary rocks that contain a wide range of particle sizes: Geol. Soc. America Bull., v. 71, p. 507–510.

——— 1960b, Diamictite, a substitute term for symmictite: Geol. Soc. America Bull., v. 71, p. 1809.

Gould, H. R., 1951, Some quantitative aspects of Lake Mead turbidity currents, in Society of Economic Paleontologists and Mineralogists, Turbidity currents and the transportation of coarse sediments to deep water—a symposium: Soc. Econ. Paleontologists and Mineralogists Spec. Pub. 2, p. 34–52.

Kuenen, Ph. H., 1951a, Mechanics of varve formation and the action of turbidity currents: Geol. föen. Stockholm Förh., v. 73, p. 69–84.

———— 1951b, Turbidity currents as the cause of glacial varves: Jour. Geology, v. 59, no. 5, p. 507–508.

Kuenen, Ph. H., and Migliorini, C. I., 1950, Turbidity currents as a cause of graded bedding: Jour. Geology, v. 58, no. 2, p. 91–127.

Menard, H. W., and Ludwick, J. C., 1951, Applications of hydraulics to the study of marine turbidity currents, in Society of Economic Paleontologists and Mineralogists, Turbidity currents and the transportation of coarse sediments to deep water—a symposium: Soc. Econ. Paleontologists and Mineralogists Spec. Pub. 2, p. 2–13.

Nichols, D. R., 1956, Permafrost and ground-water conditions in the Glennallen area, Alaska: U.S. Geol. Survey open-file report, 18 p.

Nichols, D. R., 1960, Slump structures in Pleistocene lake sediments, Copper River basin, Alaska: Art. 162 in U.S. Geol. Survey Prof. Paper 400–B. p. B353–B354.

Nichols, D. R., and Yehle, L. A., 1961, Mud volcanoes in the Copper River basin, Alaska, in Geology of the Arctic: Toronto, Univ. of Toronto Press, p. 1063–1087.

Rubin, Meyer, and Alexander, Corrinne, 1960, U.S. Geological Survey radiocarbon dates V: Am. Jour. Sci. Radiocarbon Supp., v. 2, p. 129–185.

Schmoll, H. R., 1961, Orientation of phenoclasts in laminated glaciolacustrine deposits, Copper River Basin, Alaska: Art. 218 in U.S. Geol. Survey Prof. Paper 424–C, p. C192–C195.

U.S. Geological Survey, 1960, Quantity and quality of surface waters of Alaska, 1957: U.S. Geol. Survey Water-Supply Paper 1500, 100 p.

Article 92

COMPETENCE OF TRANSPORT ON ALLUVIAL FANS

By LAWRENCE K. LUSTIG, Sacramento, Calif.

Abstract.—The competence of transport on alluvial fans in Deep Springs Valley, Calif., is estimated by using a field approximation for tractive force based on maximum particle size and on slope. The distribution of tractive force is shown on isopleth maps together with an orthogonal net that represents inferred sediment-transport paths.

One of the most important factors in the transport of sediment on alluvial fans is the competence of the transporting medium. The occurrence of large boulders on an alluvial fan implies, of course, a high degree of competence, but boulder size alone is not an entirely valid indicator of competence. The nature of the source rocks also is important, because the competence of the transporting medium may have been sufficient to move even larger particles than those occurring on a given fan, had they been available at the source. The problem considered in this article, however, is how best to estimate the competence of past flows from field data, which admittedly can yield only a rough approximation of the actual competence. Field data for this study were taken from observations in Deep Springs Valley, in eastern California, northwest of Death Valley.

Competence is usually equated with the velocity of flow, and the relation is expressed in terms of particle diameter. Leliavsky (1955, p. 34) stated that the earliest formula was provided in 1753 by Brahms, who used particle weight rather than diameter. The report of Suchier (1883), listing velocities required to transport particles of "pea," "hazelnut," and "pigeon egg" dimensions, is typical of several early treatments. Gilbert (1914) considered the transport of particles as large as 6 mm in diameter, as did Nevin (1946), who reviewed the competence problem. The basic competence curves of Hjulström (1935, p. 298) have been extended and modified to include the transport of cobbles (Menard, 1950) and boulders (Fahnestock, 1961). Even the data of Fahnestock, which cover particles as large as 1.8 feet in diameter, cannot be safely extrapolated to embrace the much larger boulders that occur on alluvial fans. The use of any velocity power law, therefore, should be avoided in determining competence of transport on alluvial fans on which large boulders have been moved downslope.

As an alternative to velocity of flow, tractive force can be used as a measure of competence. Tractive force can be expressed as $\tau = \lambda dS$, where λ is the specific weight of the transporting medium, d is the depth of flow, and S is the slope of the energy gradient. The tractive force thus defined pertains to the shear exerted on the upper layer of the bed material. The formula, or some variant thereof, is widely used in engineering studies and provides one of the few means of obtaining an approximation of competence from field data.

Substitution of field data for the variables in the tractive-force expression was suggested, in part, by personal observation in Deep Springs Valley, Calif. Boulders that contained pockets of pebbles, sand, silt, and clay on their uppermost sides, several feet above fan surfaces, were noted in several places. The lithologic diversity of the sediment in these pockets, as well as the variation in size, suggests that this material represents a portion of the finer sediment that was transported with the boulders and trapped upon cessation of movement. Either the depth of flow exceeded the diameters of the boulders or the finer sediment was acquired by the rolling of boulders through a shallower flow. Observation of mudflows and the examination of alluvial-fan deposits in section suggest that the depth of flow may have been greater than the diameters of the particles transported, at least over the upper and middle reaches of the fans. In the lower reaches of the fans, the depth of flow was probably less than these particle

diameters. In order to obtain a field approximation for tractive force, maximum particle size was substituted for d, the depth of flow. The approximations obtained in the calculations may therefore be too low for the upper fan reaches and too high for the lower reaches.

Slopes were measured in the field to the nearest 0.5 percent over a 100-foot reach upfan from each maximum-sized particle. Local runoff has undoubtedly modified the slope, but this might well consist of uniform lowering over each reach. Again, for the sake of expediency, approximation was used; the determined slope was substituted for the formula slope required. It is thought that the local slope determined at each point should at least provide a more accurate representation of the former flow conditions than could be determined from topographic maps.

The remaining variable is specific weight, or density times gravity. Sharp and Nobles (1953) have provided one of the few density values obtained for mudflows; one sample from a mudflow at Wrightwood, Calif., is reported to have had a density of 2.4 grams per cubic centimeter. Although this density seems excessively high, the density of a mudflow can vary considerably during the downfan progress of the flow. The variation may result from water loss through the permeable bed or from the addition of water from the high waters that commonly follow close behind mudflows. Because no single value for the density of any flow can reasonably be postulated for flow down an alluvial fan, substitution for the specific weight of the transporting medium has been omitted from the approximation of tractive force.

Thus, the field approximation used for determining the tractive force or competence of transport consists of substituting maximum particle size (to the nearest tenth of a foot) for depth of flow, and local slope (in feet per 100 feet) for slope of the energy gradient. The product of these variables was calculated for 496 sampling stations in Deep Springs Valley, Calif., the distribution was mapped, and the resulting isopleths were interpreted as reflecting the competence of transport. The interpretation of the maps will be considered in a future report, but the results obtained in the north end of Deep Springs Valley and for a single alluvial fan in the south end are shown here in figures 92.1 and 92.2.

If the tractive-force isopleths based on slope and maximum particle size are accepted as approximations of the competence distribution, then the orthogonals to these isopleths should represent paths of sediment transport; this assumes only that competence must de-

crease in the direction of flow. Of the infinite number of possible orthogonal paths, one set has been drawn through contour trends on figures 92.1 and 92.2. Because this drawn set closely corresponds to the location of channels on alluvial fans, which are the known paths of recent sediment transport, the method is probably valid and holds some predictive possibilities.

As stated previously, specific weight of the transporting medium has been disregarded, and one would necessarily have to select some value for density of flow to obtain the tractive force implied by the approximation. The reader can at least determine from the maps the relative order of magnitude of the tractive force, however. The zero isopleth also provides useful information. In figure 92.1 this isopleth encloses the central portion of the basin and on figure 92.2 it is shown near the lower part of the fan. Competence therefore approaches zero in these regions because the slopes approach zero, within the limits of error of the measurements. The transport of large particles extends beyond the boundary however, and is attested to in reports by McAllister and Agnew (1948), Kirk (1952), and others, of boulders on playas. This seeming anomaly of the transport of large particles across regions of negligible slope must reflect a mass-transport mechanism attended by buoyancy and momentum effects; the mass-transport mechanism in turn indicates that the method outlined here can approximate the competence of mudflows.

REFERENCES

Fahnestock, R. K., 1961, Competence of a glacial stream: Art. 87 *in* U.S. Geol. Survey Prof. Paper 424-B, p. B211–B213.

Gilbert, G. K., 1914, The transportation of debris by running water: U.S. Geol. Survey Prof. Paper 86, 263 p., 3 pls.

Hjulström, Filip, 1935, Studies of the morphological activity of rivers as illustrated by the River Fyris: Uppsala Univ. Geol. Inst. Bull., v. 25, p. 221–527.

Kirk, L. G., 1952, Trails and rocks observed on a playa in Death Valley National Monument, Calif.: Jour. Sed. Petrology, v. 22, no. 3, p. 173–181.

Leliavsky, Serge, 1955, An introduction to fluvial hydraulics: London, Constable and Co., Ltd., 257 p.

McAllister, J. F., and Agnew, A. F., 1948, Playa scrapers and furrows on Racetrack Playa, Inyo County, Calif. [abs.]: Geol. Soc. America Bull., v. 59, p. 1377.

Menard, H. W., 1950, Sediment movement in relation to current velocity: Jour. Sed. Petrology, v. 20, no. 3, p. 148–160.

Nevin, C. M., 1946, Competency of moving water to transport debris: Geol. Soc. America Bull., v. 57, p. 651–674.

Sharp, R. P., and Nobles, L. H., 1953, Mudflows of 1941 at Wrightwood, southern California: Geol. Soc. America Bull., v. 64, p. 547–560.

Suchier, A., 1883, Die Bewegung der Geschiebe des Oberrhein: Deutsche Bauzeit., no. 56, p. 331–356.
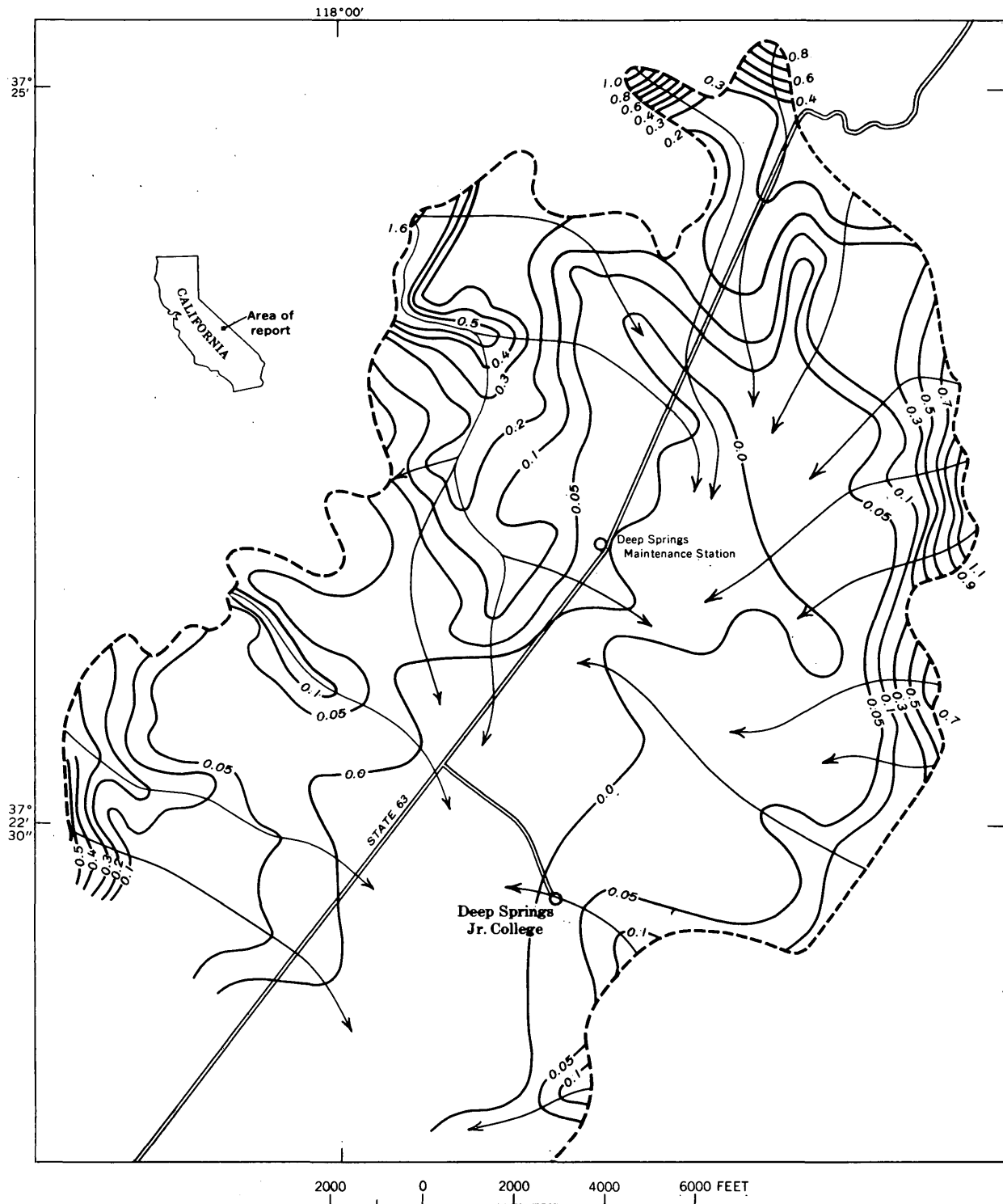
FIGURE 92.1.—Approximate tractive-force isopleths (explained in text) and inferred sediment-transport paths in the north end of Deep Springs Valley, Calif. Dashed line represents the approximate basin boundary. Isopleth interval, 0.05, 0.1, and 0.2.
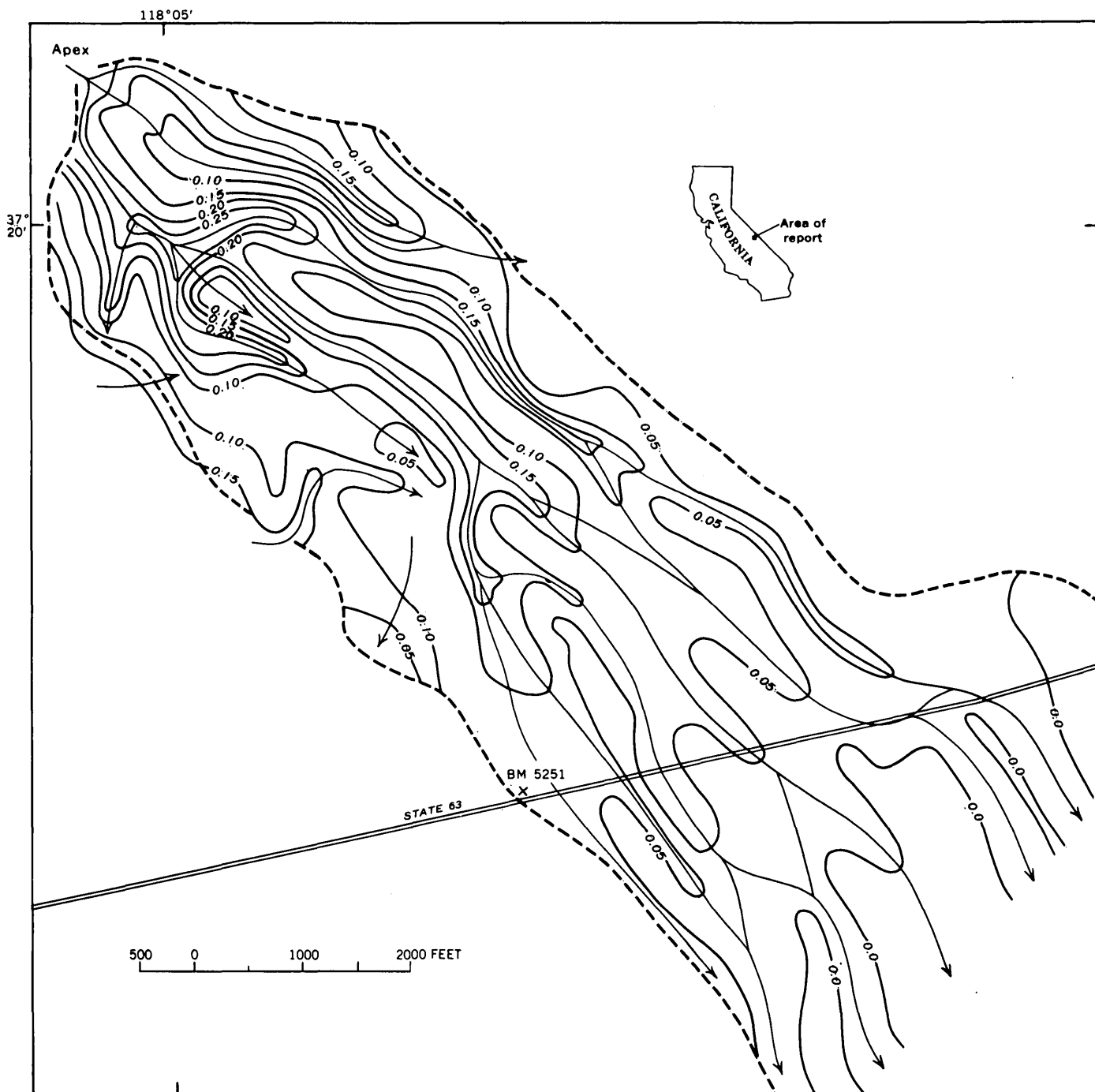
FIGURE 92.2.—Approximate tractive-force isopleths (explained in text) and inferred sediment-transport paths on the Antelope Springs fan in the south end of Deep Springs Valley, Calif. Dashed line represents the approximate fan boundary. Isopleth interval, 0.05.

Article 93

DISTRIBUTION OF GRANULES IN A BOLSON ENVIRONMENT

By LAWRENCE K. LUSTIG, Sacramento, Calif.

Abstract.—Data on the occurrence of granules (2 to 4 mm) in Deep Springs Valley, Calif., suggest that these particles are mechanically unstable polymineralic aggregates that are rapidly reduced to their sand-size components by weathering. A deficiency of mineral grains in the granule size range in the source rocks is the basic cause of the scarcity of granules in the sediments.

In a review of the various size grades, Pettijohn (1957, p. 47) noted that the results of many studies indicate that granules (2 to 4 mm) are less abundant in nature than are other size classes. He also noted that there seems to be a deficiency of very coarse sand (1 to 2 mm) as well. The basis for these statements is the fact that a sedimentary deposit consisting of both gravel and sand generally exhibits a distinct mode for each of these two fractions. The break in the frequency curve between these two modes falls within the 1- to 4-mm size range.

Various investigators have attempted to explain the deficiency of granules. Sundborg (1956, p. 191–194), for example, argues that particles between 1 and 6 mm are those most readily moved hydraulically when bed transport commences and are the last to come to rest when it ceases. Accordingly, granules are scarce in nature because they are in nearly constant motion, relative to other size classes, and therefore simply wear out. Kagani (1961, p. 523–532) also advances a hydraulic explanation and, in addition, advocates placing size-class boundaries at all conspicuous minimums in frequency curves. This would, in effect, tend to remove granules entirely from consideration as a distinct size class.

An investigation of the clastic sediments in Deep Springs Valley, Calif., in the eastern part of the State, northwest of Death Valley, provided a good opportunity to consider the problem of the scarcity of granules. Because sediment transport is typically both brief and intermittent in a bolson environment, the conditions postulated by Sundborg do not prevail. Therefore, granules should be no less abundant than other size classes if the hydraulic theory is correct.

The weight percentage of granules in the granule-to-clay size fraction was determined for 90 samples. Among these samples, 71 were obtained from alluvial-fan and valley-floor surface sediments in the north end of Deep Springs Valley (fig. 93.1) and the remainder from an alluvial channel in another part of the basin. Of the fan and valley-floor samples, 24 were unimodal and 47 were bimodal. In the unimodal group no mode coincided with the granule, very coarse sand, fine-sand,
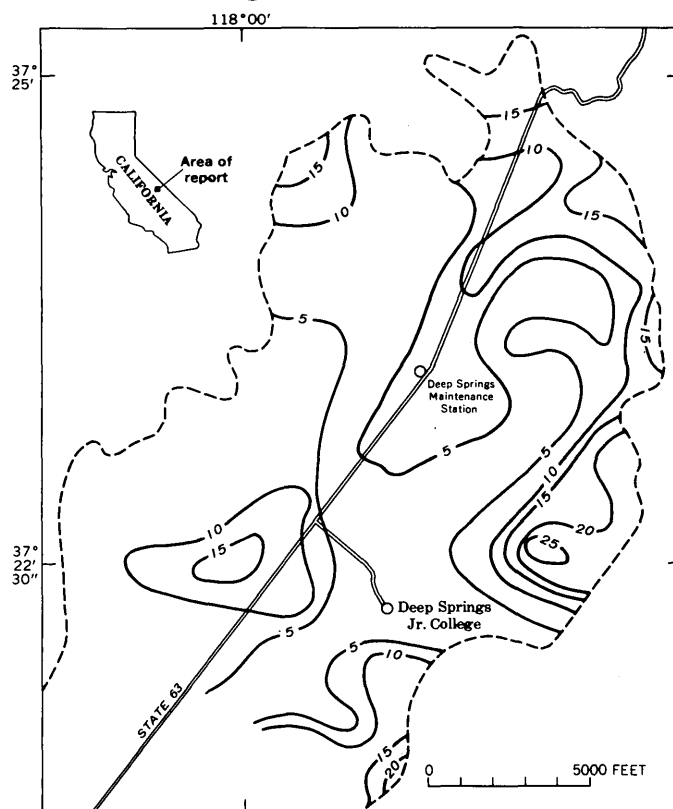
FIGURE 93.1.—Distribution of granules in the north end of Deep Springs Valley, Calif. Isopleths represent weight percentages of granules in the granule-to-clay size fraction.

and clay size classes. Granules, however, occurred as the primary mode of 4 of the bimodal samples and the secondary mode of 5. Among the 19 alluvial channel samples, 13 were unimodal and 6 were bimodal. Gran-

ules again failed to occur as the modal class in the unimodal sediments. The secondary mode of 5 of the 6 bimodal samples, however, did coincide with the granule size class. If the frequency of occurrence of each of 8 size classes as both primary and secondary modes is calculated, then one finds that granules occur more frequently than 3 of the size classes and less frequently than 4. On this basis, therefore, granules are very nearly the median mode of the bolson sediments.

The basis for this calculation is, of course, arbitrary and results in an exaggeration of the frequency of modal occurrence of granules. The arbitrary nature of modality itself is, however, often forgotten and is worthy of mention here. Only a single sample among the 90 studied was unimodal when class intervals were chosen at half-phi units; the remaining 89 samples were polymodal. When the weights were grouped to produce intervals in accord with the full-phi units of the Wentworth size classification, however, the 37 unimodal samples discussed previously were produced. Because any classification of size must be considered arbitrary rather than natural, the obvious conclusion to be drawn is that the unimodal samples result from averaging of the data. Many of the bimodal distributions could be transformed into unimodal distributions by the simple expedient of setting the class intervals equal to 2 phi units. In the limit, of course, any sediment could be shown to be not only unimodal but of the same size class as any other.

A more pertinent factor than frequency of occurrence as a modal class, however, is the absolute abundance of granules. Their abundance in the granule-to-clay size fraction (fig. 93.1) ranges from 15 to 20 percent near the basin margin to the north and east and is slightly less on the western side. At least 3 to 5 percent of this fraction consists of granules at any point in the center of the basin. Although this percentage is a maximum for the total sediment, because gravel has been omitted, it is pertinent to the observations of Yatsu (1959, p. 224–242), who argued that the break in slope along the intersection of an alluvial fan with the valley floor coincides with the modal-frequency break in the gravel-to-sand distribution referred to previously. Granules should therefore be absent below this break in slope or in the central part of the basin. The evidence from Deep Springs Valley, however, suggests a decrease in abundance of granules toward the basin center but not the disappearance of this size class.

The decrease in abundance of granules within relatively short distances from source areas not only requires explanation but serves to refute the suggestion of Sundborg (1956, p. 191–194). Because transport of the surface sediments considered here is infrequent, the granules are not in constant motion. Selective sorting in a downfan direction may appear to be a likely alternative, but if this is true, then it is difficult to understand why granule concentrations are absent in ancient as well as recent sediments, as reported in studies referred to by Pettijohn (1957, p. 47). Lag deposits would necessarily have to accumulate in some areas, but, to the writer's knowledge, none have been reported in the literature. A mechanical theory, suggested by the data from Deep Springs Valley, is thought to be the most reasonable explanation.

Approximately 80 percent of the granules examined were found to consist of polymineralic rock fragments; quartz and feldspar grains made up the remainder. This implies that the plutonic rocks that are the primary source of the clastic sediments considered must consist of mineral grains that are predominantly less than 2 mm in size. The results of Dake (1921, p. 162), who found that less than 10 percent of the quartz grains in plutonic rocks exceed 1 mm in size, tend to confirm this implication. The fact that medium or coarse sand is the dominant size class in all the unimodal samples studied, whereas granules are more abundant in the bimodal samples, suggests that the polymineralic granules are unstable aggregates of sand-size grains. These aggregates tend to disappear in nature by reason of rapid reduction to their components. The reduction is achieved by mechanical disintegration through weathering and is aided by periods of transport, however brief. The transition from polymineralic granules to sand-size components is accompanied by a consequent change from predominantly bimodal to unimodal frequency distributions. The deficiency of discrete mineral grains larger than 2 mm in plutonic source rocks should be regarded as the fundamental cause of the relative scarcity of granules in nature.

REFERENCES

Dake, C. L., 1921, The problem of the St. Peter sandstone: Missouri School Mines and Metallurgy Bull., v. 6, p. 158–163.

Kagani, H., 1961, Modal analysis of marine sediments in the southern part of Tokyo Bay: Japan Jour. Geology and Geography, v. 32, p. 523–532.

Pettijohn, F. J., 1957, Sedimentary rocks, 2d ed.: New York, Harper and Bros., 718 p.

Sundborg, Åke, 1956, The River Klaralven; A study of fluvial process: Geografiska Annaler, v. 38, p. 127–316.

Yatsu, E., 1959, On the discontinuity of grain size frequency distributions of fluvial deposits and its geomorphological significance: Geog. Union Regional Council Proc., 1957, Internat. Sci. Council of Japan, Tokyo, p. 224–242.

Article 94

SEDIMENTS ON THE CONTINENTAL MARGIN OFF EASTERN UNITED STATES [1]

By ELAZAR UCHUPI, Woods Hole, Mass.

Abstract.—Relict glacial sediments blanket most of the continental shelf north of Hudson Canyon, and relict fluvial or nearshore quartzose sands occur throughout most of the shelf from Hudson Canyon to Cape Hatteras. Calcareous organic and authigenic sediments are the dominant sediment types on the continental margin farther south. Present-day detrital sediments are restricted to a narrow zone near shore, to the outer edge of the shelf off Long Island, and to the continental slope north of Cape Hatteras. The predominance of relict and calcareous sediments indicates that present rate of deposition of detritus derived from land is very low over most of the continental shelf. The report and accompanying sediment map were compiled from published and unpublished reports.

Sediments on the continental margin along the Atlantic coast have been investigated over a long period of time. Among the earliest descriptions are those of Pourtales (1850, 1854, 1870, 1871, 1872), Bailey (1851, 1854, 1856), and Agassiz (1888). Pourtales examined 9,000 samples collected by the U.S. Coast and Geodetic Survey during its lead-line sounding program, and from these compiled the first sediment map (1871). During World War II, H. C. Stetson compiled bottom notations from Coast and Geodetic Survey smooth sheets into a series of sediment maps for use in submarine operations. Similar charts, in somewhat more detail, were also compiled by the German Navy for the same purpose and probably from the same data (Oberkommando der Kriegsmarine, 1943).

Stetson (1938, 1939) examined the shelf deposits along 13 widely spaced profiles from Cape Cod, Mass., to Cape Canaveral, Fla. More detailed studies of smaller areas off northern New England include those of Burbank (1929) and Shepard (1939) on the Gulf of Maine; Shepard and others (1934) and Wigley (1961) on Georges Bank; Phleger and Ericson [2] off

Portsmouth, N.H.; Trowbridge and Shepard (1932) on Massachusetts Bay; Hough (1942) on Cape Cod Bay; and Hough (1940) and Sanders (1958) on Buzzards Bay. Farther south, Alexander (1934), Colony (1932), McMaster (1962), and Shepard and Cohee (1936) reported on the sediment distribution and composition on the central section of the shelf from Rhode Island to Maryland. Sediments on the shelf from Maryland to Key West, Fla., were examined by Ginsburg (1956), Moore and Gorsline (1960), Pearse and Williams (1951), Thorp (1939), and Tyler (1934); and those of the Bahama Banks by Illing (1954) and Imbrie and Purdy (1962). Deposits on the continental slope and the submarine canyons were studied by Ericson and others (1961) and Stetson (1949). Sediments atop the Blake Plateau and on the plateau's marginal escarpment were described by Ericson and others, (1961), Moore and Gorsline (1960), and Stetson and others (1962). These reports are the basis for the bottom-sediment chart shown in figure 94.1; no samples were examined during the study. The compilation was a prelude to a new sampling program initiated in September 1962 by the U.S. Geological Survey in cooperation with the Woods Hole Oceanographic Institution.

CLASSIFICATION

The sediments are classified on the basis of their mineral composition and carbonate content into three groups: detrital sediments, which consist mainly of allogenic mineral grains and have a calcium carbonate content of less than 50 percent; calcareous sediments, which are composed of the skeletal debris from mollusks, algae, bryozoans, foraminiferans, and coelenterates and have a carbonate content greater than 50 percent; and authigenic sediments, which have a wide range in carbonate content and consist of a mixture of authigenic and allogenic minerals and foraminiferal tests. These three major groups are subdivided into sediment types named on the basis of the percentage distribution of

grain sizes (fig. 94.1), using triangular diagrams similar to those of Shepard (1954). The calcareous deposits are further subdivided on the basis of the composition of the organic calcareous components.

DISTRIBUTION

Continental shelf and Bahama Banks

Sediments on the Nova Scotia shelf range from rock and gravel near shore and on the banks at the outer edge of the shelf to coarse sand on the remainder of the shelf. The silty sediments off the east coast of Nova Scotia are confined to a shallow depression on the shelf. Sand is the most abundant deposit in the Bay of Fundy. Silty sand, sandy silt, and silt are limited to the upper reaches of the bay and the lee of Grand Manan Island. From the Bay of Fundy to Cape Cod the bottom deposits near the coast are scattered rock outcrops covered by a thin veneer of sand and gravel; the finer sediments are restricted to the fiordlike valleys along the Maine coast.

Topographically the floor of the Gulf of Maine is extremely irregular and consists of numerous banks and ridges separated by broad and flat basins (Murray, 1947). These topographic highs rise 25 to 50 meters above the surrounding basins and are blanketed by gravel and sand. Sediments on the flanks and in the basins surrounding these topographic highs consist of silty sand and sandy silt that grade into silt and clay toward the center of the basins. Many of the foraminiferal tests in the basin and basin-slope sediments are filled with pyrite. The two sills of the Gulf of Maine (Eastern and Great South Channels) are blanketed by coarser deposits than those present in the gulf. Great South Channel is floored by coarse sand and small patches of gravel, and the sediments in Eastern Channel are predominantly gravel.

Sediments on Georges Bank consist of coarse sand and scattered patches of gravel; the largest area of gravel occurs along the bank's northeastern margin. Clasts in the gravel are predominantly crystalline, granite and gneiss being the most abundant. Felsite and quartzite are also common, and a few fragments of calcareous sandstone and limestone containing Cretaceous fossils have also been recovered. These coarse deposits atop the topographic highs within the Gulf of Maine and the gravel in Great South and Eastern Channels are believed to have been transported to their present sites by Pleistocene glaciers. Below the coarse sand and gravel, Shepard and others (1934) found gravelly silt which they believed to be a till deposit, and they suggested that the coarse sediments above the till represent a lag formed by tidal currents which have winnowed out the fine sediments. Possibly the silty

and clayey sediments in the Gulf of Maine are the fine fractions that were winnowed out of the Georges Bank till.

From Nantucket Island to Hudson Canyon, four broad sediment zones parallel the shelf-break. A nearshore zone about 9 kilometers wide extends from shore to a depth of 28 meters. It consists of large patches of silty sand and sandy silt separated by areas of medium to fine sand. From a water depth of 28 to 59 meters there is a 50-kilometer-wide zone of coarse sand and scattered patches of gravel containing glacial erratics. The sand grains in this zone are heavily stained with iron oxide, and limonitic pellets formed by the alteration of biotite are common. Farther seaward is a 74-kilometer-wide band of silty sand, sandy silt, and silt found at a water depth of 59 to 135 meters. From Martha's Vineyard to Long Island this zone contains an admixture of frosted rounded quartz grains that are thought to be the remnants of a Pleistocene dune field. Authigenic sediments consisting of glauconite pellets and foraminiferal tests, some of which are filled with pyrite, are present near the shelf-break and at the head of Hudson Canyon. Tertiary strata that probably crop out on the shelf near these two areas may be the source of the glauconite.

From Hudson Canyon to Cape Hatteras the sediment has a simpler pattern and consists of medium to fine sand. The sand can be divided into two zones: an inner one, 56 kilometers wide, that extends from shore to a 40-meter water depth and is heterogeneous with scattered patches of gravel; and an outer one, 30 kilometers wide, that extends to a depth of 40 to 60 meters and contains finer grained and more uniform sand. There is a tendency for the sediments of the outer zone to coarsen at the shelf-break, partly because of the presence of glauconite and an increase in foraminiferal tests.

From shore to a depth of 24 to 29 meters, the shelf from Cape Hatteras to Cape Canaveral is mantled by fine sand, silty sand, and sandy silt. Beyond these depths, shell fragments, calcareous oolites, and phosphorite nodules are more abundant in the direction of the shelf-break. Phosphorite and the oolites reach their maximum concentrations in 39 meters of water, 80 kilometers from shore; the shell fragments are most abundant in 30 to 40 meters of water 70 to 80 kilometers from shore. The oolites and phosphorite range in size from 0.2 to 1.2 mm, and have a polished and waterworn appearance. Most of the shell fragments associated with the oolites and phosphorite are polished and rounded. Near the shelf-break the molluscan fragments are replaced by waterworn calcareous algae, bryozoans, barnacles, and echinoid fragments.
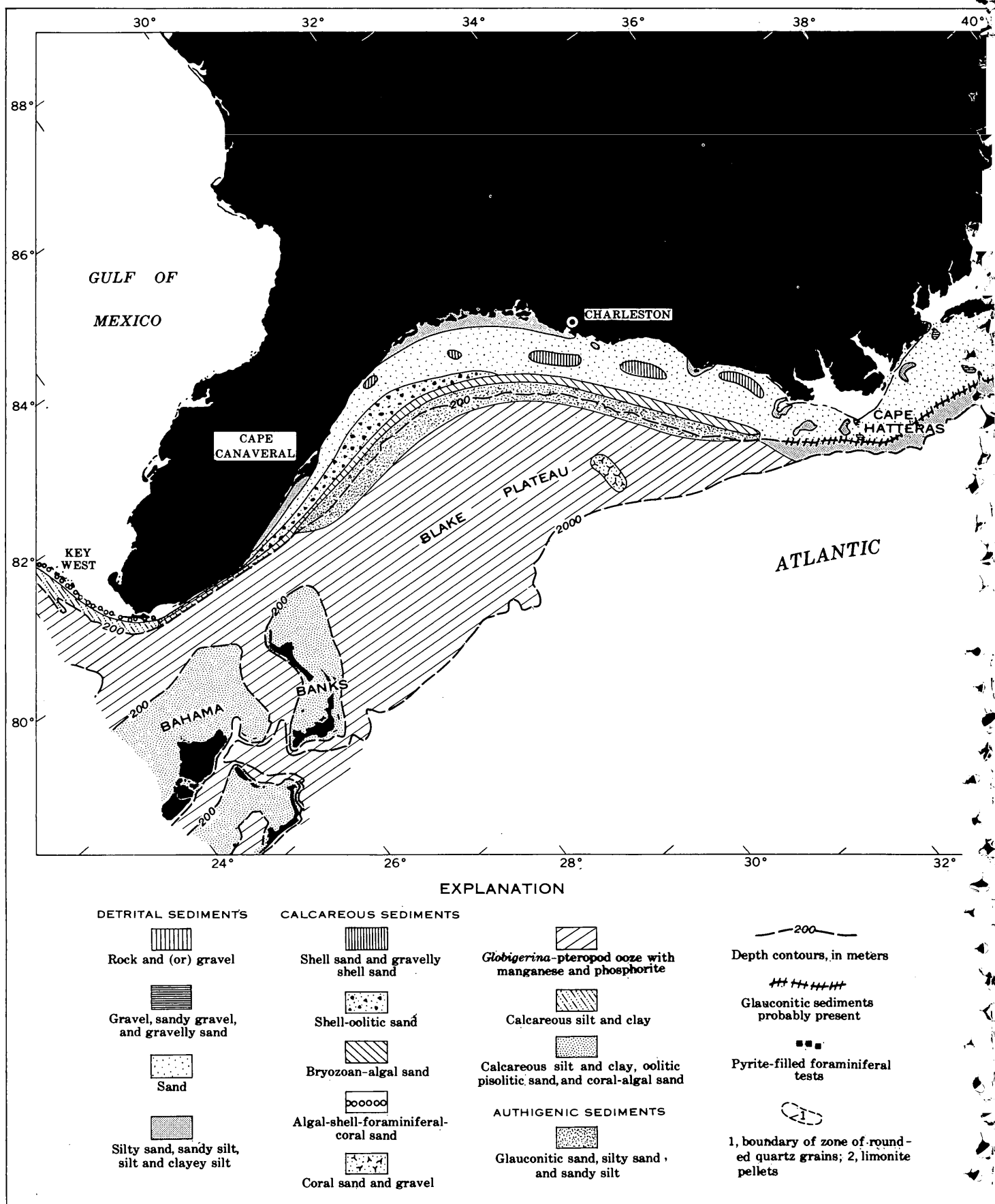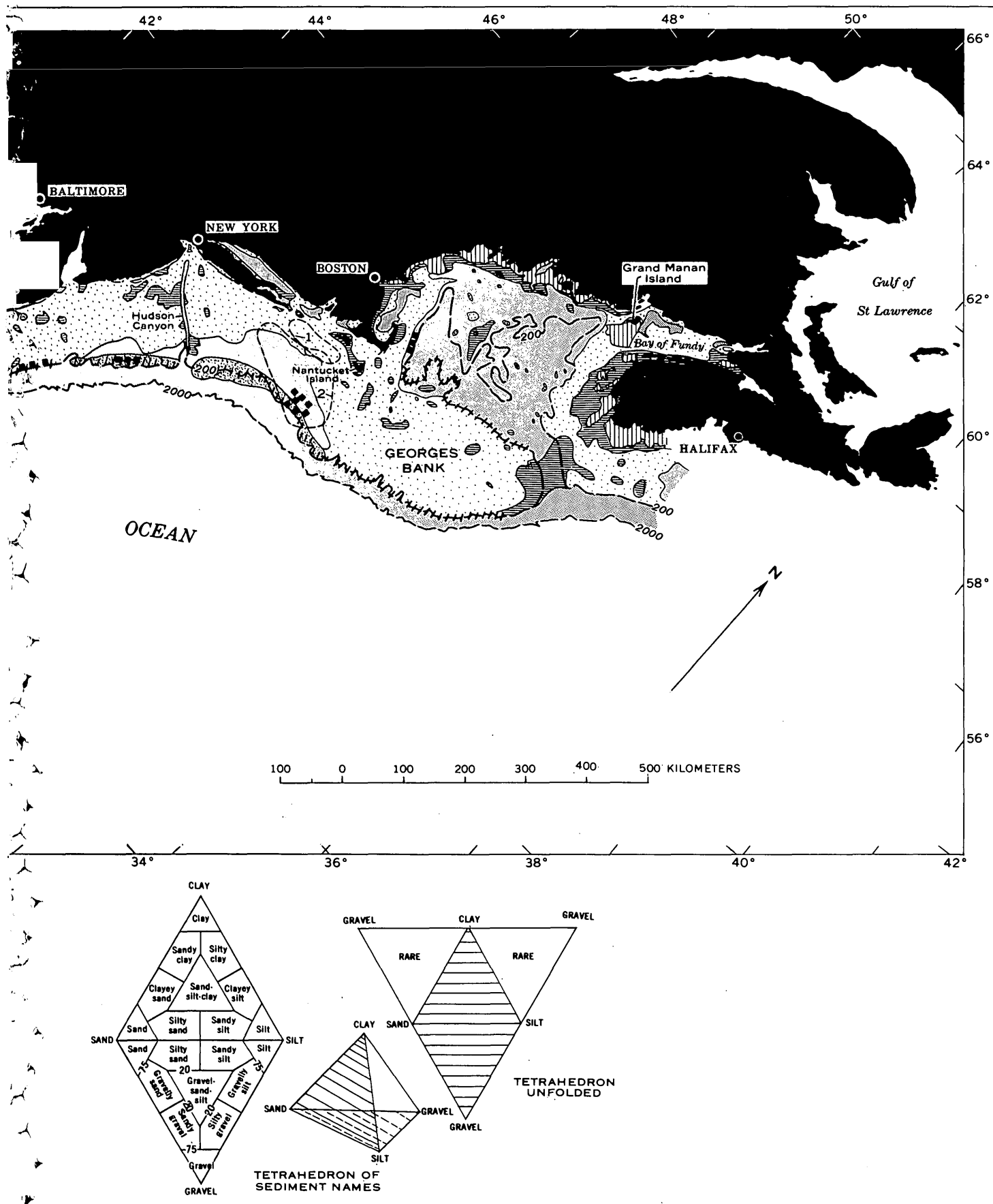
FIGURE 94.1.—Sediments of the continental margin off eastern United States

EXPLANATION

DETRITAL SEDIMENTS

Rock and (or) gravel

Gravel, sandy gravel, and gravelly sand

Sand

Silty sand, sandy silt, silt and clayey silt

CALCAREOUS SEDIMENTS

Shell sand and gravelly shell sand

Shell-oolitic sand

Bryozoan-algal sand

Algal-shell-foraminiferal-coral sand

Coral sand and gravel

Globigerina-pteropod ooze with manganese and phosphorite

Calcareous silt and clay

Calcareous silt and clay, oolitic pisolitic sand, and coral-algal sand

AUTHIGENIC SEDIMENTS

Glauconitic sand, silty sand, and sandy silt

---200---

Depth contours, in meters

Glauconitic sediments probably present

Pyrite-filled foraminiferal tests

1, boundary of zone of rounded quartz grains; 2, limonite pellets

42°   44°   46°   48°   50°   66°

64°

BALTIMORE

NEW YORK

Gulf of   62°

St Lawrence

BOSTON

Grand Manan
Island

Hudson
Canyon

Bay of Fundy

Nantucket
Island

HALIFAX   60°

GEORGES
BANK

OCEAN

58°

56°

100   0   100   200   300   400   500 KILOMETERS

34°   36°   38°   40°   42°

CLAY

Clay

Sandy   Silty
clay   clay

Clayey   Sand·   Clayey
sand   silt·clay silt

Silty   Sandy
Sand   sand   silt   Silt
SAND   SILT
Sand   Silty   Sandy   Silt
sand   silt

Gravel·
sand·
silt

Gravel

GRAVEL

GRAVEL   CLAY   GRAVEL

RARE   RARE

CLAY   SAND   SILT

SAND   GRAVEL

GRAVEL

SILT

TETRAHEDRON OF
SEDIMENT NAMES

TETRAHEDRON
UNFOLDED

tetrahedron shows names of sediments, based on percentage distribution of grain size.

Calcareous sediments dominate the shelf from Biscayne Bay to Key West, although there is a considerable amount of quartz in the sediments north and east of Marquesas Lagoon. From shore to a depth of about 5 meters the sediment consists mainly of calcareous algae, tests of Foraminifera, coral, and shell fragments. Slightly more than 1 percent of the deposit consists of friable, elongate ellipsoidal bodies of semiconsolidated calcareous material believed to be fecal pellets formed by maldanid worms. Oolites and phosphorite, ellipsoidal and 0.5 to 1.5 mm in size, are also present. The sediments on the rest of the shelf are mainly calcareous silts and clays. An unusual constituent of these fine-grained calcareous deposits is aragonite in the form of needles about 10 microns long.

Sediments mantling the Bahama Banks consist of a patchy network of oolitic-pisolitic sands, calcareous organic sands, and calcareous silts and clays.

Continental Slope

From Nova Scotia to Cape Hatteras, sediments of the continental slope consist mainly of silt and clay. Sediments in the canyons that cut the slope range from silt and clay on the walls to silty sand, sand, and gravel along the axes. These coarse deposits probably represent displaced paralic sediments. From Cape Hatteras to lat 28° N. the slope is covered by glauconitic silty sand and sandy silt. South of lat 28° N. the scarps east of the Florida peninsula, the scarp west of the Bahama Banks, and the trough between them (Florida Strait) are blanketed by *Globigerina*-pteropod ooze.

Blake Plateau and Outer Marginal Escarpment

Globigerina-pteropod ooze, nodules and slabs of manganese oxide, and a few nodules of phosphorite mantle most of the surface of the Blake Plateau. The blanket of unconsolidated ooze is only a few centimeters thick and rests on a *Globigerina*-pteropod limestone of Miocene age. The only region of the plateau not blanketed by *Globigerina*-pteropod ooze is an area of 3,600 of 4,500 square kilometers, located 90 kilometers southeast of Charleston, S.C. Scattered within it are about 200 mounds or banks, having a relief of 30 to more than 300 meters, that are formed by the accumulation of coral debris mainly from *Lophelia prolifera* and *Dendrophyllia profunda*.

Sediments on the marginal escarpment east of the Blake Plateau consist of *Globigerina*-pteropod ooze. These unconsolidated sediments are thin, as indicated by the abundant rock outcrops on most of the slope.

ORIGIN OF THE SEDIMENTS

Sediments on the continental margin can be classified according to the dominant cause of deposition, as suggested by Emery (1952). One kind is the detritus contributed to the ocean by present-day streams. The silty sediments near the shore, those at the outer edge of the shelf off Long Island, possibly the sediments in the Gulf of Maine, and the silts and clays on the continental slope north of Cape Hatteras are examples of present-day detrital sediments. A second kind, relict detrital sediments, is deposited under different environmental conditions than those existing at present. The glacial debris scattered throughout the shelf north of Hudson Canyon is an example of this type of deposit. The fine to medium quartzose sands mantling most of the shelf from Hudson Canyon to Cape Hatteras are probably also relict, as they cannot be in the process of being transported over and beyond the finer present-day detrital sediments near shore. The sands are probably of fluvial or nearshore origin and were deposited during the late Pleistocene when sea level was below its present level. A third kind of deposit is the residual debris left by in situ weathering of rocks cropping out on the sea floor. Possibly the glauconitic sediments near the shelf-break north of Hatteras were formed by in situ weathering of Tertiary glauconitic sediments. Sediments of organic origin, a fourth type, consist of calcareous foraminiferal tests, shell fragments, and calcareous algal skeletal debris. These deposits are dominant south of Cape Hatteras. A fifth kind is the chemical precipitates or authigenic sediments, chiefly glauconite, phosphorite, and manganese oxide. These deposits are scattered throughout the shelf south of Hatteras, and are very abundant on the Blake Plateau and on the slope west of the plateau.

In summary, relict detrital and calcareous organic sediments are the two dominant types on the continental margin, followed by present-day detrital, authigenic, and residual deposits. The predominance of relict and calcareous sediments indicates that present rates of deposition of detritus derived from land are very low over large areas of the continental shelf.

REFERENCES

Agassiz, Alexander, 1888, Three cruises of the United States Coast and Geodetic Survey steamer "Blake," v. I: Harvard Coll. Mus. Comp. Zoology Bull, v. XIV, 314 p.

Alexander, A. E., 1934, A petrographic and petrologic study of some continental shelf sediments: Jour. Sed. Petrology, v. 4, p. 12–22.

Bailey, J. W., 1851, Microscopical examination of soundings, made off the coast of the United States by the Coast Survey: Smithsonian Contr. Knowledge, v. 2, Art. 2, 15 p.

Bailey, J. W., 1854, Examination of some soundings from the Atlantic Ocean: Am. Jour. Sci., v. 17, p. 176–178.

———— 1856, On the origin of greensand and its formation in the oceans of the present epoch: Boston Soc. Nat. History Proc., v. 5, p. 364–368.

Burbank, W. S., 1929, The petrology of the sediment of the Gulf of Maine and Bay of Fundy: U.S. Geol. Survey open-file report, 74 p.

Colony, R. J., 1932, Source of Long Island and New Jersey sands: Jour. Sed. Petrology, v. 2, p. 150–159.

Emery, K. O., 1952, Continental shelf sediments of southern California: Geol. Soc. America Bull., v. 63, p. 1105–1108.

Ericson, D. B., Ewing, Maurice, Wollin, Goesta, and Heezen, B. C., 1961, Atlantic deep sea cores: Geol. Soc. America Bull., v. 72, p. 193–286.

Ginsburg, R. N., 1956, Environmental relationships of grain size and constituent particles in some Florida sediments: Am. Assoc. Petroleum Geologists Bull., v. 40, p. 2384–2427.

Hough, J. H., 1940, Sediments of Buzzards Bay, Massachusetts: Jour. Sed. Petrology, v. 10, p. 19–32.

———— 1942, Sediments of Cape Cod Bay, Massachusetts: Jour. Sed. Petrology, v. 12, p. 10–30.

Illing, L. V., 1954, Bahamian calcareous sands: Am. Assoc. Petroleum Geologists Bull., v. 38, p. 1–95.

Imbrie, John, and Purdy, E. G., 1962, Classification of modern Bahamian carbonate sediments. Classification of carbonate rocks: Am. Assoc. Petroleum Geologists Mem. 1, p. 253–272.

MacCarthy, G. R., 1933, Calcium carbonate in beach sands: Jour. Sed. Petrology, v. 2, p. 64–67.

McMaster, R. L., 1962, Petrography and genesis of recent sediments in Narragansett Bay and Rhode Island Sound, Rhode Island: Jour. Sed. Petrology, v. 32, p. 484–501.

Moore, J. E., and Gorsline, D. S., 1960, Physical and chemical data for bottom sediments; South Atlantic coast of the United States: U.S. Fish and Wildlife Service, Spec. Sci. Report—Fisheries Pub. 366, 84 p.

Murray, H. W., 1947, Topography of the Gulf of Maine, field season of 1940: Geol. Soc. America Bull., v. 58, p. 153–196.

Oberkommando der Kriegsmarine, 1943, Uboot handbuch der ostküste der Vereinigten Staaten von Nordameria, Nördlicher Teil (atlas): Berlin, 124 charts.

Pearse, A. S., and Williams, L. G., 1951, The biota of the reefs off the Carolinas: Jour. Elisha Mitchell Sci. Soc., v. 67, p. 133–161.

Pourtales, L. F., 1850, On the distribution of the foraminifera on the coast of New Jersey, as shown by the off-shore soundings of the Coast Survey: Am. Assoc. Adv. Sci. Proc., 3rd meeting, Charleston, S.C., p. 84–88.

———— 1854, Extracts from letters of assistant L. F. Pourtales upon examination of specimens of bottom obtained in the Gulf Stream by Lieutenants Comg. Craven and Maffit: Report of the superintendent of Coast Survey during 1853, p. 82–83.

———— 1870, Der Boden des Golfstromes und der Atlantischen Küste Nord-America: Petermanns Mitheilungen aus Justus Perthes Geographischer Anshalt, v. 16, p. 393–398.

———— 1871, Constitution of the bottom of the ocean off Cape Hateras: Boston Soc. Nat. History Proc., v. 14, p. 58–59.

———— 1872, The characteristics of the Atlantic sea bottom off the coast of the United States: Report of the Superintendent of the U.S. Coast Survey for 1869, App. 11, p. 220–225.

Sanders, H. L., 1958, Benthic studies in Buzzards Bay, I. Animal-sediment relationship: Limnology and Oceanography, v. 3, p. 245–258.

Shepard, F. P., 1939, Continental shelf sediments, in Trask, P. D., ed., Recent marine sediments, a symposium: Tulsa, Okla., Am. Assoc. Petroleum Geologists, p. 219–229.

———— 1954, Nomenclature based on sand-silt-clay ratios: Jour. Sed. Petrology, v. 24, p. 151–158.

Shepard, F. P., and Cohee, G. V., 1936, Continental shelf sediments off the mid-Atlantic states: Geol. Soc. America Bull., v. 47, p. 441–458.

Shepard, F. P., Trefethen, J. M., and Cohee, G. V., 1934, Origin of Georges Bank: Geol. Soc. America Bull., v. 45, p. 281–302.

Stetson, H. C., 1938, The sediments of the continental shelf off the eastern coast of the United States: Massachusetts Inst. Technology and Woods Hole Oceanog. Inst., Papers in Physics, Oceanography and Meteorology, v. 5, no. 4, p. 5–48.

———— 1939, Summary of sedimentary conditions on the continental shelf off the east coast of United States, in Trask, P. D., ed., Recent marine sediments, a symposium: Tulsa, Okla., Am. Assoc. Petroleum Geologists, p. 230–244.

———— 1949, The sediments and stratigraphy of the east coast continental margin; Georges Bank to Norfolk Canyon: Massachusetts Inst. Technology and Woods Hole Oceanog. Inst., Papers in Physics, Oceanography, and Meteorology, v. 11, no. 2, p. 1–60.

Stetson, T. R., Squires, D. F., and Pratt, R. M., 1962, Coral banks in deep water on the Blake Plateau: Am. Mus. Novitates, no. 2114, p. 1–39.

Thorp, E. M., 1939, Florida and Bahama marine calcareous deposits, in Trask, P. D., ed., Recent marine sediments, a symposium: Tulsa, Okla., Am. Assoc. Petroleum Geologists, p. 283–297.

Trowbridge, A. C., and Shepard, F. P., 1932, Sedimentation in Massachusetts Bay: Jour. Sed. Petrology, v. 2, p. 3–37.

Tyler, S. A., 1934, A study of sediments from the North Carolina and Florida coasts: Jour. Sed. Petrology, v. 4, p. 3–11.

Wigley, R. L., 1961, Bottom sediments of Georges Bank: Jour. Sed. Petrology, v. 3, p. 165–188.

Article 95

POSSIBLE WIND-EROSION ORIGIN OF LINEAR SCARPS ON THE SAGE PLAIN, SOUTHWESTERN COLORADO

By DANIEL R. SHAWE, Denver, Colo.

Abstract.—Low straight subparallel scarps in Pleistocene loess on the Sage Plain, southwestern Colorado, bound elongate flat areas oriented about N. 25° E. Swales between the flats probably resulted from excavation of an old weathered surface now represented by the flats. The most likely agent of excavation was prevailing southwesterly winds.

Low straight subparallel scarps 1 to 3 miles long bound broad mesalike flats trending about N. 25° E., in loess of Pleistocene age on the Sage Plain in southwestern Colorado. The scarps are conspicuous on aerial photographs but are difficult to discern on the ground. They have been mapped previously as fractures (Kelley, 1955, fig. 2, p. 14).

Study of the linear features in 1956 by W. B. Rogers and the author showed that they are formed entirely in a thin blanket of loess. Sandstone exposures along the trace of the linear scarps show no fractures parallel to the scarps but commonly are crossed by joints and faults trending about 65° to the scarps. The original interpretation of the linear features as fractures appears to be incorrect. Fractures restricted to the loess and oriented parallel to the scarps may have somehow controlled development of the scarps, but there is no evidence of such fractures.

The loess, which is of pre-Wisconsin age (Hunt, 1956, p. 38), extends nearly 100 miles along the Colorado-Utah boundary, has a maximum width of about 70 miles, and covers about 3,500 square miles. On the Sage Plain the deposit commonly is as much as 20 feet thick. The loess consists largely of silt but contains some fine sand and clay. Quartz is the dominant constituent, and feldspar is present in small amounts; heavy minerals make up about 0.5 percent of the total.

The broad mesalike flats, generally bounded by a scarp on either side, consist of relatively undissected loess and lie about 5 to 15 feet above intervening swales. All the flats narrow to the northeast (figs. 95.1 and 95.2) and are separated by broad intricately eroded, hummocky swales about the same width as the flats. Both the swales and the flats are moderately dissected by dendritic intermittent streams, along which bedrock is exposed locally. Bedrock also is exposed in many other places in the swales. The stream channels locally are cut as much as 100 feet below the level of the flats. The flats thus appear to be relict features of an older surface.

The flats have a superficial resemblance to wide longitudinal dunes illustrated by Lueder (1959, p. 236, fig. 14–5), but the resemblance probably is misleading. Several lines of evidence oppose a dune origin: the flats are relatively wide in comparison with the swales, whereas longitudinal dunes are much narrower than associated interdune areas; barchan or similar dunes usually associated with longitudinal dunes are lacking on the Sage Plain; the material of the flats is composed of silt rather than sand; and the extreme width, about half a mile, of some of the flats is greater than that of dunes.

Soil relations also rule out a dune origin. A light-colored calcareous soil horizon crops out near the top of the scarps, just below the surface of the flats. The soil horizon evidently developed during weathering of an original blanket of loess that presumably was continuous across the whole area and was exposed by excavation of the intervening swales.

The difference between the soil of the swales and that of the flats is illustrated by other properties. The

N
↑

EXPLANATION

Surficial deposits
*Largely loess of Pleistocene age
except for alluvium of Recent
age along drainage courses*

Bedrock
*Largely Dakota Sandstone of
Cretaceous age*

Scarp in loess
Hachures on low side

Fault
*Dotted where concealed; bar and
ball on downthrown side*

COLORADO

Area of
report

Area shown
on aerial
photograph

TO DOVE CREEK

0   1 MILE
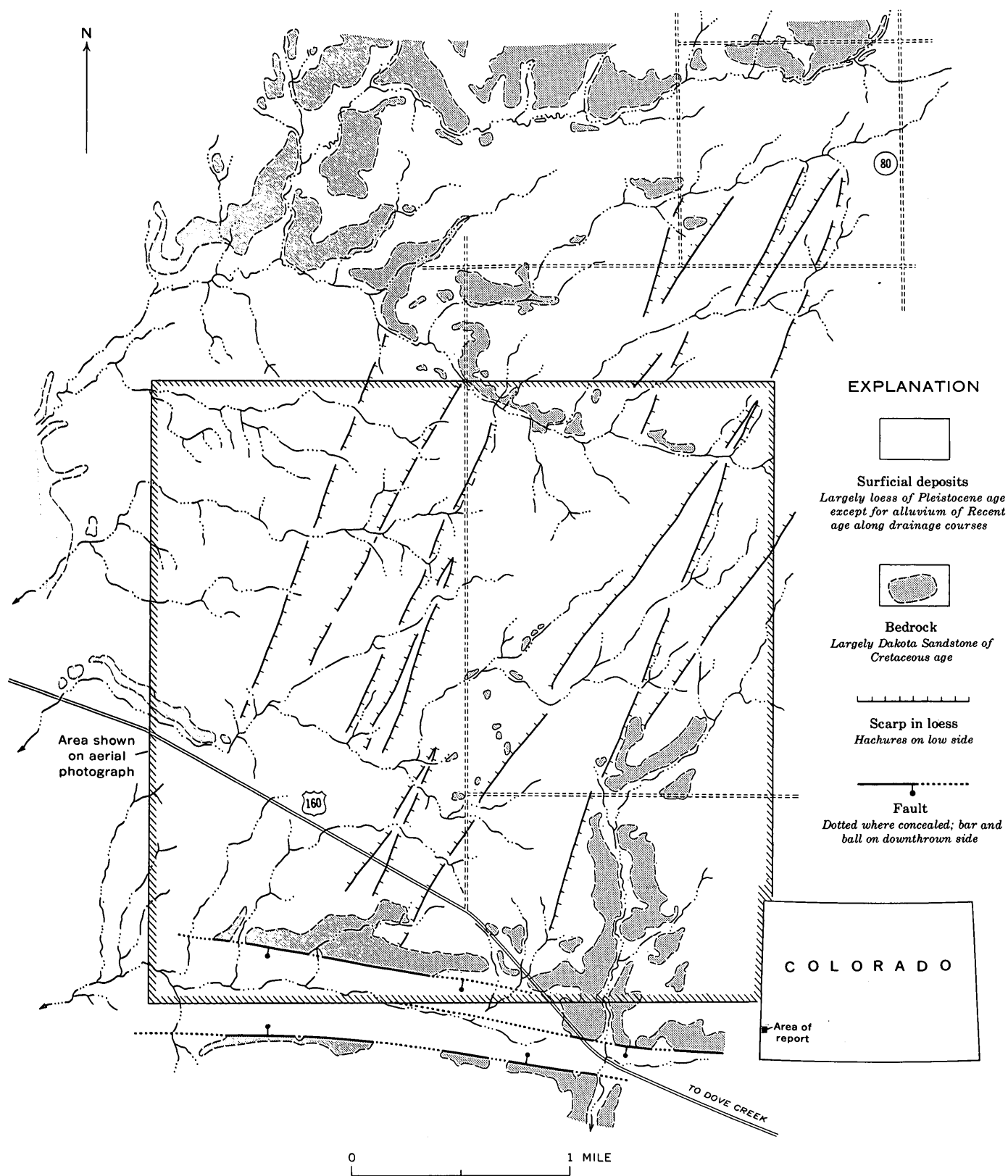
FIGURE 95.1.—Geologic sketch map of an area on the Sage Plain, southwestern Colorado, showing linear features possibly formed by wind erosion of loess. Bedrock mapping chiefly by George C. Simmons.

loess everywhere is reddish brown, but that in the swales is relatively darker and grayer than that on the flats and appears to represent a deeper soil horizon, exposed by erosion. The loess on the flats is slightly more coherent, and its greater redness suggests near-surface oxidation. Preliminary studies of the heavy-mineral content of the loess suggest that the heavy-mineral suites from flats and swales are generally similar, although resistant minerals such as zircon are more abundant in soil from the swales. Presumably, weathering has destroyed some black opaque minerals and apatite in soil on the flats.

FIGURE 95.2.—Aerial photograph showing linear features on the Sage Plain, southwestern Colorado. Location shown on figure 95.1.

The relict flats are remnants of an earlier, weathered flat-lying depositional surface, and the swales thus seem to have been formed by excavation of material. To the author it appears most likely that the excavation was performed by prevailing southwesterly winds that blew across a level deposit of loess laid down in pre-Wisconsin time. If we assume that the soil is of Pleistocene age, excavation possibly began near the end of the Pleistocene. Wind and climate changes probably were responsible for the change from deposition to excavation of loess. The swales started locally as shallow troughs scooped out by the wind; as they grew deeper and wider they developed a wedge shape in plan, the point of which migrated windward; thus the points of the flats are all oriented northeastward. The present dendritic drainage pattern probably was established upon the original loess surface prior to excavation and became entrenched as excavation proceeded. The stream directions are thus independent of the relict flats and the swales, except for local small consequent streams along the edges of some flats (fig. 95.1).

Active sand dunes in northeastern Arizona, northwestern New Mexico, and southeastern Utah are oriented about N. 45° E. (Thorp and Smith, 1952), indicating the general trend of present-day prevailing winds. The relict flats on the Sage Plain thus are oriented nearly parallel to prevailing winds, which probably have not changed direction appreciably since Pleistocene time.

REFERENCES

Hunt, C. B., 1956, Cenozoic geology of the Colorado Plateau: U.S. Geol. Survey Prof. Paper 279, 99 p.

Kelley, V. C., 1955, Regional tectonics of the Colorado Plateau and relationship to the origin and distribution of uranium: New Mexico Univ. Pubs. in Geology, no. 5, 120 p.

Lueder, D. R., 1959, Aerial photographic interpretation: New York, McGraw-Hill Book Co., Inc., 462 p.

Thorp, James, and Smith, H. T. U., co-chm., 1952, Pleistocene eolian deposits of the United States, Alaska, and parts of Canada: Washington, Natl. Research Council, map, 2 sheets.

Article 96

GLACIAL LAKES NEAR CONCORD, MASSACHUSETTS

By CARL KOTEFF, Boston, Mass.

Abstract.—Detailed mapping in the Concord 7½-minute quadrangle has revised the history of the Cherry Brook stage of glacial Lake Sudbury, and has delineated a separate lake, glacial Lake Concord. The recalculated postglacial tilt in the area is between 5 and 6 feet per mile.

Surficial geologic mapping in the Concord, Mass., 7½-minute quadrangle has resulted in a revision of the history of part of glacial Lake Sudbury, and the delineation of a separate lake, glacial Lake Concord (fig. 96.1). Lake Sudbury as first outlined by J. W. Goldthwait (1905) extended much farther south than the Cherry Brook stage shown in figure 96.1. The present article considers only the Cherry Brook stage of Lake Sudbury, and its relation to glacial Lake Concord.

The shorelines are based primarily on the distribution of lake sediments and on the present altitude of outlets; no shoreline features such as wave-cut benches and beach deposits were found. The absence of such features was noted by Goldthwait (1905, p. 273), and was explained by Hansen (1956, p. 77–78) as the result of the presence of large residual ice blocks, which reduced the area of open water and thus limited wave action. The shoreline itself consisted, at least in part, of ice. Colluvium and slope movement also may have masked or destroyed some shore features. The shoreline shown for the Cherry Brook stage was modified in the western part from Goldthwait (1905), and in the northwestern part from Hansen (1956). Hansen's data also were used in interpreting the shoreline of Lake Concord in its western part, near Maynard.

Delta deposits are distributed throughout the lake area; the more conspicuous ones are indicated in figure 96.1. The deposits consist chiefly of fine sand to very coarse gravel. Foreset beds were observed in only a few deltas, because the topset beds generally are 10 feet or more thick, and few exposures reach that depth. The collapsed form of the deltas indicates that they were built in contact with ice on one or more sides; accordingly, they are called kame deltas. The lake-bottom sediments include fine sand, silt, and clay. The clay, which is generally very silty, has been found in Bedford, Concord, and Sudbury, and according to local residents was used for making bricks in colonial times.

Six outlets, 3 for the Cherry Brook stage and 3 for Lake Concord, have been found. They are numbered in chronological order on figure 96.1.

A postglacial tilt of 5 to 6 feet per mile is calculated for this area. The divide at outlet 2 (about 155 feet in altitude) is approximately 30 feet lower than the highest foreset beds (about 185 feet) observed in a delta at the northern limit of the Cherry Brook stage, more than 5 miles north of the outlet. It is assumed that the ice retreated northward parallel to the direction of advance (approximately S. 10° E.) and that the strike of the tilt is normal to this direction. This tilt is a little less than the 7 feet per mile calculated by Goldthwait (1905, p. 286–287).

Outlet 1, at an altitude above 160 feet, represents the first major spillway of the Cherry Brook stage of Lake Sudbury. The outlet is floored in the upstream part mostly by swamp and has gentle side slopes; downstream it is narrow and its walls show bedrock outcrops through a cover of large boulders and very thin till and colluvium. The kame delta 1½ miles west of Wayland was constructed at the time when outlet 1 was used. Goldthwait (1905) originally described this delta as having an altitude of 175 feet, and placed it in an earlier and higher "Weston stage" of Lake Sudbury, with a higher outlet somewhat south of outlet 1. However, the foreset beds that underlie more than 10 feet of topset beds in this delta have an altitude of a little less

ART. 96 *IN* U.S. GEOL. SURVEY PROF. PAPER 475–C, PAGES C142–C144. 1963.

C142

than 165 feet, and outlet 1 of the Cherry Brook stage appears to be the likely control for the lake in which the delta was constructed.

When the main ice margin had retreated far enough northward to allow Cherry Brook drainage to become integrated with that of Stony Brook, outlet 2 at about 155 feet altitude became the controlling outlet, and the lake level dropped more than 5 feet. The upper part of the Cherry Brook valley has a few areas of boulder pavement, but for a mile above the junction with Stony Brook, numerous bedrock exposures and large boulders, some as much as 20 feet across, occur both in the floor and along the walls of the valley. The deltas north of Wayland were constructed at this time.

Outlet 3 came into use when the ice front had retreated to a position just south of Fairhaven Bay. This outlet, at an altitude of about 165 feet, is floored mostly by swamp, together with a few large boulders and scattered bedrock outcrops. Its walls are mostly bedrock. Out-

lets 2 and 3 probably were used contemporaneously, because a postglacial tilt of between 5 and 6 feet per mile indicates that these outlets were at the same altitude during glacial-lake time, even though there is about a 10-foot difference in altitude at present. Outlet 3 was used only temporarily, until aggrading streams choked it off with deposits 10 to 15 feet higher than the outlet. Then outlet 2 again became the only major spillway.

The northernmost part of Lake Sudbury during the Cherry Brook stage apparently became filled by large masses of delta deposits when the main ice front stood about 1 mile south of Concord. This prevented any further drainage of glacial melt water into the Lake Sudbury basin. The highest altitude determined for the delta foreset beds here is 185 feet, and the topset beds of the deltas are more than 190 feet in altitude, except at 3 places. Two of these places are railroad cuts through drift that was originally above 190 feet; the third place is the valley of the Sudbury River, where
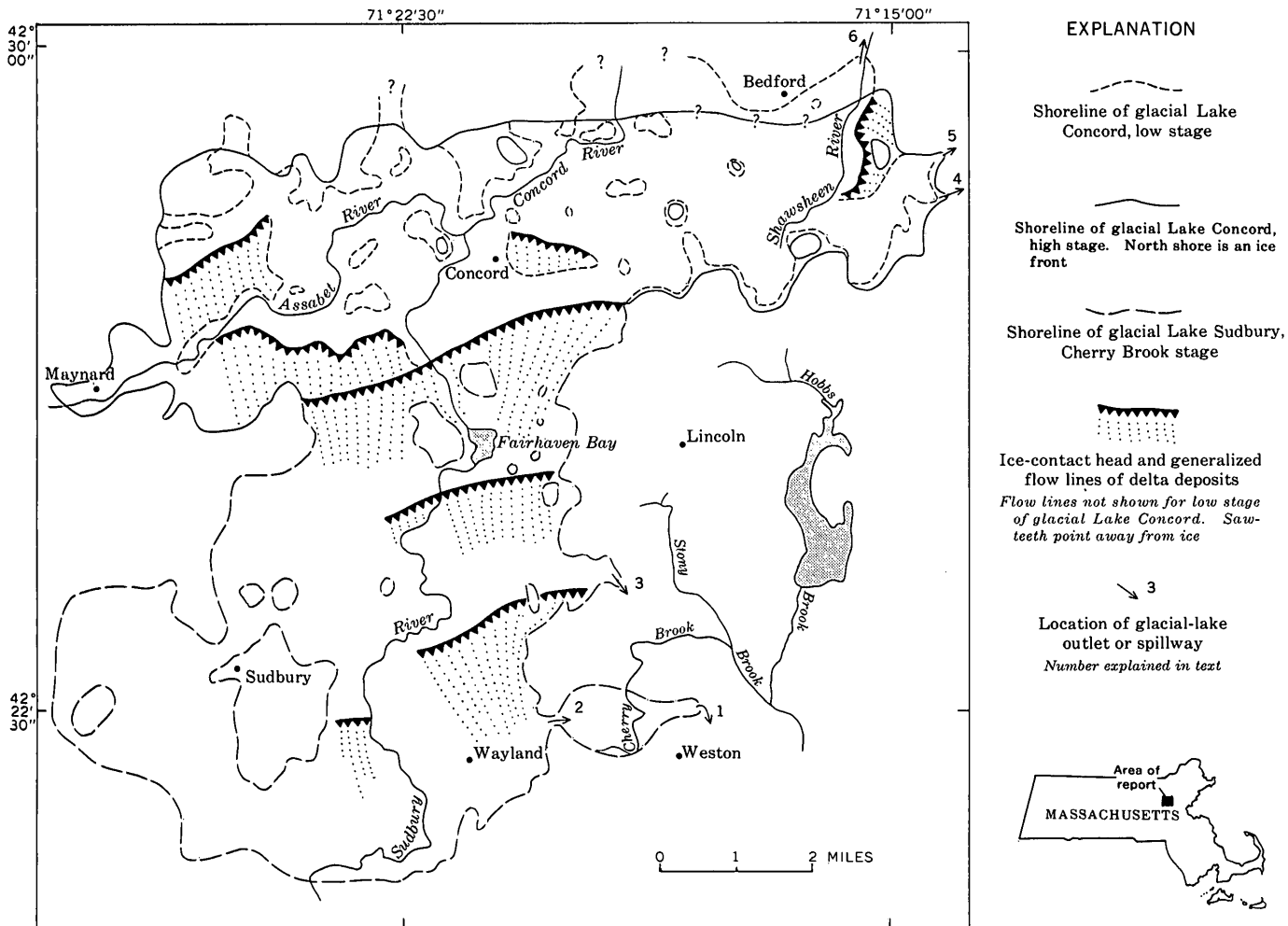
FIGURE 96.1.—Map of the Concord, Mass., area showing the maximum extent of glacial Lakes Sudbury (Cherry Brook stage) and Concord.

melt-water deposits stand on either side of the valley at an altitude of more than 190 feet and appear to have been once continuous across the valley. Large ice masses may have lain in and north of Fairhaven Bay; melting of the ice and erosion of adjacent deposits would have allowed escape of the lake waters northward at a later date.

Lake Concord came into existence immediately after retreat of the ice from its position south of Concord. The positions of ice fronts during Lake Concord time are more difficult to determine than those during the Cherry Brook stage. The lake was bordered on the north, for the most part, by ice, and on the south and west by higher ground. The ice front, hence the shoreline, is inferred to have retreated farther north during the low stage of the lake than during the earlier, high stage (fig. 96.1). Outlet 4 controlled the high stage of Lake Concord, whose altitude as determined from foreset beds was between 180 and 185 feet. The valley of outlet 4 is at an altitude of less than 180 feet, and is characterized by bedrock covered by thin till; a few outcrops occur downstream. Although it is not evident today because of postglacial tilt, the altitude of Lake Concord was relatively lower than the maximum 185-foot altitude of the Cherry Brook stage.

Outlet 5 has an altitude of about 145 feet, and is floored mostly by swamp and scattered small boulders. The south wall of the valley is composed of sand and gravel, and the north wall is composed of till, probably thin. Outlet 5 was probably covered by ice and glacial drift during the high stage of Lake Concord, but gradual dissipation and erosion of the ice and the drift lowered this outlet and the lake level to the low stage at 145 to 150 feet. Foreset bedding at an altitude of less than 170 feet in a delta west of Concord indicates a steplike lowering of Lake Concord from the high to the low stage. Three exposures in low-stage deltas show bedding dipping eastward. The ice-contact slopes of the deposits of the low stage (not shown in fig. 96.1)

indicate that large masses of ice lay in Lake Concord throughout its history.

Goldthwait (1905, p. 291) described the deposits west of Concord as belonging to what is called the low stage of Lake Concord in the present article, but he did not recognize the high stage. He also believed that the lake was controlled by a pass at the head of Hobbs Brook. However, there is no possible spillway lower than 195 feet at the head of Hobbs Brook, so that this brook could not have served as an outlet for even the high stage. Hansen (1956, p. 78–79) stated that the deposits west of Concord at altitudes of approximately 155 feet were not lacustrine, but rather were deposited in contact with ice by running melt water after the lake was drained. The deltaic bedding and consistent 150-foot altitude of these deposits for a distance of more than 6 miles, however, indicate that they are lacustrine, although large ice masses that could have affected deposition probably were present in the lake.

As the ice front retreated northward from Bedford, the Shawsheen River valley was exposed, allowing complete drainage of Lake Concord through outlet 6. Some very fragmentary evidence in the lake area indicates temporary water levels below 145 feet that may have been controlled by outlet 6, but deposits below 145 feet in altitude are included with lake-bottom deposits. The present floor of the Shawsheen is at an altitude of 100 feet or less where the river has cut down to bedrock. Water-polished bedrock on the valley walls indicates an earlier threshold at about 115 feet, but it is not clear whether most of the erosion was caused by discharge of the lake or by the present Shawsheen River.

REFERENCES

Goldthwait, J. W., 1905, The sand plains of glacial Lake Sudbury: Harvard College Mus. Comp. Zoology Bull., v. 42, p. 263–301.

Hansen, W. R., 1956, Geology and mineral resources of the Hudson and Maynard quadrangles, Massachusetts: U.S. Geol. Survey Bull. 1038.

CHANNEL CHANGES ON SANDSTONE CREEK NEAR CHEYENNE, OKLAHOMA

By DeROY L. BERGMAN and C. W. SULLIVAN,

Elk City, Okla., and Oklahoma City, Okla.

Abstract.—The cross-sectional shape of the channel of Sandstone Creek, in western Oklahoma, has changed from rectangular to V-shaped during the period 1957–62 due to sustained seepage from upstream floodwater-retarding structures, which has encouraged rapid growth of vegetation that anchors sediment within the channel. Floodwaters now flow at higher stages, and low flows are entrenching in a narrowed low-water channel.

Channel changes near the streamflow gaging station on Sandstone Creek near Cheyenne, Okla., have become very evident since 1957, and the changes are still occurring. The channel changes are of interest because of the factors causing a trend toward bank stabilization and because of the effect of the changes on the stage-discharge relation at this location. The changes appear to be related to a change in the pattern of streamflow resulting from an upstream flood-prevention work plan being applied to the watershed.

Sandstone Creek basin lies in the rolling red-plains region of extreme west-central Oklahoma. The creek drains an area of 107 square miles and is tributary to the Washita River. Elevations in the basin range from 1,750 to 2,400 feet. Valley slopes are moderate and upland slopes range from 2 to 20 percent. The climate in the area is dry subhumid, and the mean annual precipitation on the basin is about 25 inches. Most of the rainfall occurs during storms of moderate to intense severity and of short duration.

The watershed contains 24 floodwater-retarding structures and 17 gully plugs constructed by the Soil Conservation Service, U.S. Department of Agriculture, under an upstream flood-prevention work plan. By 1952, the floodwater-retarding structures had been completed, and more than 80 percent of recommended land-treatment measures had been applied.

The factors apparently causing channel changes have been: (1) the establishment of perennial streamflow from reservoir seepage, which is considered the principal factor; and (2) the resulting establishment of permanent vegetation. The vegetation anchors previously unchained deposits within the channel. The deposits thus retained have contributed to a gradual change in the cross section of the channel from rectangular to V-shaped. Though the change is marked, the total cross sectional area of the channel at bankfull stage has not changed materially.

The sequence of channel changes on Sandstone Creek during the years 1950 to 1962 is vividly pictured in figure 97.1. Streamflow characteristics during this time can be separated into two regimes: intermittent and perennial. During the period of intermittent streamflow, prior to mid-1957, the channel was barren and rectangular, with an ill-defined low-water channel (fig. 97.1A, B). Silt from the undercut and weathered banks and from basin erosion was deposited in the channel after each rise in water level, and was subsequently carried downstream during high-water periods. Days of no flow were quite common (114 days in 1954). Since mid-1957, the steamflow has been perennial. During this period the channel has been changing from barren to thickly vegetated, from rectangular to V-shaped, and the low-water channel from ill defined to well defined (fig. 97.1C, D).

The permanent vegetation established itself in the riparian area of the low-water channel during the interval from mid-1957 to mid-1959. Streamflow characteristics in the years since mid-1957 have been ideal for vegetation growth. The riparian vegetation within the channel, which is now growing above the 3½-foot stage, is inundated only about 1 percent of the time, and the perennial streamflow provides the needed moisture for growth. The kinds of vegetation, in order of appearance, are: sedge; native grasses and weeds; willow, salt-cedar, and cottonwood trees.

FIGURE 97.1.—Sandstone Creek near Cheyenne, Okla., looking upstream from gaging station.　*A*, 1950; *B*, 1954; *C*, 1960; *D*, 1962.　(Photographs A, B, and C, by U.S. Dept. of Agriculture.)

The sediment deposited in the vegetated area has constricted the low-water channel to one-third its former width, and has caused development of the **V**-shaped channel (fig. 97.1*C*).　The continued growth of the vegetation and addition of deposits from floodflows has further developed this channel shape (fig. 97.1*D*).　The constricted channel now has been scoured below the normal level of the former streambed by the relatively silt-free water from the upstream detention structures.

Instrument surveys of the channel cross section were made in 1954 and 1961.　The survey notes were plotted with the 1961 cross section superimposed upon the 1954 cross section for comparison.　The areas of erosion and deposition during the intervening period are evident in figure 97.2.　The change in cross-sectional area within the channel through the range of stage is illustrated in figure 97.3 by the stage-area curves for the cross sections.
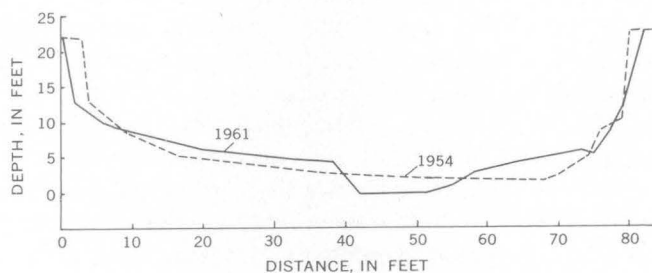
FIGURE 97.2—Comparison of channel cross section for 1954 and 1961 at gaging station.
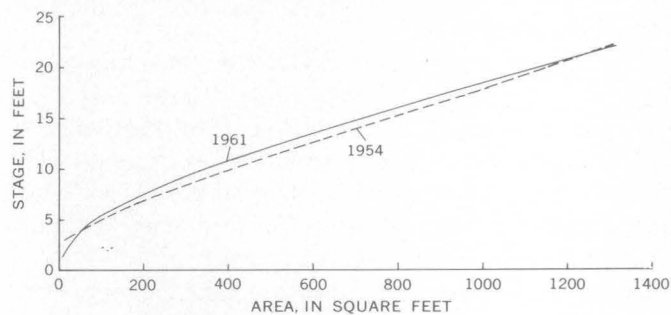
FIGURE 97.3—Comparison of stage-area curves for 1954 and 1961 for cross section at gaging station.

The overall redistribution of the channel area, coupled with the increased retarding action of the vegetation, results in a higher stage for a given discharge above the 3½-foot stage than occurred during the intermittent streamflow period. However, the well-defined channel below the 3½-foot stage has greater discharge capacity than the previous ill-defined low-water channel. To illustrate this point, figure 97.4 presents representative stage-discharge relation curves during the two periods as computed from the gaging-station records.
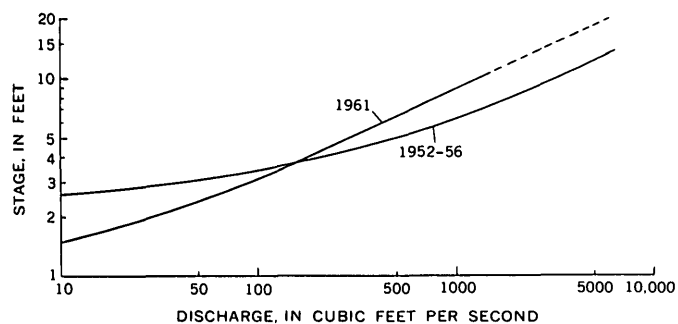
FIGURE 97.4—Comparison of average stage-discharge relation for the period 1952–56 and the year 1961 at gaging station.

The effects of the change in the streamflow capacity of the channel can be illustrated by using the flood discharge-frequency curve based on the 10 years of record for this site. This frequency curve has been converted to a comparable stage-frequency curve for each type period based on the stage-discharge relation for the respective periods (fig. 97.5). The effects of changes in the channel are illustrated also through use of the flow-duration curve of record for the stream-gaging station. The flow-duration curve has been converted to equivalent stage-duration curves by using the representative curve of stage-discharge relation for each period discussed (fig. 97.6).

The continued effect of regulation from the upstream reservoirs on the low-water channel is noticeable in two ways. First, the appearance of the bed-load material has changed from a mixture of fine-grained sand and silt to sand of fine- to medium-grain size. Very little silt is noticeable in the bed of the stream during low-water periods. Second, the continued scour has produced many small riffles composed of medium- to coarse-grained sand, shaly particles, and oblong clay balls. The drop over the riffles is usually less than half a foot, and the length of the pools is usually no more than ten times the channel width. The riffles, and the nature of the material comprising them, indicate that the present channel may have reached the level of previous maximum scour. Should this be the case, it will be interest-
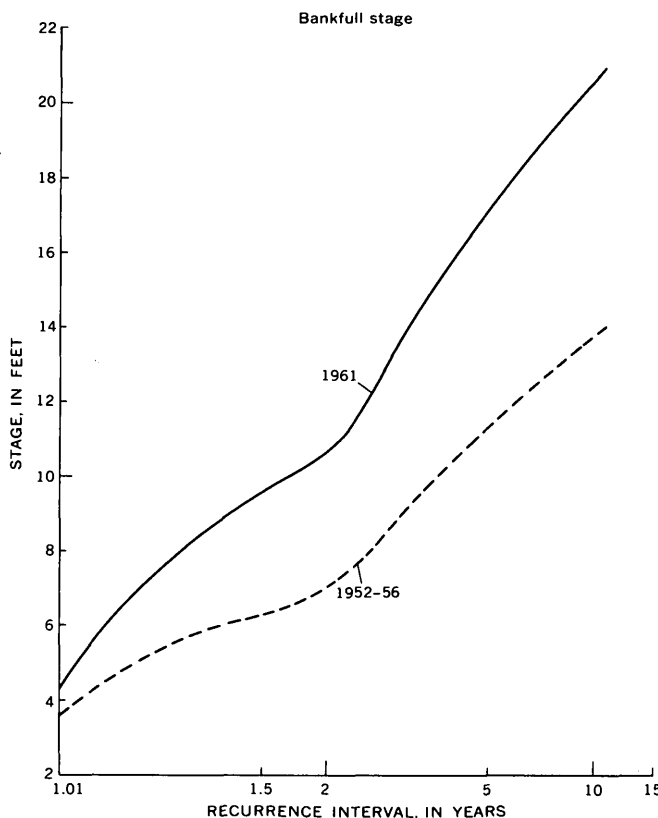
FIGURE 97.5—Comparative stage-frequency curves relative to channel characteristics during 1952–56 and 1961.
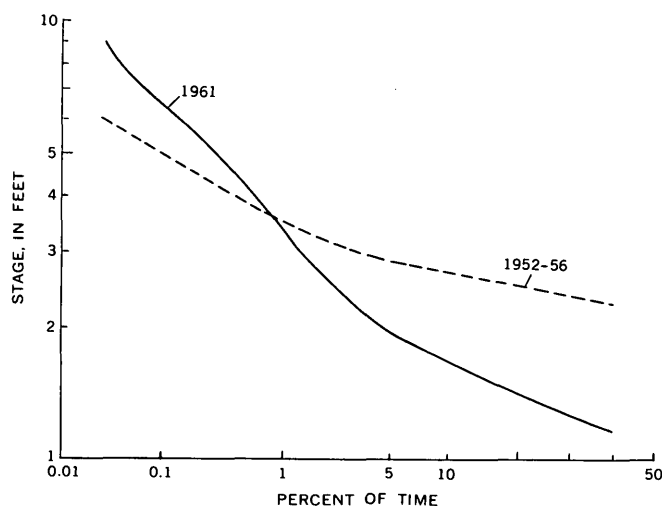
FIGURE 97.6—Comparative stage-duration curves relative to channel characteristics during 1952–56 and 1961.

ing to note whether the stream will continue to imbed in the existing channel, or whether it will begin to increase in meander amplitude and shorten in meander length.

Changes similar to those discussed above appear to be occurring throughout the length of Sandstone Creek.

A reach of channel downstream from the gaging station is in a later stage of development. Using this downstream reach as a guide, the next stage of development should be the introduction of more trees in the medium- and high-water parts of the channel, the continued weathering and grading of the old vertical banks above the tree line, and the continued deposition of sediment in the medium-water channel. Small trees growing below the top bank are evidence that this stage of development has started within the reach (fig. 97.1D).

ORIGIN AND GEOLOGIC SIGNIFICANCE OF BUTTRESS ROOTS OF BRISTLECONE PINES, WHITE MOUNTAINS, CALIFORNIA

By VALMORE C. LaMARCHE, JR., Cambridge, Mass.

Abstract.—Many roots of bristlecone pines (*Pinus aristata* Engelmann) are characterized by an asymmetrical distribution of secondary wood along the bottom of the root. The vertical buttress form develops after diametral growth and slope denudation have exposed the upper root surface to abrasion and weathering and the cambial area is reduced to a small segment of the circumference. Dating of the initial exposure indicates that local rates of denudation have been fairly uniform during the past 3,000 years.

Exposed roots of millenia-old bristlecone pines (*Pinus aristata* Engelmann) growing high in the White Mountains of eastern California are being used to measure local rates of slope denudation (LaMarche, 1961). Many of the exposed roots are asymmetrical in transverse section. One lateral root studied is 25 feet long and 3 feet high but only 6 inches wide (fig. 98.1). Such roots have been termed "buttress roots."

The asymmetry of a buttress root reflects the internal distribution of secondary wood. The older part of the root is near the top, where the root axis is enclosed in concentric growth rings. The younger wood forms a downward extension that is bounded on the lower surface by the cambium and bark. This wood is made up of gently curved annual layers that terminate at the vertical sides of the root. The buttress roots are similar in shape and internal structure to the "massive slab" type of bristlecone pine stem described by Schulman (1958). In both types, the shape results from reduction of the cambial area to a small segment of the circumference, which restricts the addition of new wood to a narrow longitudinal strip along the side of the stem or the bottom of the root.

The roots are concentrated in the upper foot of the rocky, dolomitic soil. Where exposed in roadcuts or on uprooted trees, the roots are circular in cross section and have a continuous cover of bark (fig. 98.2*A*). In contrast, where the roots of living trees have been exposed
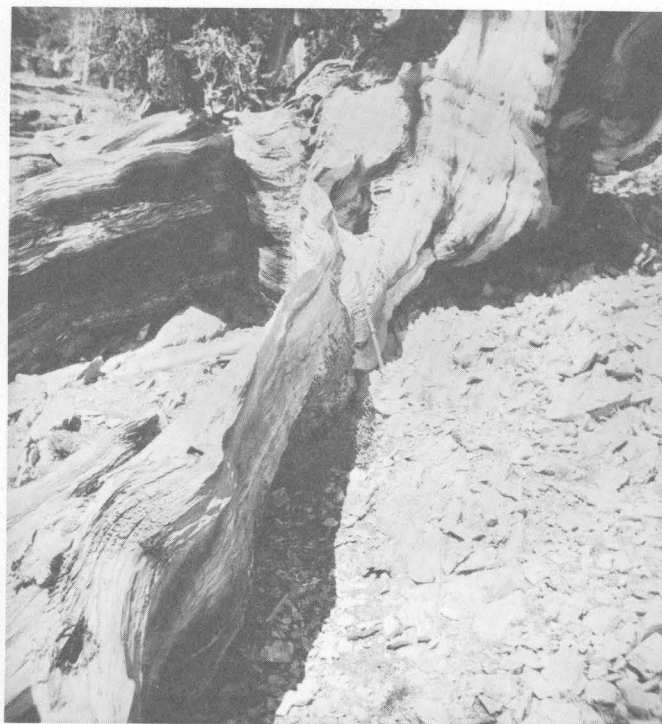
FIGURE 98.1.—Longitudinal view of a 2,500-year-old buttress root. The root is 3 feet high (1 foot is below ground), 6 inches wide, and 25 feet long. The stem and another root are in the background. The increment borer (center) is 18 inches long.

by slope denudation, they typically have the buttress form.

The slopes in the area are denuded by erosion and shallow mass movement. When diametral growth and slope recession expose the upper surface of a root (fig. 98.2*B*), angular soil particles move downslope across the top of the root. Consequent abrasion and weathering probably remove the protective layer of bark faster
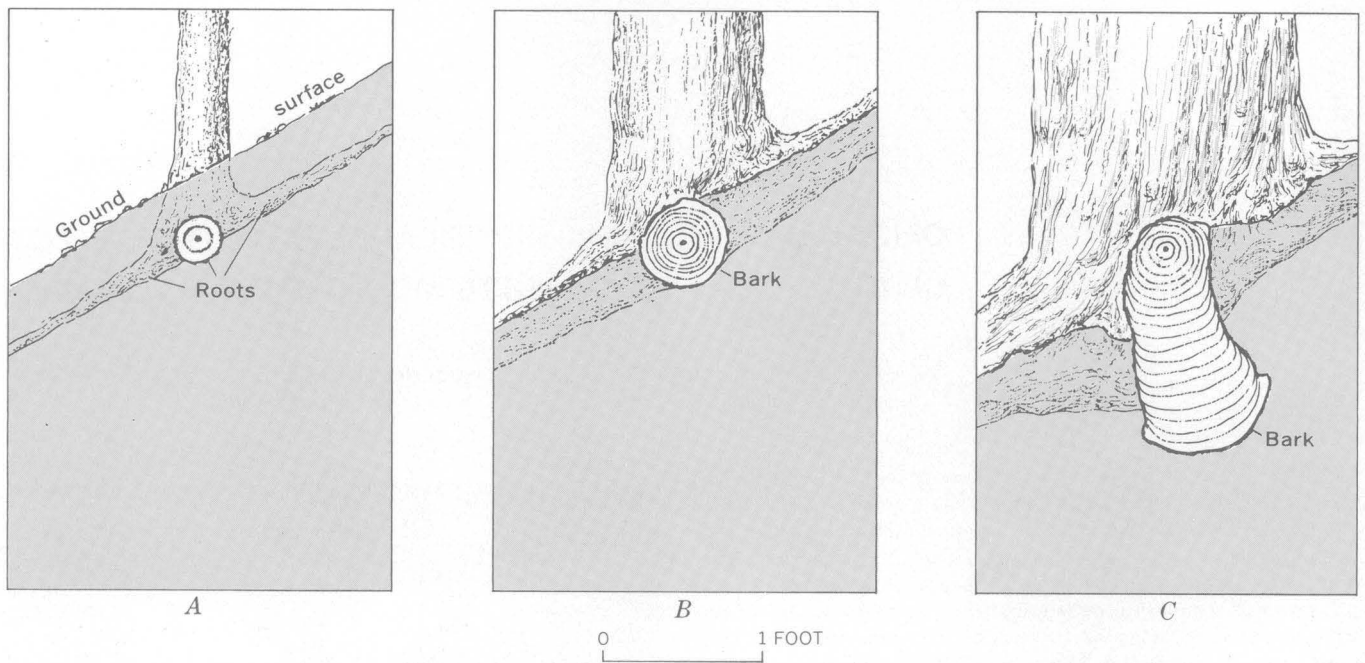
FIGURE 98.2.—Cross sections of a buttress root, showing evolution. *A*, shallow roots beneath ground surface; *B*, exposure of root and reduction of cambial area; *C*, buttress root after several hundred years of restricted growth.

than it is replaced. Stripping of the bark and cambium from the upper root surface, with continuing secondary growth on the lower side, produces the vertical buttress form (fig. 98.2*C*).

The buttress roots studied range from 400 to 3,000 years in age, as determined by counting and correlating growth rings. Further, the age of the root at the time of initial cambial reduction can be estimated from the shape and continuity of the growth rings. This estimated age gives a measure of the time that elapsed between longitudinal growth of the root and its exposure at the ground surface and consequent downward growth. The elapsed time ranges from 200 to about 1,000 years and depends on the initial depth of burial and the local denudation rate.

The roots of some bristlecone pines were first exposed at least 2,500 years ago, and initial exposure of the roots of younger trees has been taking place up to the present time. Therefore, the root exposure shown by these trees cannot be attributed to accelerated erosion in response to changes in climate or land use in recent times. Thus, it can be inferred that in the White Mountains area, local denudation rates have been fairly uniform during the past 3,000 years.

REFERENCES

LaMarche, V. C., Jr., 1961, Rate of slope erosion in the White Mountains, California: Geol. Soc. America Bull., v. 72, p. 1579.

Schulman, Edmund, 1958, Bristlecone pine, oldest known living thing: Natl. Geog. Mag., v. 113, p. 355–372.

BAUXITIZATION OF TERRA ROSSA IN THE SOUTHERN APPALACHIAN REGION

By MAXWELL M. KNECHTEL, Washington, D.C.

Abstract.—The bauxite of many deposits in the southern Appalachian region is envisaged as a product of leaching in sink holes, wherein silica is removed from aluminiferous matter present in fill (terra rossa) consisting of argillaceous, chert-bearing residual material. The terra rossa has resulted from earlier leaching of soluble corbonates from rocks of Paleozoic age.

The bauxite of many deposits in the southern Appalachian region consists primarily of gibbsite ($Al_2O_3 \cdot 3H_2O$) mixed in varying proportions with kaolinite ($Al_2O_3 \cdot 2SiO_2 \cdot 2H_2O$). Also generally present are finely divided ferruginous matter, grains of heavy minerals, and rarely a little quartz. The high alumina content presumably represents concentration by geochemical processes whereby silicates of alumina, such as feldspar, mica, and various clay minerals, have lost all or part of their silica content. Opinion has been divided, however, as to whether the parent aluminiferous materials were constituents of bedrock cropping out close to the bauxite deposits, in accordance with a view favored in this article, or were transported from distant outcrops, as suggested by Bridge (1950, p. 195–196).

The deposits occur in association with formations of Paleozoic age composed largely of chert-bearing carbonate rock interstratified with variable amounts of shaly and sandy material. Near most if not all of the bauxite deposits, however, leaching of the bedrock in the process of weathering has removed virtually all the readily soluble minerals, chiefly carbonates, as well as appreciable amounts of silica and other relatively insoluble constituents. The undissolved residue, mostly of a type called terra rossa, consists largely of chert-bearing red, yellow, or brown argillaceous material. Such material commonly forms an extensive blanket and locally underlies the surface to a depth of several hundred feet. Occurrence of bauxite deposits in close association with terra rossa elsewhere in the world has been described by Zans (1952, 1959a,b). The proportion of soluble to relatively insoluble constituents of the underlying unleached rock differs from place to place and from stratum to stratum; therefore the ratio of the volume of terra rossa to the volume of the rock through which the insoluble constituent particles were once disseminated must vary within wide limits. This ratio would be infinitesimal if the particles were derived from rock of a stratum composed almost exclusively of carbonates, but it would approach unity for rock composed of silicates that would break down, with only slight change in composition, to clay consisting chiefly of hydrous mica particles. A ratio somewhere between these extremes would result from loss of silica and of such components as calcium and potassium in the alteration of feldspathic or micaceous materials to pure kaolinite. Because of the probable wide variations in this ratio, and in such factors as porosity and water content, there is little basis for even a rough estimate of the compaction that has occurred in development of the terra rossa of given localities. Concurrence in this conclusion is implied by White and Denson (1952, p. 8) concerning the compaction of residual deposits in the northwest Georgia bauxite district.

Inasmuch as the terra rossa has not been removed by erosion during the great length of time presumably required for its development, it is reasonable to suppose that throughout most of its history any thick blanket of such noncohesive material has been overlain by a protective cover of more durable material, such as a sheet of gravel or cherty debris, in the manner described by Hack (1960a, fig. 179.2; 1960b, p. 88–89, fig. 1). During progressive decomposition of the underlying bedrock, any such protective cover presumably would settle gradually to lower altitudes.

The characteristic shape of bauxite deposits in the Appalachian region is that of subconical bodies tapering downward, and it is generally agreed that these represent sink-hole fillings (Adams, 1923; Bridge, 1950, p. 193). As such, they may be related in origin to ancient karst surfaces comparable to the pediment existing today at and near the bauxite-bearing kaolin deposit exposed in the Cold Spring clay pit in Augusta County, Va., at the southeast margin of the Ridge and Valley province (Knechtel, 1943, p. 165). The view that this deposit originated in the manner here suggested is favored by its proximity to numerous sink holes, many of which are marked by subcircular ponds. The karst terrain is underlain by dolomite, limestone, shale, slate, and sandstone belonging to formations of early Paleozoic age, whereas the adjacent mountainous terrain to the southeast is underlain by still older formations composed predominantly of quartzite and indurated shale. Beyond the crest of the Blue Ridge and in the Piedmont province are extensive outcrops of crystalline rocks. Beneath the sink-hole-studded plain, unleached dolomite rests on quartzite and is overlain by a blanket of terra rossa consisting of argillaceous to sandy residual material. In places this blanket is known to be several hundred feet thick and nearly everywhere it underlies a protective cover of coarse gravel.

In the finely divided (<2 microns) fractions of two specimens of highly argillaceous terra rossa, one from the Kennedy manganese mine, 6 miles east of the Cold Spring clay pit, and another from the Vesuvius manganese mine, 3½ miles southwest of the pit, the kaolinite content is estimated by J. C. Hathaway (written communication, 1958) to be 50 percent and 30 percent, respectively; the mica content of each is 30 percent. Hathaway estimates, further, that feldspar makes up approximately 40 percent of a finely divided (<2 microns) fraction, and approximately 60 percent of a coarser (2–62 microns) fraction, of a shale specimen from undecomposed strata of the Waynesboro Formation (Lower Cambrian) near Lyndhurst, Va., about 11 miles east of the Cold Spring pit; the estimated mica content of these two fractions is 20 percent and 10 percent, respectively. An even larger percentage of feldspar was estimated for a specimen of light-yellow sandstone of the Waynesboro Formation exposed in the city of Waynesboro, Va., about 15 miles northeast of the pit.

It seems reasonable, therefore, to infer that the clay-mineral content of the terra rossa represents alteration in situ of feldspathic and other aluminiferous mineral matter derived from the local sequence of sedimentary rocks of Paleozoic age. Furthermore, the kaolin and bauxite in the Cold Spring pit appear to represent a still more advanced stage of alteration, involving removal of a large part of the silica from the terra rossa. No necessity is therefore seen for postulating, as did Bridge (1950, p. 193, fig. 7), that the kaolin and bauxite were derived from crystalline-rock debris transported to the pit site from outcrops of igneous and metamorphic rocks in the Blue Ridge or Piedmont provinces. It is difficult to imagine a sequence of events in the evolution of the present local drainage pattern whereby appreciable quantities of debris could have been stream transported to this site from even the nearest such outcrops across intervening terrain which today is mountainous. The fragments making up the extensive deposits of gravel that rest on the terra rossa were evidently transported here from the direction of the Blue Ridge. They consist exclusively, however, of material derived from the formations of Cambrian age, chiefly quartzite, that crops out in the area between the crystalline rocks and the pit. There is no direct evidence that either the gravel or the terra rossa were derived from the crystalline rocks whose nearest outcrops today are near the crest of the Blue Ridge, 3¾ miles south-southeast of the pit.

These considerations are the basis for a hypothetical geologic history of bauxite deposits enclosed in terra rossa at imaginary sites A, B, C, and D (fig. 99.1). The bauxite deposits at these sites are conceived to be closely similar in form, mineral content, and physical environment to the J. F. Smith ore body in the Chattanooga district, Tennessee. The associated geologic phenomena and the sequence of events involved in the origin of this body are thought to apply to other deposits in the region, including the one at the Cold Spring pit in Augusta County, Va. Details of the J. F. Smith deposit are from unpublished data of J. C. Dunlap, of the U.S. Geological Survey. The two grades of bauxite shown in figure 99.1 (phases 3 and 4) are based on differences in content of alumina and silica. Grade B bauxite contains 50 to 55 percent alumina and less than 15 percent silica, and grade C contains 45 to 50 percent alumina and less than 30 percent silica.

The body of bauxite at site A has roughly the shape of an upward-flaring funnel. It encloses a subconical, downward-tapering body of material, chiefly cherty clay and sand, which is similar in composition to the terra rossa that surrounds the bauxite body. The surrounding material and the enclosed material were derived from weathering of bedrock that has been decomposing near the site during much of post-Paleozoic time. The weathered material forms part of an extensive blanket of terra rossa that rests on undecomposed bedrock and is overlain by a protective cover of gravel.

At site A the bauxite deposit is thus enclosed by protectively covered terra rossa. In the vicinity of sites B and C, the protective cover and much of the terra rossa have been stripped away, as have also the upper parts of bauxite bodies similar to the body at site A. The materials so removed have been transported downslope, as indicated by bauxite float strewn over the surface to the right of site B (fig. 99.1). Near site D, all the terra rossa has been removed and carbonate-bearing bedrock is exposed.

If it is assumed that the terra rossa removed by erosion from site D enclosed a body of bauxite similar to the body at site A, then the history of such a bauxite deposit can be illustrated by 5 phases, shown in figure 99.1, that correspond to the 5 levels numbered in downward sequence in the profile.

Phase 1.—Carbonate rock, envisaged as present in the space above site D (fig. 99.1), is overlain by a gravel-protected blanket of terra rossa more than 100 feet thick that represents a large volume of bedrock that already has been compacted by leaching during lowering of the surface from altitudes higher than level 1. A depression in the level-1 surface above site C represents an ancient sink comparable to that today marked by the pond between sites A and B. The bauxite exposed at site C owes its origin to phenomena related to this ancient sink.

Phase 2a.—Owing to further leaching of carbonate rock at site D, the terra rossa has increased slightly in thickness and the gravel has dropped to level 2a. A large cavern with downward-tapering walls has formed in the subsurface and is partly filled with debris composed largely of clay.

Phase 2b.—The roof of the cavern has collapsed, and part of the overlying terra rossa has subsided into the cavern. The gravel forms the bottom of a resulting subcircular depression or sink, presumably occupied by a pond or swamp. The carbonate-bearing rock around the walls and under the floor of the former cavern is thus in contact at this phase with a downward-tapering body of predominantly argillaceous materials. The materials in contact with the carbonate-bearing rock are permeated by water saturated with carbon dioxide that is derived in part from decay of vegetal matter in the pond. Through a process comparable to that suggested by Carroll and Starkey (1959), the materials begin to undergo intensive leaching of their silica and iron. This process of bauxitization continues so long as the contiguous carbonate-bearing rock remains intact, preserving the geochemical environment described by Carroll and Starkey as favoring the extraction of silica, but the process ceases whenever leaching has converted all of this rock to terra rossa containing little or no carbonate.

Phase 3.—All the adjacent carbonate rock has decayed and, as a result of both compaction and erosion, the land surface has been lowered still further, to level 3. Bauxitization has ceased and the partly bauxitized body of fill is surrounded by chert-bearing terra rossa. A funnel-shaped mass of bauxite separates the surrounding material from a central subconical mass of similar material that escaped bauxitization. An increase in iron content, indicated by the dotted line within the ore body (fig. 99.1), appears to have resulted from outward migration of the iron. The migration may result from the reaction of the iron oxide with organic matter that reduced the iron from the ferric to the more soluble ferrous state. The iron would thereupon move outward, possibly in the form of chelates or other organic complexes, and would precipitate in the highly ferruginous outer part of the bauxite deposit. The reduction of the ferric iron would generate the CO_2 that is required by the Carroll-Starkey hypothesis for bauxitization in the presence of carbonate rock. The concept is consistent with the marked tendency of the inner limit of the highly ferruginous material of the ore body to coincide with the outer limit of the grade-C bauxite (fig. 99.1, phase 3). As the ore body contains no fragments of chert, any silica that may once have been present in that form may be assumed to have been dissolved and carried away along with the silica that was leached from the other constituents of the parent terra rossa.

In the interval since phase 2b, compaction of the surrounding material due to loss of a large volume of soluble matter in the bedrock has greatly exceeded any reduction in the volume of the cavern fill due to removal of silica. The material within the sink hole has accordingly tended to subside more slowly than the surrounding terra rossa. Some of the terra rossa directly above the ore body has consequently tended to remain higher than that surrounding the ore and has been removed by erosion. The ore body itself has so far remained intact. In the level-3 surface above site B is a depression representing a newly formed sink wherein will develop the bauxite deposit today exposed at this site.

Phase 4.—The surface above site D has subsided from level 3 to level 4, owing to continued leaching and compaction of bedrock, as well as to a small amount of erosion that has occurred since phase 3. Reworked gravel, introduced from adjacent areas, temporarily serves as a protective cover.

Phase 5.—The gravel-capped terra rossa and bauxite have been completely removed by erosion from site D, and carbonate rock is exposed.
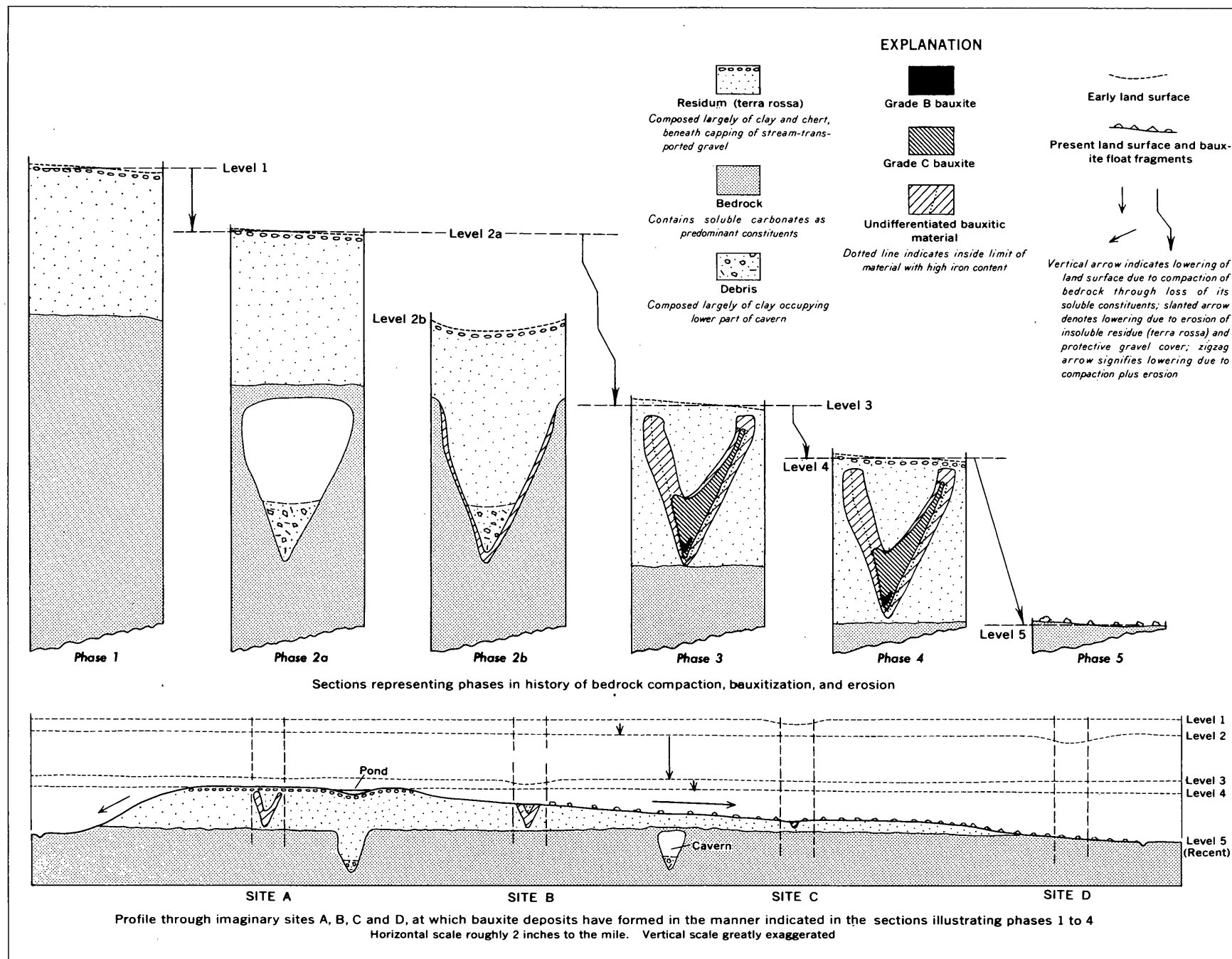
EXPLANATION

Residum (terra rossa)

Composed largely of clay and chert, beneath capping of stream-trans-ported gravel

Bedrock

Contains soluble carbonates as predominant constituents

Debris

Composed largely of clay occupying lower part of cavern

Grade B bauxite

Grade C bauxite

Undifferentiated bauxitic material

Dotted line indicates inside limit of material with high iron content

Early land surface

Present land surface and baux-ite float fragments

Vertical arrow indicates lowering of land surface due to compaction of bedrock through loss of its soluble constituents; slanted arrow denotes lowering due to erosion of insoluble residue (terra rossa) and protective gravel cover; zigzag arrow signifies lowering due to compaction plus erosion

Level 1

Level 2a

Level 2b

Level 3

Level 4

Level 5

Phase 1   Phase 2a   Phase 2b   Phase 3   Phase 4   Phase 5

Sections representing phases in history of bedrock compaction, bauxitization, and erosion

Level 1
Level 2
Level 3
Level 4
Level 5 (Recent)

Pond

Cavern

SITE A   SITE B   SITE C   SITE D

Profile through imaginary sites A, B, C and D, at which bauxite deposits have formed in the manner indicated in the sections illustrating phases 1 to 4
Horizontal scale roughly 2 inches to the mile. Vertical scale greatly exaggerated

FIGURE 99.1.—Profile and sections illustrating a hypothetical sequence of events in the geologic history of bauxite deposits in the southern Appalachian region.

At site A the protective gravel cover is still preserved above a blanket of terra rossa containing a bauxite deposit that has descended in its entirety from a higher altitude; the upper parts of comparable bauxite deposits at sites B and C have been carried away by erosion and are represented by float fragments on the surface downslope from these sites (fig. 99.1). A pond between sites A and B marks the location of a recently formed sink comparable to that which was present at level 2, site D, during phase 2b. In this sink, bauxitization of terra rossa may already be in phase 2b. The roof of a cavern between sites B and C is about to collapse, and it is possible that the bauxitization process will be repeated here again in the sink that is expected to form in the near future.

The hypothesis that has been described implies that: (1) the existing widely scattered bauxite deposits of the Appalachian region are of many different ages, (2) countless bauxite deposits similar to these have formed and disappeared in this region since the close of the Paleozoic Era, and (3) the requisite conditions for current and future evolution of bauxite deposits probably exist in sink holes within parts of the region today underlain by thick accumulations of terra rossa.

REFERENCES

Adams, G. I., 1923, The formation of bauxite in sink holes: Econ. Geology, v. 18, p. 410–412.

Bridge, Josiah, 1950, Bauxite deposits of the southeastern United States, in Snyder, F. G., ed., Symposium 'on mineral resources of the southeastern United States: Knoxville, Tenn., Univ. Tennessee Press, p. 170–201.

Carroll, Dorothy, and Starkey, H. C., 1959, Leaching of clay minerals in a limestone environment: Geochim. et Cosmochim. Acta, v. 16, p. 83–87.

Hack, J. T., 1960a, Relation of solution features to chemical character of water in the Shenandoah Valley, Virginia: Art. 179 in U.S. Geol. Survey Prof. Paper 400-B, p. B387–B390.

—— 1960b, Interpretation of erosional topography in humid, temperate regions: Am. Jour. Sci., v. 258-A, p. 80–97.

Knechtel, M. M., 1943, Manganese deposits of the Lyndhurst-Vesuvius district, Augusta and Rockbridge Counties, Virginia: U.S. Geol. Survey Bull. 940-F, p. 163–198.

White, W. S., and Denson, N. M., 1952, The bauxite deposits of Floyd, Bartow and Polk Counties, northwest Georgia: U.S. Geol. Survey Circ. 193, 27 p.

Zans, V. A., 1952, Bauxite resources of Jamaica and their development: Colonial Geology and Mineral Resources, v. 3, no. 4, p. 307–333.

—— 1959a, Recent views on the origin of bauxite: "Geonotes," Quarterly Newsletter, Geologists' Assoc. London, Jamaica Group, Geol. Survey Dept., Kingston, Jamaica, p. 123–132.

—— 1959b, Review of "Bauxites, their mineralogy and genesis," Moscow, 1958: Econ. Geology, v. 54, p. 957–965.

Article 100

AN ORE-BEARING CYLINDRICAL COLLAPSE STRUCTURE
IN THE AMBROSIA LAKE URANIUM DISTRICT, NEW MEXICO

By H. C. GRANGER and E. S. SANTOS, Denver, Colo.

Abstract.—A cylindrical collapse structure in sandstone of the Morrison Formation near Ambrosia Lake, N. Mex., has provided a structural control on a primary uranium ore body in a district in which most other deposits of the same age are controlled predominantly by sedimentary features.

The Doris No. 1 ore body is a small sandstone-type uranium deposit that is controlled by a cylindrical collapse structure. It is unique because all other primary uranium deposits of the standstone type in the Ambrosia Lake district seem to be stratigraphically controlled.[1]

The mine is in McKinley County, N. Mex., near the center of sec. 21, T. 13 N., R. 9 W.; the collar of the shaft is about 400 feet northwest of New Mexico State Highway 53, a mile southwest of its junction with New Mexico State Highway 509 (fig. 100.1).

The Doris No. 1 (Little Doris) mine was opened originally by Westvaco Corp. but was later acquired by Phillips Petroleum Corp. and mined under lease by KSN Co., Inc. Permission to map and sample the mine was granted by R. C. Kirchman of the KSN Co., but, because of reportedly high radon content in the air and dangerous rock conditions, we were not permitted to enter the western parts of the mine. For inaccessible parts of the mine we used maps and data supplied by E. D. McLaughlin, Jr., who was the first to recognize the unusual structural control of the ore body.

The mine is in a reentrant along a generally northwest-trending escarpment capped by the Dakota Sandstone (Granger and others, 1961). Near the collar of the shaft the ground surface slopes smoothly toward Arroyo del Puerto and San Mateo Creek, which occupy a fault-line valley cut through the escarpment along the

San Mateo fault (fig. 100.1). West of the mine the surface is hummocky and rises to merge with the cliff of Dakota Sandstone.

The mine is entered by a 30° inclined shaft about 170 feet long that is collared in mudstones of the Brushy Basin Member of the Morrison Formation. The workings at the foot of the shaft are in sandstone and consist of rooms that generally conform to the shape of the circular structure (fig. 100.2).

In the Ambrosia Lake area, the Morrison Formation of Late Jurassic age is divided in ascending order into the Recapture, Westwater Canyon, and Brushy Basin Members. The Doris No. 1 deposit is in the Poison Canyon Sandstone of Zitting and others (1957) of the Westwater Canyon Member. This is a local sandstone unit at the top of and generally separated from the main body of the Westwater Canyon by a few feet of typical Brushy Basin mudstone.

Most large uranium deposits in the Ambrosia Lake district are a few miles north of the Doris deposit in an area where the Poison Canyon Sandstone is not readily distinguished from the main body of the Westwater Canyon member. Several relatively small ore bodies in the Poison Canyon, however, constitute an arcuate mineralized belt (Granger and others, 1961) about 7 miles long and as much as a mile wide (fig. 100.1). The Doris No. 1 deposit is near the middle of this belt in an area where the Poison Canyon is about 40 to 50 feet thick.

Drilling from the surface showed that the ore body is largely within a part of the Poison Canyon Sandstone that is lower, structurally, than the surrounding strata. The circular pattern of the structure was identified by mapping the several arcuate segments of the bounding fault which are exposed in the mine workings (fig. 100.2). Strata within the structure are virtually unbroken and only locally warped. Some cross beds are

---

[1] Since this article was written, Clark and Havenstrite (1963) have reported on two circular collapse structures of pre-Dakota age in the Cliffside mine, about 4½ miles northeast of the Doris No. 1 mine. One of these is within an ore zone and is ore bearing; the other is just north of this zone and is reportedly barren.

nearly vertical in zones in which the bedding is contorted. No evidence of the structure can be seen at the surface outcrop over the mine, and no data are available to indicate to what depth the structure may extend.

Displacement along the east side of the structure is about 30 feet, and there is an additional few feet of sag in the central part of the collapsed cylinder. The displacement is probably less on the west side of the structure, but data here are meager.

An authigenic carbonaceous gangue material (Granger and others, 1961), which forms films on sand grains and locally fills interstices in the sandstone, is coextensive with the ore. This material causes the ore to be generally gray to black and readily distinguishes it from the lighter hued waste rock.

The ore is very spotty and occurs as several scattered thin layers and pods at various stratigraphic and structural positions. Most of the ore is inside the collapsed cylinder and largely conforms to stratigraphic features. Some ore, however, was mined from undisturbed rocks as much as 25 feet northwest of the bounding fault. Layers, or veins, of ore that are parallel to and occur within the circular fault zone are sporadic but common. This ore apparently was not dragged into position by the faulting but was emplaced after faulting and was controlled by the fault.

Oxidation has affected much of the deposit but did not completely destroy the primary ore layers. Secondary uranium minerals are sparsely disseminated within the ore, and barren sandstone near the ore contains iron oxide minerals. Secondary iron and manganese minerals are also present locally within the circular fault zone. This deposit may have contained less pyrite than is usually associated with other ore deposits in the district because oxidation has produced only a pale buff color in the rock in contrast to reddish brown and yellow seen in oxidized zones in other parts of the Ambrosia Lake district.

Attempts to identify the primary uranium mineral in the carbonaceous material have not been successful. X-ray powder patterns of the carbonaceous material show only a few diffuse unidentifiable lines, other than quartz lines; probably the uranium is now present largely as UO_3 because of the pervasive oxidation that has affected the deposit. Similar organic material from unoxidized deposits throughout the district almost invariably contains enough coffinite to produce a clearly identifiable pattern.

Uranopilite and a zippeite-like mineral (Frondel, 1958, p. 146) occur together with sparse gypsum about 15 feet north of the foot of the shaft (fig. 100.2) where they form an efflorescent coating on the exposed surface

EXPLANATION

▨   ⊢   ⚒
Vertical or inclined shaft   ' Adit   · Open pit
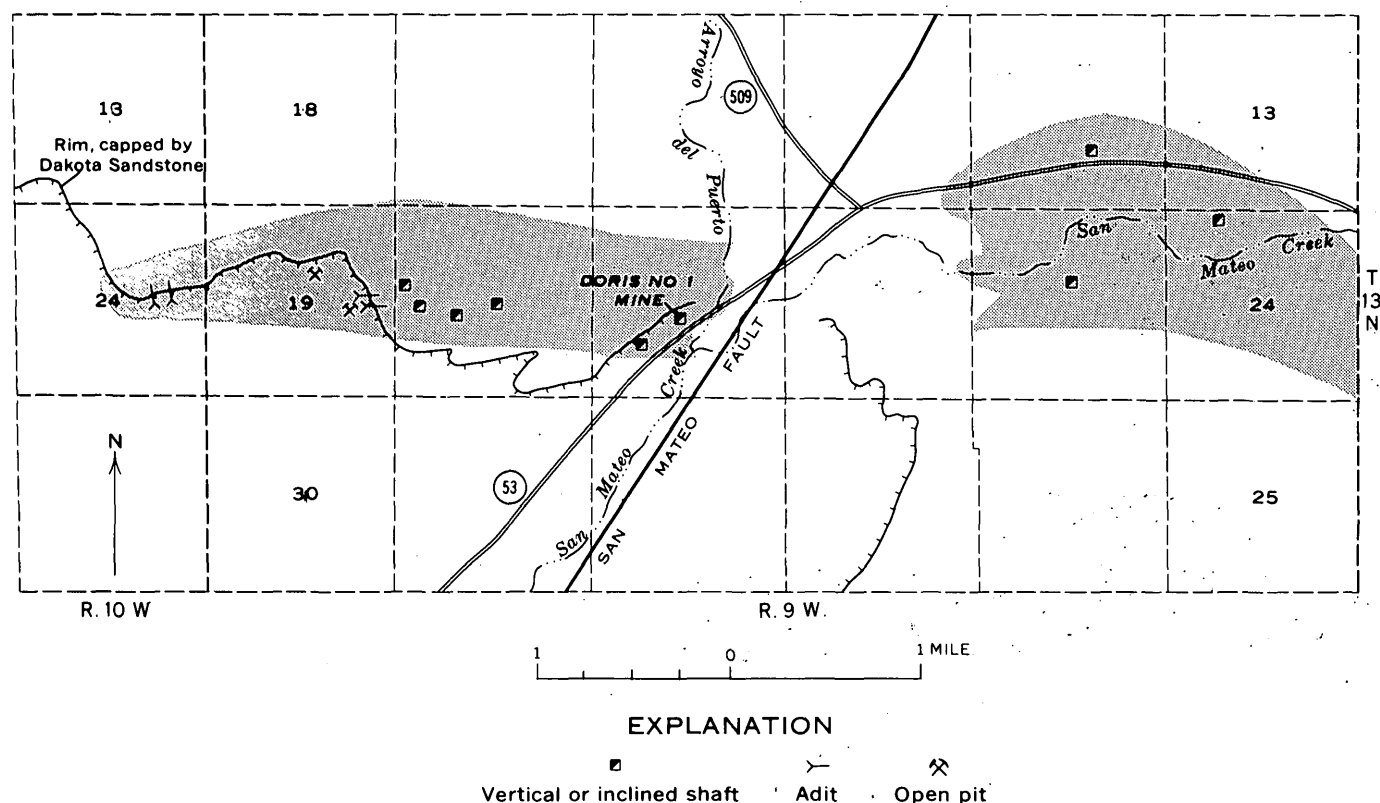
FIGURE 100.1.—Map showing location of Doris No. 1 mine within the belt (shaded) of primary deposits in the Poison Canyon Sandstone of Zitting and others (1957).

EXPLANATION

Contorted sandstone
Showing direction of dip

Inclined workings
Chevrons point downslope

Raise

Sandstone

Mudstone or
conglomerate layer

Carbonaceous ore

MAP
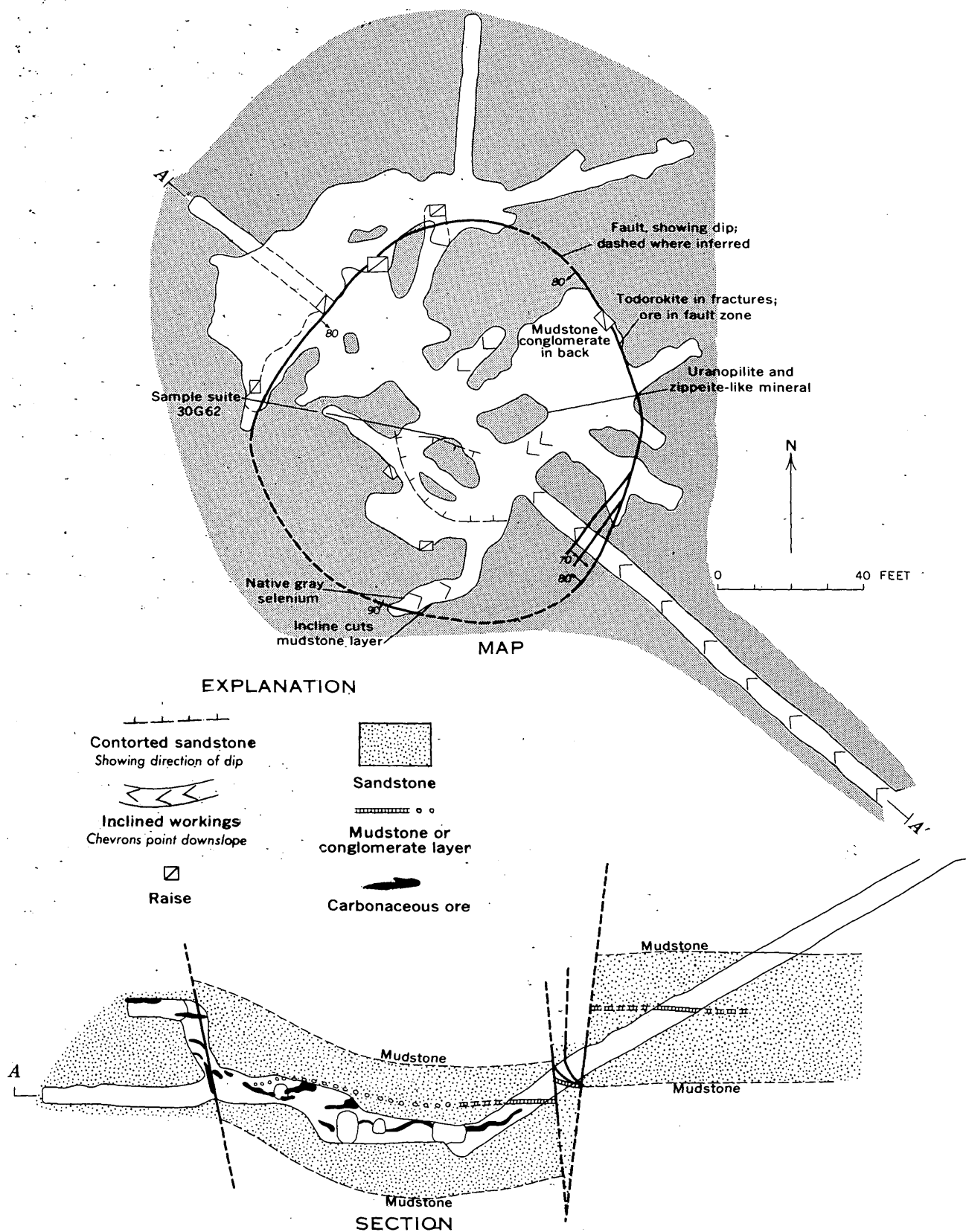
SECTION

FIGURE 100.2.—Map and section of the Doris No. 1 mine.

of a black ore layer. The uranopilite is bright yellow and has a moderately strong greenish-yellow fluorescence. It forms small aggregates with a finely felted texture made up of short disoriented bladed or needle-like crystals. The zippeite-like mineral forms minute rounded aggregates of powdery yellow crystals. The same mineral has been noted in several mines throughout the district but it generally forms minute "pincushions" of radiating needlelike crystals. Sparse coatings of the same or, perhaps, other yellow efflorescent uranium minerals also occur elsewhere on the mine walls.

Minute scattered flakes of greenish-yellow to green nonfluorescent uranium(?) minerals occur in the partly oxidized black ore layers, but no attempt has been made to identify them.

Limonitic iron oxides and partly oxidized pyrite are disseminated throughout both the mineralized and barren sandstone. Where it has been protected from oxidation by the abundant organic gangue in the ore, pyrite occurs as minute cubes and irregularly shaped masses less than 1 mm across. Calcite is scarce and may have been largely removed by acid solutions created by the oxidizing pyrite.

Elsewhere in the district, native gray selenium is common at the interfaces between oxidized and unoxidized rock. In the Doris No. 1 mine, however, the rocks are pervasively oxidized, and the only selenium noted was in fractures in mudstone above the ore and in thin gray streaks less than 2 inches long in partly oxidized sandstone adjacent to black ore layers. Tiny selenium needles are disseminated in the interstices throughout the gray streaks.

Kaolinite "nests" (Granger, 1962) are distributed throughout the host rock, forming aggregates as much as several millimeters across. They are most abundant in the coarser grained barren sandstones and are either sparse or extremely small in the finer grained sandstones and ore layers.

Walls of open fractures in the cylindrical fault zone north of the foot of the shaft (fig. 100.2) are locally coated with dull velvety-black todorokite, $2(Mn,Ca)0.5MnO_2 \cdot 4H_2O$. It forms tiny radiating crystalline pisolitic aggregates less than 0.2 mm in diameter which have grown, one upon the other, to form microbotryoidal textures and minute knobby columns. The individual crystals are fibrous platelets which are dark brown in transmitted light under a microscope. This is the only occurrence of todorokite yet known in the Ambrosia Lake area and is one of few localities known in the United States.

The results of analyses of a suite of samples (No. 30G62) that were taken across an ore layer in the central part of the mine are shown graphically in figure 100.3. The content of organic carbon, lead, molybdenum, vanadium, and selenium correlate, to some extent, with the uranium concentration. Pervasive weak oxidation of the host rock may have resulted in some redistribution of these elements, but it is believed that the effect has been minor. A sample of ore from the cylindrical fault north of the shaft has a composition similar to the samples within the ore layer described. The character and thickness of the rock sampled in suite 30G62 are given below.

Description of sample in suit 30G26

[Letters refer to zones shown in figure 100.3]

Thickness (inches)

a. Medium-grained barren sandstone 20 to 16 inches above ore layer; yellowish gray with scattered kaolinite nests 1.0 to 1.5 mm across. Limonite occurs as disseminated specks, clay stain, and thin films on quartz grains. Quartz overgrowths are sparsely present on sand grains and form minute triangular crystal faces. Calcite is extremely sparse_____ 4

b. Fine-grained moderately well sorted barren sandstone 16 to 4 inches above ore layer; ranges from very pale orange to grayish orange with small white kaolinite nests. Pyrite is mostly oxidized, leaving specks and films of limonite. Sand grains commonly coated with a film of white clay. A few thin lenticular streaks containing needles of gray selenium were noted_____ 12

c. Fine-grained barren sandstone 4 to 0 inches above ore layer; yellowish gray with local pale reddish-brown hematitic specks and stain. Kaolinite may be present but doesn't form nests. A loose claylike material fills many intertices. Minute disseminated flakes of a greenish-yellow uranium mineral are present__ 4

d. Fine-grained to very fine grained dark-gray ore in upper 2 inches of ore layer; well cemented by carbonaceous material. Pyrite is sparse and largely oxidized to limonitic stain. Kaolinite aggregates are present but very small_____ 2

e. Middle 2 inches of ore layer identical with 30G62d__ 2

f. Very fine grained grayish-black ore in lower 2 inches of ore layer. Carbonaceous material fills nearly all interstices. All interstices not completely filled by carbonaceous material are filled with kaolinite. A few scattered flakes of an unidentified greenish nonfluorescent uranium(?) mineral are present____ 2

g. Fine-grained barren sandstone 0 to 4 inches below the ore layer; yellowish gray with local moderate yellowish-brown limonite specks and stain. Sand grains all coated with a thin film of white clay____ 4

h. Fine-grained barren sandstone 4 to 16 inches below the ore layer; yellowish gray with local grayish-orange limonite stain. Some clay disseminated throughout the rock but doesn't form either nests or coatings on the sand grains_____ 12

i. Fine- to medium-grained barren sandstone 16 to 20 inches below the ore layer; yellowish gray with local grayish-orange limonite stain and specks that resemble corroded pseudomorphs. A few small scattered kaolinite nests are present, and each sand grain is coated with a film of white clay_____ 4

CLASSIFICATION OF THE DEPOSIT

Unoxidized uranium ore of two types is recognized in the Ambrosia Lake district: a prefault type, considered to be primary, and a postfault type, believed to be redistributed (Granger and others, 1961). The prefault ore is stratigraphically controlled and invariably associated with an abundant gangue of authigenic carbonaceous material; it generally contains concentrations of lead, molybdenum, and vanadium. In contrast, postfault ore is partly structurally controlled and ordinarily contains much less, if any, carbonaceous material, lead, and molybdenum but more vanadium than the prefault ore. The faults that separate these deposits in time formed long after the Morrison was deposited and displace the primary ore, the Dakota Sandstone, and at least the lower part of the overlying Mancos Shale.

Chemically, the ore in the Doris No. 1 deposit (fig. 100.3) is similar to the ores in prefault deposits elsewhere in the district and contrasts with the postfault ores. The organic carbon, lead, and molybdenum content is typical of prefault ore and much higher than in most postfault ore. Although the vanadium content is greater than in most prefault ore, it is not abnormally high for prefault ores in the Poison Canyon Sandstone, and the uranium-vanadium ratio in the ore layer is higher than in much of the postfault ore in the district.
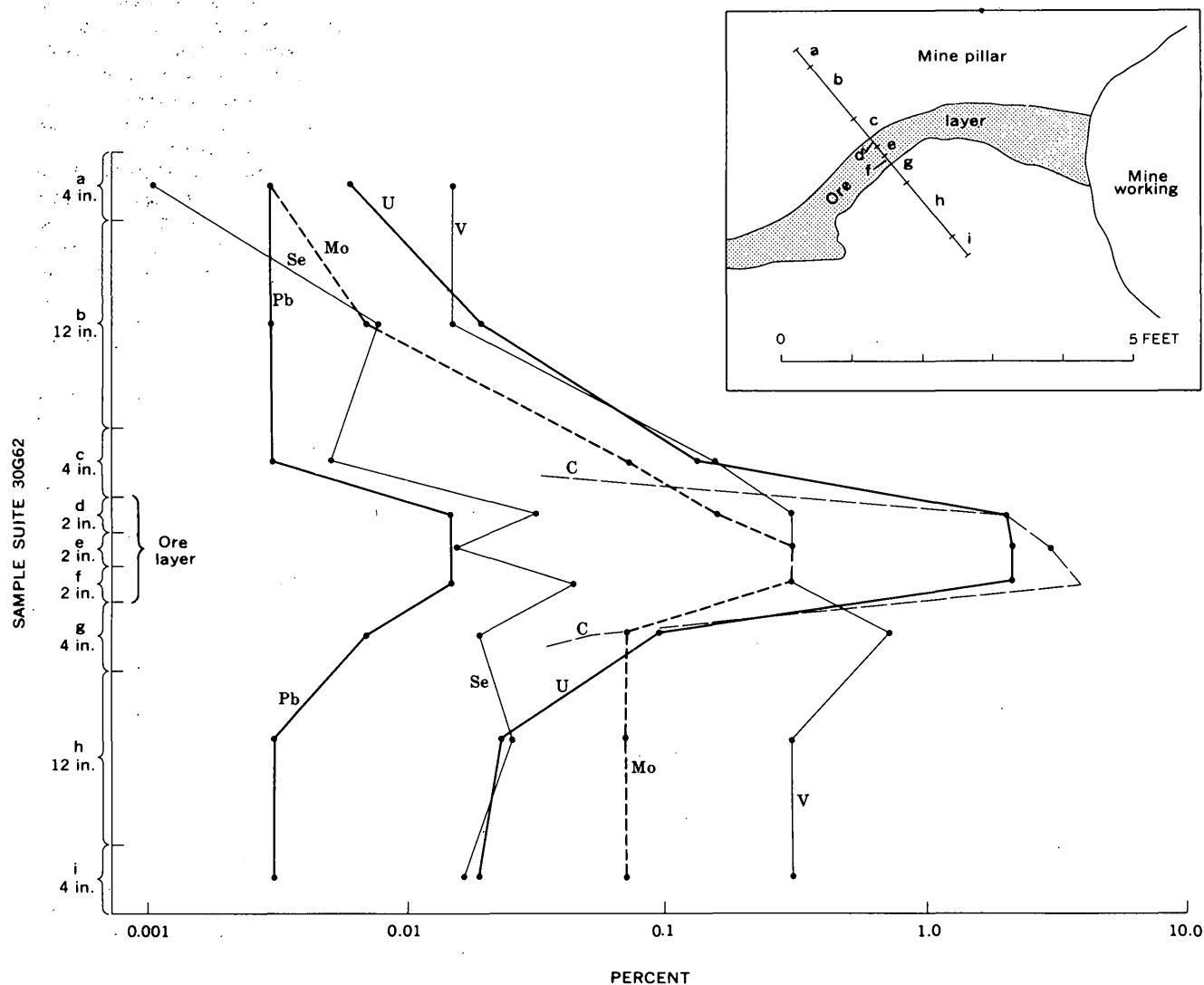
FIGURE 100.3.—Graph showing distribution of selected elements in sample suite 30G62 across an ore layer in the Doris No. 1 deposit. Pb, Mo, and V determined by semiquantitative spectrographic methods by J. C. Hamilton, U determined volumetrically by H. H. Lipp or fluorometrically by E. J. Fennelly. Organic C determined by induction furnace, gasometric difference by L. C. Frost. Se determined volumetrically by G. T. Burrow. Samples in suit 30G26 are described in text.

In the nearby Laguna district are hundreds of collapse structures, locally called sandstone pipes (Schlee, 1959; Hilpert and Moench, 1960). These pipes are known to cut only rocks of Jurassic age extending from the Summerville to the Morrison Formations. The bottoms, where exposed, are in sharp contact with little-deformed underlying strata; the tops generally sag and contain detritus from the uppermost units of rocks that contain them. Schlee (1959) considers the pipes to have been caused by gravitational foundering of sand into mud and locally by collapse resulting from the removal of underlying gypsum. The pipes commonly are concentrated along Jurassic folds of low amplitude, and they seem to be contemporaneous with Jurassic sedimentation. Two of the sandstone pipes are known to contain uranium ore: one at the Woodrow mine, and the other at the Jackpile mine (Hilpert and Moench, 1960, p. 441).

We believe that the collapse structure in the Doris No. 1 mine is genetically similar to the sandstone pipes in the Laguna area and that it was formed before the Dakota Sandstone was deposited. The collapse, therefore, is probably not related in any way to the major faults, which are post-Dakota in age and which separate, in time, the prefault and postfault ore deposits. Even though it is partly structurally controlled, the Doris No. 1 ore body was evidently deposited before the major period of faulting in the region. The ore is so similar in appearance and chemical composition to proved prefault ore, that it is probably temporally and genetically related to the other prefault deposits in the Ambrosia Lake district. The fact that the deposit is, in part, controlled by a structure necessitates a minor revision in the premise that the prefault ore bodies are entirely stratigraphically controlled.

CONCLUSIONS

It may be significant that, of the hundreds of sandstone pipes in the Laguna district, only the two which are near or in the large stratigraphically controlled sandstone-type ore deposits are known to be mineralized and thus seem to have had control on mineralization. Similarly, the Doris No. 1 deposit is one of a group of deposits which are generally stratigraphically controlled.

Although collapse structures in some places may have been conduits through which mineralizing solutions from deep-seated sources gained access to sedimentary rocks, the shallow depths to which they extend in the Ambrosia Lake and Laguna districts rules them out as pathways between a juvenile source and the ore deposits. It seems more likely that they have acted only as localizing features, in much the same way as bedding planes and disconformities, for solutions largely moving laterally through the rocks. We believe that any preexisting structure, whether sedimentary or tectonic, along the general trend of mineralization can serve as a control for sandstone-type uranium deposits.

REFERENCES

Clark, D. S., and Havenstrite, S. R., 1963, Geology and ore deposits of the Cliffside mine, Ambrosia Lake area, in Society of Economic Geologists, V. C. Kelley, chm., Uranium field conference, Geology and technology of the Grants [New Mexico] uranium region: New Mexico Bur. Mines and Mineral Resources Mem. 15, p. 108–116.

Frondel, Clifford, 1958, Systematic mineralogy of uranium and thorium: U.S. Geol. Survey Bull. 1064 [1959].

Granger, H. C., 1962, Clays in the Morrison Formation and their spatial relation to the uranium deposits at Ambrosia Lake, New Mexico: Art. 124 in U.S. Geol. Survey Prof. Paper 450–D, p. D15–D20.

Granger, H. C., Santos, E. S., Deane, B. G., and Moore, F. B., 1961, Sandstone-type uranium deposits at Ambrosia Lake, New Mexico—an interim report: Econ. Geology, v. 56, p. 1179–1210.

Hilpert, L. S., and Moench, R. H., 1960, Uranium deposits of the southern part of the San Juan Basin, New Mexico: Econ. Geology, v. 55, p. 429–464.

Schlee, J. S., 1959 Sandstone pipes of the Laguna area, New Mexico [abs.]: Geol. Soc. America Bull., v. 70, no. 12, pt. 2, p. 1669.

Zitting, R. T., Masters, J A, Groth, F. A., and Webb, M. D., 1957, Geology of the Ambrosia Lake area uranium deposits, McKinley County, New Mexico: The Mines Magazine, v. 47, no. 3, p. 53–58.

Article 101

FORMATION OF RIDGES THROUGH DIFFERENTIAL SUBSIDENCE OF PEATLANDS OF THE SACRAMENTO–SAN JOAQUIN DELTA, CALIFORNIA

By GEORGE H. DAVIS, Washington, D.C.

Abstract.—Comparison of topographic maps of 1906–08 with maps of 1952 in the peatlands of the Sacramento-San Joaquin Delta shows that local relief of more than 15 feet has developed on formerly level terrain. Relative subsidence of peat soil through surface wastage is the cause; soils of high mineral content marking old channels and dunes stand out as ridges.

Comparison of topographic mapping of 1906–08 with mapping of 1952 in the peatlands of the Sacramento-San Joaquin Delta shows that ridges having a relief of more than 15 feet (three 5-foot contour intervals) have developed on land that was nearly level in 1906–08.

The delta is an area of about a quarter of a million acres of islands and interlacing tidal channels near the confluence of the Sacramento and San Joaquin Rivers in north-central California (fig. 101.1). Under natural conditions the surface of the islands stands about at mean sea level and is inundated at high tide. Prior to reclamation the entire area was covered with a dense growth of tule (*Scirpus lacustris*). Virtually all of the delta was reclaimed from tule swamp during the period 1850–1920 by enclosing the islands with levees and draining the swamps.

The soils of the delta are predominantly peat, which in some places extends as deep as 60 feet below sea level. Around the margins of the delta, the peat soils grade into mineral soils. The mineral content of the soils within the delta is generally highest along the rims of the islands and on the sites of abandoned channels and sloughs. Wier (1950) described subsidence of peatlands in the delta and concluded that the loss of altitude was due principally to wastage of the peat through (1) oxidation by exposure to the air, (2) burning of the peat soils to destroy weeds and plant pests, and (3)
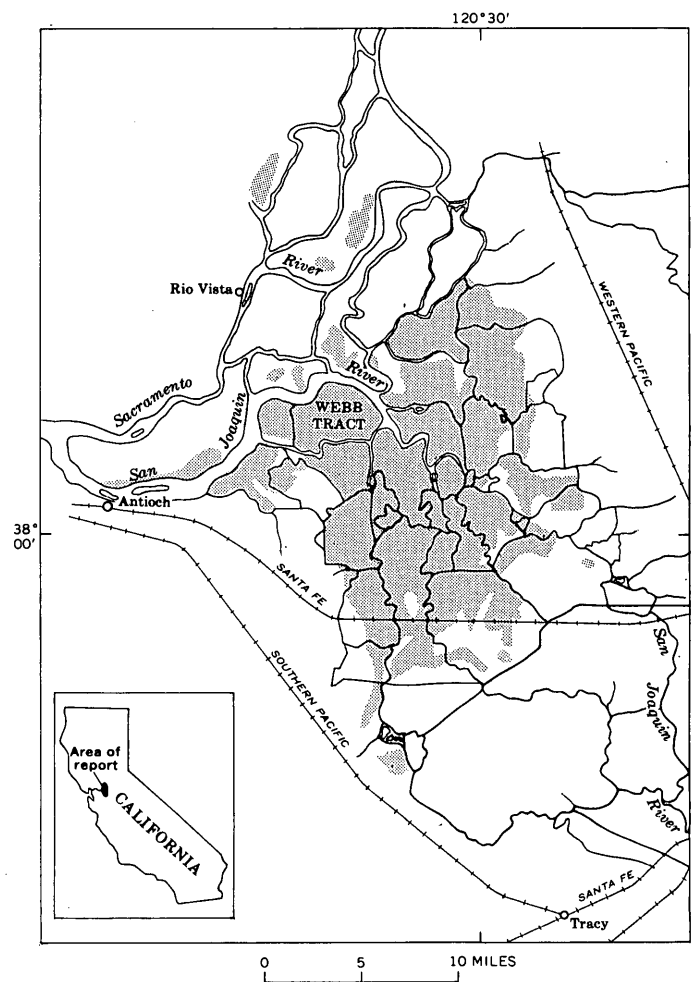
FIGURE 101.1.—Location map showing surface extent of peat (shaded) in the Sacramento–San Joaquin Delta (generalized after Cosby, 1941).

wind erosion of the loose peat. Wier (1950, p. 55) reported that the subsidence had been as much as 10 feet up to 1950 and was continuing at a rate of about 3 inches per year. Minor subsidence due to other causes may also be occurring in the delta area. For example, tectonic movement, and compaction at depth due to production of natural gas from the Rio Vista gas field, which underlies much of the delta, are likely causes. However, leveling now available is insufficient to confirm or rule out these possibilities. Releveling by the U.S. Coast and Geodetic Survey programmed for 1963 may resolve this question.

The soils of the delta islands not classified as peat (fig. 101.1) are for the most part classified as muck and organic soils (Cosby, 1941, map); the distinction is based on the content of rock material, peat consisting almost entirely of organic matter. The organic soils also are subject to surface wastage but to a lesser extent than peat. As the subsidence is due to surface wastage of organic material, the extent and amount of subsidence are closely related to the organic content of the surface soils.

Remapping of the Jersey Island 7½-minute quadrangle by the U.S. Geological Survey in 1952 at a scale of 1:24,000 offers an instructive example of the development of ridges of inorganic soils by wastage of the surrounding peat soils, as first noted by Wier (1950, p. 47). The quadrangle (formerly named the Jersey quadrangle) was first mapped in 1906–08 at a scale of 1:31,680 by the plane-table method. The remapping of the topography in the flat-lying islands was also done by the plane-table method, although the culture and drainage were compiled from aerial photographs. The same contour interval (5 feet) was used on both maps. The contours on both maps are of about the same order of accuracy and precision (C. V. Eckhardt, U.S. Geological Survey, Topographic Division, oral communication, Oct. 22, 1962); therefore, only a minor part of the differences in topography shown is believed to be due to differences in mapping. An area including Bradford Island and the western part of the Webb Tract, along the San Joaquin River in northeastern Contra Costa County, is shown as mapped in 1906–08 (fig. 101.2) and in 1952 (fig. 101.3). Both maps are reproduced here at a common scale for comparison.

The change in topography is especially obvious in the Webb Tract, which in 1906–08 stood between sea level and +5 feet (fig. 101.2); only 3 small rises, indicated by arrows, exceeded 5 feet in altitude. By 1952, the 3 small rises were the high points on a sinuous ridge that had a relief of as much as 15 feet and extended westward across the part of the Webb Tract shown on the map (fig. 101.3). Note, however, that the high points are at virtually the same altitude on both maps; the

rest of the area has subsided. Most of the island, which stood at 0 to +5 feet altitude in 1906–08 is now 10 feet or more below mean sea level. Comparable subsidence has taken place on Bradford Island and in other parts of the delta. Most of the islands have become saucer shaped, sloping away from the rimming levees, toward their centers. Although due partly to reinforcement of the levees, the saucer shape of the islands is due largely to the fact that peaty materials beneath the levees are protected from oxidation by the dredged inorganic channel deposits that are used in levee construction.

The soils map of Contra Costa County (Carpenter and Cosby, 1939) shows the ridges as formed chiefly of Piper fine sandy loam; the highest knob on the western edge of Bradford Island is shown as Oakley sand. The rest of the islands are shown almost entirely as "peat." On aerial photographs the ridges appear light colored, probably because of their sandy character and good drainage. The Piper fine sandy loam is described as having a dark-gray or dark-brownish-gray, calcareous organic surface layer over a less organic subsoil. The lower part of the subsoil layer consists of compact partly consolidated sandy material containing little organic matter. The Oakley is described as a brown or light-brown loose sand that drifts badly in high winds. Both Piper and Oakley soils are interpreted by Carpenter and Cosby (1939) as being channel deposits or dune sand.

The relation of topography and soils indicates that in the peatlands of the delta the ridges develop where the surface is formed by inorganic soils, which are not subject to wastage as are the surrounding peat and organic soils. The elongate sinuous shape of the ridge in the Webb Tract suggests that it probably represents an ancient stream channel. The isolated sandy knobs on Bradford Island, especially the highest (+20 feet in 1952), may well be dunes. The local relief can be expected to increase as the exposed peat soils in the low parts of the islands waste away. Peat that underlies the sandy soil of the ridges at some depth would be protected from oxidation and erosion by the sandy surface material. Because surface subsidence of the mineral soils of the ridges is negligible, these areas are the most favorable sites for bench marks, buildings, or other structures such as electric-power facilities that require stable foundations.

REFERENCES

Carpenter, E. J., and Cosby, S. W., 1939, Soil Survey; Contra Costa County, California: U.S. Dept. Agriculture, Ser. 1933, no. 26, 83 p., map.

Cosby, S. W., 1941, Soil survey; the Sacramento–San Joaquin Delta area, California: U.S. Dept. Agriculture, Ser. 1935, no. 21, 48 p., map.

Wier, W. W., 1950, Subsidence of the peat lands of the Sacramento–San Joaquin Delta, California: Hilgardia, v. 20, no. 3.

FIGURE 101.2.—Part of Jersey 7½-minute quadrangle showing topography as mapped in 1906–08. Contour interval, 5 feet. Parts of Bradford Island and the Webb Tract below −5 feet altitude shown by shading; above +5 feet by diagonal pattern and number.

121°40'

RIVER

SAN JOAQUIN

BRADFORD ISLAND

FISHERMANS CUT

WEBB TRACT

FALSE RIVER

FERRY

38° 05'

SEA-LEVEL

Cable Area

Beacon

BM 8

Gas Wells

Gas Well

Gas Well

Windmill

Windmill

Beacon

Windmill

Gas Well

BM 9

BM 10

Beacon

Pump

Santa Clara Shoal

Oulton Point

Windmill

Beacon

BM 8

BM 6

Beacon

SACRAMENTO CO

CONTRA COSTA CO

Fishermans Slough

Gas Well

Gas Well

Pump House

BM 13

Tide Gage

Beacon

BM 15

Beacon

PIPE

BM 14

MUD

ISLAND

BM 9

Poles

Sarpentia Slough

Slough

Short Slough

LEVEE

Pump

BM 12

BM 8

+5

+5

+5

+5

+5

FIGURE 101.3.—Part of Jersey 7½-minute quadrangle showing topography as mapped in 1952. Contour interval, 5 feet. Parts of Bradford Island and the Webb Tract below −5 feet altitude shown by shading; above +5 feet by diagnoal pattern and number.

1   ½   0   1 MILE

Article 102

CHEMICAL PREPARATION OF SAMPLES FOR LEAD ISOTOPE ANALYSIS

By JOHN C. ANTWEILER, Denver, Colo.

Abstract.—High-purity samples for lead isotope analysis are prepared by decomposing the lead minerals with hot dilute nitric acid, followed by four precipitations of lead nitrate with strong nitric acid. The lead nitrate obtained can be readily converted to the iodide, sulfide, or other compounds for isotopic analysis.

The wide application of lead isotope data to geologic problems has been discussed by Cannon and others (1961) with special emphasis on problems of ore genesis. Some of these problems can be solved with imperfect data, but others require extremely precise and accurate data. Isotope geologists can obtain far better data now than they could just a few years ago because mass spectrometrists are constantly improving the precision of mass measurements. However, advancements in mass spectrometry that contribute to more precise and accurate data may be offset if chemical purification of samples for isotope analysis is omitted. By carefully controlling sample purity and total pressure, Richards (1962) obtained with a mass spectrometer of 6-inch radius of curvature, results comparable to those obtained by others with a 12-inch instrument.

Treatment of lead ores before lead isotope analysis has varied from no treatment, as shown by Ehrenberg (1953) and Zykov and Stupnikova (1957) who made isotope analyses directly on lead ores, to the thorough and exhaustive purification by Harvard chemists of the samples analyzed by Nier (1938). Galena, the principal ore of lead, like most minerals is not a chemically pure compound. The summary of spectrographic analyses of 75 galena samples in table 102.1 shows that galena may contain half a dozen or more metal impurities in the concentration range of 100 to 10,000 parts per million. Most of these samples contain appreciable amounts of iron, silicon, bismuth, antimony, copper, silver, and zinc. Some contain significant amounts of tin, cadmium, molybdenum, or other metals such as arsenic, manganese, and cobalt.

TABLE 102.1.—*Summary of spectrographic analyses of 75 galena samples, showing number and percentage of samples having contaminating elements at four levels of concentration*

[Analyses by R. G. Havens, P. R. Barnett, N. M. Conklin, J. Haffty, C. Annell, H. W. Worthing]

Element	Level of concentration							
	1 percent or more		0.1 percent or more		0.01 percent or more		0.001 percent or more	
	Number of samples	Percentage of total	Number of samples	Percentage of total	Number of samples	Percentage of total	Number of samples	Percentage of total
Fe	12	16.0	36	48.0	62	82.7	75	100
Si	11	14.7	32	42.7	71	94.7	75	100
Bi	9	12.0	24	32.0	35	46.7	36	48.0
Zn	8	10.7	31	41.3	47	62.7	(1)	0
Sb	5	6.7	22	29.3	44	58.7	(1)	0
Cu	4	5.3	23	30.7	52	69.3	61	81.3
As	4	5.3	11	14.7	(1)	0	(1)	0
Ag	2	2.7	33	44.0	55	73.3	62	82.7
Ca	2	2.7	22	29.3	55	73.3	56	74.7
Ba	1	1.3	6	8.0	10	13.3	41	54.7
Mg	0	0	15	20.0	36	47.8	60	80.0
Al	0	0	14	18.7	45	60.0	70	93.3
Cd	0	0	3	4.0	23	30.7	(1)	0
Te	0	0	2	2.7	(1)	0	(1)	0
Ni	0	0	2	2.7	7	9.3	(1)	0
U [2]	0	0	2	2.7	3	4.0	5	6.7
Na	0	0	2	2.7	3	4.0	(1)	0
Sn	0	0	1	1.3	8	10.7	24	32.0
V	0	0	1	1.3	5	6.7	(1)	0
Mn	0	0	0	0	22	29.3	45	60.0
Co	0	0	0	0	8	10.7	(1)	0
Sr	0	0	0	0	7	9.3	25	33.3
Mo	0	0	0	0	5	6.7	12	16.0
Ti	0	0	0	0	4	5.3	20	26.7
B	0	0	0	0	3	4.0	4	5.3
Cr	0	0	0	0	2	2.7	6	8.0
La	0	0	0	0	2	2.7	(1)	0
Tl	0	0	0	0	1	1.3	(1)	0
Zr	0	0	0	0	1	1.3	3	4.0
Y	0	0	0	0	0	0	9	12.0
Sc	0	0	0	0	0	0	7	9.3
Au	0	0	0	0	0	0	4	5.3
In	0	0	0	0	0	0	2	2.7
Nb	0	0	0	0	0	0	1	1.3
K	0	0	(1)	0	(1)	0	(1)	0

[1] Below detection limit by method used.
[2] Chemical determination.

A method for preparing high-purity ore-lead samples for isotopic analysis was desired that would be simpler and shorter than the sulfate separation method (Scott, 1939) used by the U.S. Geological Survey for several years. The sulfate method is generally satisfactory when 10 milligrams or more of Pb is available, but it is time consuming and requires the use of a number of

ART. 102 *IN* U.S. GEOL. SURVEY PROF. PAPER 475-C, PAGES C166–C170. 1963.

C166

lead-free reagents. Most of the other lead-separation methods are useful in certain circumstances, but they have one or more of the following disadvantages: they are lengthy, require the use of a number of lead-free reagents, fail to achieve complete separation from other elements, are limited by interferences, or result in a compound not amenable to isotopic analysis.

The method described below overcomes most of these disadvantages. It is simple and comparatively fast, requires only two lead-free reagents (water and nitric acid), separates lead from most other elements (barium and strontium excepted), is not limited by the elements commonly found in galena, and results in a compound (the nitrate) that is readily converted to the sulfide, the iodide, or to other compounds for mass analysis. The procedure is based on the fact that lead is selectively precipitated with strong HNO_3. This selectivity was used by Baxter and Grover (1915) to purify lead for atomic-weight determination, by Schrenck and Delano (1931) to purify lead for electrodeposition studies, by Neumann and Perlman (1950) to separate radioactive bismuth from lead, and by the Oak Ridge National Laboratory (W. C. Davis, written communication, 1961) to remove all spectrographically detectable impurities from separated lead isotopes.

EXPERIMENTAL WORK

The first experiments showed that all spectrographically detectable impurities were removed by repeated precipitations of lead nitrate with concentrated (sp gr 1.42) HNO_3. The procedure was satisfactory except that lead loss was significant. Although quantitative recovery is not essential for samples prepared for isotopic analysis, small samples could be lost before being purified to the desired degree. A study was made, therefore, of the solubility of lead nitrate in various concentrations of nitric acid at room temperature and at 0°C. This was done as follows: a saturated solution of lead nitrate in nitric acid was prepared by adding to 100 ml of HNO_3 an excess of finely ground $Pb(NO_3)_2$; the mixture was warmed and stirred, allowed to reach the desired temperature, and filtered. Lead in the filtrate was determined colorimetrically by the dithizone method, or gravimetrically as the sulfate or chromate. Figure 102.1 and table 102.2 show the rapid decrease in lead solubility as nitric acid concentration is increased and temperature is decreased; less than 1 microgram of Pb dissolves in 1 ml of 100-percent HNO_3 at 0°C. It will be noted that the solubility of lead nitrate in fuming HNO_3 is greater than in 100-percent HNO_3; this is attributed to the action of nitrous acid and nitrogen oxides present in fuming HNO_3

As one would expect, several nitric acid precipita-
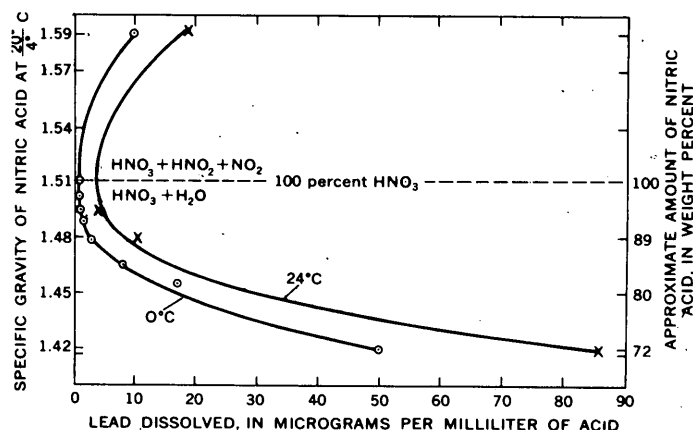
FIGURE 102.1.—Solubility of lead as a function of nitric acid concentration at 24°C. and 0°C.

TABLE 102.2.—Solubility of lead in nitric acid of various concentrations at 24°C and 0°C

Approximate HNO_3 (weight percent)	Specific gravity of HNO_3 at $\frac{20°}{4°}$ C	Solubility of Pb (micrograms per milliliter)	
		24°C	0°C
67	1.40	230	-----
72	1.42	85	50
81	1.454	-----	17
84	1.465	-----	8
88	1.478	10	2. 9
93	1.489	-----	1. 4
95	1.494	4	1. 0
98	1.503	-----	. 9
100	1.510	-----	. 9
Fuming	1.59	18	10

tions are required to remove all impurities from lead nitrate, because any precipitate may occlude small amounts of other elements in the solution. To determine the number of precipitations required, the National Bureau of Standards lead isotope reference sample (NBS–200, galena from Ivigtut, Greenland) was decomposed with nitric acid. The lead nitrate obtained was precipitated with 100-percent HNO_3, and the precipitate was collected on a filter disk, sampled, and redissolved. This procedure was repeated until a total of five precipitations had been made. Samples taken after the first, fourth, and fifth precipitations were analyzed spectrographically. The analyses, given in table 102.3, show considerable purification after just one nitric acid precipitation. Only calcium was detectable after the fourth precipitation, and it was removed by one more precipitation. The purity obtained by 4 precipitations is thought to be adequate for isotopic analysis, and therefore the recommended procedure for most ore-lead samples consists of sample decomposition with dilute HNO_3 followed by 4 consecutive precipitations with 100-percent HNO_3.

TABLE 102.3.—*Semiquantitative spectrographic analyses, in percent, of the National Bureau of Standards lead isotope reference sample (NBS–200) and of lead compounds prepared from it*

[Only elements found are shown. The "less than" (<) values were generally reported as "looked for but not found," but estimated visual detection limits have been substituted to show amounts that might be present but escape detection. Silicon was not specifically looked for. Analyses in PbI_2 column by Nancy Conklin; all others by R. G. Havens]

Element	Raw galena	PbI_2 from 1 HNO_3 precipitation	$Pb(NO_3)_2$ from 4 HNO_3 precipitations	$Pb(NO_3)_2$ from 5 HNO_3 precipitations
Al	0.015	<0.001	0.003	<0.001
Fe	.15	.0007	<.0007	<.0007
Mg	.00015	.00015	<.00015	<.00015
Ca	.0007	.0005	.0007	<.0007
Mn	.0015	<.0002	<.0002	<.0002
Ag	.7	.015	<.0001	<.0001
Bi	1.5	.01	<.001	<.001
Cu	.07	<.0001	<.0001	<.0001
Sb	.03	<.01	<.01	<.01
Sn	.015	<.001	<.001	<.001

Reagents.—To prevent the possibility of isotopic contamination, only lead-free reagents were used. Water was prepared by double distilling demineralized distilled water in an all-quartz still. "Concentrated" HNO_3 (sp gr 1.42) was prepared by distilling analytical reagent-grade HNO_3 under reduced pressure. Dilute HNO_3 (1:1 v/v) was prepared by diluting a volume of concentrated HNO_3 (sp gr 1.42) with an equal volume of water. Very strong HNO_3 (100 percent, sp gr 1.50–1.51) was prepared by carefully distilling equal volumes of analytical reagent-grade HNO_3 and H_2SO_4 at 0.01-mm Hg pressure in a still equipped with a Vigreaux fractionating column. (Rapid distillation results in carryover of some sulfate ion, which would form insoluble lead sulfate.) Very strong HNO_3 should be handled only in a well-ventilated hood, and only with protective gloves.

Procedure.—Dissolve about 0.1 g galena or other lead mineral by heating with 30 ml 1:1 (v/v) HNO_3 until decomposition is complete. If samples are small, decrease quantity of reagents accordingly. Filter and wash residue 5 times with hot 1:1 HNO_3. Collect filtrates and washings in a vycor or quartz dish and evaporate to incipient crystallization of lead nitrate. Precipitate lead nitrate by adding 15 ml of 100-percent HNO_3 (sp gr 1.50), warm, and stir to maximize solution of impurities. Chill to 0°C, and decant through a fine-porosity fritted disk. Wash precipitate with two 5-ml portions of cold HNO_3 (sp gr 1.50); discard filtrate and washings. Dissolve lead nitrate in dish and on filter with 1:1 HNO_3. Evaporate solution to incipient crystallization of lead nitrate, and precipitate lead nitrate as before. Repeat filtration, solution, and precipitation at least twice more. Dissolve lead nitrate from fourth precipitation with water, and evaporate solution to dryness. Dry purified lead nitrate crystals for 2 hours at 100°C.

Note: Some sulfuric acid is obtained by decomposing galena with nitric acid. When the lead nitrate solution is evaporated, some lead may be precipitated as lead sulfate; repeated precipitation and solution as described usually eliminates the sulfate interference by the end of the second or third precipitation.

Results.—The procedure was used to purify a large number of galena samples from Colorado for isotopic analysis. The following five of these samples were used to evaluate the procedure:

1. Specimen Co–P–Bl–1. Galena from the Boomer mine, Lake George district, Park County, Colo. Collected by W. N. Sharp and C. C. Hawley, 1959.

2. Specimen Co–L–Hg. Galena from the Homestake mine, Lake County, Colo. Collected by Ogden Tweto, 1951.

3. Specimen Co–J–Og. Galena from the Augusta lode near Evergreen, Jefferson County, Colo. Collected by R. S. Cannon, Jr., and J. C. Antweiler, 1961.

4. Specimen Co–Ch–Tg. Galena from Turret district, Chaffee County, Colo. Given to J. C. Antweiler by George Corley, Corley Mining Co., 1961.

5. Specimen Co–Ko–Vgc. Galena from Victory mine, Kokomo district, Summit County, Colo. Collected by S. C. Creasey, 1949.

Evaluation should be based upon a comparison of isotopic analyses and the chemical purity of samples prepared by this and by other methods. The isotopic analyses have not yet been made, but spectrographic analyses of the five samples are given in table 102.4. Methods of preparation used were (1) the sulfate method (Scott, 1939), (2) galena-to-lead-iodide method (Cuttita and Warr, 1960), (3) method of this article with just 1 nitric acid precipitation, and (4) method of this article with 4 nitric acid precipitations. All samples were converted to lead iodide for uniformity. The nitrate method is superior to the others in terms of product purity. Even one nitric acid precipitation results in a product with fewer impurities than is obtained by the lengthy sulfate procedure. Four nitric acid precipitations reduced all impurities to less than 0.1 percent (in the extreme example); impurities in the samples from Turret and Kokomo were reduced to a few parts per million. Comparatively little purification was obtained by use of the galena-to-lead-iodide procedure. Similarly, one would expect little purification by the use of other sample-preparation procedures, such as acid decomposition of galena followed directly by reconstitution of lead sulfide, that do not selectively isolate lead from impurities inherent in the sample.

Discussion.—The alkaline earth metals are the most serious interferences in the nitrate method. Strontium and barium, like lead, are quantitatively precipitated by strong HNO_3, and precipitates of these metals carry calcium (Meinke, 1955). The effect of the alkaline earth metals on lead isotope analysis is no better known

than the effect of other impurities. Although it might seem desirable to make certain that samples submitted for isotopic analysis are free of these metals, it is doubtful in most cases whether such effort is justified. Less than 10 percent of the samples summarized in table 102.1 contained 0.01 percent or more Sr, and less than 15 percent contained 0.01 percent or more Ba. Furthermore, strontium or barium, even though present in the purified nitrate, would be greatly reduced by subsequent conversion to either the sulfide or iodide for isotopic analysis.

TABLE 102.4.—*Semiquantitative spectrographic analyses, in percent, of galena samples and of lead iodide prepared from them by different methods*

[Analyst: Nancy Conklin. The "less than" (<) values were generally reported as "looked for but not found," but estimated visual detection limits have been substituted to show amounts that might be present but escape detection]

1. Galena sample Co-P-Bi-1

	Raw galena	PbI₂ from H₂SO₄ [1]	PbI₂ from HI [2]	PbI₂ from 1 HNO₃ precipitation	PbI₂ from 4 HNO₃ precipitations
Si	0. 03	(³)	0. 007	0. 007	<0. 0015
Fe	. 03	<0. 001	. 02	. 03	<. 001
Mg	. 0002	<. 001	<. 00015	. 002	. 005
Ca	. 0007	. 001	. 0005	. 0015	. 05
Ag	. 5	. 01	. 07	. 02	. 003
Bi	. 7	. 003	. 015	. 007	<. 001
Cu	. 3	. 0005	. 007	. 01	. 0005
Nb	. 003	<. 001	<. 001	<. 001	<. 001
Sb	. 05	<. 01	<. 01	<. 01	<. 01
Sn	. 007	<. 001	<. 001	<. 001	<. 001
Y	. 002	<. 001	<. 001	<. 001	<. 001
Yb	<. 0003	<. 0003	<. 0003	<. 0003	<. 0003
Zn	. 03	<. 02	<. 02	<. 02	<. 02

2. Galena sample Co-L-Hg

	Raw galena	PbI₂ from H₂SO₄	PbI₂ from HI	PbI₂ from 1 HNO₃	PbI₂ from 4 HNO₃
Si	0. 07	(³)	0. 015	0. 003	0. 03
Fe	2.	0. 1	. 007	. 002	<. 001
Mg	. 3	. 01	. 002	. 0007	. 0007
Ca	. 015	. 007	. 0015	<. 0005	. 0007
Mn	. 05	. 0015	<. 0002	<. 0002	<. 0002
Ag	. 07	. 001	. 02	. 0015	. 007
Bi	. 02	<. 001	. 002	. 003	<. 001
Cu	. 15	. 01	. 007	<. 0001	. 0003
Sb	. 02	<. 01	<. 01	<. 01	<. 01
Zn	. 07	<. 02	<. 02	<. 02	<. 02

TABLE 102.4.—*Semiquantitative spectrographic analyses, in percent, of galena samples and of lead iodide prepared from them by different methods*—Continued

[Analyst: Nancy Conklin. The "less than" (<) values were generally reported as "looked for but not found," but estimated visual detection limits have been substituted to show amounts that might be present but escape detection]

3. Galena sample Co-J-Og

	Raw galena	PbI₂ from H₂SO₄ [1]	PbI₂ from HI [2]	PbI₂ from .1 HNO₃ precipitation	PbI₂ from 4 HNO₃ precipitations
Si	0. 07	0. 07	0. 007	0. 003	0. 003
Fe	. 05	. 05	<. 001	. 002	. 015
Ca	. 015	. 0015	<. 0005	<. 0005	<. 0005
Ag	. 02	. 001	. 007	. 0015	<. 0001
Bi	. 02	<. 001	. 0015	. 003	<. 001
Cu	. 7	. 0005	. 02	<. 0001	. 0005
Mo	. 003	<. 0005	. 0015	<. 0005	<. 0005

4. Galena sample Co-Ch-Tg

	Raw galena	PbI₂ from H₂SO₄	PbI₂ from HI	PbI₂ from .1 HNO₃	PbI₂ from 4 HNO₃
Si	0. 03	0. 3	0. 03	<0. 001	<0. 001
Al	. 007	<. 001	. 007	<. 001	<. 001
Fe	. 001	. 003	. 005	. 0007	<. 0007
Mg	. 002	. 0005	. 0015	. 00015	. 00015
Ca	. 002	. 0007	. 0005	<. 0005	<. 0005
Mn	. 01	<. 0002	. 005	<. 0002	<. 0002
Ag	. 05	. 001	. 03	. 005	<. 0001
Bi	. 01	<. 001	. 003	<. 001	<. 001.
Cd	. 015	<. 005	. 01	<. 005	<. 005
Cu	. 3	<. 0001	. 15	<. 0001	<. 0001
In	. 002	<. 001	. 003	<. 001	<. 001
Ni	. 0007	<. 0003	<. 0003	<. 0003	<. 0003
Sb	. 03	<. 01	<. 01	<. 01	<. 01
Zn	. 7	<. 02	1.	<. 02	<. 02

5. Galena sample Co-Ko-Vgc

	Raw galena	PbI₂ from H₂SO₄	PbI₂ from HI	PbI₂ from .1 HNO₃	PbI₂ from 4 HNO₃
Si	0. 007	0. 007	0. 07	<0. 001	<0. 001
Fe	. 005	<. 001	<. 001	<. 001	<. 001
Mg	. 0005	. 00015	. 00015	<. 00015	<. 00015
Ca	. 00015	<. 0005	<. 0005	. 0005	. 0005
Mn	. 0005	<. 0002	<. 0002	<. 0002	<. 0002
Ag	. 1	. 003	. 03	. 015	<. 0001
Bi	. 005	<. 001	. 001	. 0015	<. 001
Cd	. 005	<. 005	<. 005	<. 005	<. 005
Cu	. 0015	. 00015	. 001	. 003	<. 0001
Sb	<. 07	<. 01	. 03	<. 01	<. 01
Sn	. 005	<. 001	. 003	<. 001	<. 001

¹ PbSO₄ transformed to PbI₂; PbSO₄ prepared for gravimetric Pb determination as described by Scott (1939).
² Method described by Cuttita and Warr (1960).
³ Not specifically looked for.

REFERENCES

Baxter, G. P., and Grover, F. L., 1915, A revision of the atomic weight of lead. The analysis of lead bromide and chloride: Am. Chem. Soc. Jour., v. 37, p. 1027–1061.

Cannon, R. S., Jr., Pierce, A. P., Antweiler, J. C., and Buck, K. L., 1961, The data of lead isotope geology related to problems of ore genesis: Econ. Geology, v. 56, p. 1–38.

Cuttita, Frank, and Warr, J. J., 1960, Preparation of lead iodide for mass spectrometry: Art. 221 in U.S. Geol. Survey Prof. Paper 400–B, p. B487–B488.

Ehrenberg, H. Fr., 1953, Isotopenanalysen an Blei aus Mineralen: Zeitschr. Physik, v. 134, p. 317–333.

Meinke, W. W., 1955, Nuclear chemical research and radiochemical separations, progress report 4, Nov. 1954–Oct. 1955, Project No. 7, Contract No. AT(11–1)70: Michigan Univ. 81 p.; Atomic Energy Comm. U–3116.

Neumann, N. M., and Perlman, I., 1950, Isotopic assignments of bismuth isotopes produced with high energy particles: Phys. Rev., v. 78, p. 192.

Nier, A. O., 1938, Variations in the relative abundances of the isotopes of common lead from various sources: Am. Chem. Soc. Jour., v. 60, p. 1571–1576.

Richards, J. R., 1962, Interpretation of lead isotope abundances: Nature, v. 195, p. 590–591.

Schrenck, W. T., and Delano, P. H., 1931, Electrolytic determination of lead as lead dioxide: Indus. Eng. Chemistry, Anal. Ed., v. 3, p. 27.

Scott, W. W., (N. H. Furman, ed.), 1939, Standard methods of chemical analysis, 5th ed., v. 1, The elements: New York, D. Van Nostrand Co., Inc., p. 504–505.

Zykov, S. I., and Stupnikova, N. I., 1957, Izotopny analiz svintsa bez predvaritel'noy khimicheckoy podrotovki minerala [Isotopic lead analysis without preliminary chemical preparation of the mineral]: Geokhimiya, 1957, no. 5, p. 430–434. [See also Geochemistry, a translation of Geokhimiya, 1957, no. 5, p. 506–510.]

PERCENT-CONSTITUENT PRINTING ACCESSORY
AND FLOW-THROUGH CELL FOR A SPECTROPHOTOMETER

By LEONARD SHAPIRO and EDWARD L. CURTIS, Washington, D.C.

Abstract.—An accessory has been designed which converts an ordinary spectrophotometer to one which uses the color density of a solution to automatically calculate and print on tape the concentration of the constituent in the solution. No computations are required, and the results are obtained more rapidly and are more dependable than by conventional methods. A newly designed simple flow-through cell provides greater convenience and speed of operation.

An accessory has been designed to convert an ordinary spectrophotometer to one which automatically calculates and prints on tape the percent constituent of a solution. The accessory, which can be built with commercially available components, is designed for use with a Model B Beckman spectrophotometer.

An additional convenience in operating the accessory-equipped spectrophotometer is a newly designed flow-through cell for holding the solution to be tested. The cell, which is made of Lucite and glass, is relatively inexpensive and easy to make in the average machine shop.

PRINTING ACCESSORY

General description

The sensitivity of the spectrophotometer is varied so that the reading on the spectrophotometer meter is always 100-percent transmission. This is done by rotating a logarithmically wound potentiometer automatically with a small servomotor. The angular rotation required to vary the sensitivity to maintain 100-percent transmission is directly proportional to the change in concentration from one solution to another. A gear on the shaft of the logarithmic potentiometer drives a linear potentiometer which serves as a read-out device. An external voltage is applied across the ends of the read-out potentiometer, and the voltage between one end and the movable contact is measured and printed with a digital-voltmeter–printer. Any change in this measured voltage is directly proportional to the change in angular rotation, which in turn is directly proportional to the difference in concentration of the different solutions. The external voltage is adjusted so that the voltage being read out for a known standard solution is numerically equal to the known concentration expressed as percent constituent. All subsequent readings are then printed automatically in terms of percent constituent.

Components

The components for the printing accessory are shown in the semischematic diagram of figure 103.1. All components except the digital voltmeter and printer can be placed into the instrument box which serves as a support for the spectrophotometer (fig. 103.1).

The ON–OFF toggle switch below the spectrophotometer turns on the line and battery power. The AUTO–MANUAL toggle switch is a 4-pole double-throw type which in the MANUAL position causes the spectrophotometer to operate in the normal manner. When the switch is thrown to the AUTO position a logarithmically wound potentiometer is switched into the sensitivity circuit of the spectrophotometer, and the pre-existing set of resistors which normally controls the sensitivity in three steps is switched out. The same switch also turns on the servomotor, which drives the potentiometer and introduces a 3-volt battery and resistor across pins 11 and 13 at the back of the spectrophotometer.

Normally, when the meter needle indicates 100-percent transmission, the voltage at pins 11 and 13 of the Model B Beckman spectrophotometer is 3 volts. This voltage varies in the same direction as the percent transmission. When the accessory is switched in, the 3-volt battery and resistor are placed across these pins, as

ART. 103 *IN* U.S. GEOL. SURVEY PROF. PAPER 475-C, PAGES C171–C174. 1963.

694–027 O—63——12

C171

shown in figure 103.1. A current flows through the resistor when the voltage is other than 3 volts at pins 11 and 13. The input leads of a servoamplifier are connected across the resistor, which causes the servomotor to rotate whenever a current flows through the resistor. Whenever a new solution is poured into the spectrophotometer, the servoamplifier causes the logarithmically wound potentiometer to restore 3 volts at pins 11 and 13 and to give a meter reading of 100-percent transmission.

The read-out potentiometer, which is geared to the logarithmic potentiometer, provides a measurement of the rotation required to restore equilibrium from one solution to another. By manually adjusting the read-out potentiometer across a 45-volt battery when a standard solution is in the spectrophotometer, the operator can make the digital-voltmeter reading numerically the same as the percent-constituent reading for the known

standard. (A PERCENT-CONSTITUENT knob is provided as shown in figure 103.1 for this adjustment.) Then when other solutions are placed into the spectrophotometer the digital voltmeter will automatically read percent constituent, provided that the color system follows Beers' law.

Two other controls are shown in figure 103.1. One is a SERVO-SENSITIVITY knob, which varies the servoamplifier sensitivity by changing the value of R in the 3-volt circuit to a point where the servo does not hunt excessively. The other is a ZERO-ADJUSTMENT knob, which turns another potentiometer to balance the 3-volt battery exactly with the spectrophotometer output, so that the meter reading will be right at 100-percent transmission when it is to be automatically maintained at balance. These last two controls, once they have been adjusted, should rarely need readjustment.
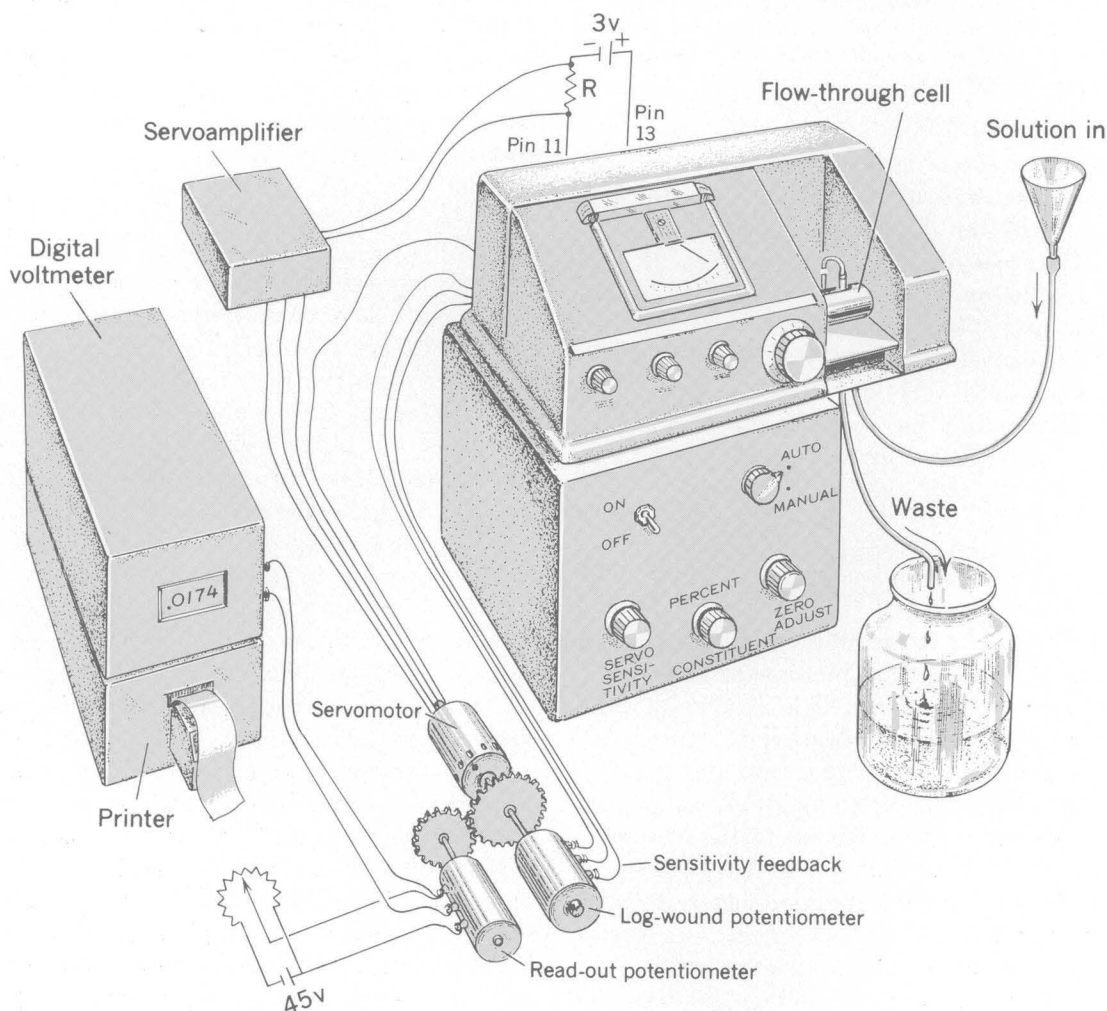
FIGURE 103.1.—Semischematic diagram of percent-constituent printing spectrophotometer. The log-wound potentiometer, read-out potentiometer, servomotor, and servoamplifier are contained in the instrument box under the spectrophotometer.

Circuitry

Two separate circuits are used. One is wired into the spectrophotometer through the 4-pole double-throw switch (AUTO-MANUAL switch, figs. 103.1 and 103.2) so that it may be introduced into or eliminated from the normal existing circuit, as shown in figure 103.2; the other is a read-out circuit (fig. 103.3) not connected electrically with the previous circuit.

The toggle switches used for placing the 3-volt and 45-volt batteries into operation, and for turning on the 115-volt a-c for the whole instrument, may be placed on one 3-pole double-throw toggle switch (ON-OFF switch, fig. 103.1).

The special components purchased from commercial sources included the log-wound potentiometer, special Helipot model 7603, function $y = 10^{2(x-1)}$, resistance $16K \pm 5$ percent, conformity ± 0.4 percent; and a Brown "Elektronik" amplifier continuous-balance unit, model 356358–1, with a 56-rpm servomotor. A Beckman digital voltmeter and printer, measuring to the nearest millivolt, were used in the print-out circuit.

FLOW-THROUGH CELL

A simple flow-through cell (fig. 103.4E') and mounting bracket were designed to simplify and speed up operation of the accessory-equipped spectrophotometer.

The following procedure was used in building the cell: A 7/32-inch-diameter hole was drilled through a 1-inch length of 1⅜-inch-diameter Lucite rod, half an inch from the end and perpendicular to the axis, as shown in figure 103.4A. Next, a ³⁄₁₆-inch mill was used to cut a slit half an inch high through the length of the bar, perpendicular to the $7⁄32$-inch hole (fig. 103.4B). The mill was then used at an angle to create a tapered cut (fig. 103.4C). This is important, as the sloped sides prevent the accumulation of air bubbles during use.

Two ¼-inch-OD (⅛-inch-ID) Lucite tubes about 1 inch long were tapered and then force fitted and cemented into the top and bottom of the hole as shown in figure 103.4D. Finally, two 1-inch round microscope cover slips were cemented to the ends of the rod with epoxy cement (fig. 103.4E).

A simple metal or plastic mounting bracket was built to fit into the spectrophotometer (fig. 103.5). It provides a light-tight holder for the flow-through cell, which can be readily removed or inserted.

The cell was mounted in its bracket, and a plastic inlet tube with a ⅛-inch ID and about a 16-inch length was attached to the bottom tube of the cell. The outlet was made of a short bent glass tube leading from the top of the cell into a larger drain tube that passes through a hole in the bracket, with an air break between the tubes to prevent a siphon effect.

The volume of the cell is a few milliliters. A solution is almost completely displaced (>99.9 percent) by passing 30 to 40 ml of a new solution through the cell.

FIGURE 103.2.—Circuitry of wiring into spectrophotometer.
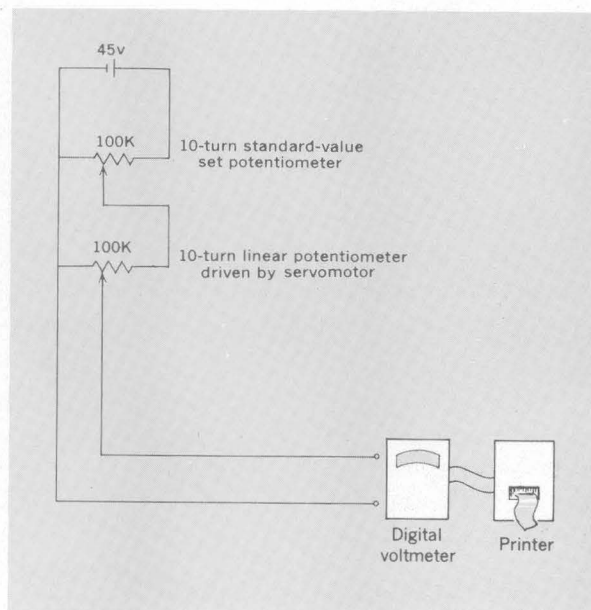
FIGURE 103.3.—Circuitry of read-out and print-out system.
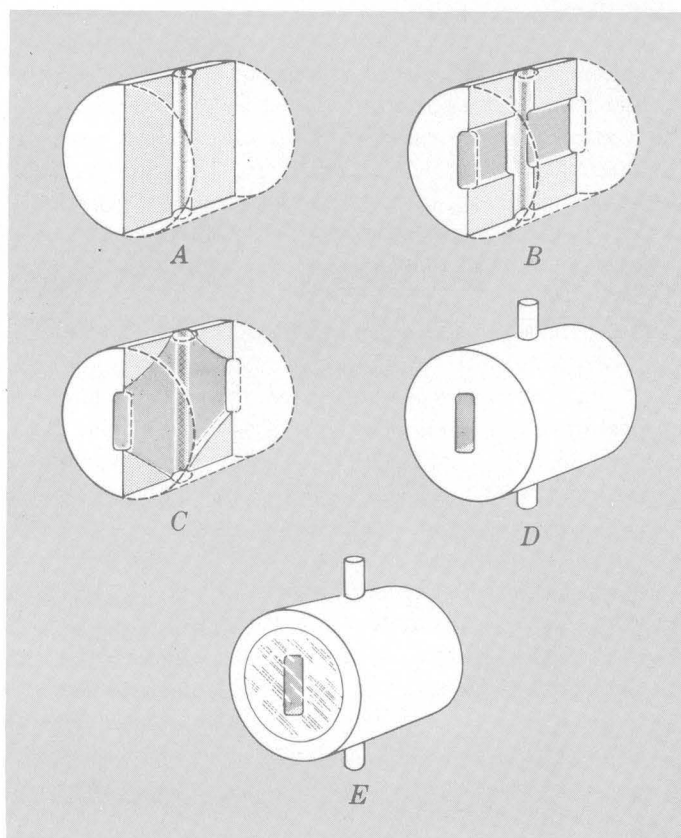
FIGURE 103.4.—Step-by-step construction of flow-through cell.
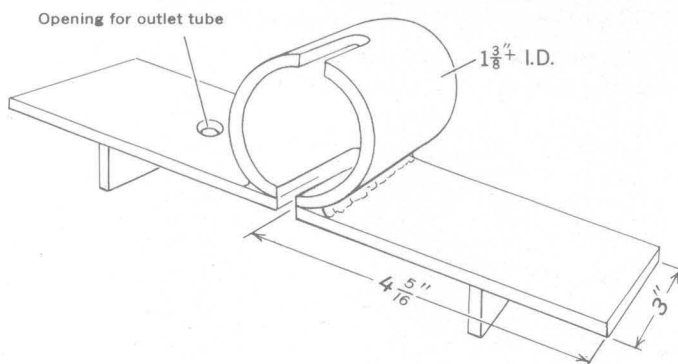
FIGURE 103.5.—Mounting bracket for flow-through cell.

PROCEDURE

The following procedure is suggested for operating the spectrophotometer with the percent-constituent printing accessory and flow-through cell:

Turn on the instrument and allow it to warm up for at least 30 minutes.

Prepare a blank, a known standard, and a series of unknown solutions in the usual manner for spectrophotometry.

Pour about 40 ml of the blank solution into the funnel. When the solution stops flowing, adjust the slit to any position so that the meter needle is automatically resetting itself. If this position is not 100 percent transmission ±1 percent, turn the ZERO ADJUSTMENT knob to bring the transmission within this limit. Note the exact meter reading. Open the slit to a point where the meter reading goes well above 100 and then close it carefully to bring the needle just to the previously noted balance position. It is now at the zero position of the log-wound potentiometer. Pour about 40 ml of the standard solution into the funnel. When the overflow of the liquid has stopped, adjust the reading on the digital voltmeter with the PERCENT-CONSTITUENT knob to read the same value as the known standard. Press the print button to print the value of the standard. Pour each of the unknown solutions into the funnel in sequence, and each time the liquid stops flowing, press print button to print the percent constituent of the solution.

DISCUSSION

The use of the electronic arrangement described provides a uniform sensitivity across the full scale of the instrument because the amplifier receives the same voltage change for the same change in absorbance. A deviation of 0.001 in optical density is sufficient to initiate corrective action. Theoretically, the servoamplifier-servomotor combination can provide a more sensitive response to color change than is obtained by normal manual operation. In practice the accuracy of the system may be limited by any deviation of the log coil from its designed curve and any mechanical lag in the links between the servomotor and the two potentiometers. A special pair of gears cut to a logarithmic relation is feasible and might be an improvement over the existing log coil plus gearing.

Results obtained with the printing spectrophotometer for the determination of SiO_2, Al_2O_3, Fe_2O_3, TiO_2, MnO, and P_2O_5 in silicate rocks do not differ significantly in accuracy and precision from those obtained with a manual spectrophotometer.

The benefits of this instrument include not only time saved by eliminating computations but also more dependability by eliminating human errors that arise in the computations.

DISSIPATION OF HEAT FROM A THERMALLY LOADED STREAM

By HARRY MESSINGER, Washington, D.C.

Abstract.—Energy-budget analysis of a heated stream failed to account for the observed rapid cooling. Discrepancies between predicted and actual downstream temperatures are attributed mainly to inadequacies in existing methods for measuring the effective solar and atmospheric irradiation of partially shaded water surfaces.

Effective planning for industrial and recreational utilization of streams commonly requires foreknowledge of water-temperature variations that may be expected throughout the year. Where water temperatures are raised significantly above the natural level, as by steam powerplants using water-cooled condensers, a knowledge of the rate at which water temperatures are reduced downstream by natural cooling processes is important. A theoretically sound approach to the problem is the energy-budget concept, which has been used extensively to calculate evaporation rates from lakes and reservoirs (Harbeck and others, 1958).

THEORY

In applying energy-budget methods to streams, the various inflow, outflow, and stored-heat terms are evaluated for successive short subreaches. In each of the subreaches, temperature change is assumed to be linear with distance. The energy budget for each subreach, over any arbitrarily selected time period, may be written as:

$$Q_R + Q_i = Q_B + Q_E + Q_H + Q_O + Q_C + Q_S, \quad (1)$$

where Q_R = net incoming atmospheric and solar radiation,

Q_i = heat content of water flowing into subreach,

Q_B = back radiation (long-wave) from water surface,

Q_E = energy lost by evaporation,

Q_H = energy lost by convection to atmosphere,

Q_O = heat content of water flowing out of subreach,

Q_C = heat conducted to streambed, and

Q_S = increase of heat storage in subreach.

Each of the preceding terms, except Q_C, may be evaluated, either by direct measurement or by calculation, by standard procedures developed for determining evaporation losses (U.S. Geological Survey, 1954). Conductive loss to the streambed can be computed, with reasonable accuracy, by multiplying the measured temperature gradient in the bed at a representative point in the subreach by the average thermal conductivity of the bed material.

Equation 1 may be rearranged thus:

$$(Q_i - Q_o) = Q_B + Q_E + Q_H + Q_C + Q_S - Q_R, \quad (2)$$

where the left-hand term denotes the loss in sensible heat of the water as it passes through the subreach. If the subreach originally selected is just long enough to produce a small, known temperature drop (for example, 1°C) and if all the right-hand terms are expressed in units of heat flow per unit area, then the required length, l, may be expressed as:

$$l = \frac{KF\Delta T}{W(Q_i - Q_o)}, \quad (3)$$

where F = average flow rate in subreach;

ΔT = temperature drop in subreach;

W = average width of subreach; and

K = a constant, whose value depends on the units employed in the other terms.

APPLICATION

The energy-budget method was used to predict the temperature profile of a heated section of the West Branch of the Susquehanna River below Shawville, Pa. Use of the stream water for condensing steam from the turbines of the Shawville powerplant, which operates at a constant load of 600,000 kw, raised the temperature of the river about 15°C during the period of study. (October 17 and 18, 1962).

Over a 24-hour period beginning at 0600 hours on October 17, 1962, temperature measurements were made

approximately bihourly at several sections downstream and one upstream from the powerplant. Ten measurements were made at equal distances across the width of each section. Only one measurement was necessary at each point because vertical mixing was virtually complete. Calibrated thermistor probes, accurate to 0.1°C, were used in the measurements. Average temperatures at each of 4 sections downstream and 1 upstream from the powerplant are shown in figure 104.1. Station 1, about 0.4 mile downstream from the powerplant diversion dam, included the flow from a small, unheated tributary (Trout Run). No other appreciable surface inflow occurred in the 4.9-mile reach between stations 1 and 4 during the period of study. Streamflow was virtually constant at 370 cubic feet per second, by actual measurement, and ground-water inflow in the reach was insignificant.

Wind velocity was measured with sensitive 3-cup totalizing anemometers that were installed in midstream at stations 2 and 3, exactly 2 meters above the mean water surface, and were read at 2-hour intervals.
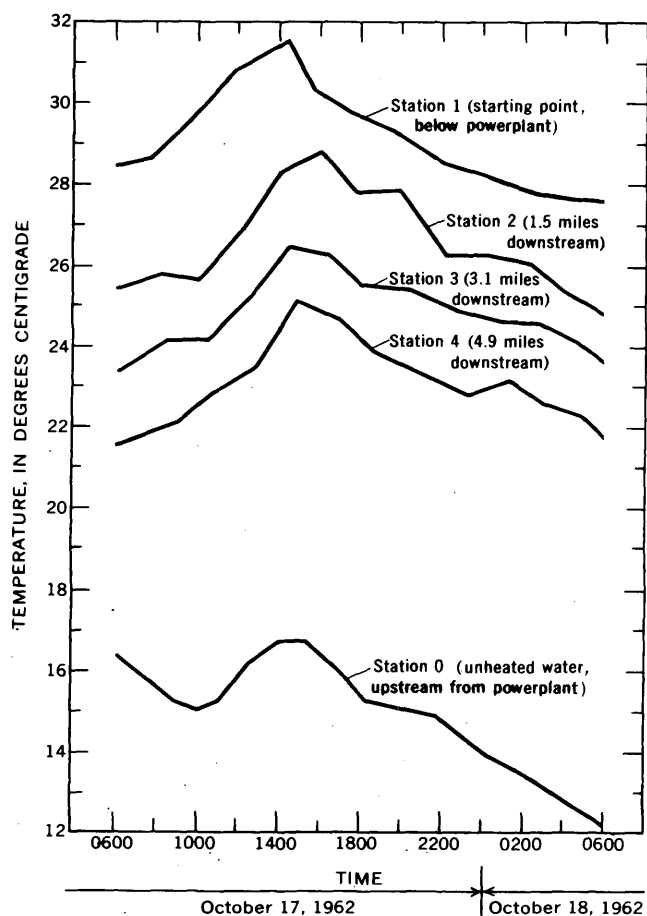
Bed temperatures were measured by means of a hollow plastic probe driven into the streambed at station 1. Three thermistors which were embedded 6 inches apart in the surface of the probe were connected to a portable wheatstone bridge circuit. The bed-temperature readings were taken simultaneously with the stream-temperature readings. Total radiation, solar radiation, and humidity measurements were made in a well-exposed area on the roof of a local school about 0.1 mile north of the river, between stations 3 and 4.

In calculating heat conduction to the streambed, Q_C, an average thermal conductivity of 0.004 cal per sec cm °C was used, corresponding to a value about midway between that of wet mud and sandstone (Ingersoll and others, 1948, p. 244). The bed loss in each successive subreach below station 1 was estimated by assuming that it was approximately proportional to the difference between the average water temperature in the subreach and the natural water temperature, as measured upstream from the powerplant. No really serious errors can result from this assumption, because the actual value of the Q_C term was only about 5 percent that of the sensible heat loss, $(Q_i—Q_o)$, in each subreach.

Conduction and convection losses to the atmosphere, Q_H, were calculated by multiplying the evaporation losses, Q_E, by a modified Bowen ratio, R_B. The method has been used in previous energy-budget studies. The modified Bowen ratio was calculated to fit a recently developed theory (W. D. Sellers, oral communication, 1962) that involves the ratio of the heat and momentum transfer coefficients $(K_H$ and $K_M)$. In his original work, Bowen (1926) assumed that K_H/K_M was virtually unity, whereas Sellers considers it to be a function of the Richardson number Ri. For the large differences between water and air temperatures measured in this study, the ratio K_H/K_M had an average value of about 1.30. The effect of applying this factor to the Bowen ratio was to increase Q_H by an amount approximately equal to 7 percent of the $(Q_i—Q_o)$ term.

The actual rate of cooling of the stream, as determined by the average temperature at each measuring station over the 24-hour study period, was considerably greater than that predicted by theory (fig. 104.2). The average stream temperature fell 3°C in slightly less than 2 miles of flow, whereas the predicted length of reach, to effect the same temperature decrease was 3.3 miles. Several possible explanations for the discrepancy, in decreasing order of probability, are:

1. Excessive values were assigned to Q_R in the calculation. The total radiant energy falling on the stream surface may be considerably less than that measured by the radiometer, because of shading by nearby hills and trees. The degree

FIGURE 104.1.—Variation of stream temperature with time in the West Branch of the Susquehanna River, near Shawville, Pa.

of shading is a complex function of the sun angle, time of year, direction of flow, type and amount of adjacent vegetation, and surrounding topography.

2. Errors were made in windspeed measurements. The average windspeed measured at station 3, during the last 10 hours of the study period, was less than 0.4 miles per hour. Accuracy of the measurement at such low velocities is questionable, because of friction losses in the bearings and gear trains.

3. Knowledge of water-surface temperatures, relative to the measured bulk temperatures, was in-

adequate. Surface temperatures directly affect the Q_B, Q_E, and Q_H terms of the energy budget. If, for example, during periods of high thermal radiation, the surface temperature were only 1°C higher than the bulk value, the $(Q_i - Q_o)$ term would be increased about 7 percent.

In an attempt to determine the causes of the discrepancy, separate energy-budget computations were made for each 4-hour period. The results, shown in the six curves of figure 104.3, suggest the explanation for the discrepancy.

The curves show that the greatest deviation from theory occurred during the daylight hours; especially, between 1000 and 1400 hours, when the net incoming radiation was highest (288 cal per cm²). During the next 4-hour period (Q_R=211 cal per cm²), the deviation was only slightly less. Conversely, the smallest deviations are noted for the two 4-hour nighttime periods beginning at 1200 hours (Q_R=78 and 81 cal per cm², respectively).

These observations give greater weight to the possibility of errors in the Q_R terms and in the assumed water-surface temperatures, as discussed above. On the other hand, windspeed inaccuracies become somewhat less important, because the lowest speeds occurred during the nighttime hours when deviations from the theory were smallest.

Future energy-budget studies of streams will center about the development of more reliable techniques for evaluating the Q_R term. The use of noncontacting, infrared thermometry should establish whether or not temperature differences at the water surface are of sufficient magnitude to affect the energy budget materially.

FIGURE 104.2.—Variation of average stream temperature with distance downstream from station 1 for entire 24-hour study period.

REFERENCES

Bowen, I. S., 1926, The ratio of heat losses by conduction and by evaporation from any water surface: Phys. Rev., v. 27, p. 779–787.

Ingersoll, L. R., Zobel, O. J., and Ingersoll, A. C., 1948, Heat conduction, 1st ed.: New York, McGraw-Hill Book Co., 278 p.

U.S. Geological Survey, 1954, Water-loss investigations—Lake Hefner studies, technical report: U.S. Geol. Survey Prof. Paper 269, 158 p.
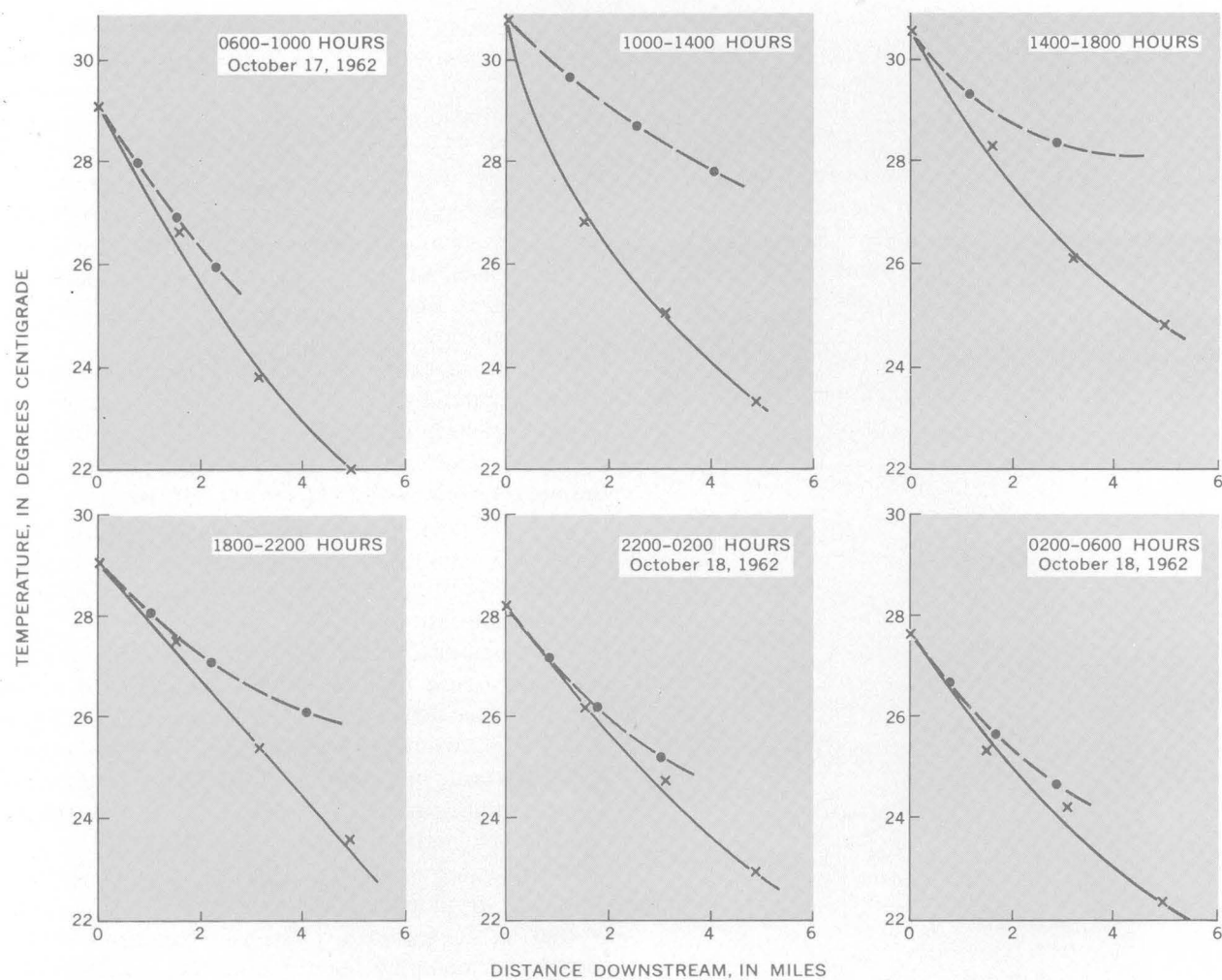
FIGURE 104.3.—Variation of stream temperature with distance downstream for various 4-hour study periods. Solid line, measured temperature; dashed line, predicted temperature.

MOVEMENT OF WATERBORNE CADMIUM AND HEXAVALENT CHROMIUM WASTES IN SOUTH FARMINGDALE, NASSAU COUNTY, LONG ISLAND, NEW YORK

By N. M. PERLMUTTER; MAXIM LIEBER,[1] and H. L. FRAUENTHAL;[2]

Mineola, N.Y.; and Hempstead, N.Y.

Abstract.—A slug of contaminated ground water moving through glacial outwash and containing as much as 3.7 parts per million of cadmium and 14 ppm of hexavalent chrominum was investigated by test drilling and sampling in 1962. The slug extends about 4,200 feet from recharge basins at a plating plant to Massapequa Creek, where part of the waste discharges naturally and part moves a short distance downgradient beneath and into the stream.

A slug of contaminated ground water containing high concentrations of cadmium and chromium from plating wastes, which have been discharged during the past 20 years by an industrial plant in South Farmingdale in east-central Nassau County, was defined in detail by test drilling in 1962 (figs. 105.1 and 105.2). The slug has been mapped four times since 1949 to determine changes in its size and to follow its course downgradient. Hexavalent chromimum in excess of 0.05 parts per million and cadmium in excess of 0.01 ppm are considered objectionable in public-water supplies (U.S. Public Health Service, 1962), although the cumulative toxicity of these metals as a result of long-term consumption by humans and animals is uncertain. Short-term ingestion of the metals may produce some ill effects, but fortunately much of the contamination seems to be eliminated from the body by natural processes.

[1] Assistant Director, in charge of Sanitation Laboratories, Division of Laboratories and Research, Nassau County Department of Health.
[2] Hydraulic Engineer, Division of Sanitation and Water Supply, Nassau County Department of Public Works.
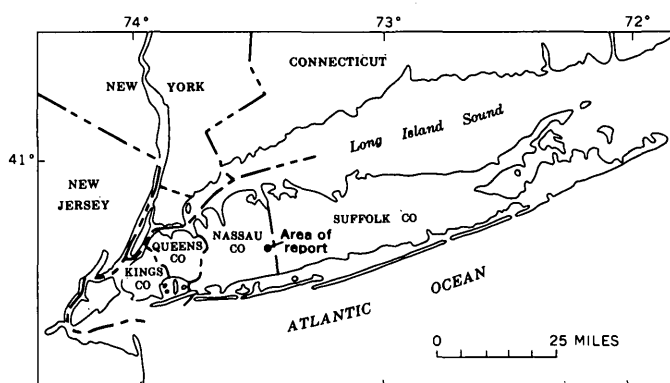
FIGURE 105.1.—Map of Long Island, N.Y., showing location of South Farmingdale, Nassau County.

We wish to thank all the Nassau County and U.S. Geological Survey personnel who participated in the field and office work, particularly Mr. Charles Kirsner, Department of Public Works who supervised the well-drilling program, Commissioner Eugene F. Gibbons and Deputy Commissioner John H. Peters, Nassau County Department of Public Works, and Dr. Joseph H. Kinnaman, Commissioner, Department of Health, for their support and interest.

Hexavalent chromium was detected first in a supply well at the industrial plant in South Farmingdale in 1942, but no further study was made of the problem for several years owing to a shortage of personnel during
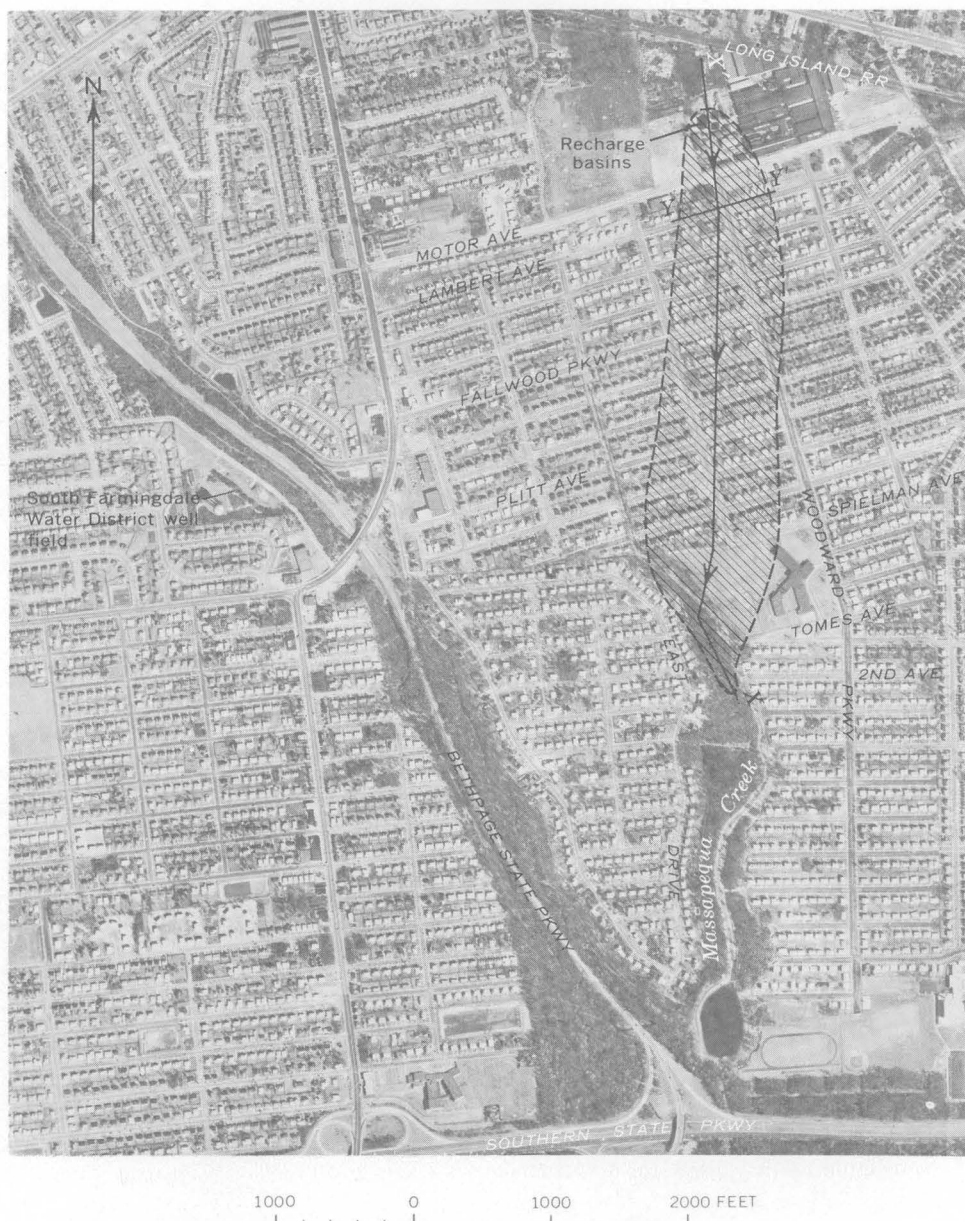
FIGURE 105.2.—Aerial photograph of South Farmingdale area showing extent of contamination in 1962 (ruled area), and location of sections X–X' and Y–Y'.

World War II. In 1945, seven shallow test wells were installed, as far as 900 feet south of the plant, by the New York City Department of Water Supply, Gas, and Electricity to investigate the potential hazard to the city's infiltration gallery at Massapequa, about $3\frac{1}{2}$ miles south of the source of contamination. The test wells, which were bottomed only a short distance below the water table, showed little or no contamination in 1945, but a resampling of several of the wells by the New York State Department of Health in 1948 showed as much as 3.5 ppm of hexavalent chromium in the water. On the basis of these early studies, a chromium

treatment plant recommended by the State Health Department was put into operation at the industrial plant in 1949.

Because of continued concern over the effectiveness of the treatment for chromium and the fact that cadmium and other metals were being removed from the waste water only incidentally, if at all, the Nassau County Departments of Health and of Public Works made a series of surveys of the contaminated slug, including test drilling, in 1949, 1953, 1958, and 1962. The results of the first two surveys were reported by Davids and Lieber (1951), Lieber and Welsch (1954), and Welsch

(1955). Their reports showed that the slug extended at least 3,600 feet from the plant by 1949. The 1958 survey was incomplete and the results were never published.

INVESTIGATION IN 1962

The 1962 investigation of the geologic, hydrologic, and chemical aspects of the contaminated water was the most intensive to date. About 90 test wells were drilled in and near the slug by the Nassau County Department of Public Works, and a series of water samples were collected from Massapequa Creek. The test wells were drilled in the vicinity of the recharge basins at the plating plant, along Motor Avenue, Lambert Avenue, Fallwood Parkway, Plitt Avenue, Spielman Avenue, East Drive, and in the bed of Massapequa Creek and along its banks between Spielman and Second Avenues (fig. 105.2). Most of the wells were driven with 1¼-inch drive points, and ranged in depth from about 8 to 75 feet. The final depth of the driven wells was sufficient to determine the full thickness of the slug at most locations. Wells were drilled by cable tool to depths of 97 to 140 feet at 3 sites to check for contamination in the deeper beds and to collect geologic samples.

Water samples collected at 5-foot intervals were analysed mainly for hexavalent chromium and cadmium by the Nassau County Health Department, Division of Laboratories. Hexavalent chromium was determined by the use of s-diphenylcarbazide and colorimetric comparison, and cadmium was determined by dithizone extraction (American Public Health Association and others, 1960). The chromium determinations are believed to be reliable to the nearest 0.01 ppm. Because the test for cadmium is still considered to be tentative owing to problems in the analytical procedure that are probably caused by interfering metallic ions, some doubt exists about the reliability of cadmium determinations below concentrations of about 0.05 ppm. Results of chemical and spectrographic analyses of several water samples by the Geological Survey were not available at the time of preparation of this article.

GEOHYDROLOGIC ENVIRONMENT

The land surface in the South Farmingdale area (fig. 105.2) is a gently sloping outwash plain notched by several south-flowing shallow tributaries of Massapequa Creek. It ranges in altitude from about 40 to 70 feet above sea level and is underlain by 2 geologic units of significance in this study (fig. 105.3A): an upper unit of glacial outwash, called the upper Pleistocene deposits, and a lower unit of stream deposits of Late Cretaceous age, called the Magothy(?) Formation. The upper Pleistocene deposits consist chiefly of highly permeable beds of brown fine to coarse sand and gravel containing a trace of silt, and some subordinate thin scattered lenses of silt and silty clay. The lower 20 to 30 feet of the unit generally contains more clay than the upper part. The total thickness of the upper Pleistocene deposits ranges from about 80 to 130 feet. The Magothy(?) Formation consists chiefly of beds and lenses of gray fine sand and sandy and silty clay containing lignite, some beds of brown fine sand, and, in a few places, thin beds of coarse sand containing some gravel. The strata of the Magothy(?) Formation have a lower average permeability than those of the upper Pleistocene deposits, because of their higher clay content and poorer sorting. Neither of the geologic units in the report area contains lenses of silt and clay that are either thick or extensive enough to act as significant hydraulic barriers to the movement of water. However, the lenses of silt and clay doubtless have an important geochemical influence on local concentrations of cadmium and chromium ions.

About half the average annual rainfall of 45 inches percolates down to the upper Pleistocene deposits, where the ground water occurs under unconfined conditions. The water table, which is the upper surface of the zone of saturation in the ground-water reservoir, ranges in depth from about 15 feet below land surface in the northern part of the area to within a foot of the land surface at Massapequa Creek in the southern part. It has an average gradient of about 12 feet per mile. Water in the underlying Cretaceous deposits is connected hydraulically with the water in the Pleistocene deposits but is increasingly confined at depth by layers of silt and clay. However, the two geologic units form a single aquifer having a wide range in permeability.

Water enters the aquifer beneath the South Farmingdale area by (1) direct recharge from rainfall, (2) underflow from the adjoining area to the north, (3) return of industrial waste water through recharge basins, and (4) seepage from hundreds of domestic cesspools. The ground water moves generally southward (fig. 105.3A); some discharges into Massapequa Creek, and some moves as underflow beneath the creek and the adjoining area. Most of the report area is supplied with water from deep wells owned by the South Farmingdale Water District. A small number of home-owners maintain shallow wells that are used for lawn sprinkling only.

EXTENT AND MOVEMENT OF CONTAMINATION

Sampling of the test wells and Massapequa Creek shows that the contaminated slug of ground water is a cigar-shaped body in plan view, and extends south from the industrial recharge basins to the valley of Massapequa Creek, where it is moving slowly downgradient
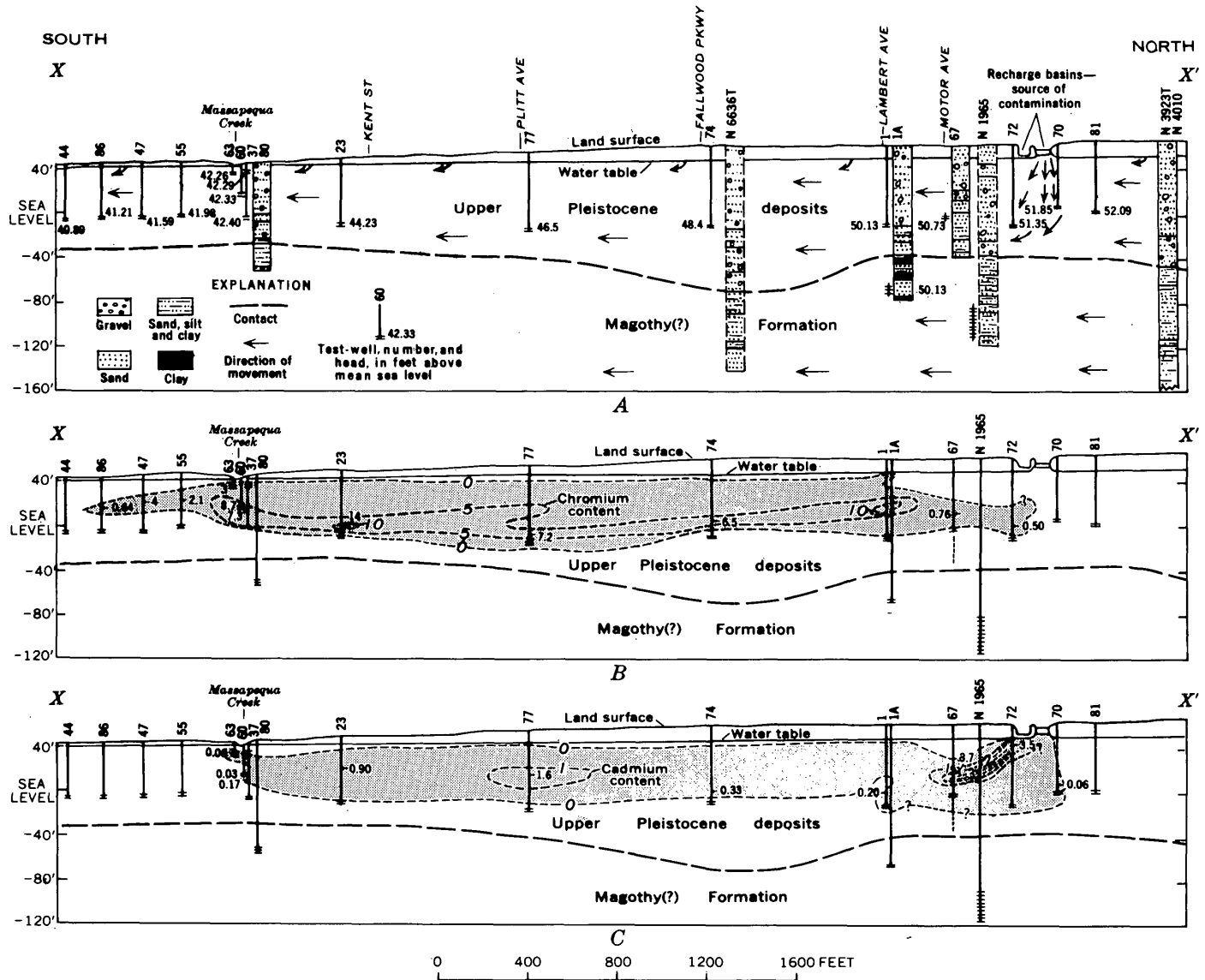
FIGURE 105.3.—Sections showing geology and direction of movement of ground water (A), and lines of equal chromium (B) and cadmium (C) content, in parts per million, along line X–X' (fig. 105.2) in 1962. Contaminated water body shaded.

into and beneath the stream (figs. 105.2 and 105.3 B, C). The slug was about 4,200 feet long and had a maximum width of about 1,000 feet in 1962. It is elongated generally in the direction of natural ground-water flow and is widest near Spielman Avenue. The width of the slug actually doubles in a distance of 2,700 feet between Motor and Spielman Avenues, owing largely to dispersion. Further widening of the slug is apparently deterred by Massapequa Creek, which acts hydraulically as a line sink or line discharge and hence deflects the flow from its original path. The slug narrows considerably at its southern extremity as it moves beneath the valley toward points of discharge in Massapequa Creek.

, Section X–X' (fig. 105.3 B, C) shows the vertical extent and concentration of hexavalent chromium and cadmium in a plane oriented along the approximate direction of flow in the center of the slug. The maximum concentration of hexavalent chromium detected in 1962 was 14 ppm at well 23 near Spielman Avenue, and the maximum cadmium content was 3.7 ppm at well 67, a short distance south of the recharge basins. Figure 105.3B shows that the concentration of hexavalent chromium is decreasing at the north end of the slug, and comparison of figures 105.3B and 105.3C shows that the chromium ions have migrated farther south than the cadmium ions. Chemical analyses made in 1962 of the treated effluent from the plating plant show that the effluent is generally relatively free of hexavalent chromium but at times contains as much as 3.5 ppm of cadmium.

Section $Y-Y'$ (fig. 105.4) shows the concentration of hexavalent chromium beneath Lambert Avenue in a vertical plane approximately perpendicular to the direction of ground-water flow. Two centers of contamination are illustrated on the section. The main center is near the intersection of Woodward Parkway and Lambert Avenue. A second and smaller center of contamination at the east end of the section may be due to relatively minor leakage from one of the plating buildings east of the main line of flow from the recharge basins.

The 1962 survey showed for the first time that the contamination had not only reached Massapequa Creek but was present in the stream as well as in the beds beneath it. The maximum concentration of hexavalent chromium in Massapequa Creek was 2.1 ppm, about 300 feet north of Tomes Avenue (fig. 105.2), and a concentration of 0.01 ppm was found in a sample from the creek about a mile south of Southern State Parkway. The maximum load of hexavalent chromium carried by the stream was calculated to be about 4.5 pounds per day at 2d Avenue. The cadmium concentration in the stream ranged from 0 to 0.07 ppm north of Southern State Parkway; it was not detectable south of Southern State Parkway.

The public-supply wells nearest the contaminated slug are those of the South Farmingdale Water District (fig. 105.2). The wells are screened to a depth of about 150 to 600 feet in the Magothy (?) Formation and, owing to their depth and the direction of movement of the slug, are in no danger of contamination now or in the foreseeable future under present hydraulic conditions. No general-purpose domestic wells are known to be in use in the present path of the slug. The Massapequa infiltration gallery, which serves as a standby source of water for New York City, is about 2½ miles south of the southern extremity of the slug. No water has been drawn from the gallery since February 1958. Because of the great dilution of the slug after it discharges into Massapequa Creek, no significant concentrations of metallic contaminants have reached or are likely to reach the vicinity of the gallery via the stream. Also, the opportunity for dilution, by millions of gallons of fresh ground water, of any remnant of the slug which might move to the gallery as underflow suggests that potential operation of the gallery in the future should not be seriously influenced by this source of contamination.

Because of the slow rate of ground-water flow, the age of the contaminated water in different parts of the
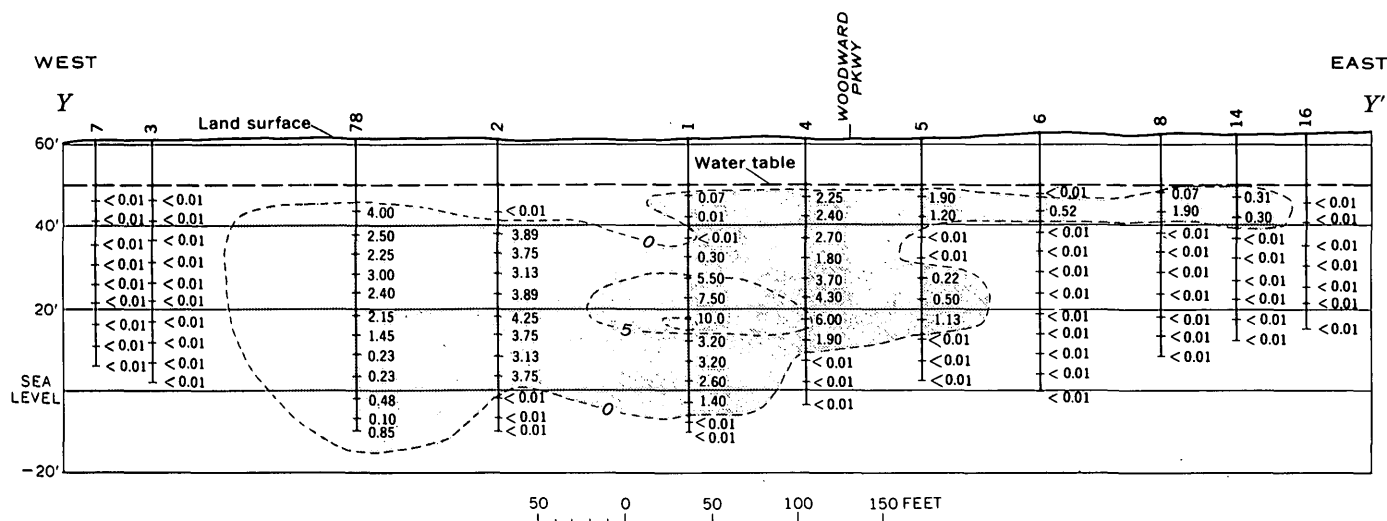
FIGURE 105.4.—Section along line $Y-Y'$ (fig. 105.2) showing concentration of hexavalent chromium and lines of equal chromium content, in parts per million, in wells along Lambert Ave., South Farmingdale, Nassau County, N.Y., in 1962.

slug may span a 10-year interval or more, and is greatest to the south. The concentrations of hexavalent chromium and cadmium reflect transient conditions. Those concentrations observed in 1962 are the result of past and present intermittent recharge of varying concentrations and quantities of plating wastes, dilution by rainfall and ground-water underflow, adsorption of contaminants on mineral grains, particularly clay minerals, and discharge into Massapequa Creek. Concentrations of the contaminants in most parts of the slug are generally much lower than in previous years, although the overall shape and dimensions of the slug have not changed appreciably since 1949, except for substantial widening at Spielman Avenue and movement into and beneath Massapequa Creek and vicinity.

Contemplated improvements in treatment procedures at the plating plant may result in further reduction in the concentration, if not elimination, of most of the contaminants, including cadmium and other minor constituents such as nickel, copper, and cyanide in the waste water from the plating plant. However, because of the slow rate of movement of the ground water and the slowness of dilution by fresh ground-water recharge, it might be 10 to 15 years before the contaminated water could be completely flushed out under natural conditions, even if the treatment were 100-percent effective.

REFERENCES

American Public Health Association and others, 1960, Standard methods for the examination of water and waste water, 11th ed.: New York, Am. Public Health Assoc., Inc., 626 p.

Davids, H. W., and Lieber, Maxim, 1951, Underground water contamination by chromium wastes: Water and Sewage Works, v. 98, no. 12, p. 528–534.

Lieber, Maxim, and Welsch, F. W., 1954, Contamination of ground water by cadmium: Am. Water Works Assoc. Jour., v. 46, no. 6, p. 541–547.

U.S. Public Health Service, 1962, Drinking water standards: Federal Register, Mar. 6, p. 2152–2155.

Welsch, F. W., 1955, Ground-water pollution from industrial wastes: Sewage and Industrial Wastes, v. 27, no. 9, p. 1065–1069.

EFFECT OF URBANIZATION ON STORM DISCHARGE AND GROUND-WATER RECHARGE IN NASSAU COUNTY, NEW YORK

By R. M. SAWYER, Mineola, N.Y.

Abstract.—Urbanization in the East Meadow Brook drainage basin has decreased recharge to the ground-water reservoir from which most water supplies on Long Island are taken. The loss of recharge during the period 1952–60 was equivalent to about 63,000 gallons per day.

Nassau County, N.Y., on Long Island, is one of the fastest growing counties in the Nation. The large expansion of housing and highway construction, with the ensuing replacement of permeable surfaces by impervious ones, has reduced infiltration of precipitation to the water table. A dual problem is created by this rapid urbanization—loss of replenishment of underground water supplies, and collection and disposal of storm waters.

The change from a rural to a suburban environment was accompanied by a program of storm-sewer construction. A system of short sewer lines and seepage basins provides a means of water conservation comparable in effectiveness to natural surface conditions. Storm runoff is carried through relatively short sewer lines to excavated collecting basins termed "recharge basins". From these basins the water percolates down through the underlying natural deposits of sand and gravel and enters the ground-water reservoir from which most water supplies on Long Island are taken.

Recharge basins may be used in the interior of the island where the depth to water table is as much as 200 feet. Near the south shore, however, the depth to water table decreases, becoming very shallow at the shore. In the near-shore areas there is at present no other recourse than to discharge storm-water runoff to streams or to Great South Bay.

In order to test the change in regimen of streams, two streams were chosen for study (fig. 106.1)—one affected by urbanization (East Meadow Brook at Freeport), and one unaffected (Mill Neck Creek at Mill Neck). East Meadow Brook flows south through a highly urbanized section of housing developments, shop-
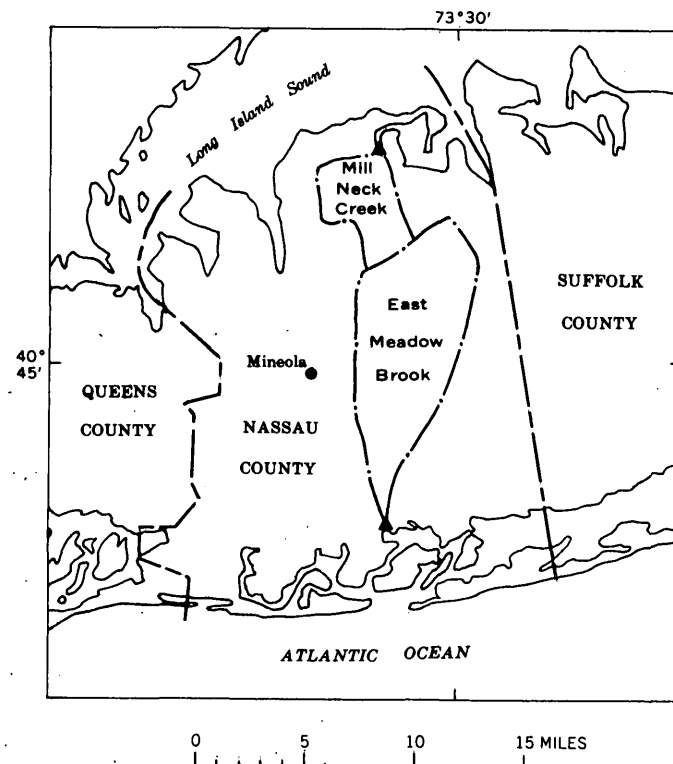
FIGURE 106.1.—Map showing the drainage basins of East Meadow Brook and Mill Neck Creek in Nassau County, N.Y. Triangles are stream-gaging stations.

ping centers, and light industrial areas. Mill Neck Creek, on the other hand, flows north through an area consisting mostly of large estates and a few farms. Gaging stations on both streams have the same length of record, 1938 to 1960.

The following population figures prepared by the Nassau County Planning Commission (1959) show the increase in population in the drainage basins of the two streams in the period 1950–55:

Drainage basin	Population 1950	1955
East Meadow Brook	43,821	101,019
Mill Neck Creek	12,120	15,727

In the densely populated East Meadow Brook basin (about 10 square miles) population increased about 130 percent in the 5-year period 1950–55, while in the Mill Neck Creek basin (about 31 square miles) it increased only about 30 percent.

The data in table 106.1 indicate that this increase in population in the East Meadow Brook drainage basin probably occurred mostly in the period 1951–52. There was a slight increase previously in the immediate postwar years of 1945 and 1946. Peak discharge for Mill Neck Creek shows no apparent change in trend over the years, while that of East Meadow Brook shows an increasing or rising trend starting about 1952.

TABLE 106.1.—*Annual precipitation at Mineola and discharge of Mill Neck Creek and East Meadow Brook*

Water year	Precipitation at Mineola (inches)	Peak discharge (cfs)		Annual mean discharge (cfs)		Direct discharge, in percentage of total discharge	
		Mill Neck Creek	East Meadow Brook	Mill Neck Creek	East Meadow Brook	Mill Neck Creek	East Meadow Brook
1938	57.88	86	149	9.25	·16.19	13.2	9.0
1939	36.32	36.6	72	10.41	21.35	7.0	5.6
1940	42.01	38.7	130	9.77	15.28	8.5	8.1
1941	38.97	76.1	(1)	9.01	14.29	7.4	7.6
1942	46.90	50.1	121	8.70	13.35	12.4	12.2
1943	38.76	32.6	78	9.09	16.03	5.9	6.5
1944	49.20	104	297	9.60	18.31	13.8	14.9
1945	45.51	61.8	74	9.98	16.74	9.3	7.6
1946	46.16	46.7	129	10.44	18.23	8.2	8.7
1947	32.60	31.6	105	9.11	13.05	6.7	6.4
1948	50.43	51.9	190	9.99	20.87	8.9	9.9
1949	47.98	40.8	134	10.28	21.19	8.8	8.7
1950	33.77	21.6	170	8.32	12.94	5.9	7.9
1951	39.91	39.0	100	8.49	15.02	8.1	10.6
14-year average	43.31			9.46	16.63		
1952	57.11	44.2	224	10.70	22.04	8.3	14.5
1953	47.20	56.8	234	10.59	20.61	8.5	13.6
1954	45.02	67.8	270	9.46	14.90	9.0	19.0
1955	48.45	135	355	9.88	20.52	11.4	19.3
1956	43.70	59.6	185	10.75	22.02	7.3	11.8
1957	36.33	68.8	170	9.23	15.30	6.4	13.0
1958	57.64	61.7	172	10.72	21.18	9.9	19.4
1959	38.74	30.9	250	9.70	18.42	6.7	16.0
1960	52.44	137	835	10.2	18.3	11.7	28.9
9-year average	47.40			10.1	19.3		

1 Not computed.

Annual precipitation data for Mineola, the station nearest the headwaters of both streams, are given in table 106.1. The annual precipitation for the period 1952–60 averaged 47.40 inches, an increase of 4.09 inches, or 9.4 percent, over the 1938–51 average of 43.31 inches.

Annual mean discharge of both East Meadow Brook and Mill Neck Creek (table 106.1) shows an increase in the average for the period 1952–60, as compared with 1938–51, due at least in part to the increase in precipitation.

Figures for direct discharge, as a percentage of total discharge (table 106.1) were obtained by subtracting the base flow from the quantity shown on the discharge hydrograph during periods of direct runoff. The base flow during these periods was estimated from the base flow before and after the storm. Mill Neck Creek shows no break in trend in these figures for the period of record. East Meadow Brook shows no break in trend for the period up to 1951, but shows a new upward trend starting with 1952. In several years prior to 1951 (1938, 1939, 1940, 1942, 1945, 1947, 1949) the percentage of direct discharge for Mill Neck Creek is larger than that for East Meadow Brook, but after 1951, the Mill Neck Creek percentage in every year is considerably below that for East Meadow Brook.

Average annual total, direct, and base runoff for both streams for the periods 1938–51 and 1952–60 are shown in table 106.2. At Mill Neck Creek, the increases in percentage of total runoff, direct runoff, and base runoff are similar, ranging from 6.1 to 7.3 percent, and are closely comparable to the 9.4 percent increase in precipitation. At East Meadow Brook, on the other hand, total runoff increased 1.15 inches, or 15.8 percent; direct runoff increased 0.80 inch, or 123.1 percent; base runoff increased 0.35 inch, or only 5.3 percent. The changes at East Meadow Brook are probably due to the change in land surface from pervious to impervious material as well as to the increase in precipitation.

Base runoff is the discharge from the shallow, water-table aquifer. In and near the East Meadow Brook drainage basin, ground-water pumpage is almost entirely from the deeper, confined Magothy(?) Formation. Increased pumpage, therefore, would have only a slight net effect on the water table. Moreover, sewers were not built in this area prior to 1960 and most of the ground-water pumped was, therefore, returned to the water table by septic tanks and cesspools. Consumptive use in this area is not a significant factor; hence, the difference in base flow between these two drainage basins is due to increased direct runoff in the East Meadow Brook basin.

TABLE 106.2.—*Average annual precipitation at Mineola and runoff of Mill Neck Creek and East Meadow Brook*

[All figures are in inches per year unless otherwise indicated]

	Precip-itation	Runoff of Mill Neck Creek			Runoff of East Meadow Brook		
		Total	Direct	Base	Total	Direct	Base
14 years (1938–51)	43.31	11.17	0.99	10.18	7.29	0.65	6.64
9 years (1952–60)	47.40	11.97	1.05	10.92	8.44	1.45	6.99
Increase	4.09	.80	.06	.74	1.15	.80	.35
Increase, in percent	9.4	7.2	6.1	7.3	15.8	123.1	5.3

Had total runoff and direct runoff at East Meadow Brook increased at about the same rate as at Mill Neck Creek, the increase of base runoff at both streams should have been comparable. It appears, therefore, that 2 percent of the base runoff at East Meadow Brook—or 2 percent of the recharge to the ground-water reservoir—has been lost because of the change in the land surface. This loss amounts to 0.1328 inch per year, or 63,000 gallons per day.

REFERENCE

Nassau County Planning Commission, 1959, Population analysis for Nassau County, State of New York.

Article 107

MAPPING TRANSMISSIBILITY OF ALLUVIUM IN THE LOWER ARKANSAS RIVER VALLEY, ARKANSAS

By M. S. BEDINGER and L. F. EMMETT, Little Rock, Ark.

Abstract.—Areal differences in transmissibility were mapped by using information from aquifer tests, specific-capacity tests, and lithologic logs. Aquifer-test results served as a basis for estimating transmissibility from specific capacity, and laboratory determinations of the relation of permeability to grain size were used in estimating transmissibility from lithologic logs.

Areal differences in transmissibility of the alluvial aquifer in the lower Arkansas River valley have been mapped as a prerequisite to construction of an electric-analog model (Robinove, 1962; Stallman, 1963) of the alluvial aquifer in an area about 20 miles wide along the Arkansas River from Little Rock, Ark., to the Mississippi River (fig. 107.1).

The coefficient of transmissibility of the alluvial aquifer at 26 sites in and near the area was known from aquifer tests made during this and previous studies. The aquifer-test results were used as a basis for estimating transmissibility from the specific capacity of wells, and laboratory determinations of the relation of permeability to grain size were used in estimating transmissibility from lithologic logs.

The specific capacity of a well is computed from the yield and drawdown, measured after equilibrium conditions have been reached, and usually is expressed in gallons per minute per foot of drawdown. For wells of equal diameter and equal efficiency, the specific capacity is directly proportional to the transmissibility of the aquifer. Even where the efficiency is variable, the specific capacity affords a reasonably good rough measure of the ability of the aquifer to transmit water.

Specific-capacity tests were made on 54 wells in and near the project area. The specific-capacity values were converted to transmissibility values by using the graph in figure 107.2, which is based on a modified version of the Thiem equation for determining the coefficient of transmissibility, T, in gallons per day per foot (Ferris and others, 1962, p. 91):

$$T = \frac{527.7Q \log_{10}\left(\frac{r_2}{r_1}\right)}{s_1 - s_2}, \qquad (1)$$

where Q is the well discharge, in gallons per minute, and s_1 and s_2 are the drawdowns, in feet, at distances r_1 and s_2, in feet, respectively, from the axis of the pumped well.

If r_2 is assumed to be the radius at which s_2 is zero, the equation may be written as

$$T = 527.7 \frac{Q}{s_1} \log_{10}\left(\frac{r_2}{r_1}\right). \qquad (2)$$

Then, if s_1 is assumed to be the drawdown at the casing of the well (where r_1 is the radius of the well), the term Q/s_1 is approximately equal to the specific capacity of the well. The distance r_2 is given by the following equation (modified from Ferris and others, 1962, p. 100):

$$r_2{}^2 = \frac{0.30Tt}{S}, \qquad (3)$$

where t is the time in days since pumping started, S is the storage coefficient of the well, and r_2 and T are as previously defined.

Values of r_2 were computed for various times from the average transmissibility and storage coefficients as determined from the 26 aquifer tests. The use of aver-

ART. 107 *IN* U.S. GEOL. SURVEY PROF. PAPER 475-C, PAPER C188-C190. 1963.

C188
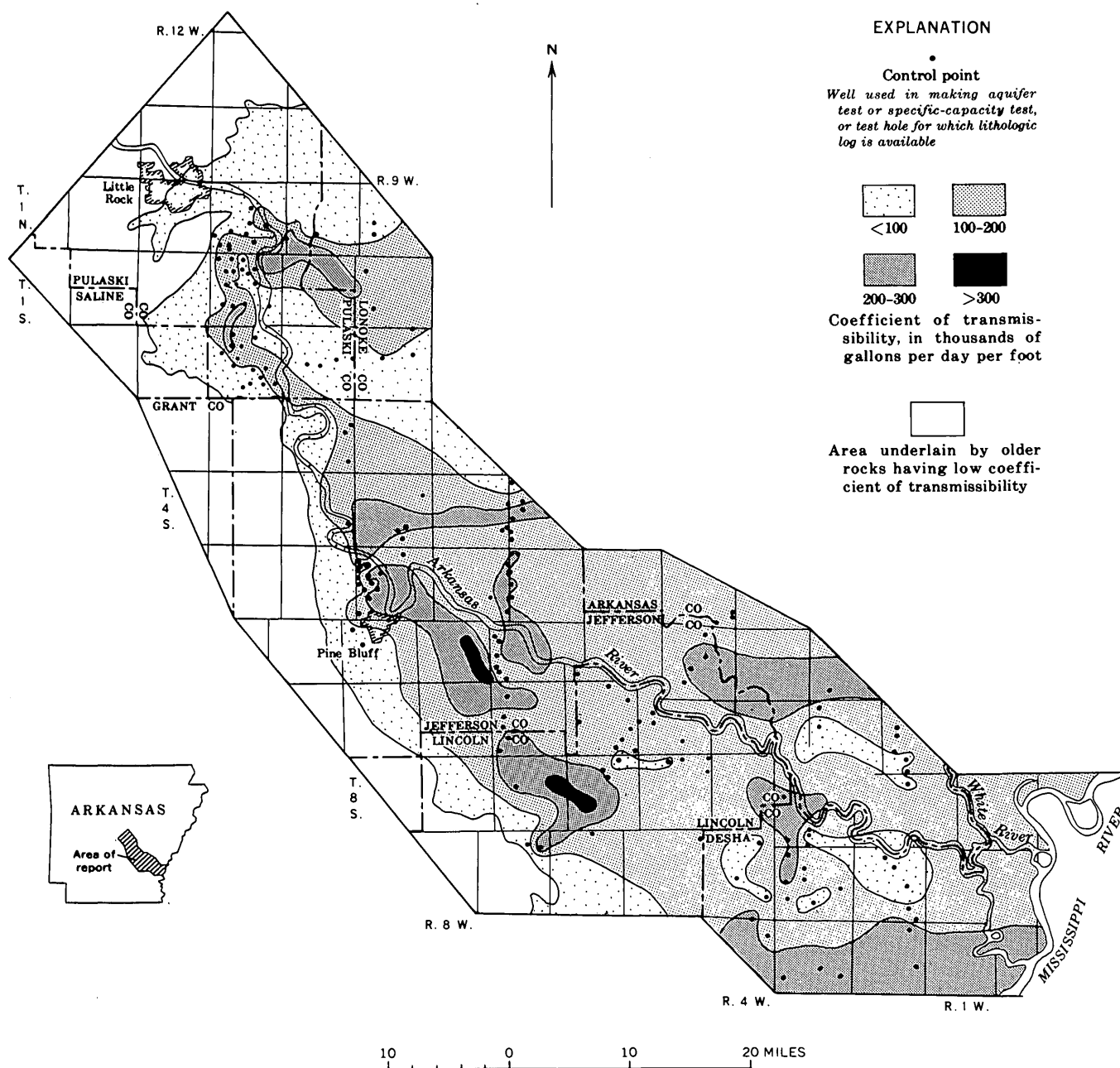
FIGURE 107.1.—Transmissibility of the alluvial aquifer in the lower Arkansas River valley.

age values for T and S in equation 3 has little effect on the T value computed from equation 2 because the ratio r_2/r_1 enters equation 2 as the $\log_{10}$. The value of r_2 from equation 3 was used to compute the term 527.7 $\log_{10}$ (r_2/r_1). This was done for various pumping durations and well radii (fig. 107.2).

The graph in figure 107.2 was used to determine the transmissibility at the sites of the 54 specific-capacity tests in the study area by multiplying the specific capacity of the well, Q/s_1, by a factor 527.7 $\log_{10}$ (r_2/r_1),

which is dependent upon the well diameter and duration of pumping.

Lithologic logs of 135 test holes in the area were obtained and 59 samples were analyzed by the Survey's hydrologic laboratory for particle-size distribution and permeability. The following table, which shows the range in field coefficient of permeability for various types of material, has been derived from the relation between grain size and permeability in the Arkansas River valley (Bedinger, 1961).
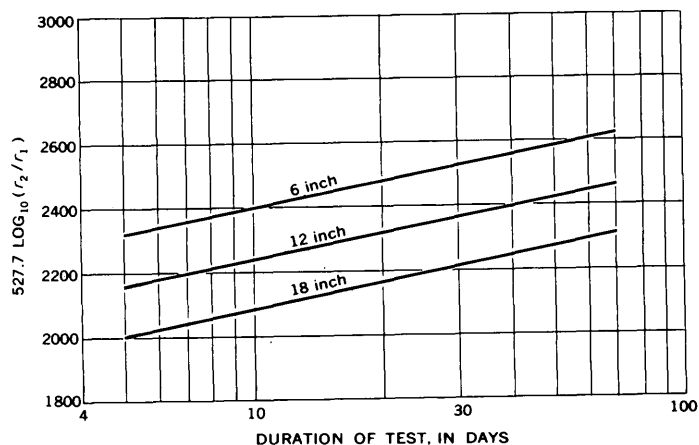
FIGURE 107.2.—Values of 527.7 $\log_{10}(r_2/r_1)$ for selected well diameters and durations of pumping.

Permeability of alluvial materials of the Arkansas River valley

[Gallons per day per square foot]

Material	Field coefficient of permeability
Sand, very coarse, and very fine gravel	6,000–15,000
Sand, very coarse	3,000– 9,000
Sand, coarse and very coarse	1,500– 4,000
Sand, coarse	800– 2,000
Sand, medium and coarse	400– 1,000
Sand, medium	200– 500
Sand, fine and medium	100– 250
Sand, fine	50– 140
Sand, very fine and fine	20– 60
Sand, very fine	10– 30

In using such tables to estimate transmissibility from lithologic logs, the choice of permeability within the indicated range for a given material involves subjective judgment in examination of the drill cuttings. However, with experience in an area, one generally can estimate permeability by this method with fair to good accuracy.

The three methods of computing transmissibility—aquifer tests, specific-capacity tests, and estimates from lithologic logs—were used in the preparation of figure 107.1. This map, which shows the areal differences in transmissibility in the alluvial deposits, was the basis for selecting the resistors used in constructing an electric-analog model of the area.

This technique of mapping areal differences in transmissibility should be applicable in many areas. However, the permeability values for different types of material and the values of 527.7 $\log_{10}$ (r_2/r_1) given above are not necessarily applicable to other areas. Comparisons between field and laboratory determinations of permeability should be made and values adjusted as needed for each area in order to apply this technique elsewhere.

REFERENCES

Bedinger, M. S., 1961, Relation between median grain size and permeability in the Arkansas River valley, Arkansas: Art. 157 *in* U.S. Geol. Survey Prof. Paper 424–C, p. C31–C32.

Ferris, J. G., Knowles, D. B., Brown, R. H., and Stallman, R. W., 1962, Theory of aquifer tests: U.S. Geol. Survey Water-Supply Paper 1536–E, p. 69–174.

Robinove, C. J., 1962, Ground-water studies and analog models: U.S. Geol. Survey Circ. 468, 12 p.

Stallman, R. W., 1963, Calculation of resistivity and error in an electric analog of steady flow through nonhomogeneous aquifers: U.S. Geol. Survey Water-Supply Paper 1544–G, 20 p.

SNOWMELT HYDROLOGY OF THE NORTH YUBA RIVER BASIN, CALIFORNIA

By S. E. RANTZ, Menlo Park, Calif.

Work done in cooperation with California Department of Water Resources

Abstract.—Formulas previously derived for computing daily snowmelt during the melting season in three small mountain watersheds were tested in the North Yuba River basin, a larger, gaged watershed. Observed and synthesized hydrographs compared well, but they showed that better estimates of snowmelt can be made when the snowpack is heavy than when it is light.

Formulas for estimating snowmelt runoff from mountainous river basins were derived in an intensive cooperative investigation of three small laboratory watersheds in the Sierra Nevada by the U.S. Army, Corps of Engineers, and the U.S. Weather Bureau during the years 1945–56. Other Federal agencies were minor participants in the investigation; the author, as a representative of the U.S. Geological Survey, was assigned as an analyst.

The formulas are based on physical laws of heat exchange, and contain constants that account for the effect of environmental influences such as forest cover and basin exposure. These formulas, and the theory upon which they are based, are not discussed here, but an excellent treatment of the subject appears in a summary report of the snow investigations (U.S. Army, Corps of Engineers, 1956) and in a condensed version of that report (U.S. Army, Corps of Engineers, 1960).

This article describes a study to test the applicability of the derived formulas to larger river basins. The 245-square-mile basin of the North Yuba River upstream from the Geological Survey gaging station below Goodyears Bar, Calif., in the Sierra Nevada, was selected for testing, partly because the river is unregulated and partly because the altitude of its watershed ranges widely (2,450 to 8,590 feet above sea level). Three years were selected for study: 1956 and 1958, when the snowpack was the heaviest of the last decade, and 1959, when the snowpack was the lightest of the last decade. The snow-survey data collected in late March and early April of each of those years, and daily meteorological observations of the Weather Bureau during the snowmelt seasons, were used in the formulas to compute synthetic records of daily discharge of the North Yuba River at the gaging station.

Many preliminary steps were necessary before the snowmelt formulas could be applied. Because of its wide range in altitude, the basin was divided into 1,000-foot altitude zones, and the area and percentage of forest cover for each zone were determined from topographic maps. From snow-survey data a relation was obtained between altitude and the water equivalent of the snowpack at the start of each melt season. The snowmelt formulas require daily values of many meteorological elements of which only air temperature and precipitation are observed in the North Yuba River basin. It was necessary, therefore, to transpose records from other Weather Bureau stations, or to derive by other means the daily values of such elements as dewpoint, windspeed, solar radiation, and snow-suface albedo.

After all the necessary meteorological elements were obtained, either by observation or by synthesis, the snowmelt in each altitude zone was computed. The formulas were used to compute the daily magnitude of the various components of snowmelt; namely, the melt from short-wave and long-wave radiation, convection, condensation, and rain, and the melt at the ground surface. These melt components were added together and routed to the gaging station as runoff (Carter and Godfrey, 1960). The maximum snowmelt computed for any one day was 2 inches. Rain that falls on a melting snowpack is transmitted through the snow with only minor lag; therefore, any rain that fell during the melt period was added to the snowmelt for that day. As a final step, the daily increment of melt water, in inches,

ART. 108 *IN* U.S. GEOL. SURVEY PROF. PAPER 475-C, PAGES C191–C193. 1963.

C191

produced in each altitude zone was converted to equivalent depth of water over the entire basin. It is this equivalent depth of water that is considered in the following paragraphs.

Because the rate (inches per hour) at which snow melts is slow, and because large parts of the basin become bare of snow as the season progresses, a large part of the melt reaches the river as subsurface flow. Consequently it was necessary to separate the melt and rainwater into surface runoff and subsurface flow and route each separately to the gaging station. After a few trial computations the following assumptions were adopted as criteria for this separation:

1. Throughout the melt season, the daily evapotranspiration loss is 0.10 inch.

2. When the snowline is at or below an altitude of 6,000 feet, the daily infiltration is 0.45 inch.

3. When the snowline is between 6,000 and 7,000 feet in altitude, the daily infiltration is 0.35 inch.

4. When the snowline is above an altitude of 7,000 feet, the daily infiltration is 0.25 inch.

5. The surface-runoff increment is the difference between available supply and infiltration. (On those days when infiltration exceeds available supply, the surface runoff is zero and the increment to ground water is the difference between available supply and evapotranspiration loss. On days when surface runoff occurs, the increment to ground water is the difference between infiltration and loss.)

6. There is a 5-day time lag between the infiltration of snowmelt or rain and the arrival of this infiltrated water in the ground-water reservoir.

The daily increment of water reaching the ground-water body was routed to the gaging station by a simple reservoir-type procedure to give the base-flow component of river discharge (Carter and Godfrey, 1960, p. 102). The daily increment of surface runoff was routed by using unit hydrographs. In the years of heavy snowfall, 1956 and 1958, the ratio of computed base flow to computed surface runoff was 5 to 3; in the year of light snowfall, 1959, this ratio was 14 to 1. The computed daily values of base flow and surface runoff were added together to give the synthesized total streamflow for each day of the three snowmelt seasons. Figure 108.1 is a comparison of synthesized and observed daily discharge.

The observed and the synthesized graphs agree satisfactorily, in general, thereby attesting to the soundness of the method used. It is not surprising that the synthesized discharge is too high during most of the snow-deficient year, 1959, when observed daily discharge ranged from a low of 750 cubic feet per second to a high of only 1,300 cf. Whenever the snowpack is very light, many areas within the snowfield soon become bare of snow. As the depth and water content of the snow are measured at snow courses, which are few in number and are mostly in sheltered sites, the estimate of water content of the snow over the basin tends to be too high. The hydrographs of synthesized and observed runoff would undoubtedly have agreed more closely in all 3 years had there been a wider coverage of snow-measurement data and weather data within the basin.

REFERENCES

Carter, R. W., and Godfrey, R. G., 1960, Storage and flood routing: U.S. Geol. Survey Water-Supply Paper 1543–B.

U.S. Army, Corps of Engineers, 1956, Snow hydrology, Summary report of the snow investigations: Portland, Oreg., North Pacific Division.

—— 1960, Runoff from snowmelt: Eng. Manual 1110–2–1406.
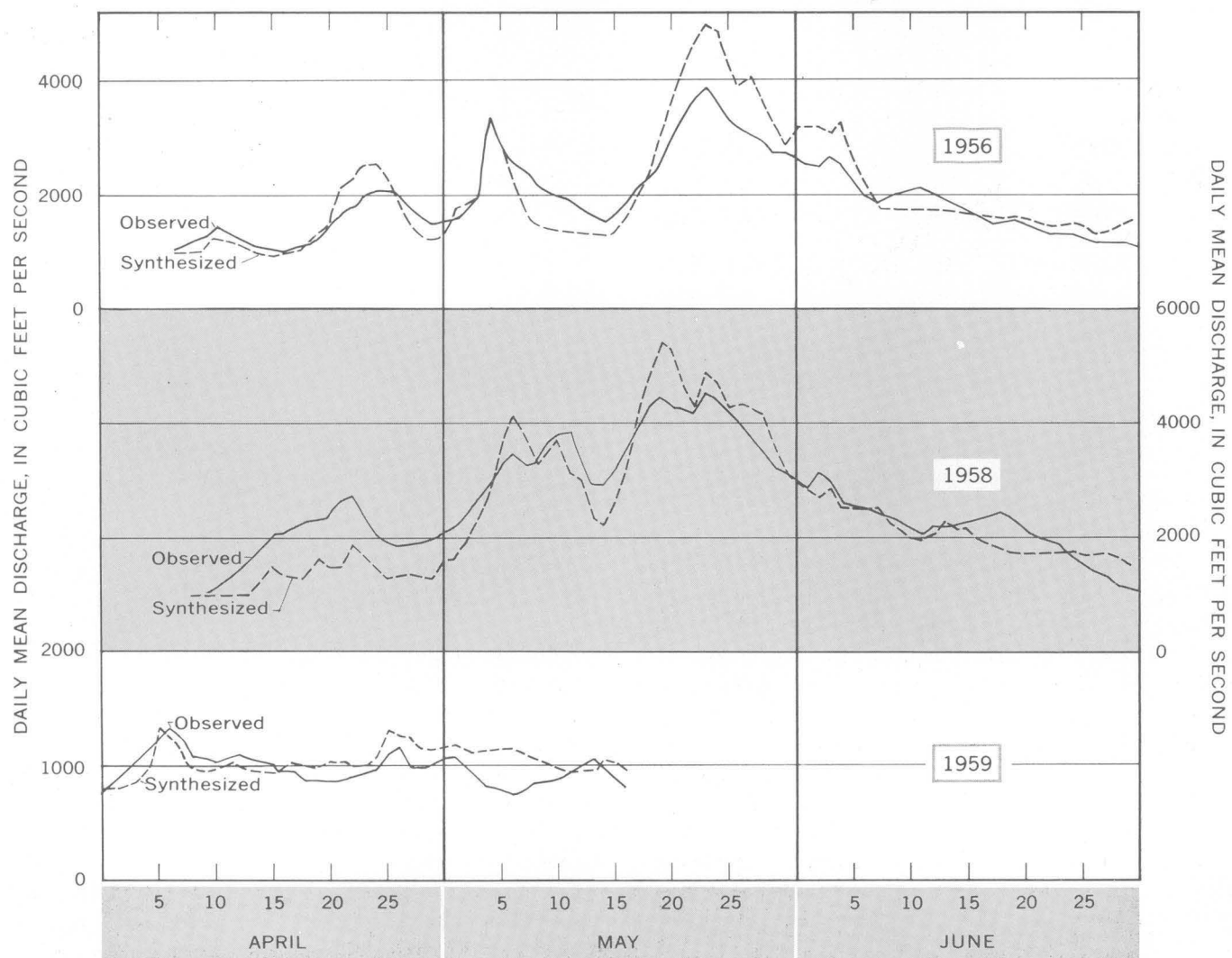
FIGURE 108.1.—Synthesized and observed daily runoff during the snowmelt seasons, North Yuba River below Goodyears Bar, Calif.

Article 109

FIELD VERIFICATION OF COMPUTATION OF PEAK DISCHARGE THROUGH CULVERTS

By C. T. JENKINS, Denver, Colo.

Abstract.—Tests on a battery of five 58- by 36-inch pipe-arch culverts show that, for the range tested, agreement is good between measured discharges and those computed indirectly from studies of small-scale models.

Tests made at a battery of five pipe-arch culverts indicate good agreement between results of indirect methods for computation of peak discharge at culverts and the results of current-meter measurements made under the most favorable conditions. The tests were made on the Colorado River about a mile downstream from Lake Granby, Colo., during March and April 1962. The methods of indirect computation are those outlined by Carter (1957), based on laboratory model tests made by the U.S. Geological Survey at Georgia Institute of Technology and on the results of previous tests by other investigators.

Carter (1957, p. 2 and pl. 1) identified six types of flow, classified according to the factor or factors that control the discharge through the culvert, and defined coefficients of discharge for each type for a large range in entrance geometry. Generally, flow conditions in a culvert at the time of peak discharge are not observed in the field, and the flow type must be deduced from criteria based on culvert geometry and relative elevations of high-water marks. However, during the tests below Lake Granby it was possible to classify the flow types by observation as Carter's types II and VI. The control for type II is critical depth at the outlet; for type VI, entrance and barrel geometry. Carter's coefficients for type-II flow are based generally on tests on models with barrel diameters of 4 to 6 inches, and those for type VI on tests on models 18 to 36 inches in diameter. The small models were either circular or rectangular in cross section; the larger models included corrugated pipe arches. Carter (1957, p. 19) specified that his type-VI coefficients apply to pipe arches, but did not state whether or not his type-II coefficients apply to shapes other than those tested. In practice, they are used for pipe arches as well as for circular sections.

Each of the culverts below Lake Granby was a 58- by 36-inch standard corrugated metal pipe arch 51 feet long. The culverts were about 9 feet apart center-to-center, and were laid on slopes ranging from 0.004 to 0.01. The entrance projections ranged from 1.2 to 2.8 feet from the embankment. The openings differed only slightly from the standard dimensions and shape given by the manufacturer.

During the test period, four discharges were held steady long enough for flow to stabilize through the culverts. Each flow was measured with a current meter at an excellent measuring section just below the lake. Surveys were made of the geometry of the culverts and the approach section and of water-surface elevations for each flow. Values of the discharges computed as outlined by Carter (1957, p. 2–10, 14) are shown in the accompanying table. Carter (1957, pl. 1) indicated that type-VI flow occurs only when the ratio of the height (h_1-z) of water above the upstream invert to the diameter (D) of the culvert is greater than 1.5; type-V flow was observed in the field in all five culverts when $(h_1-z)/D$ ranged from 1.34 to 1.45. However, Carter implied that the $(h_1-z)/D$ criterion is not inflexible, because he listed coefficients for "high-head" flow for $(h_1-z)/D$ ratios as small as 1.3.

Agreement between computed and measured discharge is good, indicating that, within the range tested,

ART. 109 *IN* U.S. GEOL. SURVEY PROF. PAPER 475–C, PAGES C194–C195. 1963.

C194

no serious error is introduced by applying the results of model tests to prototypes much larger than the model, and in some instances, substantially different in shape. However, similar field tests on other prototypes, especially at larger $(h_1-z)/D$ ratios, would be required to confirm completely the results of the model study. During such tests, the type of flow should be noted so that criteria for flow classification, as well as discharge coefficients, can be tested.

REFERENCE

Carter, R. W., 1957, Computation of peak discharge at culverts: U.S. Geol. Survey Circ. 376.

Comparison of measured and computed discharge for five culverts

Range of $(h_1-z)/D$	Type of flow [1]		Discharge		
	Observed in field	From Carter's criteria	Measured (cfs)	Computed (cfs)	Difference (percent)
0.92–1.03	II	II	244	246	+0. 8
.99–1.10	II	II	275	268	−2. 5
1.34–1.45	VI		373	374	+ .3
1.34–1.45		II	373	354	−5. 1
1.58–1.69	VI	VI	413	445	+7. 8

[1] Types of flow described by Carter (1957).

Article 110

USE OF LOW-FLOW MEASUREMENTS TO ESTIMATE FLOW-DURATION CURVES

By OLIVER P. HUNT, Albany, N.Y.

Abstract.—Flow-duration curves for streams where only a few low-flow measurements are available can be estimated on the basis of nearby gaged streams. The low-flow measurements must be made under base-flow conditions. A new technique is described for estimating low flows under these conditions.

Flow-duration curves for streams where only a few low-flow measurements have been made can be estimated by relating the discharge of these measurements to the concurrent discharge at gaging stations on one or more comparable streams for which flow-duration curves are already available. A method of estimating the flow-duration curves is described by Searcy (1959). A shorter method that gives practically the same results is described in this article. In both methods, the flow measurements must be made during periods when the flow consists largely of ground-water effluent (Langbein and Iseri, 1960, p. 5), and measurements must be made under several rates of base flow.

The records for three recording gages in Dutchess County, N.Y., were selected to illustrate the use of this method. Sites with actual gaging-station records were selected so that the duration curve developed by this method could be compared with the actual duration curve defined by many years of record. The stations used, with period of record available, are listed below:

Fishkill Creek at Beacon, N.Y. (1944–55).

Tenmile River near Gaylordsville, Conn. (1929–55).

Wappinger Creek near Wappingers Falls, N.Y. (1928–55).

As the records for the above stations were for different periods of time, all were extrapolated to a common base period, 1926–55. (See Searcy, 1959, p. 12–14).

On the assumption that Wappinger Creek is the unknown, a duration curve of daily flow was developed

on the basis of nine selected base-flow discharge measurements. The dates and discharges used are shown in columns 1 and 2 of table 110.1 Columns 3 and 4 are corresponding daily discharges from Tenmile River and Fishkill Creek, respectively. Columns 5 and 6 show the percentage of time that discharges in columns 3 and 4 were equaled or exceeded, obtained from base-period duration curves of daily flow for the Tenmile River and Fishkill Creek gaging stations.

Two independent duration curves of daily flow for Wappinger Creek were developed using logarithmic-probability paper (fig. 110.1). One of these curves was based on the Tenmile River record and one on the Fishkill Creek record. For the curve based on the Tenmile River record, discharges shown in column 2 of table 110.1 were plotted at percentages listed for the same date in column 5 of table 1. The smooth curve (solid line) on figure 110.1 was then drawn on the basis of these plotted points. A curve based on Fishkill Creek record (dashed line) was drawn in the same manner, using percentages shown in column 6 of table 110.1.

The hypothetical flow of Wappinger Creek estimated as described above is compared in table 110.2 with the actual flow as recorded at the gaging station near Wappingers Falls, N.Y., for the period 1926–55. The discharges shown in column 2 of table 110.2 were taken from the correlation curve based on the Tenmile River record (solid line) on figure 110.1 for selected percentages of time. Similarly, the discharges in column 3 of table 110.2 were taken from the correlation curve based on the Fishkill Creek record (dashed line) on figure 110.1. The average of columns 2 and 3 is listed in column 4. Column 5 lists the discharges taken from the actual duration curve of daily flow for Wappinger Creek for the base period 1926–55. Columns 6 and 7 indicate the difference (in cubic feet per second and in percent) between the mean of the duration curves

based on nine selected discharge measurements and that based on the 30-year base period 1926-55.

The mean duration curve of daily flow for Wappinger Creek developed by use of the nine discharge measurements compares very favorably. This close comparison is believed due to the fact that (1) the centroid of each drainage area used for correlation is within 20 miles of the Wappinger Creek site, (2) the precipitation pattern is similar for all three basins, and (3) discharge measurements, column 2 of table 110.1, were of base flow.

In any study involving the derivation of duration curves from base-flow measurements it is essential that precipitation patterns be comparable in the basins considered.

A substantial saving in time (about 50 percent) has been achieved by using the method described in this article in low-flow duration studies in New York. The results compare very closely with those obtained by using the procedure described by Searcy (1959).

TABLE 110.1.—Base-flow measurements for Wappinger Creek and concurrent daily discharges and percentage of duration for Tenmile River and Fishkill Creek

Date	Discharge measurement, Wappinger Creek (cfs)	Daily discharge (cfs)		Percent of time discharge equaled or exceeded that shown	
		Tenmile River	Fishkill Creek	Tenmile River	Fishkill Creek
1	2	3	4	5	6
1956:					
May 10_____	380	492	519	18	16
June 30_____	49	80	79	73	71
Aug. 18_____	20	25	24	95. 8	91
1957:					
May 10_____	118	139	130	60	60
July 11_____	14	17	11	98. 9	97
Sept. 13_____	4. 8	10	6. 0	99. 96	99. 3
1958:					
June 20_____	71	113	118	65	62
Aug. 20_____	17	31	18	92. 8	93. 7
Sept. 25_____	58	89	44	71	82. 5

FIGURE 110.1—Estimated duration curve of daily flow, Wappinger Creek, near Wappingers Falls, N.Y.

TABLE 110.2.—Comparison of estimated discharge for selected percent duration with discharge from base-period duration curve for Wappinger Creek

Percentage of time discharge equaled or exceeded that shown	Discharge from correlation curve (cfs)			Discharge of Wappinger Creek, from 1926-55 duration curve (cfs)	Difference between correlation curve and 1926-55 curve	
	Tenmile River	Fishkill Creek	Average of columns 2 and 3		cfs	Percent
1	2	3	4	5	6	7
20_____	355	340	348	390	−42	−10. 8
30_____	265	255	260	280	−20	−7. 1
40_____	200	190	195	200	−5	−2. 5
50_____	148	138	143	142	+1	+. 7
60_____	102	92	97	98	−1	−1. 0
70_____	61	57	59	63	−4	−6. 3
80_____	38	36	37	39	−2	−5. 1
85_____	30	28	29	30	−1	−3. 3
90_____	23	22	22. 5	22. 5	0	0
95_____	17	15	16	16	0	0
99_____	10	8. 4	9. 2	10. 2	−1. 0	−9. 8

REFERENCES

Searcy, J. K., 1959, Flow-duration curves, in Manual of hydrology, pt. 2, Low-flow techniques: U.S. Geol. Survey Water-Supply Paper 1542-A., p. 1-33.

Langbein, W. B., and Iseri, K. T., 1960, General introduction and hydrologic definitions, in Manual of hydrology, pt. 1, General surface-water techniques, U.S. Geol. Survey Water-Supply Paper 1541-A, p. 1-29.

Article 111

GRAPHICAL MULTIPLE-REGRESSION ANALYSIS OF AQUIFER TESTS

By C. T. JENKINS, Denver, Colo.

Abstract.—The graphical method of multiple regression described is well adapted to estimating the permeabilities of various layers of an aquifer from well-log and pumping-test data. Results of graphical analysis of a set of hypothetical data agree closely with the results of algebraic analysis of the same data.

Multiple regression has been used to solve several problems in hydraulics and hydrology. Among these are determination of stage-fall discharge relations, relations between basin characteristics and index floods, and low-flow characteristics of streams. Although, to the knowledge of the writer, the technique has not been widely used in analysis of well logs and of the results of pumping tests to estimate the permeabilities of various layers of an aquifer, it seems to be particularly well adapted to that purpose. The procedure in no way enhances the data. The results are subject to errors introduced by departure of the aquifer from the ideal and to errors in the data, but the "best" answers can be obtained quickly and simply.

The method used may be either algebraic or graphical. A graphical method probably is faster, if there are only a few tests and only 2 or 3 layers to be considered, and it has the advantage of revealing anomalous data readily. Curvilinear relations between the thickness of a material and its permeability hardly would be expected, but if such relations exist, they can be detected much more readily by the graphical method than by the algebraic method. On the other hand, the dependability of the results can be calculated if the algebraic method is used.

Both graphical and algebraic methods are described in many textbooks (for example, Ezekiel, 1941). The illustrations presented here are specific applications of long-known standard methods.

Selection of a "model" that the data are expected to follow is essential if the algebraic method is used, and highly desirable if the graphical method is used. The model for pumping-test analyses is obvious. Mathematically, the relation expected is expressed by the equation

$$X_1 = bX_2 + cX_3 + dX_4 \cdots, \qquad (1)$$

where X_1 is the transmissibility of the aquifer (the dependent variable), the coefficients b, c, d, $\cdots$ are the permeabilities of the various layers, and X_2, X_3, X_4, $\cdots$ are the corresponding thicknesses (the independent variables). The expected relation is the simplest form of multiple regression. The terms on the right side of the equation can be described graphically by straight lines through the origin with slopes b, c, d, $\cdots$ if X_2, X_3, X_4, $\cdots$ are plotted as abscissas against the parts of X_1 that are due to the transmissibilities of the corresponding layers as ordinates. Rigorous solution of the equation generally will show an intercept; that is, the calculations will indicate a finite value, either positive or negative, for transmissibility of the aquifer when all thicknesses are zero. A large value of the intercept is one indication that the data are not consistent.

The graphical method of evaluating the intercept and the coefficients b, c, d, $\cdots$ for the hypothetical data shown in the accompanying table is illustrated in figure. 111.1.

The steps are:

1. Plot the transmissibility of the aquifer as the ordinate against the independent variable that is estimated to have the greatest effect (in this case, the thickness of the gravel, X_2). Draw curve 1 as the average of the points.

2. Draw curve 2 through the origin parallel to curve 1.

3. Measure the vertical deviation of each point from curve 2 with dividers and plot it as the ordinate against the variable that has the second greatest effect (in this case, the thickness of sand and gravel mixed, X_3) as the abscissa. Draw curve 3 as the average of these points.

4. Draw curve 4 through the origin parallel to curve 3.

5. Plot the vertical deviations from curve 4 of each point against the thickness of sand. Draw curve 5 as the average of these points. This line generally will not pass through the origin. Because it is known that there should be no intercept for the curve showing the estimated transmissibilities of various thicknesses of sand, it might seem logical to draw a line through the origin parallel to curve 5. This can be done, but it is not necessary. At this point in the analysis, the posi-

tions of the curves make little difference; it is their slopes that are important, because the slopes represent the first estimates of the permeabilities.

6. The next step is to remove the estimated effects of the last two variables from the plotted position of the points that defined curve 1. For example, well 9 penetrates 20 feet of sand and 24 feet of sand and gravel (see table). From curve 5, the estimated effect for 20 feet of sand is 80,000 gallons per day per foot and for 24 feet of sand and gravel, 110,000 gpd per ft—a total of 190,000. The transmissibility is 750,000 gpd per ft,
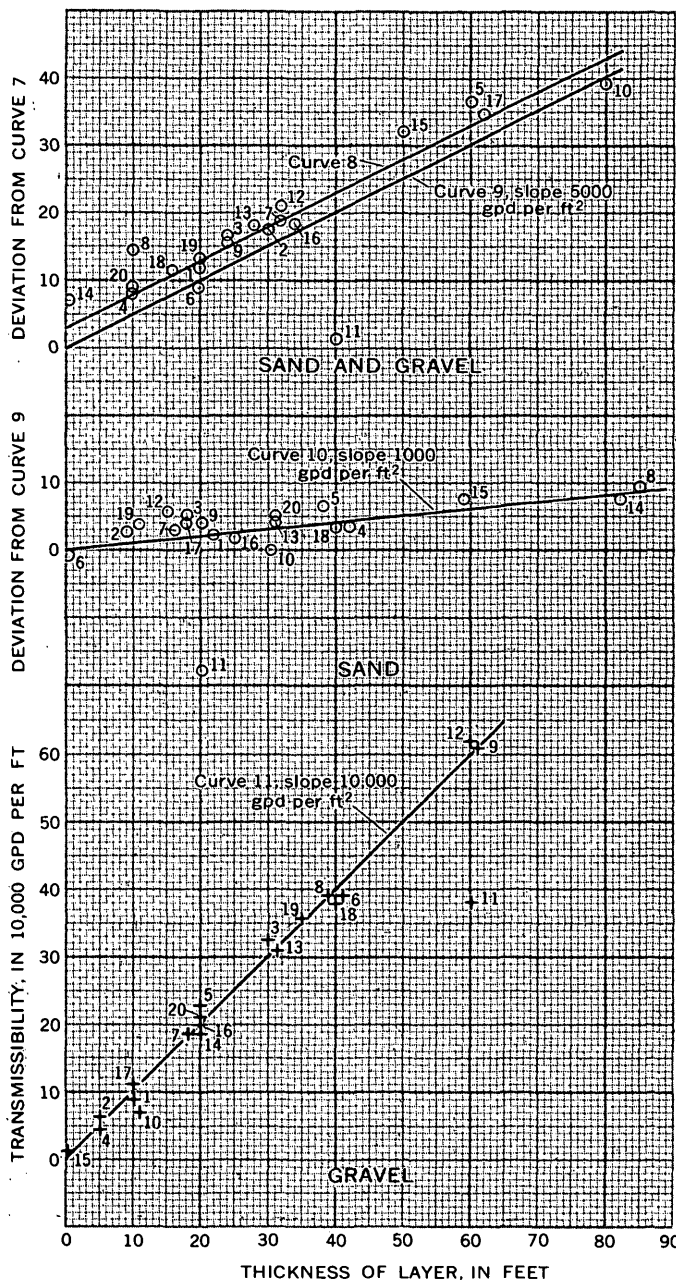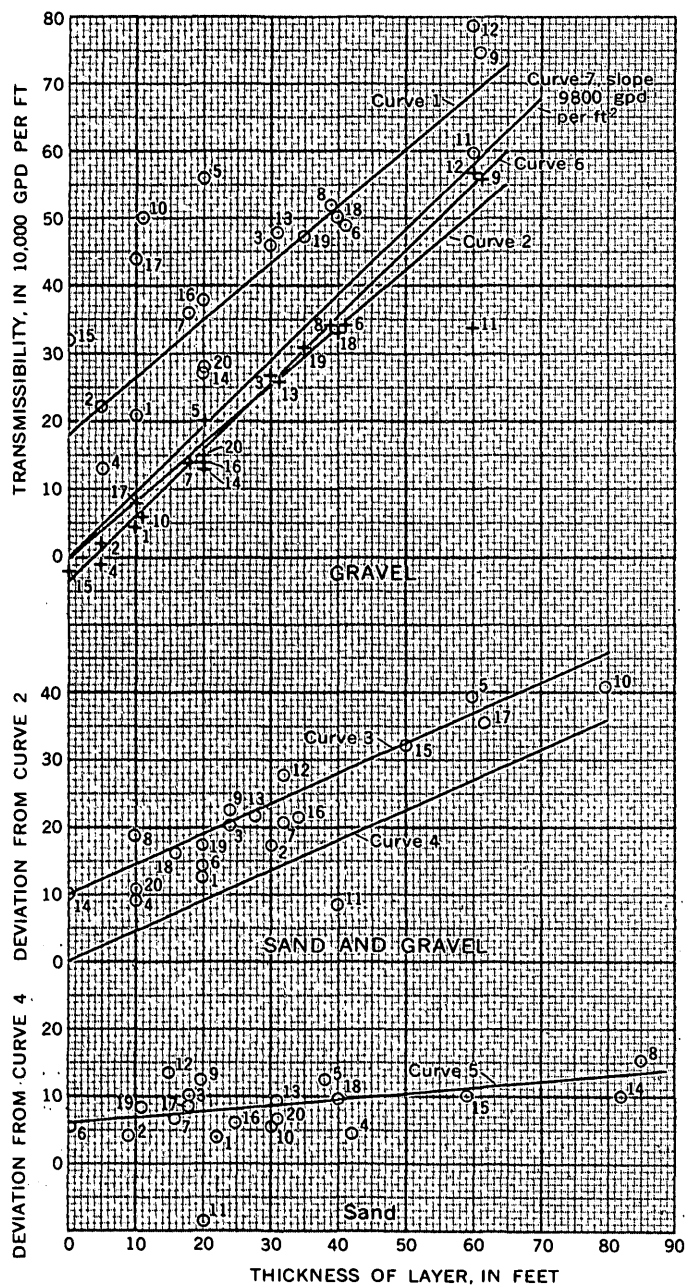
FIGURE 111.1.—Graphical determination of multiple-regression equation from pumping-test data and well logs.

so the adjusted ordinate value in units of 10,000 gpd per ft is 75−19=56. This value represents the new estimate of the transmissibility of 61 feet of gravel, and the plotted position is indicated by a plus sign on the first diagram. Similar treatment of the other points results in a new scatter diagram.

The excessive deviation of the point for well 11 indicates that the data from well 11 are anomalous. Either the data are in error, or the aquifer differs from that penetrated by the other 19 wells. Data from well 11 were not considered in the rest of the analysis.

7. Draw curve 6 as the average of the plotted plus signs.

8. Draw curve 7 through the origin parallel to curve 6.

9. Plot the vertical deviations from curve 6 of the originally plotted points against the thickness of the sand and gravel mixture. Draw curve 8 as the average of the plotted points. Draw curve 9 through the origin parallel to curve 8.

10. Draw curve 10 through the origin if possible.

If the intercept of curve 10 differs appreciably from zero, or if the remaining scatter seems excessive, steps 6 through 10 can be repeated; otherwise, the slopes of curves 7, 9, and 10 are the "best" estimates of the permeabilities of the materials. The scatter about curve 10 and its intercept, if any, are related to the scatter and intercepts of all three curves, 7, 9, and 10, and are measures of the consistency of the data and the completeness of the solution.

Hypothetical data from pumping tests and well logs

Well No.	Transmissibility, (gpd per ft) X_1	Thickness of gravel (ft) X_2	Thickness of sand and gravel (ft) X_3	Thickness of sand (ft) X_4
1	210,000	10	20	22
2	220,000	5	30	9
3	460,000	30	24	18
4	130,000	5	10	42
5	560,000	20	60	38
6	490,000	41	20	0
7	360,000	18	32	16
8	520,000	39	10	85
9	750,000	61	24	20
10	500,000	11	80	30
11	600,000	60	40	20
12	790,000	60	32	15
13	480,000	31	28	31
14	270,000	20	0	82
15	320,000	0	50	59
16	380,000	20	34	25
17	440,000	10	62	18
18	500,000	40	16	40
19	470,000	35	20	11
20	280,000	20	10	31

The lack of an intecept by curve 10 and the small scatter about the curve probably would satisfy most investigators, but the procedure outlined in step 6 has been repeated, resulting in curve 11, to illustrate that a further reduction in scatter can be attained. The slope of curve 11 is nearer to the correct permeability of gravel than that of curves 6 and 7.

The regression equation resulting from the graphical analysis is

$$X_1 = 10,000 \text{ gpd/ft}^2 X_2 + 5,000 \text{ gpd/ft}^2 X_3 + 1,000 \text{ gpd/ft}^2 X_4 \qquad (2)$$

The coefficients of X_2, X_3, and X_4 are, respectively, the permeabilities of gravel, sand and gravel mixture, and sand.

The technique illustrated has been outlined in great detail in the interests of clarity, but several variations that entail a little less labor can be used. The two most important involve steps 1 and 6.

In many analyses, it may be possible to make a better first estimate of the slope of curve 1 than that of a line through the average of the points. The investigator may know intuitively the approximate value of the permeability of the gravel. If so, he can eliminate curve 1 and draw curve 2 initially. In some analyses, a good estimate of the slope of curves 1 and 2 can be made by considering only those data that have equal, or nearly equal, values of the second (and the third, if possible) most important independent variable. For example, in the illustration given, wells 2, 7, 12, and 16 penetrate between 30 and 34 feet of the sand and gravel mixture, and the range both in the transmissibilities of the sections penetrated and thicknesses of gravel is wide. If curve 1 had been drawn through these 4 points, the resulting slope would have been 9,400 gpd per ft^2, much closer to the final value of 10,000 than the slope of 8,600 that resulted from drawing curve 1 as the average of all the points.

The arithmetic involved in step 6 can be eliminated by applying, with dividers, the vertical deviation of the plotted points from curve 5 to curve 2, thus determining the position of the points that define curve 6. For example, point 9 is about 40,000 gpd per ft above curve 5, and its position as a plus sign in the first diagram is about 40,000 gpd per ft above curve 2, plotted against 61 feet, the thickness of gravel in well 9. Similarly, point 20 is about 20,000 gpd per ft below curve 5, and it is plotted as a plus sign 20,000 gpd per ft below curve 2.

The best estimate of the permeabilities can be obtained without using curves 2, 4, 7, and 9, but if curves 7 and 9 are not used, it will not be possible to measure the intercept, if any, of curve 10.

All variations of the graphical method will give the same results within the limitations of plotting accuracy and individual judgment as to what represents acceptable scatter.

The mechanics of the algebraic method will not be discussed herein (see Ezekiel, 1941, or other texts), but the resulting equation (excluding data from well 11) is

$$X_1 = -800 \text{ gpd per ft} + 10{,}000 \text{ gpd per ft}^2 X_2 + 5{,}020 \text{ gpd per ft}^2 X_3 + 900 \text{ gpd per ft}^2 X_4$$

$$(3)$$

The close agreement between equations 2 and 3 illustrates that the graphical method, used with a reasonable degree of care, gives results consistent with those computed algebraically.

REFERENCE

Ezekiel, Mordecai, 1941, Methods of correlation analysis 2d ed.: New York, John Wiley and Sons, Inc., 531 p.

Article 112

NOMOGRAPH FOR COMPUTING EFFECTIVE SHEAR ON STREAMBED SEDIMENT

By BRUCE R. COLBY, Lincoln, Nebr.

Abstract.—A nomograph for computing effective shear on bed-sediment particles from known mean velocities is given and explained. It is based on a slightly different velocity equation from the one that is commonly used, and it eliminates the need for trial-and-error computations of effective shear.

Unless a streambed is approximately plane, only part of the total shear on the bed is effective in moving sediment on the bed, and this part is related to mean velocity and to bed configuration (Einstein, 1950, p. 9–10). Because bed configuration may vary widely and somewhat unpredictably in alluvial streams, the effective shear frequently is computed from known mean velocity. This article presents a nomograph for computing one measure of the effective shear from known mean velocity.

Probably the most commonly used equation for computing effective shear is one based on work by Keulegan (1938) and given by Einstein (1950, p. 10) as

$$\frac{\bar{u}}{\sqrt{gR'S}}=5.75 \log_{10}\left(\frac{12.27\,R'x}{k_s}\right), \qquad (1)$$

in which

$\bar{u}$=mean velocity for a cross section;

$\sqrt{gR'S}$=shear velocity with respect to sediment particles (a specific form of effective shear on bed sediment);

g=acceleration caused by gravity;

R'=hydraulic radius with respect to particles;

S=energy gradient;

x=parameter for transition from a hydraulically rough to a hydraulically smooth boundary; and

k_s=grain roughness, usually assumed equal to diameter for which 65 percent of bed sediment by weight is finer.

The two numerical constants in this equation need further explanation. The constant 5.75 equals 2.30, the natural logarithm of 10, divided by the turbulence constant, k, which is here assumed to equal 0.40. The constant 12.27 is based on an equation given by Keulegan (1938, p. 722, eq. 60) and should be about correct for the particular form correction that applies to a rectangular channel whose hydraulic radius is 0.10 of the width. The constant would be about 11.6 rather than 12.27 for a rectangular channel whose hydraulic radius is 0.05 of its width. For such a channel the ratio of hydraulic radius to average depth, R/d, is 0.90, which is lower than the ratio for many natural channels. For an infinitely wide rectangular channel, the constant is the antilog of 6.00/5.75 (Keulegan, 1938, p. 717, eq. 38) or 11.1. The effect of a change from 11.1 to 12.27 under the log sign is usually small, so that a precise constant is not required, but a logical constant might be 11.4 or 11.5 for many natural channels.

However, the use of average depth rather than hydraulic radius is convenient and is, in general, sufficiently accurate for most natural streams. Hence, in the following discussion and definition of a practical nomograph, $11.1d$, a quantity that is theoretically indicated for infinitely wide rectangular channels, has been used as follows:

$$\frac{\bar{u}}{\sqrt{g(RS)_m}}=5.75 \log_{10}\left(\frac{11.1\,dx}{k_s}\right). \qquad (2)$$

The use of the hydraulic radius R under the log sign is consistent with Keulegan's (1938) equations, but Einstein (1950, p. 10) changed the R under the log sign to R', presumably when he changed the shear velocity u_* (equals $\sqrt{gR'S}$) to the shear velocity with respect to the particles u_*' (equals $\sqrt{gRS}$).

Two items should be noted with respect to the use of R rather than R' under the log sign. One item is that the equation 2 can be derived directly by integration of the point-velocity equation that was used by Einstein (1950, p. 8, eq. 3) from the streambed to a distance d

above the bed. Hence, equation 2 correctly gives the average velocity at a stream vertical whose point velocities conform to the point-velocity equation used by Einstein. The second item is that the measure of depth, whether R or d, under the log sign has the nature of an upper limit for the integration of point velocities along a vertical. If R' is used under the log sign, the mean velocity $\bar{u}$ presumably should represent a mean for only that part of the cross section that is within a distance R' from the channel boundary, and this is a difficult mean velocity to determine by measurement.

Because of the change under the log sign from R' to R or to d, a change that is usually far greater than the relatively insignificant change from 12.27 to 11.1, $\sqrt{gR'S}$ or u'_* computed from equation 1 may differ appreciably for some flows from u_*, computed from equation 2.

Several other uncertainties may arise with respect to the applicability of equation 2, but the only one of these to be discussed in this short article is the variability of k. Einstein and Chien (1954, fig. 12) showed a decrease of k with an increase in a measure of the energy that is required to transport suspended sediment over relatively smooth sand beds. Hubbell and Matejka (1959, p. 71, 72, and 74) reported values for k much higher than 0.40 for some flows over dune beds. Sayre and Albertson (1961, p. 144–147) also found k much higher than 0.40 for flows over relatively widely spaced rigid baffles. (The term k is used here although some of the constants probably should not be called turbulence constants.) An experimentally determined turbulence constant for a given flow may be used, if it is considered to be more suitable than 0.40, by replacing 5.75 in equation 2 with 2.30/k.

The mean-velocity equation in the form

$$\frac{\bar{u}}{\sqrt{(RS)_m}}=5.75\sqrt{g}\,\log_{10}\left(\frac{11.1\,dx}{k_s}\right)$$

$$=34.0+32.6\left(\log_{10}\frac{d}{k_s}+\log_{10}x\right) \tag{3}$$

can be solved for $\sqrt{(RS)_m}$ by trial and error, either arithmetically by estimating a value of x and repeating the computation for $\sqrt{(RS)_m}$ or graphically according to a method given by Colby and Hubbell (1961, p. 3–5 and pl. 1). The trial-and-error feature of the computation can be eliminated by use of the nomograph shown on figure 112.1.

The principles involved in the nomograph are fairly simple. Equation 3 shows that the ratio $\bar{u}/\sqrt{(RS)_m}$

has a constant relation to the logarithm of (xd/k_s) if g and the turbulence constant k are both constant. That is, according to equation 3, $\bar{u}/\sqrt{(RS)_m}$ is determined uniquely by xd/k_s, if g and k are constant. Thus, a horizontal line on the main graph of figure 112.1 represents both a single value of $\bar{u}/\sqrt{(RS)_m}$ on the left-hand scale and the uniquely equivalent value of xd/k_s on the right-hand scale. When $x=1.00$ on the right-hand part of the graph, the boundary is hydraulically rough, and $d/k_s=xd/k_s$. If x is not equal to 1.00, $\log x$ is not zero, and the curved line for a particular value of d/k_s is below or above the horizontal line for a hydraulically rough boundary by 32.6 $\log x$ units on the $\bar{u}/\sqrt{(RS)_m}$ scale.

The horizontal scale of the graph is expressed as a function of x and the ratio $\bar{u}/\sqrt{(RS)_m}$. Einstein defined x in terms of $k_s\sqrt{gR'S}/(11.6\nu)$ in which ν is the kinematic viscosity. The experimental basis for the definition of x is given by Keulegan (1938, p. 713–715). For the nomograph, x is in terms of the quantity 1,000 $k_s\sqrt{(RS)_m}/(\nu\,10^5)$, which requires a reduction from Einstein's function of x in the ratio of 11.6 · 1,000/(100,000$\sqrt{g}$) or 0.0204. This quantity multiplied by $\bar{u}/\sqrt{(RS)_m}$ gives 1,000 $k_s\bar{u}/(\nu\,10^5)$. If $\bar{u}$, k_s, and ν are known, the horizontal scale determines a vertical line that corresponds to the logarithm of the product of the function of x and $\bar{u}/\sqrt{(RS)_m}$. The intersection of this vertical line with the curve for a known d/k_s ratio determines a $\bar{u}/\sqrt{(RS)_m}$ ratio from which $\sqrt{(RS)_m}$ can be computed directly for the known $\bar{u}$. If the quantity P (Einstein, 1950, p. 40) is needed for computing sediment discharge, it is directly proportional to $\bar{u}/\sqrt{(RS)_m}$ and can be taken from the scale near the left side of the nomograph. In other words, a horizontal line from the intersection of the vertical line and a curve for the d/k_s ratio gives $\bar{u}/\sqrt{(RS)_m}$ and P on the two left-hand scales.

The small graph at the right of figure 112.1 shows $\nu \cdot 10^5$ in terms of temperature.

The measures on the horizontal scale and on the right-hand vertical scale are dimensionless. The ratio $\bar{u}\sqrt{(RS)_m}$ is in units of feet and seconds but can readily be made dimensionless by dividing each ratio by 5.68 which is the square root of 32.2. The small graph at the right is not in dimensionless quantities but a new horizontal scale and curve can easily be added for cgs units.

If a variable k is to be used rather than a constant k of 0.40 the adjustment for the variable k can be made on the nomograph by multiplying the left-hand scale by 0.40/k.

The $\sqrt{(RS)_m}$ values from the nomograph are roughly 1 percent lower, at least for many flows, than the $\sqrt{(RS)_m}$

values that can be obtained from equation 2 with 12.27 substituted for 11.1. The values can be determined considerably more rapidly and conveniently from the nomograph than by arithmetic trial-and-error computation and a little more rapidly and conveniently than from the procedure given by Colby and Hubbell (1961).

REFERENCES

Colby, B. R., and Hubbell, D. W., 1961, Simplified methods for computing total sediment discharge with the modified Einstein procedure: U.S. Geol. Survey Water-Supply Paper 1593, 17 p.

Einstein, H. A., 1950, The bed-load function for sediment transportation in open channel flows: U.S. Dept. Agriculture Tech. Bull. 1026, 70 p.

Einstein, H. A., and Chien, Ning, 1954, Second approximation to the solution of the suspended load theory: California Univ. Inst. Eng. Research, Missouri River Div. Sediment Ser. 3, 30 p.

Hubbell, D. W., and Matejka, D. Q., 1959, Investigations of sediment transportation, Middle Loup River at Dunning, Nebr.: U.S. Geol. Survey Water-Supply Paper 1476, 123 p.

Keulegan, G. H., 1938, Laws of turbulent flow in open channels: U.S. Natl. Bur. Standards Jour. Research, v. 21, p. 707–741.

Sayre, W. W., and Albertson, M. L., 1961, Roughness spacing in rigid open channels: Am. Soc. Civil Engineers Proc., v. 87, no. HY 3, p. 121–150.
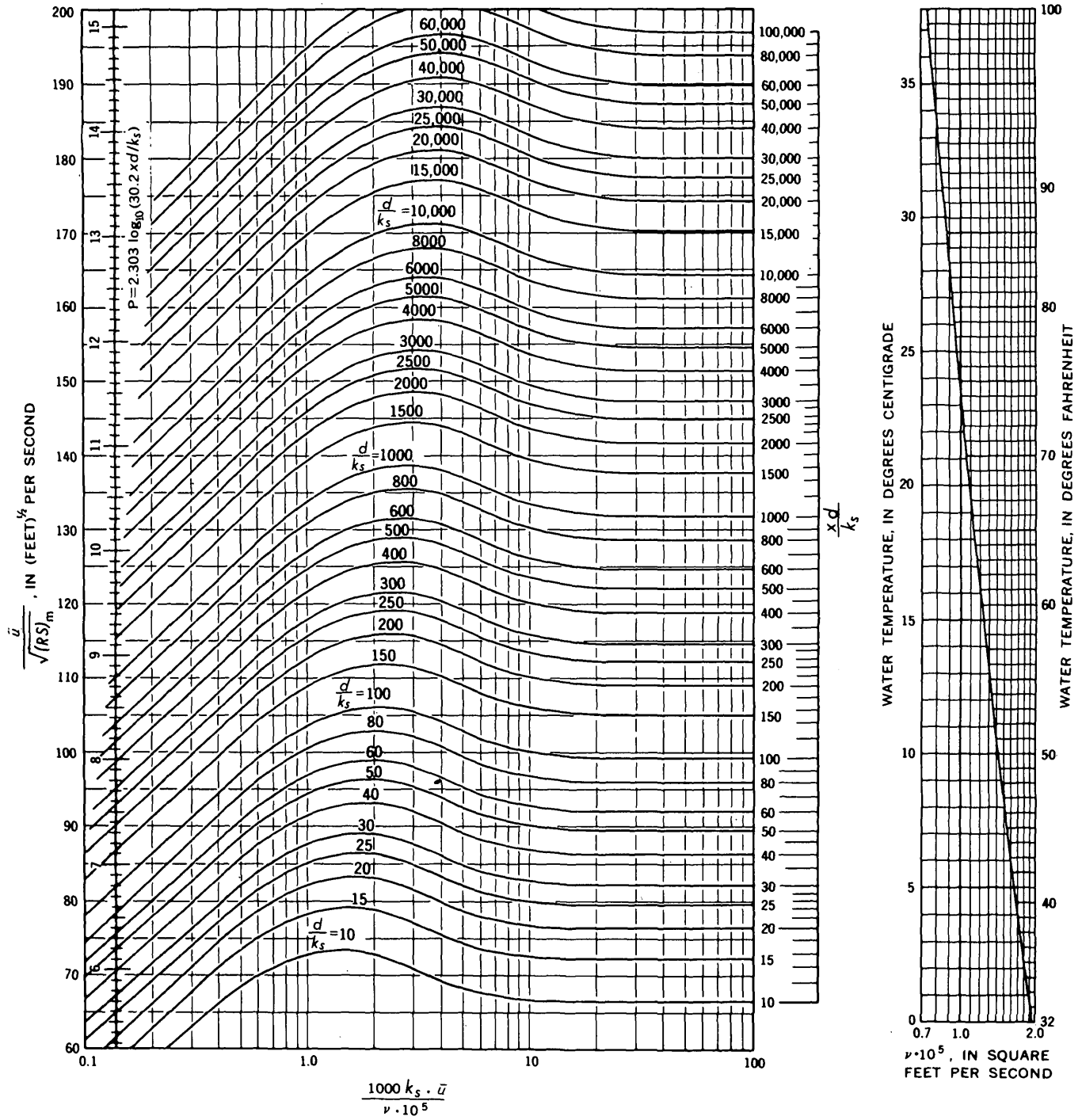
FIGURE 112.1.—Nomograph for computing $\sqrt{(RS)_m}$.

Article 113

DISTRIBUTION OF SHEAR IN RECTANGULAR CHANNELS

By JACOB DAVIDIAN and D. I. CAHAL, Washington, D.C.

Abstract.—Distribution patterns of boundary shear, measured with a Preston tube, were determined in a smooth, rectangular flume at depths of 5 and 8 inches. A shift in aspect ratio towards two-dimensional flow, or an increase in Froude number from 0.1 to 1.5, tended to produce a more uniform shear distribution throughout the boundary.

An analysis of the distribution of shear in open-channel flow will materially contribute to an understanding of the hydraulic geometry and geomorphic evolution of channel systems. Therefore, shear values along the boundary of an open rectangular channel were computed from Preston-tube measurements, and their distribution was examined with the view toward understanding the basic principles governing the self-formation of natural river channels.

The Preston method for the determination of local skin friction with the use of a surface pitot tube has been well described by Hsu (1955). It is assumed that in turbulent flow there is a region in the boundary layer near the wall or floor surface where the conditions are a function only of the surface friction, the physical properties of fluid, and a representative length. A universal, nondimensional relation is obtained between surface friction, the difference between the pressure in the pitot tube and the static pressure on the surface, and the pitot diameter,

$$\log \tau_o d^2/4\rho\nu^2 = -1.372 + (7/8) \log (p_t - p_o)d^2/4\rho\nu^2,$$

with its limits of applicability, $4.5 < \log (p_t - p_o)d^2/4\rho\nu^2 < 6.5$, where τ_o is boundary shear, d is the pitot diameter, ρ and ν are mass density and kinematic viscosity of water, and $(p_t - p_o)$ is the pressure difference.

All experimental data were collected at the National Bureau of Standards Hydraulic Laboratory at a cross section about 118 feet downstream from the entrance of a smooth tiltable flume 140 feet long, 18 inches wide, and at normal depths of flow of 5 inches and 8 inches.

The variation of the friction factor f, within a Froude number range from $F = 0.1$ to 1.5, and a Reynolds number range from $R = 6 \times 10^4$ to 6×10^5, is well described by the equation $1/\sqrt{f} = 2.03 \log R \sqrt{f} - 1.21$.

The shear values computed from the Preston-tube measurements around the wetted perimeter of the cross section were all plotted, and, by means of a planimeter, average shears were determined for the walls, floor, and entire cross section. The average shear thus computed for an entire cross section was compared with the value of shear as determined by the du Boys equation, $\tau_o = \gamma RS$, in which γ is the unit weight of water, R is the hydraulic radius, and S is the floor slope. In general, the measured (Preston-tube) shear was about 5 percent less than the computed (du Boys) shear.

The patterns that the shear distributions around the boundaries take, as determined by the Preston tube, are of interest from the viewpoint of fluvial mechanics. In figure 113.1, an increase in Froude number is associated with the following changes in shear distribution:

(1) the ratio of the maximum wall shear to the average wall shear decreases towards unity,

(2) the ratio of the average floor shear to the average total cross-sectional shear decreases towards unity,

(3) the ratio of the average wall shear to the average floor shear increases towards unity.

In figure 113.2 the ratio of average floor shear to average total cross-sectional shear is plotted as the ordinate, and the ratio of depth to width of flow is plotted as the abscissa. The short horizontal lines show the center of gravity of the data points for each depth-width ratio, and suggest a decrease in the shear ratio towards unity with a decrease in the depth-width ratio. For each aspect-ratio set of data, those points having the smaller shear-ratio values also tend to have the higher Froude numbers, a tendency also noted in the middle curve of figure 113.1.
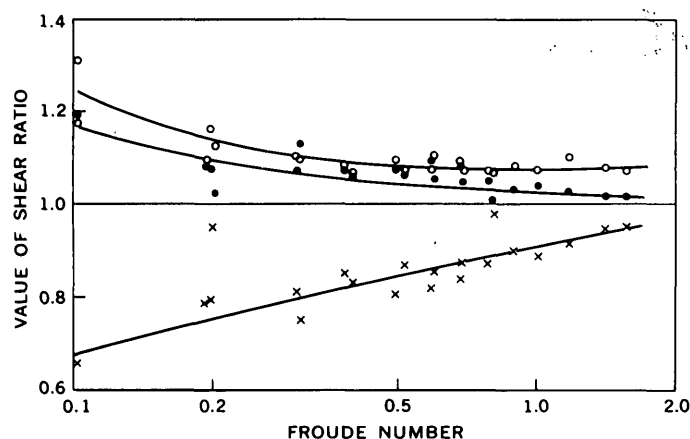
FIGURE 113.1.—Variation in shear distribution with Froude number. Top curve (circles), ratio of maximum wall shear to average wall shear; middle curve (dots), ratio of average floor shear to average cross-sectional shear; bottom curve (X's), ratio of average wall shear to average floor shear. Plotted data include 5-inch and 8-inch depths.
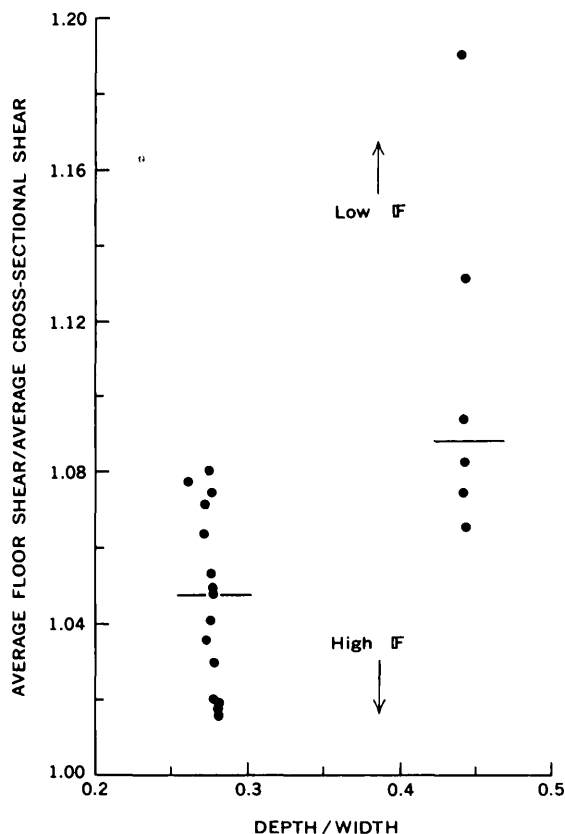
FIGURE 113.2.—Variation in shear distribution with aspect ratio.

Along with the increasingly more uniform shear distributions at the boundary, velocity distributions in the channel also tend to become more uniform with an increase in Froude number, as would be expected. Complete velocity traverses for each run were made at the test cross section. At all depths, the transverse velocity distributions are more parabolic in shape for low than for high Froude numbers, having more of a lag at the side walls and more of a peak at the center of the flume.

From these tests, it is apparent that a shift in aspect ratio toward two-dimensional flow, or an increase in Froude number (trends similar to figure 113.1 would have been evident if velocity or Reynolds number were used as the abscissa instead of F), will tend to produce a more uniform shear distribution in the boundary. The relations shown in figures 113.1 and 113.2 can be examined for an appreciation of the geomorphic evolution of channel systems.

Most natural streams flow at values of F below 0.3, and are reasonably stable. Instances of natural stream flow at $F > 0.6$ are infrequent. The trend for proportionately larger wall shears along with larger Froude numbers (bottom curve, fig. 113.1) suggests the possibility that banks in a natural stream will erode until the Froude number and wall-floor shear ratio are decreased again to values associated with stream stability. For any given discharge and a given "stable" value of F for a particular stream, an increase in width due to erosion will tend to bring about a decrease in depth, and a larger width-depth ratio. Leopold and Maddock (1953, p. 29) bring attention to the works of others who claim that natural streams do indeed tend to develop large width-depth ratios:

. . . To be stable, the channel carrying bed loads, therefore, should have a higher velocity along the bed, but the same velocity along the banks, and this could only occur with a wider, shallower section. . . . Indian rivers tend to adopt broad, shallow sections, and . . . this type of cross section is best adapted for the transportation of heavy silt.

The rigid test flume cannot adjust its shape, of course, but at low Froude numbers (and also at large depths or small width-depth ratios), it is evident from figures 113.1 and 113.2 that the values of shear around the perimeter tend to be more peaked or less uniform on the wall (top curve, fig. 113.1), higher on the floor than the average shear (middle curve, fig. 113.1; fig. 113.2), and smaller on the wall than on the floor (bottom curve, fig. 113.1).

An alluvial stream will react to nonuniform shear stresses by erosion and deposition. Such a natural stream, which has had opportunity to adjust and react to the shear patterns of figures 113.1 and 113.2 imposed by the flow of water through it and which has achieved a reasonably stable shape for the low Froude-number range at which it usually flows, could develop a cross section that is broad, has a large width-depth ratio, and is gently curved upwards towards the shores from a slightly deeper middle region.

REFERENCES

Leopold, L. B., and Maddock, Thomas, Jr., 1953, The hydraulic geometry of stream channels and some physiographic implications: U.S. Geol. Survey Prof. Paper 252, 57 p.

Hsu, E. Y., 1955, The measurement of local turbulent skin friction by means of surface pitot tubes: The David W. Taylor Model Basin Research and Devel. Rept. 957.

⚒

SULFATE AND NITRATE CONTENT OF PRECIPITATION OVER PARTS OF NORTH CAROLINA AND VIRGINIA

By A. W. GAMBELL, Washington, D.C.

Abstract.—Preliminary data from a precipitation-sampling network covering a 34,000-square-mile study area suggest that the atmosphere is a major source of sulfate and nitrate in the stream waters of southern Virginia and eastern North Carolina.

The chemical composition of atmospheric precipitation has been the subject of several investigations in recent years. Studies by Junge and Werby (1958) and Eriksson (1959; 1960) are only two of the more recent investigations indicating that the atmosphere is a potential source of large quantities of water-soluble material. To learn more about the origin of this material, the processes by which it is introduced into precipitation, and, ultimately, its role in determining the quality of water, a network of precipitation-sampling stations has been established covering a well-defined drainage area. This article presents data obtained from the first month of network operation. Average concentration and approximate total load of the major ionic constituents in precipitation have been computed. Some general comparisons with river-quality data illustrate the magnitude of atmospheric contributions to stream waters. Interpretation of the data is, of necessity, quite limited. Detailed interpretation will be reserved for a later time when data for a longer period are available.

NETWORK DESIGN AND EQUIPMENT

In July 1962, 28 precipitation-sampling stations were established in North Carolina and Virginia. These stations form a network covering approximately 34,000 square miles, drained by 5 major streams: the Chowan, Roanoke, Tar, Neuse, and Cape Fear Rivers. The area included in the network is shown in figure 114.1 and location of the stations is shown in figures 114.2 and 114.3. Each sampling station is located at a U.S. Weather Bureau cooperative observer site. With one or two exceptions, sampling stations were purposely located outside the larger metropolitan areas. This was done to minimize contamination from local sources. The principal exception is the sampling station at Norfolk, Va. It is in the center of the city; accordingly, the precipitation has a high sulfate content.

Each sampling station is equipped with a standard 8-inch precipitation gage and a special collecting device. The collecting device consists of a 5-inch-diameter glass funnel mounted in the top of an insulated enclosure. The funnel drains through a polyethylene tube into a polyethylene bottle in the interior of the enclosure. The entire device is mounted with the rim of the collecting funnel 5 feet from the ground. The funnel is continuously open and therefore collects a certain amount of dry fallout as well as precipitation. Composite samples are collected monthly from each station and analyzed for sulfate, chloride, nitrate, sodium, calcium, and potassium.

MINERAL CONTENT OF RAINFALL AND STREAM WATERS

Precipitation over the network area during August 1962 averaged slightly less than 4 inches. The heaviest precipitation fell in the southeastern part of the network; however, the amounts were reasonably uniform throughout the area.

The areal variations of the major ionic constituents in precipitation are of considerable interest because they furnish valuable clues as to the source of these materials.

ART 114 *IN* U.S. GEOL. SURVEY PROF. PAPER 475-C, PAGES C209–C211. 1963.

C209

Although only sulfate and nitrate are discussed here, the distribution of sodium, chloride, and calcium also displayed discernible patterns during August.

Figure 114.2 illustrates two important features of the areal variation in sulfate concentration. It shows first that sulfate is widely prevalent in precipitation on the study area in August 1962 and, second, that the sulfate concentration increases inland from less than 1.5 parts per million along the Atlantic Ocean to more than 4.5 ppm in the northwestern part of the area. This trend of increasing concentration landward is contrary to what would be anticipated if the ocean were the principal source of atmospheric sulfate.

The occurrence of sulfur in the atmosphere was discussed by Junge (1960). In unpolluted areas sulfur occurs primarily in three forms: as SO_4^{-2} in aerosols, and as SO_2 and H_2S gas. Sea-salt aerosols, soil dust, and the oxidation of SO_2 and H_2S are sources of SO_4^{-2}. A large part of the SO_2 in the atmosphere originates from the combustion of fossil fuels. Most of the H_2S in the atmosphere is probably of natural origin, resulting from the decay of organic material. Although the role played by these substances is not completely understood, previous studies suggest that industrial activity and sea-salt aerosols are the predominant sources of atmospheric sulfur. Because there is little industry in the western part of the network area, a source other

EXPLANATION

A
Location of river-quality sampling stations

Drainage area represented by river-quality sampling stations

Boundary of drainage area

Figure 114.2.—Sulfate content of precipitation (parts per million) on study area, August 1962. Isopleth interval, 1.0 ppm.

Figure 114.1.—Precipitation-sampling network (shaded area).

EXPLANATION

A
Location of river-quality sampling stations

Drainage area represented by river-quality sampling stations

Boundary of drainage area
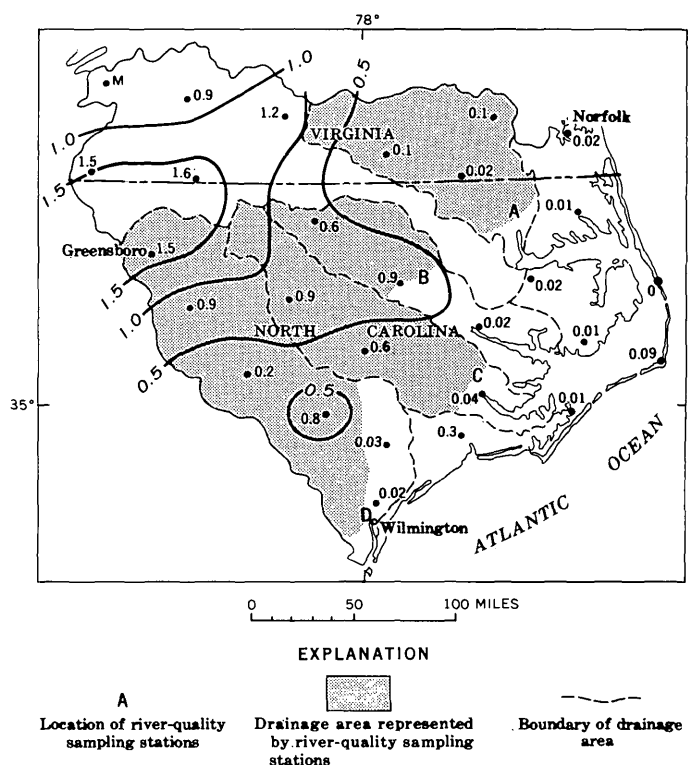
Figure 114.3.—Nitrate content of precipitation (parts per million) on study area, August 1962. Isopleth interval, 1.0 ppm.

than local industry must account for the trend observed in figure 114.2. Either sulfur has been brought in by advection from a nearby area, or some presently unexplained natural source is responsible. The lines of equal sulfate content (fig. 114.2) clearly indicate that the ocean was not the major source of atmospheric sulfur in this area during August 1962.

Figure 114.3 shows a distinct pattern in the areal variation of nitrate. Precipitation occurring over the coastal plain is almost devoid of nitrate. Farther inland, however, the precipitation contains nitrate in relatively large concentrations. Several explanations might account for this striking difference.

The fixation of atmospheric nitrogen by lightning discharges is one known source of nitrate. Sixteen thunderstorm-precipitation samples collected by the author contained nitrate concentrations ranging from 0.7 to 8.1 ppm; the average concentration was 2.9 ppm. Because August is a month of frequent thunderstorm occurrence, at least part of the nitrate shown in figure 114.3 is probably the result of thunderstorm activity. The fact that convective storms are more frequent along the mountains than near the coast further strengthens this contention.

The soil may be an indirect source of atmospheric nitrate, as ammonia is produced in the later stages of decay of most organic matter. If the pH of the soil is relatively high, some ammonia will escape to the atmosphere. Junge (1958) proposed that the oxidation of this ammonia may produce much of the nitrate found in precipitation. Therefore, areal differences in soil composition may account for differences in the nitrate content of precipitation. The addition to the soil of commercial fertilizers containing nitrate may also be significant.

Another possibility is that much of the sulfate and nitrate in the western part of the area may have a common source. Oxides of both sulfur and nitrogen are produced in the combustion of most fuels. Data for the winter months should help greatly to clarify the picture.

A summary of the data concerning sulfate and nitrate, as well as the other major ionic constituents for August 1962, is presented in table 114.1. The values in table 114.1 are based on the total volume of precipitation on the 34,000-square-mile, five-basin area.

One important purpose of the network study is to determine what fraction of the dissolved solids in the natural water of the area is of direct atmospheric origin. Although data for a single month are insufficient to make such an evaluation, it appears that the atmos-

pheric contribution will prove to be substantial. Table 114.2 illustrates this point with respect to sulfate and nitrate. The river values are time-weighted averages. The precipitation values are based on the volume of precipitation on the respective drainage areas. The shaded sections of figures 114.2 and 114.3 correspond to the drainage areas represented. Although the averages in table 114.2 cannot be used for direct comparison, the general implications are evident. In an area where the natural water is of relatively low dissolved-solids content, such as that covered by the network, the atmosphere may be the principal source for a variety of constituents.

TABLE 114.1—*Average concentrations and approximate total loads of major ionic constituents in precipitation on the study area during August 1962*

Ion	Average concentration (ppm)	Total load (tons)
SO_4^{-2}	2.8	25,000
Ca^{+2}	1.1	10,000
Na^{+1}	.8	7,500
NO_3^{-1}	.6	5,300
Cl^{-1}	.4	3,800
K^{+1}	.1	1,200

TABLE 114.2.—*Comparison of sulfate and nitrate content of river waters with that of precipitation in August 1962*

Sampling station (figs. 114.2 and 114.3)	Drainage area upstream from station (sq mi)	Sulfate (ppm)		Nitrate (ppm)	
		River water	Precipitation	River water	Precipitation
A. Chowan River at Winton, N.C.	4,198	5.6	2.5	0.9	0.1
B. Tar River at Tarboro, N.C.	2,140	5.1	2.9	2.3	.5
C. Neuse River at Cowen Landing near Vanceboro, N.C.	4,027	7.4	2.7	4.6	.4
D. Cape Fear River at Navassa, N.C.	7,060	9.4	3.1	.8	.5

REFERENCES

Eriksson, Erik, 1959, The yearly circulation of chloride and sulfur in nature; meteorologic, geochemical and pedalogical implications, pt. 1: Tellus, v. 11, p. 375–403.

——— 1960, The yearly circulation of chloride and sulfur in nature; meteorologic, geochemical and pedalogical implications, pt. 2: Tellus, v. 12, p. 63–109.

Junge, C. E., 1958, The distribution of ammonia and nitrate in rain water over the United States: Am. Geophys. Union Trans., v. 39, no. 2, p. 241–248.

——— 1960, Sulfur in the atmosphere: Jour. Geophys. Research, v. 65, p. 227–237.

Junge, C. E., and Werby, R. T., 1958, The concentrations of chloride, sodium, potassium, calcium, and sulfate in rain water over the United States: Jour. Meteorology, v. 15, p. 417–425.

Article 115

DIFFERENCES BETWEEN FIELD AND LABORATORY DETERMINATIONS OF pH, ALKALINITY, AND SPECIFIC CONDUCTANCE OF NATURAL WATER

By C. E. ROBERSON, J. H. FETH; PAUL R. SEABER; and PETER ANDERSON,

Menlo Park, Calif.; Trenton, N.J.; and Philadelphia, Pa.

Abstract.—Determinations of pH and alkalinity of ground and surface water from the Sierra Nevada, Calif., and ground water from the coastal plain of New Jersey indicate appreciable differences between laboratory and field measurements. Special caution is required for geochemical interpretations based on laboratory determinations of these properties.

Scientific literature cites few if any data supporting the widely held belief that field measurements of some water-quality properties are more representative than laboratory measurements. Because of this lack of data, the U.S. Geological Survey has made two widely separated studies, comparing field and laboratory measurements of alkalinity (as bicarbonate) and pH of water samples collected in the Sierra Nevada of California (Roberson and Feth) and in the Atlantic Coastal Plain of New Jersey (Seaber and Anderson). The New Jersey study also compared field and laboratory measurements of specific conductance. This article presents some of the data obtained in these studies.

CALIFORNIA STUDY

In the California study, field and laboratory determinations of pH and alkalinity were made of 88 samples of water. Of these samples, 73 were from springs and 15 were from streams. Most of the samples (76) were from areas of granitic rock, and the rest were from other geologic environments such as volcanic rocks, alluvium, and serpentine. Most of the samples had a low dissolved-solids content, only 3 exceeding 350 parts per million in calculated dissolved solids. Samples for laboratory determinations were stored in 350-ml pressure-sealed soft-glass ("citrate") bottles filled virtually to capacity to minimize contact with air during transport and storage.

Field determinations of pH and alkalinity were made in a truck-mounted laboratory that provided electrostatic shielding and protection from the wind. These determinations were made immediately after the samples were collected. Field pH of samples was measured by a portable battery-operated meter (Beckman model N or model G). The meter was standardized using buffer solutions whose temperatures had been brought to that of the water to be tested. Field alkalinity of samples was determined by potentiometric titration to pH 4.5 (Rainwater and Thatcher, 1960, p. 94).

Laboratory determinations of pH and alkalinity were made in a temperature-controlled room where temperatures of buffer solutions and samples were allowed to equilibrate with the ambient air temperature of the room. The time interval between field and laboratory determinations ranged from 5 to 120 days. Laboratory pH of samples was measured with a line-operated (Beckman model H) pH meter. Laboratory alkalinity of samples was determined by potentiometric titration to pH 4.5 (Rainwater and Thatcher, 1960, p. 94).

Results obtained for the 88 samples studied are shown in table 115.1. The difference between field and laboratory determinations of pH (ΔpH) ranged from 0.0 to 2.8 pH units. The average difference is 0.3, and the standard deviation is 0.5 pH units. For alkalinity (as bicarbonate), the difference between field and laboratory determinations ranged from 0 to 26 ppm. The average difference is 3 ppm, and standard deviation is 5 ppm. In general, the changes in alkalinity between field and laboratory determinations are less pronounced than the changes in pH. This difference in the two sets of results indicates that field pH is a more critical determination than field alkalinity.

TABLE 115.1.—*Comparison of field and laboratory determinations of water samples collected in the Sierra Nevada, Calif.*

[G, ground water; SW, surface water]

Laboratory No.	Source	pH		Alkalinity as HCO$_3^{-1}$ (ppm)		Time interval (days)	Temperature of sample at source (°F)	Calculated dissolved solids (ppm)
		Laboratory	Field	Laboratory	Field			
1204	G	8.1	8.1	200	202	60	58	242
1205	G	6.7	7.1	54	56	60	52	97
1207	G	7.2	7.5	64	62	60	52	106
1216	G	8.0	8.2	109	107	21	58	135
1218	G	7.4	7.5	31	30	15	57	50
1224	G	7.1	7.0	66	64	19	47	82
1225	SW	7.5	7.8	57	58	18	38	71
1226	G	6.9	8.2	42	37	13	51	73
1228	SW	6.0	8.1	3	6	18	60	9
1229	SW	6.3	7.0	4	4	18	53	11
1230	SW	6.0	8.8	3	6	18	36	8
1232	G	6.1	6.3	5	5	17	53	12
1233	G	5.8	5.9	20	19	12	47	35
1234	SW	6.9	7.0	11	11	12	41	23
1236	SW	5.8	6.1	2	2	12	40	3
1245	G	6.2	6.8	23	26	30	40	54
1246	G	7.7	7.9	93	96	29	64	98
1247	G	7.7	7.5	67	68	48	55	72
1248	G	6.8	7.4	35	38	29	52	49
1249	G	7.3	7.7	75	78	28	53	88
1250	G	7.6	7.9	76	80	28	52	87
1251	G	6.9	7.3	70	72	28	61	79
1252	G	7.4	7.4	88	89	28	69	93
1255	G	6.2	6.2	17	19	28	50	35
1256	G	6.2	6.3	19	21	27	47	32
1257	G	6.6	6.9	10	13	27	49	21
1258	G	5.9	6.2	8	8	27	59	18
1259	G	5.7	5.6	10	14	27	41	23
1261	G	7.3	7.5	83	84	60	50	93
1287	G	5.9	5.9	9	10	13	56	23
1290	G	7.0	7.2	100	103	12	70	154
1291	G	7.1	7.8	76	80	19	54	91
1292	G	6.7	6.4	148	152	11	67	203
1293	G	6.9	6.4	120	119	11	53	154
1295	G	6.1	5.5	26	24	11	50	54
1296	G	6.2	5.5	48	46	11	52	91
1297	G	6.4	6.0	54	57	11	48	99
1304	SW	7.6	8.1	63	65	45	55	78
1309	SW	7.8	8.1	74	64	45	58	89
1324	G	8.1	7.8	59	55	90	126	2,990
1325	G	7.7	7.6	93	86	19	48	119
1326	G	7.6	7.3	81	79	19	40	177
1328	G	6.8	6.8	740	738	90	86	1,870
1330	G	7.2	7.1	67	71	16	51	84
1381	G	7.4	7.2	105	107	16	49	100
1478	SW	7.7	8.2	273	280	120	48	347
1479	G	7.1	7.3	108	103	120	38	--------
1481	SW	7.3	7.4	47	49	6	46	59
1482	SW	7.3	7.4	47	49	6	41	57
1500	G	5.8	5.8	11	14	6	43	28
1507	SW	6.3	6.8	5	8	20	48	11
1508	SW	6.2	6.4	6	8	20	48	13
1510	SW	7.2	7.2	21	23	20	42	34
1526	G	6.6	6.8	101	103	7	48	139
1527	G	6.7	6.7	72	75	7	60	120
1528	G	6.5	6.6	77	67	6	47	128
1529	G	7.4	7.4	84	95	6	53	127
1530	G	5.6	5.8	14	14	6	51	29
1531	G	6.8	6.9	34	32	6	62	53
1532	G	7.0	6.9	97	100	6	51	133
1534	G	5.4	5.8	12	14	5	52	25
1535	G	5.6	5.8	17	20	5	44	32
1539	G	7.5	6.7	36	40	90	50	60
1541	G	7.5	7.9	88	90	90	50	101
1542	G	6.6	6.6	91	92	90	45	101
1543	G	6.6	6.6	73	76	90	45	90
1544	SW	7.6	7.9	80	91	90	62	96
1559	G	6.6	6.8	33	35	75	54	65
1560	G	8.0	8.2	190	216	75	56	172
1561	G	7.1	7.6	109	93	75	56	150
1564	G	7.5	8.0	143	168	60	60	149
1565	G	6.2	6.5	31	34	60	44	54
1566	G	7.7	7.6	59	64	60	50	71
1567	G	5.8	6.2	19	21	60	44	53
1568	G	7.4	7.1	68	70	60	50	82
1569	G	6.3	6.7	40	41	60	41	64
1570	G	6.3	6.5	49	52	60	46	78
1571	G	7.4	7.5	63	63	60	48	79
1572	G	7.4	7.7	103	108	60	48	106
1573	G	6.5	7.3	13	15	60	44	32
1574	G	6.8	7.2	37	38	60	44	54
1575	G	7.8	7.4	108	111	60	83	1,190
1576	G	7.6	7.4	88	81	60	44	102
1577	G	5.8	6.2	18	18	60	48	41
1578	G	7.4	7.5	146	150	60	65	335
1579	G	5.9	6.1	42	45	60	50	78
1580	G	5.8	6.0	28	30	60	54	57
1581	G	6.8	7.1	119	113	60	70	162

Water samples having a low dissolved-solids content showed, in general, slightly greater change in pH than water having a higher mineral content. Similarly, samples having a low total dissolved carbonate-species content generally showed appreciable variation between pH determined in the field and in the laboratory.

Although the time interval between field and laboratory determinations ranged from 5 to 120 days, comparison of pH with time of storage shows little correlation. However, as a group, laboratory determinations made within 1 week of the time that the samples were collected showed somewhat smaller changes than determinations made after longer storage.

Some possible reasons for the differences between determination of pH in the field and in the laboratory are worth noting. Determinations made in the laboratory would be lower than those made in the field if, during transport and storage, the water sample absorbed CO_2 from the atmosphere. This could happen if the pressure stopper of the sample bottles leaked or if the samples stood open in the laboratory for a significant length of time before pH measurements were made. The latter possibility is ruled out because readings were made as soon as the samples were removed from the bottles, but the possibility of leakage cannot be entirely eliminated. Reactions within the water samples during storage, such as release of CO_2 by microorganisms, would also lower the pH.

Laboratory pH values higher than those measured in the field would result from loss of CO_2 in water taken in the field at low temperature and stored at a higher temperature in a bottle having some air space above the water surface. Reaction between the water samples and the soft glass of the bottles might also raise the pH.

The change in pH between field and laboratory analyses with the logarithm of total dissolved carbonate-species content calculated from the field pH and alkalinity measurements is shown in figure 115.1. The points scatter, but the trend suggests that exchange of CO_2 between water sample and atmosphere may be largely responsible for observed changes in pH. Water having a low content of carbonate species (larger negative value of the logarithm) apparently tends to gain CO_2 and to show a decrease in pH, whereas water having a high total carbonate-species content may lose CO_2 to the atmosphere and show an increase in pH. Absence of persistent trends in study graphs of other variables, however, suggests that more than one factor is involved and that two or more may interact to cause changes in pH and alkalinity in some samples.

The changes observed in bicarbonate content and in pH, when field and laboratory determinations are com-
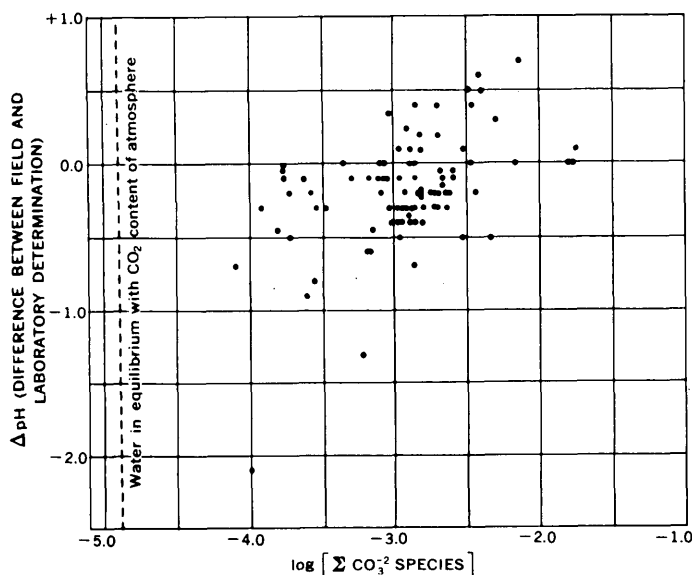
FIGURE 115.1.—Graph comparing change in pH with calculated total dissolved carbonate-species content in sample.

pared, indicate that laboratory determinations of these variables are not reliable for use in geochemical equilibrium calculations. The lack of correlation between pairs of variables, such as pH and temperature, pH and time of storage, and pH and HCO_3^{-1}, suggests that projection of laboratory-determined data to calculated data indicative of conditions prevailing in the field cannot be made with confidence. Therefore, pH, and preferably also bicarbonate, should be determined in the field if the data are to be used in thermodynamic calculations. Field determinations of pH can be made to close limits of tolerance (± 0.05) if considerable care is exercised.

NEW JERSEY STUDY

In the New Jersey study, field and laboratory determinations of pH, alkalinity, and specific conductance were made on water samples collected from 38 wells tapping the Englishtown Formation. At each wellhead, samples were collected in 1-gallon polyethylene bottles, which were kept capped as much as possible during the field determinations. For laboratory determinations, two citrate bottles were filled from each polyethylene bottle. One sample was used for determinations of pH, alkalinity, and specific conductance. The other sample was acidified and used for the determination of iron.

Field determinations of pH, alkalinity, and specific conductance were made on all samples immediately after the samples were collected at the well site. The pH was determined by a battery-operated pH meter (Beckman Model M). Although this meter can be read to the nearest 0.02 pH unit, pH data in table 115.2

were rounded to the nearest 0.1 pH unit. Alkalinity (as bicarbonate) was determined by titrating the samples with a standard solution of sulfuric acid using phenolphthalein and methyl orange as acid-base indicators (American Public Health Association, 1960, p. 44-48). On several water samples, alkalinity was determined by both this indicator method and a modification of the potentiometric method described by Rainwater and Thatcher (1960, p. 94-95). Results obtained by the two methods agreed within 1 percent. Alkalinity was reported to the nearest part per million. Specific conductance was measured to the nearest micromho (at 25°C) by a battery-operated instrument (Industrial Instruments Solu-Bridge). All instruments were calibrated before and after fieldwork and were found to be within the accuracy of the determination as described by Hem (1959).

Laboratory determinations were made by the standard methods of the U.S. Geological Survey (Rainwater and Thatcher, 1960), which also are the ones used in the California study. All laboratory determinations were made within 1 month of date of collection.

The data obtained in the New Jersey study are shown in table 115.2. Except for one sample, field pH was greater than laboratory pH. The maximum difference between field and laboratory determinations of pH was 2.5. For all samples, field alkalinity was greater than laboratory alkalinity. The maximum difference between field and laboratory alkalinities was 33 ppm, but most differences (29 samples) were in the range from 5 to 15 ppm. The difference between field and laboratory determinations of alkalinity was greater than 5 percent for all but 1 of the 38 groundwater samples. According to Hem (1959, p. 97), agreement closer than 2 to 5 percent cannot be expected for duplicate alkalinity determinations. For all but five samples, field specific conductance was greater than that determined in the laboratory.

The greatest differences between field and laboratory determinations of pH, alkalinity, and specific conductance were found in samples whose iron precipitated during storage of the sample. Samples having a visible precipitate of iron had average differences of 0.9 pH units, 19 ppm of alkalinity, and 28 micromhos of specific conductance. Samples having no visible precipitate of iron had average differences of 0.6 pH units, 11 ppm of alkalinity, and 17 micromhos of specific conductance.

Iron precipitated in all 7 samples in which the field pH was 7.0 or less and in 3 of the 5 samples in which the field pH ranged from 7.1 to 7.3. Iron did not precipitate in any of the remaining 26 samples, which had a field pH of 7.4 or greater. Average differences be-

tween field and laboratory pH, alkalinity, and specific conductance for these pH ranges are shown in table 115.3.

TABLE 115.2.—*Field and laboratory determinations of physica and chemical properties of water from the Englishtown Formation in New Jersey*

[Chemical analyses, in parts per million]

Well No.	pH		Alkalinity (as HCO_3)		Specific conductance (in micromhos at 25° C)		Iron (Fe)	Precipitate in sample bottle
	Field	Lab.	Field	Lab.	Field	Lab.	Lab.	
1	4.8	3.8	3	0	148	166	11	Yellow.
2	5.0	4.4	5	0	480	446	11	Red.
3	6.6	5.2	22	3	67	37	7.8	Yellow.
4	6.6	7.0	70	49	175	134	9.8	Do.
5	6.7	4.2	32	0	82	43	11	Red.
6	6.9	5.8	48	16	110	59	11	Do.
7	7.0	6.3	94	74	181	159	8.6	Yellow.
8	7.1	6.6	72	65	145	130	3.0	Clear.
9	7.2	6.8	106	93	203	193	2.0	Yellow.
10	7.3	6.7	156	132	285	270	.14	Do.
11	7.3	6.8	56	52	141	133	.36	Clear.
12	7.3	7.0	152	129	260	242	3.4	Yellow.
13	7.4	6.9	98	88	215	195	1.6	Clear.
14	7.4	6.9	60	49	130	104	1.6	Do.
15	7.6	7.1	104	94	181	175	.68	Do.
16	7.7	7.3	138	129	230	214	1.5	Do.
17	7.7	7.2	106	93	182	182	1.9	Do.
18	7.8	7.3	106	988	218	228	.62	Do.
19	7.8	7.2	108	97	184	173	.47	Do.
20	7.8	7.5	112	104	202	175	.45	Do.
21	7.9	7.3	106	99	180	178	.46	Do.
22	8.0	7.4	164	150	255	242	.65	Do.
23	8.0	7.5	132	121	235	211	2.0	Do.
24	8.0	7.4	96	91	183	171	1.7	Do.
25	8.0	7.4	99	84	158	153	.26	Do.
26	8.0	7.5	160	149	270	244	.35	Do.
27	8.0	7.3	164	151	265	267	.45	Do.
28	8.0	7.3	106	100	167	177	.22	Do.
29	8.0	7.5	138	129	238	228	.64	Do.
30	8.0	7.2	114	106	185	184	.31	Do.
31	8.1	7.5	96	83	180	159	.59	Do.
32	8.1	7.2	126	116	219	198	.24	Do.
33	8.1	7.6	118	111	208	193	.30	Do.
34	8.2	7.7	122	120	208	191	.20	Do.
35	8.3	7.9	[1] 149	140	235	214	1.0	Do.
36	8.3	7.9	[2] 184	166	244	271	.24	Do.
37	8.5	7.5	[3] 246	218	[3] 352	351	--------	Do.
38	8.5	8.0	[4] 251	218	348	233	.19	Do.

[1] Includes equivalent of 2 ppm of carbonate (CO_3).
[2] Includes equivalent of 6 ppm of carbonate (CO_3).
[3] Includes equivalent of 10 ppm of carbonate (CO_3).
[4] Includes equivalent of 8 ppm of carbonate (CO_3).

TABLE 115.3.—*Average differences, ignoring sign, between field and laboratory determinations of pH, alkalinity, and specific conductance of water samples collected in the Englishtown Formation of New Jersey*

Range in field pH	No. of samples	Average differences between field and laboratory determinations		
		pH	Alkalinity (as HCO_3)	Specific conductance (in micromhos at 25°C)
4.8–7.0	7	1.1	19	34
7.1–7.3	5	.5	14	13
7.4–8.5	26	.6	11	17
4.8–8.5	38	.7	13	19

The differences between field and laboratory data possibly can be explained by the precipitation of iron compounds, changes in temperature of the samples, and changes in chemical equilibrium between the time of field analysis and laboratory analysis (Rainwater and Thatcher, 1960, p. 31–32). Because precipitations of iron compounds and changes in temperatures would result in a decrease in the bicarbonate concentration, the pH and the alkalinity concentration would be expected to decrease; possibly the specific conductance would decrease also.

The following observations are based on a comparison of the analytical data for water samples from 38 wells tapping the Englishtown Formation in New Jersey:

1. The field determinations of pH, alkalinity, and specific conductance generally are higher than laboratory determinations.

2. Samples in which iron precipitated between the time of the field determinations and the laboratory determinations showed the greatest differences between the field and laboratory values of pH, alkalinity, and specific conductance.

3. Iron precipitates appeared in all samples having a field pH of 7.0 or less, in some samples having a field pH of 7.1 and 7.3, and in no samples having a field pH of 7.4 or more.

4. The highest concentrations of iron and the greatest differences in pH, alkalinity, and specific conductance characterized samples collected in areas where little or no calcium carbonate is present in the natural aquifer materials.

Because field determinations of pH, alkalinity, and specific conductance probably are more representative of the actual state of the water in the Englishtown Formation, they should be preferred for geochemical interpretations of this aquifer system. On the other hand, if water is being rated as to its suitability for various uses after storage, laboratory determinations probably are more useful.

CONCLUSIONS

In summary, both studies showed that field determinations of pH and alkalinity are generally higher than laboratory determinations of these variables, and that field determinations of pH and alkalinity are more representative of water in its natural environment than are laboratory determinations.

REFERENCES

American Public Health Association, 1960, Standard methods for the examination of water and waste water: New York, Am. Public Health Assoc., Inc., 11th ed., 626 p.

Hem, J. D., 1959, Study and interpretation of the chemical characteristics of natural water: U.S. Geol. Survey Water-Supply Paper 1473, 269 p.

Rainwater, F. H., and Thatcher, L. L., 1960, Methods for collection and analysis of water samples: U.S. Geol. Survey Water-Supply Paper 1454, 301 p.

Article 116

INCREASED OXIDATION RATE OF MANGANESE IONS
IN CONTACT WITH FELDSPAR GRAINS

By JOHN D. HEM, Denver, Colo.

Abstract.—Solutions of Mn^{+2} in contact with feldspathic sand lose manganese by ion-exchange adsorption on the feldspar grains and by oxidation followed by precipitation of manganese oxide. Removal of manganese is substantially faster in solutions at pH 8 than at pH 7.

Laboratory studies reported here indicate that feldspathic sand moderately catalyzes the oxidation of Mn^{+2} in water and that pH strongly influences the rate of oxidation. In these studies the effect of feldspathic sand on the rate of loss of Mn^{+2} from solution was studied by means of two series of batch-type experiments.

In the first series of experiments, 500-ml volumes of aqueous solution containing 10 ppm of Mn^{+2} and adjusted to pH 7.70 with sodium hydroxide were placed in each of 6 polyethylene bottles. Five of these bottles contained feldspathic sand, in amounts ranging from 10 to 100 g, that had been pretreated with sodium chloride solution and washed so that ion-exchange sites were occupied by sodium ions; the sixth contained no sand. The sand used in these studies consisted of rounded grains in the range 0.10 to 0.80 mm. Microscopic examination of a representative sample of the sand showed that it consisted of approximately 45 percent quartz, 21 percent orthoclase feldspar, and 34 percent plagioclase feldspar. The cation-exchange capacity of the sand, determined by equilibration with 1.0 molar solution of manganese chloride, was 0.66 milliequivalents per hundred grams.

The solutions were kept in the laboratory at a temperature of $25°\pm1°C$. Periodic sampling and analysis of the solutions indicated that both the pH and the manganese concentration of the test solutions decreased with time.

A second series of experiments was made with solutions at a higher and more constant pH. The six solutions of this series differed from those of the first series only in that they contained 100 parts per million of HCO_3^{-1} added as sodium bicarbonate. The pH of these solutions was adjusted to 8.03 and remained near 8.0 throughout the experiments. In the second series, as in the first, the solutions were sampled and analyzed periodically.

Results of some of the experiments are shown in figure 116.1. Test solutions that were not exposed to feldspathic sand showed little change in concentration of Mn^{+2} at either pH near 7 or near 8, even after more than 350 hours. At pH near 8.0, the oxidation rates of Mn^{+2} were too slow to be reliably measured. Test solutions that were in contact with feldspathic sand
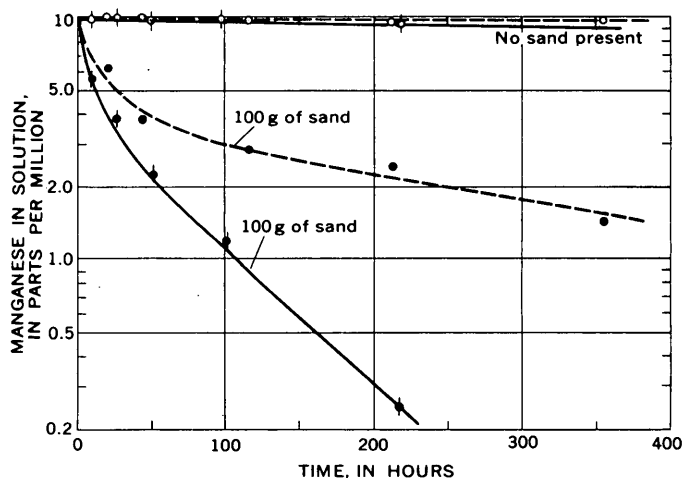
FIGURE 116.1.—Rate of loss of manganese from solutions near pH 7 (dashed lines) and pH 8 (solid lines) in presence and absence of feldspathic sand.

ART 116 *IN* U.S. GEOL. SURVEY PROF. PAPER 475–C, PAGES C216–C217. 1963.

C216

showed a rapid initial decrease in Mn^{+2} concentration, followed by a slower, steady decrease. The decrease in Mn^{+2} concentration was approximately proportional to the weight of sand in the test bottles and was greater at pH near 8 (solid line, fig. 116.1) than at pH near 7 (dashed line).

The results of these studies are most readily explained by the hypothesis that some Mn^{+2} is adsorbed on the sand and some is oxidized to form a precipitate of manganese oxide. Manganese is removed rapidly from solution at first, mostly by exchange for sodium on the sand. As the solution and the exchange surfaces approach equilibrium, the effect of ion exchange disappears and the manganese-loss curve (fig. 116.1) becomes a straight line as the manganese is removed only by oxidation catalyzed by the sand-grain surfaces.

Several lines of evidence support this hypothesis. For example, when other conditions were comparable, the slopes of the straight segments of the curves were steeper for solutions in contact with larger amounts of sand. Also, the slopes were steepened by increasing the pH and were flattened by adding bicarbonate and sulfate ions, as observed in earlier work with manganese oxidation rates (Hem, 1963). The catalysis mechanism was not closely studied, but such an effect of solid surfaces on reaction rates is not particularly unusual.

In order to compare the behavior of Mn^{+2} with a similar ion that is not subject to oxidation, a series of experiments was run using calcium solutions in place of manganese solutions. The ionic radius of Mn^{+2} is slightly smaller than that of Ca^{+2}, and manganese is a little more strongly adsorbed by the sand than calcium. The calcium experiments showed an initial period of rapid loss, but after 4 days the solutions stabilized and no further loss occurred, regardless of the amount of sand present.

Natural mineral surfaces probably catalyze the formation and precipitation of manganese oxide from weathering solutions. The effect helps to explain the chemical behavior of manganese in natural water.

REFERENCE

Hem, J. D., 1963, Chemical equilibria and rates of manganese oxidation: U.S. Geol. Survey Water-Supply Paper 1667–A.

Article 117

SOLUTION OF MANGANESE DIOXIDE BY TANNIC ACID

By JACK RAWSON, Austin, Tex.

Abstract.—Although manganese dioxide is nearly insoluble in distilled water, tannic (digallic) acid may bring considerable amounts of manganese into solution. The study suggests a possible mechanism for the solution of insoluble manganese from soils and sediments by natural waters containing tannic acid or similar organic extracts.

Manganese is usually present in soils and sediments in an oxidized, insoluble state. Most of the manganese found in natural waters probably results from the solution of manganese from soils and sediments aided by organic matter and bacterial action (Hem, 1959, p. 66). Manganese in excess of 0.3 parts per million is objectionable in public water supplies and may require removal for some industrial processes.

Manganese dioxide is nearly insoluble in distilled water but is moderately soluble in tannic acid, which is common in organic soils and sediments. The action of aqueous solutions of tannic acid on manganese dioxide was studied with a view to a more thorough understanding and explanation of phenomena that occur when natural waters containing organic extracts come into contact with soils and sediments containing insoluble manganese.

Tannins are a large group of complex substances found in many plants. Gallotannin, the common tannic acid of commerce, is obtained principally from gallnuts (Conant and Blatt, 1947, p. 506). This particular tannin is a mixture of gallic acid esters of glucose. According to Hem (1960, p. 77) the gallotannin molecule, in water solution, hydrolyzes to give glucose and digallic acid. Digallic acid has the following semistructural formula:

$$(HO)_3C_6H_2 \cdot CO_2 \cdot C_6H_2(OH)_2CO_2H$$
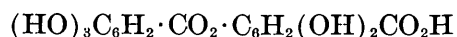
The tannic acid used in the experiments reported here is represented by the above formula.

Solutions containing 10, 100, and 1,000 ppm of tannic acid were prepared, and each solution was divided into six aliquots. The pH of each aliquot was adjusted with carbonate-free potassium hydroxide to a predetermined value ranging in unit steps from 4.5 to 9.5. The aliquots were poured into polyethylene bottles, and 1 g of reagent-grade manganese dioxide was added to each. The bottles were tightly stoppered and were placed in a constant-temperature room at about 25°C.

Periodically for 56 days, the Eh (redox potential) and pH of samples from each bottle were determined. The samples were then passed through plastic-membrane filters (average pore diameter of 0.45 micron) to remove precipitated or colloidal manganese. The concentration of the manganese in the filtrates was then determined by the permanganate method as described by Rainwater and Thatcher (1960, p. 205–207).

After 56 days of storage, the 100-ppm tannic acid solutions were separated from the solid manganese dioxide and were filtered through plastic-membrane filters. To determine whether or not collodial manganese passed through the filters, portions of these filtrates were centrifuged at 3,000 revolutions per minute for 30 minutes and then refiltered. No appreciable loss of manganese from the filtrates occurred. Though not conclusive, the retention of manganese in a filterable state suggests that the manganese was not colloidal.

The remaining portions of the filtrates from the 100-ppm tannic acid solutions were stored in tightly stoppered plastic bottles to determine whether or not the manganese would be retained in solution in the absence of excess solid manganese dioxide. After 111 days of storage, no significant loss of manganese occurred from the solutions.

The final portions of the 100-ppm tannic acid solutions were aerated by passing air, presaturated with water, through them for 10 hours. Two weeks later, the pH of the samples was raised to 9.0 with carbonate-free potassium hydroxide. The samples were filtered and the concentration of manganese in the filtrates was determined. The results indicated that the manganese content had decreased only slightly. This retention of manganese in solution indicates a manganese-tannic acid complex that strongly resists oxidation.

The table summarizes the effect of tannic acid on the solution of manganese dioxide. The results indicate that tannic acid, even in dilute solutions, may bring considerable amounts of manganese into solution.

Figure 117.1 shows the relation between storage time, pH, and manganese concentration in test solutions containing tannic acid. The results indicate that the rate of solution of manganese is a function of both the initial pH and the tannic acid concentration of the test samples. In test solutions having the same initial pH, the rate of manganese solution increases with the tannic acid concentration. In test solutions having the same tannic acid concentration, however, the reaction rate is greater in those samples having the lower initial pH.

The exact mechanism of manganese solution by tannic acid was not determined in this study. The permanganate method, though quite sensitive and specific for manganese, does not permit distinction of the forms in which manganese was originally present in the solutons. Manganese dioxide, however, is a strong oxidizing agent. Tannic acid, on the other hand, is a reducing agent. In his study of complexes of iron with tannic acid, Hem (1960, p. 84–85) demonstrated that the reduction of ferric iron to ferrous iron in acid solutions was effected by tannic acid. Manganese is chemically related to iron. The solution of manganese by tannic acid, therefore, probably results from chemical reduction. If this assumption is correct, complexing of tannic acid with divalent manganese also occurs. The retention of manganese in solution in the 100-ppm tannic acid solutions supports this argument.

The experiments suggest a mechanism for manganese solution from soils and sediments by natural waters containing tannic acid or similar organic extracts leached from decaying organic debris.
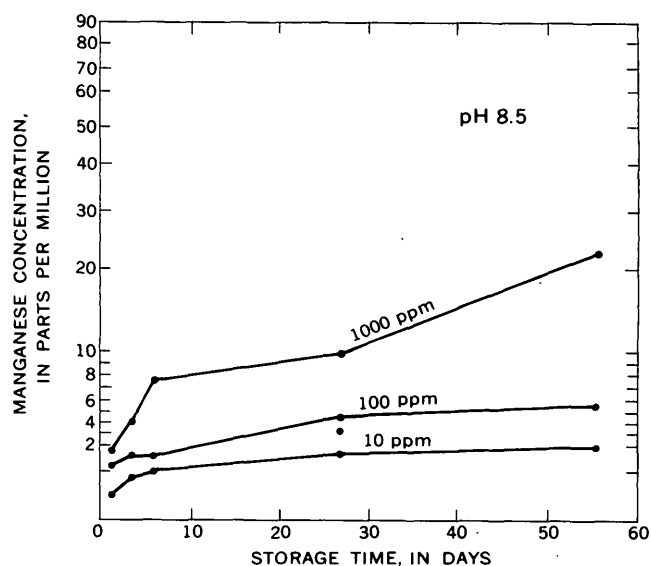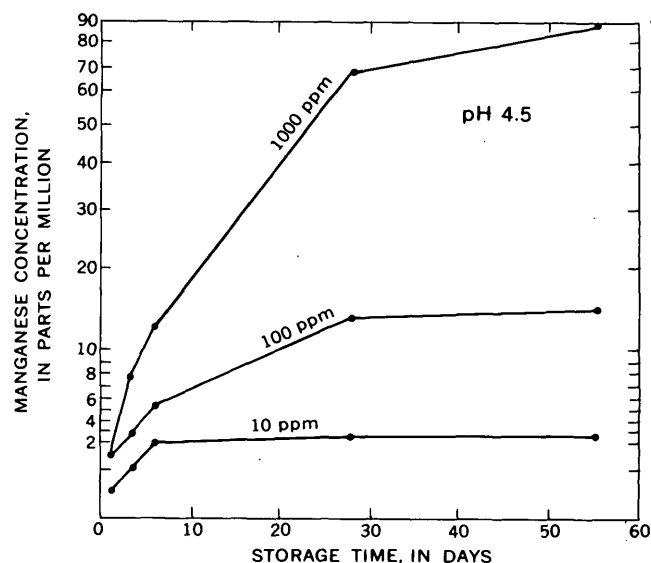
FIGURE 117.7—Solution of manganese by tannic acid.

Effect of tannic acid concentration on solution of manganese dioxide

[Eh in volts, Mn concentrations in parts per million]

| Initial pH | 10 ppm | | | | | 100 ppm | | | | | 1,000 ppm | | | | |
| | After 3 hours | | After 56 days | | | After 3 hours | | After 56 days | | | After 3 hours | | After 56 days | | |
	pH	Eh	pH	Eh	Mn	pH	Eh	pH	Eh	Mn	pH	Eh	pH	Eh	Mn
4.5	5.3	0.577	6.2	0.598	3.6	5.6	0.539	6.9	0.565	21	4.9	0.547	6.4	0.512	112
5.5	6.2	.527	6.6	.586	3.5	6.0	.521	6.8	.568	14	5.9	.478	6.2	.515	90
6.5	6.6	.492	6.6	.586	2.4	6.5	.490	6.9	.563	13	6.5	.477	6.4	.537	80
7.5	7.0	.471	6.6	.579	1.8	7.0	.490	6.9	.578	10	7.1	.477	6.4	.547	54
8.5	7.3	.465	6.6	.579	2.0	7.4	.483	6.9	.576	5.2	8.3	.428	6.6	.545	21
9.5	8.7	.389	6.7	.562	.79	8.6	.407	7.0	.571	5.2	9.2	.357	6.8	.531	15

REFERENCES

Conant, J. B., and Blatt, A. H., 1947, The chemistry of organic compounds: New York, Macmillan Co., 640 p.

Hem, J. D., 1959, Study and interpretation of the chemical characteristics of natural water: U.S. Geol. Survey Water-Supply Paper 1473, 254 p.

Hem, J. D., 1960, Complexes of ferrous iron with tannic acid: U.S. Geol. Survey Water-Supply Paper 1459–D, p. 75–94.

Rainwater, F. H., and Thatcher, L. L., 1960, Methods for collection and analysis of water samples: U.S. Geol. Survey Water-Supply Paper 1454, 297 p.

Article 118

EFFECTIVENESS OF COMMON AQUATIC ORGANISMS IN REMOVAL OF DISSOLVED LEAD FROM TAP WATER

By EUGENE T. OBORN, Denver, Colo.

Abstract.—Lead sorbed by four kinds of aquatic plants is approximately in proportion to the area of the plant-body surface in contact with the water. Symbiotic bacteria were the most active of the organisms studied.

Small amounts of lead taken in drinking water are not easily eliminated by the body, but accumulate, instead, until irreparable body damage has been done (Offner, 1944, p. 284). In a study of this danger the author investigated the effectiveness of aquatic vegetation and associated microbiological symbionts in removing lead and other dissolved ions from tap water. Experiments for this study were made during the summer of 1961.

Limnologists generally agree that soil-rooted aquatic plants, although wholly submerged, obtain their mineral salts from the substratum and not from the surrounding water. Floating plants that are not rooted in the soil, however, obtain their mineral salts directly from the surrounding water (Butcher, 1933). The plants used in the experiments reported here were all of the water-rooted variety.

Submerged hornwort (*Ceratophyllum demersum* L.) has an abbreviated root system. Common bladderwort (*Utricularia vulgaris* L.) likewise has an abbreviated root system, but additional sorption may take place through the many bladders present. With common pond scum (*Cladophora glomerata* [L.] Kütz) direct sorption is possible over most of the plant surface except for the part floating above water. Rust-colored bacterial water slime used in this study was a very mucoid symbiotic growth on which sorption could take place through any part of the completely submersed irregular mucous envelope. The bacteria[1] consisted of 53 percent gram-negative rods, unable to reduce nitrates to nitrites, but capable of growing both

[a] Determined by Bacteriology Laboratory, School of Medicine, University of Colorado.

at room temperature and at 37°F. The remaining 47 percent were gram-positive cocci, able to reduce nitrates to nitrites and capable of growing at 37°F but not at room temperature.

The plants (each 1.0-g blotter-dry weight) were placed in 250-ml Erlenmeyer flasks containing 200 ml of tap water. The water contained 10 to 20 micrograms of lead tagged with 0.1 microcurie of carrier-free Pb^{210} (equivalent to 1.2×10^{-3} μg of radioactive lead) as lead nitrate. The flask tops were covered with cellophane, secured with rubber bands, and the flasks were allowed to stand undisturbed in natural light at the ambient temperature of the laboratory for 2 weeks. The plants were then removed from the water, and the radioactive lead content of plants and water was determined.

The accompanying table, which lists the plants in increasing order of surface area per unit weight, shows the relative effectiveness of the bacteria and the three species of aquatic plants in removing radioactive lead from tap water. (Determinations by Division of Industrial Medicine, School of Medicine, University of Colorado, with the cooperation of Dr. R. F. Bell.)

	Radioactive lead (percent)	
Plant	In or on the plant	In the water
Hornwort	41	59
Bladderwort	58	42
Pond scum	79	21
Bacterial slime	87	13

Evidently, removal of radioactive lead by the plants was approximately proportional to the amount of body sorptive surface of the aquatic plants in contact with the surrounding water.

REFERENCES

Butcher, R. W., 1933, Studies on the ecology of rivers, pt. 1, On the distribution of macrophytic vegetation in the rivers of Britain: Jour. Ecology, v. 21, p. 58–91.

Offner, M. M., 1944, Fundamentals of chemistry: New York, Barnes and Noble, Inc., 408 p.

ART. 118 *IN* U.S. GEOL. SURVEY PROF. PAPER 475-C, PAGE C220. 1963.

C220

ADSORPTION OF THE SURFACTANT ABS^{35} ON ILLITE

By C. H. WAYMAN, H. G. PAGE, and J. B. ROBERTSON, Denver, Colo

Abstract.—A radiochemical-tracer technique was used to study the adsorption of the surfactant ABS^{35} on illite. The length of the alkyl chain, presence of phosphate ion, pH, and the amount and type of ionic salt present influence this adsorption. Illite and other clay minerals are inefficient adsorbents for ABS in comparison with synthetic materials (colloidal alumina and activated charcoal).

Incompletely degradable surfactants injected into the ground in household waste water have in many areas polluted ground-water supplies. One of the natural means by which these surfactants are removed from waste water is by their adsorption on soil minerals. The ability of illite to adsorb alkylbenzenesulfonate (ABS), an essential incompletely degradable surfactant in detergents, is described in this article. As in similar studies of the adsorption of ABS on kaolinite (Wayman, Robertson, and Page, 1963) and on montmorillonite (Wayman, Page, and Robertson, 1963) the ABS was tagged with S^{35} (ABS^{35}). The adsorption of ABS on clay minerals is also compared with that on synthetic materials (activated charcoal and colloidal alumina).

A radiochemical-tracer technique identical to that described for the kaolinite study was used in this study. The effects of such variables as alkyl-chain length (C$_{12}$ and C$_{15}$), pH, phosphate ion, and type and amount of dissolved ionic salts (NaCl, CaCl$_2$, and AlCl$_3$) on ABS adsorption by illite were studied. ABS was added as the sodium salt and can be represented in solution as the anion

$$(R\text{-}C_6H_4\text{-}SO_3)^{-1},$$
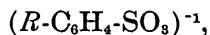
where R represents the alkyl chain.

The preparation of the illite and the experimental procedures were identical with those used in the study of kaolinite. The illite used was the standard clay mineral (No. 35) of the American Petroleum Institute.

The composition of the mineral can be represented in a broad sense (Warshaw, 1958, p. 304) by

$$[K_{0.5\text{-}0.7}(H_3O)_{0\text{-}0.3}]_{0.5\text{-}1.0}[Al_{1.7\text{-}2.0}Mg_{0\text{-}0.3}]_{2.0}$$
$$[Si_{3.3\text{-}3.6}Al_{0.4\text{-}0.7}]_{4.0}O_{10}(OH)_2$$
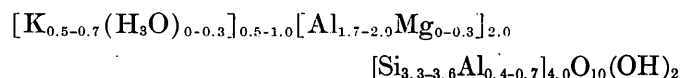
or in the form (Grim and others, 1937, p. 823)

$$(OH)_4K_y(Al_4Fe_4Mg_4Mg_6)(Si_{8\text{-}y}Al_y)O_{10}.$$
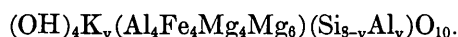
Microscopic and X-ray diffraction examination indicated that the clay contained about 12 percent impurities in the form of sericite, quartz, plagioclase, calcite, pyrite, and a trace of carbonaceous material. The cation-exchange capacity of the clay is 25.0 milliequivalents per 100 g, and the pH of a suspension of 200 mg of the clay in 35 ml of distilled water is about 6.8.

Figure 119.1 shows that both pH and length of the alkyl chain influence adsorption in solutions containing 5.0 parts per million of ABS. Dodecyl (C$_{12}$) ABS is only slightly adsorbed (maximum of 50 μg of ABS per g of clay) even at pH 4. Pentadecyl (C$_{15}$) ABS is adsorbed most readily at pH 4, but desorption seems to occur with time. Significant amounts of negative adsorption are indicated for both dodecyl and pentadecyl ABS at pH 10; this effect can be explained by repulsion of anionic ABS by the potential-determining hydroxyl ions (OH)$^{-1}$ on the clay surface at pH 10 and by disparities in the electrical double layer at the clay-solution interface. The increased adsorption of both types of ABS at low pH can be explained by significant numbers of positive sites on clay. In addition, pentadecyl ABS exhibits a greater adsorption than dodecyl ABS because the longer chain material (C$_{15}$) has a higher free energy of adsorption. Detailed supporting data for these effects have been given previously (Wayman, Page, and Robertson, 1963).
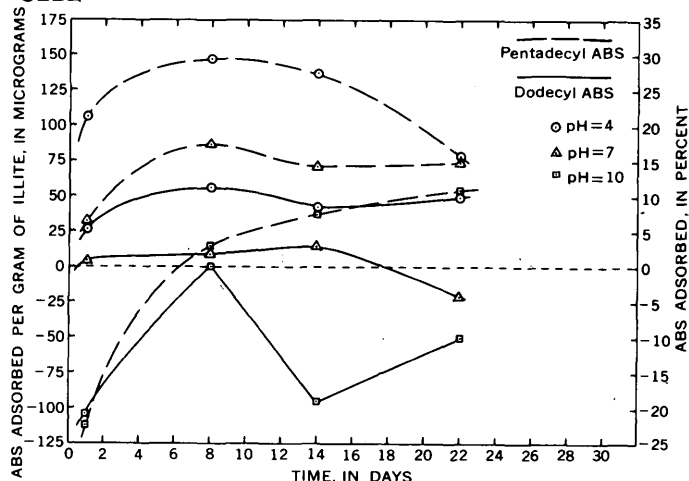
FIGURE 119.1—Influence of pH, length of alkyl chain, and time on adsorption of ABS by illite. Test solutions contained 5 ppm of pentadecyl ABS and 5 ppm of dodecyl ABS.

Figure 119.2 shows the results of adsorption of ABS on illite when 10 ppm of phosphate and either 5 ppm of dodecyl or 5 ppm of pentadecyl ABS are in solution. Maximum adsorption of ABS takes place for both forms of ABS at pH 4; apparent equilibrium adsorption is attained in about 6 days. For dodecyl ABS, adsorption at pH 7 is similar to that at pH 10. For pentadecyl ABS, adsorption-desorption are indicated. However, after lengthy periods of equilibration, the amount of either type of ABS adsorbed at a specified pH seems to approach the same value. In acid solutions (pH 4), phosphate seems to increase the amount of ABS adsorbed by illite. The effect of enhanced adsorption with phosphate in solutions might be attributed to adsorption of ABS in the form of an aluminum-phosphate-ABS complex; reasons for such an adsorption mechanism have been given elsewhere (Wayman, Page, and Robertson, 1963).

Figure 119.3 shows the influence of salt concentration, valence, and pH on the adsorption of ABS by illite. The data shown represent apparent equilibrium adsorption measured for as long as 10 days. At any pH the amount of ABS adsorbed increases with increase in salt concentration. The optimum conditions for removal are at high salt concentrations and in acid solutions (pH 4). Trivalent (AlCl₃) and divalent (CaCl₂) salts influence ABS adsorption to a greater extent than NaCl, except in alkaline solutions (pH 10). These adsorption phenomena can most readily be explained as being due to the combined effects of availability of positive sites on clay at low pH, lowering of the critical micelle concentration of surfactants by ionic salts, relation of valency to action of cations as described by the Schulze-Hardy rule, and adsorption by an aluminum-hydroxy-ABS complex. Details of these considerations

have been described previously (Wayman, Page, and Robertson, 1963).

Figure 119.4 shows the relative adsorption capacity of kaolinite, illite, and montmorillonite in comparison with synthetic adsorbents (colloidal alumina and activated charcoal). Colloidal alumina is positively charged in acid solution. It consists of fibrils of boehmite (AlOOH) approximately 5mμ in diameter and 100 to 150mμ in length, a surface area of 274 m² per g, a pore diameter of 77 A, and a pore volume of 0.53 cc per g. Activated carbon is quite variable in physical dimensions. Particle diameters range from less than 100 A to 5,000 A; average open-pore volumes range from about 0.1 to 0.3 cc per g, total surface areas are
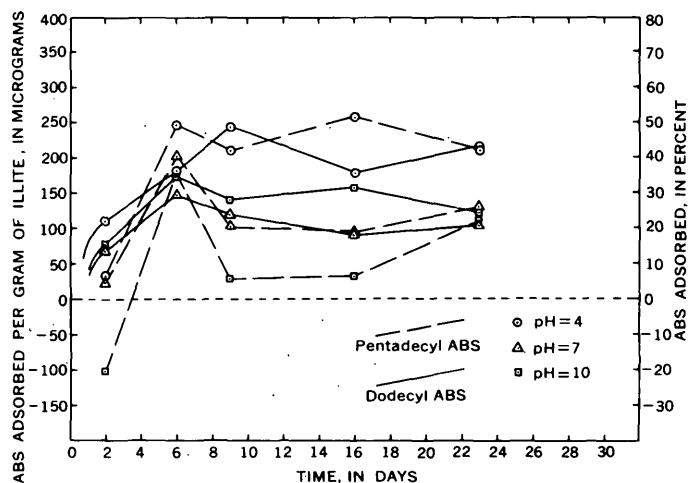
FIGURE 119.2.—Influence of pH, phosphate, and time on ABS adsorption by illite. Test solutions contained 5 ppm of dodecyl or pentadecyl ABS and 10 ppm of phosphate.
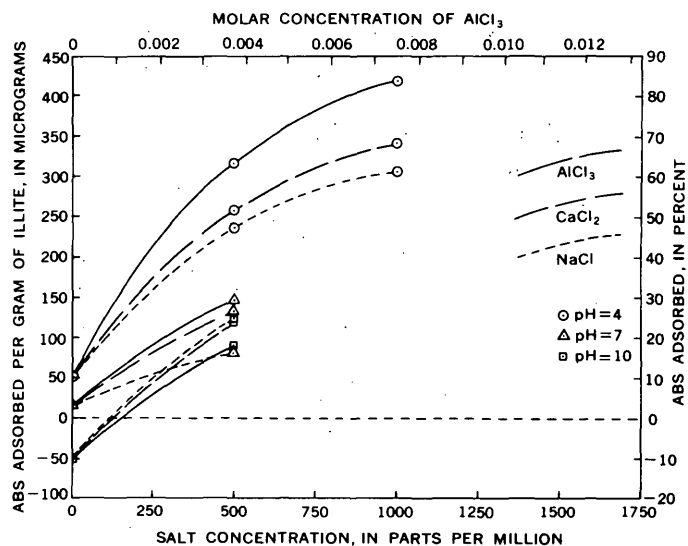
FIGURE 119.3.—Influence of salt concentration, valence, and pH on adsorption of ABS by illite. Test solutions contained 5 ppm of dodecyl ABS.

as much as 1,000 m² per g, and average pore diameters are about 20 A. The experimental method for the synthetic adsorbents was identical with that used for the clays. Figure 119.4 shows that, compared with the synthetic adsorbents, natural clays are inefficient adsorbents for ABS. These disparities in adsorption of ABS can be attributed to the exclusively positive surface and large pore diameter of colloidal alumina and to the high external and internal surface area of activated carbon.

REFERENCES

Grim, R. E., Bray, R. M., and Bradley, W. F., 1937, The mica in argillaceous sediments: Am. Mineralogist, v. 22, p. 813–829.

Warshaw, C. M., 1958, Experimental studies of illite, v. 7 of Clays and clay minerals: London, Pergamon Press, p. 303–316.

Wayman, C. H., Robertson, J. B., and Page, H. G., 1963, Adsorption of the surfactant ABS [35] on kaolinite: Art. 238 in U.S. Geol. Survey Prof. Paper 450–E, p. E181–E183.

Wayman, C. H., Page, H. G., and Robertson, J. B., 1963, Adsorption of the surfactant ABS [35] on montmorillonite: Art. 59 in U.S. Geol. Survey Prof. Paper 475–B, p. B213–B216.
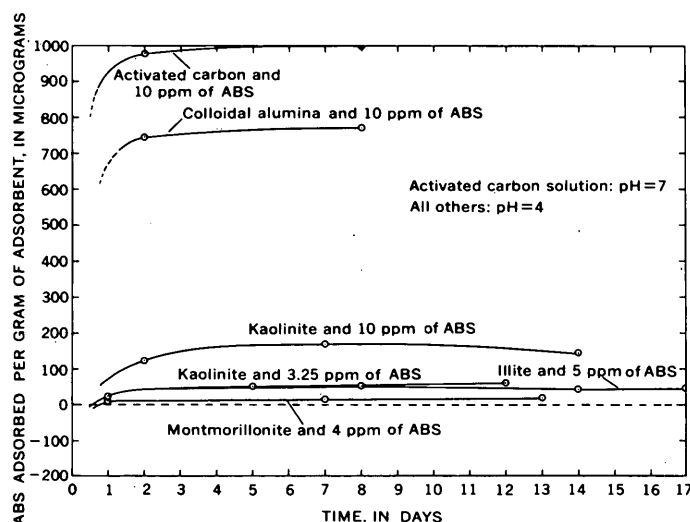
FIGURE 119.4—Adsorption of ABS by clay minerals as compared to synthetic adsorbents.

Article 120

BIODEGRADATION OF SURFACTANTS IN SYNTHETIC DETERGENTS UNDER AEROBIC AND ANAEROBIC CONDITIONS AT 10°C

By C. H. WAYMAN and J. B. ROBERTSON, Denver, Colo.

Abstract.—Studies of bacterial degradation of ABS at 10°C under aerobic and anaerobic conditions indicate significant reduction of ABS in samples containing 1,450,000 bacteria per ml. Straight-chain ABS is degraded to a greater extent than branched-chain ABS, and the aerobic environment is more effective than the anaerobic in ABS reduction.

Since World War II, more than 500,000 new synthetic chemicals have been placed at public disposal, and this amount is increased by about 10,000 per year. Many of these products are discharged directly into surface water or into the ground. Unless these compounds can be chemically degraded (by dissolution or hydrolysis) or oxidized by aerobic bacteria, pollution of ground water or surface water may result. Anionic surfactants in synthetic detergents resist biochemical degradation. Thus, when sewage effluents containing these refractory substances are dumped into rivers or streams, pollution of ground water may occur from natural infiltration from the streams. Likewise, septic-tank effluents containing surfactants may pollute ground water unless the surfactants are adsorbed by soils during infiltration.

In commercial detergents, alkylbenzenesulfonate (ABS) is the anionic surfactant that is responsible for pollution problems. The alkyl chain in this compound probably contains 12 to 15 carbon atoms and apparently is highly branched (Continental Oil Co., 1955), as indicated by the following structure:

$$CH_3-CH_2-CH_2-\underset{\underset{CH_3}{|}}{CH}-CH_2-\underset{\underset{CH_3}{|}}{CH}-CH_2-\underset{\underset{CH_3}{|}}{C}-CH_3$$

NaSO₃ (1)
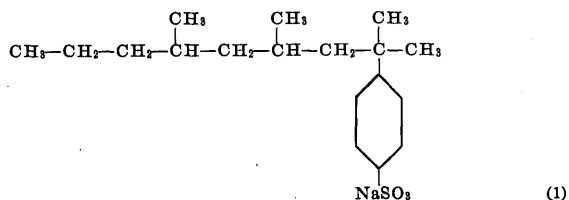
Other forms of ABS branched structures may be represented as follows:

$$CH_3-CH_2-CH_2-CH_2-\underset{\underset{CH_3}{|}}{\overset{\overset{CH_3}{|}}{C}}-CH_2-CH_2-\overset{\overset{CH_3}{|}}{\underset{\underset{CH_3}{|}}{C}}$$

NaSO₃ (2)

$$\underset{\underset{CH_3}{|}}{\overset{\overset{CH_3}{|}}{HC}}-CH_2-\underset{\underset{CH_3}{|}}{\overset{\overset{CH_3}{|}}{C}}-CH_2-CH_2-\overset{\overset{CH_3}{|}}{C}$$

NaSO₃ (3)
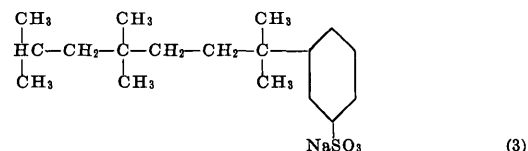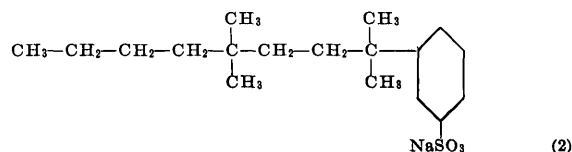
Because ABS is not completely degraded by bacteria in water, pollution of surface water and ground water by ABS has been reported from many localities throughout the Nation (Lauman, 1959; Nichols and Koepp, 1961; Walton, 1960). McKinney and Symons (1956) indicated that common soil or water bacteria, such as *Alcaligenes, Pseudomonas, Aerobacter, Escherichia,* and *Flavobacterium* are capable of surviving and growing in ABS agar when ABS is the only source of carbon for metabolism. Wayman and others (1963) have shown also that concentrations of ABS normally found in sewage or surface water are not toxic to bacteria, especially *Escherichia coli.* These data suggest that bacteria can metabolize ABS, but not completely. The inability of bacteria to degrade ABS completely seems related to the structure of ABS. For activated-sludge systems in sewage plants, McKinney and Symons (1959) point out that ABS metabolism starts with the terminal methyl group (CH₃) on the hydrocarbon side chain. The terminal methyl group is oxidized by enzymes to a carboxyl group. Then the hydrocarbon side

ART. 120 *IN* U.S. GEOL. SURVEY PROF. PAPER 475–C, PAGES C224–C227. 1963.

C224

chain is metabolized until it reaches the quaternary carbon. The quaternary carbon is probably located at the point where the hydrocarbon side chain joins the benezene ring. This oxidation scheme would apply to the type 1 ABS structure shown above. In the normal mechanism of oxidation, two hydrogen atoms are removed at a time and oxidized to water. When the oxidation reaches the quaternary carbon, only one hydrogen is available. This effect blocks ABS metabolism and terminates the oxidation. Hence, the complex branching of ABS prevents complete degradation by bacteria. Other investigators (Hammerton, 1955; and Truesdale, 1962) also attribute incomplete degradation of ABS to the branched structure.

To remedy or to ameliorate this effect of incomplete degradation of ABS, the development of ABS with a straight-chain configuration as shown below has been suggested:

$$CH_3-(CH_2)_6-CH-\underset{CH_3}{\bigcirc}-NaSO_3 \qquad (4)$$

$$CH_3-(CH_2)_6-\overset{CH_3}{\underset{CH_3}{C}}-\bigcirc-NaSO_3 \qquad (5)$$

The ABS structures represented by types 1 to 3 are referred to as "hard" substances, whereas those for 4 and 5 are called "soft." Studies of ABS degradation by activated sludge indicate that about 67 percent of the "hard" type of ABS and 94 percent of the "soft" type of ABS in solution can be degraded and thus be removed from solution.

In surface water or in water infiltrating the ground, degradation of ABS can be achieved only by bacterial activity. For surface water, the process involves an aerated system, and for infiltrating water, especially from septic tanks, an anaerobic system. Because previous studies on ABS degradation by activated-sludge treatment cannot be applied directly to surface water or to ground water, the authors studied the effects of aerobic and anaerobic systems on ABS in the temperature range 10° to 35°C. This article summarizes experimental results for aerobic and anaerobic systems at 10°C.

The source of bacteria utilized in the study consisted of the effluent from the Denver sewage treatment plant. The composition of selected constituents of this effluent over a 1-year period indicated the following ranges: bacteria, 100,000 to 4,000,000 per ml; detergent (ABS), 3 to 8 parts per million; dissolved solids, 450 to 1,000 ppm; dissolved oxygen, 0 to 5 ppm; biological oxygen demand (BOD), 125 to 250 ppm; and pH, 6.2 to 8.1.

Solutions were prepared by either no dilution or dilution of the sewage effluent with distilled water to give starting concentrations of total or coliform bacteria that ranged from 6,000 to 1,500,000 per ml. Then three types of ABS were added to various solutions, giving starting concentrations of as much as 13 ppm: sample 1, branched-chain ABS; sample 2, domestic straight-chain ABS; and sample 3, German straight-chain ABS. All samples were prepared in 1-liter volumetric containers and reduced to 500 ml for testing purposes. Samples were placed in a constant-temperature bath (10° ± 0.1°C). Periodically, samples were removed from solution and analyzed for ABS, total bacteria, and coliform bacteria. ABS was determined by the methylene-blue method. Total bacteria and coliform bacteria were determined by the pour-plate technique using Nutrient and MacConkey agars, respectively, at an incubation temperature of 37° for 72 hours.

Figure 120.1 shows the rate of degradation of both branched-chain ABS and domestic straight-chain ABS under anaerobic conditions at 10°C. The starting concentrations of ABS and bacteria studied were:

Sample 1:

Branched-chain ABS	13 ppm.
Coliform bacteria	2,000 per ml.
Total bacteria	6,000 per ml.

Sample 2:

Domestic straight-chain ABS	12 ppm.
Coliform bacteria	2,000 per ml.
Total bacteria	6,000 per ml.

The data indicate that about 6 days is required for bacteria to become acclimated to the environment. After 6 days, bacteria thrive more readily on straight-chain ABS than on branched-chain ABS. The bacteria were unable to metabolize significant amounts of either form of ABS even after 50 days. Bacteria probably exist for long periods of time on other constituents in the diluted sewage. The dying off of bacteria with time might be attributed to the toxic effect of constituents concentrated in solution from bacterial metabolism.

Figure 120.2 shows the effect of degradation of ABS under the conditions indicated in figure 120.1, but the starting concentrations were 15,000 per ml and 60,000 per ml for coliform and total bacteria, respectively. No significant degradation of ABS was observed; with increased concentration of bacteria, the period for acclimation to the environment increases. Both figures 120.1 and 120.2 indicate that in moderate anaerobic environments coliform bacteria die off more rapidly when branched-chain ABS is in solution. Thus, even in anaerobic environments coliform bacteria may persist for significant periods of time through metabolism of sewage constituents other than ABS.
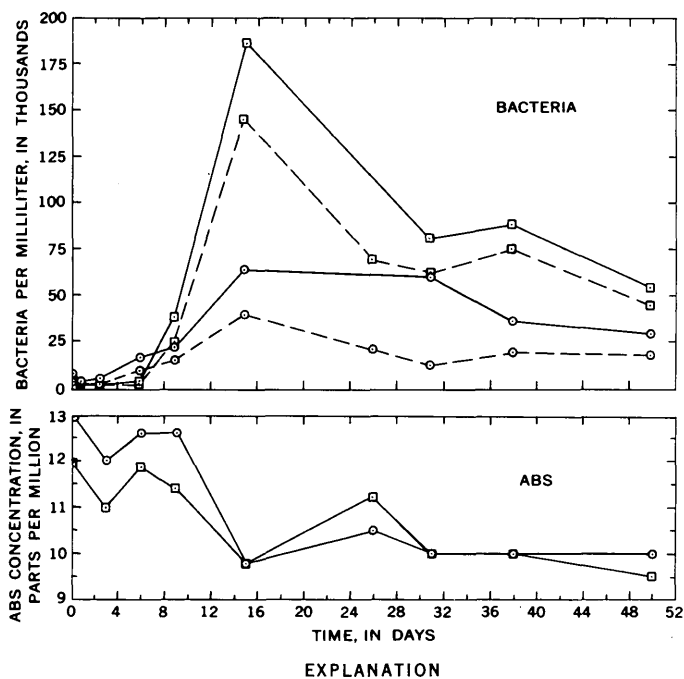
FIGURE 120.1.—Rate of degradation of ABS under anaerobic conditions at 10°C for initial concentrations of coliform bacteria (2,000 per ml) and total bacteria (6,000 per ml).
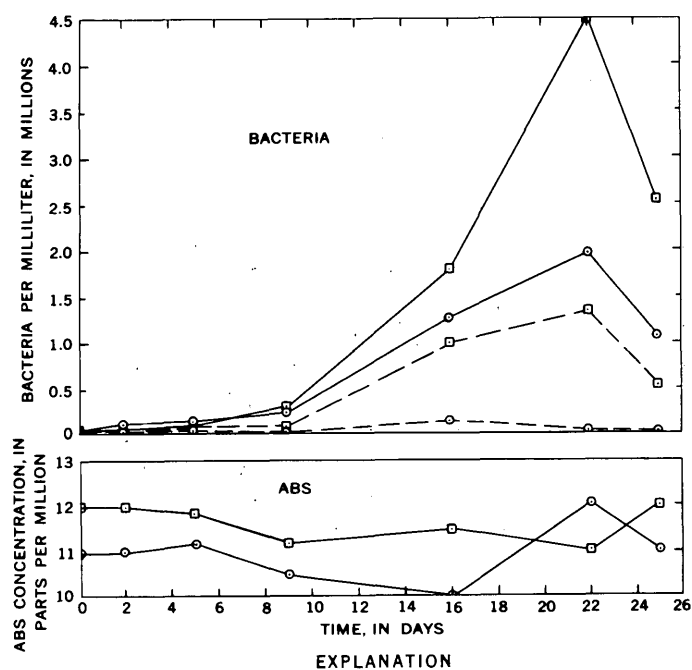
FIGURE 120.2.—Rate of degradation of ABS under anaerobic conditions at 10°C for initial concentrations of coliform bacteria (15,000 per ml) and total bacteria (60,000 per ml).

Figure 120.3 shows the results of experiments on undiluted sewage effluent for starting concentrations of 1,450,000 total bacteria per ml. These solutions had an original content of branched-chain ABS of 4 ppm in a somewhat degraded condition. Additional branched-chain or straight-chain ABS was added to raise the initial ABS concentrations to between 10 and 11 ppm. Data are given for both anaerobic and aerobic systems. Aerobic conditions were maintained by bubbling filtered air through solutions at a constant flow rate. Figure 120.3 shows that the time required for equilibrium degradation of ABS in both aerobic and anaerobic systems is more than 10 days. In anaerobic environments, about 50 percent of both branched-chain and straight-chain types of ABS added to the undiluted sewage waste can be degraded. There seems to be little difference between degradation of the German straight-chain ABS in aerobic as compared to anaerobic environments; significant amounts of the German
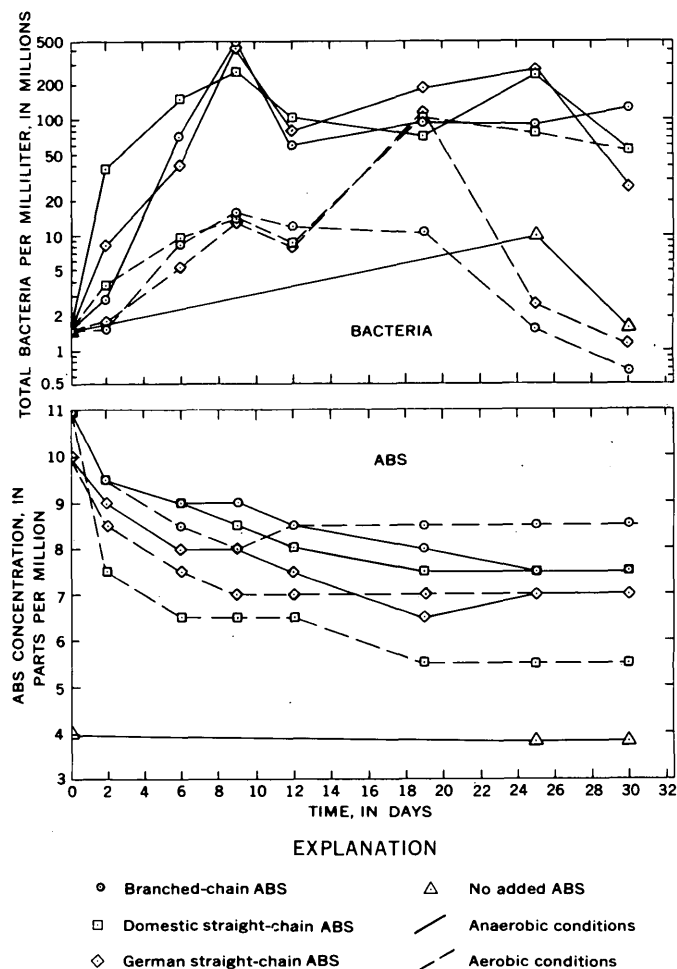
FIGURE 120.3.—Rate of degradation of ABS under anaerobic and aerobic conditions at 10°C for initial total bacterial concentrations of 1,450,000 per ml.

straight-chain ABS can be degraded in both environments. After about 19 days in an aerobic environment, as much as 75 percent of the domestic straight-chain ABS added to the undiluted sewage effluent can be degraded. The significant and rapid growth curves of bacteria might be attributed to combined effects of metabolizing both ABS and other nutrients in the sewage solutions. Results for coliform bacteria can be explained on a basis identical to that for figure 120.2.

This study suggests the following conclusions:

1. For both aerobic and anaerobic environments, at 10°C and having initial total bacterial counts of 1,450,000 per ml, the time required for equilibrium degradation of ABS is more than 10 days.

2. In anaerobic environments described in (1), about 50 percent of both branched-chain and straight-chain types of ABS added to undiluted sewage waste can be degraded under conditions of equilibrium.

3. In aerobic environments described in (1), about 40 percent of the branched-chain ABS, 75 percent of the domestic straight-chain ABS, and 50 percent of a German straight-chain ABS can be degraded under conditions of equilibrium.

4. As much as 50 percent degradation of domestic straight chain occurs after 2 days in the aerobic environment described in (1). This may be compared with degradations of 25 percent or less for the other ABS types in both anaerobic and aerobic environments for 2 days.

REFERENCES

Continental Oil Co., 1955, Structure of alkyl benzene sulfonates: Continental Oil Co. Central Research Labs. Rept. 139–55–503.

Hammerton, C., 1955, Observations on the decay of synthetic anionic detergents in natural waters: Jour. Appl. Chemistry, (London), v. 5, p. 517–524.

Lauman, H. E., 1959, Study of synthetic detergents in ground water, Suffolk County Area, Long Island: Prepared for the Long Island Home Builders Inst., Inc., 9 p.

McKinney, R. E., and Symons, J. M., 1959, Bacterial degradation of ABS, I. Fundamental biochemistry: Sewage and Indus. Wastes Jour., v. 31, p. 549–556.

Nichols, M. S., and Koepp, E., 1961, Synthetic detergents as a criterion of Wisconsin ground water pollution: Am. Water Works Assoc. Jour., v. 53, p. 303–306.

Truesdale, G.A., 1962, Pollution by synthetic detergents: Chem. Products, Jan. 1962, p. 1–8.

Walton, Graham, 1960, ABS contamination: Am. Water Works Assoc. Jour., v. 52, p. 1354–1362.

Wayman, C. H., Robertson, J. B., and Page, H. G., 1963, Factors influencing the survival of *Escherichia coli* in detergent solutions: Art. 57 *in* U.S. Geol. Survey Prof. Paper 475–B, p. B205–B208.

Article 121

DIRECT MEASUREMENT OF SHEAR IN OPEN-CHANNEL FLOW

By JACOB DAVIDIAN and D. I. CAHAL, Washington, D.C.

Abstract.—A floating-plate and knife-edge beam-balance device designed for the direct measurement of the shear along the boundary of an open rectangular channel was built and tested. The instrument was found to be unsatisfactory; its accuracy was inadequate and its operation was erratic.

The standard method for the determination of shear in open-channel flow utilizes a pitot tube as described by Hsu (1955). In an effort to make direct measurements of shear in open rectangular channels, a floating-plate beam-balance instrument was designed and built by the U.S. Geological Survey. Tests of the instrument in a laboratory flume indicated that its operation was unsatisfactory and its accuracy was inadequate. A schematic sketch of the instrument is shown in figure 121.1.

The shear-plate device was tested at the National Bureau of Standards Hydraulic Laboratory in a smooth tiltable flume 140 feet long and 18 inches wide. Tests were made at normal depths of flow of 5 and 8 inches. The shear plate, 1 inch high, 6 inches long, and $3/16$ inch thick, floats within an opening in the wall of the flume 118 feet from the entrance and has a clearance of 0.015 inch all around. The plate is set with its bottom 2 inches off the floor of the flume. Behind the plate, on the outside of the flume, is a water-filled plastic compartment so arranged that the plate is completely surrounded by fluid. Four vertical fins are attached to the back side of the plate, allowing free circulation of water between the flume and the outside well, and serving as hydraulic dampeners to lessen the tendency of the plate to flutter. The shear plate is mounted on the vertical arm of a knife-edge beam balance.

The upstream end of the horizontal arm of the balance has suspended from it the core of a linear variable-differential transformer. The shear plate is positioned free and flush with the flume wall in still water, then exposed to the moving water in the flume. Any devia-tion from the null or centered position of the plate is indicated on the dial of a transformer indicator.

On the downstream end of the horizontal arm is a pan to hold the weights necessary to maintain the null position of the plate. Because the ratio between the plate arm and the pan arm is unity, and because the knife edge of the balance is practically frictionless, the shear can be computed as the ratio of the weight in the pan
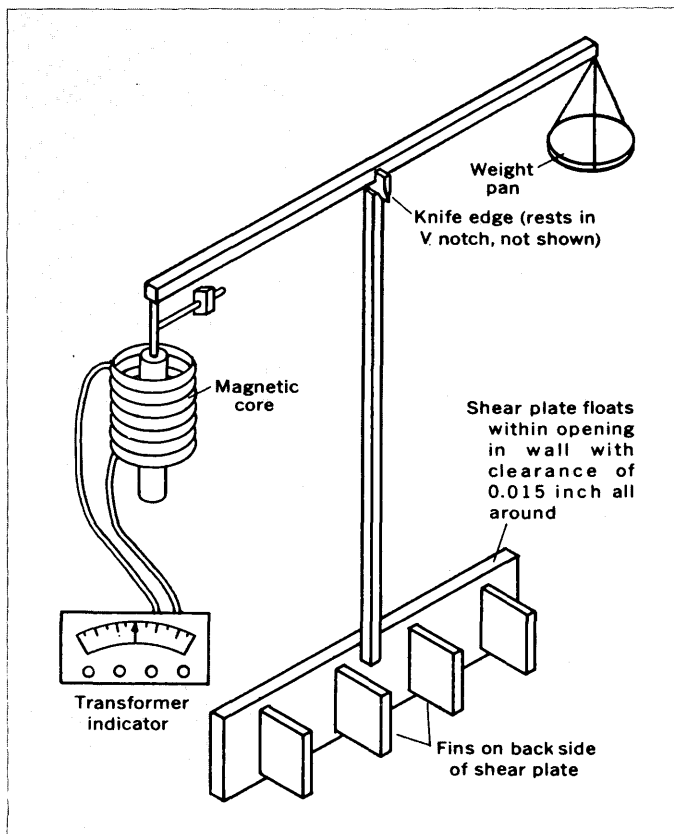
FIGURE 121.1—Schematic sketch of shear-plate knife-edge beam-balance device.

ART. 121 *IN* U.S. GEOL. SURVEY PROF. PAPER 475-C. PAGES C228–C229. 1963.

C228

to the area of the plate. The variation of the friction factor f, within a Reynolds number range from $\mathbb{R} = 6 \times 10^4$ to 6×10^5, is well described by the equation $1/\sqrt{f} = 2.03 \log \mathbb{R} \sqrt{f} - 1.21$.

The relationship between the velocity of the flow and the plate shear as computed from the balance weights is shown in figure 121.2 (top curve). All the tests at 8 inches water depth and most of the tests at 5 inches depth show a relation well described by the solid line. The dashed line shows that at 5 inches depth and between velocities of 2 and 5 feet per second (corresponding to Froude numbers, $\mathbb{F}$, of about 0.6 to 1.2) the measured plate shear is too high. Although it was not possible to achieve critical flow in the 8-inch depth series, there seems to be no shear increase at velocities in the 8-inch series which are critical in the 5-inch series. This apparent reaction of the shear plate in the neighborhood of the critical Froude number has not been checked at other depths of water, but has been affirmed in a repetition of the measurements at the 5-inch depth.

Figure 121.2 (bottom curve) shows the straight-line relationship between velocity and the plate shear as determined by measurements of local surface friction made by the Preston-tube method, using a round pitot at the wall surface in the vicinity of the plate. The 5-inch-depth measurements do not show an increase in shear at the critical Froude number. Additional studies of boundary shear in this flume, using a Preston tube are reported in Article 113.

Although the reason for the high indicated shear values at $\mathbb{F} = 1.0$ is not known, it is not this phenomenon alone which makes the shear-plate beam-balance device an unreliable instrument. The difficulty in visually adjusting the plate and in setting and keeping it free within its niche and flush with the wall becomes greater with increase in velocity and associated increases in opacity and turbulence. Furthermore, although it presents no difficulties if regularly removed, mineral matter deposited from the water and from the aerosol wetting agent used, gradually builds up on various parts of the mechanism; however, it is easily cleaned off. In some tests, the weight required to bal-
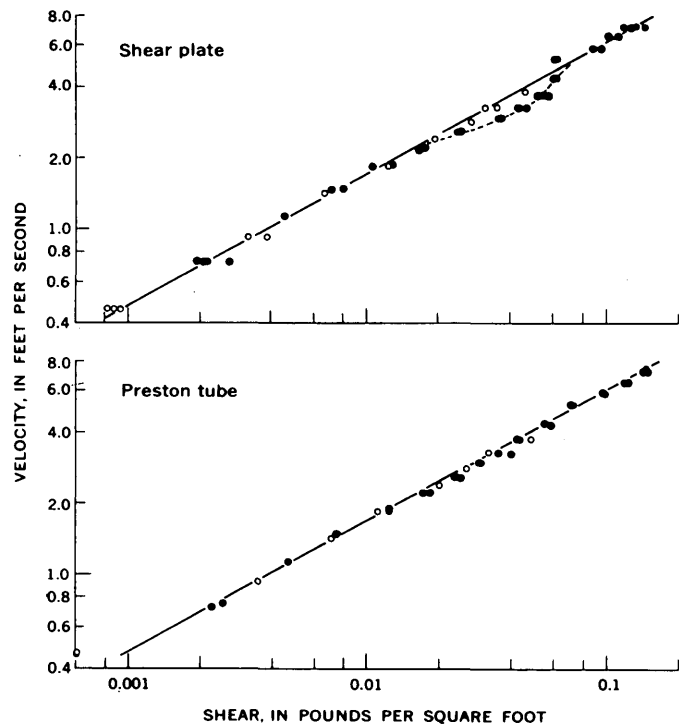
FIGURE 121.2.—Variation of shear with velocity. Top, shear computed with shear-plate beam-balance device; bottom, shear computed with Preston tube. Circles, 8-inch depth; dots, 5-inch depth.

ance the shear force varied as much as ± 20 percent. It is doubtful that an accuracy much better than ± 10 percent can be ascribed to computations of shear based on the shear-plate data, particularly for higher Froude numbers, even though repeatability was excellent in some runs.

The shear-plate device in its present form is an unsatisfactory means of measuring boundary-wall shear directly in water. Its accuracy is limited by the characteristics of the medium in which it is intended to operate.

REFERENCE

Hsu, E. Y., 1955, The measurement of local turbulent skin friction by means of surface pitot tubes: The David W. Taylor Model Basin Research and Devel. Rept. 957.

SUBJECT INDEX

[For major subject heading such as "Economic geology," "Ground water," "Stratigraphy," see under State names or refer to table of contents]

AUTHOR INDEX